Nuclear Safety
NEA/CSNI/R(2012)6
February 2012
www.oecd-nea.org

OECD

International Standard Problem No. 50

ATLAS Test, SB-DVI-09:
50% (6-inch) Break of DVI line
of the APR1400
Final Integration Report

Volume II
Figures and Participants' Reports
of Blind Calculations

AEN
NEA

NUCLEAR ENERGY AGENCY

Organisation de Coopération et de Développement Économiques
Organisation for Economic Co-operation and Development

27-Feb-2012

English text only

NUCLEAR ENERGY AGENCY
COMMITTEE ON THE SAFETY OF NUCLEAR INSTALLATIONS

NEA/CSNI/R(2012)6/PART2
Unclassified

International Standard Problem N° 50
ATLAS Test, SB-DVI-09: 50% (6-inch) Break of DVI line of the APR1400
Final Integration Report

Volume II
Figures and Participants' Reports of Blind Calculations

This document is only available in PDF.

JT03316611

English text only

ORGANISATION FOR ECONOMIC CO-OPERATION AND DEVELOPMENT

The OECD is a unique forum where the governments of 34 democracies work together to address the economic, social and environmental challenges of globalisation. The OECD is also at the forefront of efforts to understand and to help governments respond to new developments and concerns, such as corporate governance, the information economy and the challenges of an ageing population. The Organisation provides a setting where governments can compare policy experiences, seek answers to common problems, identify good practice and work to co-ordinate domestic and international policies.

The OECD member countries are: Australia, Austria, Belgium, Canada, Chile, the Czech Republic, Denmark, Estonia, Finland, France, Germany, Greece, Hungary, Iceland, Ireland, Israel, Italy, Japan, Luxembourg, Mexico, the Netherlands, New Zealand, Norway, Poland, Portugal, the Republic of Korea, the Slovak Republic, Slovenia, Spain, Sweden, Switzerland, Turkey, the United Kingdom and the United States. The European Commission takes part in the work of the OECD.

OECD Publishing disseminates widely the results of the Organisation's statistics gathering and research on economic, social and environmental issues, as well as the conventions, guidelines and standards agreed by its members.

This work is published on the responsibility of the OECD Secretary-General.
The opinions expressed and arguments employed herein do not necessarily reflect the official views of the Organisation or of the governments of its member countries.

NUCLEAR ENERGY AGENCY

The OECD Nuclear Energy Agency (NEA) was established on 1 February 1958. Current NEA membership consists of 30 OECD member countries: Australia, Austria, Belgium, Canada, the Czech Republic, Denmark, Finland, France, Germany, Greece, Hungary, Iceland, Ireland, Italy, Japan, Luxembourg, Mexico, the Netherlands, Norway, Poland, Portugal, the Republic of Korea, the Slovak Republic, Slovenia, Spain, Sweden, Switzerland, Turkey, the United Kingdom and the United States. The European Commission also takes part in the work of the Agency.

The mission of the NEA is:

– to assist its member countries in maintaining and further developing, through international co-operation, the scientific, technological and legal bases required for a safe, environmentally friendly and economical use of nuclear energy for peaceful purposes, as well as

– to provide authoritative assessments and to forge common understandings on key issues, as input to government decisions on nuclear energy policy and to broader OECD policy analyses in areas such as energy and sustainable development.

Specific areas of competence of the NEA include the safety and regulation of nuclear activities, radioactive waste management, radiological protection, nuclear science, economic and technical analyses of the nuclear fuel cycle, nuclear law and liability, and public information.

The NEA Data Bank provides nuclear data and computer program services for participating countries. In these and related tasks, the NEA works in close collaboration with the International Atomic Energy Agency in Vienna, with which it has a Co-operation Agreement, as well as with other international organisations in the nuclear field.

THE COMMITTEE ON THE SAFETY OF NUCLEAR INSTALLATIONS

"The Committee on the Safety of Nuclear Installations (CSNI) shall be responsible for the activities of the Agency that support maintaining and advancing the scientific and technical knowledge base of the safety of nuclear installations, with the aim of implementing the NEA Strategic Plan for 2011-2016 and the Joint CSNI/CNRA Strategic Plan and Mandates for 2011-2016 in its field of competence.

The Committee shall constitute a forum for the exchange of technical information and for collaboration between organisations, which can contribute, from their respective backgrounds in research, development and engineering, to its activities. It shall have regard to the exchange of information between member countries and safety R&D programmes of various sizes in order to keep all member countries involved in and abreast of developments in technical safety matters.

The Committee shall review the state of knowledge on important topics of nuclear safety science and techniques and of safety assessments, and ensure that operating experience is appropriately accounted for in its activities. It shall initiate and conduct programmes identified by these reviews and assessments in order to overcome discrepancies, develop improvements and reach consensus on technical issues of common interest. It shall promote the co-ordination of work in different member countries that serve to maintain and enhance competence in nuclear safety matters, including the establishment of joint undertakings, and shall assist in the feedback of the results to participating organisations. The Committee shall ensure that valuable end-products of the technical reviews and analyses are produced and available to members in a timely manner.

The Committee shall focus primarily on the safety aspects of existing power reactors, other nuclear installations and the construction of new power reactors; it shall also consider the safety implications of scientific and technical developments of future reactor designs.

The Committee shall organise its own activities. Furthermore, it shall examine any other matters referred to it by the Steering Committee. It may sponsor specialist meetings and technical working groups to further its objectives. In implementing its programme the Committee shall establish co-operative mechanisms with the Committee on Nuclear Regulatory Activities in order to work with that Committee on matters of common interest, avoiding unnecessary duplications.

The Committee shall also co-operate with the Committee on Radiation Protection and Public Health, the Radioactive Waste Management Committee, the Committee for Technical and Economic Studies on Nuclear Energy Development and the Fuel Cycle and the Nuclear Science Committee on matters of common interest."

NEA/CSNI/R(2012)6

OECD/NEA/CSNI
International Standard Problem No. 50

ATLAS Test, SB-DVI-09: 50% (6-inch) Break of DVI line of the APR1400

Final Integration Report

Volume II

Figures and Participants' Reports of Blind Calculations

K.Y. Choi, W.P. Baek, S.Cho, H.S. Park, K.H. Kang, Y.S. Kim, H.T. Kim

Thermal Hydraulics Safety Research Division

Korea Atomic Energy Research Institute

Table of Contents

Volume II

Appendix-B: Figures Comparing Blind Predictions with Selected Data B-1
Appendix-C: Blind Reports Provided by Participants C-1

List of Appendix-B Figures

Figure B.1 Total core power (D01) B-2
Figure B.1-A Total core power (D01) B-3
Figure B.1-B Total core power (D01) B-3
Figure B.1-C Total core power (D01) B-4
Figure B.1-D Total core power (D01) B-4
Figure B.2 Heat removal rate of SG1 (D02) B-5
Figure B.2-A Heat removal rate of SG1 (D02) B-6
Figure B.2-B Heat removal rate of SG1 (D02) B-6
Figure B.2-C Heat removal rate of SG1 (D02) B-7
Figure B.2-D Heat removal rate of SG1 (D02) B-7
Figure B.3 Heat removal rate of SG2 (D03) B-8
Figure B.3-A Heat removal rate of SG2 (D03) B-9
Figure B.3-B Heat removal rate of SG2 (D03) B-9
Figure B.3-C Heat removal rate of SG2 (D03) B-10
Figure B.3-D Heat removal rate of SG2 (D03) B-10
Figure B.4 Upper head pressure (D04) B-11
Figure B.4-A Upper head pressure (D04) B-12
Figure B.4-B Upper head pressure (D04) B-12
Figure B.4-C Upper head pressure (D04) B-13
Figure B.4-D Upper head pressure (D04) B-13
Figure B.5 Pressure of the pressurizer (D05) B-14
Figure B.5-A Pressure of the pressurizer (D05) B-15
Figure B.5-B Pressure of the pressurizer (D05) B-15
Figure B.5-C Pressure of the pressurizer (D05) B-16
Figure B.5-D Pressure of the pressurizer (D05) B-16
Figure B.6 Pressure in SG-1 dome (D06) B-17
Figure B.6-A Pressure in SG-1 dome (D06) B-18
Figure B.6-B Pressure in SG-1 dome (D06) B-18
Figure B.6-C Pressure in SG-1 dome (D06) B-19
Figure B.6-D Pressure in SG-1 dome (D06) B-19
Figure B.7 Pressure in SG-2 dome (D07) B-20
Figure B.7-A Pressure in SG-2 dome (D07) B-21
Figure B.7-B Pressure in SG-2 dome (D07) B-21
Figure B.7-C Pressure in SG-2 dome (D07) B-22
Figure B.7-D Pressure in SG-2 dome (D07) B-22
Figure B.8 Pressure in SIT-01 (D08) B-23

Figure B.8-A Pressure in SIT-01 (D08) B-24
Figure B.8-B Pressure in SIT-01 (D08) B-24
Figure B.8-C Pressure in SIT-01 (D08) B-25
Figure B.8-D Pressure in SIT-01 (D08) B-25
Figure B.9 Pressure in SIT-02 (D09) B-26
Figure B.9-A Pressure in SIT-02 (D09) B-27
Figure B.9-B Pressure in SIT-02 (D09) B-27
Figure B.9-C Pressure in SIT-02 (D09) B-28
Figure B.9-D Pressure in SIT-02 (D09) B-28
Figure B.10 Pressure in SIT-03 (D10) B-29
Figure B.10-A Pressure in SIT-03 (D10) B-30
Figure B.10-B Pressure in SIT-03 (D10) B-30
Figure B.10-C Pressure in SIT-03 (D10) B-31
Figure B.10-D Pressure in SIT-03 (D10) B-31
Figure B.11 Containment pressure (D11) B-32
Figure B.11-A Containment pressure (D11) B-33
Figure B.11-B Containment pressure (D11) B-33
Figure B.11-C Containment pressure (D11) B-34
Figure B.11-D Containment pressure (D11) B-34
Figure B.12 Pressure difference between SG-1 inlet and outlet plenum 1 (D12) B-35
Figure B.12-A Pressure difference between SG-1 inlet and outlet plenum 1 (D12) B-36
Figure B.12-B Pressure difference between SG-1 inlet and outlet plenum 1 (D12) B-36
Figure B.12-C Pressure difference between SG-1 inlet and outlet plenum 1 (D12) B-37
Figure B.12-D Pressure difference between SG-1 inlet and outlet plenum 1 (D12) B-37
Figure B.13 DP Pressure difference between SG-1 inlet and outlet plenum 2 (D13) B-38
Figure B.13-A DP Pressure difference between SG-1 inlet and outlet plenum 2 (D13) B-39
Figure B.13-B DP Pressure difference between SG-1 inlet and outlet plenum 2 (D13) B-39
Figure B.13-C DP Pressure difference between SG-1 inlet and outlet plenum 2 (D13) B-40
Figure B.13-D DP Pressure difference between SG-1 inlet and outlet plenum 2 (D13) B-40
Figure B.14 DP Pressure difference between SG-2 inlet and outlet plenum 1 (D14) B-41
Figure B.14-A DP Pressure difference between SG-2 inlet and outlet plenum 1 (D14) B-42
Figure B.14-B DP Pressure difference between SG-2 inlet and outlet plenum 1 (D14) B-42
Figure B.14-C DP Pressure difference between SG-2 inlet and outlet plenum 1 (D14) B-43
Figure B.14-D DP Pressure difference between SG-2 inlet and outlet plenum 1 (D14) B-43
Figure B.15 DP Pressure difference between SG-2 inlet and outlet plenum 2 (D15) B-44
Figure B.15-A DP Pressure difference between SG-2 inlet and outlet plenum 2 (D15) B-45
Figure B.15-B DP Pressure difference between SG-2 inlet and outlet plenum 2 (D15) B-45
Figure B.15-C DP Pressure difference between SG-2 inlet and outlet plenum 2 (D15) B-46

Figure B.15-D DP Pressure difference between SG-2 inlet and outlet plenum 2 (D15) B-46
Figure B.16 Water temperature in the core inlet plenum (D16) B-47
Figure B.16-A Water temperature in the core inlet plenum (D16) B-48
Figure B.16-B Water temperature in the core inlet plenum (D16) B-48
Figure B.16-C Water temperature in the core inlet plenum (D16) B-49
Figure B.16-D Water temperature in the core inlet plenum (D16) B-49
Figure B.17 Water temperature in the core outlet plenum (D17) B-50
Figure B.17-A Water temperature in the core outlet plenum (D17) B-51
Figure B.17-B Water temperature in the core outlet plenum (D17) B-51
Figure B.17-C Water temperature in the core outlet plenum (D17) B-52
Figure B.17-D Water temperature in the core outlet plenum (D17) B-52
Figure B.18 Water temperature in the pressurizer (D18) B-53
Figure B.18-A Water temperature in the pressurizer (D18) B-54
Figure B.18-B Water temperature in the pressurizer (D18) B-54
Figure B.18-C Water temperature in the pressurizer (D18) B-55
Figure B.18-D Water temperature in the pressurizer (D18) B-55
Figure A19 Water temperature in the hot leg 1 (D19) B-56
Figure B.19-A Water temperature in the hot leg 1 (D19) B-57
Figure B.19-B Water temperature in the hot leg 1 (D19) B-57
Figure B.19-C Water temperature in the hot leg 1 (D19) B-58
Figure B.19-D Water temperature in the hot leg 1 (D19) B-58
Figure B.20 Water temperature in the hot leg 2 (D20) B-59
Figure B.20-A Water temperature in the hot leg 2 (D20) B-60
Figure B.20-B Water temperature in the hot leg 2 (D20) B-60
Figure B.20-C Water temperature in the hot leg 2 (D20) B-61
Figure B.20-D Water temperature in the hot leg 2 (D20) B-61
Figure B.21 Water temperature in the cold leg 1A (D21) B-62
Figure B.21-A Water temperature in the cold leg 1A (D21) B-63
Figure B.21-B Water temperature in the cold leg 1A (D21) B-63
Figure B.21-C Water temperature in the cold leg 1A (D21) B-64
Figure B.21-D Water temperature in the cold leg 1A (D21) B-64
Figure B.22 Water temperature in the cold leg 1B (D22) B-65
Figure B.22-A Water temperature in the cold leg 1B (D22) B-66
Figure B.22-B Water temperature in the cold leg 1B (D22) B-66
Figure B.22-C Water temperature in the cold leg 1B (D22) B-67
Figure B.22-D Water temperature in the cold leg 1B (D22) B-67
Figure B.23 Water temperature in the cold leg 2A (D23) B-68
Figure B.23-A Water temperature in the cold leg 2A (D23) B-69

Figure B.23-B Water temperature in the cold leg 2A (D23) B-69
Figure B.23-C Water temperature in the cold leg 2A (D23) B-70
Figure B.23-D Water temperature in the cold leg 2A (D23)....B-70
Figure B.24 Water temperature in the cold leg 2B (D24) B-71
Figure B.24-A Water temperature in the cold leg 2B (D24) B-72
Figure B.24-B Water temperature in the cold leg 2B (D24)....B-72
Figure B.24-C Water temperature in the cold leg 2B (D24) B-73
Figure B.24-D Water temperature in the cold leg 2B (D24)....B-73
Figure B.25 Water temperature in SG-1 inlet plenum (D25) B-74
Figure B.25-A Water temperature in SG-1 inlet plenum (D25) B-75
Figure B.25-B Water temperature in SG-1 inlet plenum (D25)....B-75
Figure B.25-C Water temperature in SG-1 inlet plenum (D25)....B-76
Figure B.25-D Water temperature in SG-1 inlet plenum (D25) B-76
Figure B.26 Water temperature in SG-1 outlet plenum (D26) B-77
Figure B.26-A Water temperature in SG-1 outlet plenum (D26) B-78
Figure B.26-B Water temperature in SG-1 outlet plenum (D26)....B-78
Figure B.26-C Water temperature in SG-1 outlet plenum (D26) B-79
Figure B.26-D Water temperature in SG-1 outlet plenum (D26)....B-79
Figure B.27 Water temperature in SG-2 inlet plenum (D27) B-80
Figure B.27-A Water temperature in SG-2 inlet plenum (D27) B-81
Figure B.27-B Water temperature in SG-2 inlet plenum (D27)....B-81
Figure B.27-C Water temperature in SG-2 inlet plenum (D27)....B-82
Figure B.27-D Water temperature in SG-2 inlet plenum (D27) B-82
Figure B.28 Water temperature in SG-2 outlet plenum (D28) B-83
Figure B.28-A Water temperature in SG-2 outlet plenum (D28) B-84
Figure B.28-B Water temperature in SG-2 outlet plenum (D28)....B-84
Figure B.28-C Water temperature in SG-2 outlet plenum (D28) B-85
Figure B.28-D Water temperature in SG-2 outlet plenum (D28)....B-85
Figure B.29 Steam temperature in SG-1 steam dome (D29)....B-86
Figure B.29-A Steam temperature in SG-1 steam dome (D29)....B-87
Figure B.29-B Steam temperature in SG-1 steam dome (D29) B-87
Figure B.29-C Steam temperature in SG-1 steam dome (D29)....B-88
Figure B.29-D Steam temperature in SG-1 steam dome (D29)....B-88
Figure B.30 Steam temperature in SG-2 steam dome (D30)....B-89
Figure B.30-A Steam temperature in SG-2 steam dome (D30)....B-90
Figure B.30-B Steam temperature in SG-2 steam dome (D30) B-90
Figure B.30-C Steam temperature in SG-2 steam dome (D30)....B-91
Figure B.30-D Steam temperature in SG-2 steam dome (D30)....B-91

Figure B.31 Water temperature in the SIT-1 (D31) B-92
Figure B.31-A Water temperature in the SIT-1 (D31) B-93
Figure B.31-B Water temperature in the SIT-1 (D31) B-93
Figure B.31-C Water temperature in the SIT-1 (D31) B-94
Figure B.31-D Water temperature in the SIT-1 (D31) B-94
Figure B.32 Water temperature in the SIT-2 (D32) B-95
Figure B.32-A Water temperature in the SIT-2 (D32) B-96
Figure B.32-B Water temperature in the SIT-2 (D32) B-96
Figure B.32-C Water temperature in the SIT-2 (D32) B-97
Figure B.32-D Water temperature in the SIT-2 (D32) B-97
Figure B.33 Water temperature in the SIT-3 (D33) B-98
Figure B.33-A Water temperature in the SIT-3 (D33) B-99
Figure B.33-B Water temperature in the SIT-3 (D33) B-99
Figure B.33-C Water temperature in the SIT-3 (D33) B-100
Figure B.33-D Water temperature in the SIT-3 (D33) B-100
Figure B.34 Water temperature in the SIP-2 (D34) B-101
Figure B.34-A Water temperature in the SIP-2 (D34) B-102
Figure B.34-B Water temperature in the SIP-2 (D34) B-102
Figure B.34-C Water temperature in the SIP-2 (D34) B-103
Figure B.34-D Water temperature in the SIP-2 (D34) B-103
Figure B.35 Temperature in the containment (D35) B-104
Figure B.35-A Temperature in the containment (D35) B-105
Figure B.35-B Temperature in the containment (D35) B-105
Figure B.35-C Temperature in the containment (D35) B-106
Figure B.35-D Temperature in the containment (D35) B-106
Figure B.36 Steam temperature in the hot leg 1 (D36) B-107
Figure B.36-A Steam temperature in the hot leg 1 (D36) B-108
Figure B.36-B Steam temperature in the hot leg 1 (D36) B-108
Figure B.36-C Steam temperature in the hot leg 1 (D36) B-109
Figure B.36-D Steam temperature in the hot leg 1 (D36) B-109
Figure B.37 Steam temperature in the hot leg 2 (D37) B-110
Figure B.37-A Steam temperature in the hot leg 2 (D37) B-111
Figure B.37-B Steam temperature in the hot leg 2 (D37) B-111
Figure B.37-C Steam temperature in the hot leg 2 (D37) B-112
Figure B.37-D Steam temperature in the hot leg 2 (D37) B-112
Figure B.38 Steam temperature in the cold leg 1A (D38) B-113
Figure B.38-A Steam temperature in the cold leg 1A (D38) B-114
Figure B.38-B Steam temperature in the cold leg 1A (D38) B-114

Figure B.38-C Steam temperature in the cold leg 1A (D38) B-115
Figure B.38-D Steam temperature in the cold leg 1A (D38) B-115
Figure B.39 Steam temperature in the cold leg 1B (D39) B-116
Figure B.39-A Steam temperature in the cold leg 1B (D39) B-117
Figure B.39-B Steam temperature in the cold leg 1B (D39) B-117
Figure B.39-C Steam temperature in the cold leg 1B (D39) B-118
Figure B.39-D Steam temperature in the cold leg 1B (D39) B-118
Figure B.40 Steam temperature in the cold leg 2A (D40) B-119
Figure B.40-A Steam temperature in the cold leg 2A (D40) B-120
Figure B.40-B Steam temperature in the cold leg 2A (D40) B-120
Figure B.40-C Steam temperature in the cold leg 2A (D40) B-121
Figure B.40-D Steam temperature in the cold leg 2A (D40) B-121
Figure B.41 Steam temperature in the cold leg 2B (D41) B-122
Figure B.41-A Steam temperature in the cold leg 2B (D41) B-123
Figure B.41-B Steam temperature in the cold leg 2B (D41) B-123
Figure B.41-C Steam temperature in the cold leg 2B (D41) B-124
Figure B.41-D Steam temperature in the cold leg 2B (D41) B-124
Figure B.42 Wall temperature in the active core region 1 (D42) B-125
Figure B.42-A Wall temperature in the active core region 1 (D42) B-126
Figure B.42-B Wall temperature in the active core region 1 (D42) B-126
Figure B.42-C Wall temperature in the active core region 1 D42) B-127
Figure B.42-D Wall temperature in the active core region 1 (D42) B-127
Figure B.43 Wall temperature in the active core region 2 (D43) B-128
Figure B.43-A Wall temperature in the active core region 2 (D43) B-129
Figure B.43-B Wall temperature in the active core region 2 (D43) B-129
Figure B.43-C Wall temperature in the active core region 2 (D43) B-130
Figure B.43-D Wall temperature in the active core region 2 (D43) B-130
Figure B.44 Wall temperature in the active core region 3 (D44) B-131
Figure B.44-A Wall temperature in the active core region 3 (D44) B-132
Figure B.44-B Wall temperature in the active core region 3 (D44) B-132
Figure B.44-C Wall temperature in the active core region 3 (D44) B-133
Figure B.44-D Wall temperature in the active core region 3 (D44) B-133
Figure B.45 Wall temperature in the active core region 4 (D45) B-134
Figure B.45-A Wall temperature in the active core region 4 (D45) B-135
Figure B.45-B Wall temperature in the active core region 4 (D45) B-135
Figure B.45-C Wall temperature in the active core region 4 (D45) B-136
Figure B.45-D Wall temperature in the active core region 4 (D45) B-136
Figure B.46 Wall temperature in the active core region 5 (D46) B-137

Figure B.46-A Wall temperature in the active core region 5 (D46) B-138
Figure B.46-B Wall temperature in the active core region 5 (D46) B-138
Figure B.46-C Wall temperature in the active core region 5 (D46) B-139
Figure B.46-D Wall temperature in the active core region 5 (D46) B-139
Figure B.47 Wall temperature in the active core region 6 (D47) B-140
Figure B.47-A Wall temperature in the active core region 6 (D47) B-141
Figure B.47-B Wall temperature in the active core region 6 (D47) B-141
Figure B.47-C Wall temperature in the active core region 6 (D47) B-142
Figure B.47-D Wall temperature in the active core region 6 (D47) B-142
Figure B.48 Wall temperature in the active core region 7 (D48) B-143
Figure B.48-A Wall temperature in the active core region 7 (D48) B-144
Figure B.48-B Wall temperature in the active core region 7 (D48) B-144
Figure B.48-C Wall temperature in the active core region 7 (D48) B-145
Figure B.48-D Wall temperature in the active core region 7 (D48) B-145
Figure B.49 Wall temperature in the active core region 8 (D49) B-146
Figure B.49-A Wall temperature in the active core region 8 (D49) B-147
Figure B.49-B Wall temperature in the active core region 8 (D49) B-147
Figure B.49-C Wall temperature in the active core region 8 (D49) B-148
Figure B.49-D Wall temperature in the active core region 8 (D49) B-148
Figure B.50 Wall temperature in the active core region 9 (D50) B-149
Figure B.50-A Wall temperature in the active core region 9 (D50) B-150
Figure B.50-B Wall temperature in the active core region 9 (D50) B-150
Figure B.50-C Wall temperature in the active core region 9 (D50) B-151
Figure B.50-D Wall temperature in the active core region 9 (D50) B-151
Figure B.51 Wall temperature in the active core region 10 (D51) B-152
Figure B.51-A Wall temperature in the active core region 10 (D51) B-153
Figure B.51-B Wall temperature in the active core region 10 (D51) B-153
Figure B.51-C Wall temperature in the active core region 10 (D51) B-154
Figure B.51-D Wall temperature in the active core region 10 (D51) B-154
Figure B.52 Wall temperature in the active core region 11 (D52) B-155
Figure B.52-A Wall temperature in the active core region 11 (D52) B-156
Figure B.52-B Wall temperature in the active core region 11 (D52) B-156
Figure B.52-C Wall temperature in the active core region 11 (D52) B-157
Figure B.52-D Wall temperature in the active core region 11 (D52) B-157
Figure B.53 Wall temperature in the active core region 12 (D53) B-158
Figure B.53-A Wall temperature in the active core region 12 (D53) B-159
Figure B.53-B Wall temperature in the active core region 12 (D53) B-159
Figure B.53-C Wall temperature in the active core region 12 (D53) B-160

Figure B.53-D Wall temperature in the active core region 12 (D53) B-160
Figure B.54 Flow rate in DC-UH bypass line (D54) B-161
Figure B.54-A Flow rate in DC-UH bypass line (D54) B-162
Figure B.54-B Flow rate in DC-UH bypass line (D54) B-162
Figure B.54-C Flow rate in DC-UH bypass line (D54) B-163
Figure B.54-D Flow rate in DC-UH bypass line (D54) B-163
Figure B.55 Flow rate in DC-HL bypass line (D55) B-164
Figure B.55-A Flow rate in DC-HL bypass line (D55) B-165
Figure B.55-B Flow rate in DC-HL bypass line (D55) B-165
Figure B.55-C Flow rate in DC-HL bypass line (D55) B-166
Figure B.55-D Flow rate in DC-HL bypass line (D55) B-166
Figure B.56 Flow rate in the hot leg 1 (D56) B-167
Figure B.56-A Flow rate in the hot leg 1 (D56) B-168
Figure B.56-B Flow rate in the hot leg 1 (D56) B-168
Figure B.56-C Flow rate in the hot leg 1 (D56) B-169
Figure B.56-D Flow rate in the hot leg 1 (D56) B-169
Figure B.57 Flow rate in the hot leg 2 (D57) B-170
Figure B.57-A Flow rate in the hot leg 2 (D57) B-171
Figure B.57-B Flow rate in the hot leg 2 (D57) B-171
Figure B.57-C Flow rate in the hot leg 2 (D57) B-172
Figure B.57-D Flow rate in the hot leg 2 (D57) B-172
Figure B.58 Flow rate in the hot leg 1A (D58) B-173
Figure B.58-A Flow rate in the hot leg 1A (D58) B-174
Figure B.58-B Flow rate in the hot leg 1A (D58) B-174
Figure B.58-C Flow rate in the hot leg 1A (D58) B-175
Figure B.58-D Flow rate in the hot leg 1A (D58) B-175
Figure B.59 Flow rate in the hot leg 1B (D59) B-176
Figure B.59-A Flow rate in the hot leg 1B (D59) B-177
Figure B.59-B Flow rate in the hot leg 1B (D59) B-177
Figure B.59-C Flow rate in the hot leg 1B (D59) B-178
Figure B.59-D Flow rate in the hot leg 1B (D59) B-178
Figure B.60 Flow rate in the hot leg 2A (D60) B-179
Figure B.60-A Flow rate in the hot leg 2A (D60) B-180
Figure B.60-B Flow rate in the hot leg 2A (D60) B-180
Figure B.60-C Flow rate in the hot leg 2A (D60) B-181
Figure B.60-D Flow rate in the hot leg 2A (D60) B-181
Figure B.61 Flow rate in the hot leg 2B (D61) B-182
Figure B.61-A Flow rate in the hot leg 2B (D61) B-183

Figure B.61-B Flow rate in the hot leg 2B (D61) B-183
Figure B.61-C Flow rate in the hot leg 2B (D61) B-184
Figure B.61-D Flow rate in the hot leg 2B (D61) B-184
Figure B.62 Feedwater flow rate to the economizer of SG-1 (D62) B-185
Figure B.62-A Feedwater flow rate to the economizer of SG-1 (D62) B-186
Figure B.62-B Feedwater flow rate to the economizer of SG-1 (D62) B-186
Figure B.62-C Feedwater flow rate to the economizer of SG-1 (D62) B-187
Figure B.62-D Feedwater flow rate to the economizer of SG-1 (D62) B-187
Figure B.63 Feedwater flow rate to the down-comer of SG-1 (D63) B-188
Figure B.63-A Feedwater flow rate to the down-comer of SG-1 (D63) B-189
Figure B.63-B Feedwater flow rate to the down-comer of SG-1 (D63) B-189
Figure B.63-C Feedwater flow rate to the down-comer of SG-1 (D63) B-190
Figure B.63-D Feedwater flow rate to the down-comer of SG-1 (D63) B-190
Figure B.64 Feedwater flow rate to the economizer of SG-2 (D64) B-191
Figure B.64-A Feedwater flow rate to the economizer of SG-2 (D64) B-192
Figure B.64-B Feedwater flow rate to the economizer of SG-2 (D64) B-192
Figure B.64-C Feedwater flow rate to the economizer of SG-2 (D64) B-193
Figure B.64-D Feedwater flow rate to the economizer of SG-2 (D64) B-193
Figure B.65 Feedwater flow rate to the down-comer of SG-2 (D65) B-194
Figure B.65-A Feedwater flow rate to the down-comer of SG-2 (D65) B-195
Figure B.65-B Feedwater flow rate to the down-comer of SG-2 (D65) B-195
Figure B.65-C Feedwater flow rate to the down-comer of SG-2 (D65) B-196
Figure B.65-D Feedwater flow rate to the down-comer of SG-2 (D65) B-196
Figure B.66 Flow rate of the SIT-1 (D66) B-197
Figure B.66-A Flow rate of the SIT-1 (D66) B-198
Figure B.66-B Flow rate of the SIT-1 (D66) B-198
Figure B.66-C Flow rate of the SIT-1 (D66) B-199
Figure B.66-D Flow rate of the SIT-1 (D66) B-199
Figure B.67 Flow rate of the SIT-2 (D67) B-200
Figure B.67-A Flow rate of the SIT-2 (D67) B-201
Figure B.67-B Flow rate of the SIT-2 (D67) B-201
Figure B.67-C Flow rate of the SIT-2 (D67) B-202
Figure B.67-D Flow rate of the SIT-2 (D67) B-202
Figure B.68 Flow rate of the SIT-3 (D68) B-203
Figure B.68-A Flow rate of the SIT-3 (D68) B-204
Figure B.68-B Flow rate of the SIT-3 (D68) B-204
Figure B.68-C Flow rate of the SIT-3 (D68) B-205
Figure B.68-D Flow rate of the SIT-3 (D68) B-205

Figure B.69 Flow rate of the SIP-2 (D69) B-206
Figure B.69-A Flow rate of the SIP-2 (D69) B-207
Figure B.69-B Flow rate of the SIP-2 (D69) B-207
Figure B.69-C Flow rate of the SIP-2 (D69) B-208
Figure B.69-D Flow rate of the SIP-2 (D69) B-208
Figure B.70 Total break flow rate (D70) B-209
Figure B.70-A Total break flow rate (D70) B-210
Figure B.70-B Total break flow rate (D70) B-210
Figure B.70-C Total break flow rate (D70) B-211
Figure B.70-D Total break flow rate (D70) B-211
Figure B.71 Accumulated mass of the break flow (D71) B-212
Figure B.71-A Accumulated mass of the break flow (D71) B-213
Figure B.71-B Accumulated mass of the break flow (D71) B-213
Figure B.71-C Accumulated mass of the break flow (D71) B-214
Figure B.71-D Accumulated mass of the break flow (D71) B-214
Figure B.72 Collapsed water level in the down-comer (D72) B-215
Figure B.72-A Collapsed water level in the down-comer (D72) B-216
Figure B.72-B Collapsed water level in the down-comer (D72) B-216
Figure B.72-C Collapsed water level in the down-comer (D72) B-217
Figure B.72-D Collapsed water level in the down-comer (D72) B-217
Figure B.73 Collapsed water level in the active core region (D73) B-218
Figure B.73-A Collapsed water level in the active core region (D73) B-219
Figure B.73-B Collapsed water level in the active core region (D73) B-219
Figure B.73-C Collapsed water level in the active core region (D73) B-220
Figure B.73-D Collapsed water level in the active core region (D73) B-220
Figure B.74 Collapsed water level in the pressurizer (D74) B-221
Figure B.74-A Collapsed water level in the pressurizer (D74) B-222
Figure B.74-B Collapsed water level in the pressurizer (D74) B-222
Figure B.74-C Collapsed water level in the pressurizer (D74) B-223
Figure B.74-D Collapsed water level in the pressurizer (D74) B-223
Figure B.75 Collapsed water level in the intermediate leg 1A (D75) B-224
Figure B.75-A Collapsed water level in the intermediate leg 1A (D75) B-225
Figure B.75-B Collapsed water level in the intermediate leg 1A (D75) B-225
Figure B.75-C Collapsed water level in the intermediate leg 1A (D75) B-226
Figure B.75-D Collapsed water level in the intermediate leg 1A (D75) B-226
Figure B.76 Collapsed water level in the intermediate leg 1B (D76) B-227
Figure B.76-A Collapsed water level in the intermediate leg 1B (D76) B-228
Figure B.76-B Collapsed water level in the intermediate leg 1B (D76) B-228

Figure B.76-C Collapsed water level in the intermediate leg 1B (D76).................................... B-229
Figure B.76-D Collapsed water level in the intermediate leg 1B (D76) B-229
Figure B.77 Collapsed water level in the intermediate leg 2A (D77) B-230
Figure B.77-A Collapsed water level in the intermediate leg 2A (D77) B-231
Figure B.77-B Collapsed water level in the intermediate leg 2A (D77).................................... B-231
Figure B.77-C Collapsed water level in the intermediate leg 2A (D77) B-232
Figure B.77-D Collapsed water level in the intermediate leg 2A (D77).................................. B-232
Figure B.78 Collapsed water level in the intermediate leg 2B (D78) B-233
Figure B.78-A Collapsed water level in the intermediate leg 2B (D78).................................... B-234
Figure B.78-B Collapsed water level in the intermediate leg 2B (D78).................................... B-234
Figure B.78-C Collapsed water level in the intermediate leg 2B (D78).................................... B-235
Figure B.78-D Collapsed water level in the intermediate leg 2B (D78).................................... B-235
Figure B.79 Collapsed water level in SG-1 U-tube upward section (D79).............................. B-236
Figure B.79-A Collapsed water level in SG-1 U-tube upward section (D79) B-237
Figure B.79-B Collapsed water level in SG-1 U-tube upward section (D79)........................... B-237
Figure B.79-C Collapsed water level in SG-1 U-tube upward section (D79)........................... B-238
Figure B.79-D Collapsed water level in SG-1 U-tube upward section (D79).......................... B-238
Figure B.80 Collapsed water level in SG-1 U-tube downward section (D80) B-239
Figure B.80-A Collapsed water level in SG-1 U-tube downward section (D80) B-240
Figure B.80-B Collapsed water level in SG-1 U-tube downward section (D80)..................... B-240
Figure B.80-C Collapsed water level in SG-1 U-tube downward section (D80) B-241
Figure B.80-D Collapsed water level in SG-1 U-tube downward section (D80).................... B-241
Figure B.81 Collapsed water level in SG-2 U-tube upward section (D81).............................. B-242
Figure B.81-A Collapsed water level in SG-2 U-tube upward section (D81) B-243
Figure B.81-B Collapsed water level in SG-2 U-tube upward section (D81)........................... B-243
Figure B.81-C Collapsed water level in SG-2 U-tube upward section (D81)........................... B-244
Figure B.81-D Collapsed water level in SG-2 U-tube upward section (D81).......................... B-244
Figure B.82 Collapsed water level in SG-2 U-tube downward section (D82) B-245
Figure B.82-A Collapsed water level in SG-2 U-tube downward section (D82) B-246
Figure B.82-B Collapsed water level in SG-2 U-tube downward section (D82)..................... B-246
Figure B.82-C Collapsed water level in SG-2 U-tube downward section (D82) B-247
Figure B.82-D Collapsed water level in SG-2 U-tube downward section (D82).................... B-247
Figure B.83 RCP 1A speed (D83) B-248
Figure B.83-A RCP 1A speed (D83).. B-249
Figure B.83-B RCP 1A speed (D83).. B-249
Figure B.83-C RCP 1A speed (D83).. B-250
Figure B.83-D RCP 1A speed (D83) B-250
Figure B.84 RCP 1B speed (D84)... B-251

Figure B.84-A RCP 1B speed (D84) B-252
Figure B.84-B RCP 1B speed (D84) B-252
Figure B.84-C RCP 1B speed (D84) B-253
Figure B.84-D RCP 1B speed (D84) B-253
Figure B.85 RCP 2A speed (D85) B-254
Figure B.85-A RCP 2A speed (D85) B-255
Figure B.85-B RCP 2A speed (D85) B-255
Figure B.85-C RCP 2A speed (D85) B-256
Figure B.85-D RCP 2A speed (D85) B-256
Figure B.86 RCP 2B speed (D86) B-257
Figure B.86-A RCP 2B speed (D86) B-258
Figure B.86-B RCP 2B speed (D86) B-258
Figure B.86-C RCP 2B speed (D86) B-259
Figure B.86-D RCP 2B speed (D86) B-259

Appendix-B:
Figures Comparing Blind Predictions with Selected Data

List of Appendix-B Figures

Figure B.1 Total core power (D01) B-1
Figure B.1-A Total core power (D01) B-2
Figure B.1-B Total core power (D01) B-2
Figure B.1-C Total core power (D01) B-3
Figure B.1-D Total core power (D01) B-3
Figure B.2 Heat removal rate of SG1 (D02) B-4
Figure B.2-A Heat removal rate of SG1 (D02) B-5
Figure B.2-B Heat removal rate of SG1 (D02) B-5
Figure B.2-C Heat removal rate of SG1 (D02) B-6
Figure B.2-D Heat removal rate of SG1 (D02) B-6
Figure B.3 Heat removal rate of SG2 (D03) B-7
Figure B.3-A Heat removal rate of SG2 (D03) B-8
Figure B.3-B Heat removal rate of SG2 (D03) B-8
Figure B.3-C Heat removal rate of SG2 (D03) B-9
Figure B.3-D Heat removal rate of SG2 (D03) B-9
Figure B.4 Upper head pressure (D04) B-10
Figure B.4-A Upper head pressure (D04) B-11
Figure B.4-B Upper head pressure (D04) B-11
Figure B.4-C Upper head pressure (D04) B-12
Figure B.4-D Upper head pressure (D04) B-12
Figure B.5 Pressure of the pressurizer (D05) B-13
Figure B.5-A Pressure of the pressurizer (D05) B-14
Figure B.5-B Pressure of the pressurizer (D05) B-14
Figure B.5-C Pressure of the pressurizer (D05) B-15
Figure B.5-D Pressure of the pressurizer (D05) B-15
Figure B.6 Pressure in SG-1 dome (D06) B-16
Figure B.6-A Pressure in SG-1 dome (D06) B-17
Figure B.6-B Pressure in SG-1 dome (D06) B-17
Figure B.6-C Pressure in SG-1 dome (D06) B-18
Figure B.6-D Pressure in SG-1 dome (D06) B-18
Figure B.7 Pressure in SG-2 dome (D07) B-19
Figure B.7-A Pressure in SG-2 dome (D07) B-20
Figure B.7-B Pressure in SG-2 dome (D07) B-20
Figure B.7-C Pressure in SG-2 dome (D07) B-21
Figure B.7-D Pressure in SG-2 dome (D07) B-21

Figure B.8 Pressure in SIT-01 (D08) B-22
Figure B.8-A Pressure in SIT-01 (D08) B-23
Figure B.8-B Pressure in SIT-01 (D08) B-23
Figure B.8-C Pressure in SIT-01 (D08) B-24
Figure B.8-D Pressure in SIT-01 (D08) B-24
Figure B.9 Pressure in SIT-02 (D09) B-25
Figure B.9-A Pressure in SIT-02 (D09) B-26
Figure B.9-B Pressure in SIT-02 (D09) B-26
Figure B.9-C Pressure in SIT-02 (D09) B-27
Figure B.9-D Pressure in SIT-02 (D09) B-27
Figure B.10 Pressure in SIT-03 (D10) B-28
Figure B.10-A Pressure in SIT-03 (D10) B-29
Figure B.10-B Pressure in SIT-03 (D10) B-29
Figure B.10-C Pressure in SIT-03 (D10) B-30
Figure B.10-D Pressure in SIT-03 (D10) B-30
Figure B.11 Containment pressure (D11) B-31
Figure B.11-A Containment pressure (D11) B-32
Figure B.11-B Containment pressure (D11) B-32
Figure B.11-C Containment pressure (D11) B-33
Figure B.11-D Containment pressure (D11) B-33
Figure B.12 Pressure difference between SG-1 inlet and outlet plenum 1 (D12) B-34
Figure B.12-A Pressure difference between SG-1 inlet and outlet plenum 1 (D12) B-35
Figure B.12-B Pressure difference between SG-1 inlet and outlet plenum 1 (D12) B-35
Figure B.12-C Pressure difference between SG-1 inlet and outlet plenum 1 (D12) B-36
Figure B.12-D Pressure difference between SG-1 inlet and outlet plenum 1 (D12) B-36
Figure B.13 DP Pressure difference between SG-1 inlet and outlet plenum 2 (D13) B-37
Figure B.13-A DP Pressure difference between SG-1 inlet and outlet plenum 2 (D13) B-38
Figure B.13-B DP Pressure difference between SG-1 inlet and outlet plenum 2 (D13) B-38
Figure B.13-C DP Pressure difference between SG-1 inlet and outlet plenum 2 (D13) B-39
Figure B.13-D DP Pressure difference between SG-1 inlet and outlet plenum 2 (D13) B-39
Figure B.14 DP Pressure difference between SG-2 inlet and outlet plenum 1 (D14) B-40
Figure B.14-A DP Pressure difference between SG-2 inlet and outlet plenum 1 (D14) B-41
Figure B.14-B DP Pressure difference between SG-2 inlet and outlet plenum 1 (D14) B-41
Figure B.14-C DP Pressure difference between SG-2 inlet and outlet plenum 1 (D14) B-42
Figure B.14-D DP Pressure difference between SG-2 inlet and outlet plenum 1 (D14) B-42
Figure B.15 DP Pressure difference between SG-2 inlet and outlet plenum 2 (D15) B-43
Figure B.15-A DP Pressure difference between SG-2 inlet and outlet plenum 2 (D15) B-44
Figure B.15-B DP Pressure difference between SG-2 inlet and outlet plenum 2 (D15) B-44

Figure B.15-C DP Pressure difference between SG-2 inlet and outlet plenum 2 (D15)........B-45
Figure B.15-D DP Pressure difference between SG-2 inlet and outlet plenum 2 (D15) B-45
Figure B.16 Water temperature in the core inlet plenum (D16) B-46
Figure B.16-A Water temperature in the core inlet plenum (D16) B-47
Figure B.16-B Water temperature in the core inlet plenum (D16)........B-47
Figure B.16-C Water temperature in the core inlet plenum (D16) B-48
Figure B.16-D Water temperature in the core inlet plenum (D16) B-48
Figure B.17 Water temperature in the core outlet plenum (D17) B-49
Figure B.17-A Water temperature in the core outlet plenum (D17) B-50
Figure B.17-B Water temperature in the core outlet plenum (D17)........B-50
Figure B.17-C Water temperature in the core outlet plenum (D17) B-51
Figure B.17-D Water temperature in the core outlet plenum (D17) B-51
Figure B.18 Water temperature in the pressurizer (D18) B-52
Figure B.18-A Water temperature in the pressurizer (D18)........B-53
Figure B.18-B Water temperature in the pressurizer (D18)........B-53
Figure B.18-C Water temperature in the pressurizer (D18)........B-54
Figure B.18-D Water temperature in the pressurizer (D18) B-54
Figure A19 Water temperature in the hot leg 1 (D19) B-55
Figure B.19-A Water temperature in the hot leg 1 (D19)........B-56
Figure B.19-B Water temperature in the hot leg 1 (D19) B-56
Figure B.19-C Water temperature in the hot leg 1 (D19)........B-57
Figure B.19-D Water temperature in the hot leg 1 (D19)........B-57
Figure B.20 Water temperature in the hot leg 2 (D20)........B-58
Figure B.20-A Water temperature in the hot leg 2 (D20)........B-59
Figure B.20-B Water temperature in the hot leg 2 (D20) B-59
Figure B.20-C Water temperature in the hot leg 2 (D20)........B-60
Figure B.20-D Water temperature in the hot leg 2 (D20)........B-60
Figure B.21 Water temperature in the cold leg 1A (D21)........B-61
Figure B.21-A Water temperature in the cold leg 1A (D21) B-62
Figure B.21-B Water temperature in the cold leg 1A (D21) B-62
Figure B.21-C Water temperature in the cold leg 1A (D21) B-63
Figure B.21-D Water temperature in the cold leg 1A (D21)........B-63
Figure B.22 Water temperature in the cold leg 1B (D22) B-64
Figure B.22-A Water temperature in the cold leg 1B (D22) B-65
Figure B.22-B Water temperature in the cold leg 1B (D22)........B-65
Figure B.22-C Water temperature in the cold leg 1B (D22) B-66
Figure B.22-D Water temperature in the cold leg 1B (D22) B-66
Figure B.23 Water temperature in the cold leg 2A (D23)........B-67

Figure B.23-A Water temperature in the cold leg 2A (D23) B-68
Figure B.23-B Water temperature in the cold leg 2A (D23) B-68
Figure B.23-C Water temperature in the cold leg 2A (D23) B-69
Figure B.23-D Water temperature in the cold leg 2A (D23) B-69
Figure B.24 Water temperature in the cold leg 2B (D24) B-70
Figure B.24-A Water temperature in the cold leg 2B (D24) B-71
Figure B.24-B Water temperature in the cold leg 2B (D24) B-71
Figure B.24-C Water temperature in the cold leg 2B (D24) B-72
Figure B.24-D Water temperature in the cold leg 2B (D24) B-72
Figure B.25 Water temperature in SG-1 inlet plenum (D25) B-73
Figure B.25-A Water temperature in SG-1 inlet plenum (D25) B-74
Figure B.25-B Water temperature in SG-1 inlet plenum (D25) B-74
Figure B.25-C Water temperature in SG-1 inlet plenum (D25) B-75
Figure B.25-D Water temperature in SG-1 inlet plenum (D25) B-75
Figure B.26 Water temperature in SG-1 outlet plenum (D26) B-76
Figure B.26-A Water temperature in SG-1 outlet plenum (D26) B-77
Figure B.26-B Water temperature in SG-1 outlet plenum (D26) B-77
Figure B.26-C Water temperature in SG-1 outlet plenum (D26) B-78
Figure B.26-D Water temperature in SG-1 outlet plenum (D26) B-78
Figure B.27 Water temperature in SG-2 inlet plenum (D27) B-79
Figure B.27-A Water temperature in SG-2 inlet plenum (D27) B-80
Figure B.27-B Water temperature in SG-2 inlet plenum (D27) B-80
Figure B.27-C Water temperature in SG-2 inlet plenum (D27) B-81
Figure B.27-D Water temperature in SG-2 inlet plenum (D27) B-81
Figure B.28 Water temperature in SG-2 outlet plenum (D28) B-82
Figure B.28-A Water temperature in SG-2 outlet plenum (D28) B-83
Figure B.28-B Water temperature in SG-2 outlet plenum (D28) B-83
Figure B.28-C Water temperature in SG-2 outlet plenum (D28) B-84
Figure B.28-D Water temperature in SG-2 outlet plenum (D28) B-84
Figure B.29 Steam temperature in SG-1 steam dome (D29) B-85
Figure B.29-A Steam temperature in SG-1 steam dome (D29) B-86
Figure B.29-B Steam temperature in SG-1 steam dome (D29) B-86
Figure B.29-C Steam temperature in SG-1 steam dome (D29) B-87
Figure B.29-D Steam temperature in SG-1 steam dome (D29) B-87
Figure B.30 Steam temperature in SG-2 steam dome (D30) B-88
Figure B.30-A Steam temperature in SG-2 steam dome (D30) B-89
Figure B.30-B Steam temperature in SG-2 steam dome (D30) B-89
Figure B.30-C Steam temperature in SG-2 steam dome (D30) B-90

Figure B.30-D Steam temperature in SG-2 steam dome (D30)....B-90
Figure B.31 Water temperature in the SIT-1 (D31)....B-91
Figure B.31-A Water temperature in the SIT-1 (D31)....B-92
Figure B.31-B Water temperature in the SIT-1 (D31)....B-92
Figure B.31-C Water temperature in the SIT-1 (D31)....B-93
Figure B.31-D Water temperature in the SIT-1 (D31)....B-93
Figure B.32 Water temperature in the SIT-2 (D32)....B-94
Figure B.32-A Water temperature in the SIT-2 (D32)....B-95
Figure B.32-B Water temperature in the SIT-2 (D32)....B-95
Figure B.32-C Water temperature in the SIT-2 (D32)....B-96
Figure B.32-D Water temperature in the SIT-2 (D32)....B-96
Figure B.33 Water temperature in the SIT-3 (D33)....B-97
Figure B.33-A Water temperature in the SIT-3 (D33)....B-98
Figure B.33-B Water temperature in the SIT-3 (D33)....B-98
Figure B.33-C Water temperature in the SIT-3 (D33)....B-99
Figure B.33-D Water temperature in the SIT-3 (D33)....B-99
Figure B.34 Water temperature in the SIP-2 (D34)....B-100
Figure B.34-A Water temperature in the SIP-2 (D34)....B-101
Figure B.34-B Water temperature in the SIP-2 (D34)....B-101
Figure B.34-C Water temperature in the SIP-2 (D34)....B-102
Figure B.34-D Water temperature in the SIP-2 (D34)....B-102
Figure B.35 Temperature in the containment (D35)....B-103
Figure B.35-A Temperature in the containment (D35)....B-104
Figure B.35-B Temperature in the containment (D35)....B-104
Figure B.35-C Temperature in the containment (D35)....B-105
Figure B.35-D Temperature in the containment (D35)....B-105
Figure B.36 Steam temperature in the hot leg 1 (D36)....B-106
Figure B.36-A Steam temperature in the hot leg 1 (D36)....B-107
Figure B.36-B Steam temperature in the hot leg 1 (D36)....B-107
Figure B.36-C Steam temperature in the hot leg 1 (D36)....B-108
Figure A36-D Steam temperature in the hot leg 1 (D36)....B-108
Figure B.37 Steam temperature in the hot leg 2 (D37)....B-109
Figure B.37-A Steam temperature in the hot leg 2 (D37)....B-110
Figure B.37-B Steam temperature in the hot leg 2 (D37)....B-110
Figure B.37-C Steam temperature in the hot leg 2 (D37)....B-111
Figure B.37-D Steam temperature in the hot leg 2 (D37)....B-111
Figure B.38 Steam temperature in the cold leg 1A (D38)....B-112
Figure B.38-A Steam temperature in the cold leg 1A (D38)....B-113

Figure B.38-B Steam temperature in the cold leg 1A (D38) B-113
Figure B.38-C Steam temperature in the cold leg 1A (D38) B-114
Figure B.38-D Steam temperature in the cold leg 1A (D38) B-114
Figure B.39 Steam temperature in the cold leg 1B (D39) B-115
Figure B.39-A Steam temperature in the cold leg 1B (D39) B-116
Figure B.39-B Steam temperature in the cold leg 1B (D39) B-116
Figure B.39-C Steam temperature in the cold leg 1B (D39) B-117
Figure B.39-D Steam temperature in the cold leg 1B (D39) B-117
Figure B.40 Steam temperature in the cold leg 2A (D40) B-118
Figure B.40-A Steam temperature in the cold leg 2A (D40) B-119
Figure B.40-B Steam temperature in the cold leg 2A (D40) B-119
Figure B.40-C Steam temperature in the cold leg 2A (D40) B-120
Figure B.40-D Steam temperature in the cold leg 2A (D40) B-120
Figure B.41 Steam temperature in the cold leg 2B (D41) B-121
Figure B.41-A Steam temperature in the cold leg 2B (D41) B-122
Figure B.41-B Steam temperature in the cold leg 2B (D41) B-122
Figure B.41-C Steam temperature in the cold leg 2B (D41) B-123
Figure B.41-D Steam temperature in the cold leg 2B (D41) B-123
Figure B.42 Wall temperature in the active core region 1 (D42) B-124
Figure B.42-A Wall temperature in the active core region 1 (D42) B-125
Figure B.42-B Wall temperature in the active core region 1 (D42) B-125
Figure B.42-C Wall temperature in the active core region 1 D42) B-126
Figure B.42-D Wall temperature in the active core region 1 (D42) B-126
Figure B.43 Wall temperature in the active core region 2 (D43) B-127
Figure B.43-A Wall temperature in the active core region 2 (D43) B-128
Figure B.43-B Wall temperature in the active core region 2 (D43) B-128
Figure B.43-C Wall temperature in the active core region 2 (D43) B-129
Figure B.43-D Wall temperature in the active core region 2 (D43) B-129
Figure B.44 Wall temperature in the active core region 3 (D44) B-130
Figure B.44-A Wall temperature in the active core region 3 (D44) B-131
Figure B.44-B Wall temperature in the active core region 3 (D44) B-131
Figure B.44-C Wall temperature in the active core region 3 (D44) B-132
Figure B.44-D Wall temperature in the active core region 3 (D44) B-132
Figure B.45 Wall temperature in the active core region 4 (D45) B-133
Figure B.45-A Wall temperature in the active core region 4 (D45) B-134
Figure B.45-B Wall temperature in the active core region 4 (D45) B-134
Figure B.45-C Wall temperature in the active core region 4 (D45) B-135
Figure B.45-D Wall temperature in the active core region 4 (D45) B-135

Figure B.46 Wall temperature in the active core region 5 (D46) B-136
Figure B.46-A Wall temperature in the active core region 5 (D46) B-137
Figure B.46-B Wall temperature in the active core region 5 (D46) B-137
Figure B.46-C Wall temperature in the active core region 5 (D46) B-138
Figure B.46-D Wall temperature in the active core region 5 (D46) B-138
Figure B.47 Wall temperature in the active core region 6 (D47) B-139
Figure B.47-A Wall temperature in the active core region 6 (D47) B-140
Figure B.47-B Wall temperature in the active core region 6 (D47) B-140
Figure B.47-C Wall temperature in the active core region 6 (D47) B-141
Figure B.47-D Wall temperature in the active core region 6 (D47) B-141
Figure B.48 Wall temperature in the active core region 7 (D48) B-142
Figure B.48-A Wall temperature in the active core region 7 (D48) B-143
Figure B.48-B Wall temperature in the active core region 7 (D48) B-143
Figure B.48-C Wall temperature in the active core region 7 (D48) B-144
Figure B.48-D Wall temperature in the active core region 7 (D48) B-144
Figure B.49 Wall temperature in the active core region 8 (D49) B-145
Figure B.49-A Wall temperature in the active core region 8 (D49) B-146
Figure B.49-B Wall temperature in the active core region 8 (D49) B-146
Figure B.49-C Wall temperature in the active core region 8 (D49) B-147
Figure B.49-D Wall temperature in the active core region 8 (D49) B-147
Figure B.50 Wall temperature in the active core region 9 (D50) B-148
Figure B.50-A Wall temperature in the active core region 9 (D50) B-149
Figure B.50-B Wall temperature in the active core region 9 (D50) B-149
Figure B.50-C Wall temperature in the active core region 9 (D50) B-150
Figure B.50-D Wall temperature in the active core region 9 (D50) B-150
Figure B.51 Wall temperature in the active core region 10 (D51) B-151
Figure B.51-A Wall temperature in the active core region 10 (D51) B-152
Figure B.51-B Wall temperature in the active core region 10 (D51) B-152
Figure B.51-C Wall temperature in the active core region 10 (D51) B-153
Figure B.51-D Wall temperature in the active core region 10 (D51) B-153
Figure B.52 Wall temperature in the active core region 11 (D52) B-154
Figure B.52-A Wall temperature in the active core region 11 (D52) B-155
Figure B.52-B Wall temperature in the active core region 11 (D52) B-155
Figure B.52-C Wall temperature in the active core region 11 (D52) B-156
Figure B.52-D Wall temperature in the active core region 11 (D52) B-156
Figure B.53 Wall temperature in the active core region 12 (D53) B-157
Figure B.53-A Wall temperature in the active core region 12 (D53) B-158
Figure B.53-B Wall temperature in the active core region 12 (D53) B-158

Figure B.53-C Wall temperature in the active core region 12 (D53) B-159
Figure B.53-D Wall temperature in the active core region 12 (D53) B-159
Figure B.54 Flow rate in the DC-UH bypass line (D54) B-160
Figure B.54-A Flow rate in the DC-UH bypass line (D54) B-161
Figure B.54-B Flow rate in the DC-UH bypass line (D54) B-161
Figure B.54-C Flow rate in the DC-UH bypass line (D54) B-162
Figure B.54-D Flow rate in the DC-UH bypass line (D54) B-162
Figure B.55 Flow rate in the DC-HL bypass line (D55) B-163
Figure B.55-A Flow rate in the DC-HL bypass line (D55) B-164
Figure B.55-B Flow rate in the DC-HL bypass line (D55) B-164
Figure B.55-C Flow rate in the DC-HL bypass line (D55) B-165
Figure B.55-D Flow rate in the DC-HL bypass line (D55) B-165
Figure B.56 Flow rate in the hot leg 1 (D56) B-166
Figure B.56-A Flow rate in the hot leg 1 (D56) B-167
Figure B.56-B Flow rate in the hot leg 1 (D56) B-167
Figure B.56-C Flow rate in the hot leg 1 (D56) B-168
Figure B.56-D Flow rate in the hot leg 1 (D56) B-168
Figure B.57 Flow rate in the hot leg 2 (D57) B-169
Figure B.57-A Flow rate in the hot leg 2 (D57) B-170
Figure B.57-B Flow rate in the hot leg 2 (D57) B-170
Figure B.57-C Flow rate in the hot leg 2 (D57) B-171
Figure B.57-D Flow rate in the hot leg 2 (D57) B-171
Figure B.58 Flow rate in the hot leg 1A (D58) B-172
Figure B.58-A Flow rate in the hot leg 1A (D58) B-173
Figure B.58-B Flow rate in the hot leg 1A (D58) B-173
Figure B.58-C Flow rate in the hot leg 1A (D58) B-174
Figure B.58-D Flow rate in the hot leg 1A (D58) B-174
Figure B.59 Flow rate in the hot leg 1B (D59) B-175
Figure B.59-A Flow rate in the hot leg 1B (D59) B-176
Figure B.59-B Flow rate in the hot leg 1B (D59) B-176
Figure B.59-C Flow rate in the hot leg 1B (D59) B-177
Figure B.59-D Flow rate in the hot leg 1B (D59) B-177
Figure B.60 Flow rate in the hot leg 2A (D60) B-178
Figure B.60-A Flow rate in the hot leg 2A (D60) B-179
Figure B.60-B Flow rate in the hot leg 2A (D60) B-179
Figure B.60-C Flow rate in the hot leg 2A (D60) B-180
Figure B.60-D Flow rate in the hot leg 2A (D60) B-180
Figure B.61 Flow rate in the hot leg 2B (D61) B-181

Figure B.61-A Flow rate in the hot leg 2B (D61) B-182
Figure B.61-B Flow rate in the hot leg 2B (D61) B-182
Figure B.61-C Flow rate in the hot leg 2B (D61) B-183
Figure B.61-D Flow rate in the hot leg 2B (D61) B-183
Figure B.62 Feed water flow rate to the economizer of SG-1 (D62) B-184
Figure B.62-A Feed water flow rate to the economizer of SG-1 (D62) B-185
Figure B.62-B Feed water flow rate to the economizer of SG-1 (D62) B-185
Figure B.62-C Feed water flow rate to the economizer of SG-1 (D62) B-186
Figure B.62-D Feed water flow rate to the economizer of SG-1 (D62) B-186
Figure B.63 Feed water flow rate to the down-comer of SG-1 (D63) B-187
Figure B.63-A Feed water flow rate to the down-comer of SG-1 (D63) B-188
Figure B.63-B Feed water flow rate to the down-comer of SG-1 (D63) B-188
Figure B.63-C Feed water flow rate to the down-comer of SG-1 (D63) B-189
Figure B.63-D Feed water flow rate to the down-comer of SG-1 (D63) B-189
Figure B.64 Feed water flow rate to the economizer of SG-2 (D64) B-190
Figure B.64-A Feed water flow rate to the economizer of SG-2 (D64) B-191
Figure B.64-B Feed water flow rate to the economizer of SG-2 (D64) B-191
Figure B.64-C Feed water flow rate to the economizer of SG-2 (D64) B-192
Figure B.64-D Feed water flow rate to the economizer of SG-2 (D64) B-192
Figure B.65 Feed water flow rate to the down-comer of SG-2 (D65) B-193
Figure B.65-A Feed water flow rate to the down-comer of SG-2 (D65) B-194
Figure B.65-B Feed water flow rate to the down-comer of SG-2 (D65) B-194
Figure B.65-C Feed water flow rate to the down-comer of SG-2 (D65) B-195
Figure B.65-D Feed water flow rate to the down-comer of SG-2 (D65) B-195
Figure B.66 Flow rate of the SIT-1 (D66) B-196
Figure B.66-A Flow rate of the SIT-1 (D66) B-197
Figure B.66-B Flow rate of the SIT-1 (D66) B-197
Figure B.66-C Flow rate of the SIT-1 (D66) B-198
Figure B.66-D Flow rate of the SIT-1 (D66) B-198
Figure B.67 Flow rate of the SIT-2 (D67) B-199
Figure B.67-A Flow rate of the SIT-2 (D67) B-200
Figure B.67-B Flow rate of the SIT-2 (D67) B-200
Figure B.67-C Flow rate of the SIT-2 (D67) B-201
Figure B.67-D Flow rate of the SIT-2 (D67) B-201
Figure B.68 Flow rate of the SIT-3 (D68) B-202
Figure B.68-A Flow rate of the SIT-3 (D68) B-203
Figure B.68-B Flow rate of the SIT-3 (D68) B-203
Figure B.68-C Flow rate of the SIT-3 (D68) B-204

Figure B.68-D Flow rate of the SIT-3 (D68) B-204
Figure B.69 Flow rate of the SIP-2 (D69) B-205
Figure B.69-A Flow rate of the SIP-2 (D69) B-206
Figure B.69-B Flow rate of the SIP-2 (D69) B-206
Figure B.69-C Flow rate of the SIP-2 (D69) B-207
Figure B.69-D Flow rate of the SIP-2 (D69) B-207
Figure B.70 Total break flow rate (D70) B-208
Figure B.70-A Total break flow rate (D70) B-209
Figure B.70-B Total break flow rate (D70) B-209
Figure B.70-C Total break flow rate (D70) B-210
Figure B.70-D Total break flow rate (D70) B-210
Figure B.71 Accumulated mass of the break flow (D71) B-211
Figure B.71-A Accumulated mass of the break flow (D71) B-212
Figure B.71-B Accumulated mass of the break flow (D71) B-212
Figure B.71-C Accumulated mass of the break flow (D71) B-213
Figure B.71-D Accumulated mass of the break flow (D71) B-213
Figure B.72 Collapsed water level in the down-comer (D72) B-214
Figure B.72-A Collapsed water level in the down-comer (D72) B-215
Figure B.72-B Collapsed water level in the down-comer (D72) B-215
Figure B.72-C Collapsed water level in the down-comer (D72) B-216
Figure B.72-D Collapsed water level in the down-comer (D72) B-216
Figure B.73 Collapsed water level in the active core region (D73) B-217
Figure B.73-A Collapsed water level in the active core region (D73) B-218
Figure B.73-B Collapsed water level in the active core region (D73) B-218
Figure B.73-C Collapsed water level in the active core region (D73) B-219
Figure B.73-D Collapsed water level in the active core region (D73) B-219
Figure B.74 Collapsed water level in the pressurizer (D74) B-220
Figure B.74-A Collapsed water level in the pressurizer (D74) B-221
Figure B.74-B Collapsed water level in the pressurizer (D74) B-221
Figure B.74-C Collapsed water level in the pressurizer (D74) B-222
Figure B.74-D Collapsed water level in the pressurizer (D74) B-222
Figure B.75 Collapsed water level in the intermediate leg 1A (D75) B-223
Figure B.75-A Collapsed water level in the intermediate leg 1A (D75) B-224
Figure B.75-B Collapsed water level in the intermediate leg 1A (D75) B-224
Figure B.75-C Collapsed water level in the intermediate leg 1A (D75) B-225
Figure B.75-D Collapsed water level in the intermediate leg 1A (D75) B-225
Figure B.76 Collapsed water level in the intermediate leg 1B (D76) B-226
Figure B.76-A Collapsed water level in the intermediate leg 1B (D76) B-227

Figure B.76-B Collapsed water level in the intermediate leg 1B (D76) B-227
Figure B.76-C Collapsed water level in the intermediate leg 1B (D76) B-228
Figure B.76-D Collapsed water level in the intermediate leg 1B (D76) B-228
Figure B.77 Collapsed water level in the intermediate leg 2A (D77) B-229
Figure B.77-A Collapsed water level in the intermediate leg 2A (D77) B-230
Figure B.77-B Collapsed water level in the intermediate leg 2A (D77) B-230
Figure B.77-C Collapsed water level in the intermediate leg 2A (D77) B-231
Figure B.77-D Collapsed water level in the intermediate leg 2A (D77) B-231
Figure B.78 Collapsed water level in the intermediate leg 2B (D78) B-232
Figure B.78-A Collapsed water level in the intermediate leg 2B (D78) B-233
Figure B.78-B Collapsed water level in the intermediate leg 2B (D78) B-233
Figure B.78-C Collapsed water level in the intermediate leg 2B (D78) B-234
Figure B.78-D Collapsed water level in the intermediate leg 2B (D78) B-234
Figure B.79 Collapsed water level in SG-1 U-tube upward section (D79) B-235
Figure B.79-A Collapsed water level in SG-1 U-tube upward section (D79) B-236
Figure B.79-B Collapsed water level in SG-1 U-tube upward section (D79) B-236
Figure B.79-C Collapsed water level in SG-1 U-tube upward section (D79) B-237
Figure B.79-D Collapsed water level in SG-1 U-tube upward section (D79) B-237
Figure B.80 Collapsed water level in SG-1 U-tube downward section (D80) B-238
Figure B.80-A Collapsed water level in SG-1 U-tube downward section (D80) B-239
Figure B.80-B Collapsed water level in SG-1 U-tube downward section (D80) B-239
Figure B.80-C Collapsed water level in SG-1 U-tube downward section (D80) B-240
Figure B.80-D Collapsed water level in SG-1 U-tube downward section (D80) B-240
Figure B.81 Collapsed water level in SG-2 U-tube upward section (D81) B-241
Figure B.81-A Collapsed water level in SG-2 U-tube upward section (D81) B-242
Figure B.81-B Collapsed water level in SG-2 U-tube upward section (D81) B-242
Figure B.81-C Collapsed water level in SG-2 U-tube upward section (D81) B-243
Figure B.81-D Collapsed water level in SG-2 U-tube upward section (D81) B-243
Figure B.82 Collapsed water level in SG-2 U-tube downward section (D82) B-244
Figure B.82-A Collapsed water level in SG-2 U-tube downward section (D82) B-245
Figure B.82-B Collapsed water level in SG-2 U-tube downward section (D82) B-245
Figure B.82-C Collapsed water level in SG-2 U-tube downward section (D82) B-246
Figure B.82-D Collapsed water level in SG-2 U-tube downward section (D82) B-246
Figure B.83 RCP 1A speed (D83) B-247
Figure B.83-A RCP 1A speed (D83) B-248
Figure B.83-B RCP 1A speed (D83) B-248
Figure B.83-C RCP 1A speed (D83) B-249
Figure B.83-D RCP 1A speed (D83) B-249

Figure B.84 RCP 1B speed (D84) B-250
Figure B.84-A RCP 1B speed (D84) B-251
Figure B.84-B RCP 1B speed (D84) B-251
Figure B.84-C RCP 1B speed (D84) B-252
Figure B.84-D RCP 1B speed (D84) B-252
Figure B.85 RCP 2A speed (D85) B-253
Figure B.85-A RCP 2A speed (D85) B-254
Figure B.85-B RCP 2A speed (D85) B-254
Figure B.85-C RCP 2A speed (D85) B-255
Figure B.85-D RCP 2A speed (D85) B-255
Figure B.86 RCP 2B speed (D86) B-256
Figure B.86-A RCP 2B speed (D86) B-257
Figure B.86-B RCP 2B speed (D86) B-257
Figure B.86-C RCP 2B speed (D86) B-258
Figure B.86-D RCP 2B speed (D86) B-258

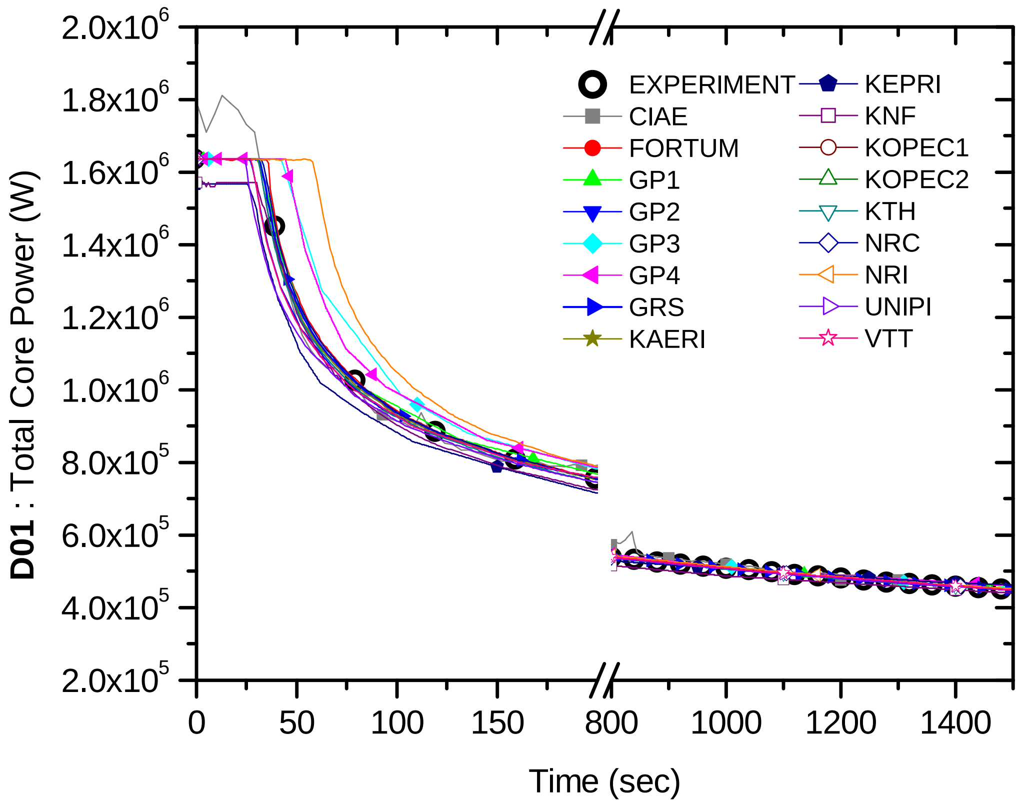

Figure B.1 Total core power (D01)

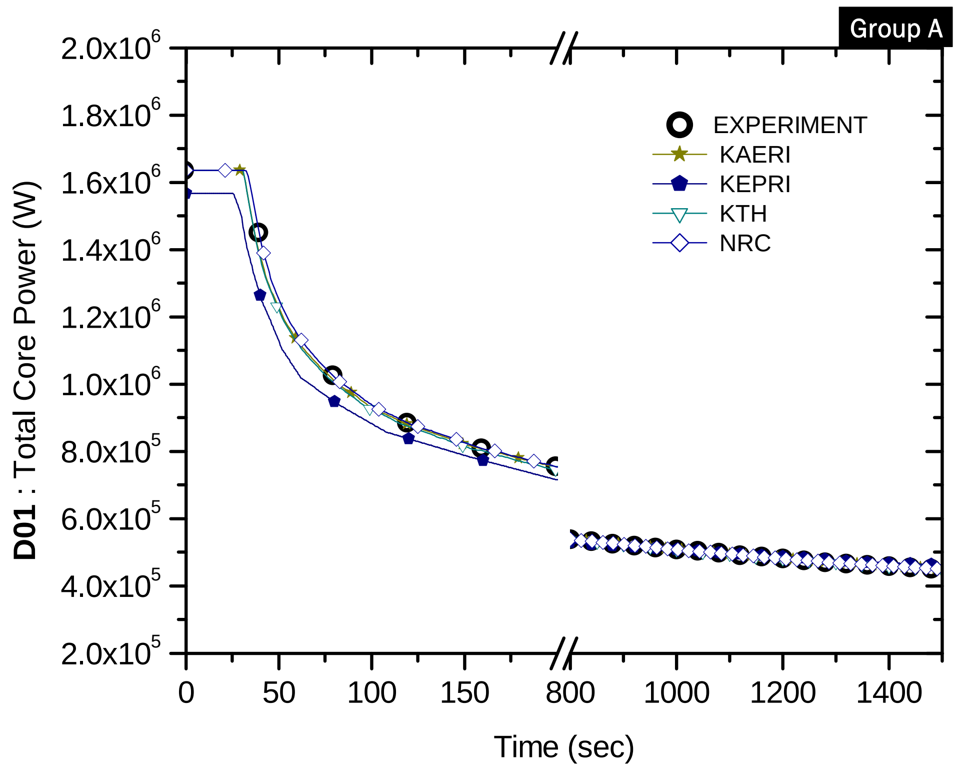

Figure B.1-A Total core power (D01)

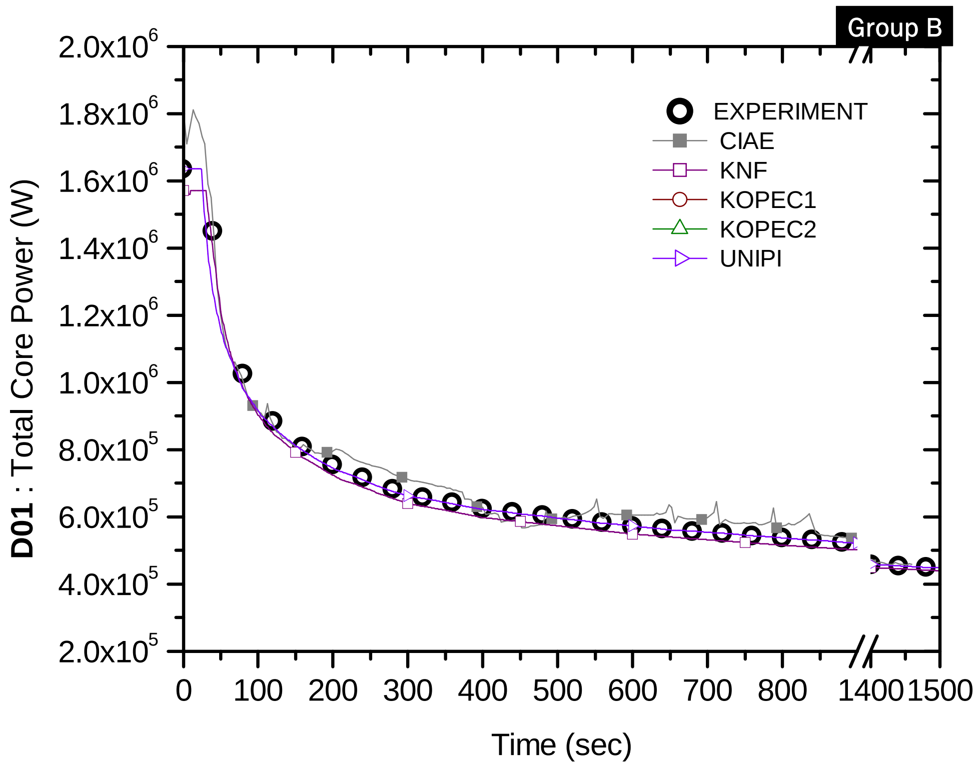

Figure B.1-B Total core power (D01)

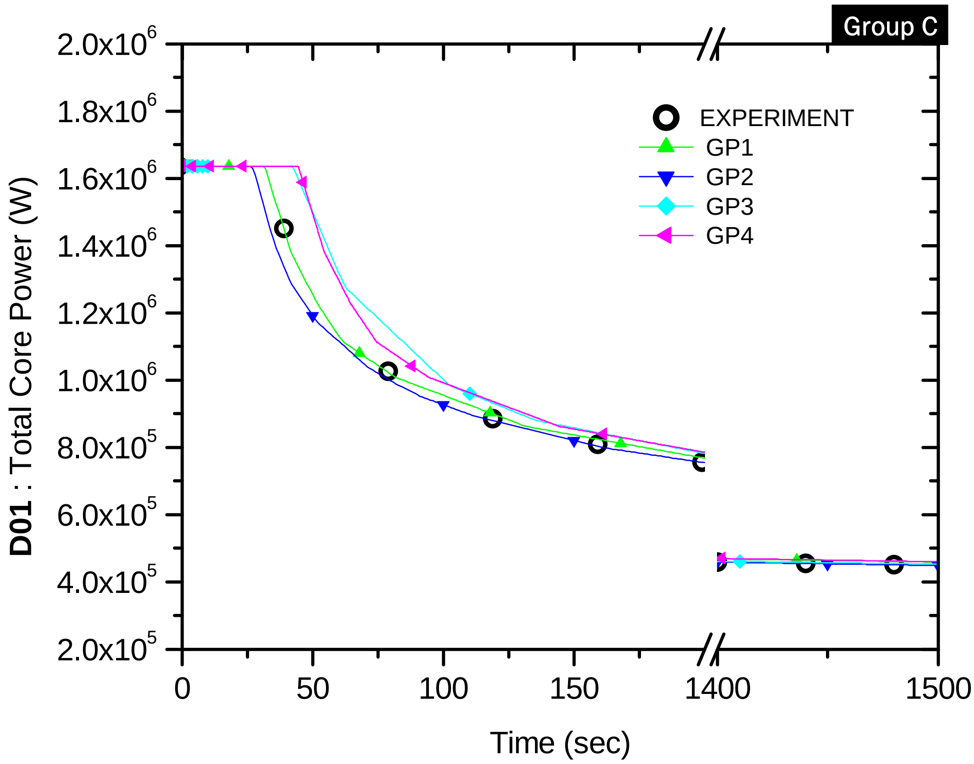

Figure B.1-C Total core power (D01)

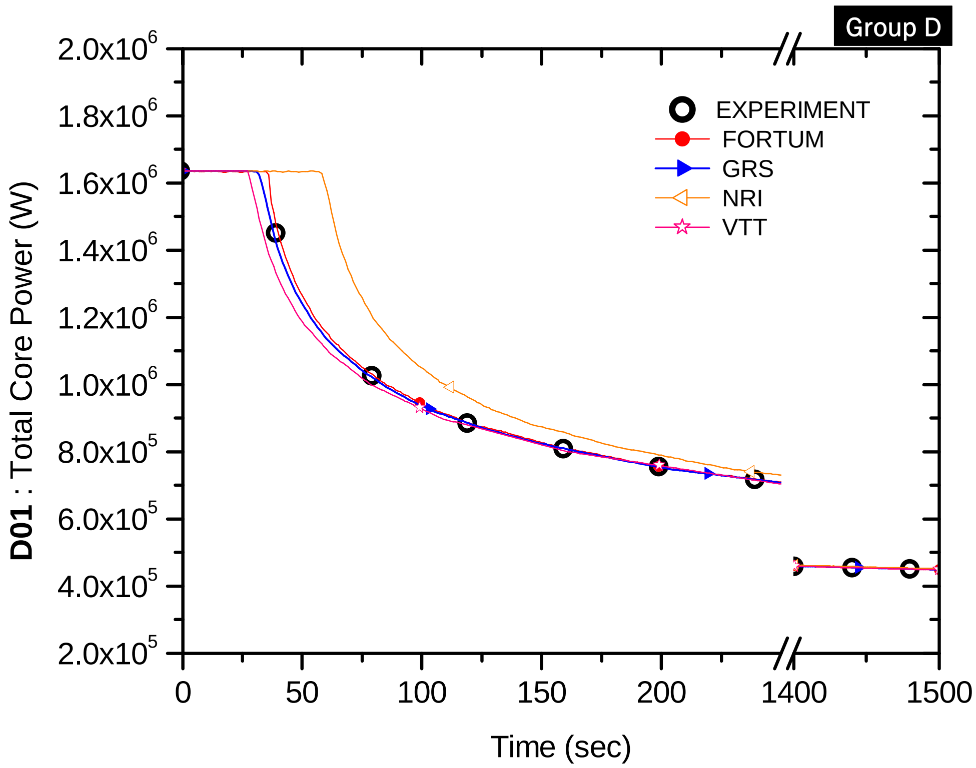

Figure B.1-D Total core power (D01)

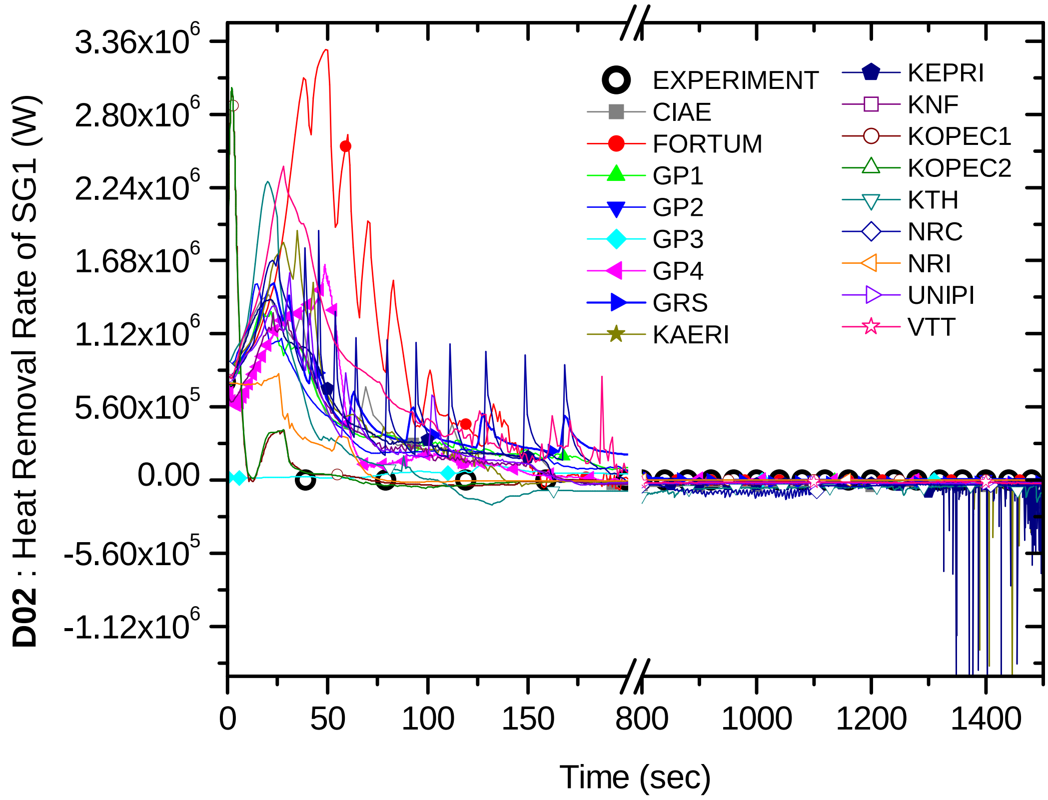

Figure B.2 Heat removal rate of SG1 (D02)

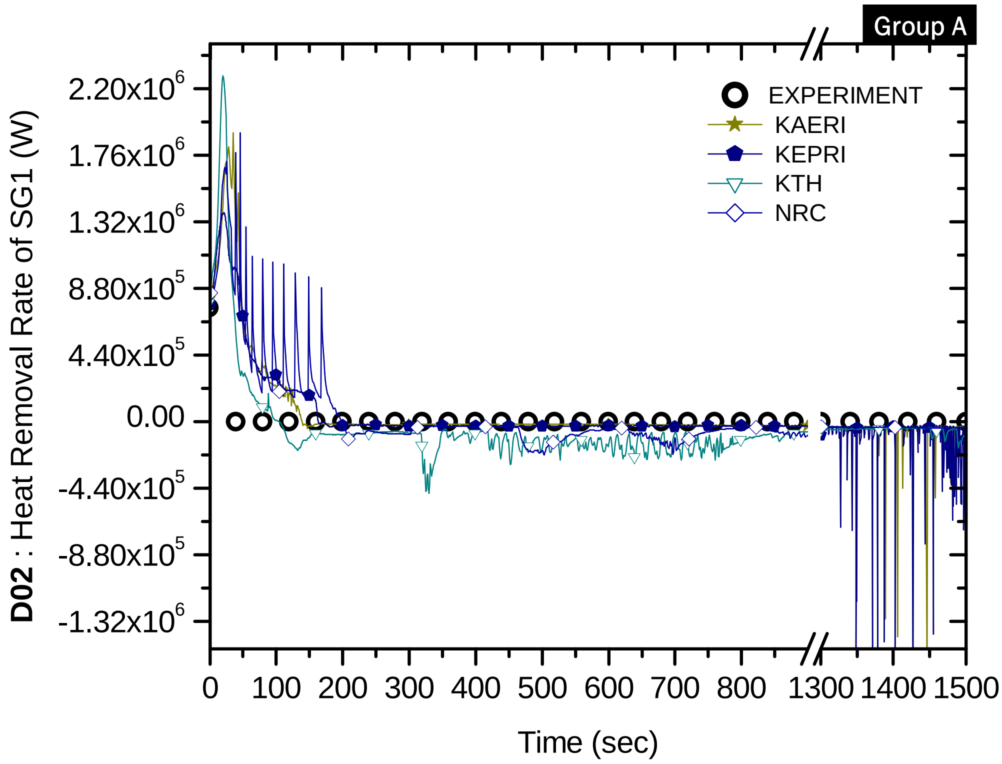

Figure B.2-A Heat removal rate of SG1 (D02)

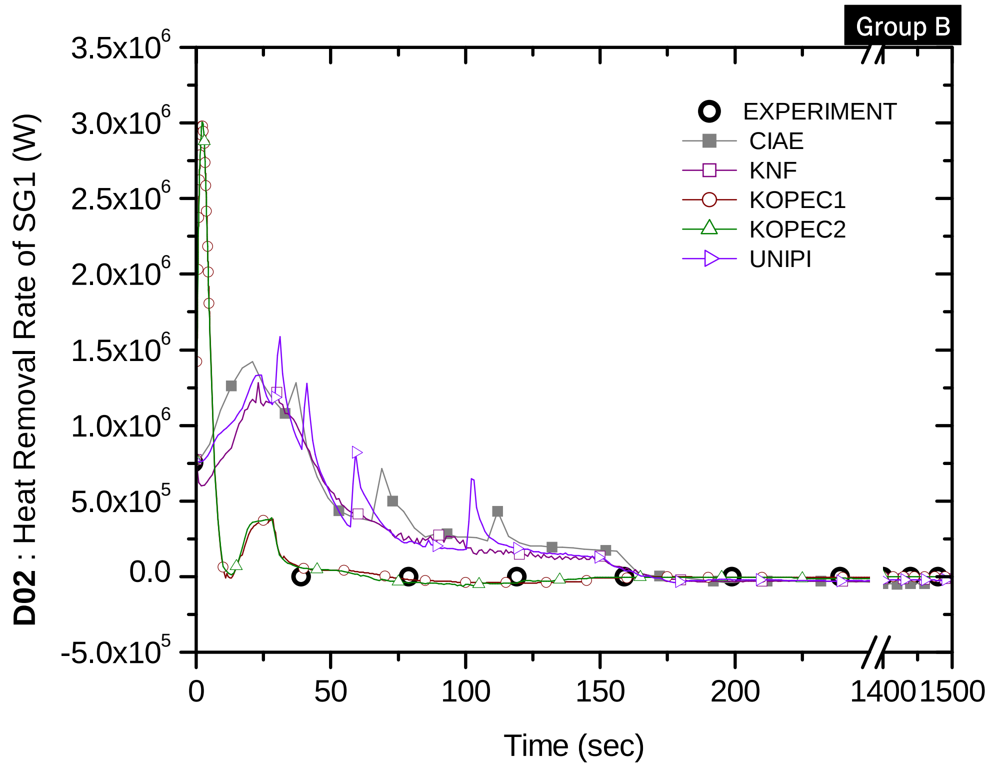

Figure B.2-B Heat removal rate of SG1 (D02)

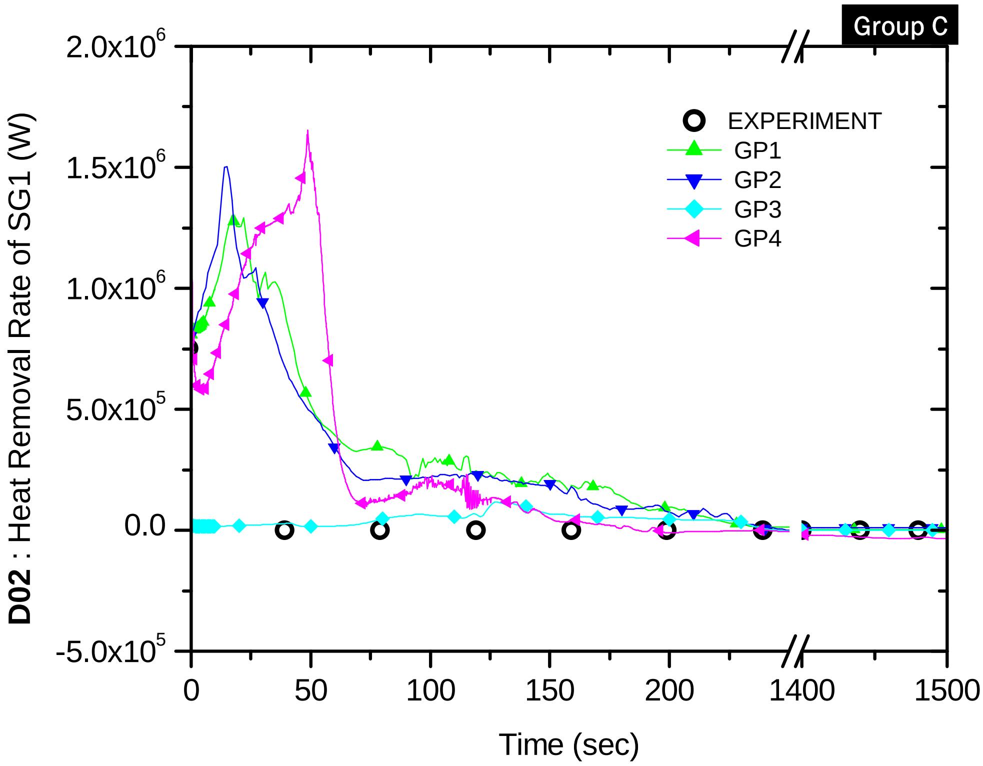

Figure B.2-C Heat removal rate of SG1 (D02)

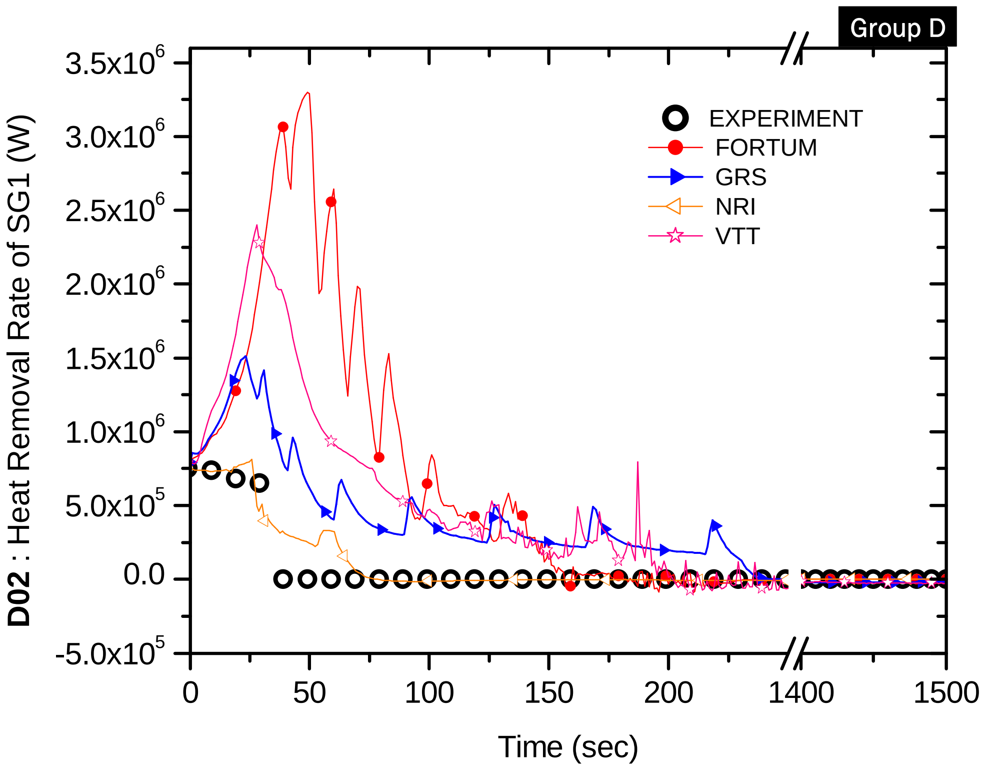

Figure B.2-D Heat removal rate of SG1 (D02)

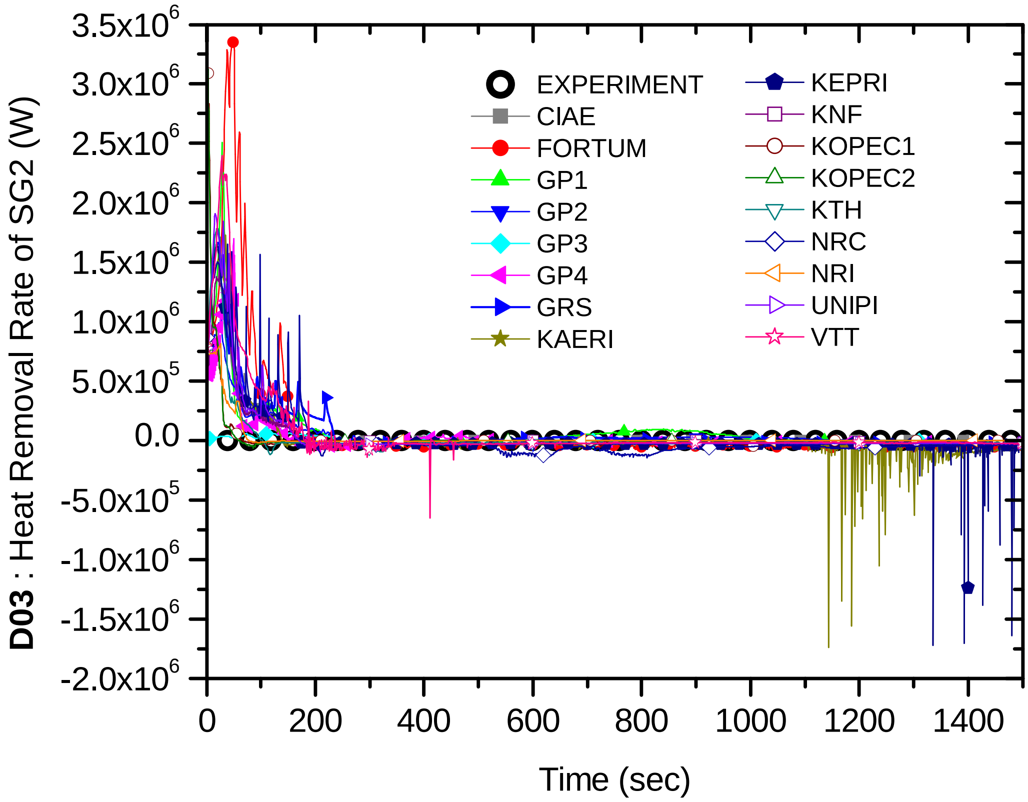

Figure B.3 Heat removal rate of SG2 (D03)

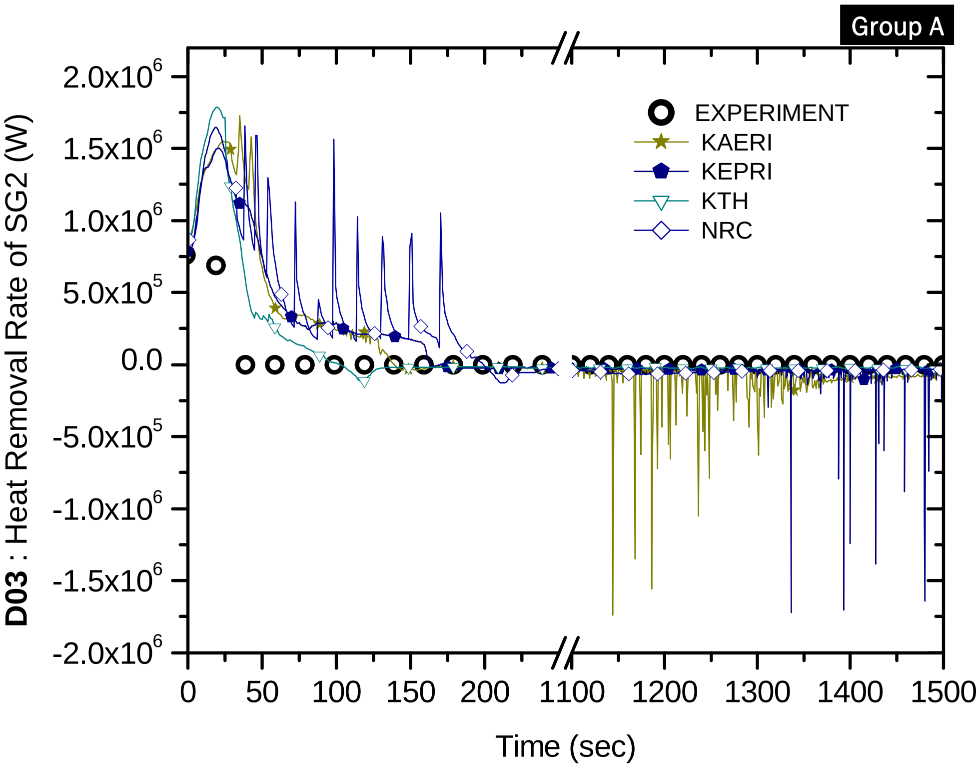

Figure B.3-A Heat removal rate of SG2 (D03)

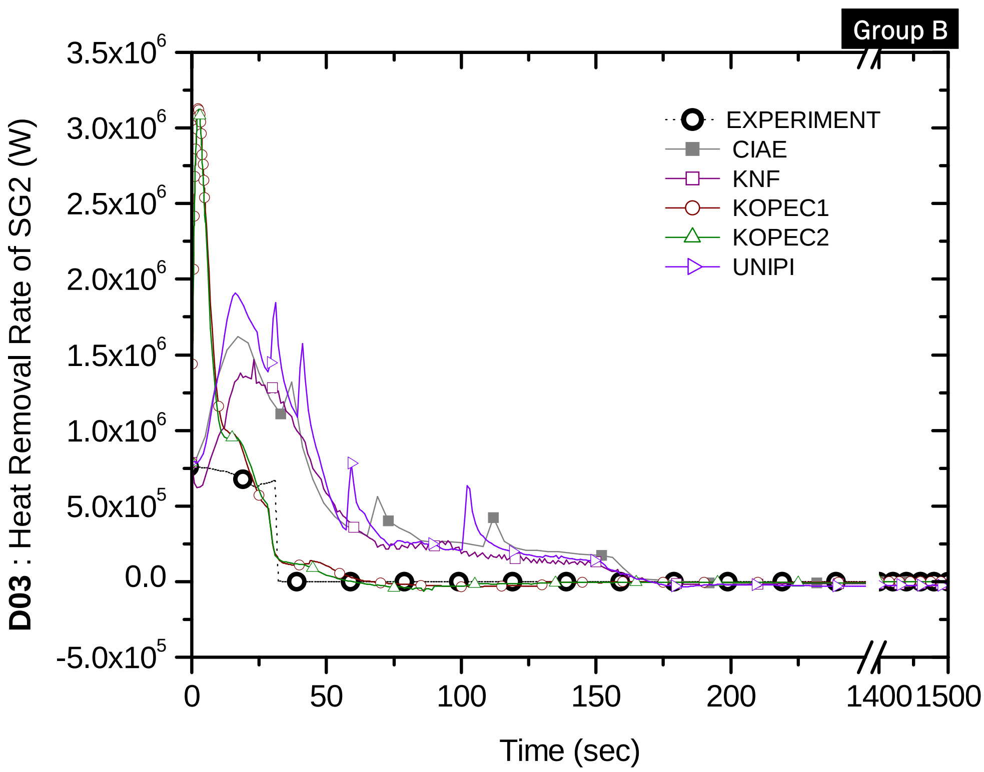

Figure B.3-B Heat removal rate of SG2 (D03)

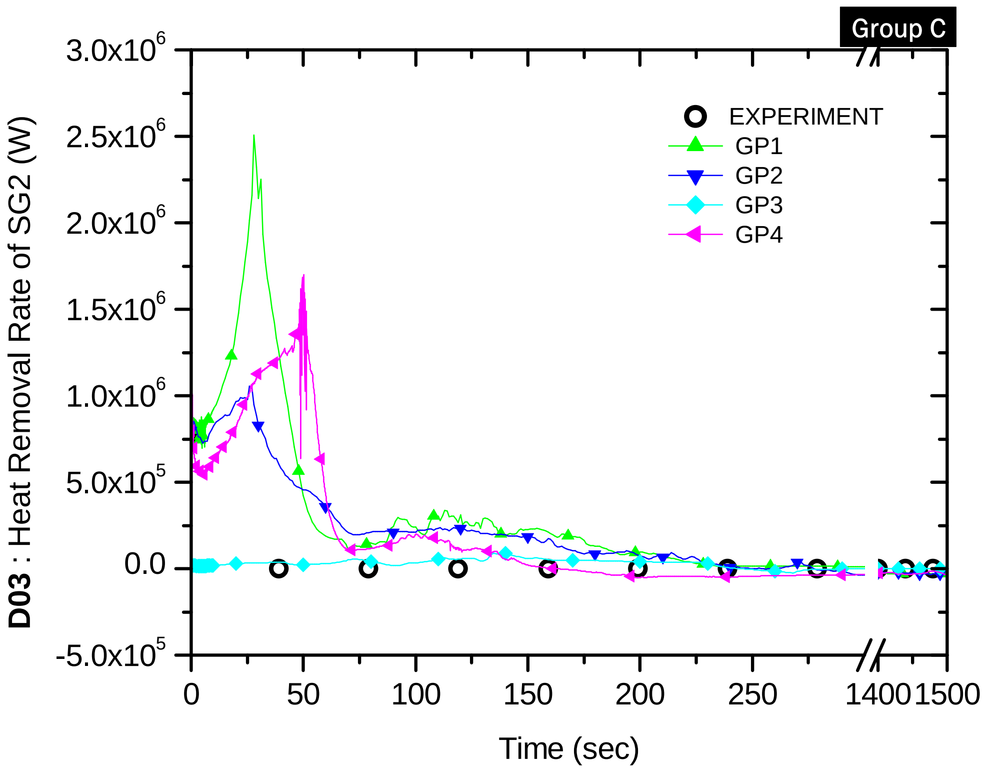

Figure B.3-C Heat removal rate of SG2 (D03)

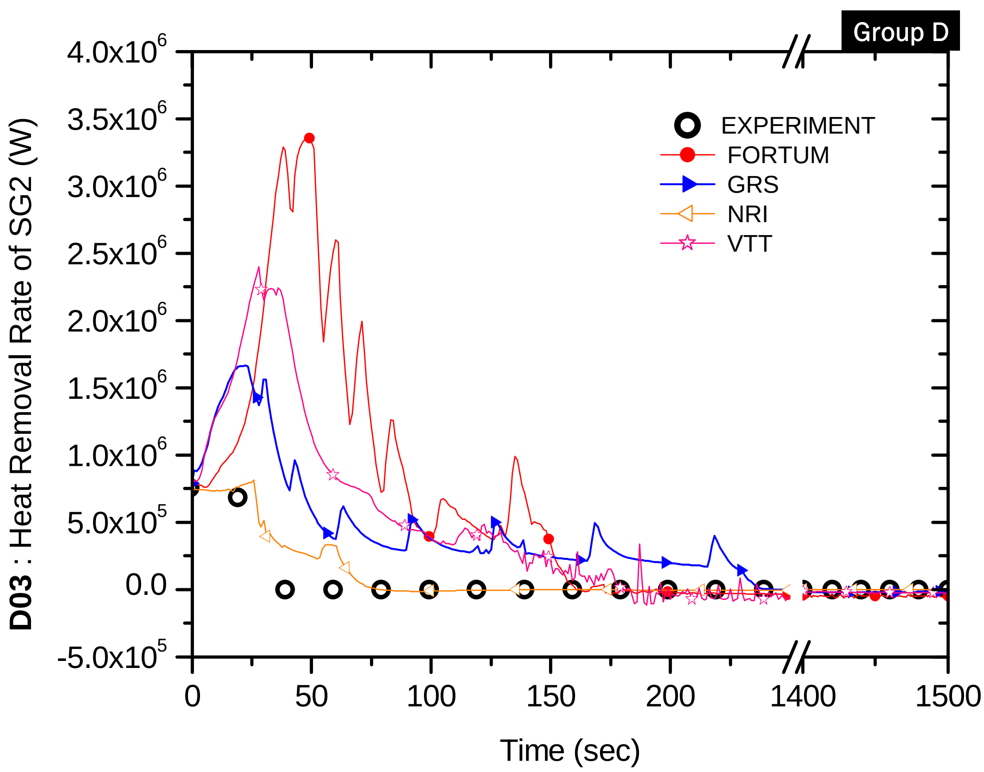

Figure B.3-D Heat removal rate of SG2 (D03)

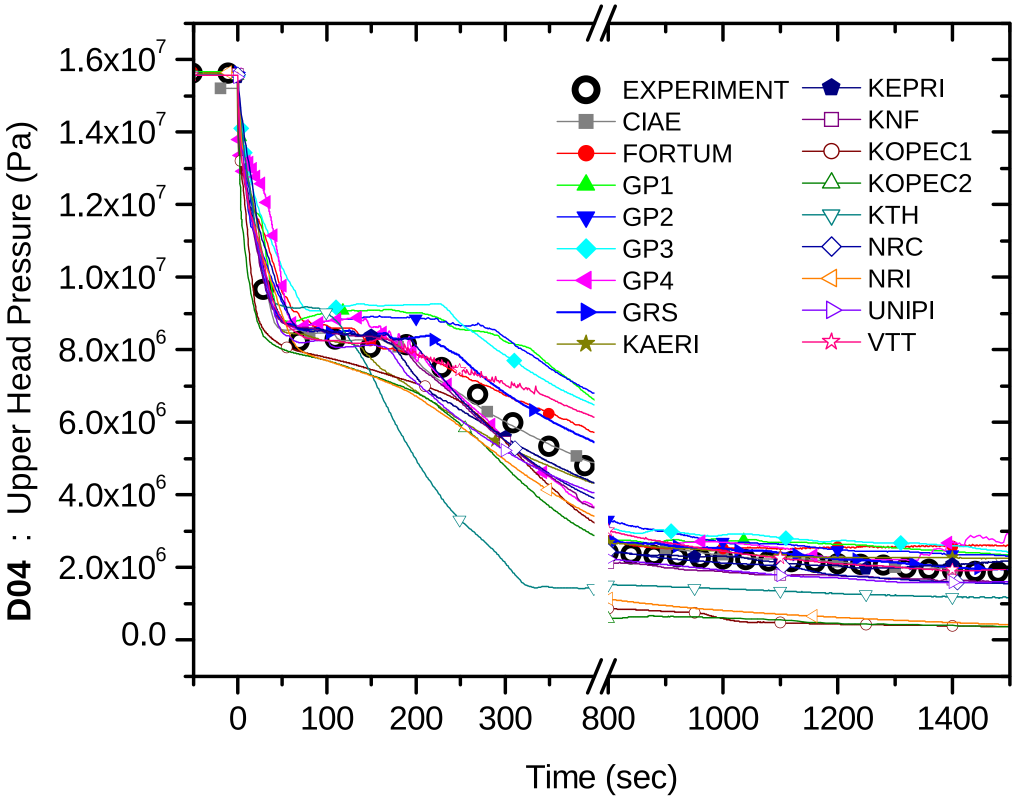

Figure B.4 Upper head pressure (D04)

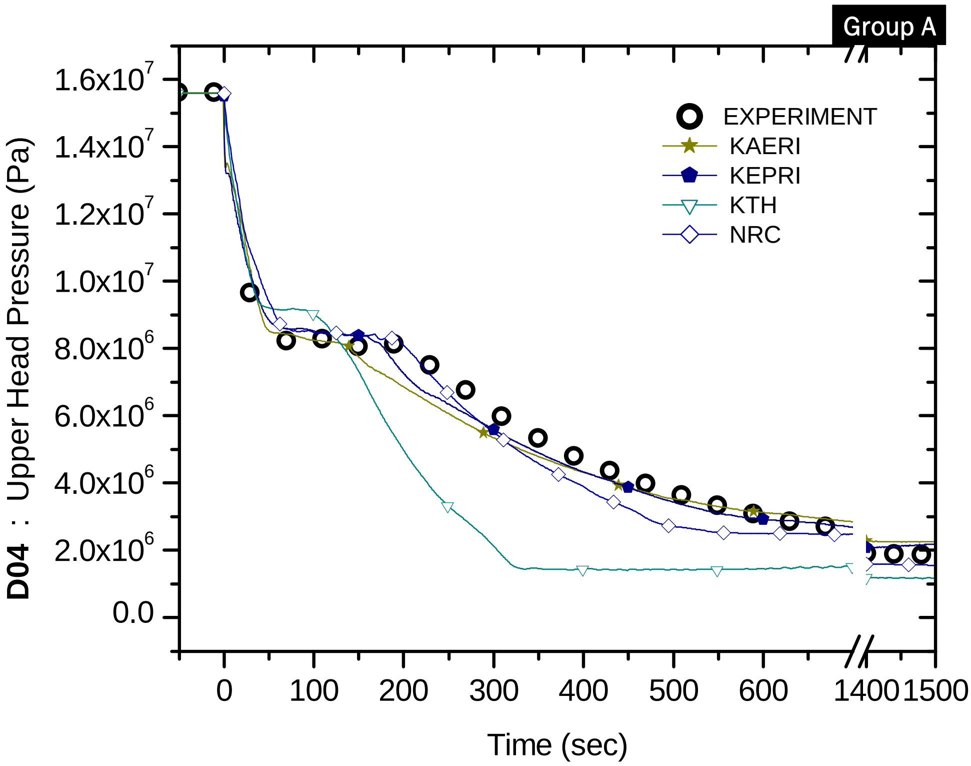

Figure B.4-A Upper head pressure (D04)

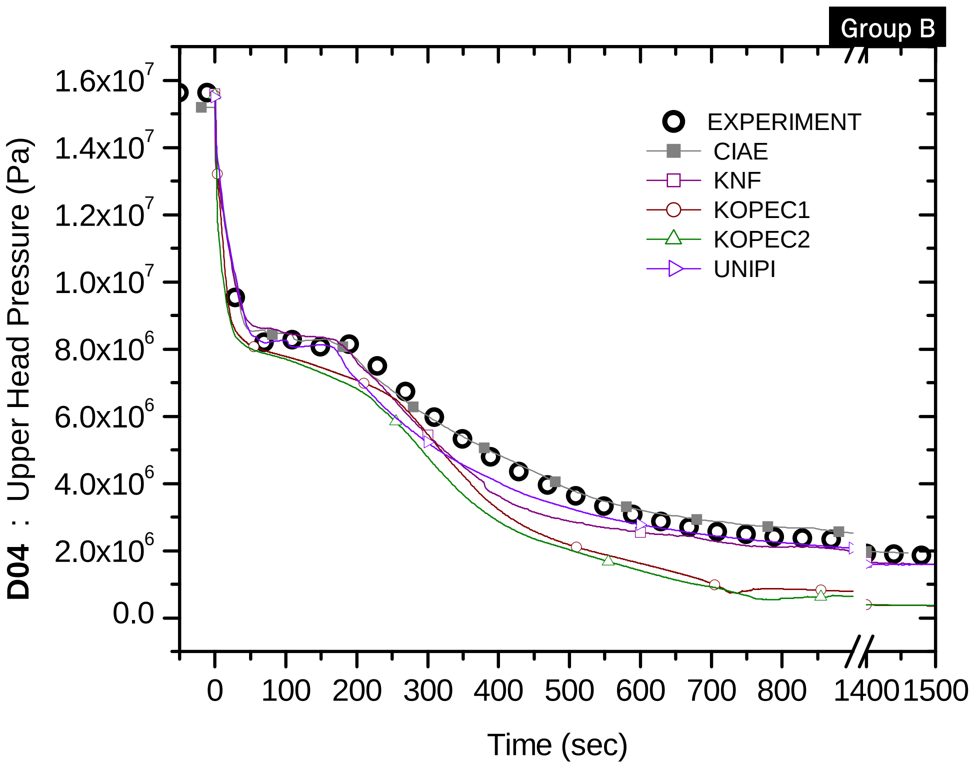

Figure B.4-B Upper head pressure (D04)

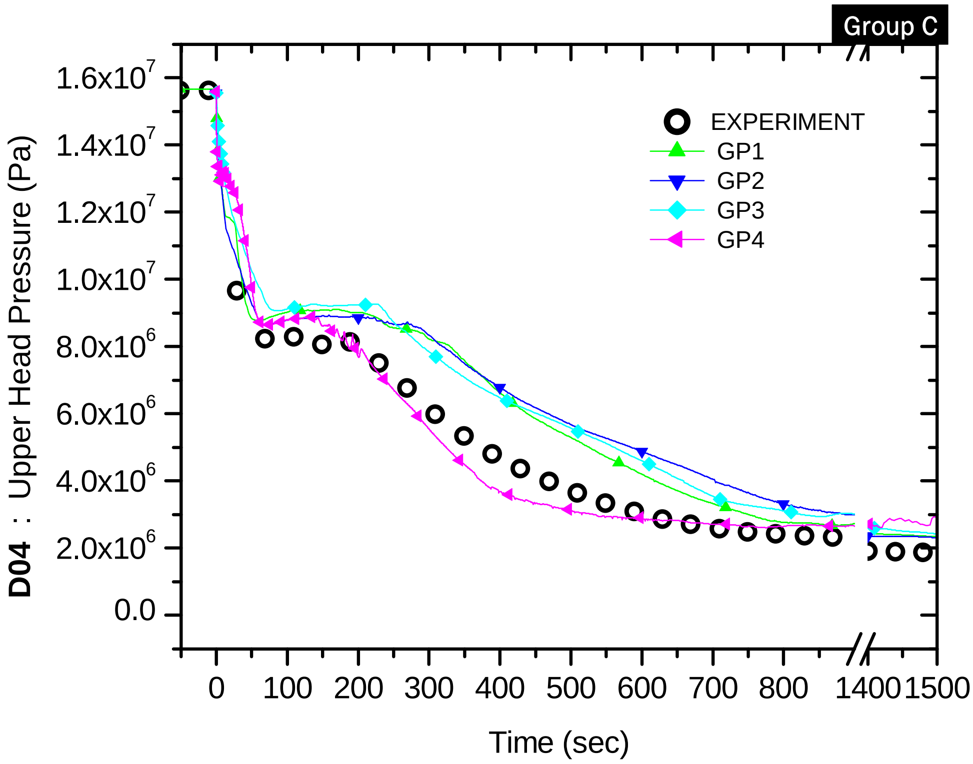

Figure B.4-C Upper head pressure (D04)

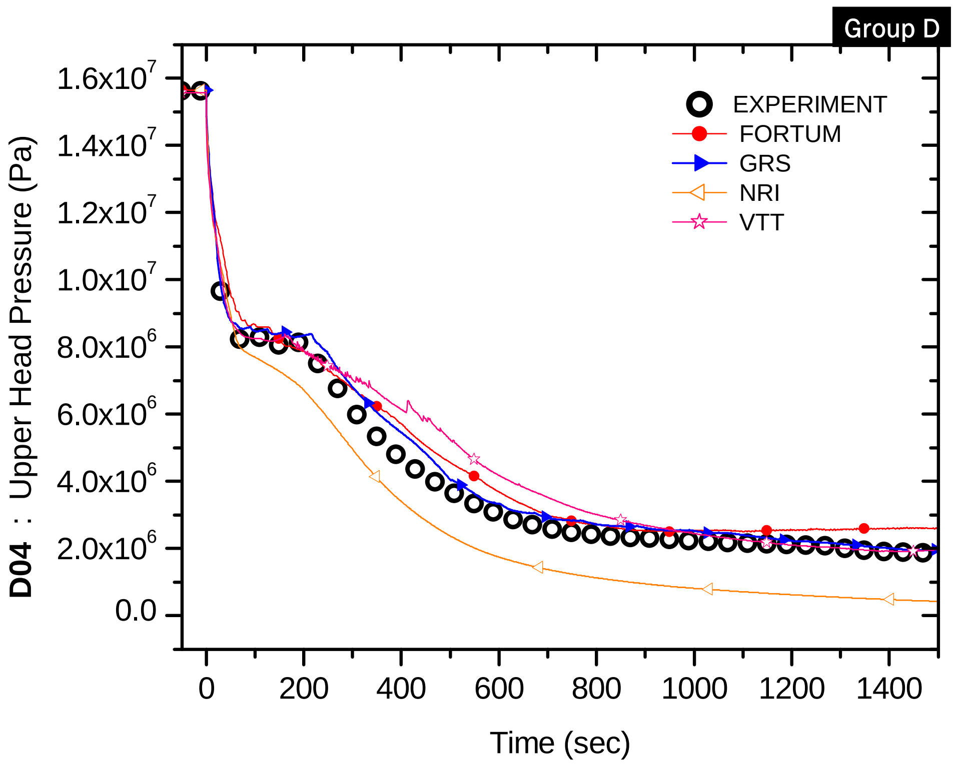

Figure B.4-D Upper head pressure (D04)

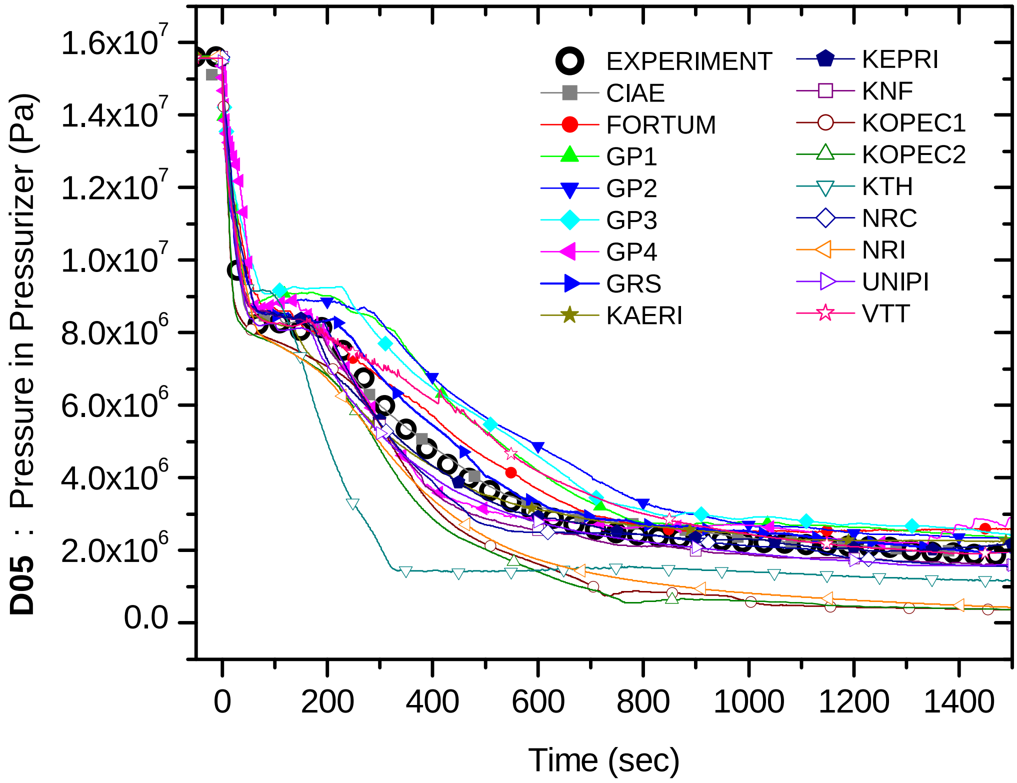

Figure B.5 Pressure of the pressurizer (D05)

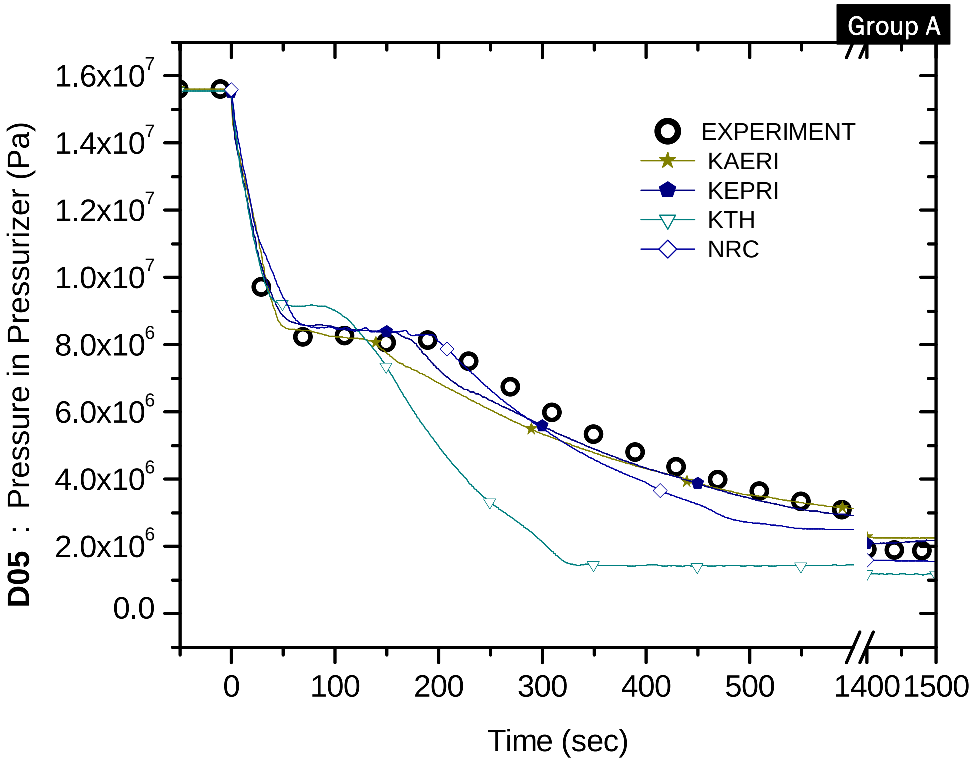

Figure B.5-A Pressure of the pressurizer (D05)

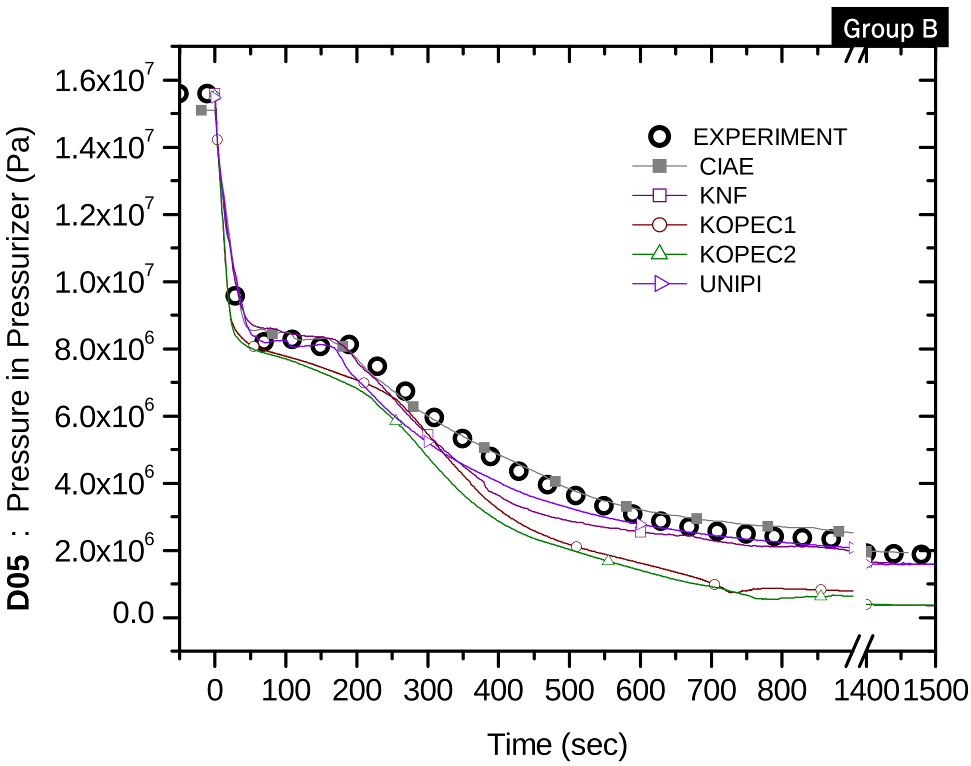

Figure B.5-B Pressure of the pressurizer (D05)

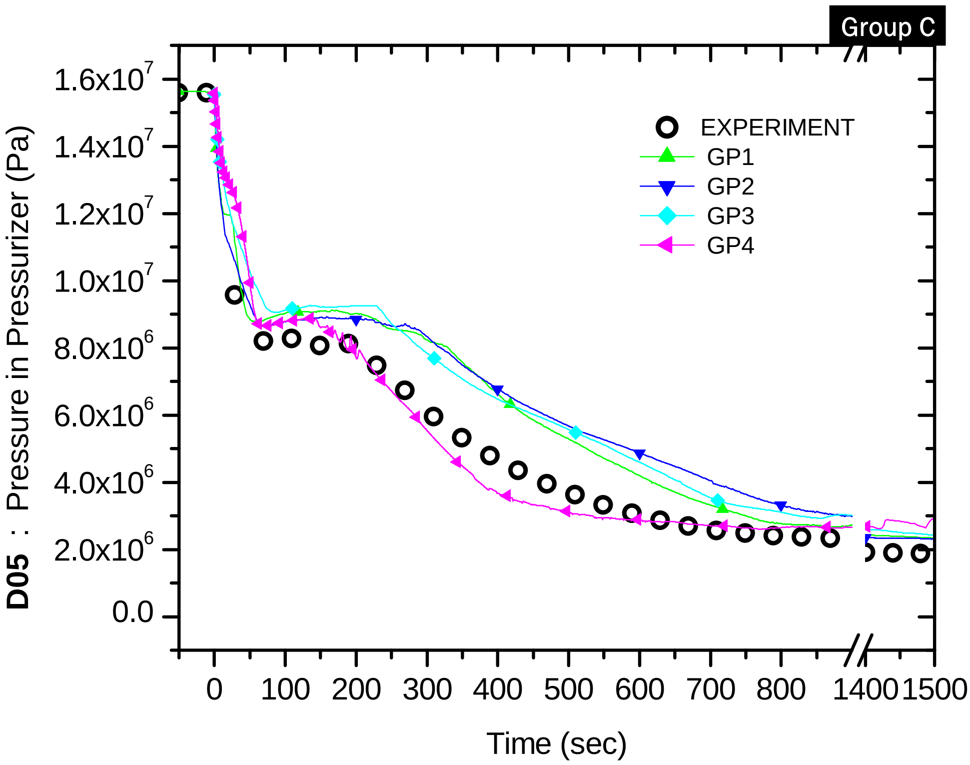

Figure B.5-C Pressure of the pressurizer (D05)

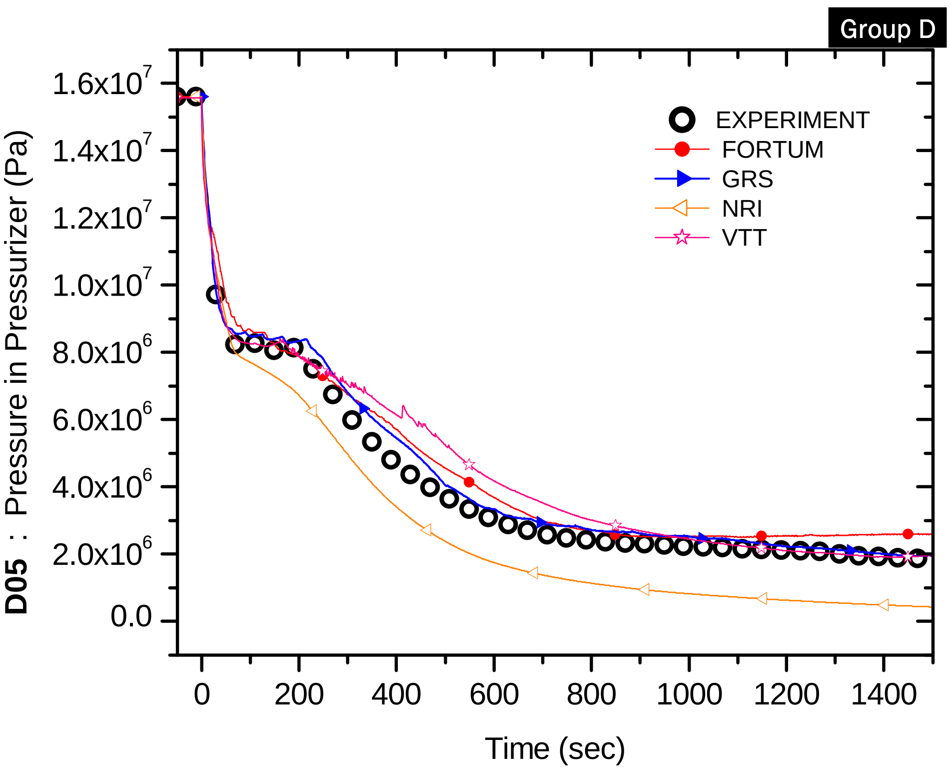

Figure B.5-D Pressure of the pressurizer (D05)

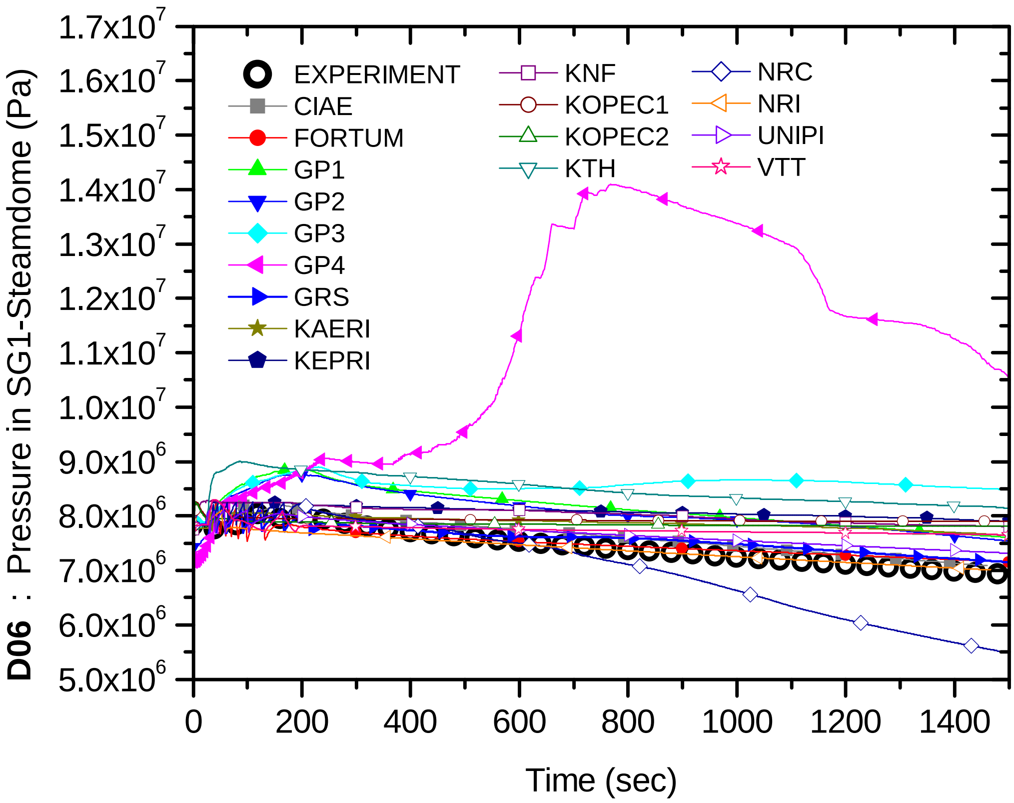

Figure B.6 Pressure in SG-1 dome (D06)

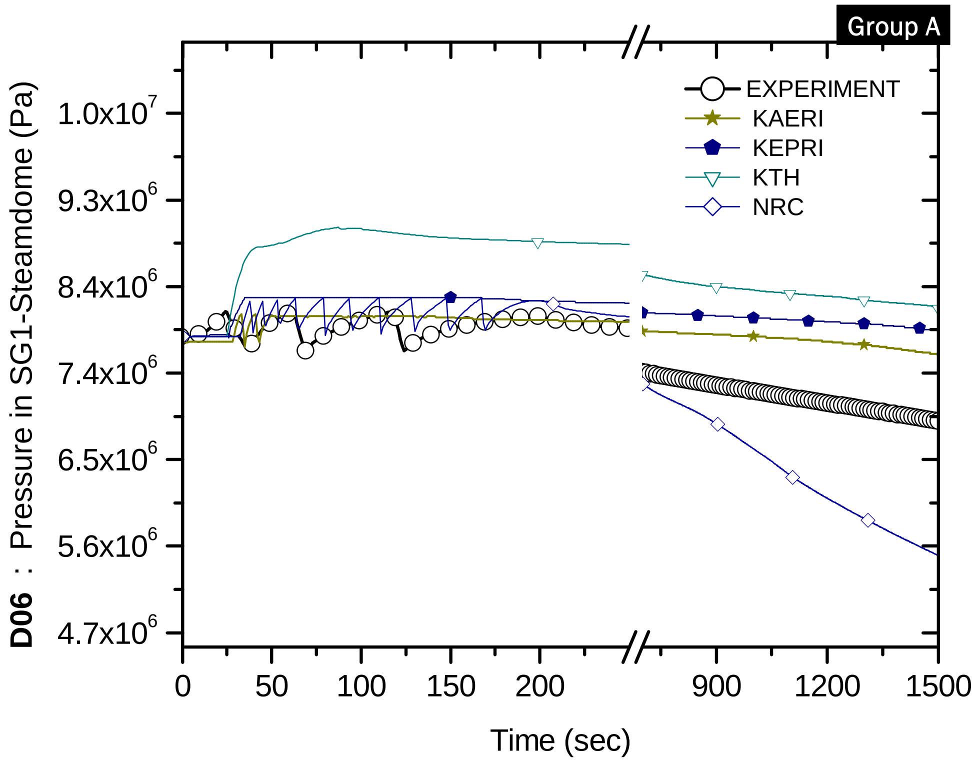

Figure B.6-A Pressure in SG-1 dome (D06)

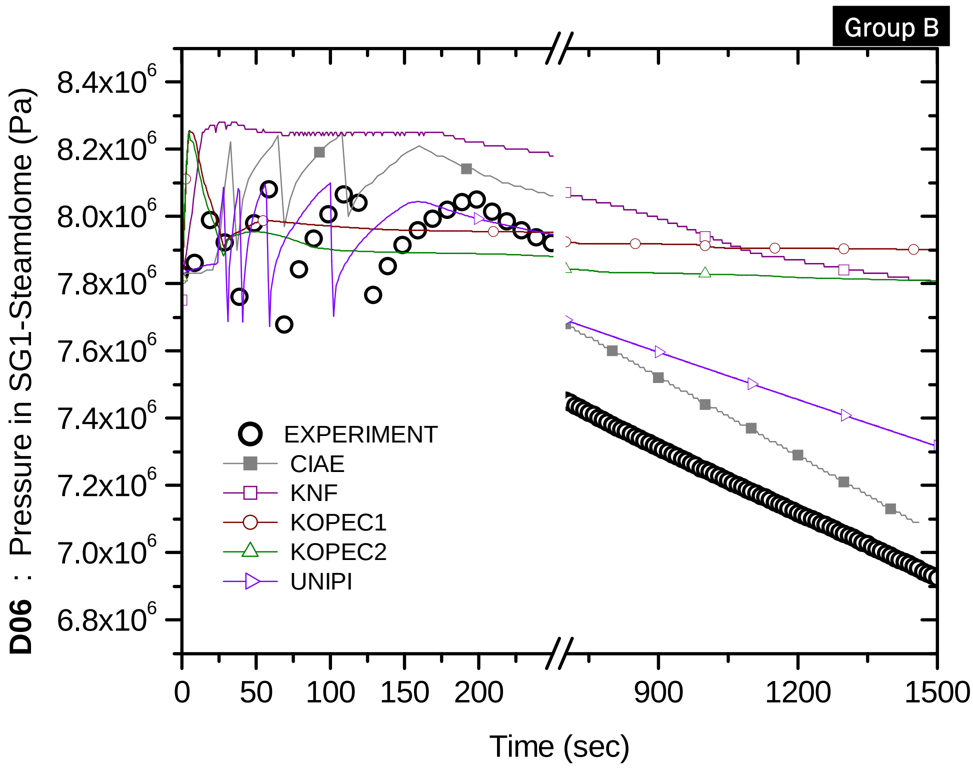

Figure B.6-B Pressure in SG-1 dome (D06)

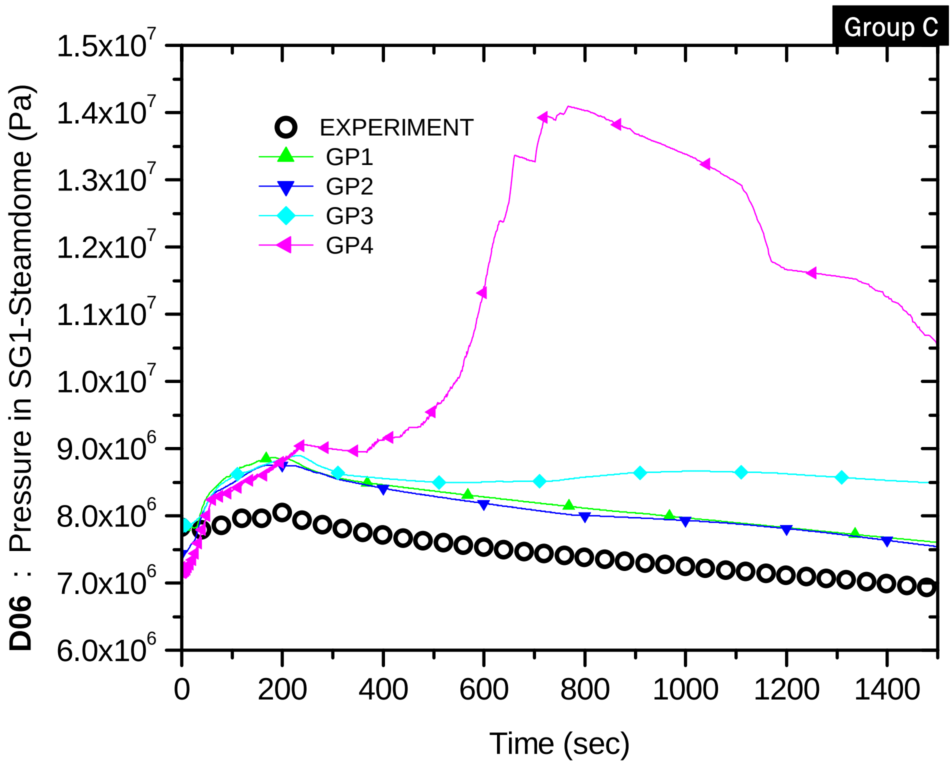

Figure B.6-C Pressure in SG-1 dome (D06)

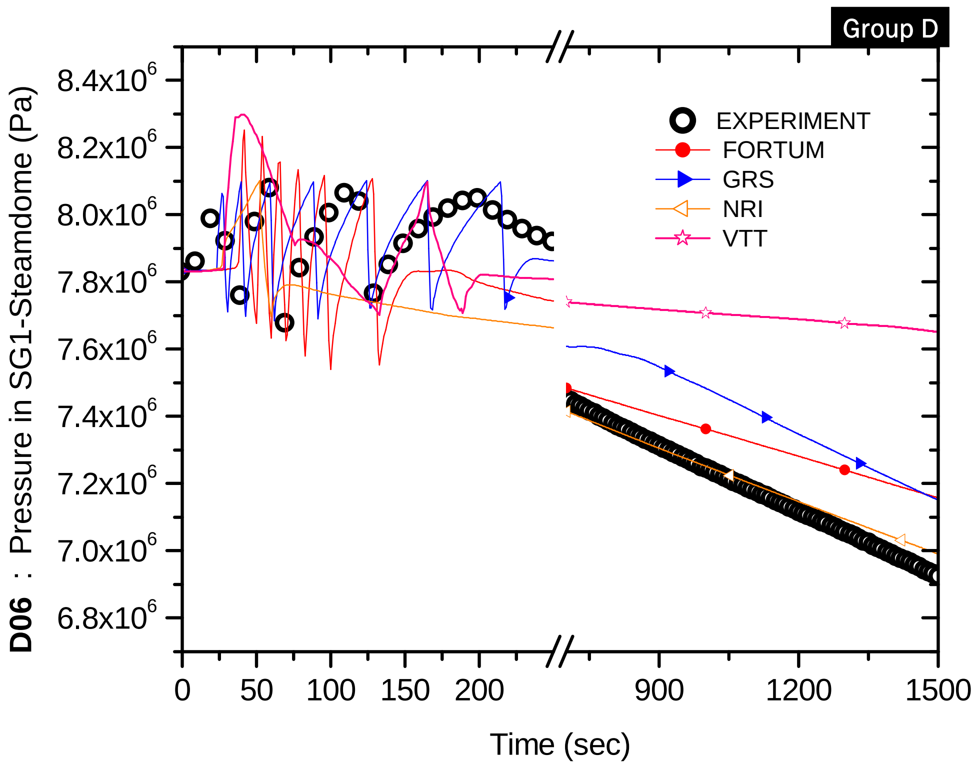

Figure B.6-D Pressure in SG-1 dome (D06)

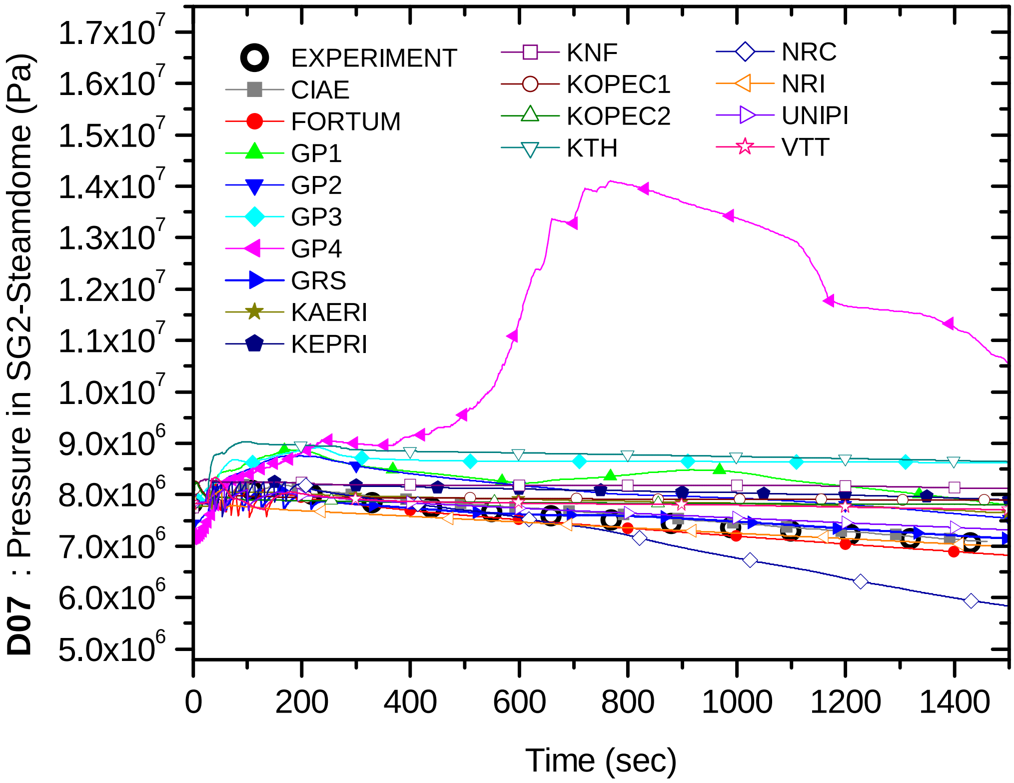

Figure B.7 Pressure in SG-2 dome (D07)

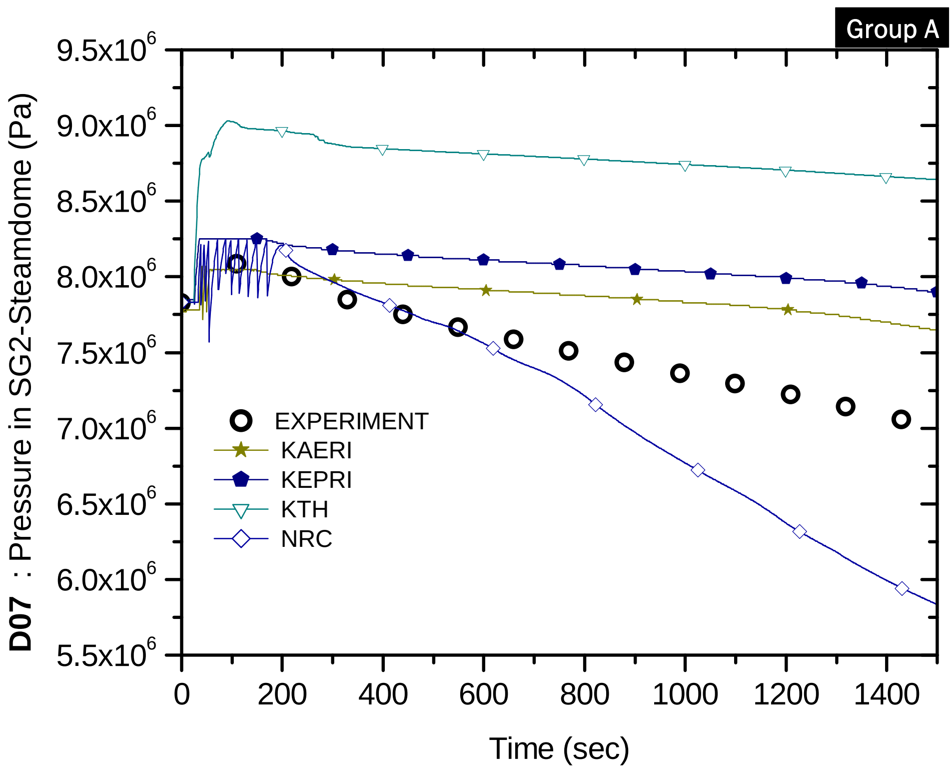

Figure B.7-A Pressure in SG-2 dome (D07)

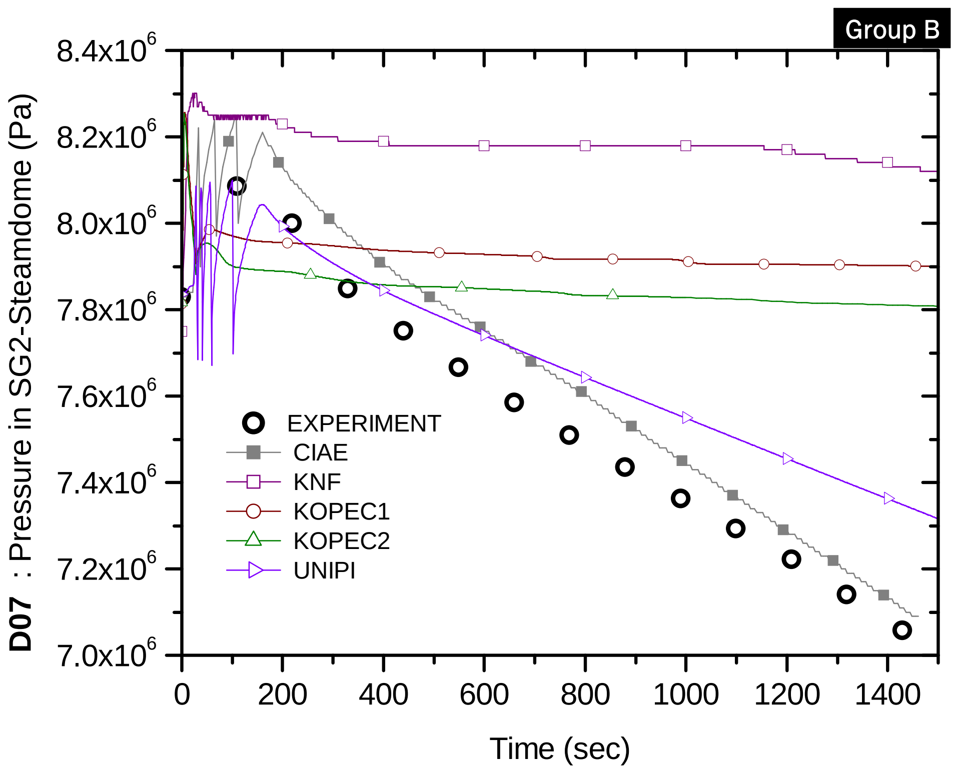

Figure B.7-B Pressure in SG-2 dome (D07)

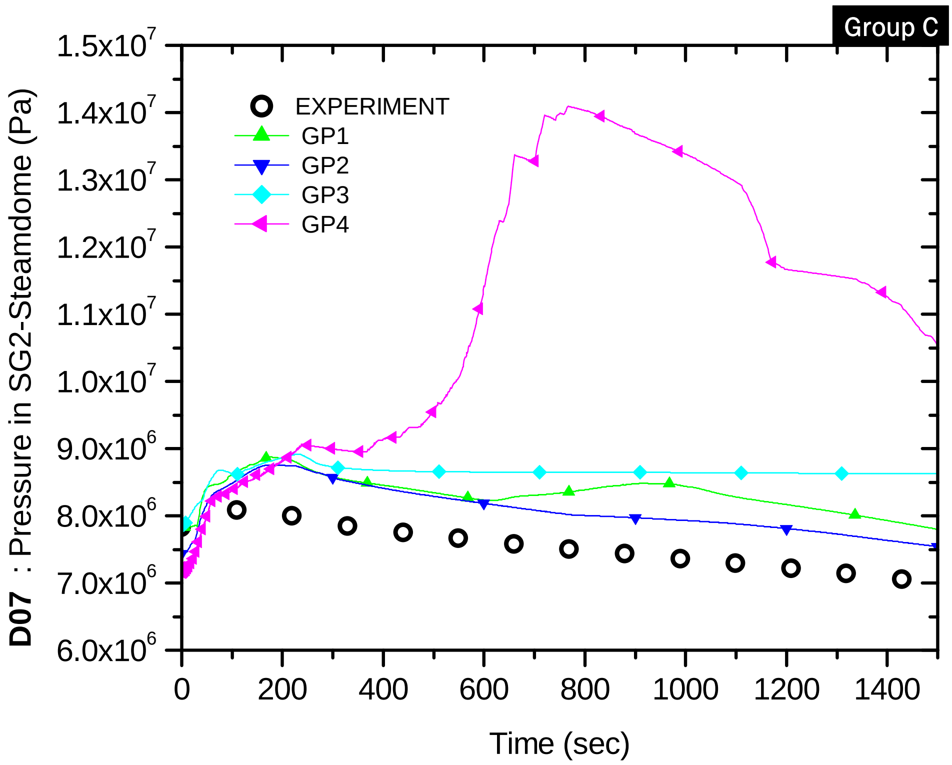

Figure B.7-C Pressure in SG-2 dome (D07)

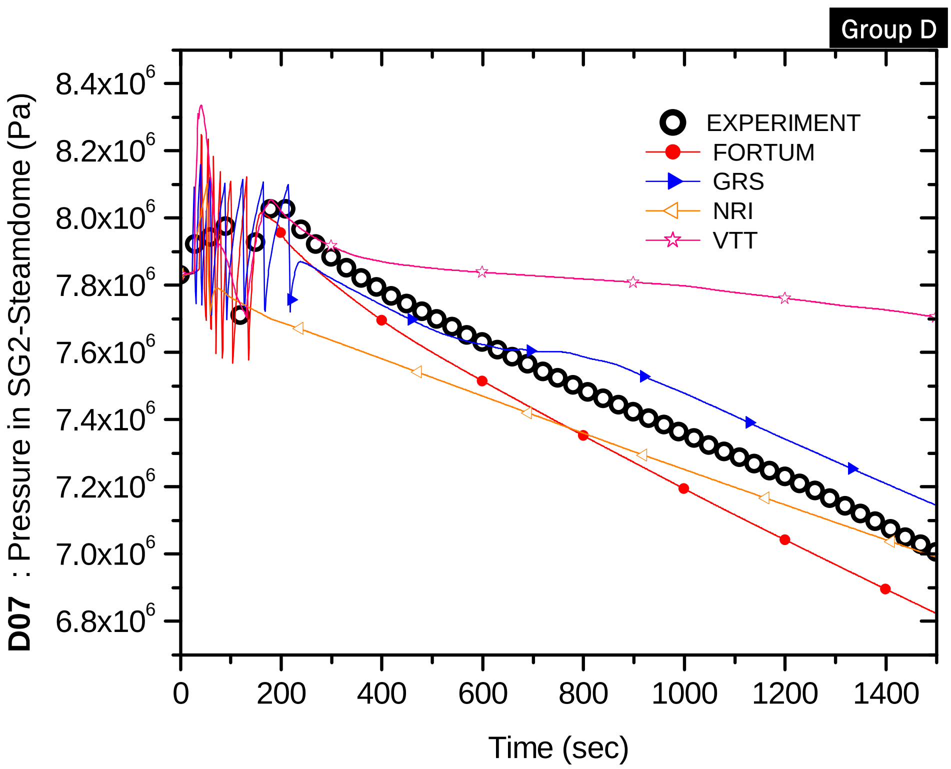

Figure B.7-D Pressure in SG-2 dome (D07)

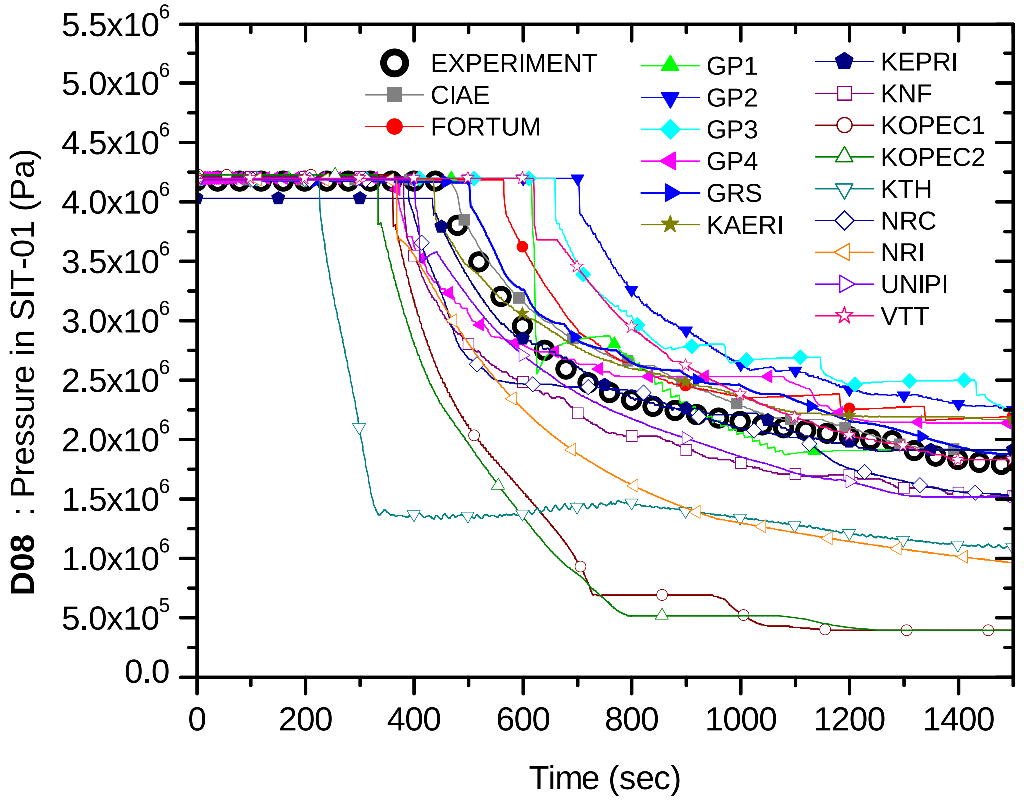

Figure B.8 Pressure in SIT-01 (D08)

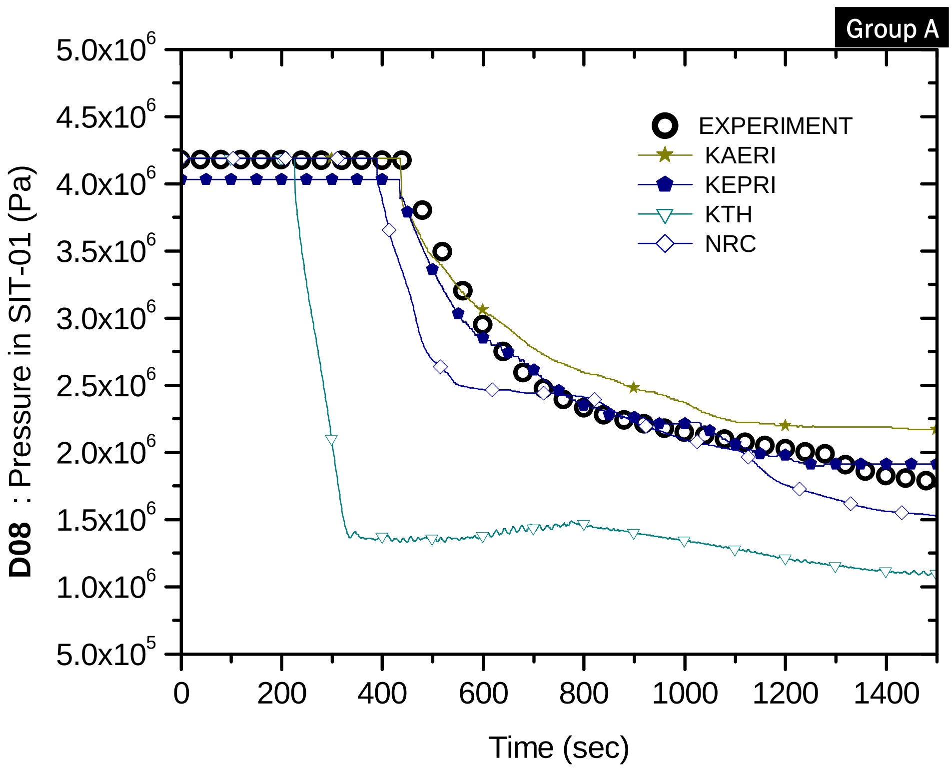

Figure B.8-A Pressure in SIT-01 (D08)

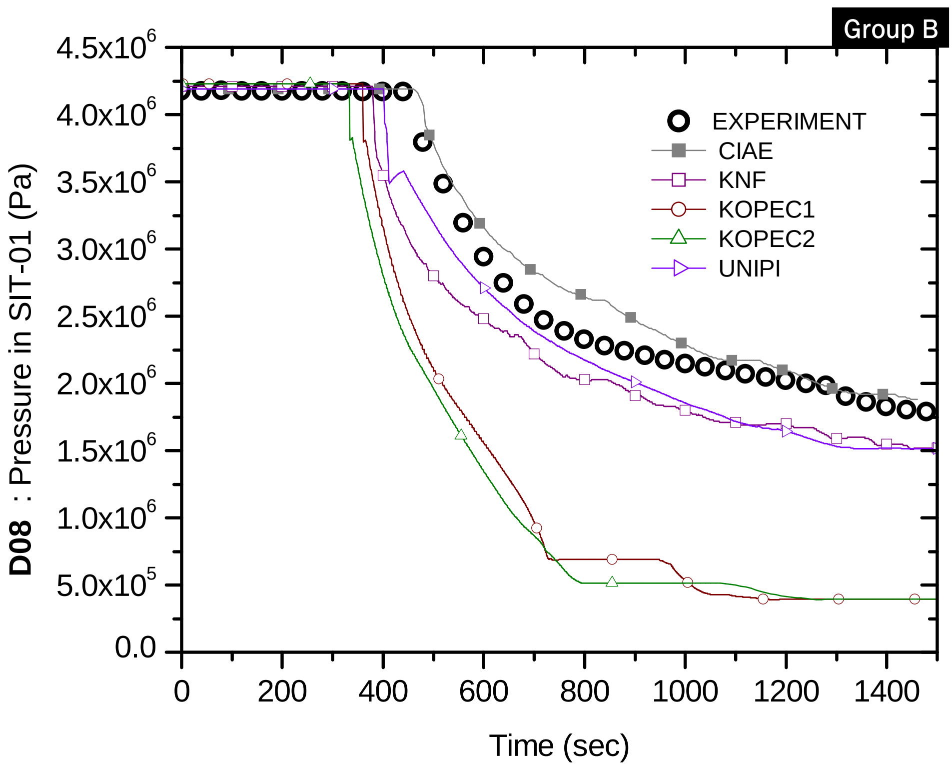

Figure B.8-B Pressure in SIT-01 (D08)

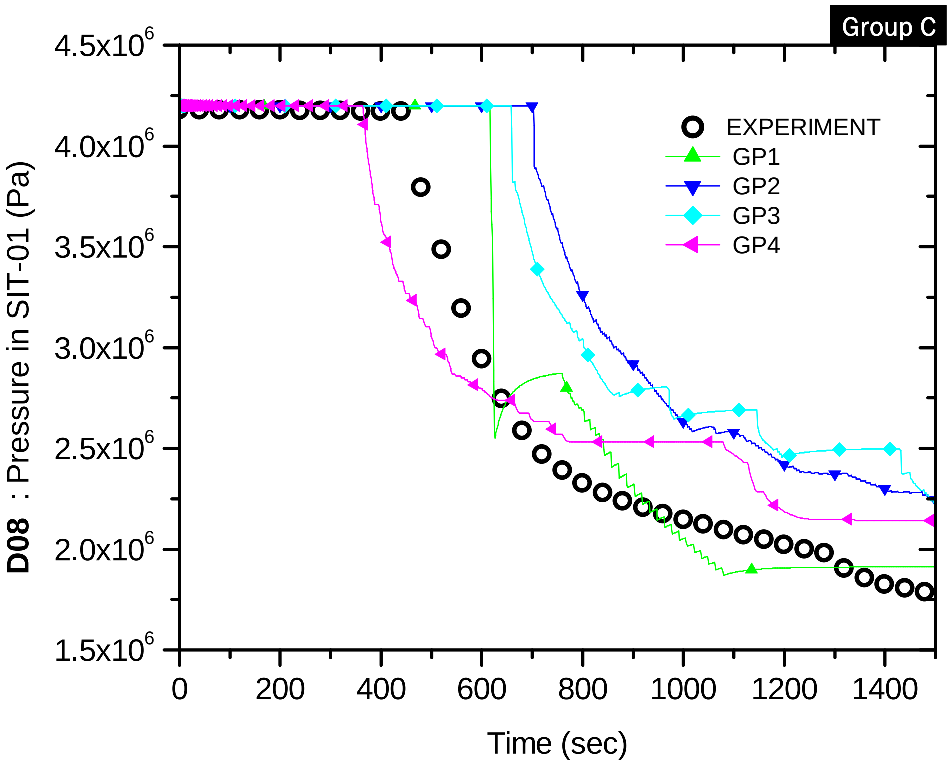

Figure B.8-C Pressure in SIT-01 (D08)

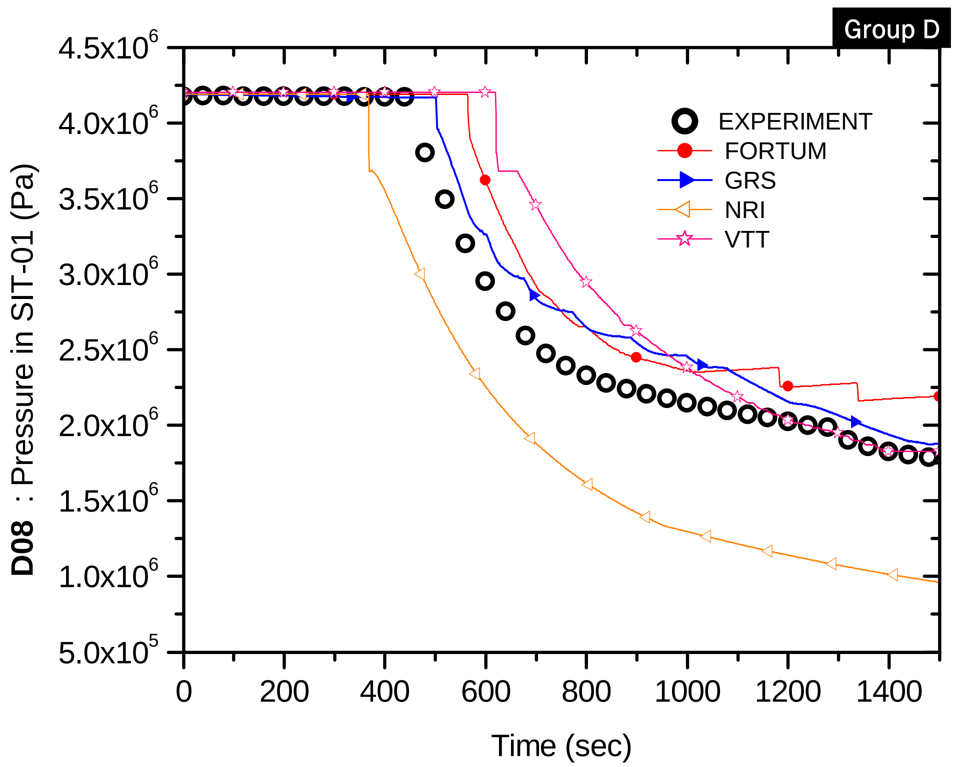

Figure B.8-D Pressure in SIT-01 (D08)

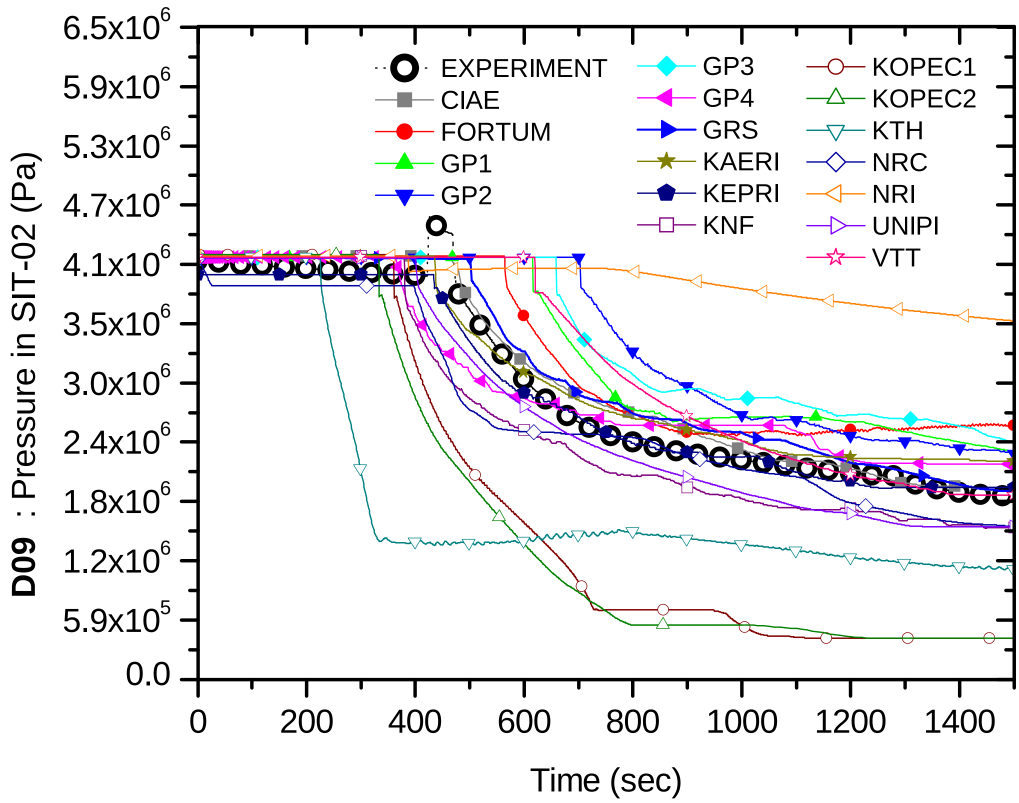

Figure B.9 Pressure in SIT-02 (D09)

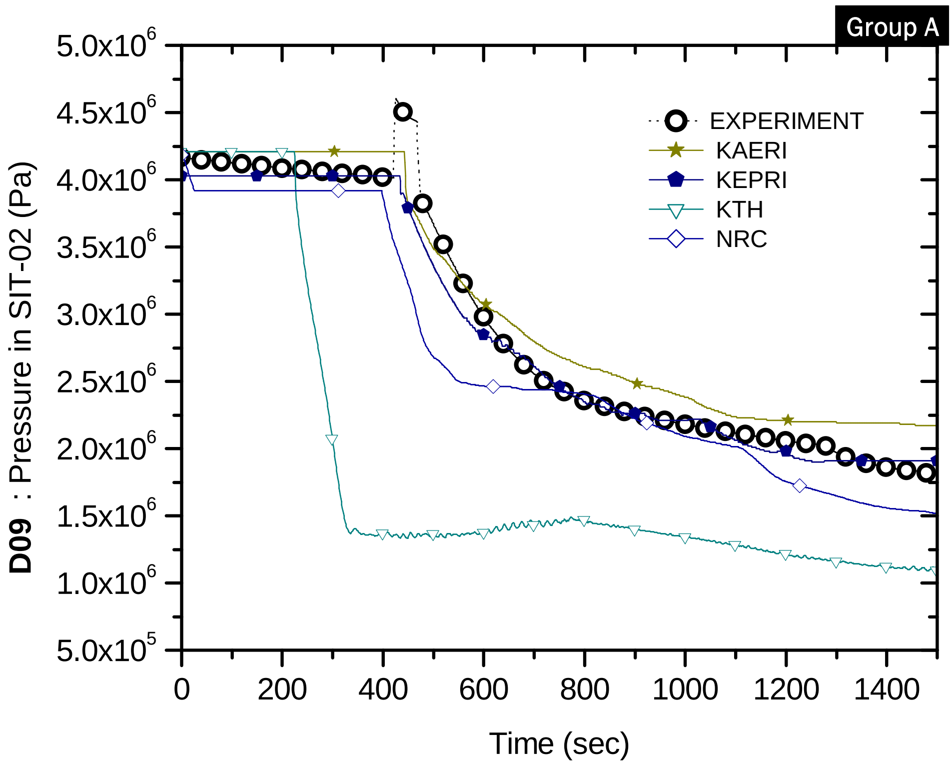

Figure B.9-A Pressure in SIT-02 (D09)

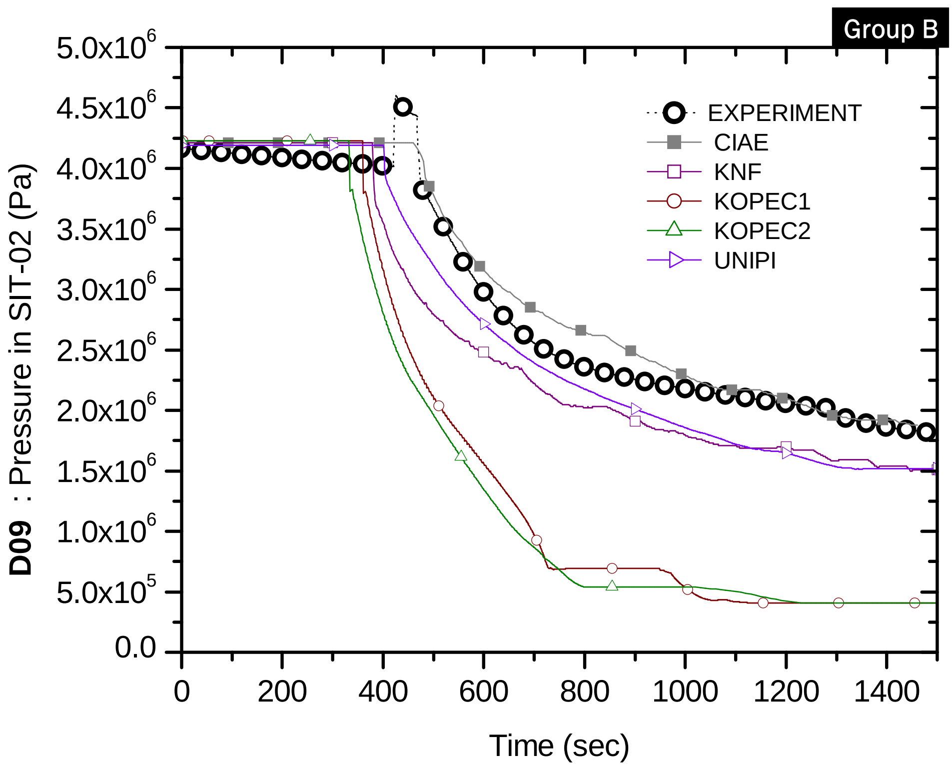

Figure B.1-B Pressure in SIT-02 (D09)

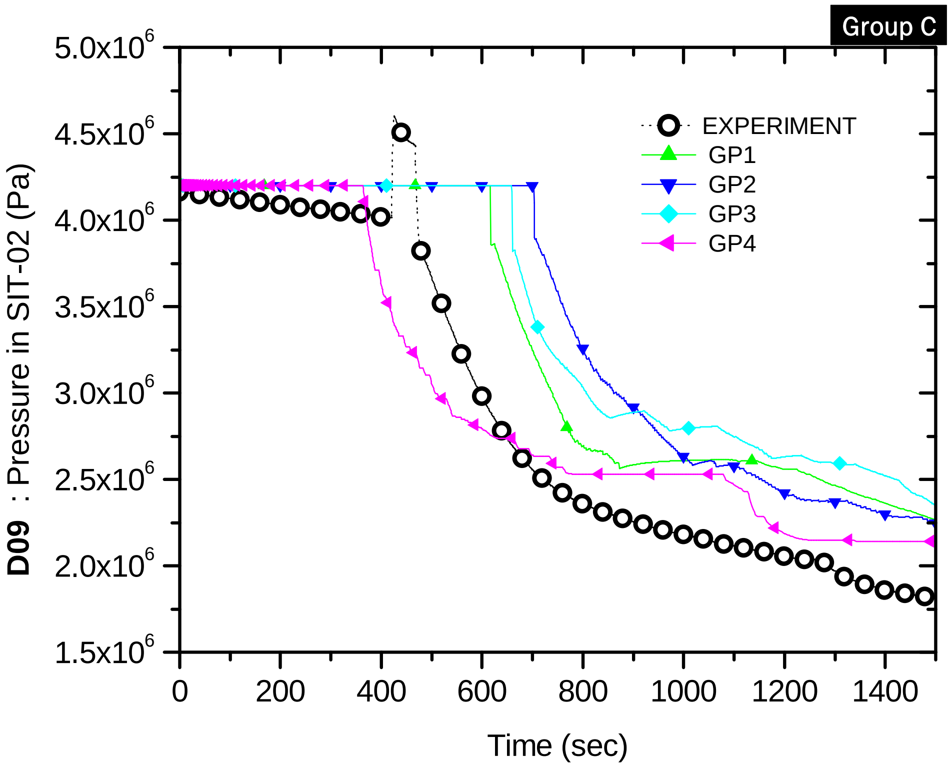

Figure B.9-C Pressure in SIT-02 (D09)

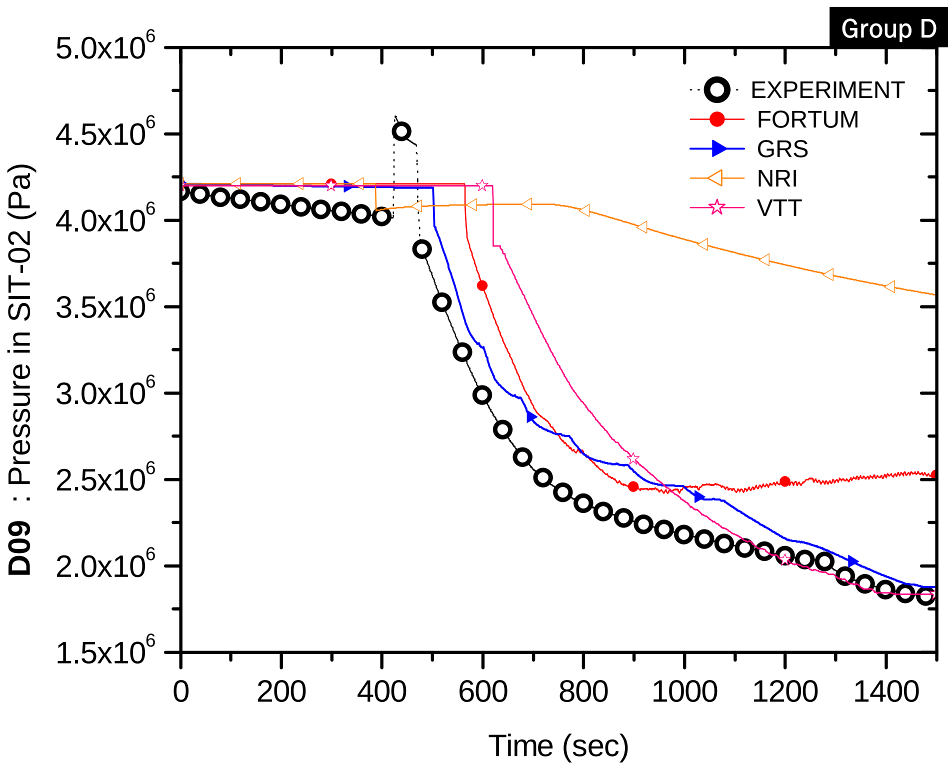

Figure B.9-D Pressure in SIT-02 (D09)

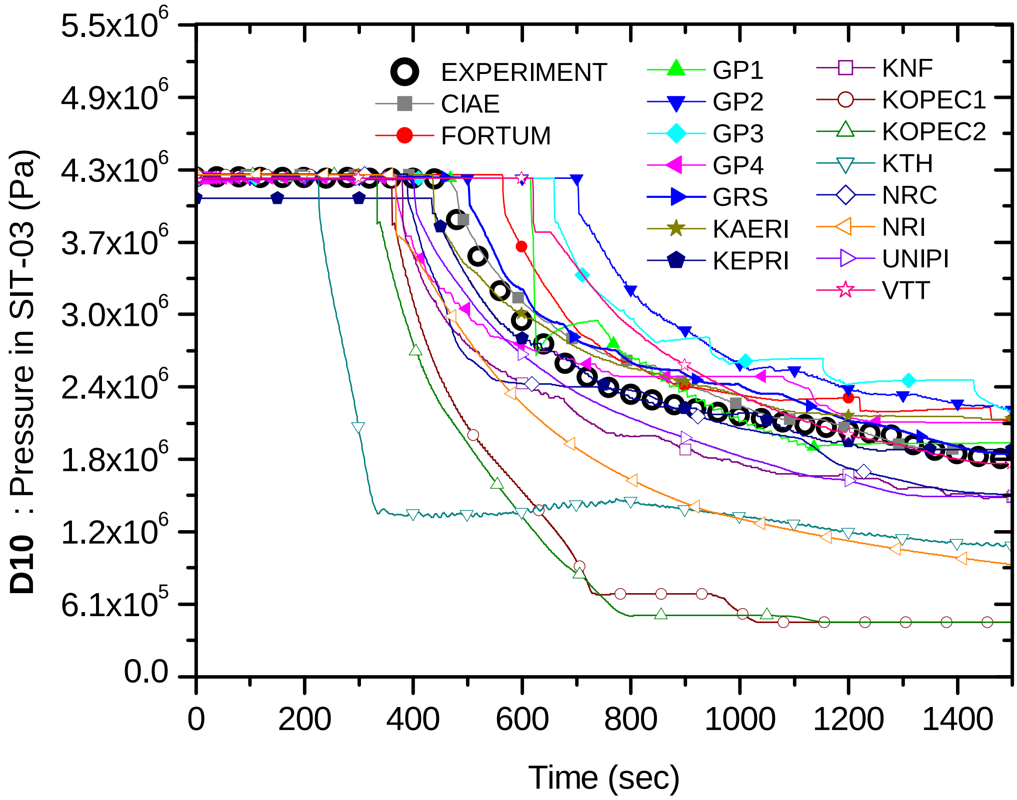

Figure B.10 Pressure in SIT-03 (D10)

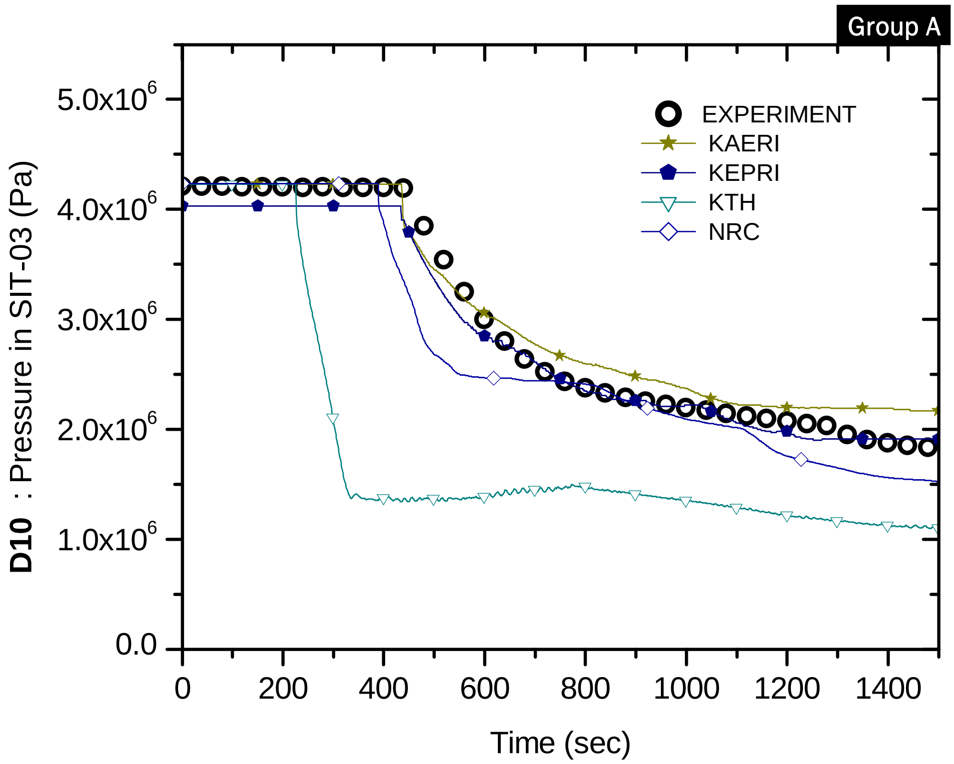

Figure B.10-A Pressure in SIT-03 (D10)

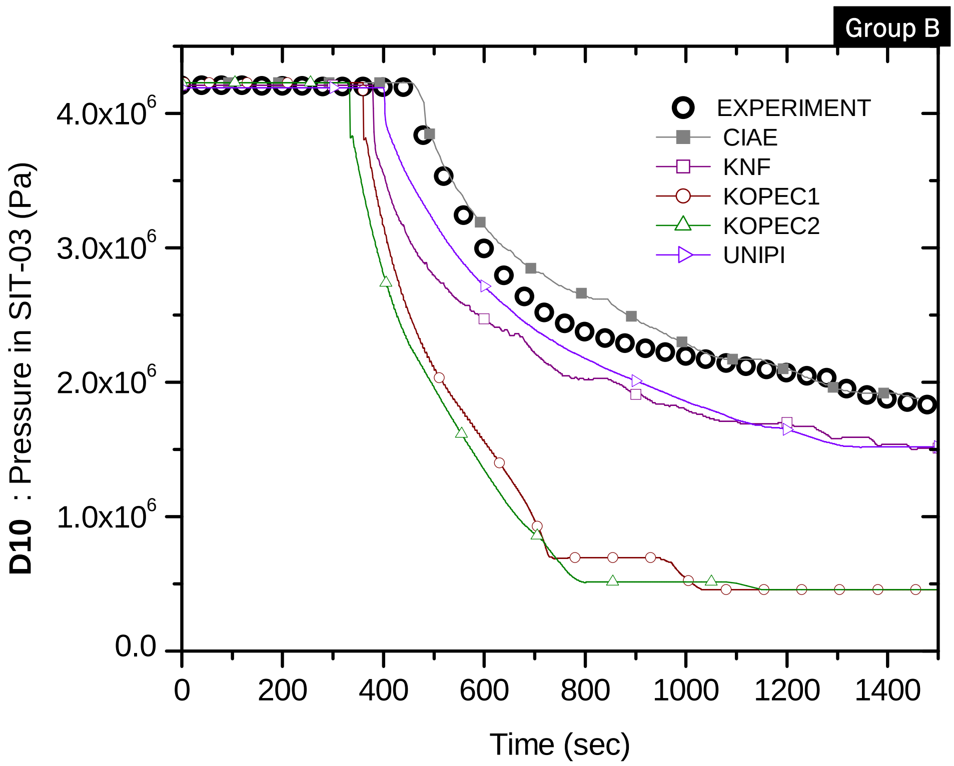

Figure B.10-B Pressure in SIT-03 (D10)

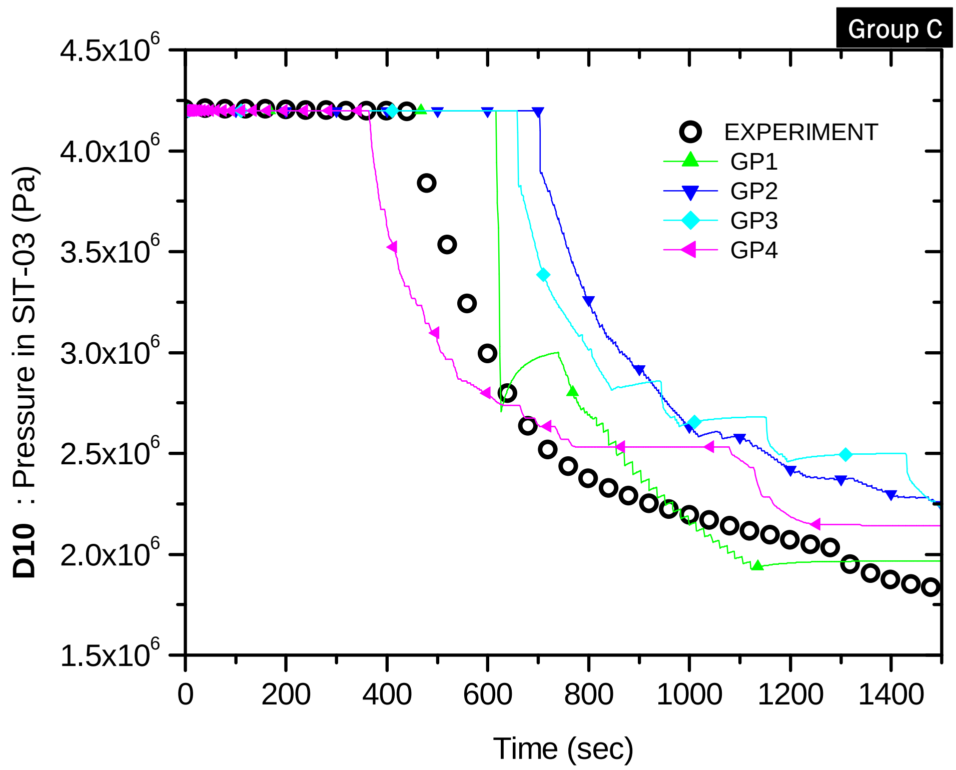

Figure B.10-C Pressure in SIT-03 (D10)

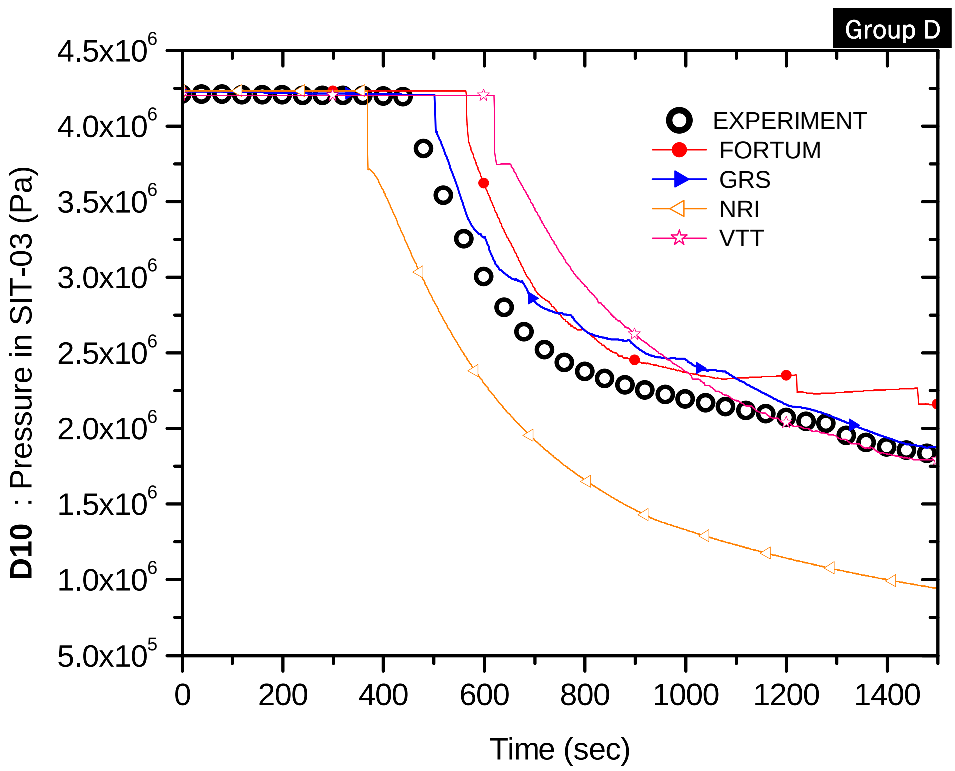

Figure B.10-D Pressure in SIT-03 (D10)

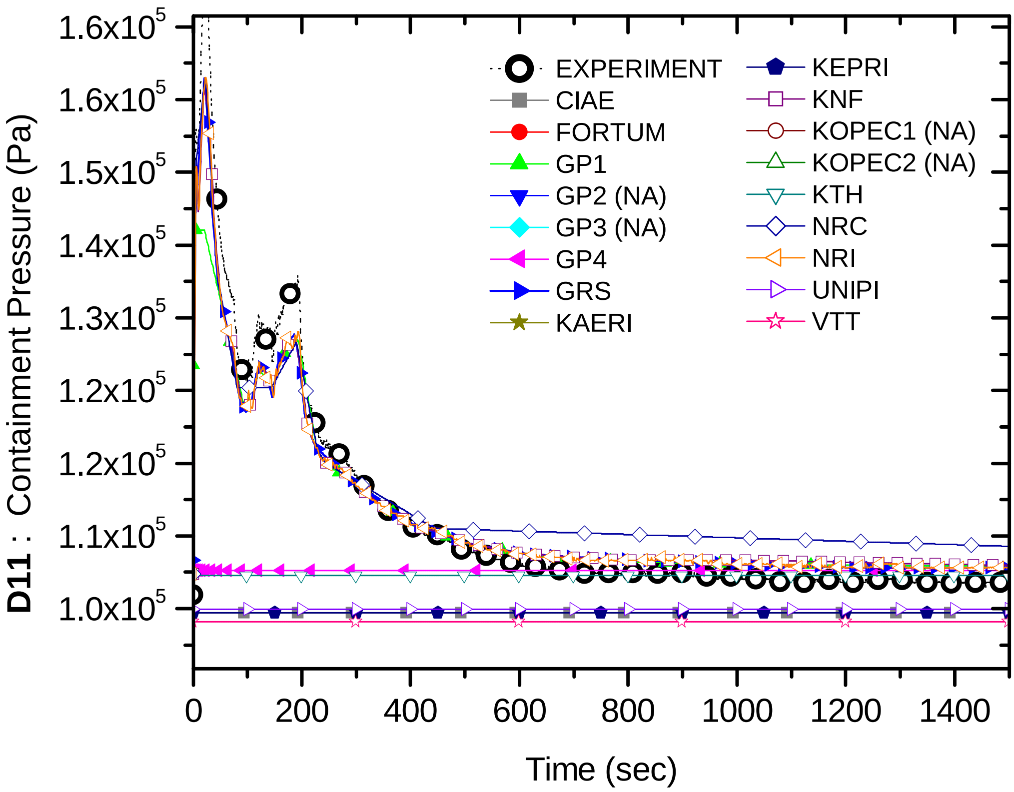

Figure B.11 Containment pressure (D11)

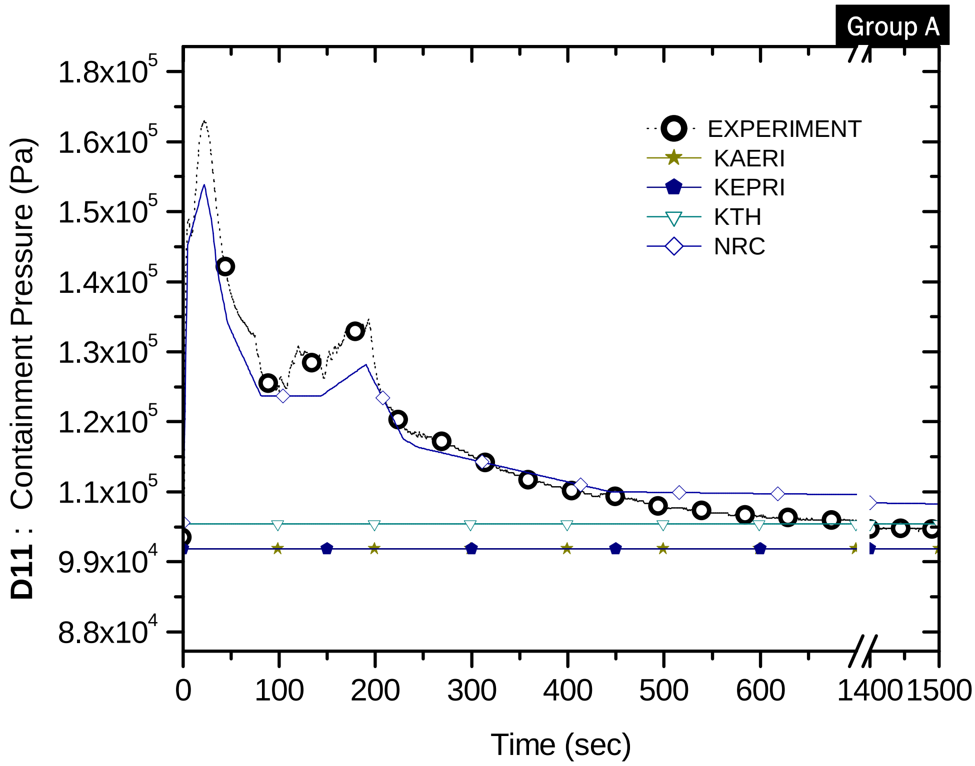

Figure B.11-A Containment pressure (D11)

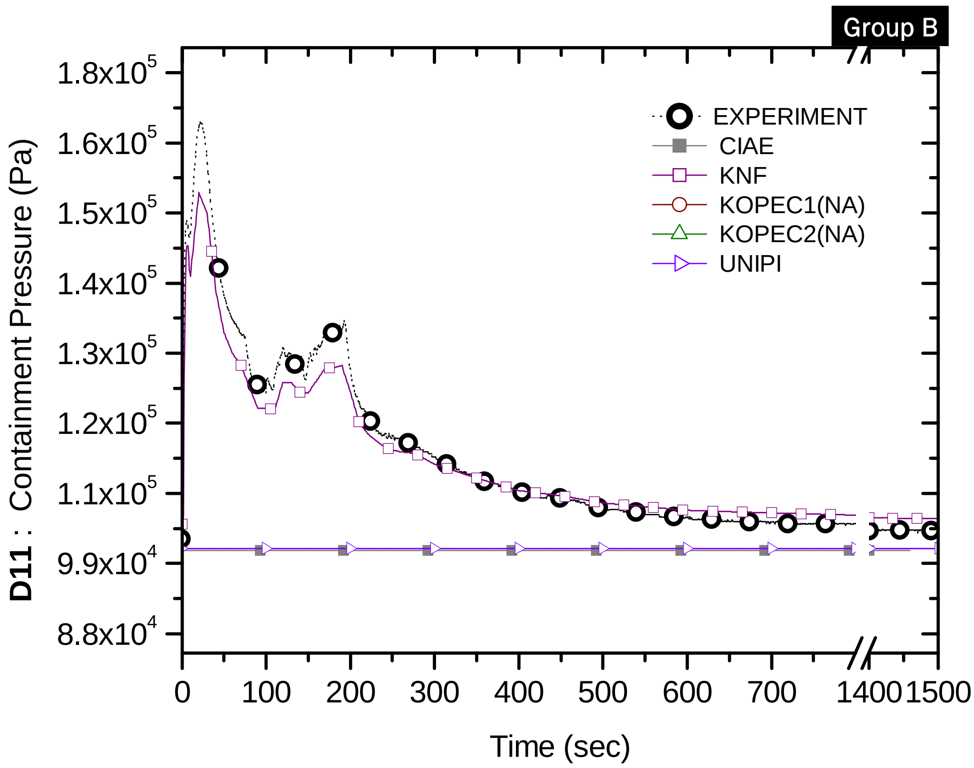

Figure B.11-B Containment pressure (D11)

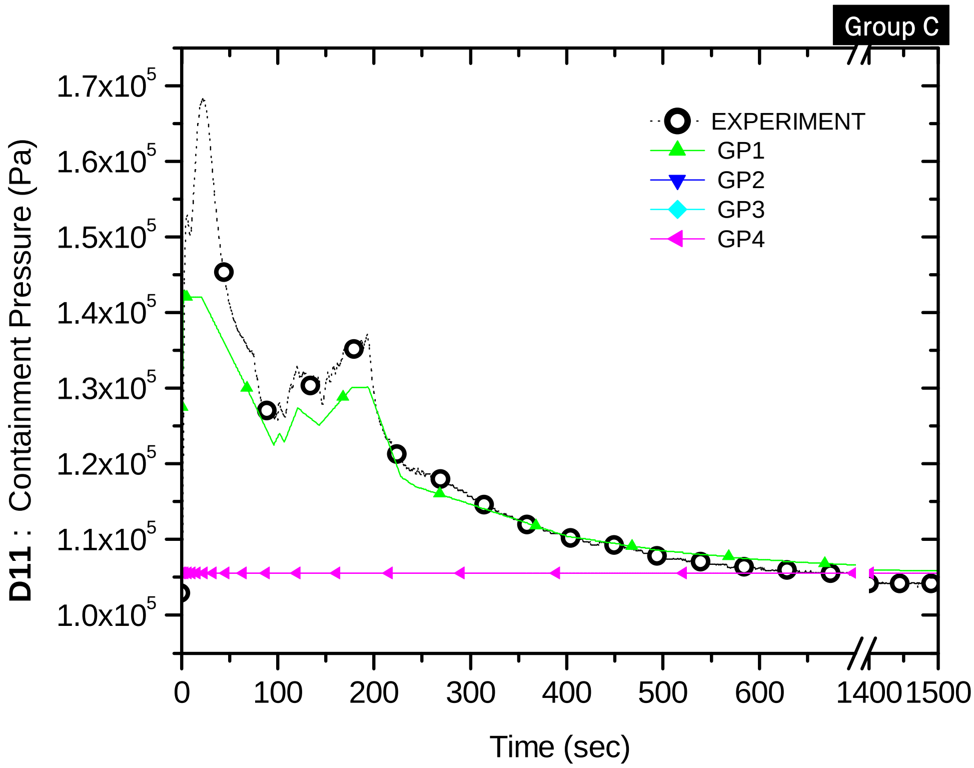

Figure B.11-C Containment pressure (D11)

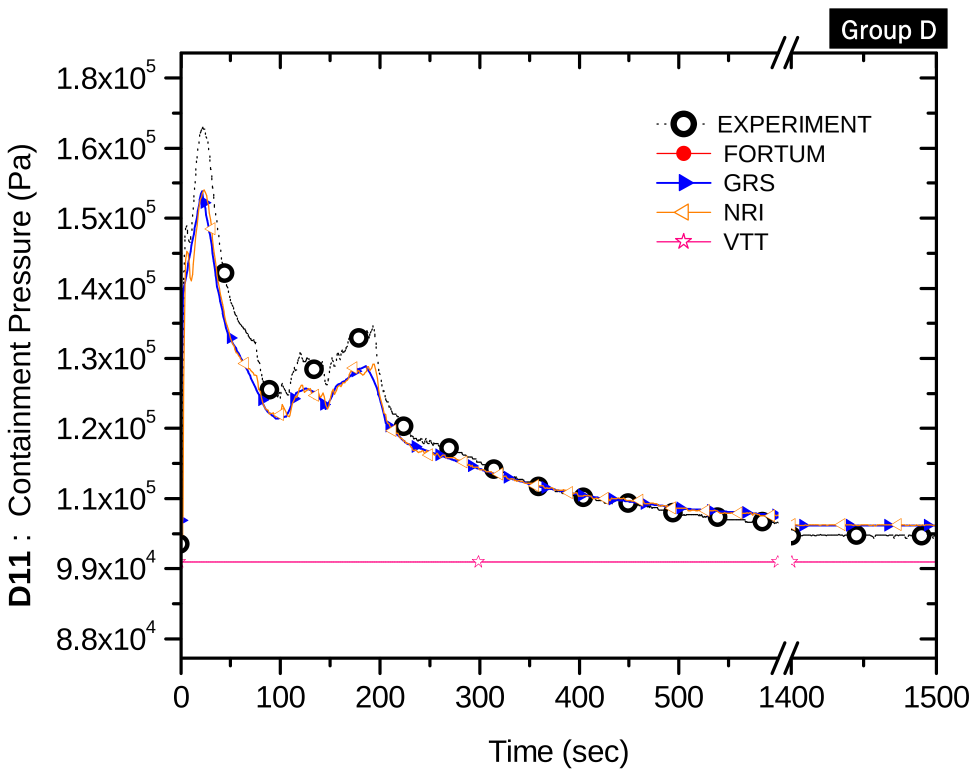

Figure B.11-D Containment pressure (D11)

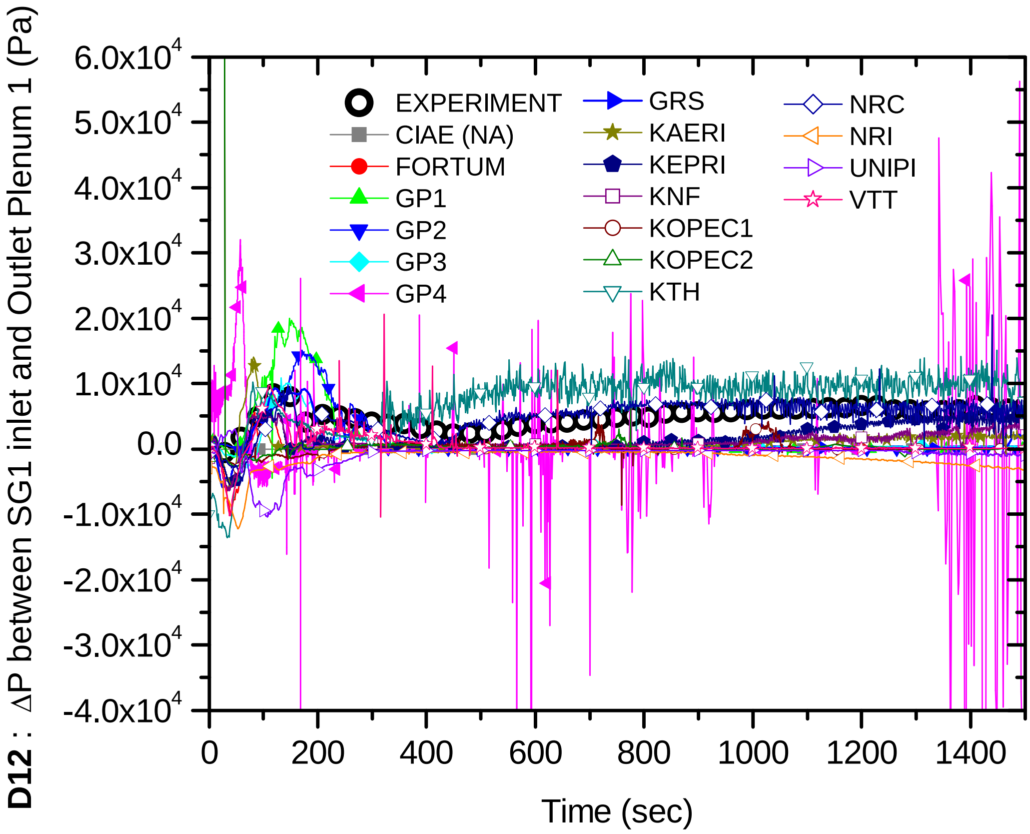

Figure B.12 Pressure difference between SG-1 inlet and outlet plenum 1 (D12)

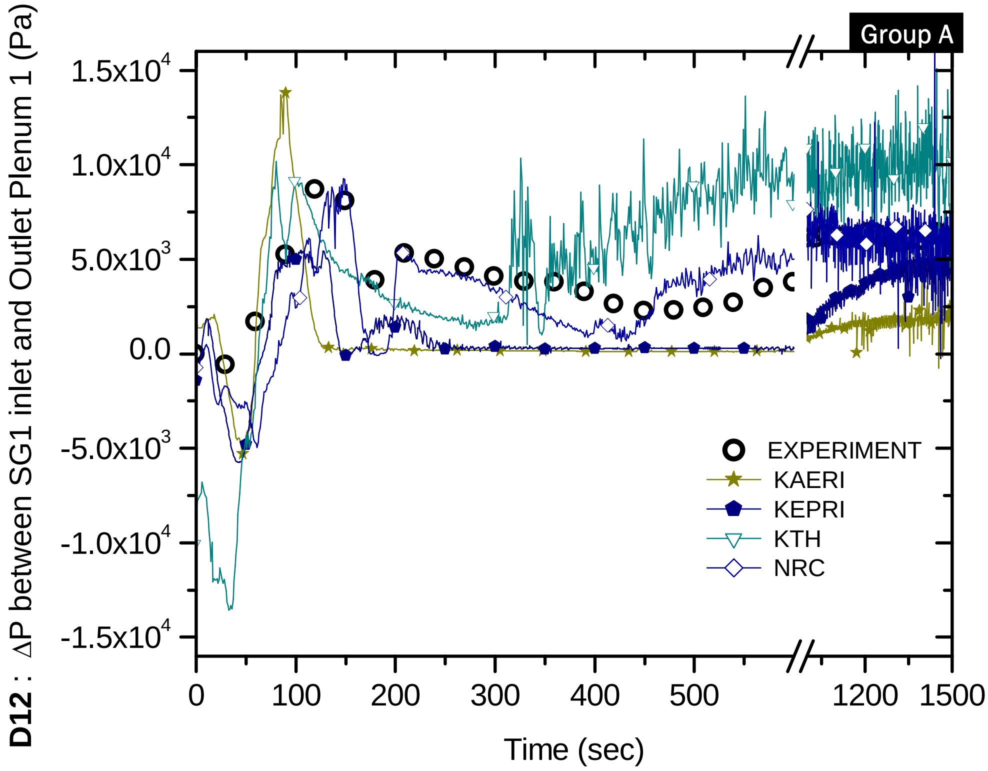

Figure B.12-A Pressure difference between SG-1 inlet and outlet plenum 1 (D12)

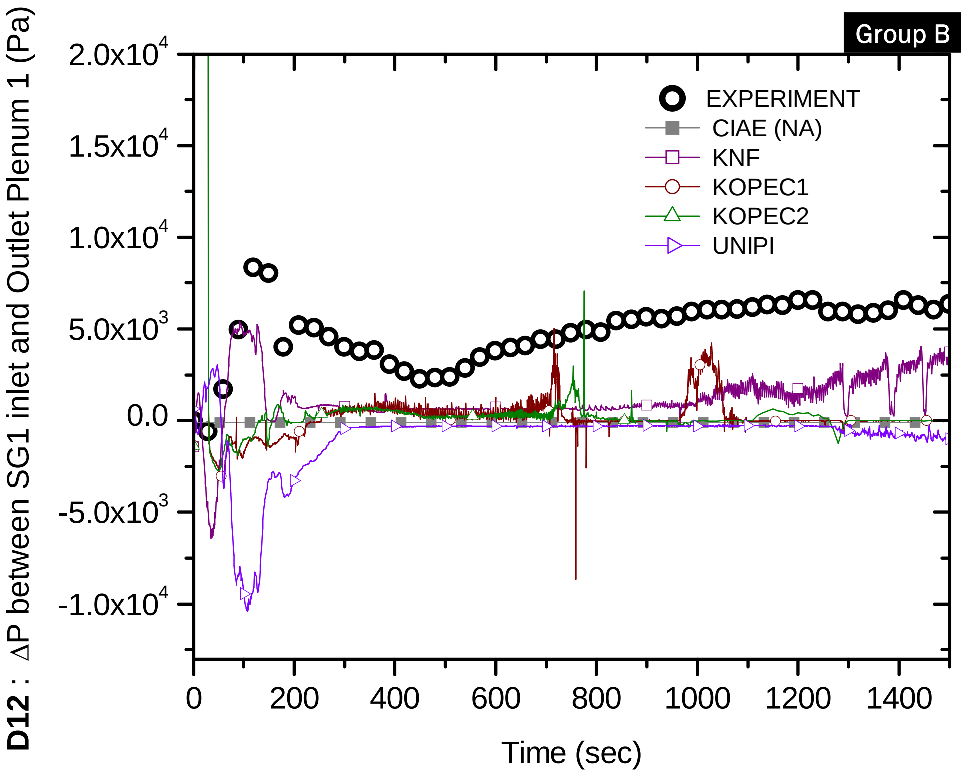

Figure B.12-B Pressure difference between SG-1 inlet and outlet plenum 1 (D12)

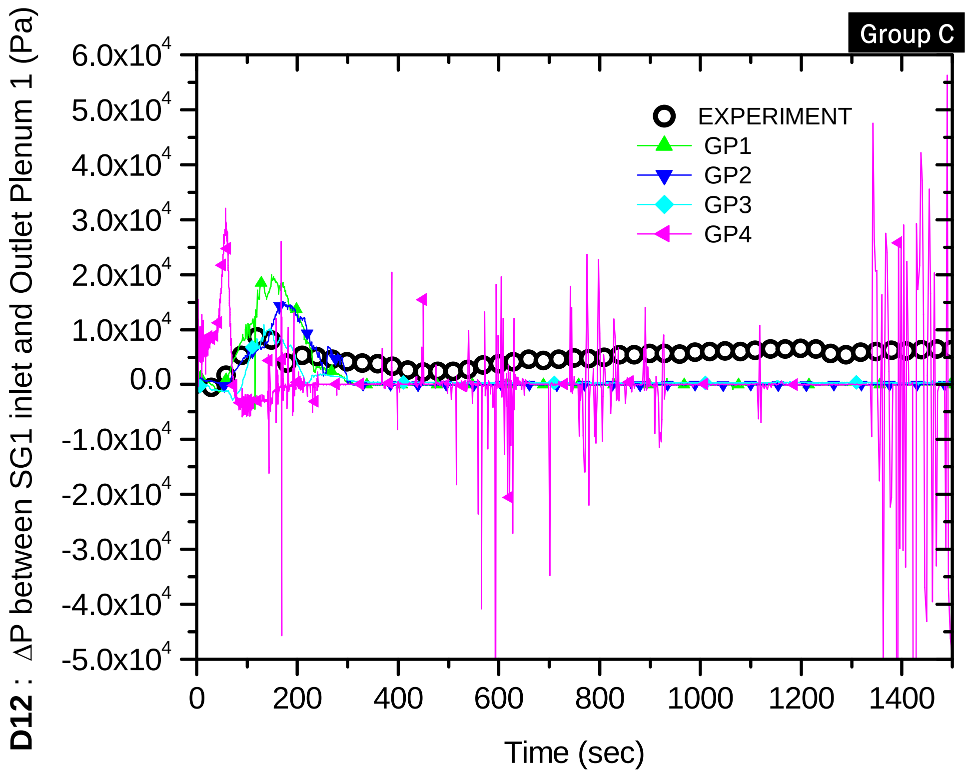

Figure B.12-C Pressure difference between SG-1 inlet and outlet plenum 1 (D12)

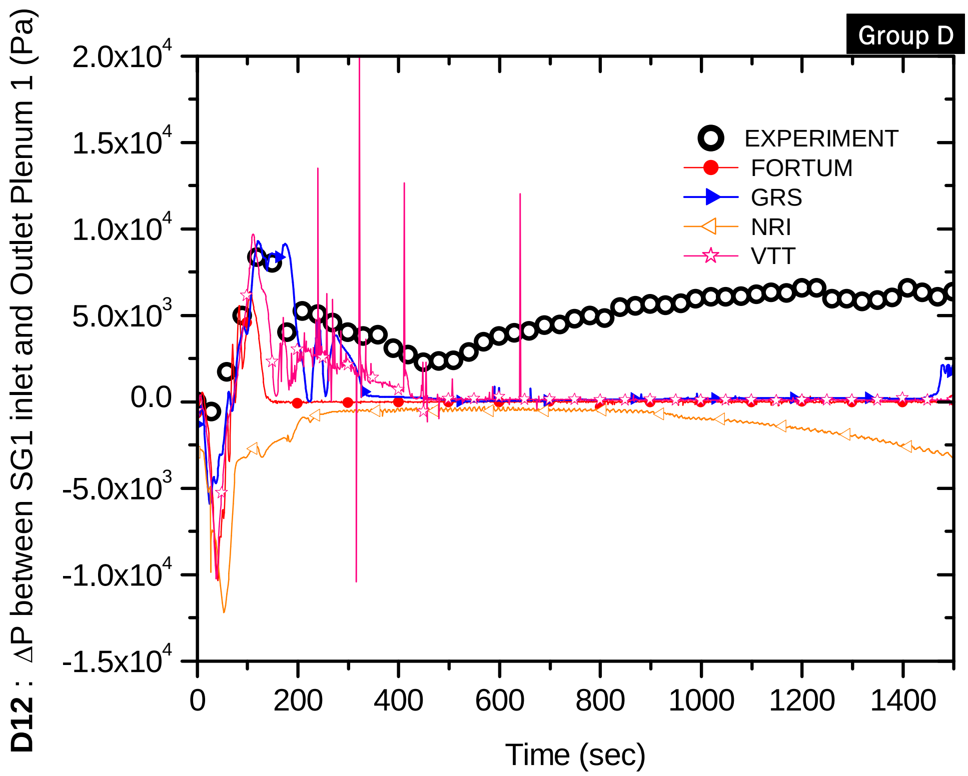

Figure B.12-D Pressure difference between SG-1 inlet and outlet plenum 1 (D12)

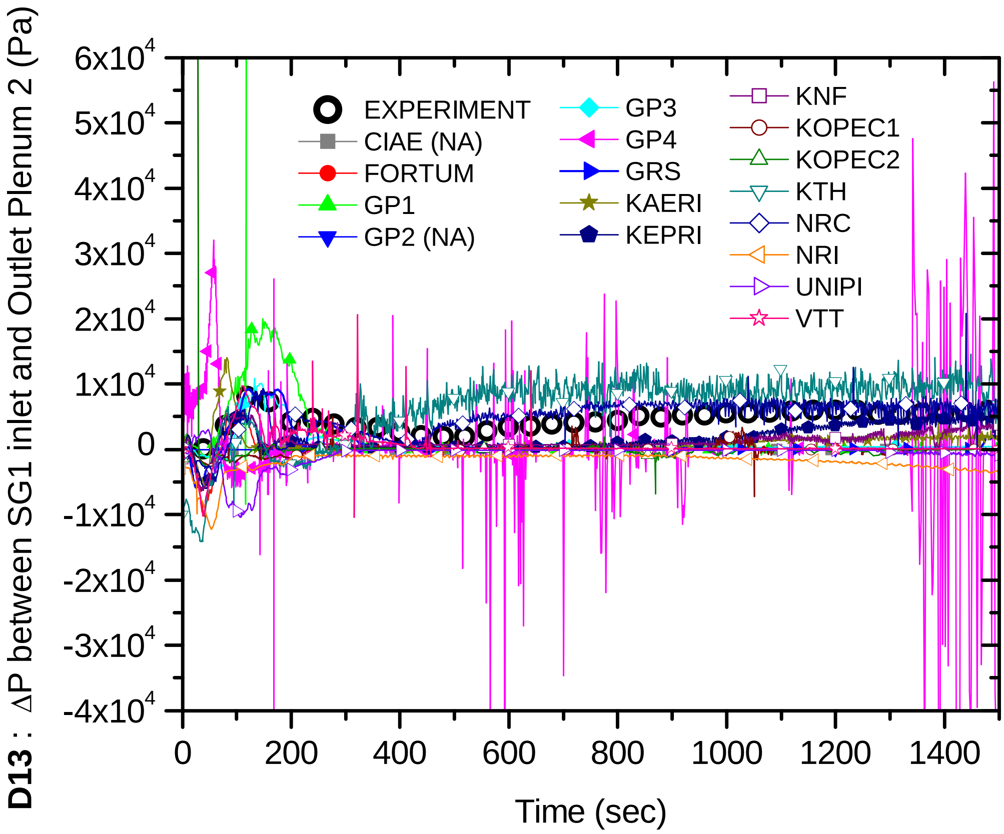

Figure B.13 Pressure difference between SG-1 inlet and outlet plenum 2 (D13)

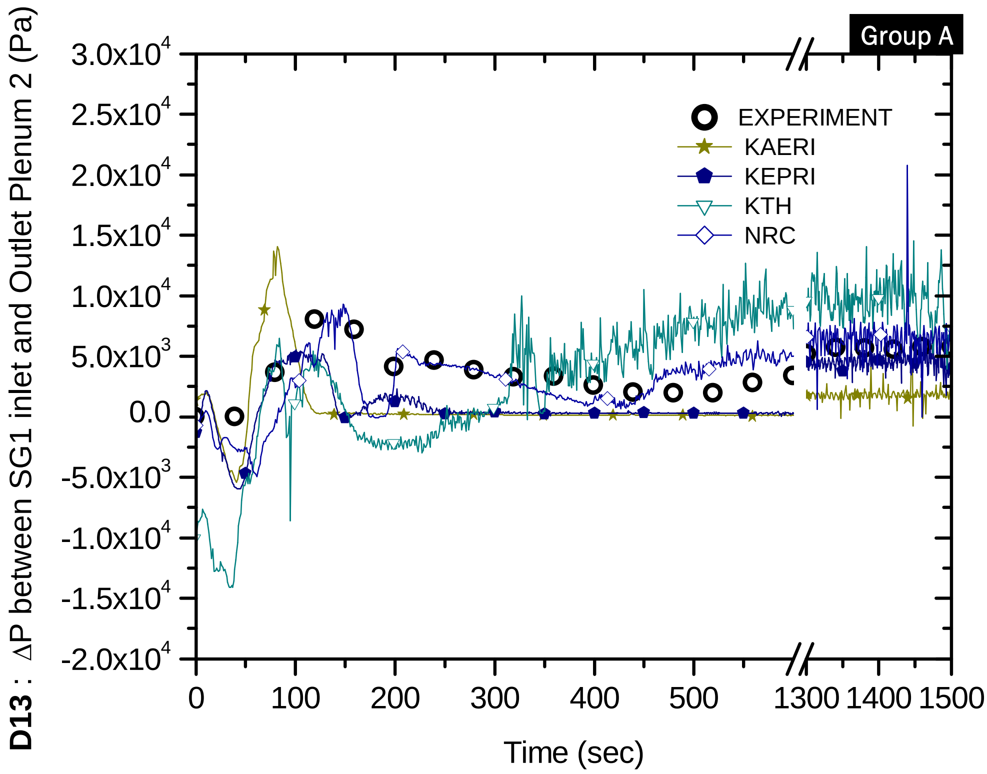

Figure B.13-A Pressure difference between SG-1 inlet and outlet plenum 2 (D13)

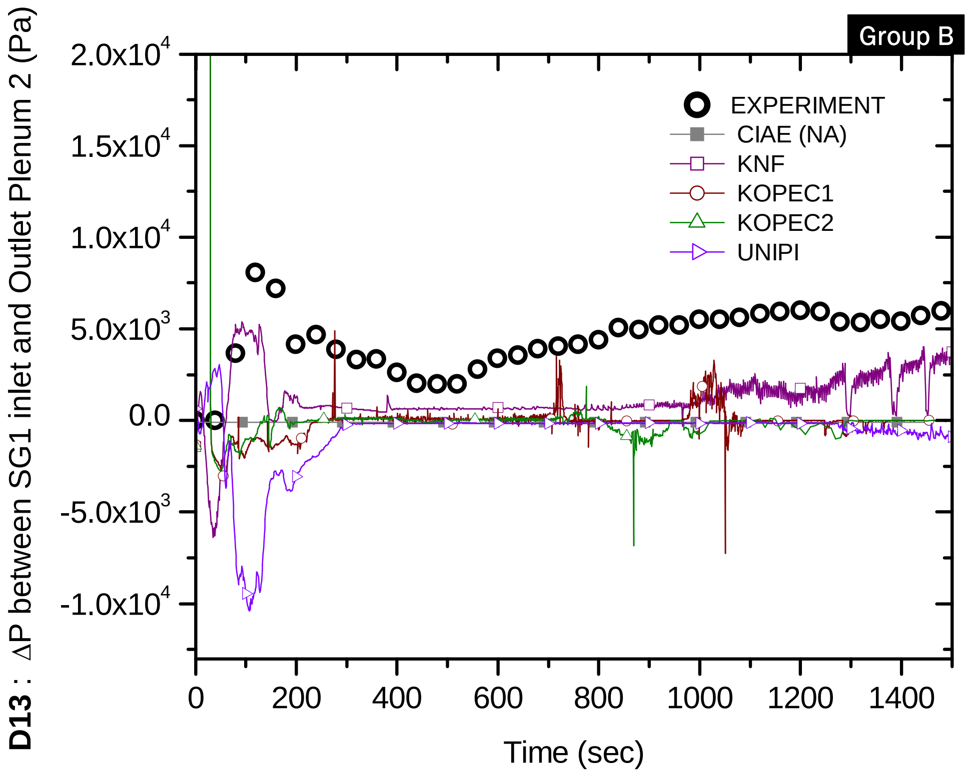

Figure B.13-B Pressure difference between SG-1 inlet and outlet plenum 2 (D13)

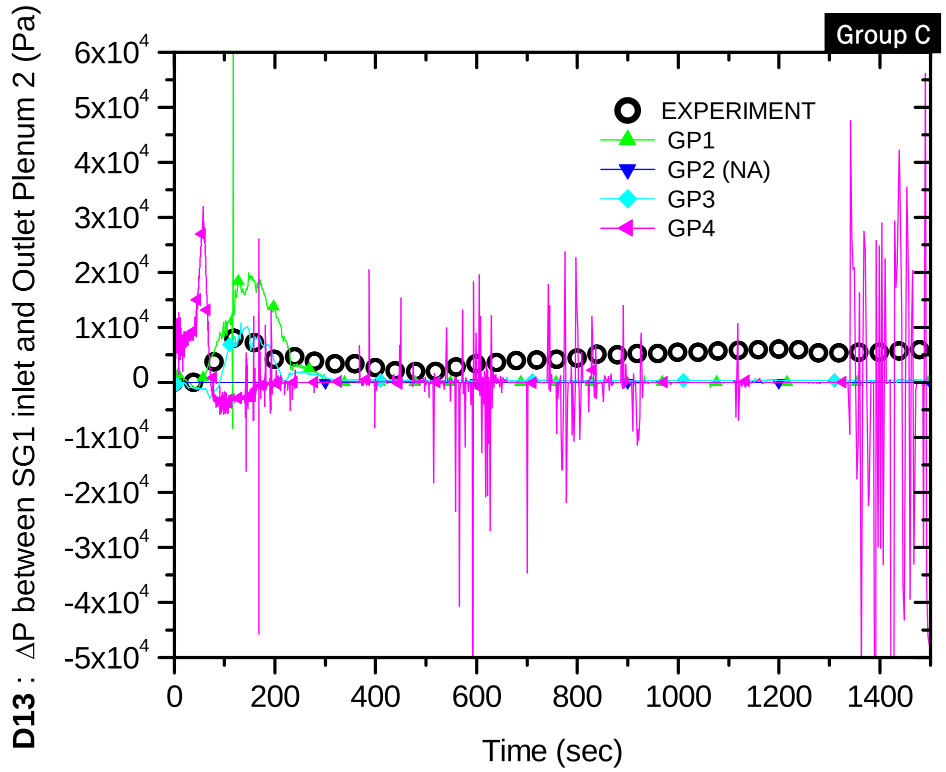

Figure B.13-C Pressure difference between SG-1 inlet and outlet plenum 2 (D13)

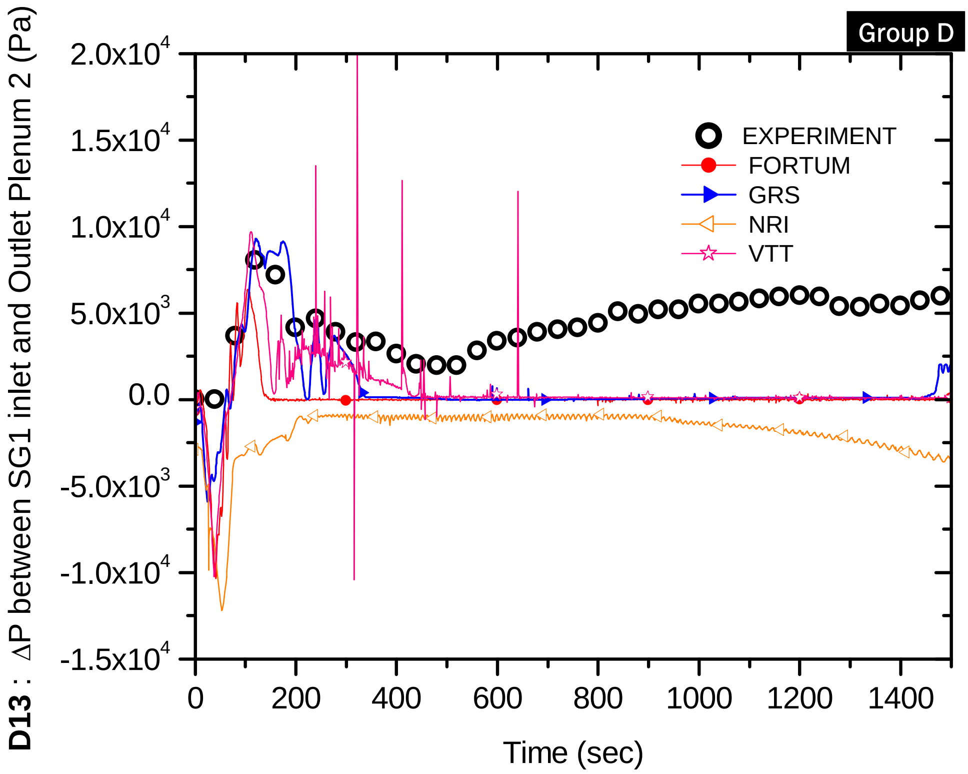

Figure B.13-D Pressure difference between SG-1 inlet and outlet plenum 2 (D13)

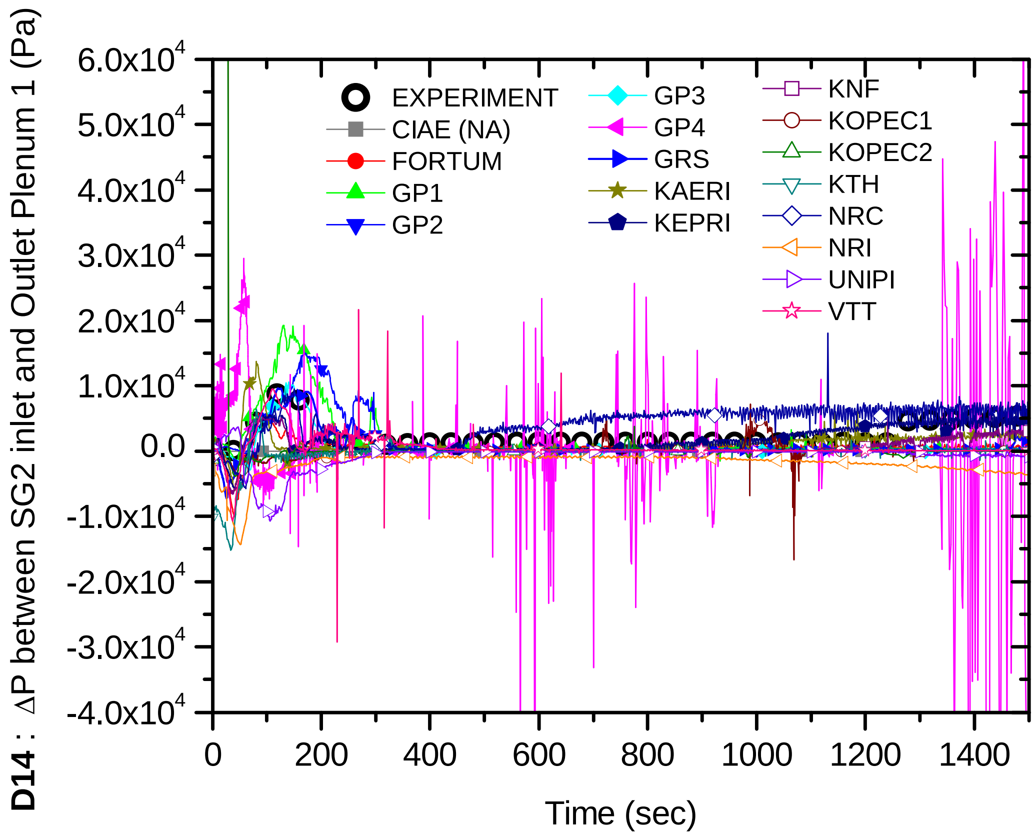

Figure B.14 Pressure difference between SG-2 inlet and outlet plenum 1 (D14)

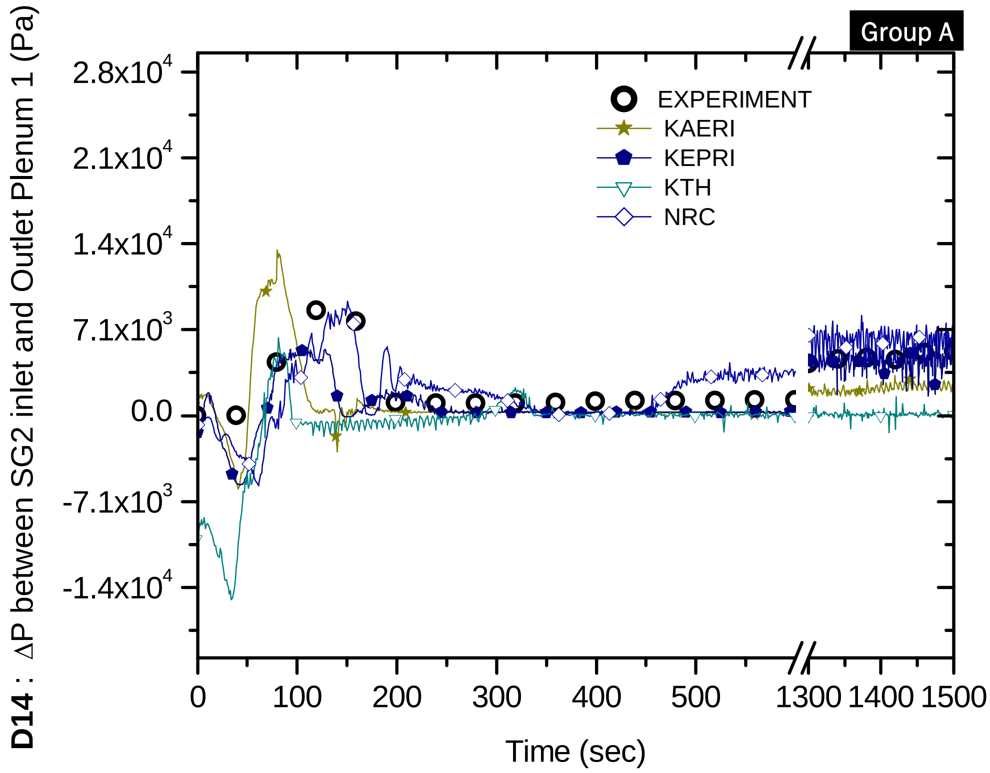

Figure B.14-A Pressure difference between SG-2 inlet and outlet plenum 1 (D14)

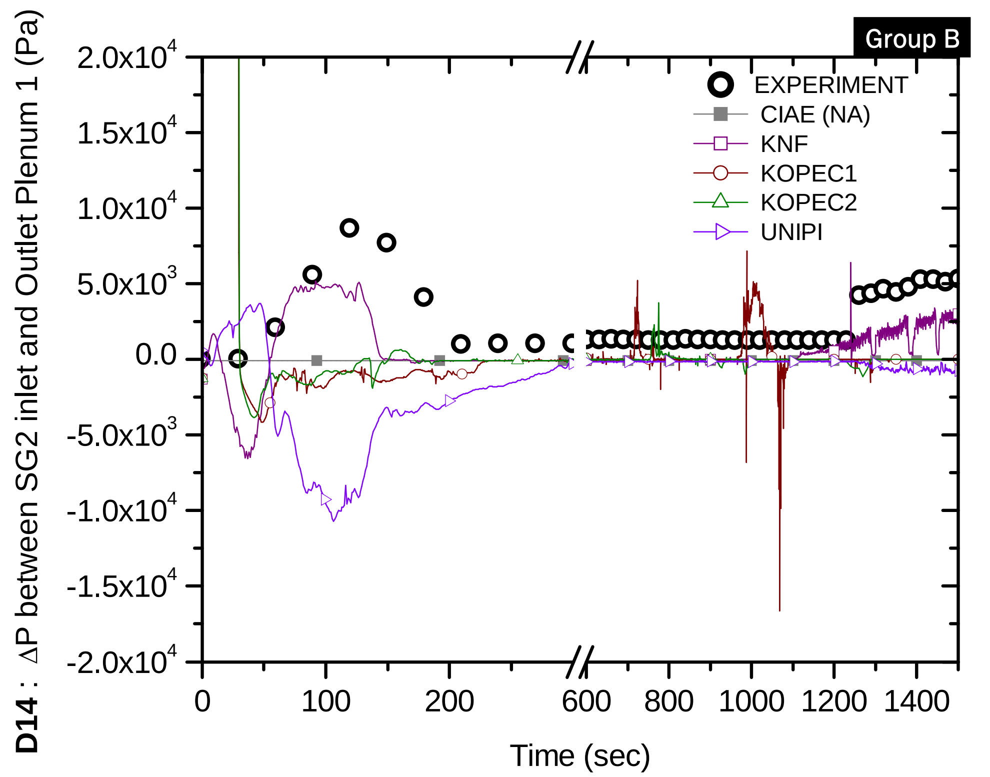

Figure B.14-B Pressure difference between SG-2 inlet and outlet plenum 1 (D14)

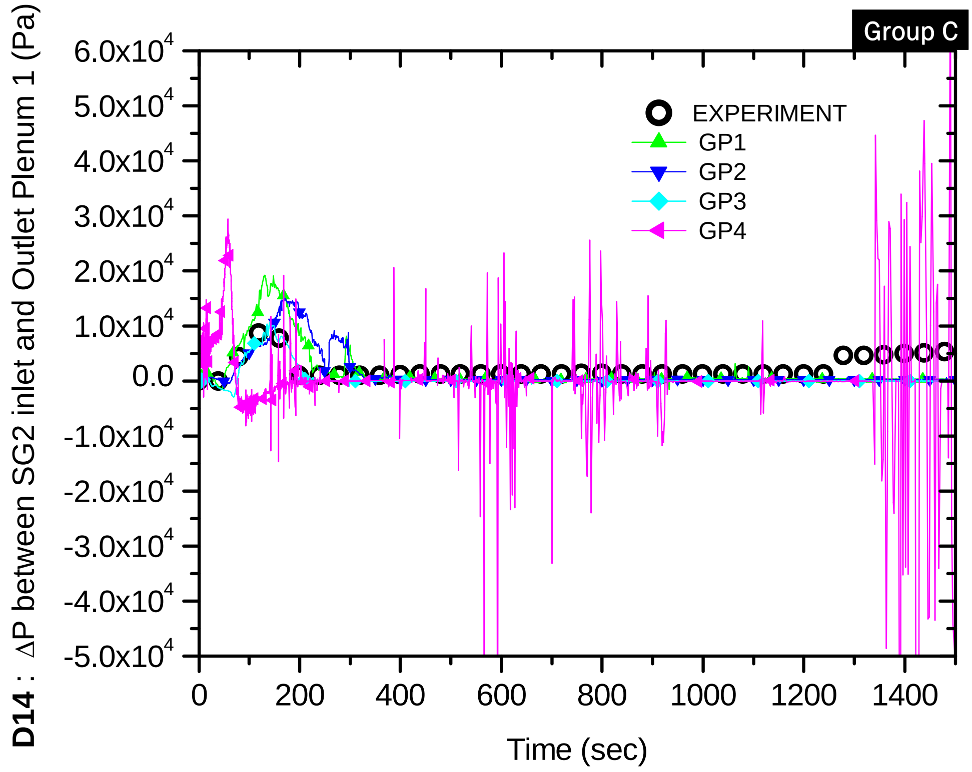

Figure B.14-C Pressure difference between SG-2 inlet and outlet plenum 1 (D14)

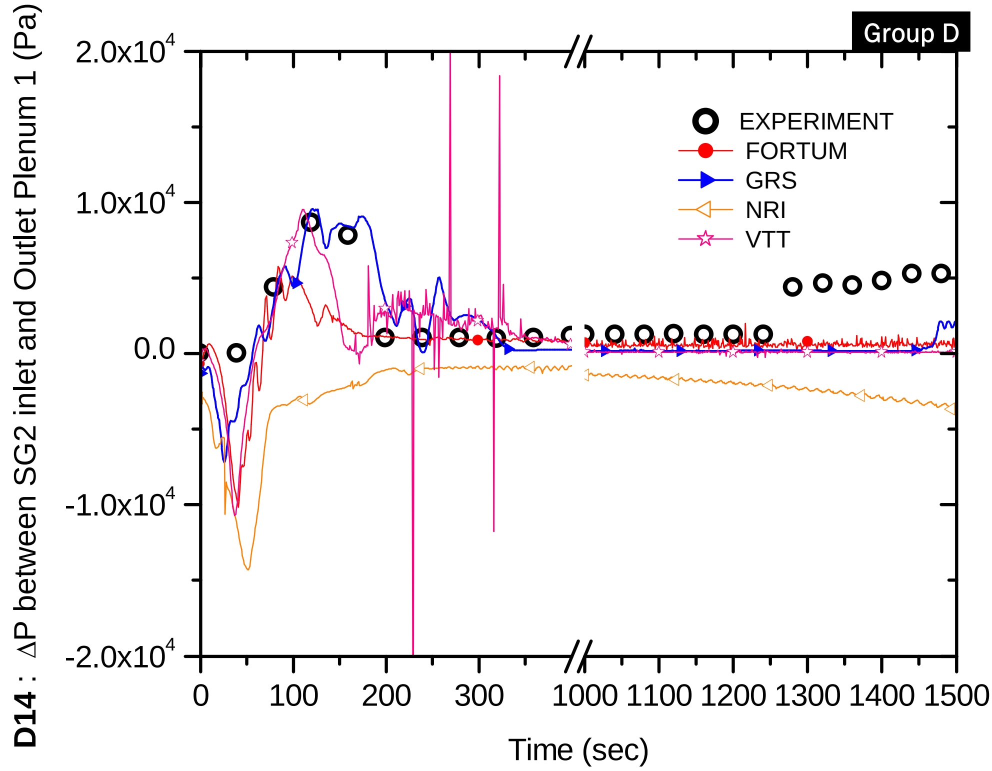

Figure B.14-D Pressure difference between SG-2 inlet and outlet plenum 1 (D14)

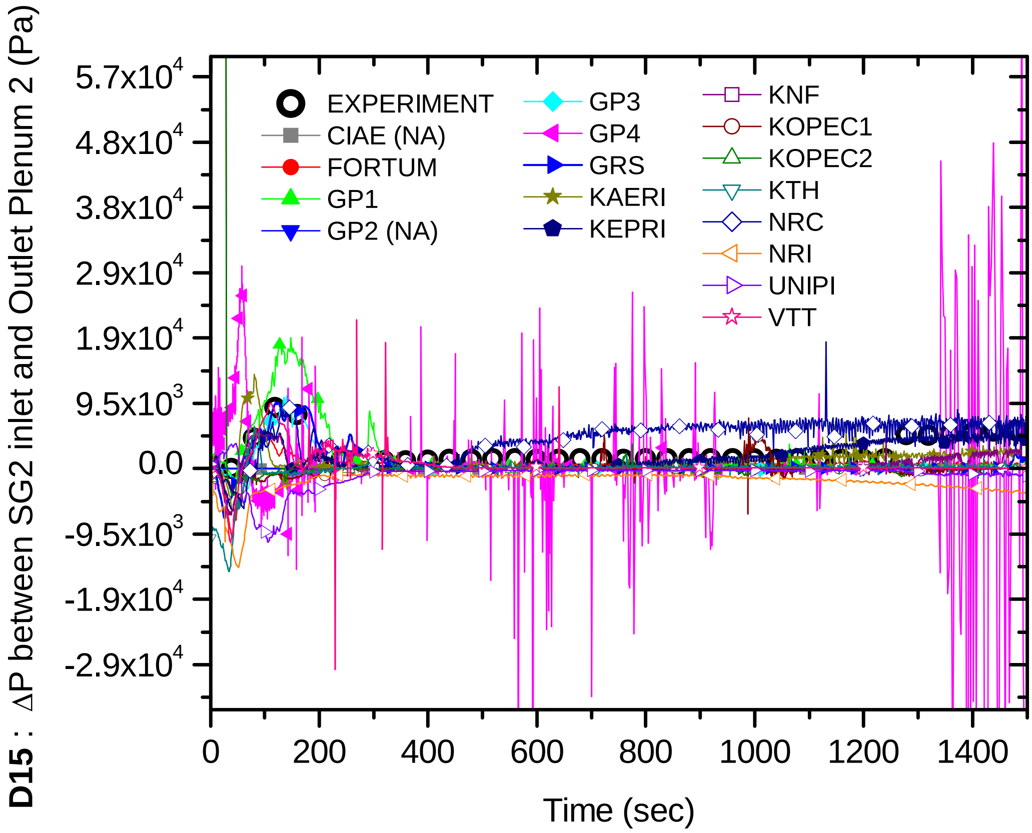

Figure B.15 Pressure difference between SG-2 inlet and outlet plenum 2 (D15)

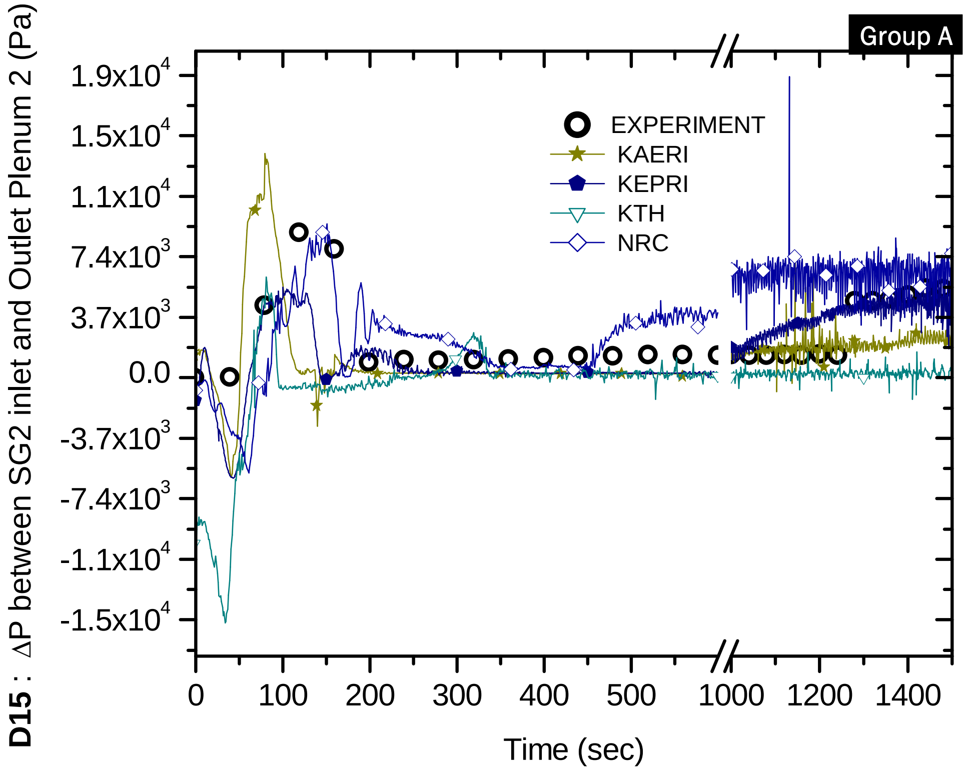

Figure B.15-A Pressure difference between SG-2 inlet and outlet plenum 2 (D15)

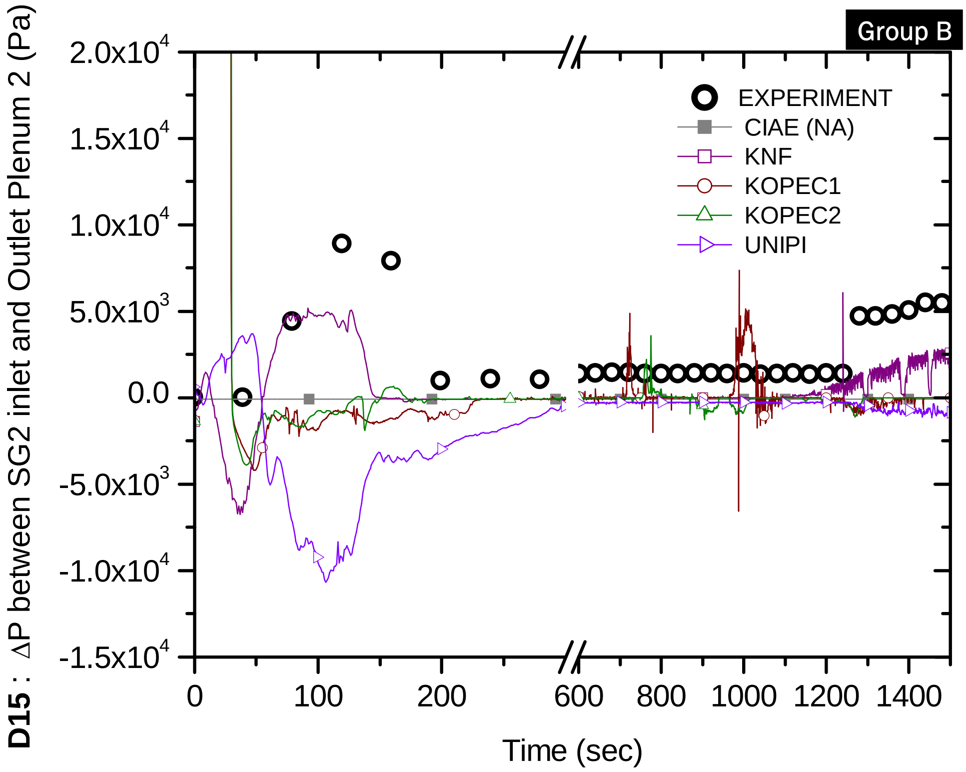

Figure B.15-B Pressure difference between SG-2 inlet and outlet plenum 2 (D15)

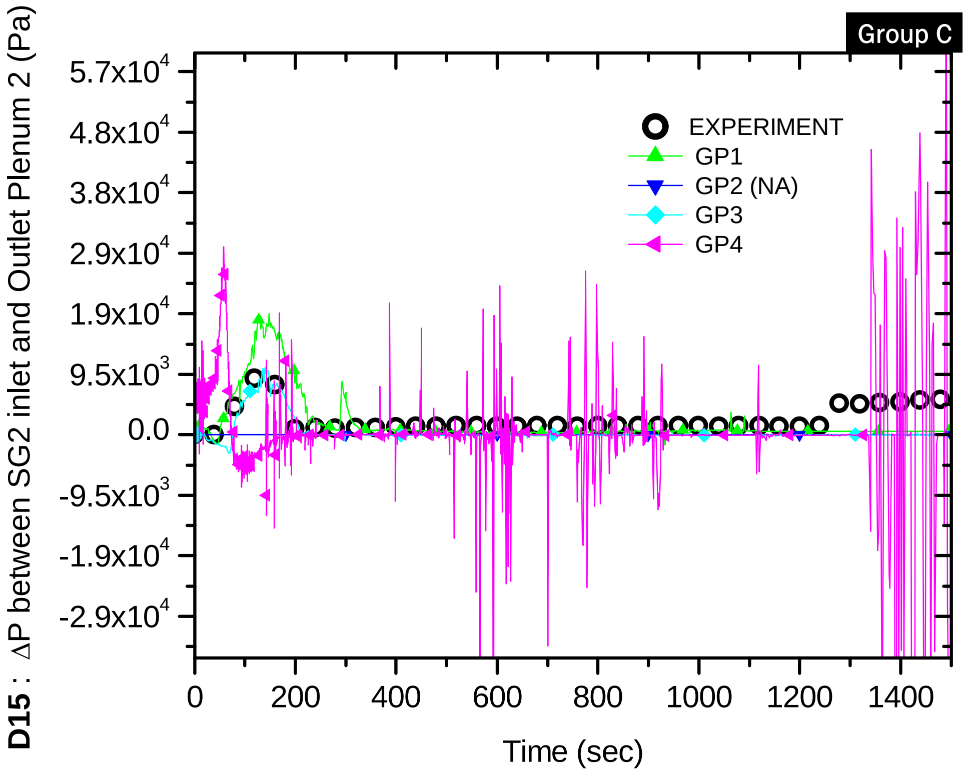

Figure B.15-C Pressure difference between SG-2 inlet and outlet plenum 2 (D15)

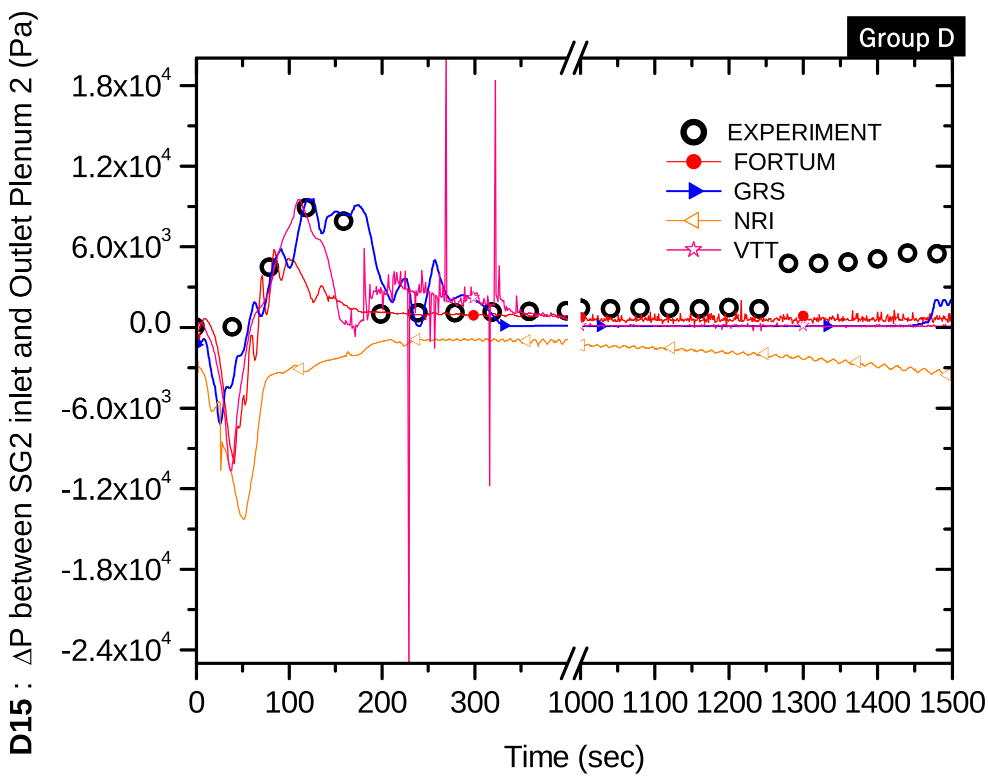

Figure B.15-D Pressure difference between SG-2 inlet and outlet plenum 2 (D15)

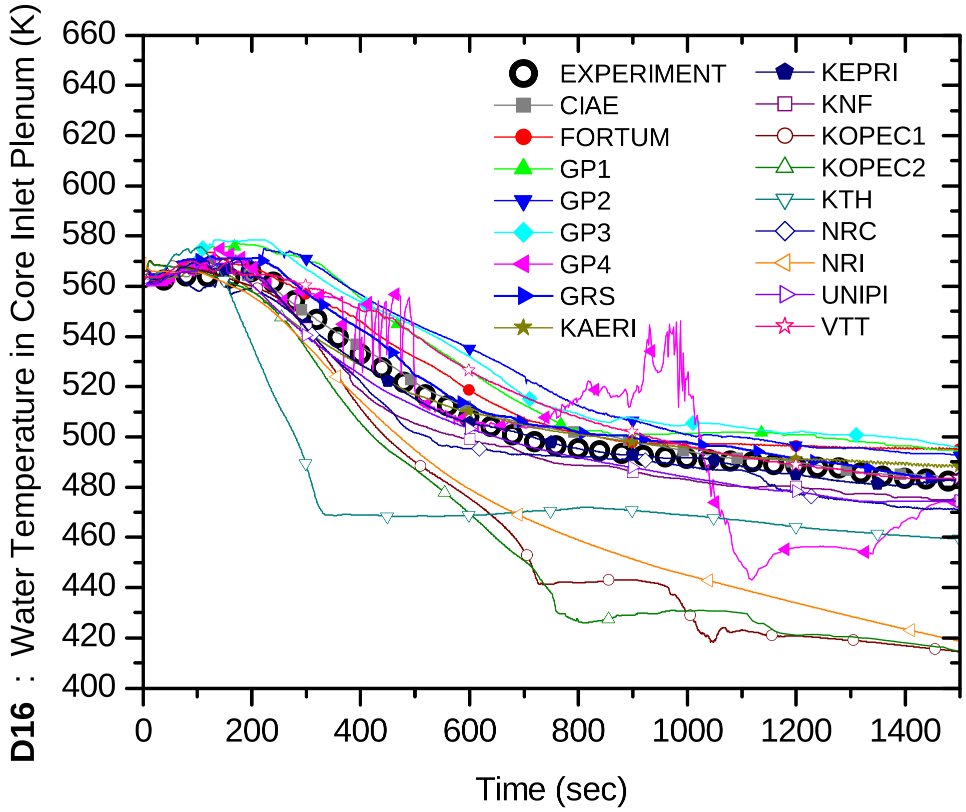

Figure B.16 Water temperature in the core inlet plenum (D16)

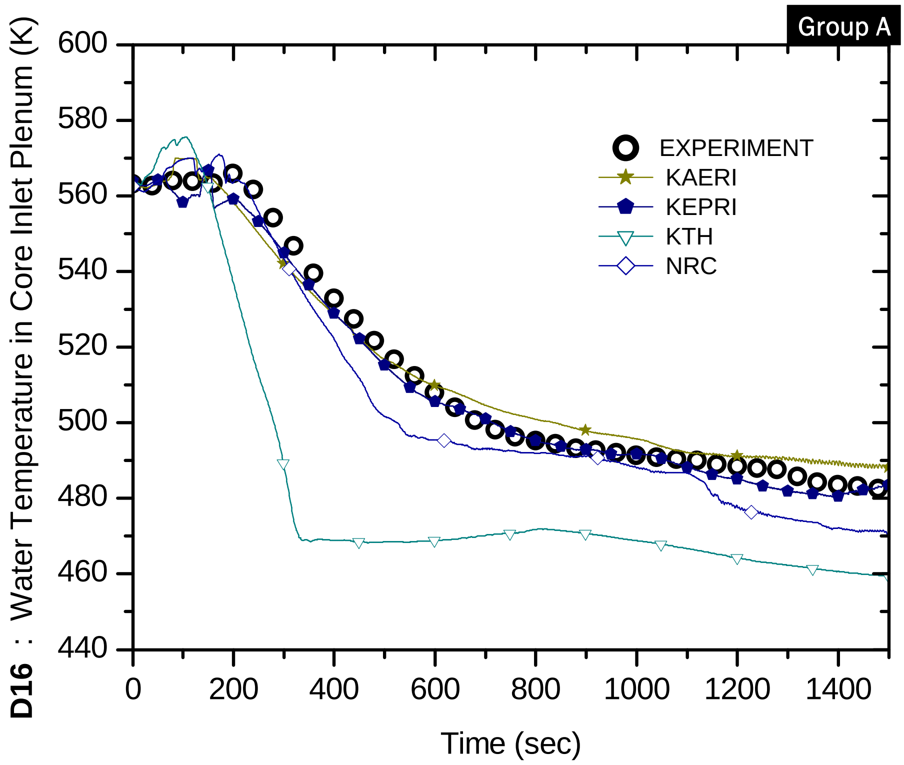

Figure B.16-A Water temperature in the core inlet plenum (D16)

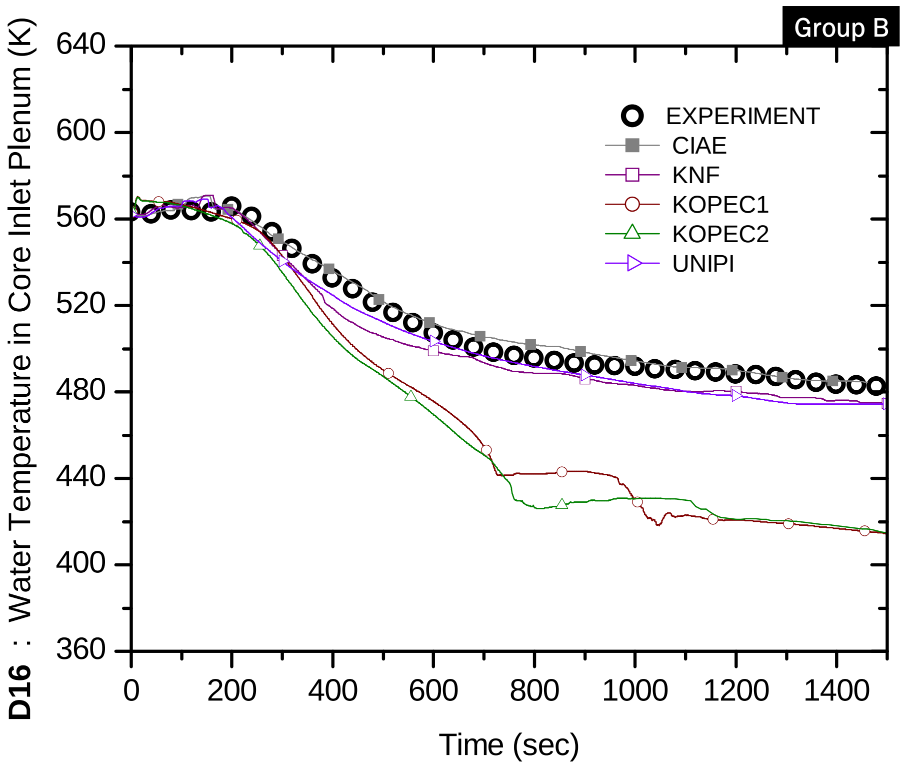

Figure B.16-B Water temperature in the core inlet plenum (D16)

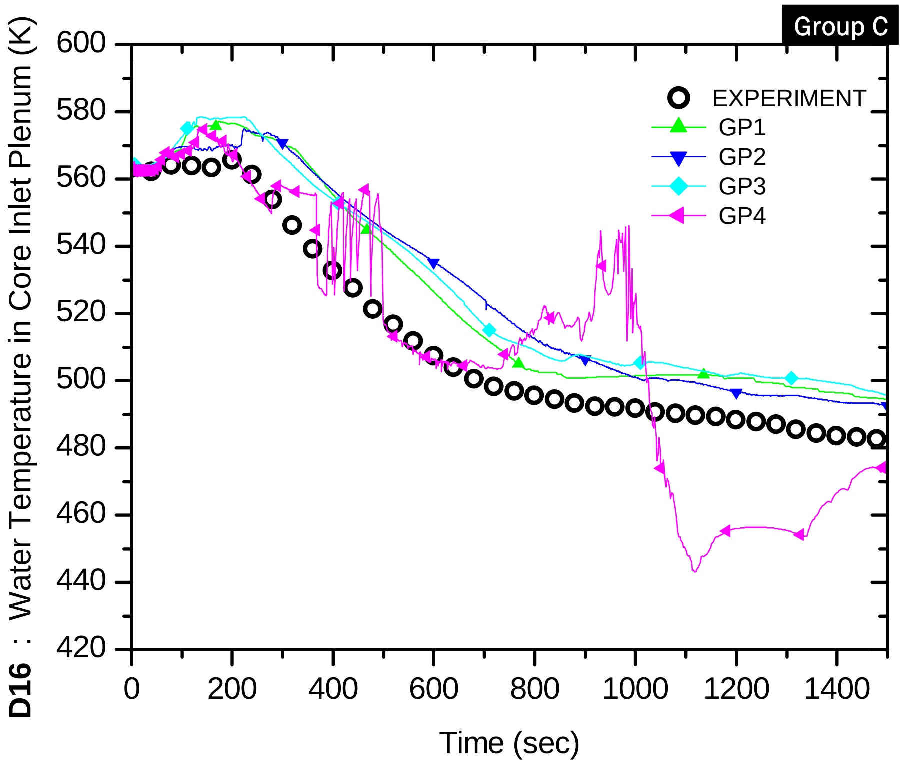

Figure B.16-C Water temperature in the core inlet plenum (D16)

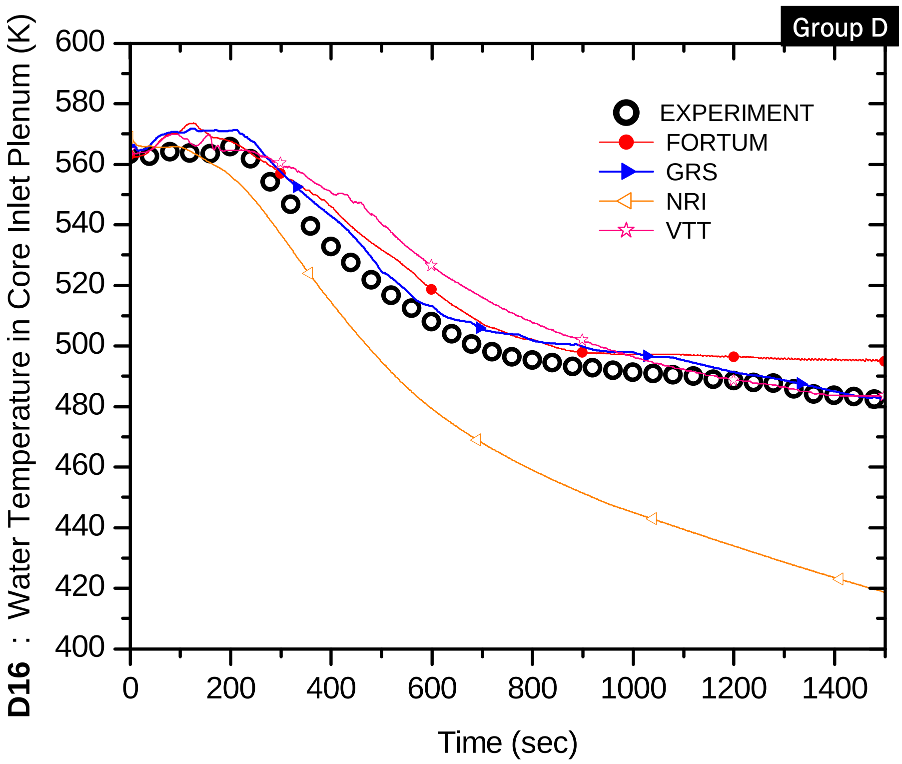

Figure B.16-D Water temperature in the core inlet plenum (D16)

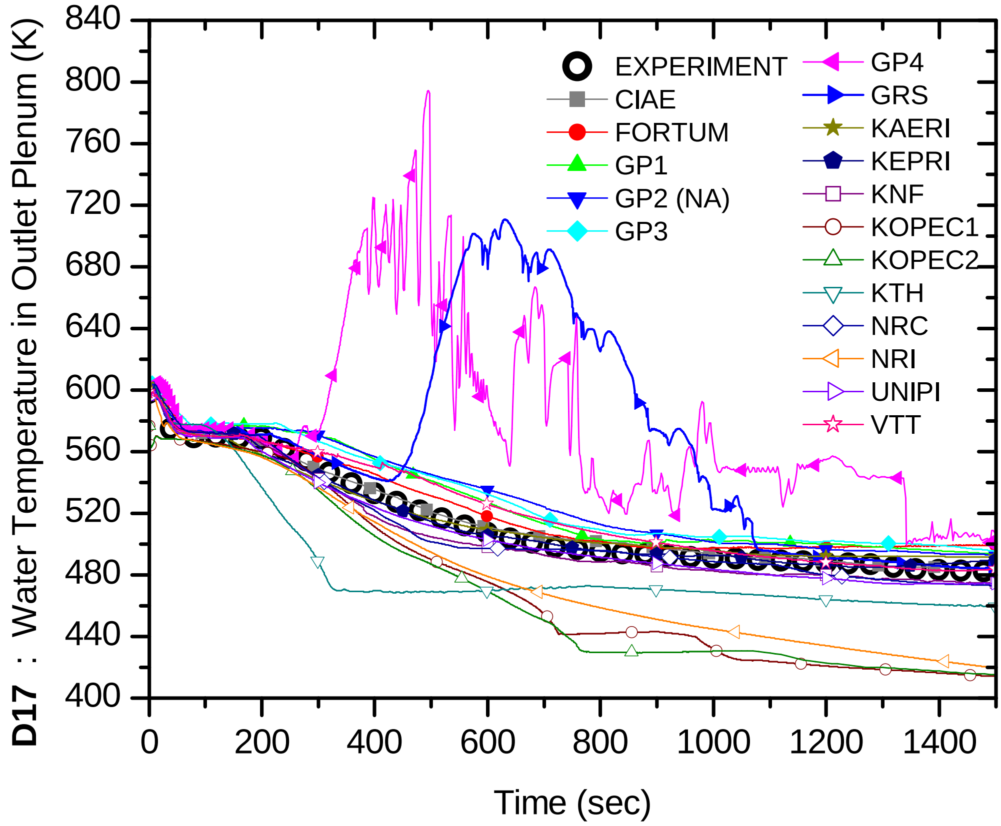

Figure B.17 Water temperature in the core outlet plenum (D17)

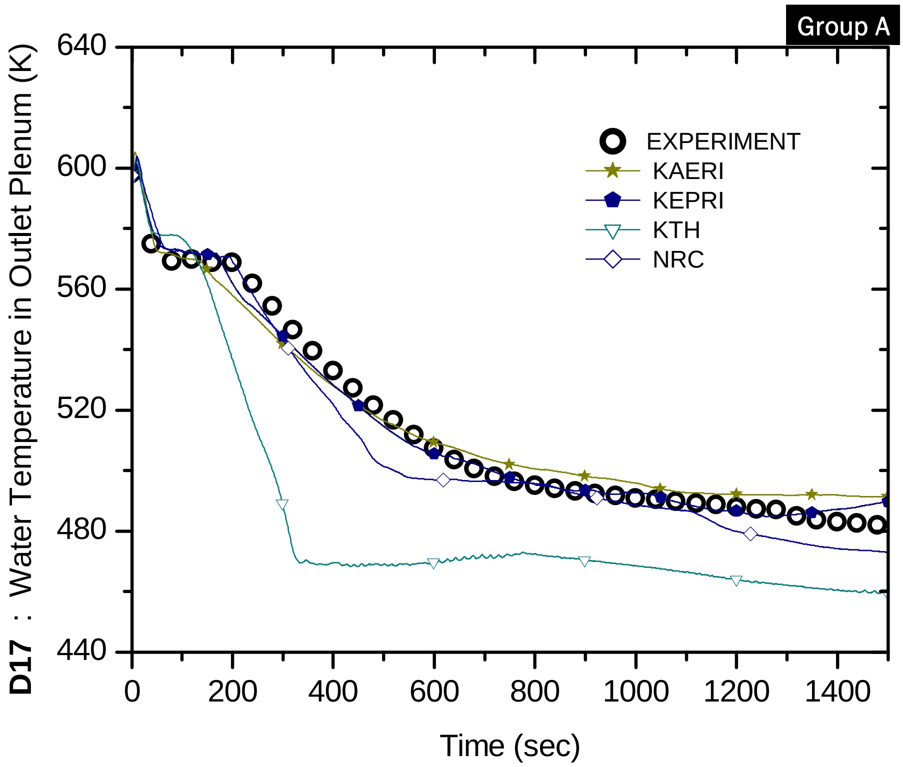

Figure B.17-A Water temperature in the core outlet plenum (D17)

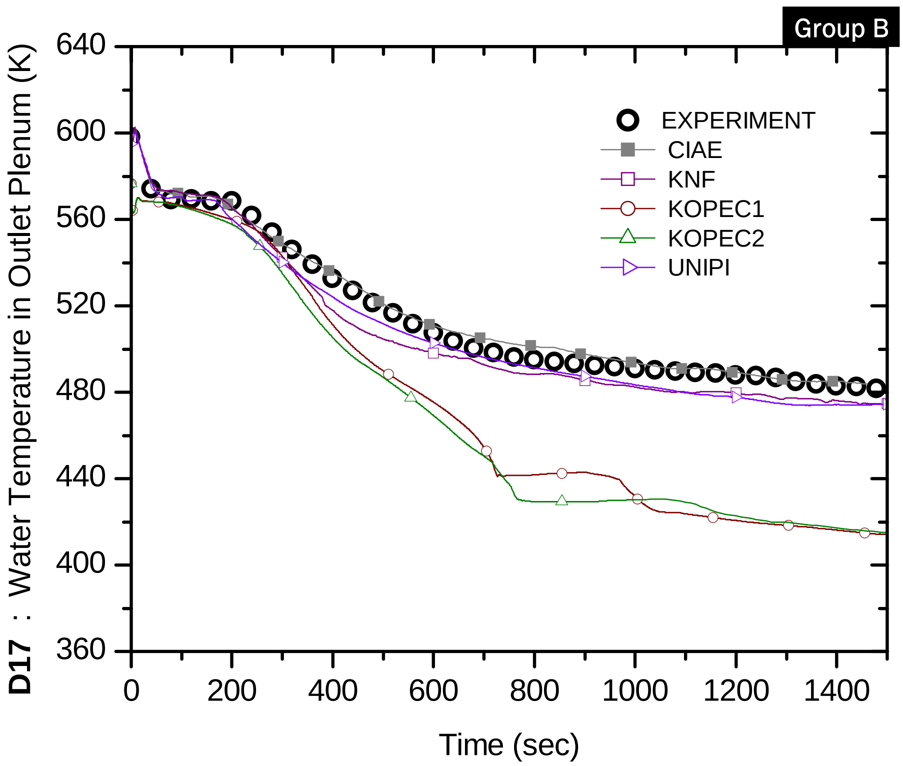

Figure B.17-B Water temperature in the core outlet plenum (D17)

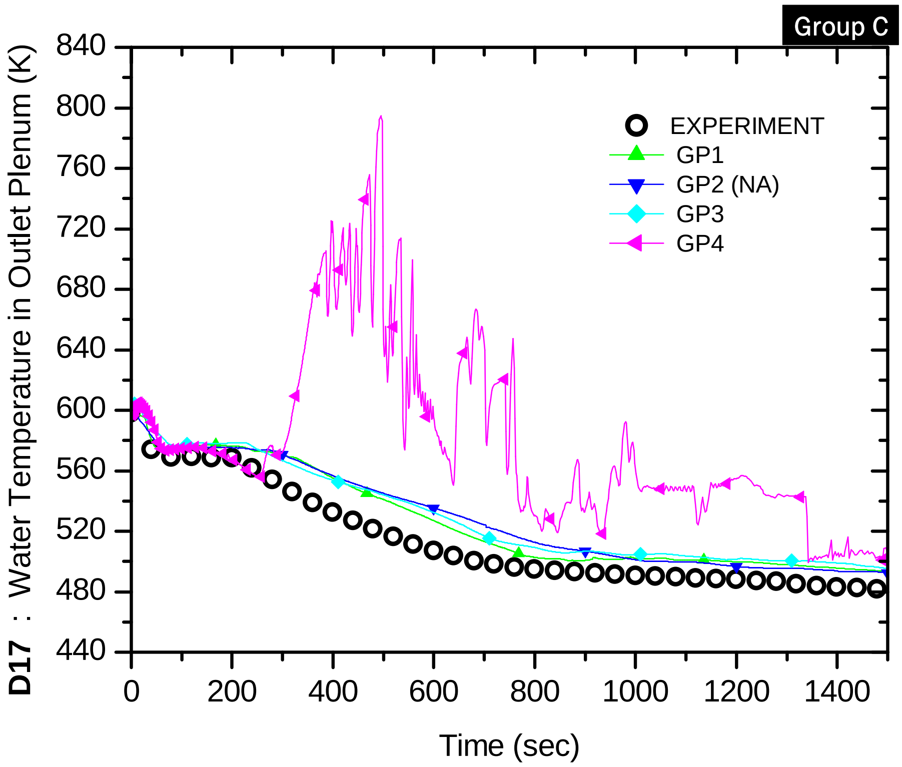

Figure B.17-C Water temperature in the core outlet plenum (D17)

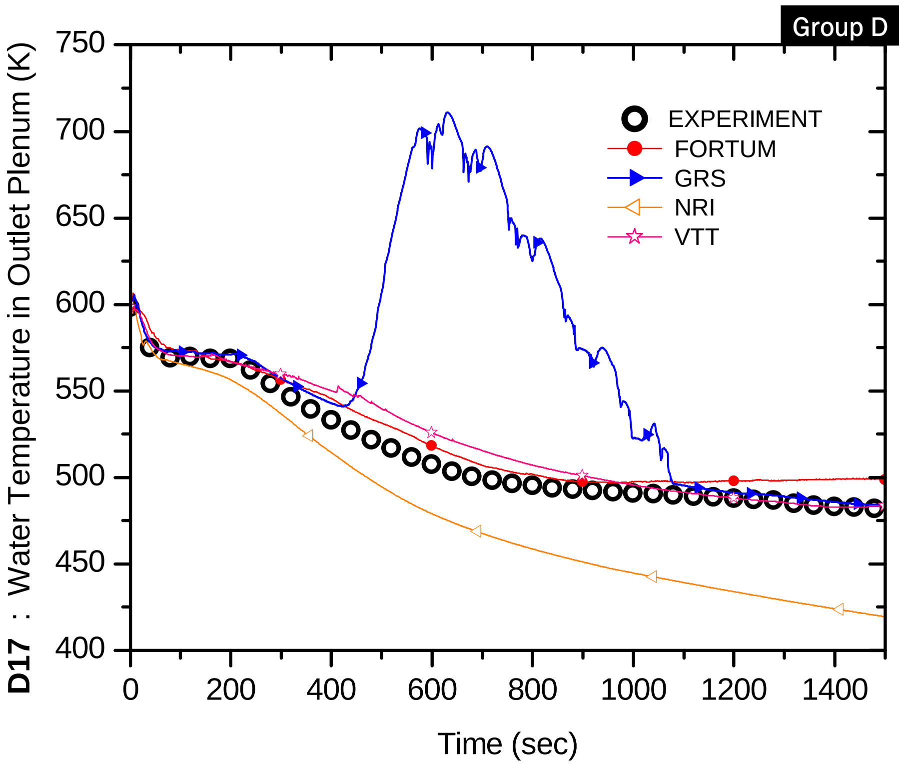

Figure B.17-D Water temperature in the core outlet plenum (D17)

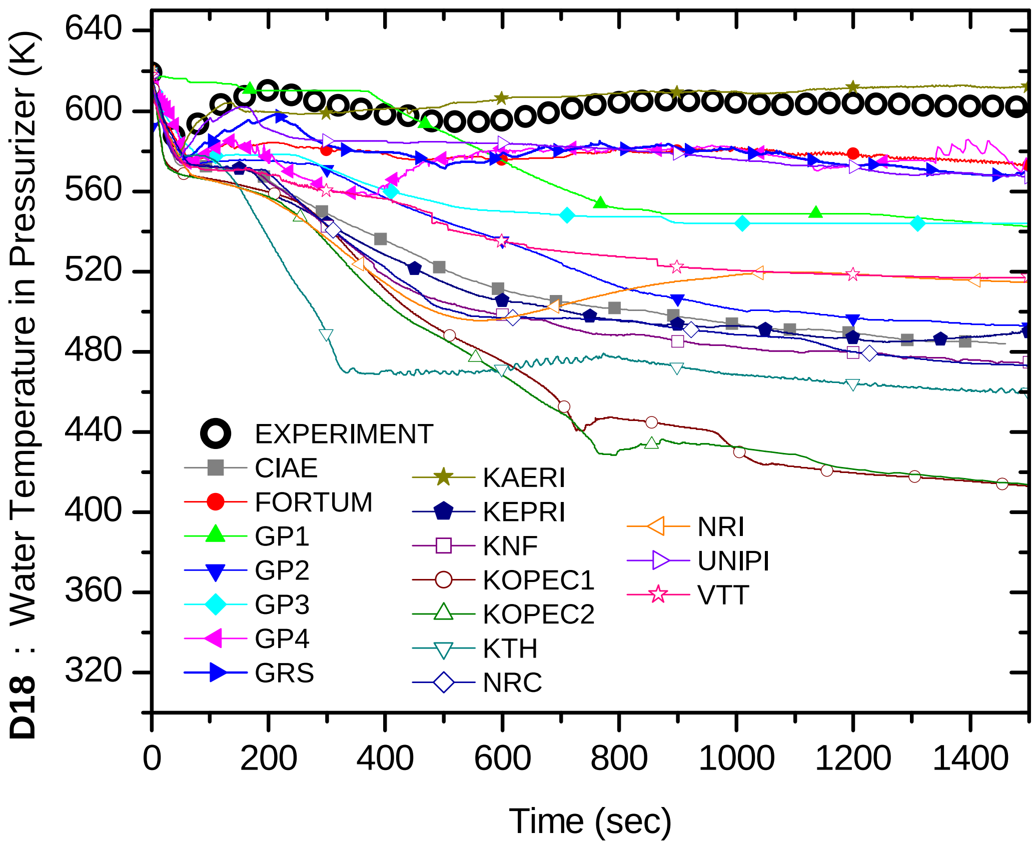

Figure B.18 Water temperature in the pressurizer (D18)

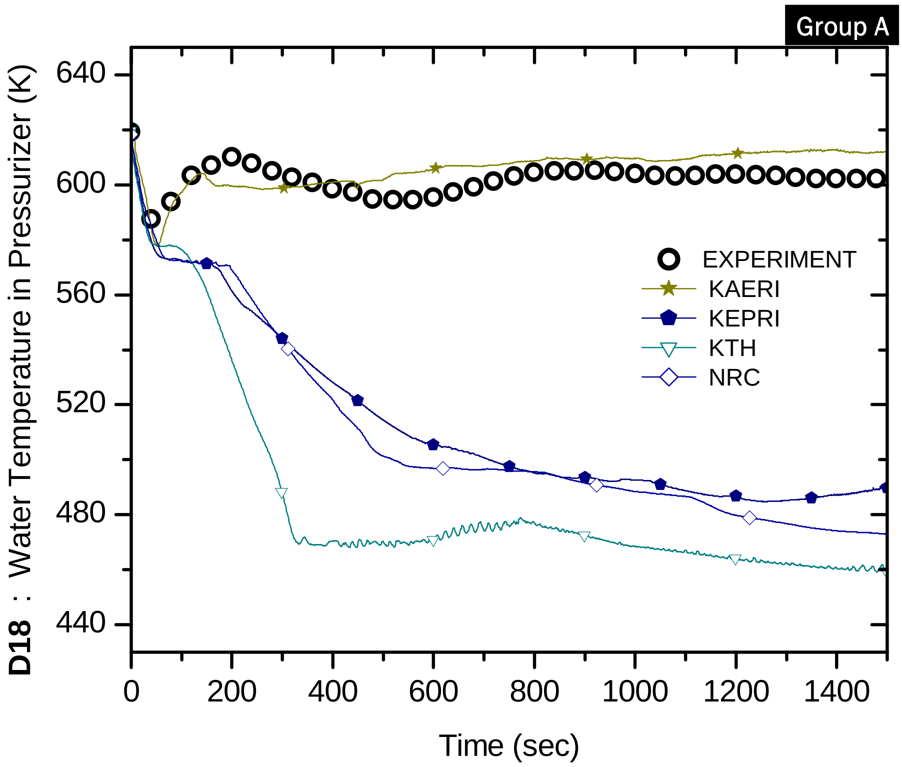

Figure B.18-A Water temperature in the pressurizer (D18)

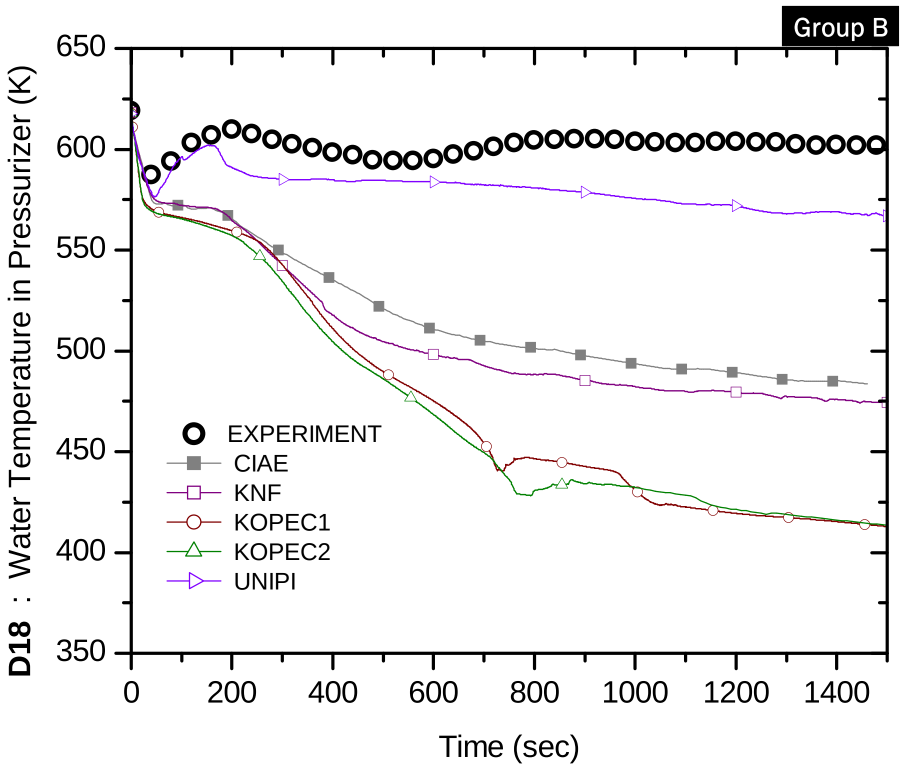

Figure B.18-B Water temperature in the pressurizer (D18)

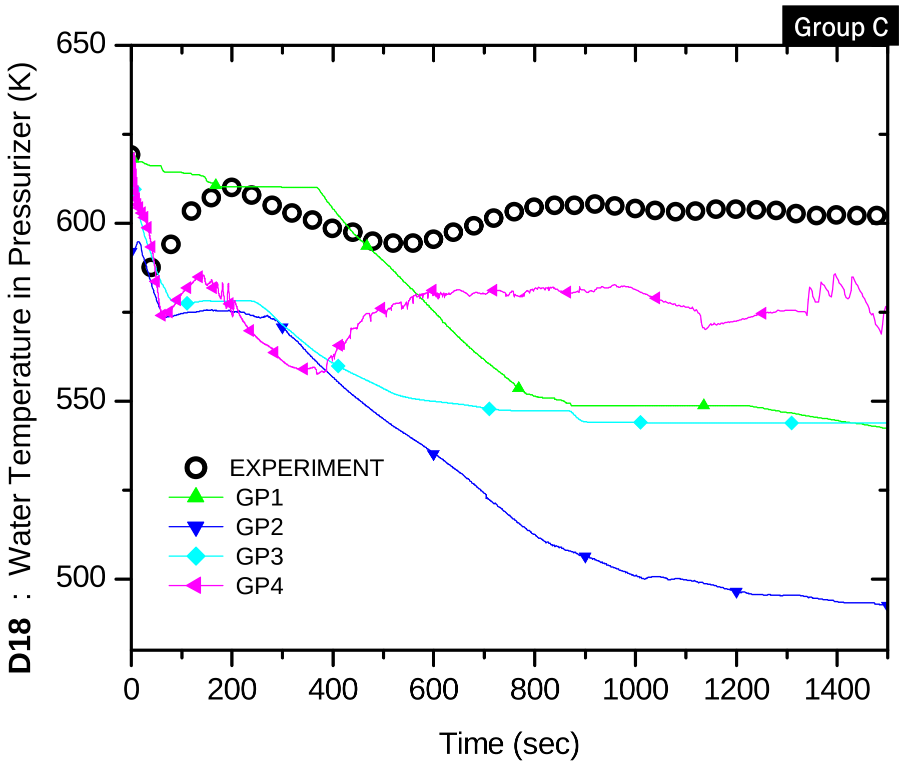

Figure B.18-C Water temperature in the pressurizer (D18)

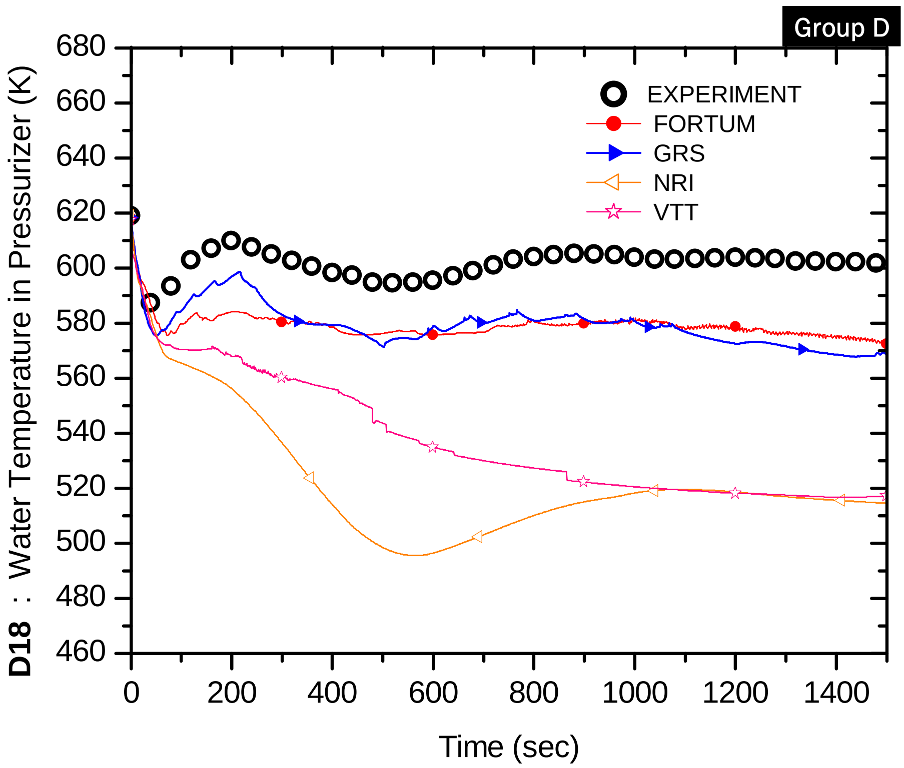

Figure B.18-D Water temperature in the pressurizer (D18)

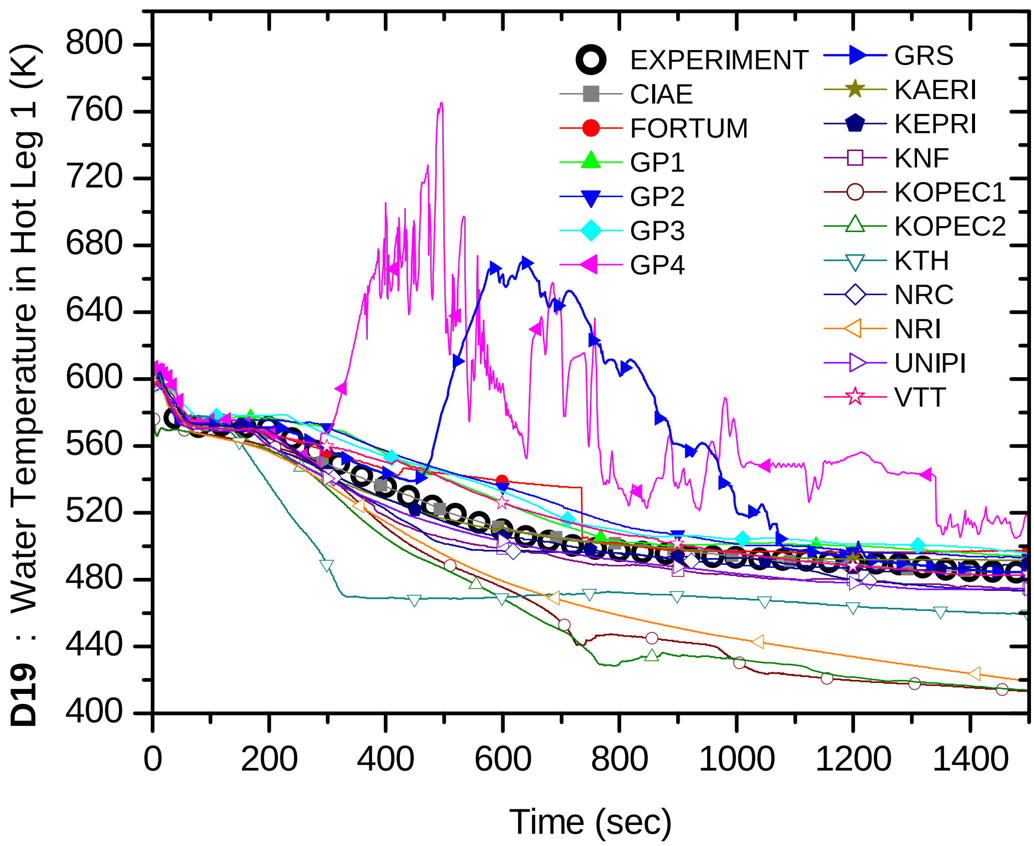

Figure B.19 Water temperature in the hot leg 1 (D19)

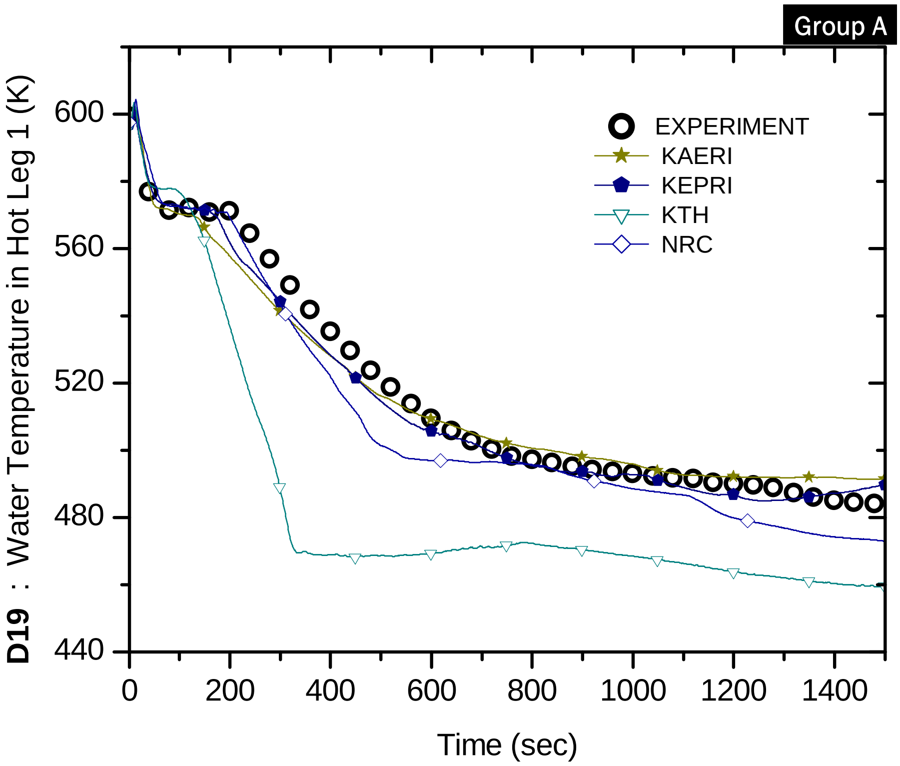

Figure B.19-A Water temperature in the hot leg 1 (D19)

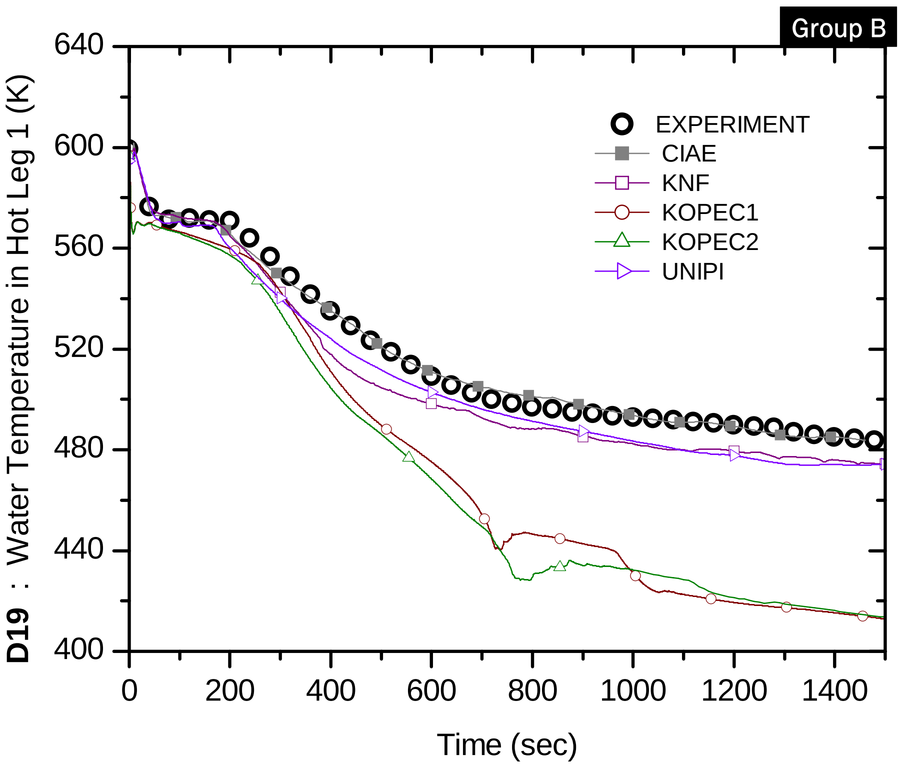

Figure B.19-B Water temperature in the hot leg 1 (D19)

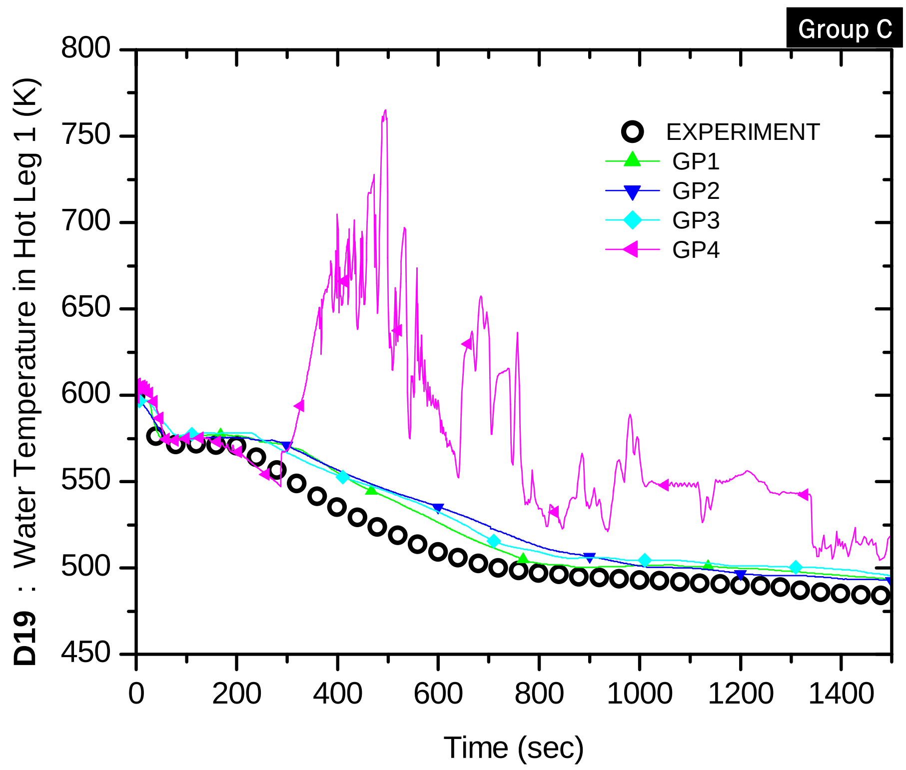

Figure B.19-C Water temperature in the hot leg 1 (D19)

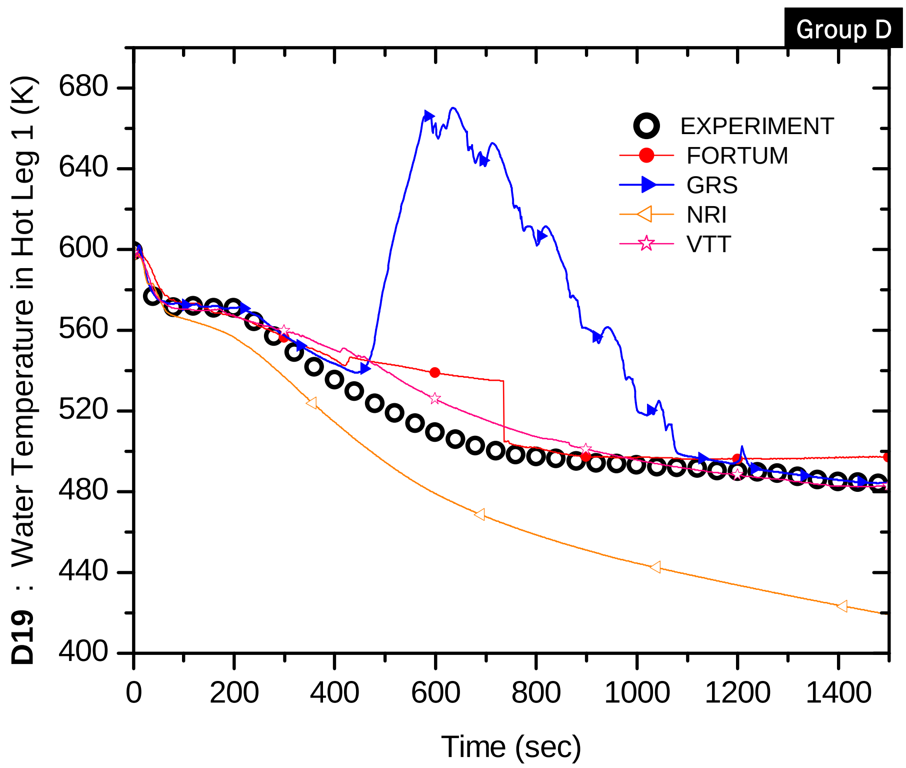

Figure B.19-D Water temperature in the hot leg 1 (D19)

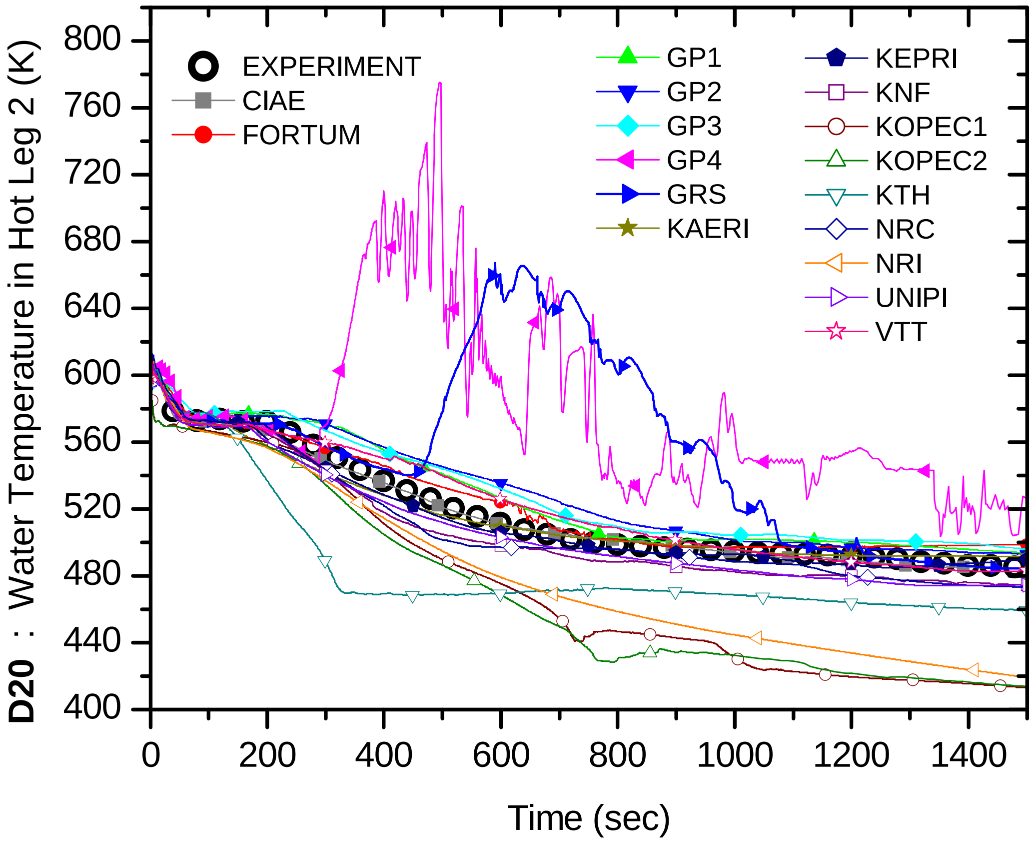

Figure B.20 Water temperature in the hot leg 2 (D20)

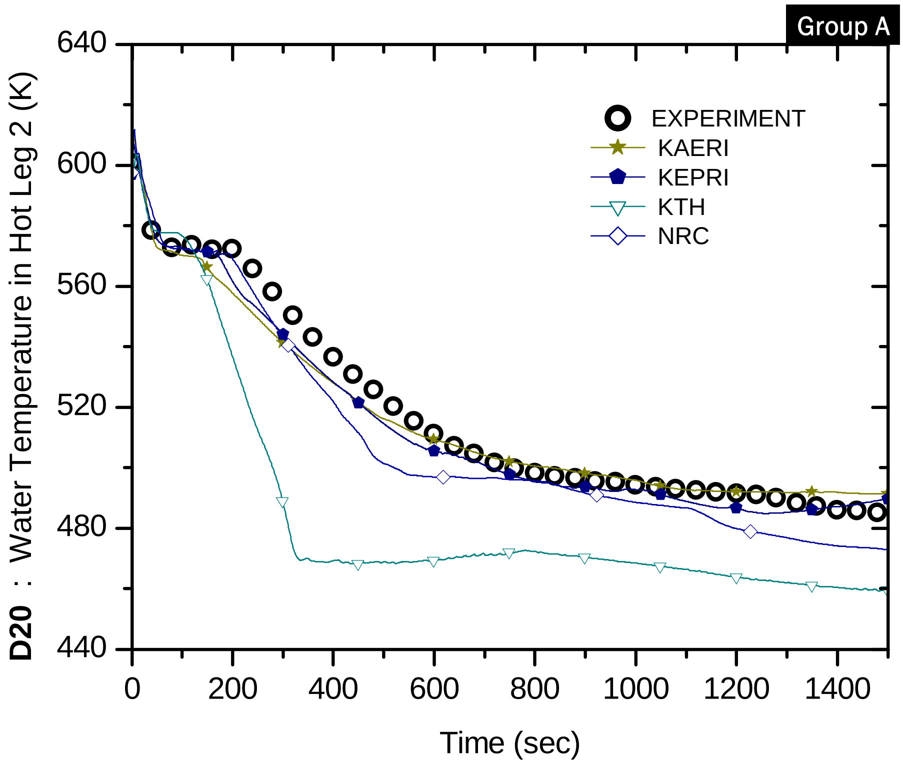

Figure B.20-A Water temperature in the hot leg 2 (D20)

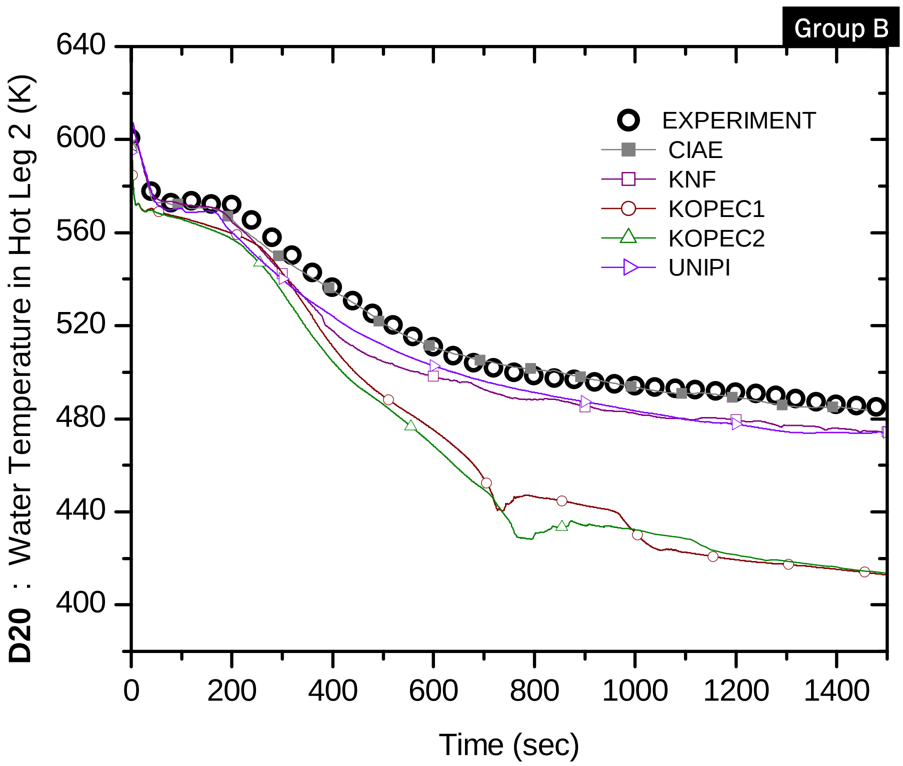

Figure B.20-B Water temperature in the hot leg 2 (D20)

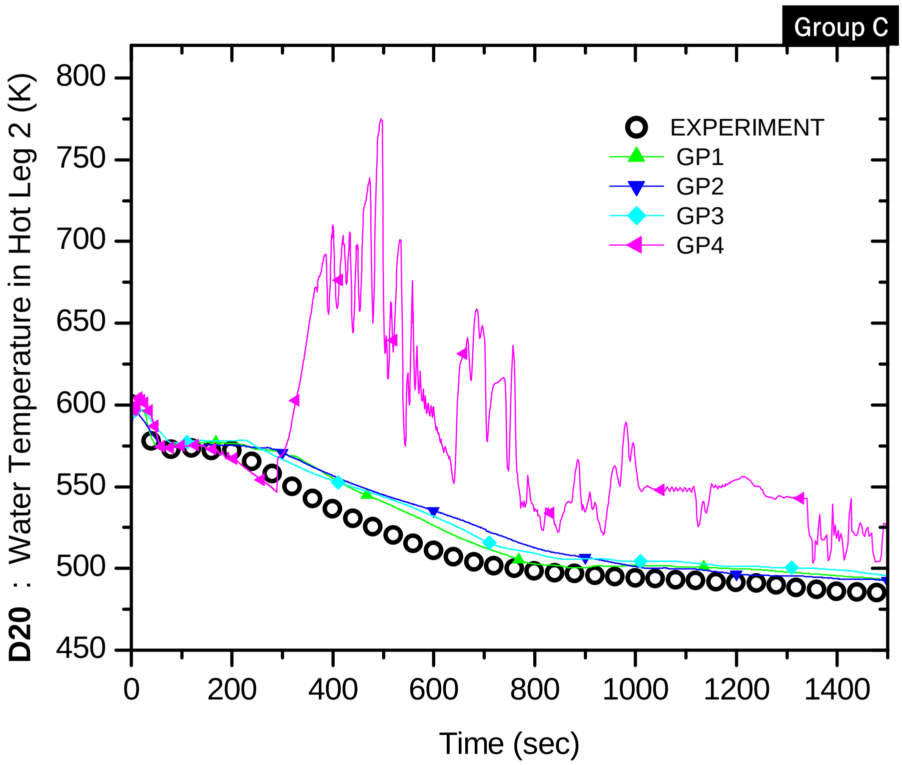

Figure B.20-C Water temperature in the hot leg 2 (D20)

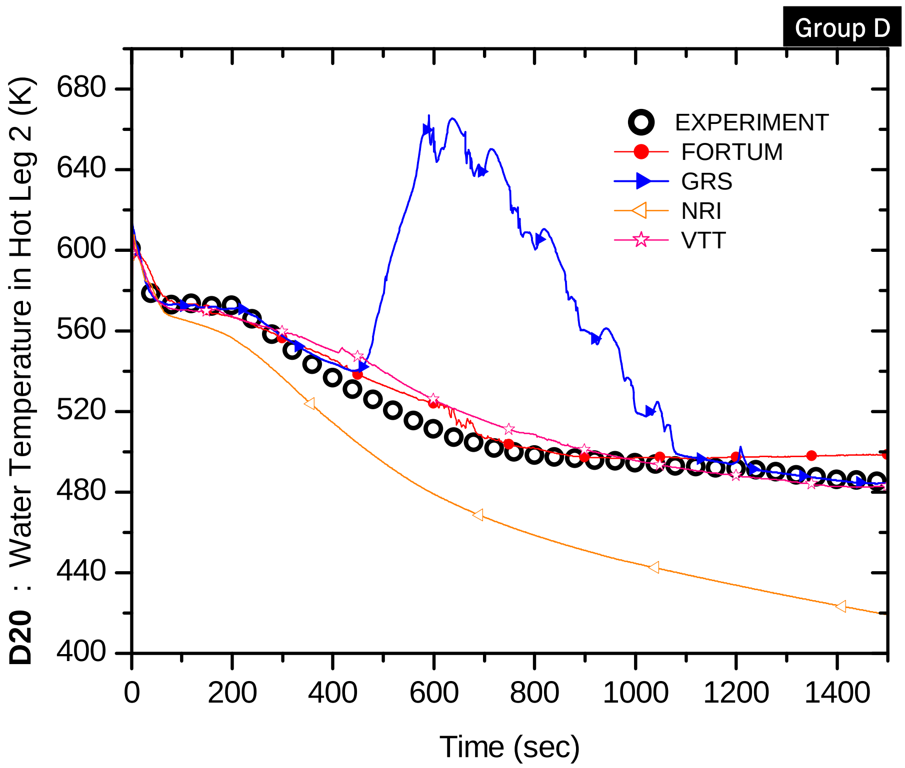

Figure B.20-D Water temperature in the hot leg 2 (D20)

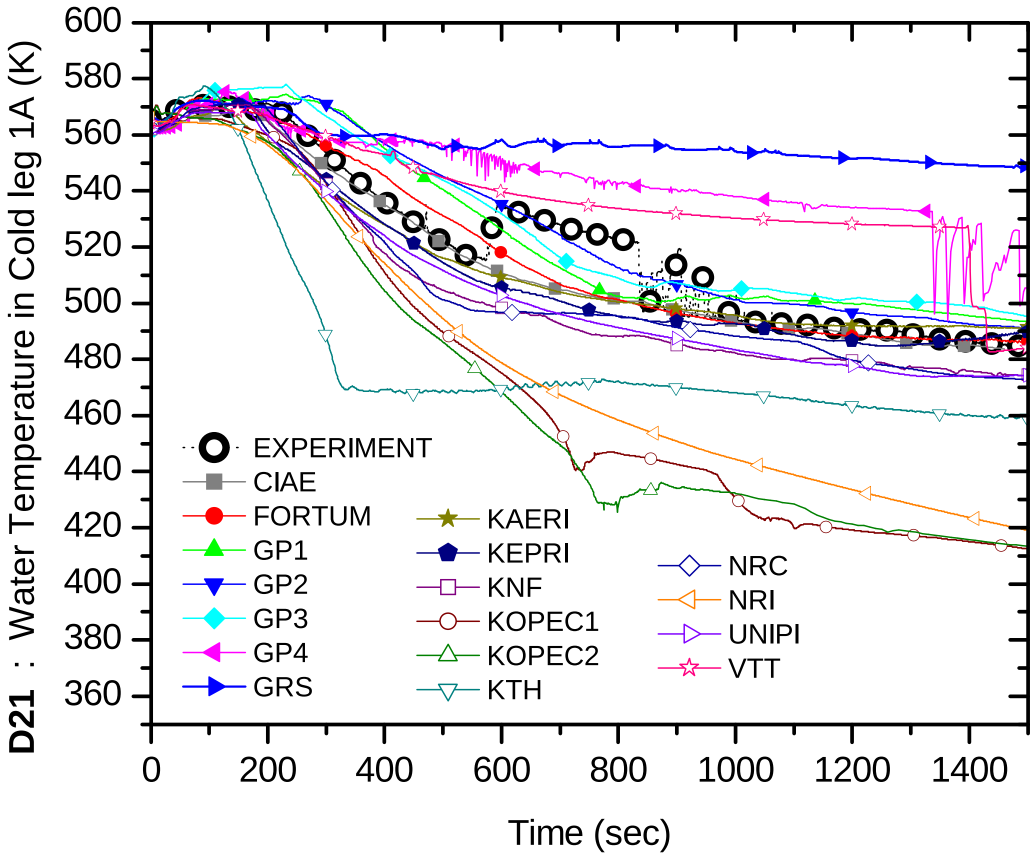

Figure B.21 Water temperature in the cold leg 1A (D21)

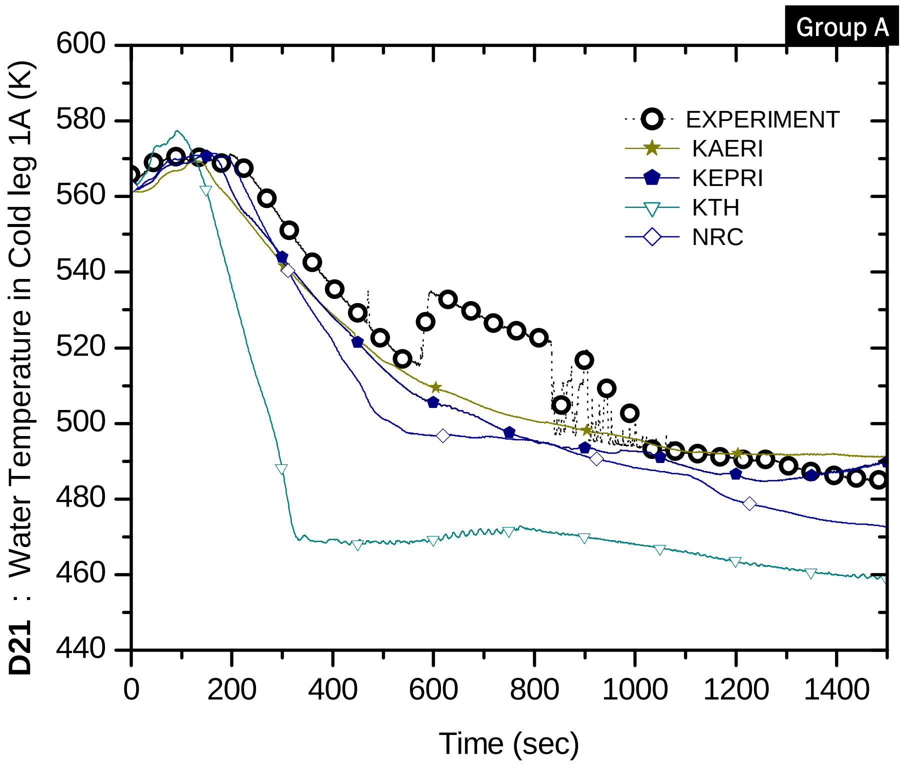

Figure B.21-A Water temperature in the cold leg 1A (D21)

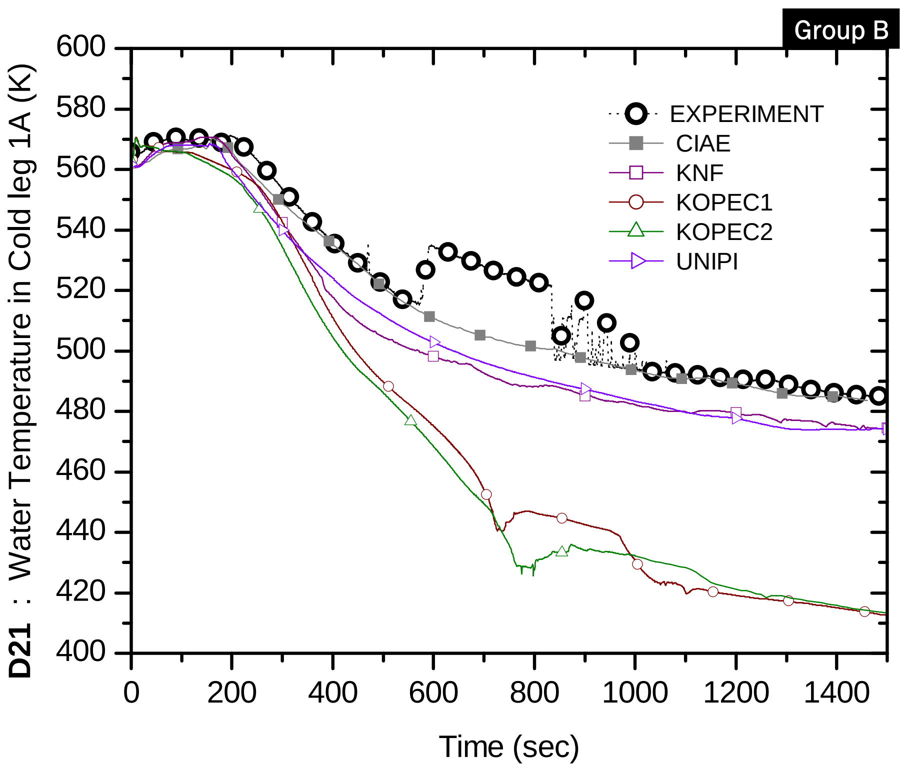

Figure B.21-B Water temperature in the cold leg 1A (D21)

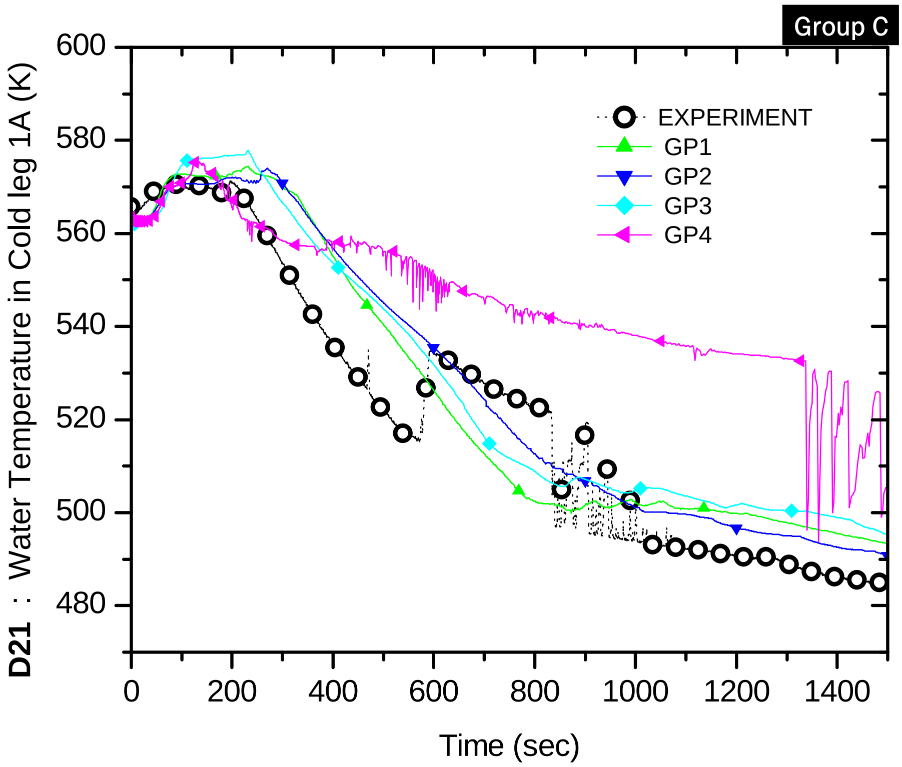

Figure B.21-C Water temperature in the cold leg 1A (D21)

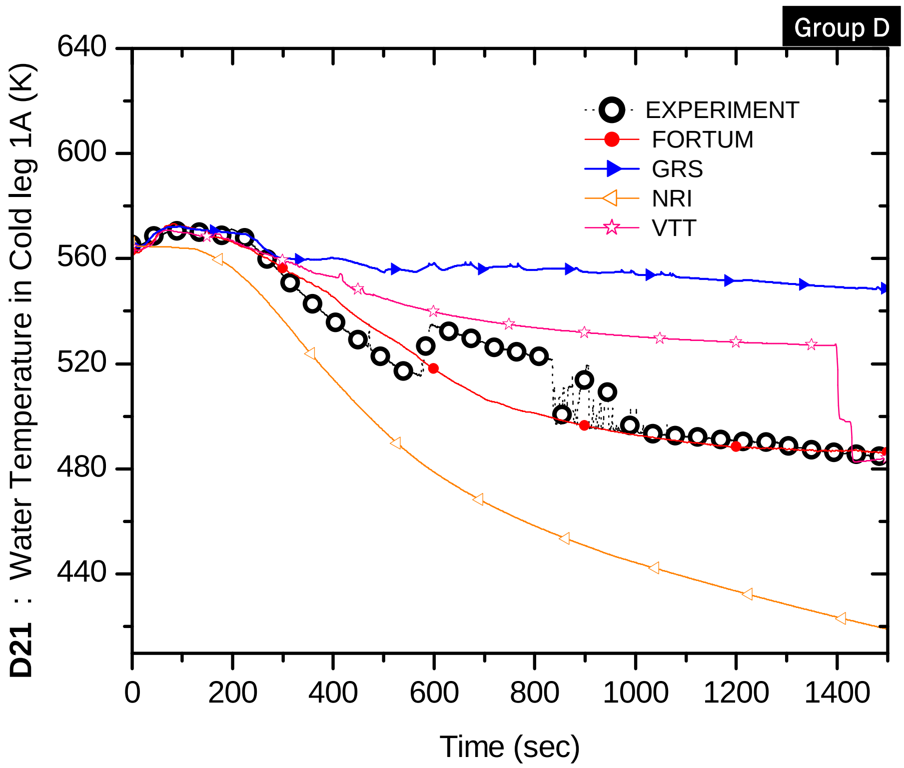

Figure B.21-D Water temperature in the cold leg 1A (D21)

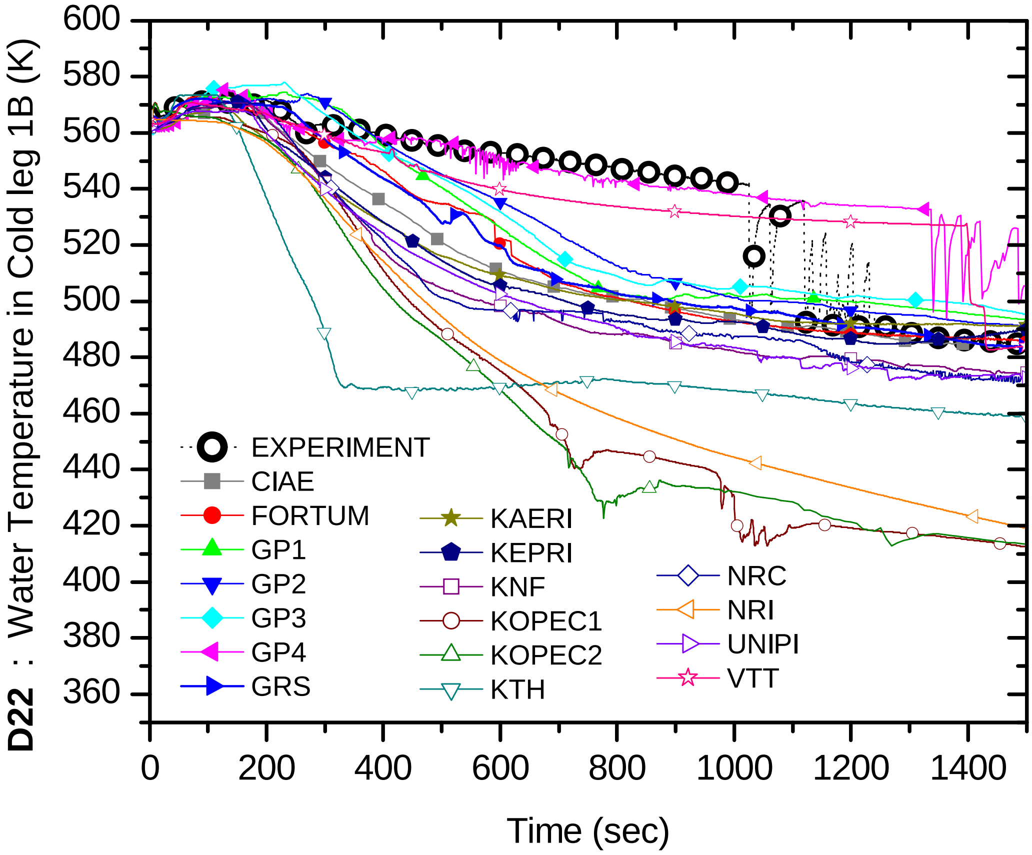

Figure B.22 Water temperature in the cold leg 1B (D22)

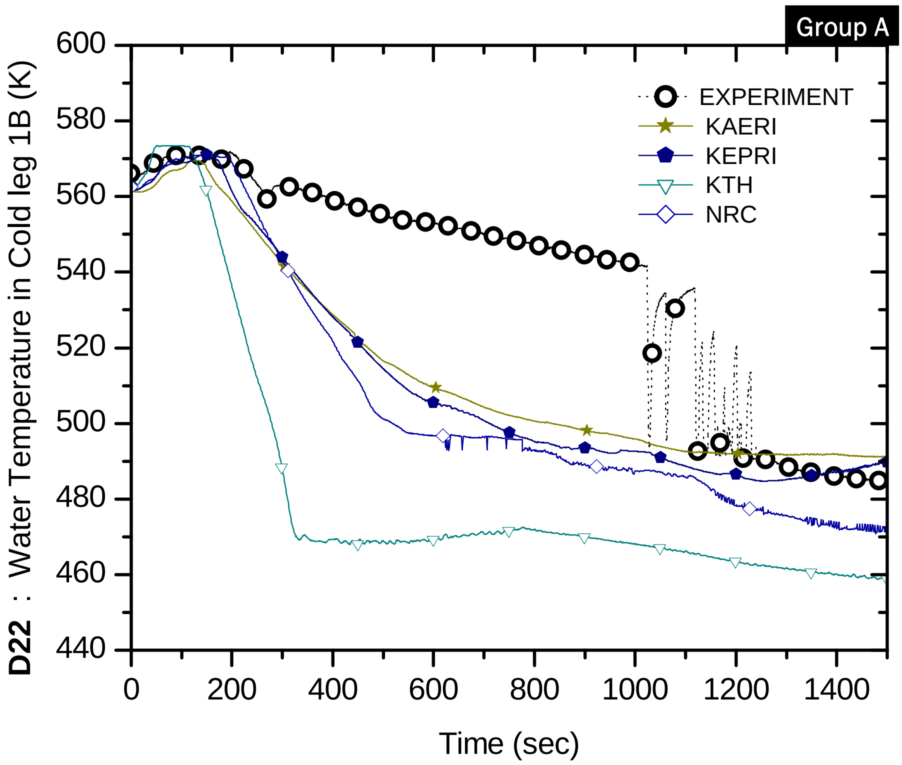

Figure B.22-A Water temperature in the cold leg 1B (D22)

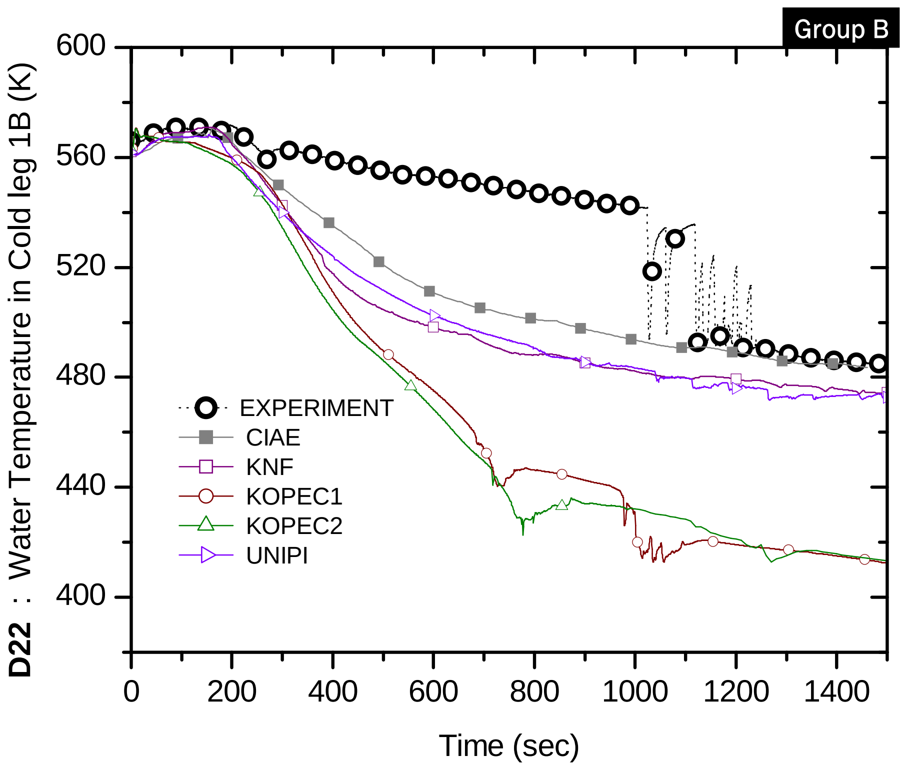

Figure B.22-B Water temperature in the cold leg 1B (D22)

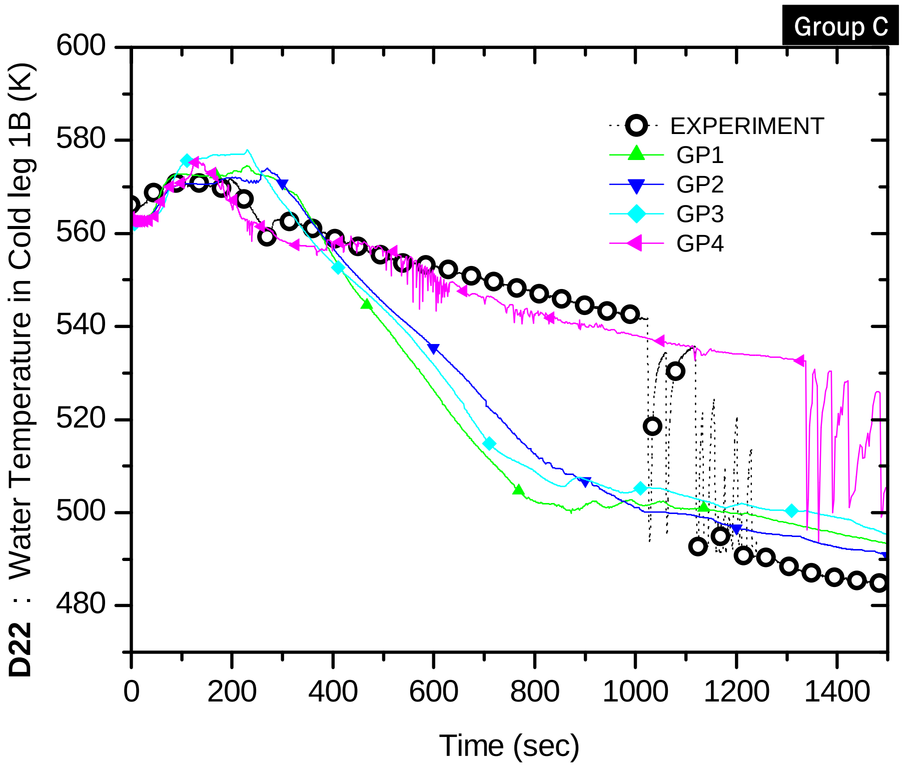

Figure B.22-C Water temperature in the cold leg 1B (D22)

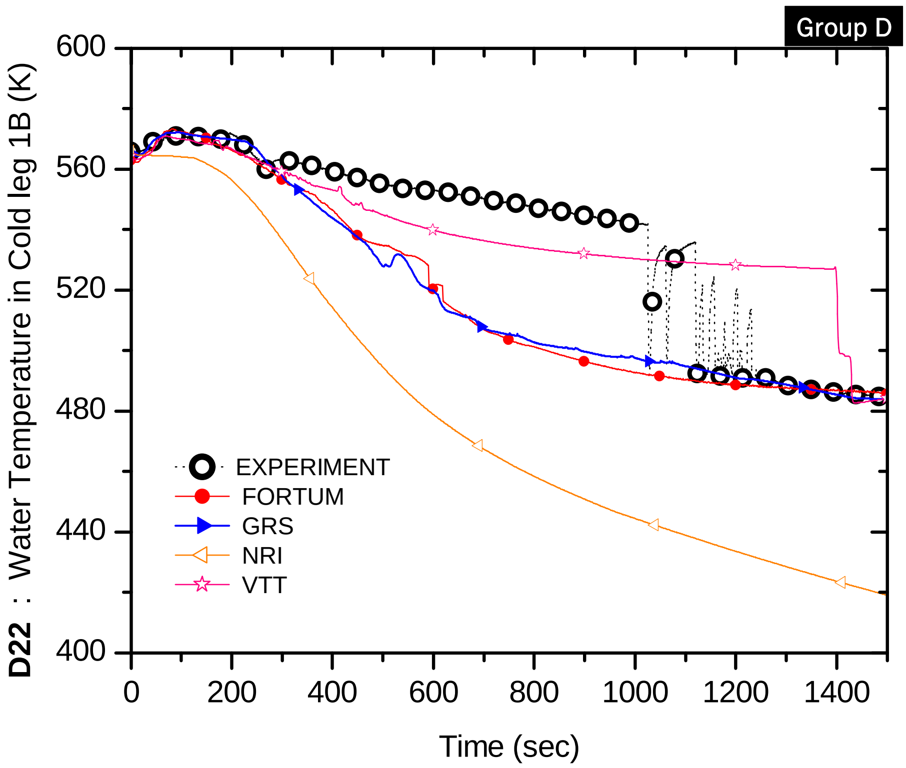

Figure B.22-D Water temperature in the cold leg 1B (D22)

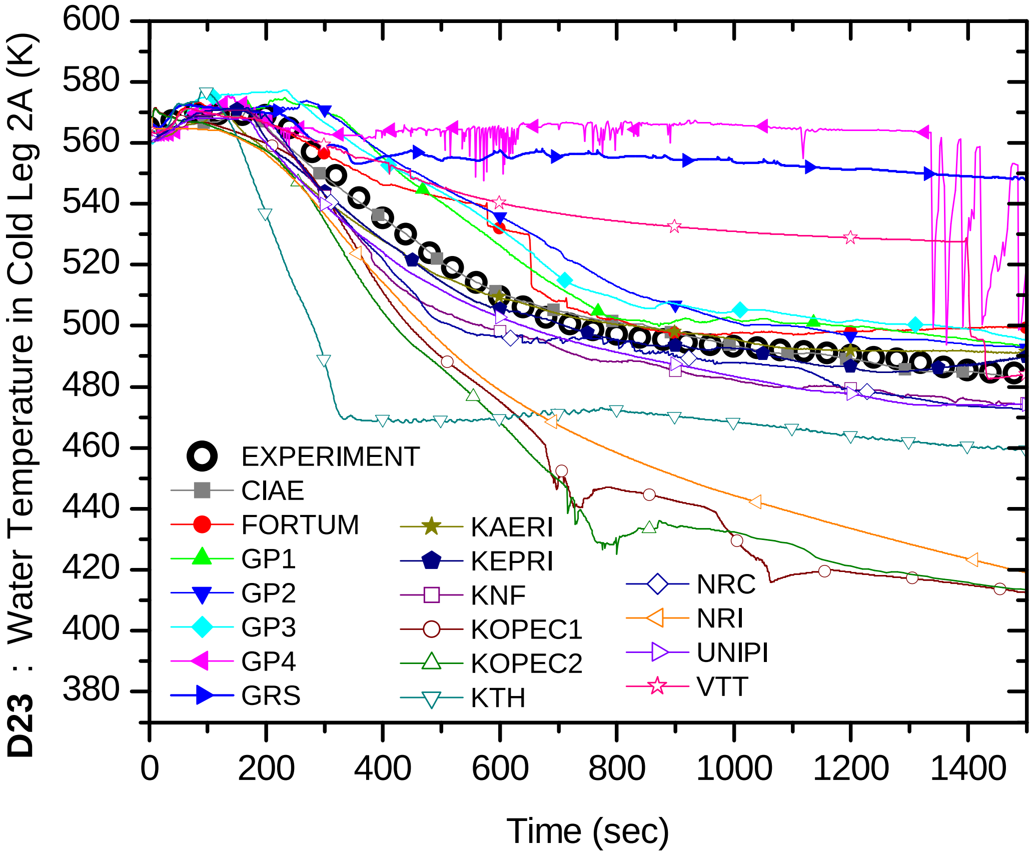

Figure B.23 Water temperature in the cold leg 2A (D23)

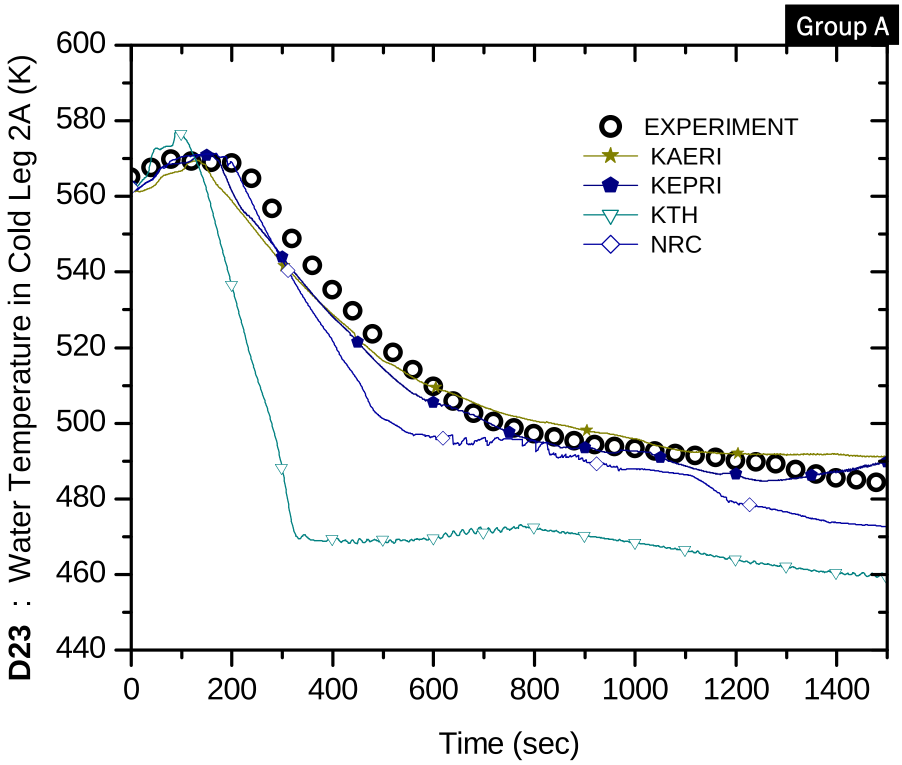

Figure B.23-A Water temperature in the cold leg 2A (D23)

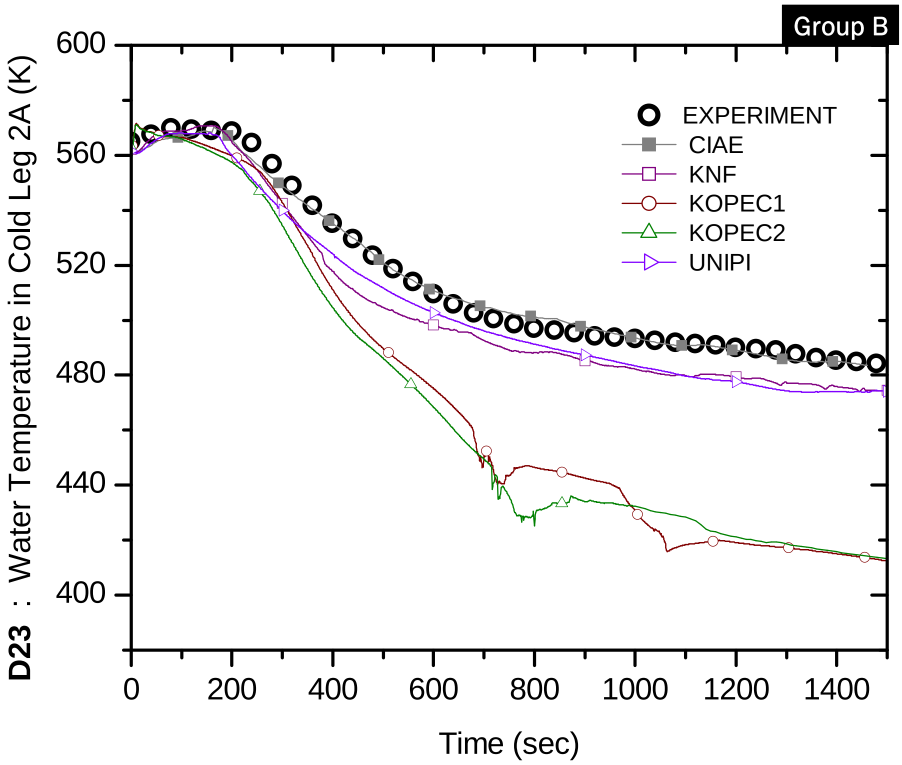

Figure B.23-B Water temperature in the cold leg 2A (D23)

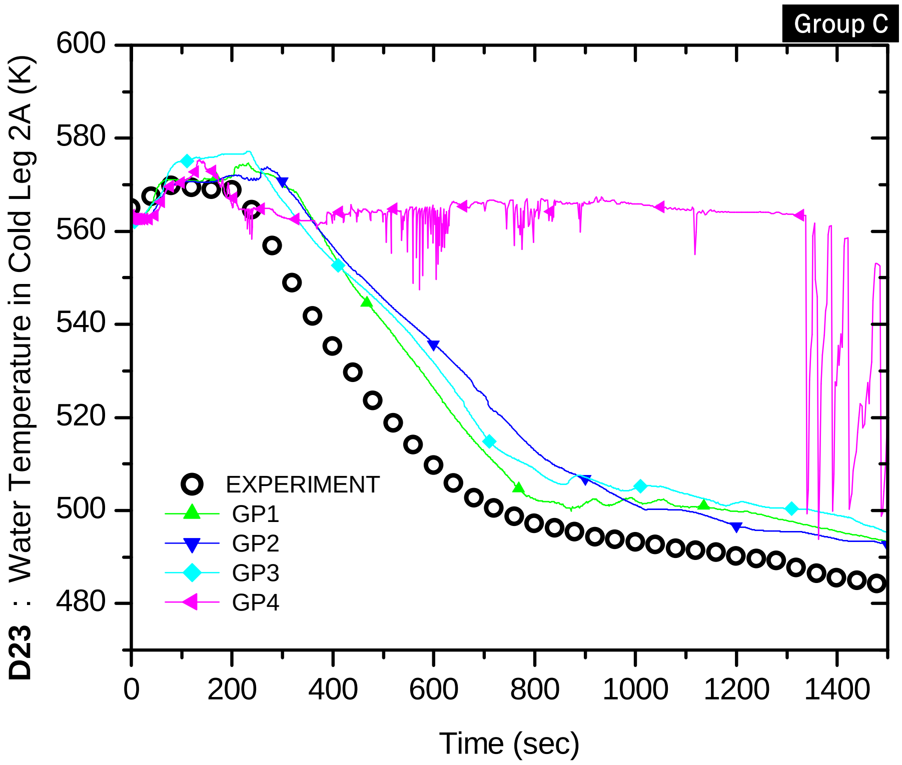

Figure B.23-C Water temperature in the cold leg 2A (D23)

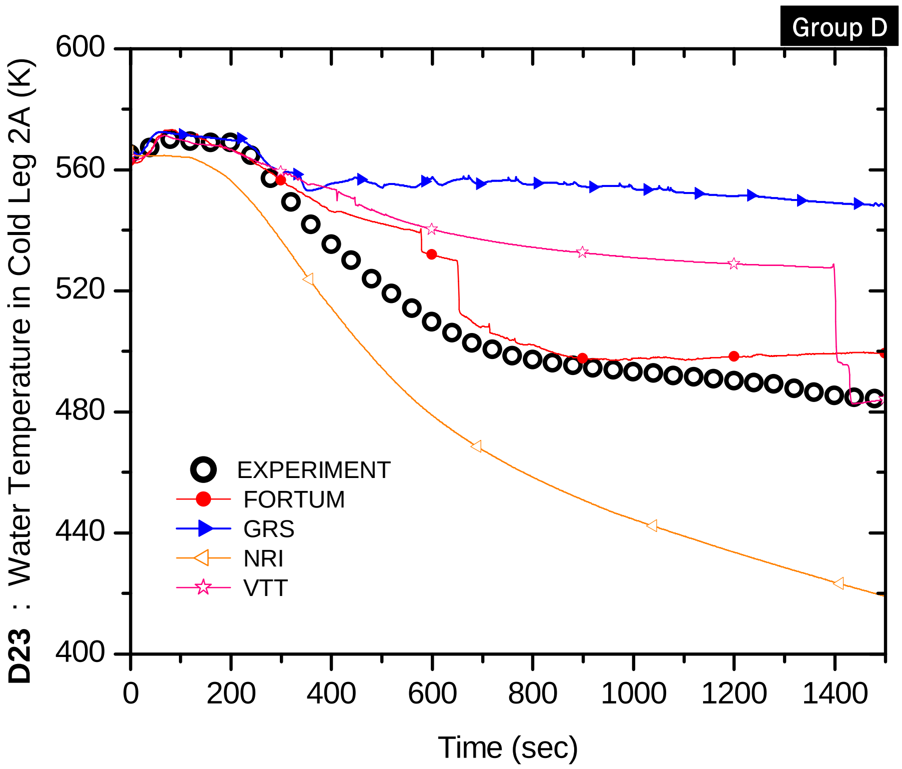

Figure B.23-D Water temperature in the cold leg 2A (D23)

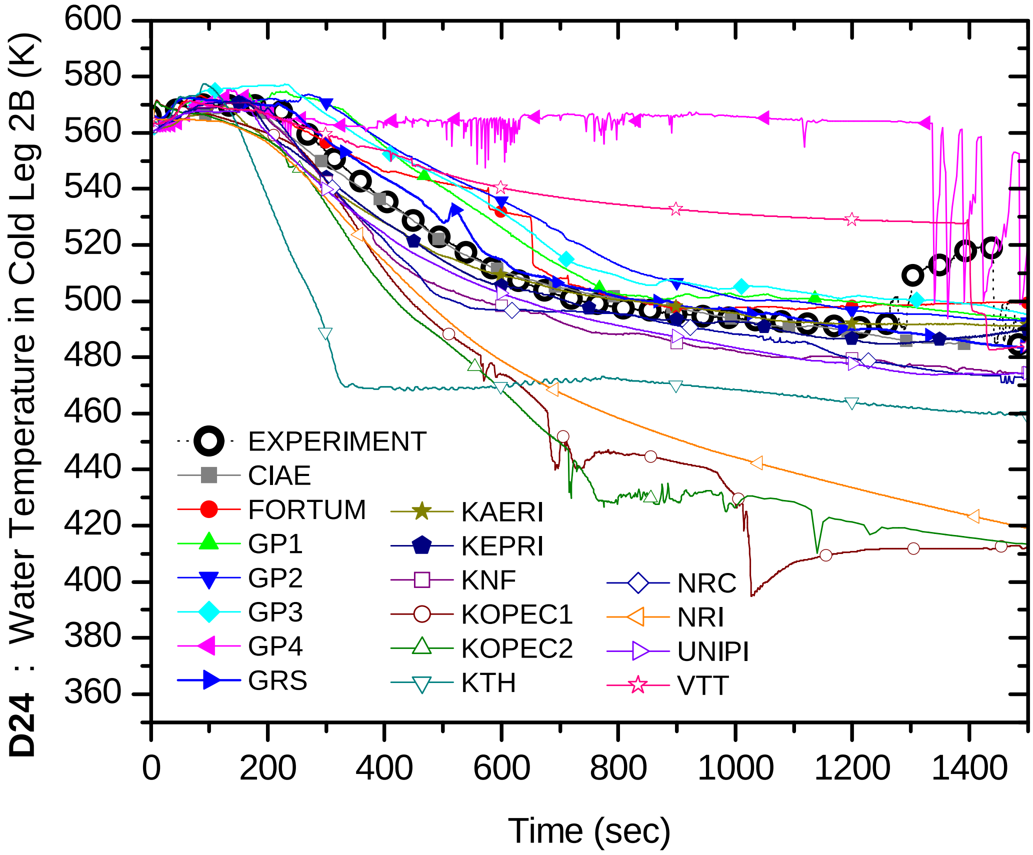

Figure B.24 Water temperature in the cold leg 2B (D24)

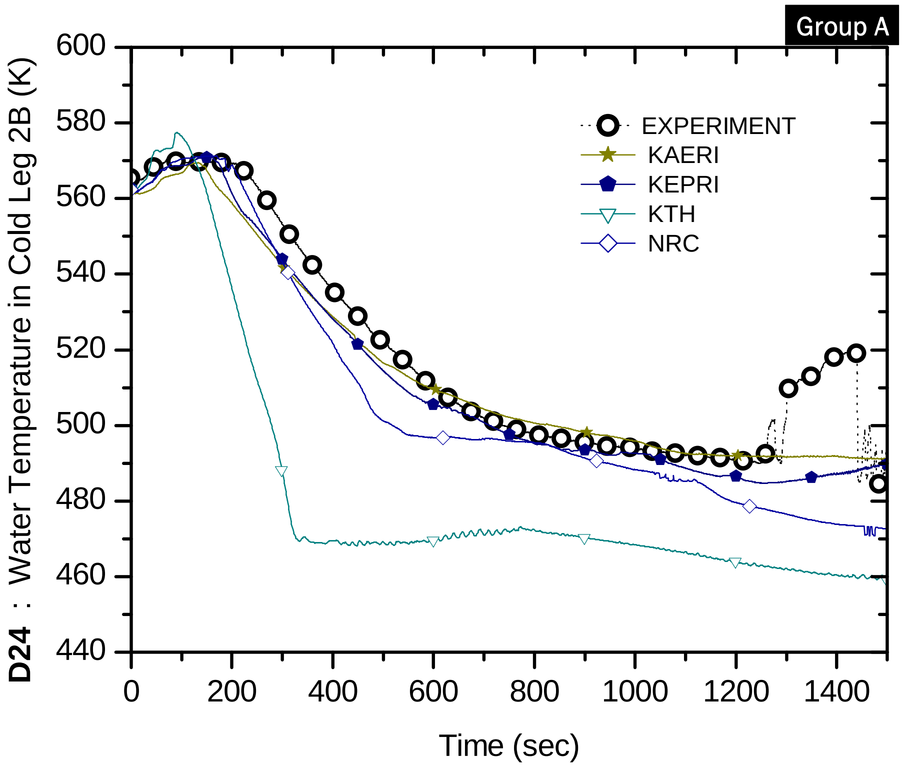

Figure B.24-A Water temperature in the cold leg 2B (D24)

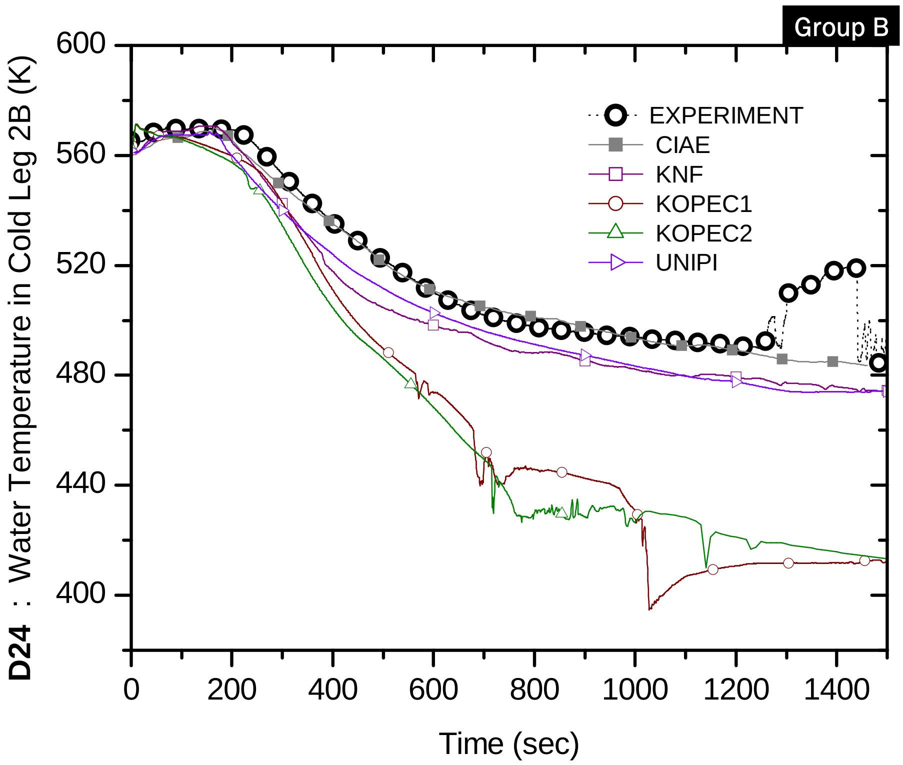

Figure B.24-B Water temperature in the cold leg 2B (D24)

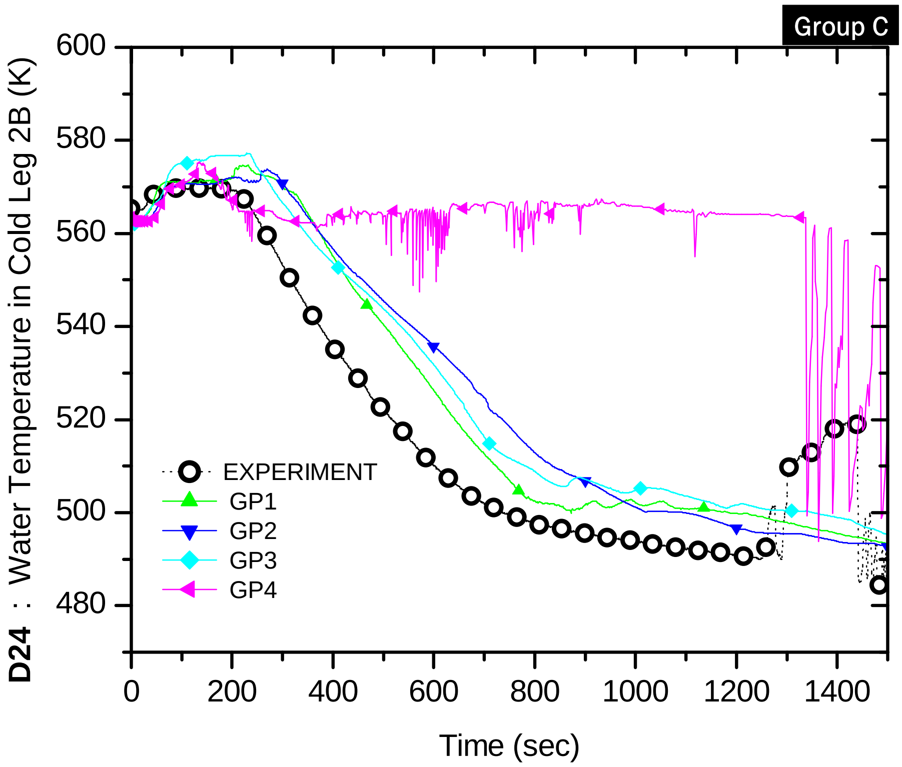

Figure B.24-C Water temperature in the cold leg 2B (D24)

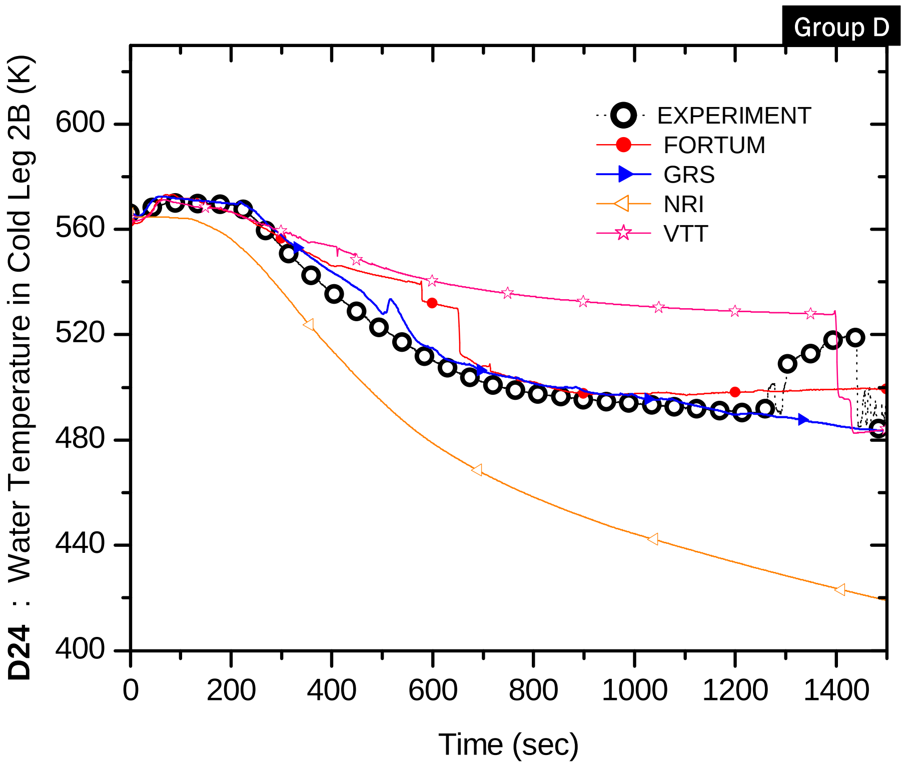

Figure B.24-D Water temperature in the cold leg 2B (D24)

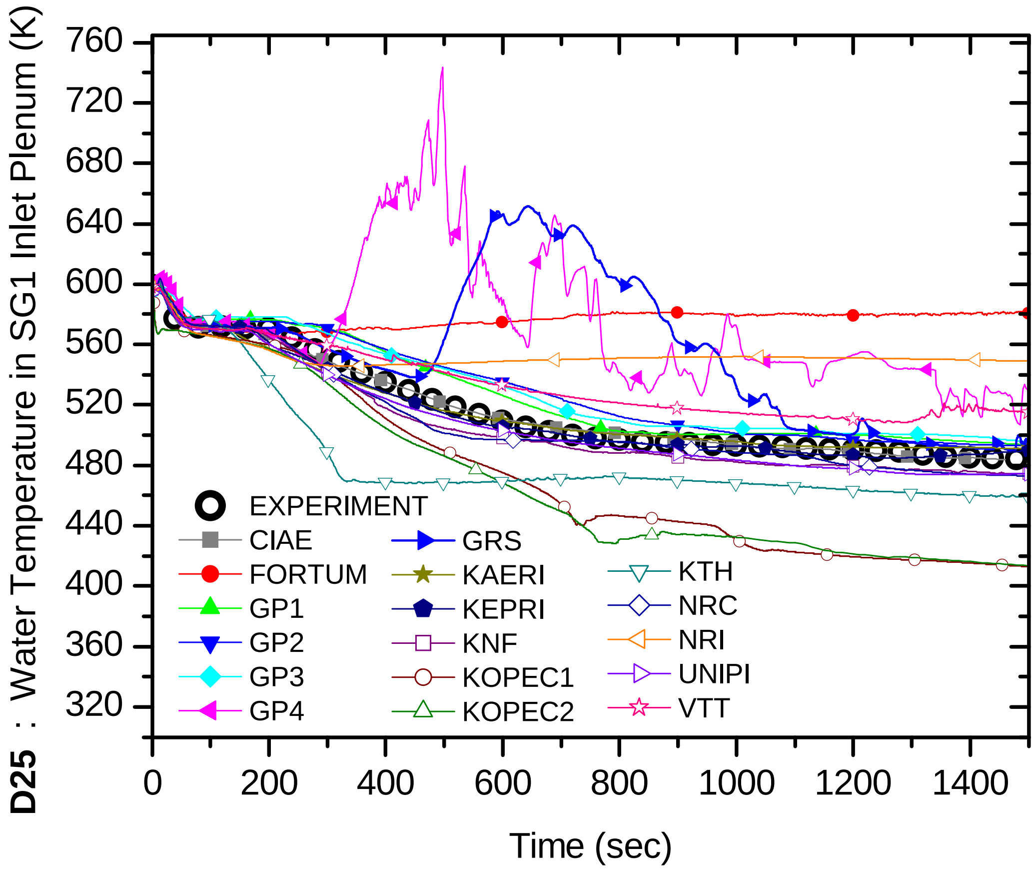

Figure B.25 Water temperature in SG-1 inlet plenum (D25)

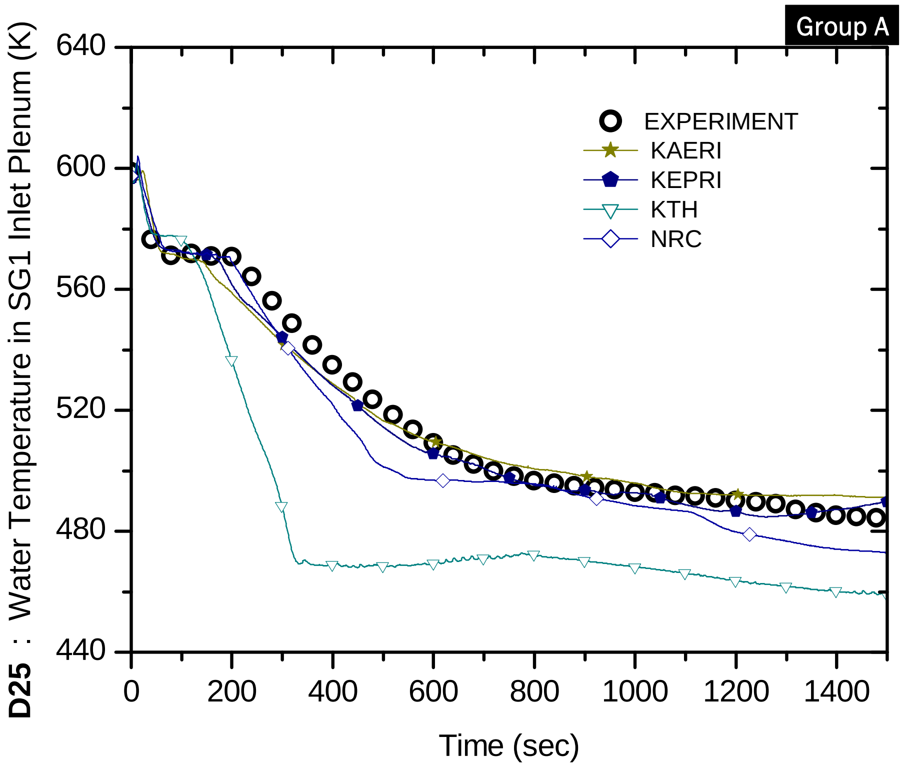

Figure B.25-A Water temperature in SG-1 inlet plenum (D25)

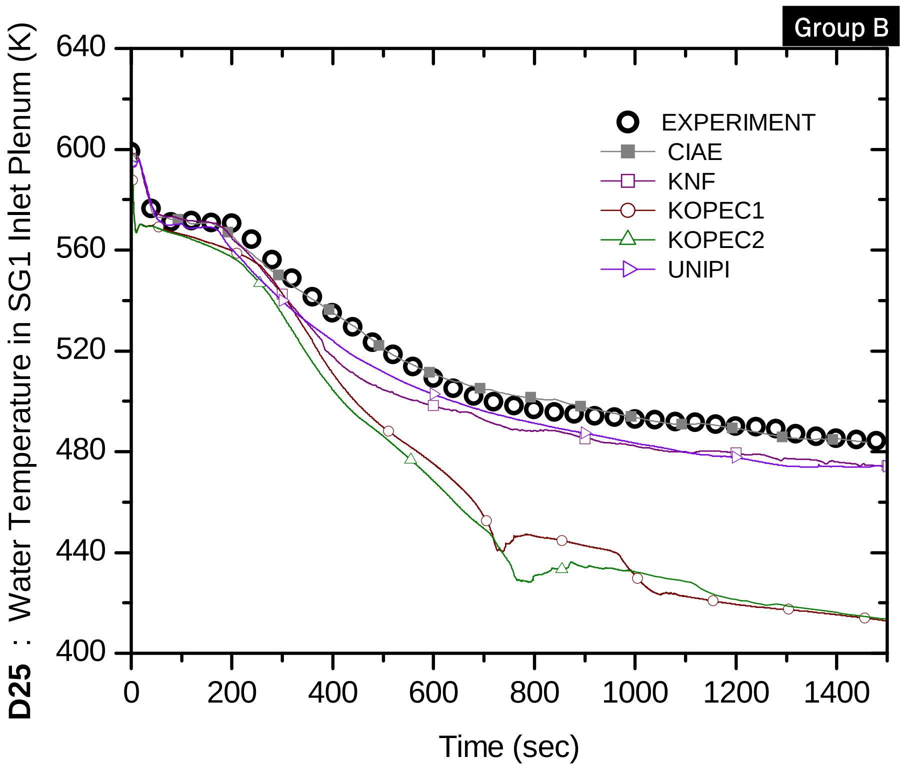

Figure B.25-B Water temperature in SG-1 inlet plenum (D25)

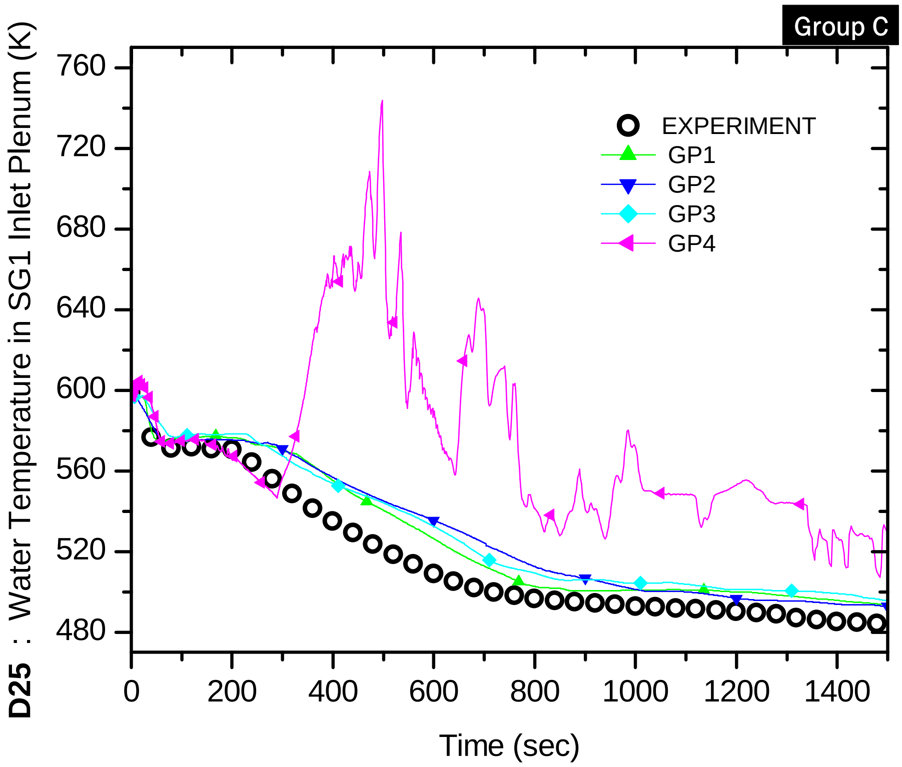

Figure B.25-C Water temperature in SG-1 inlet plenum (D25)

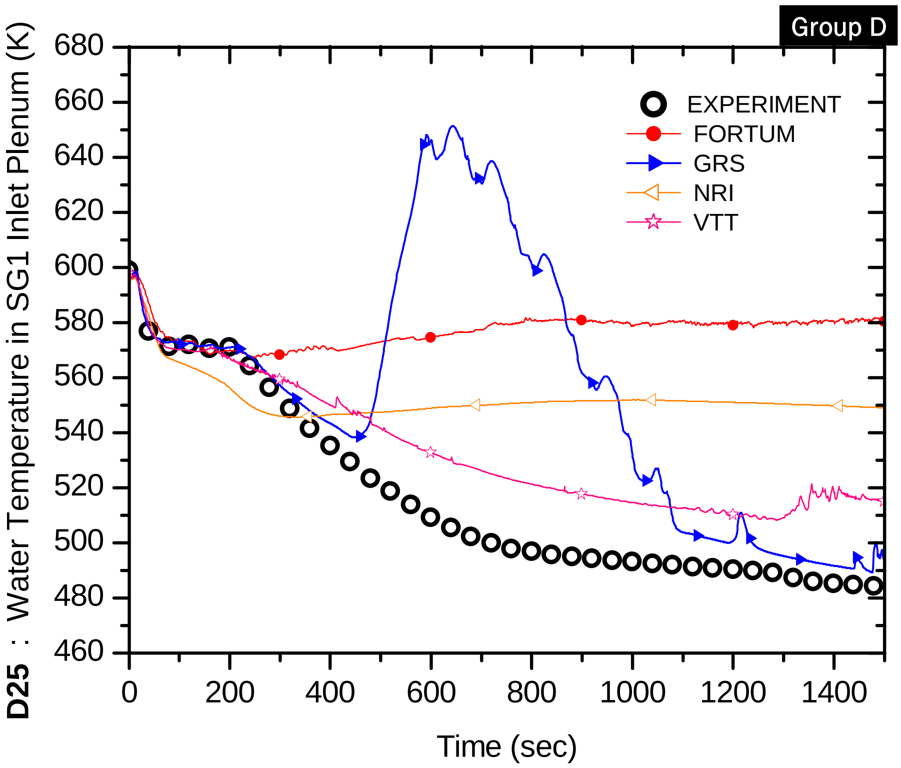

Figure B.25-D Water temperature in SG-1 inlet plenum (D25)

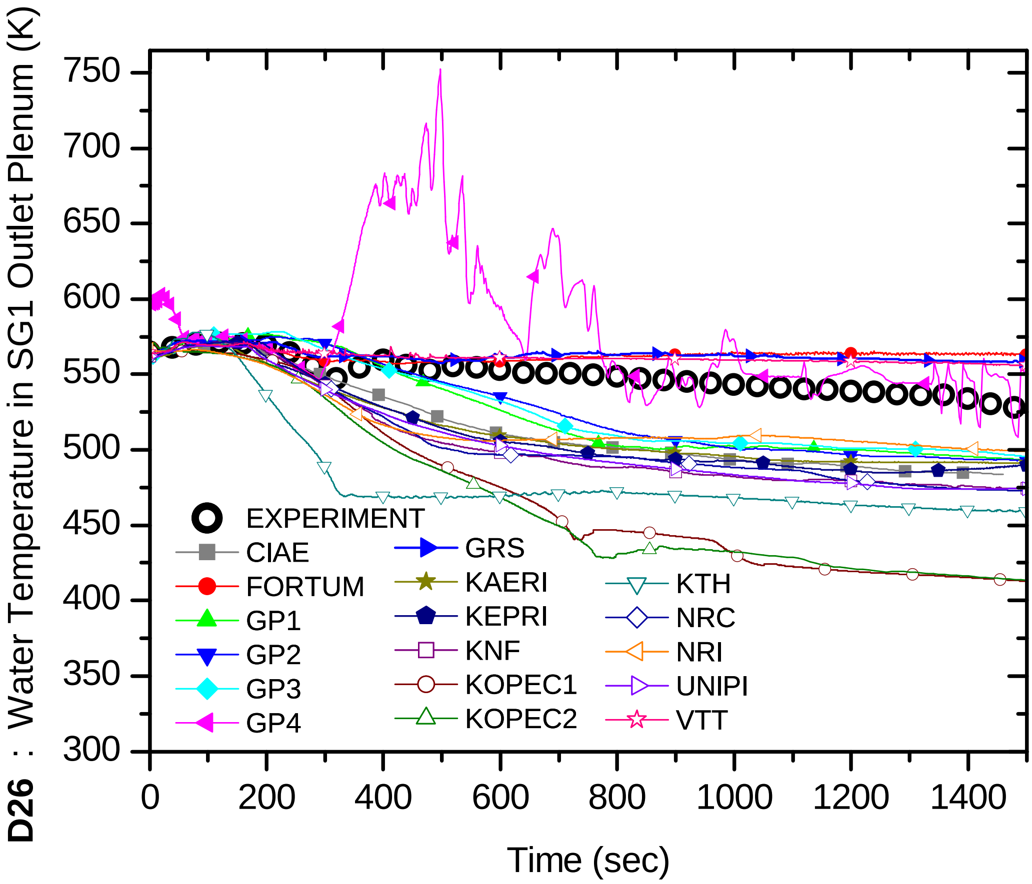

Figure B.26 Water temperature in SG-1 outlet plenum (D26)

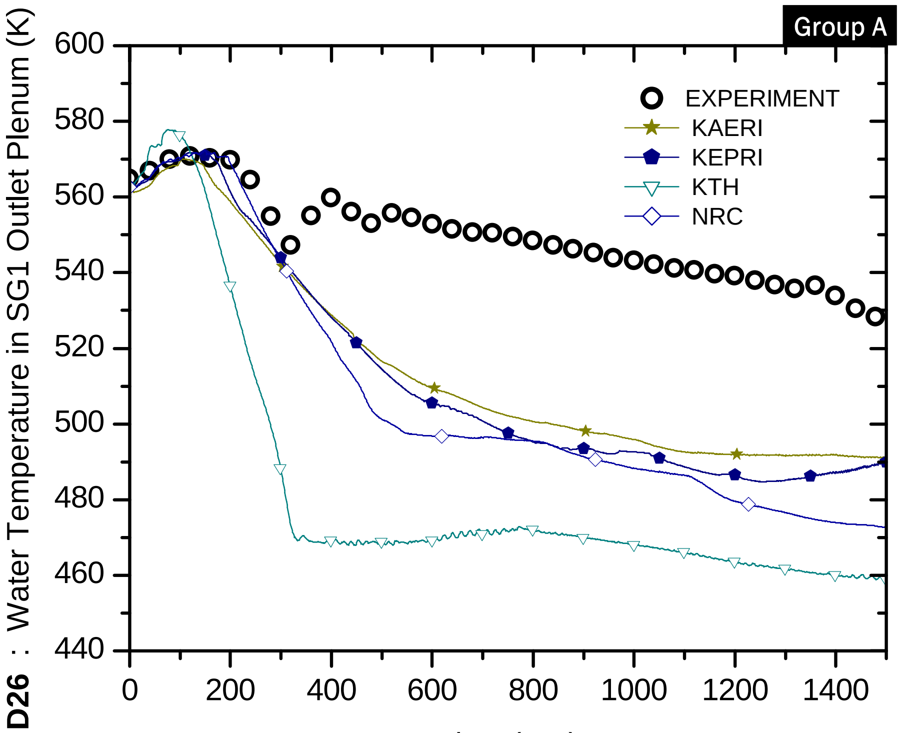

Figure B.26-A Water temperature in SG-1 outlet plenum (D26)

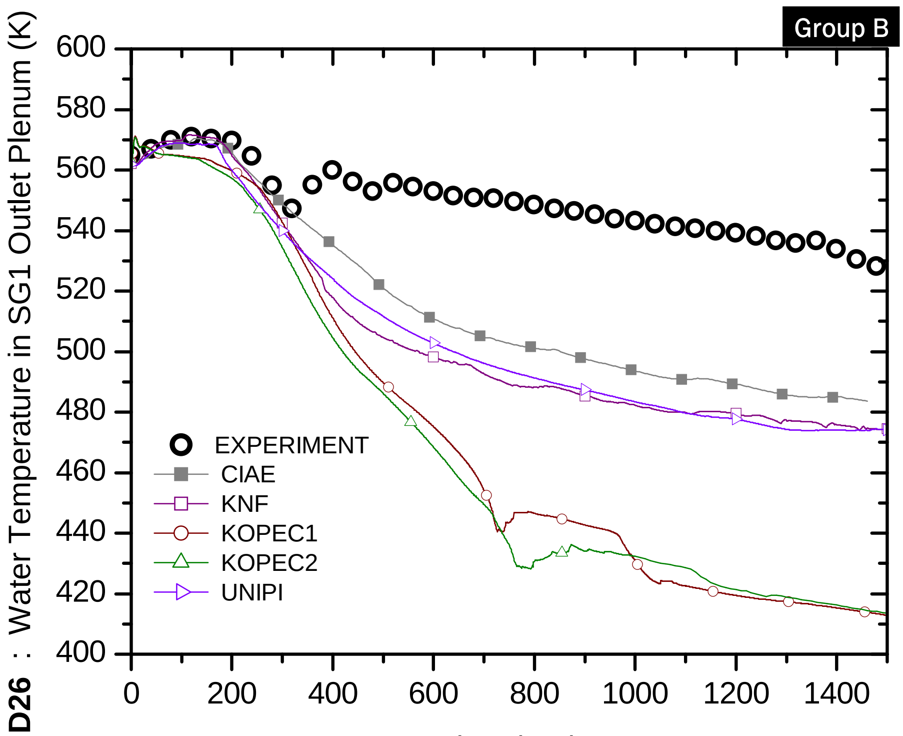

Figure B.26-B Water temperature in SG-1 outlet plenum (D26)

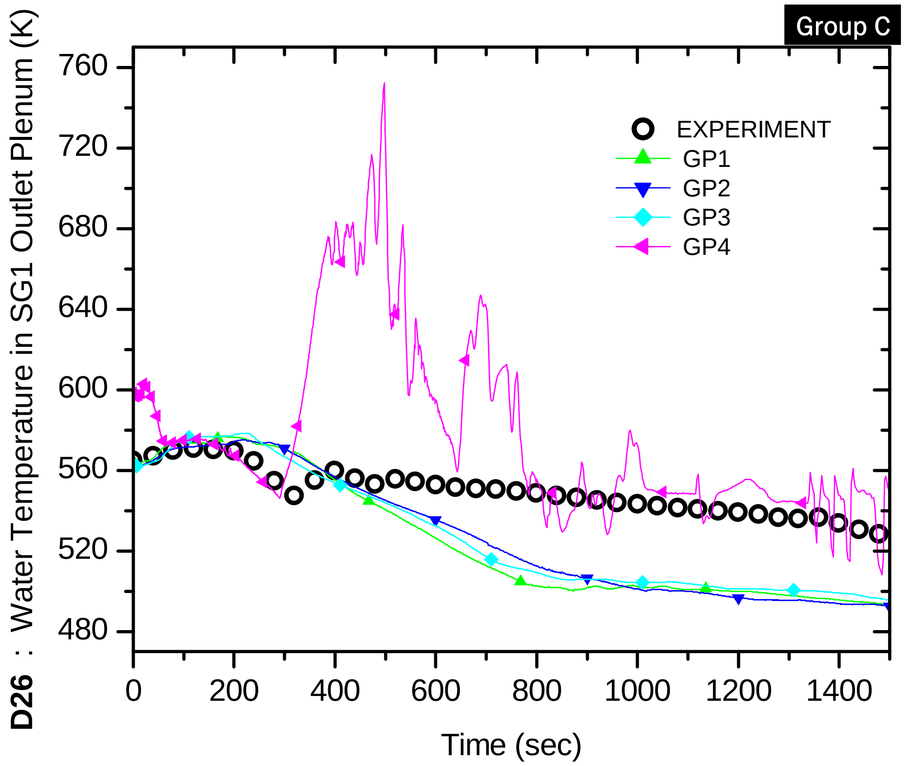

Figure B.26-C Water temperature in SG-1 outlet plenum (D26)

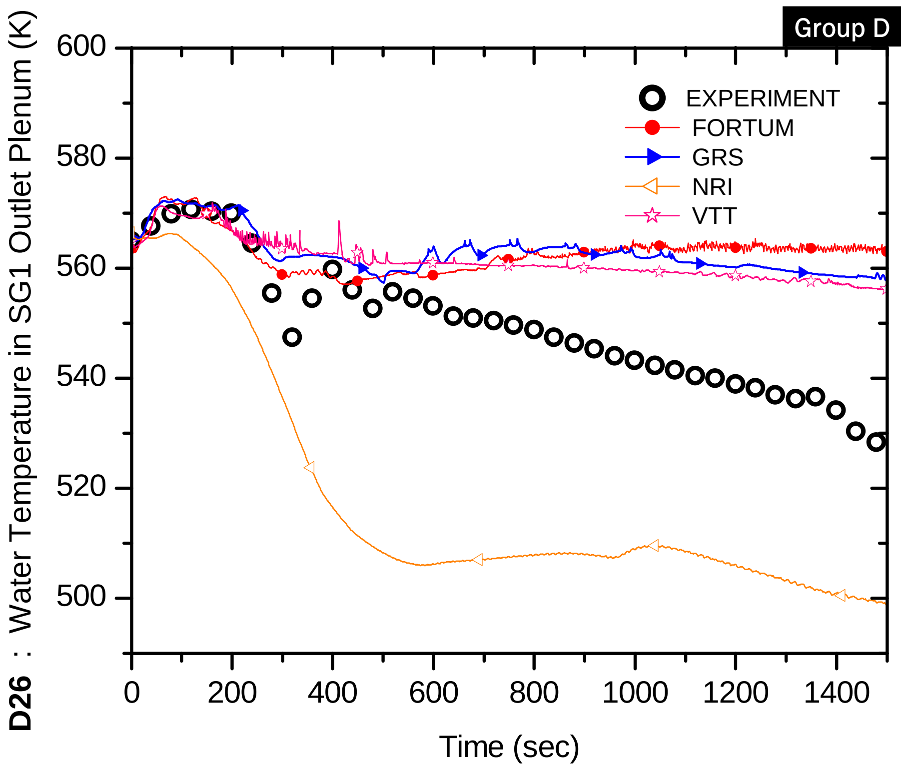

Figure B.26-D Water temperature in SG-1 outlet plenum (D26)

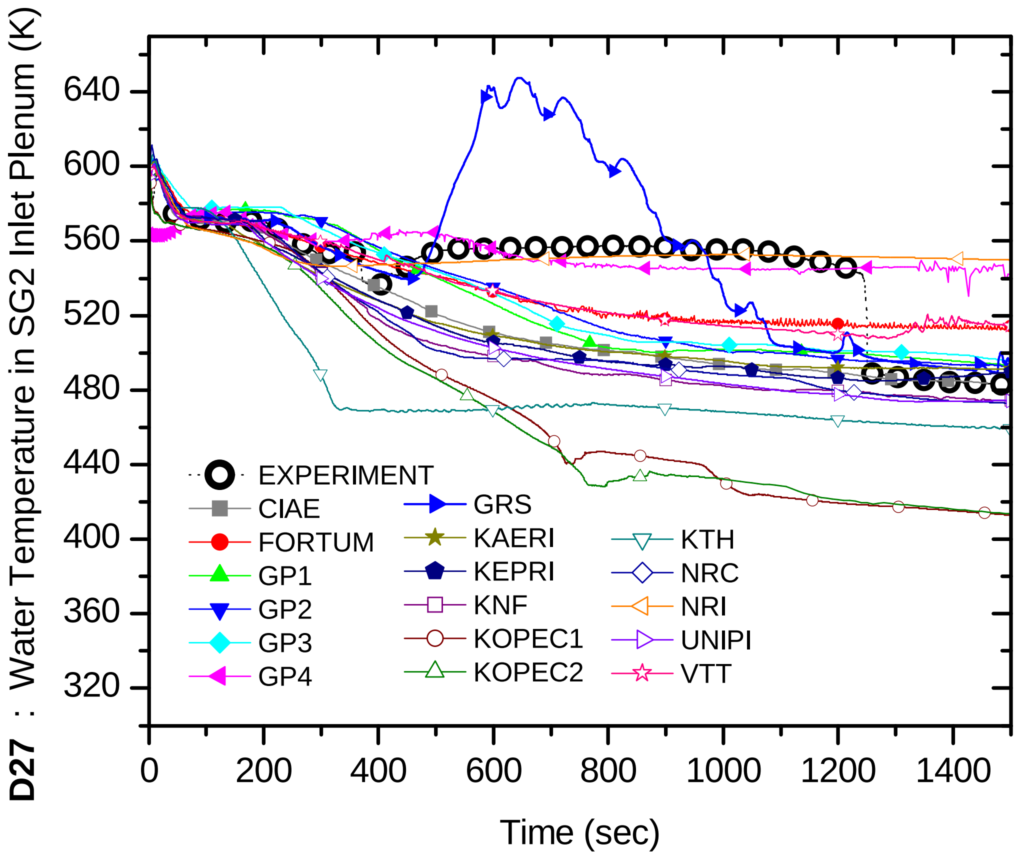

Figure B.27 Water temperature in SG-2 inlet plenum (D27)

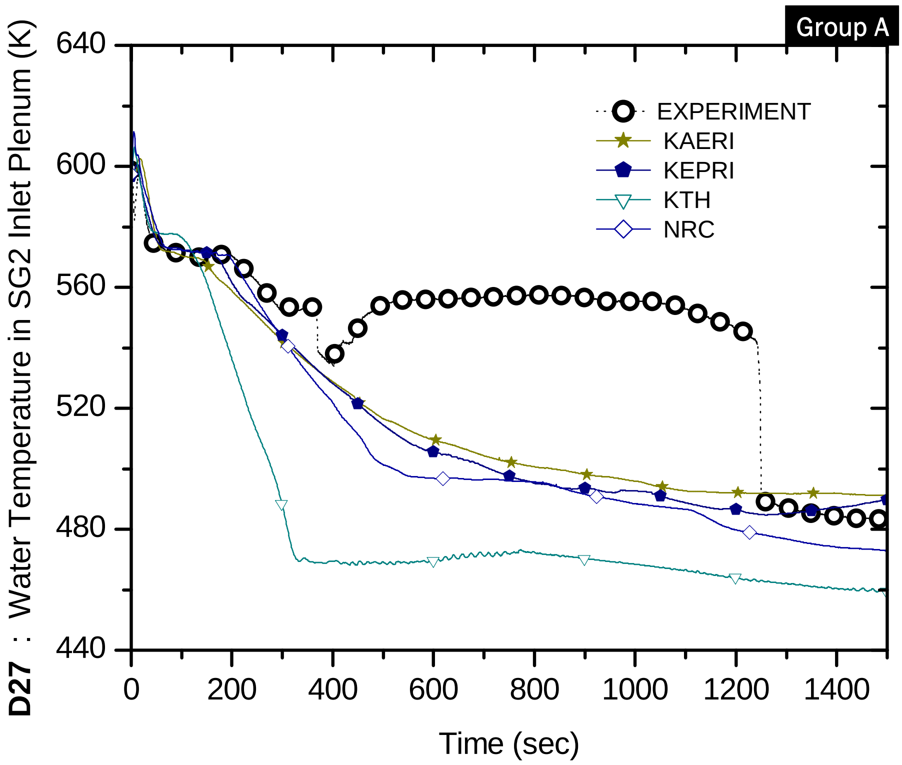

Figure B.27-A Water temperature in SG-2 inlet plenum (D27)

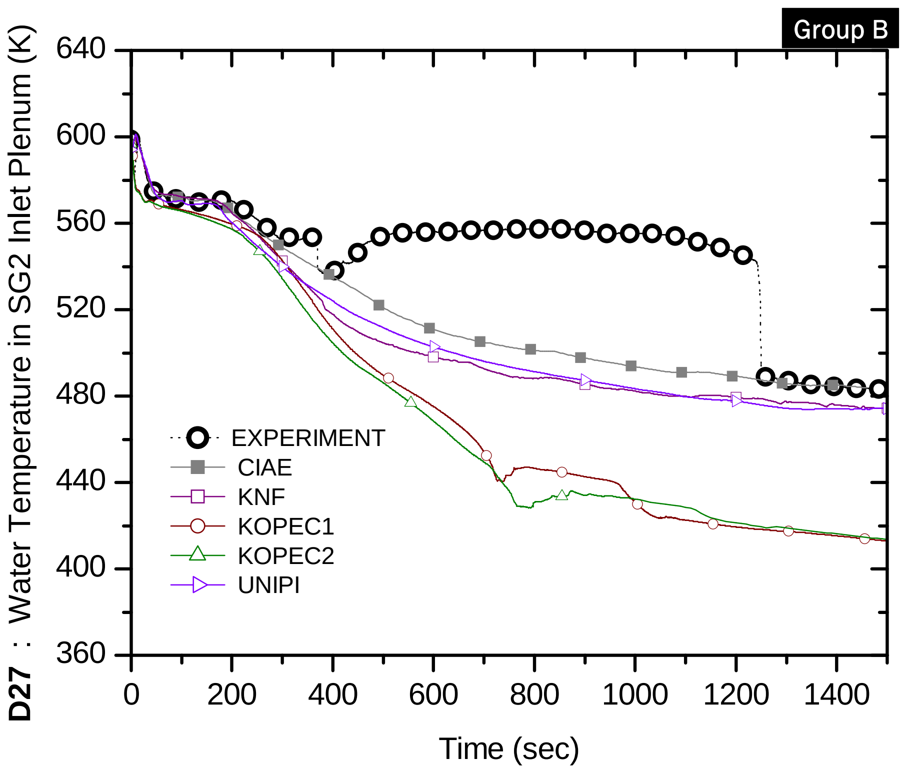

Figure B.27-B Water temperature in SG-2 inlet plenum (D27)

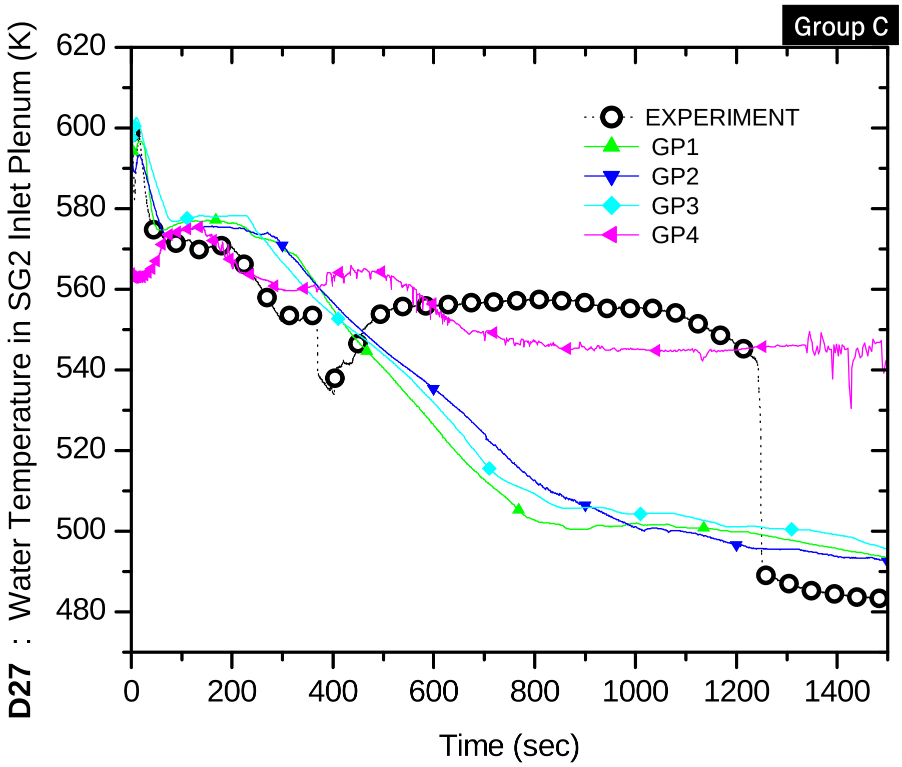

Figure B.27-C Water temperature in SG-2 inlet plenum (D27)

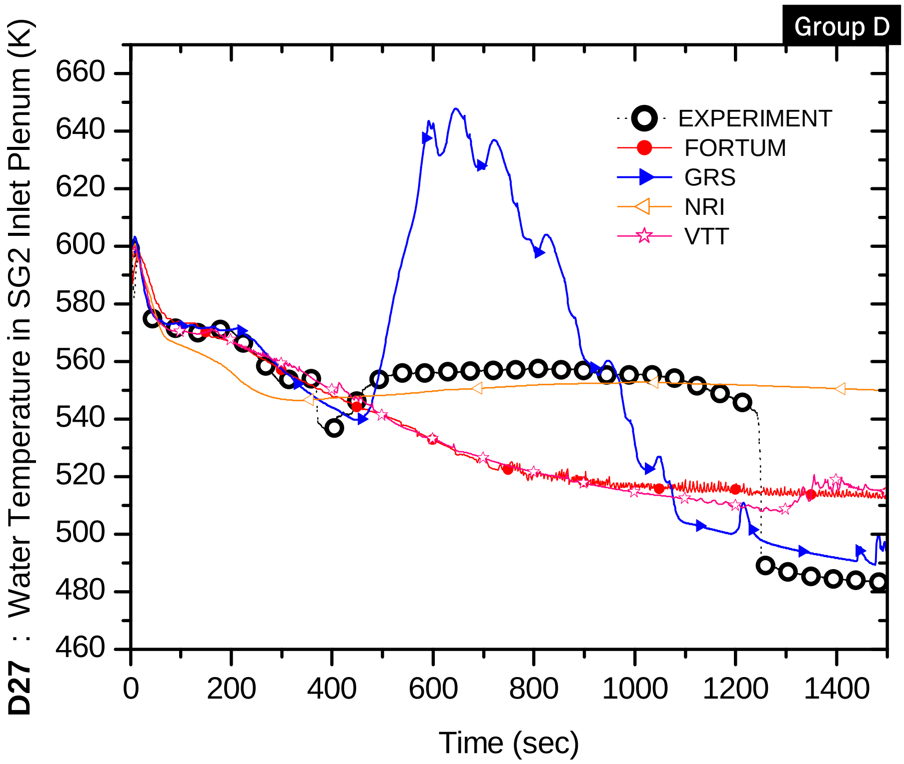

Figure B.27-D Water temperature in SG-2 inlet plenum (D27)

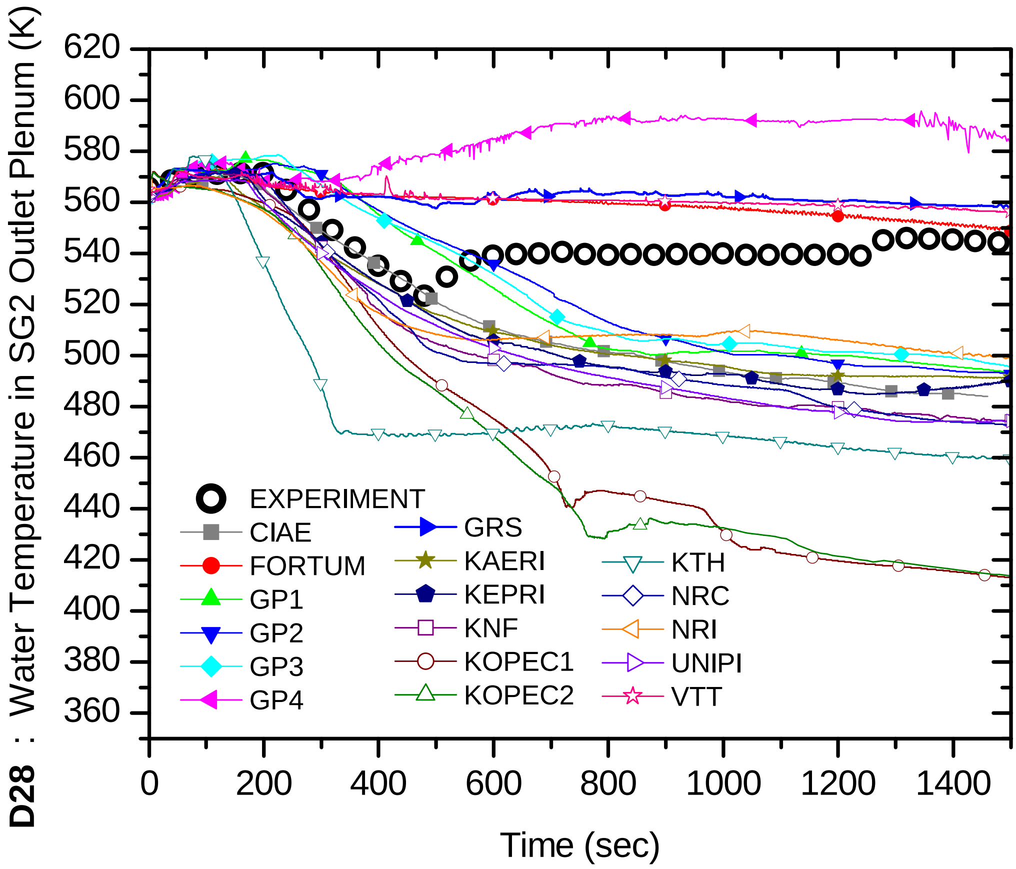

Figure B.28 Water temperature in SG-2 outlet plenum (D28)

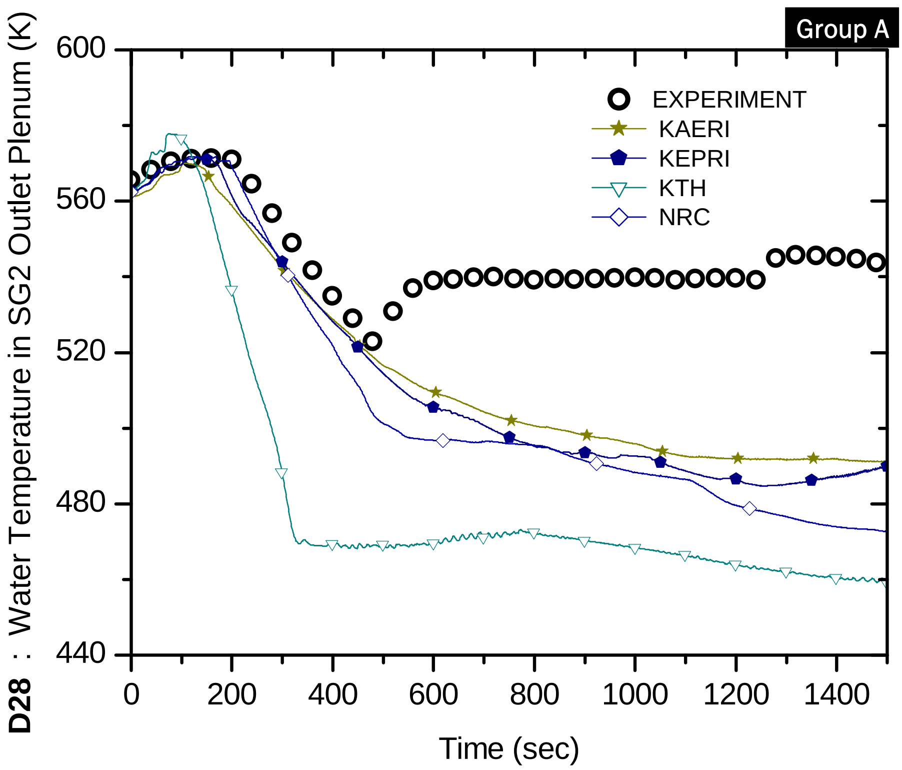

Figure B.28-A Water temperature in SG-2 outlet plenum (D28)

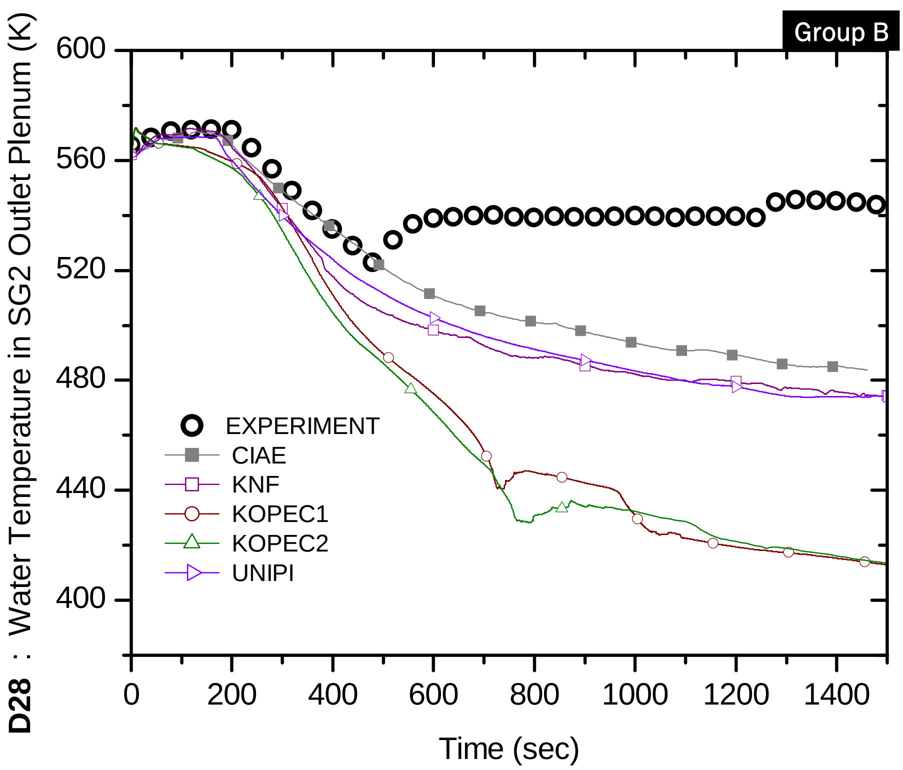

Figure B.28-B Water temperature in SG-2 outlet plenum (D28)

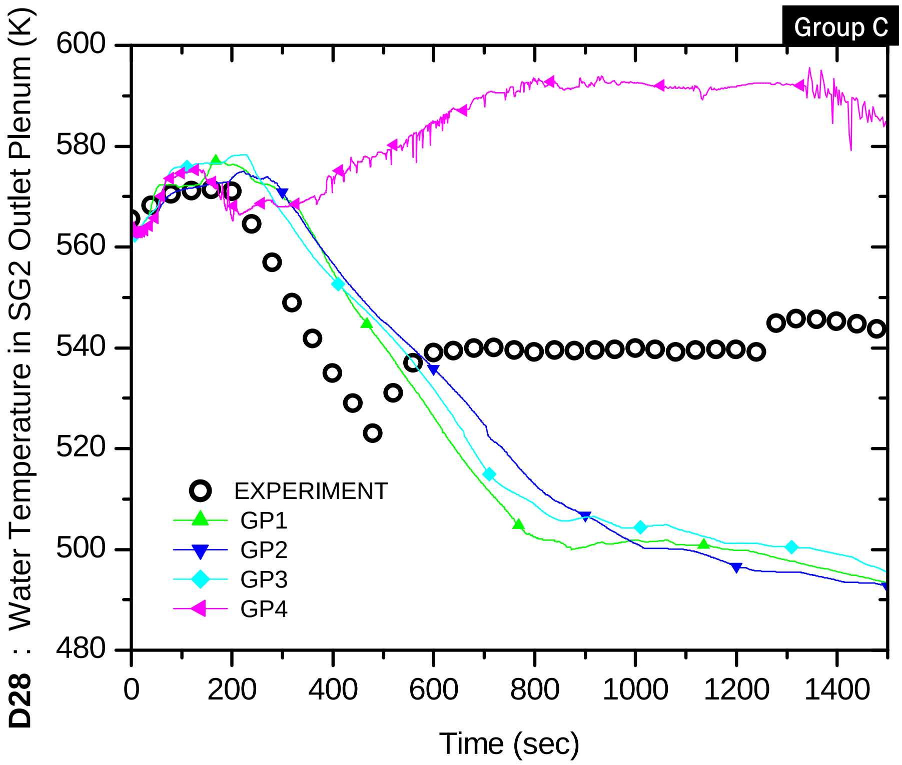

Figure B.28-C Water temperature in SG-2 outlet plenum (D28)

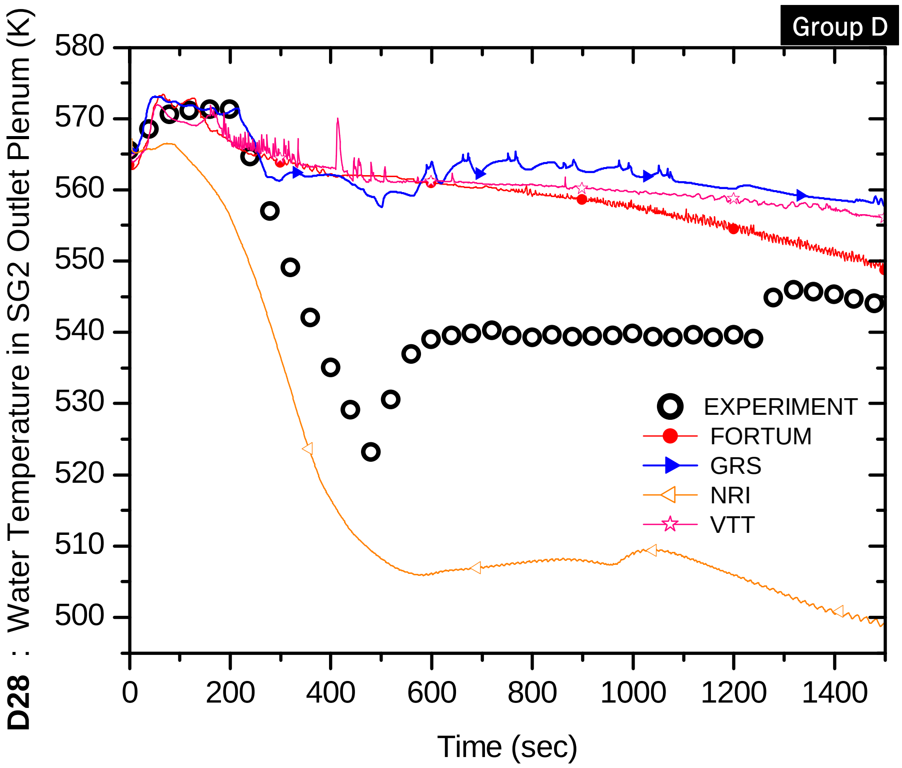

Figure B.28-D Water temperature in SG-2 outlet plenum (D28)

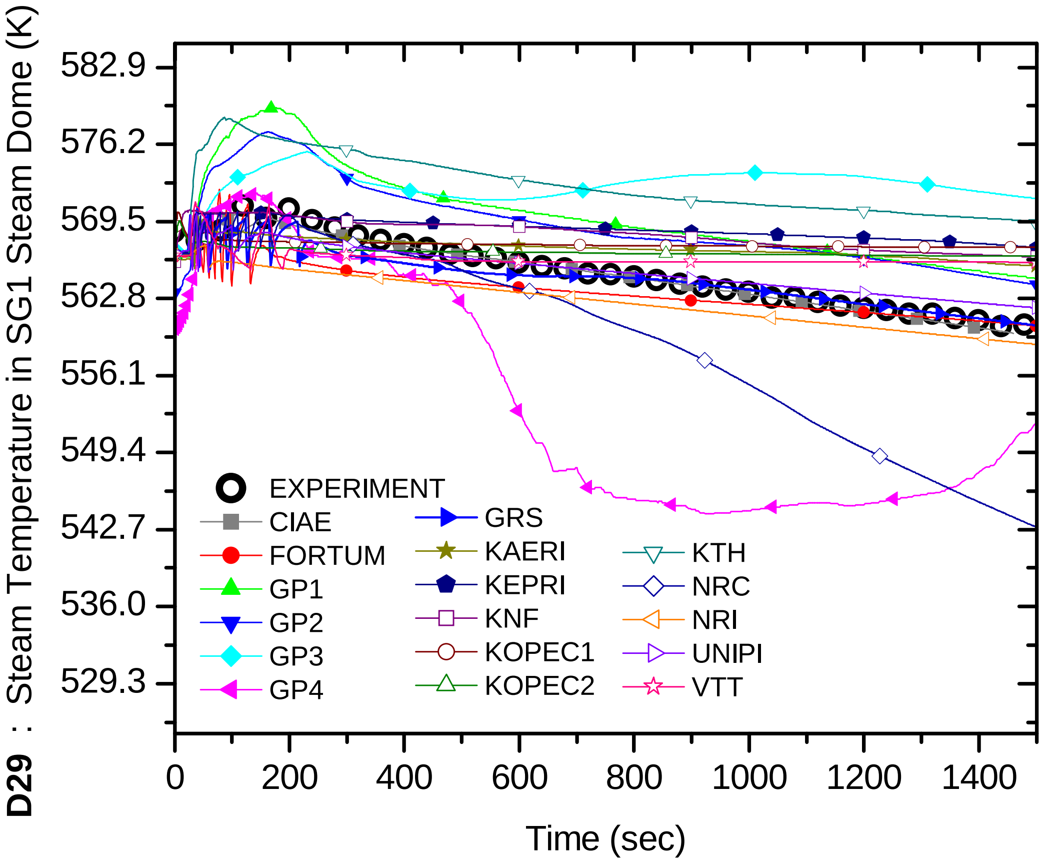

Figure B.29 Steam temperature in SG-1 steam dome (D29)

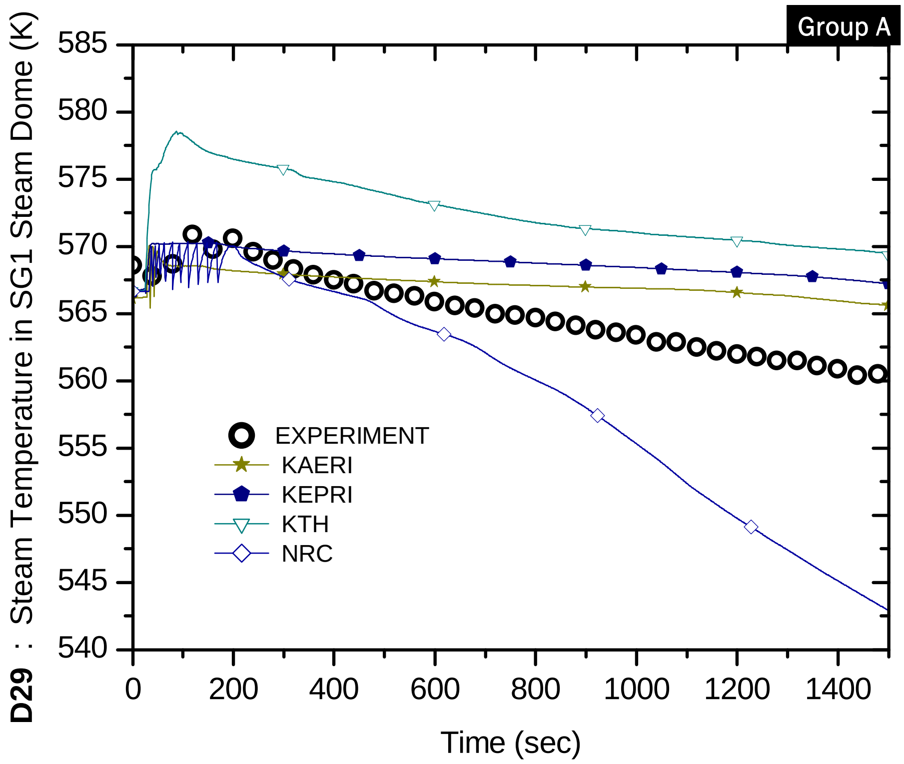

Figure B.29-A Steam temperature in SG-1 steam dome (D29)

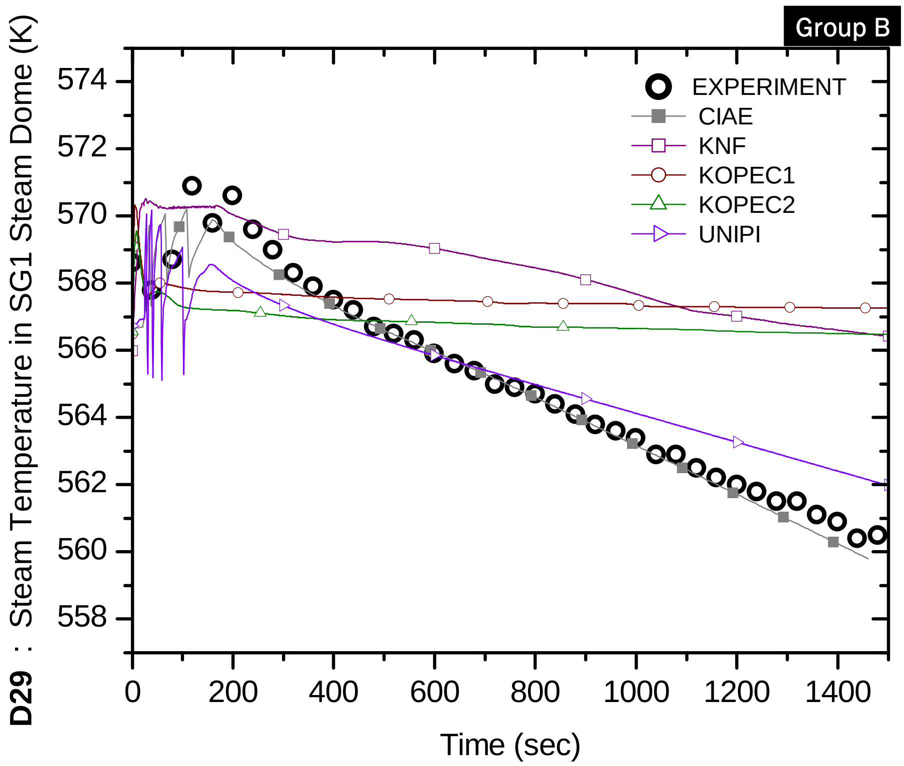

Figure B.29-B Steam temperature in SG-1 steam dome (D29)

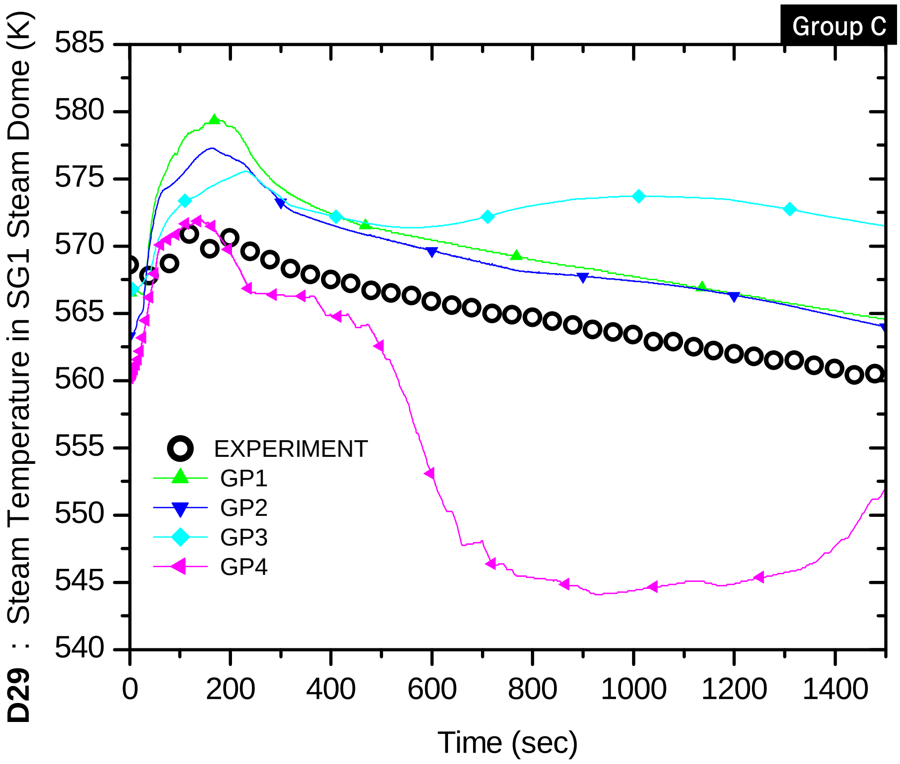

Figure B.29-C Steam temperature in SG-1 steam dome (D29)

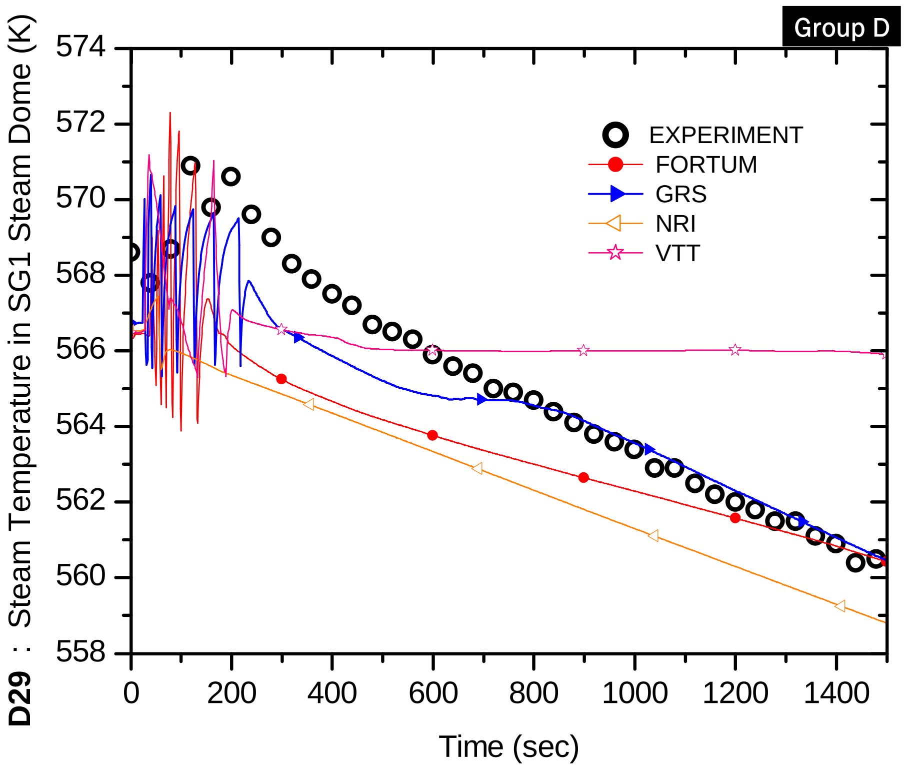

Figure B.29-D Steam temperature in SG-1 steam dome (D29)

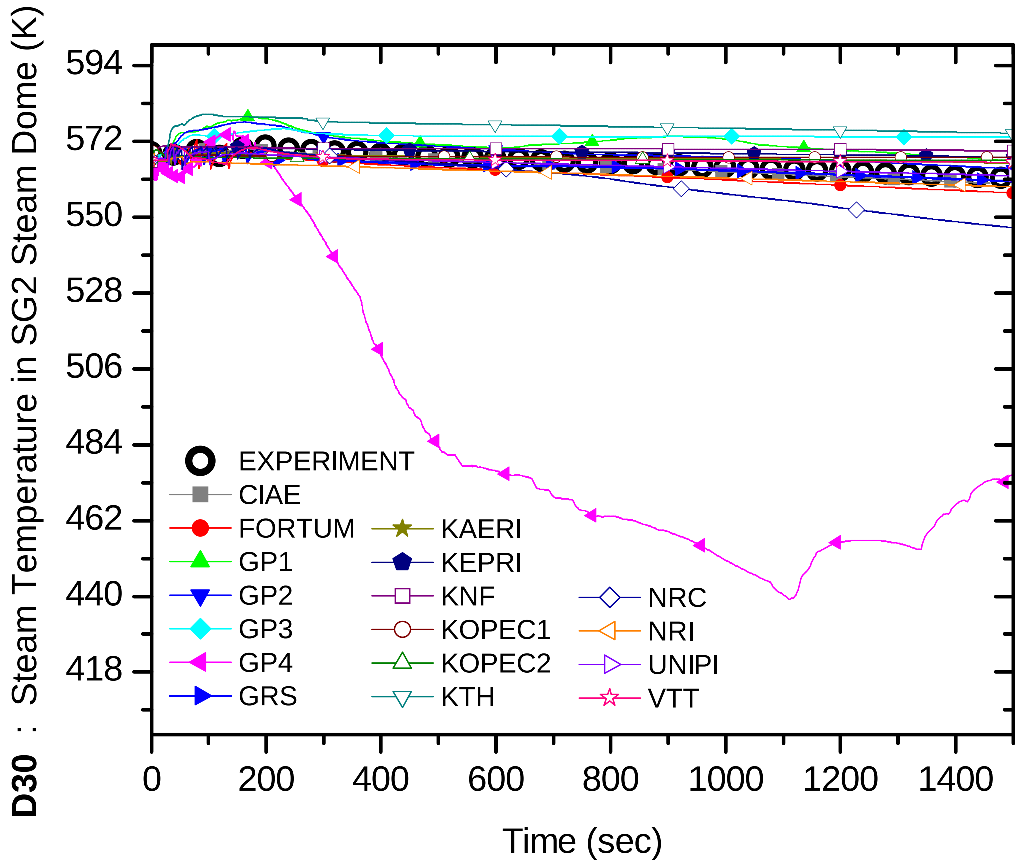

Figure B.30 Steam temperature in SG-2 steam dome (D30)

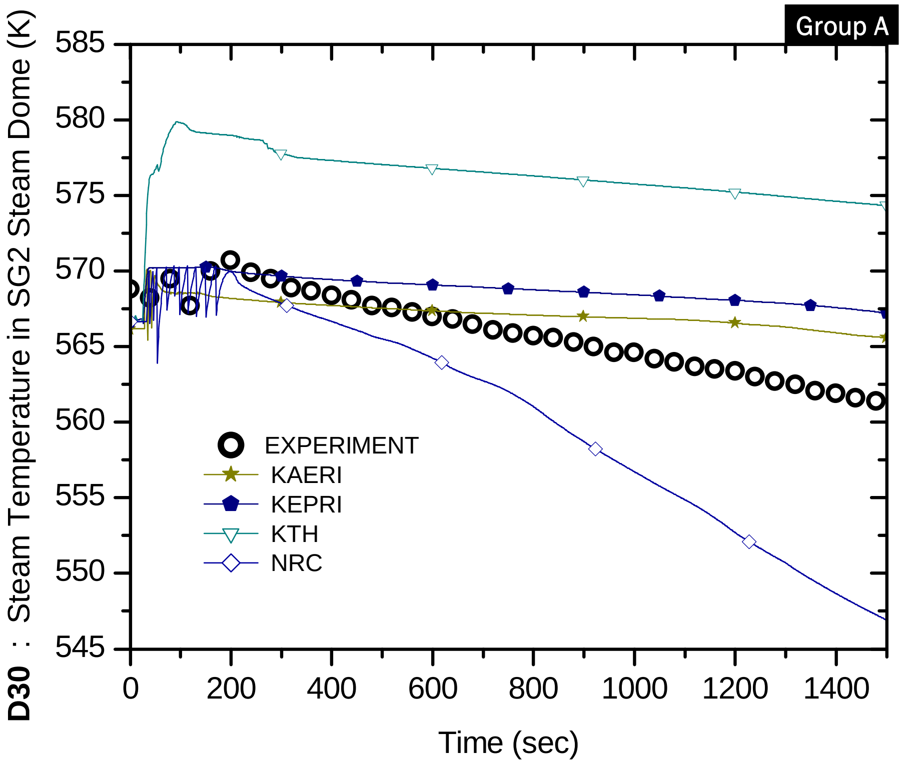

Figure B.30-A Steam temperature in SG-2 steam dome (D30)

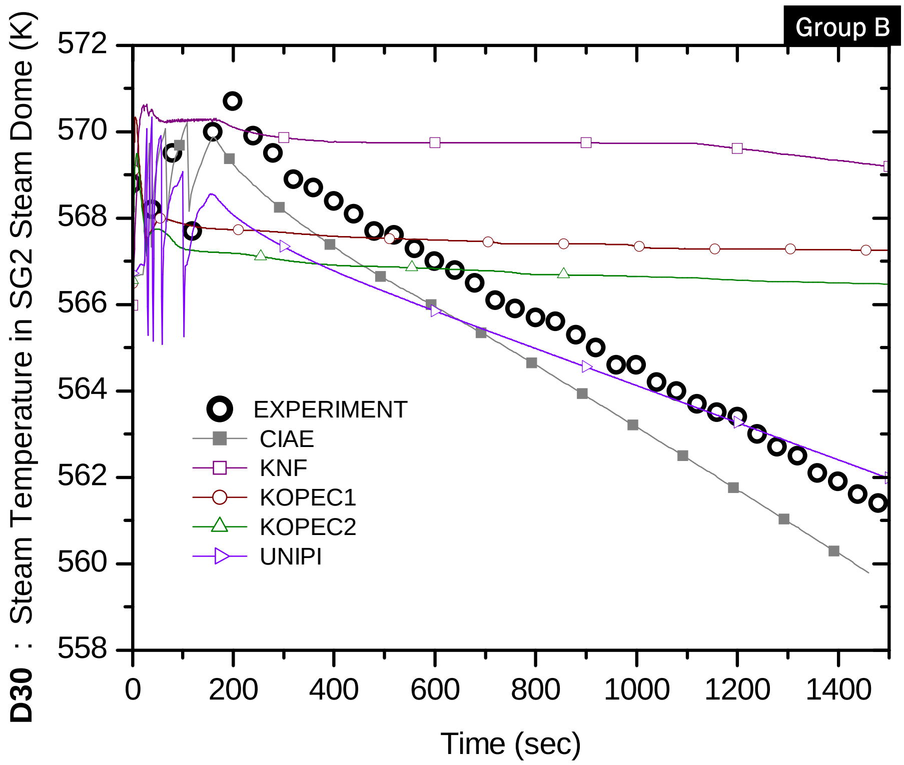

Figure B.30-B Steam temperature in SG-2 steam dome (D30)

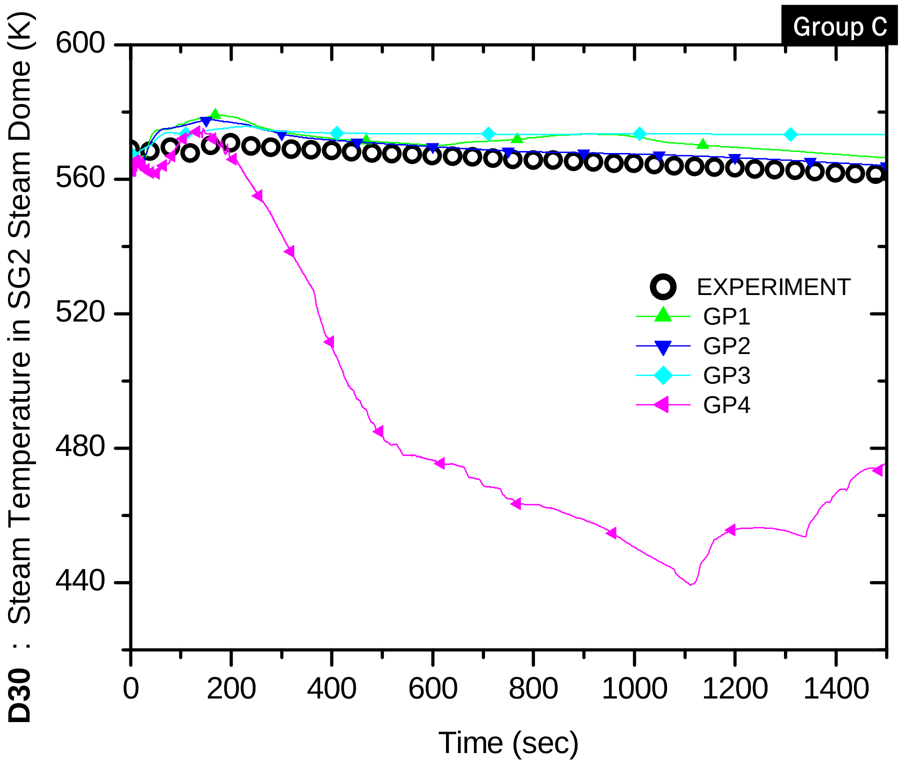

Figure B.30-C Steam temperature in SG-2 steam dome (D30)

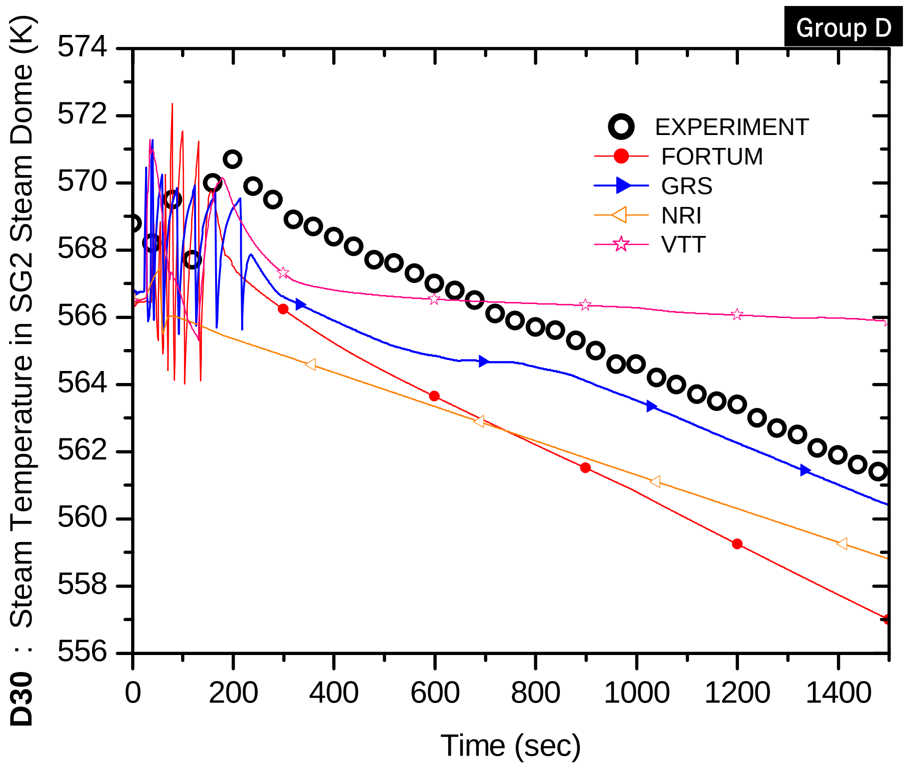

Figure B.30-D Steam temperature in SG-2 steam dome (D30)

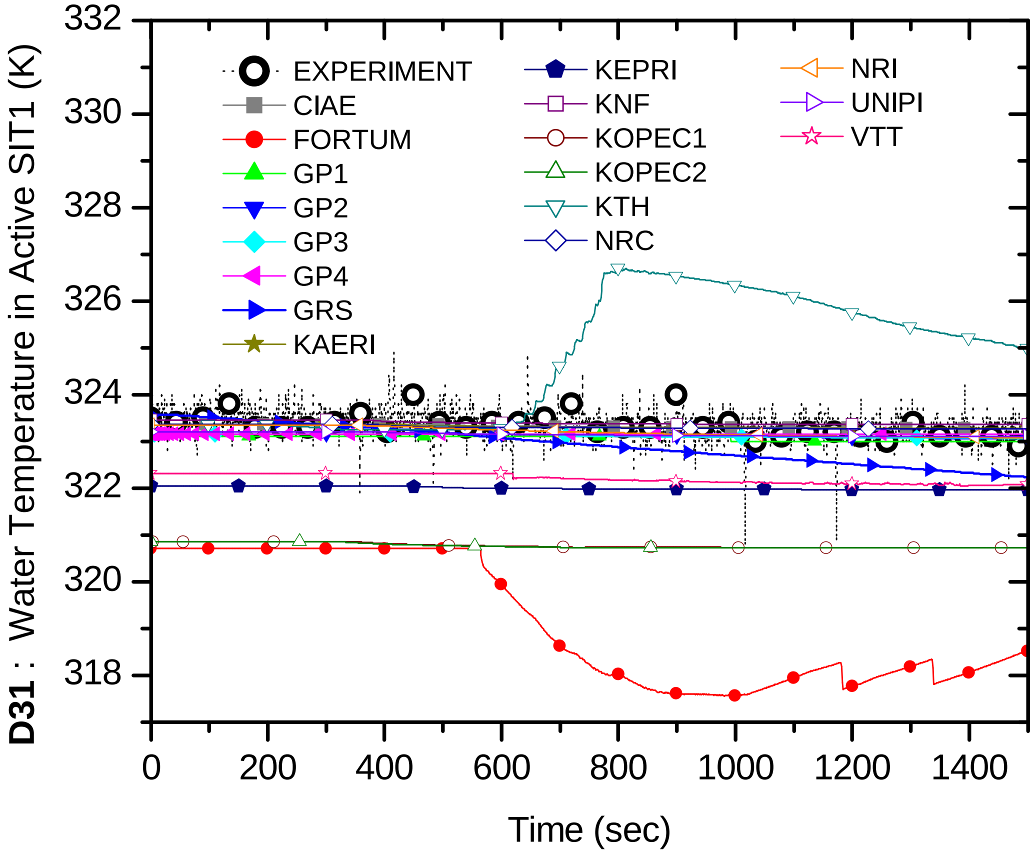

Figure B.31 Water temperature in the SIT-1 (D31)

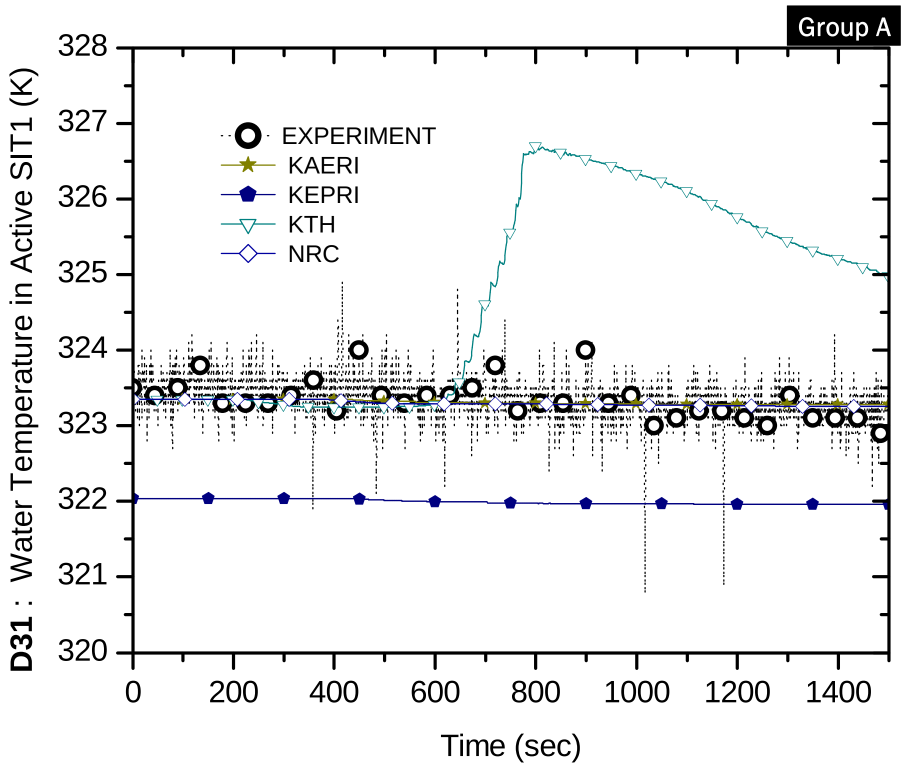

Figure B.31-A Water temperature in the SIT-1 (D31)

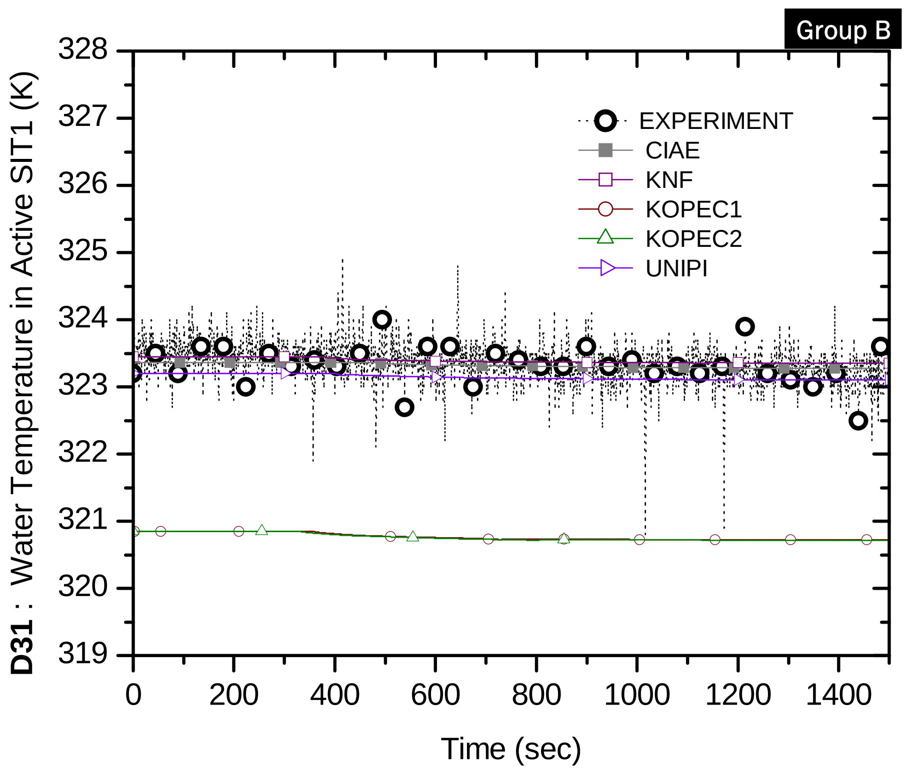

Figure B.31-B Water temperature in the SIT-1 (D31)

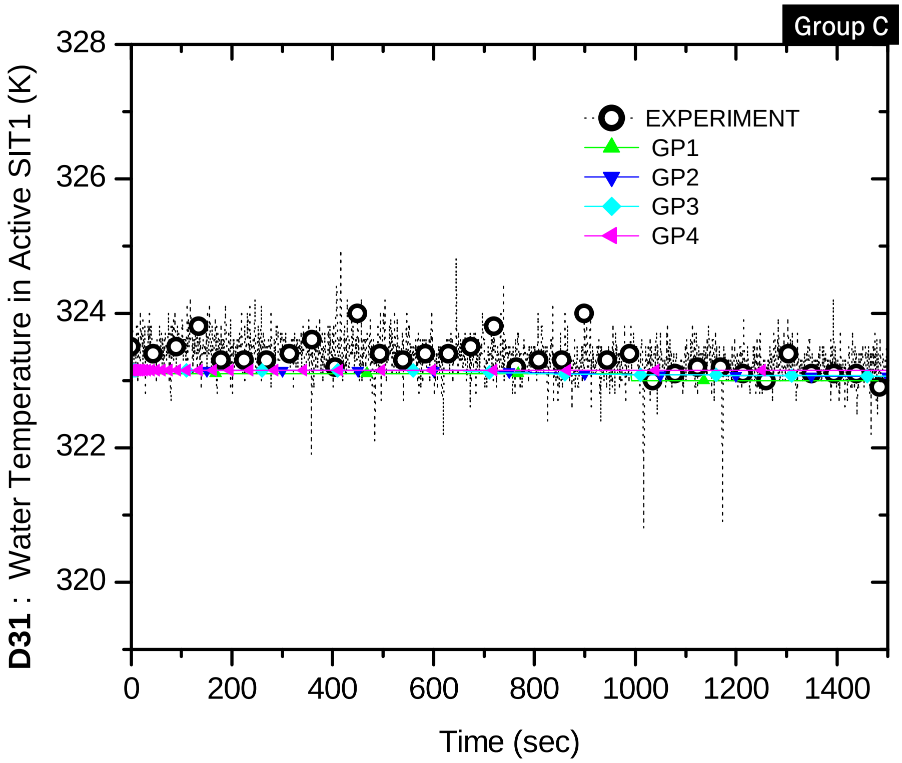

Figure B.31-C Water temperature in the SIT-1 (D31)

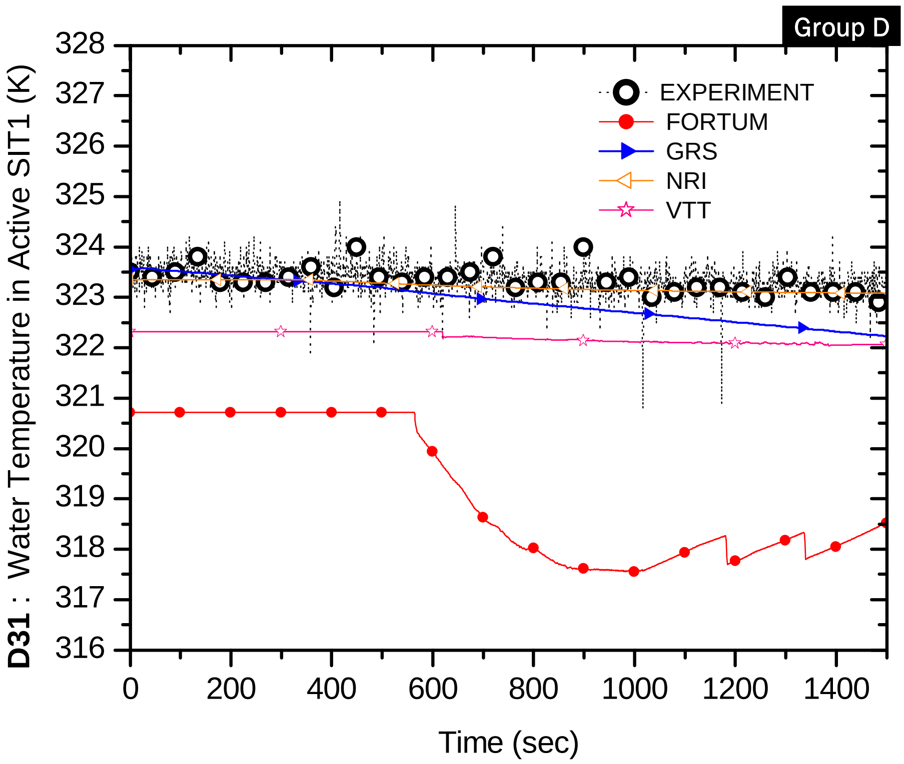

Figure B.31-D Water temperature in the SIT-1 (D31)

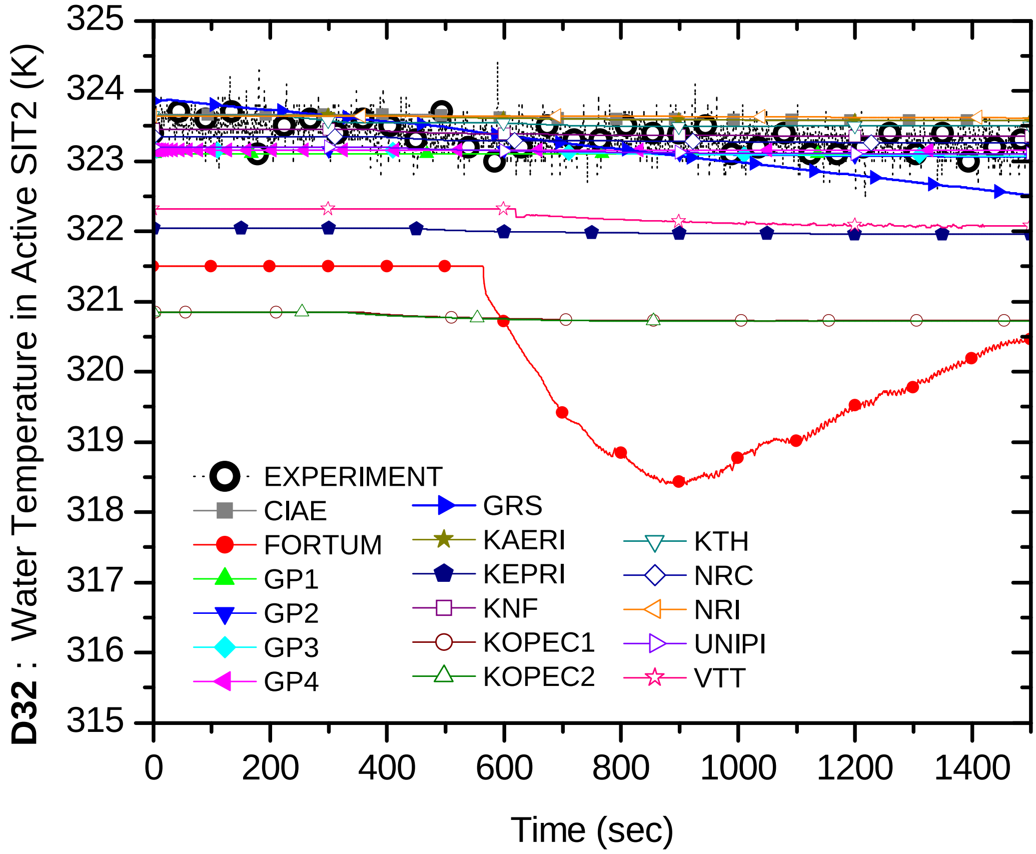

Figure B.32 Water temperature in the SIT-2 (D32)

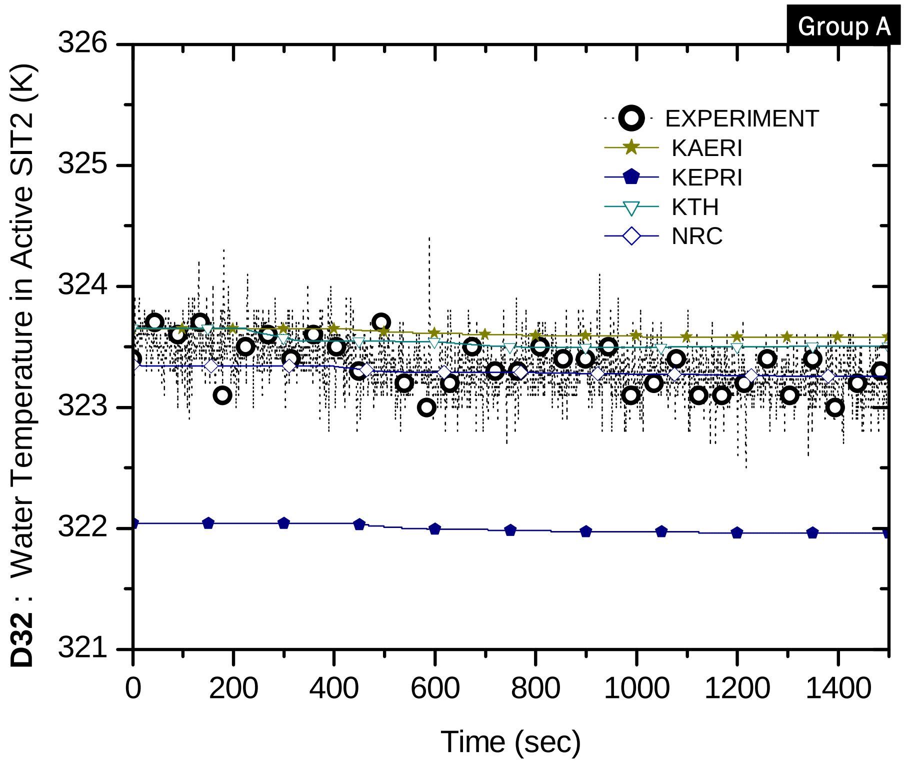

Figure B.32-A Water temperature in the SIT-2 (D32)

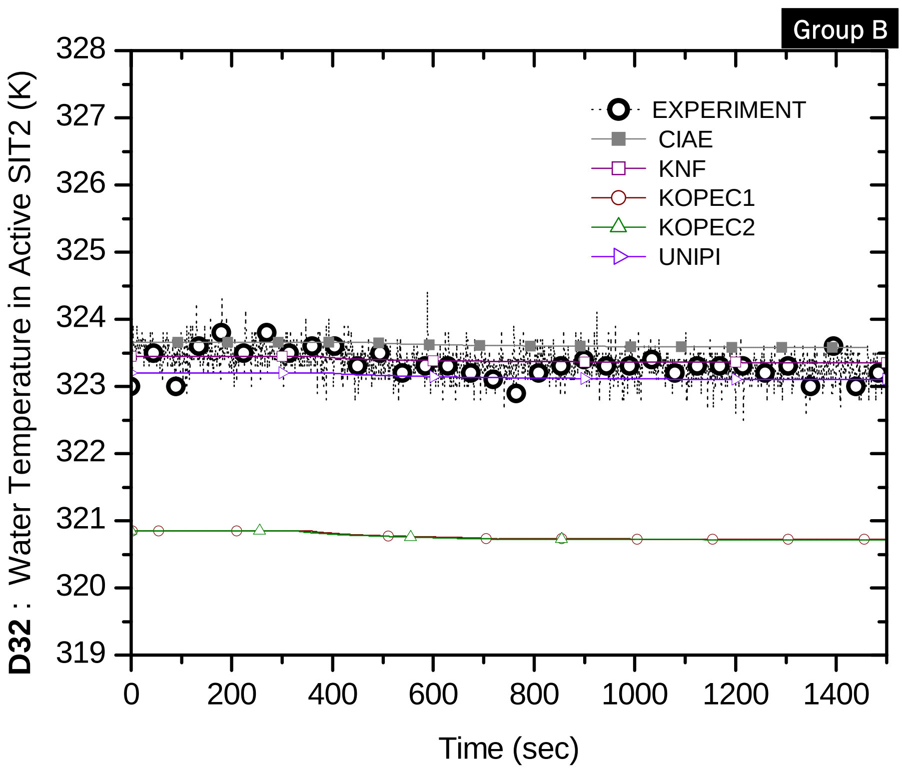

Figure B.32-B Water temperature in the SIT-2 (D32)

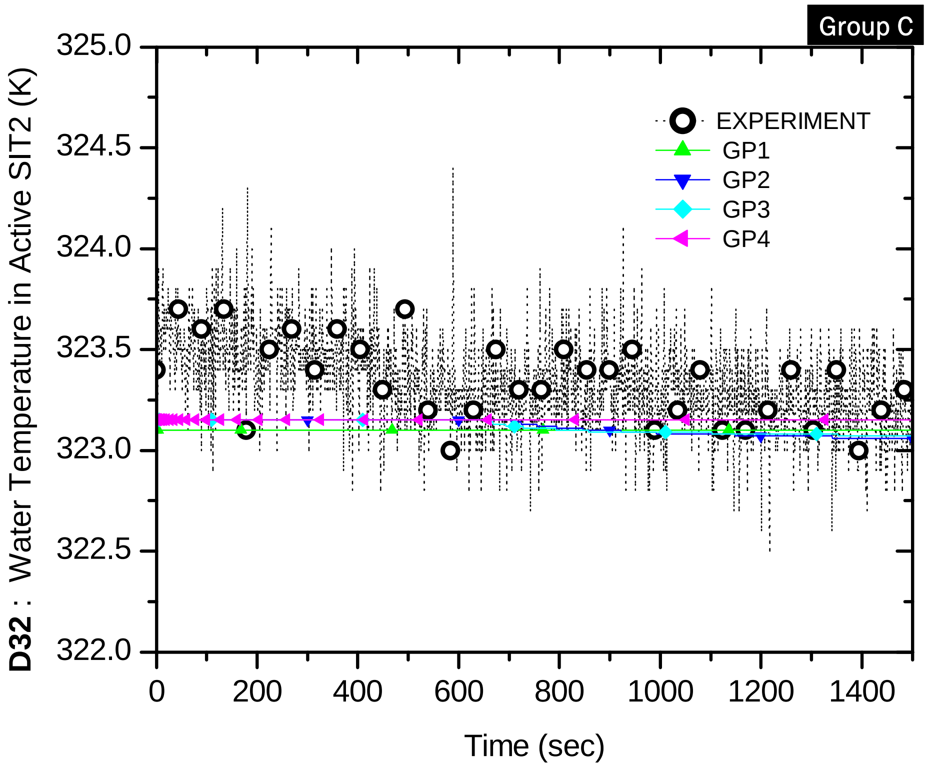

Figure B.32-C Water temperature in the SIT-2 (D32)

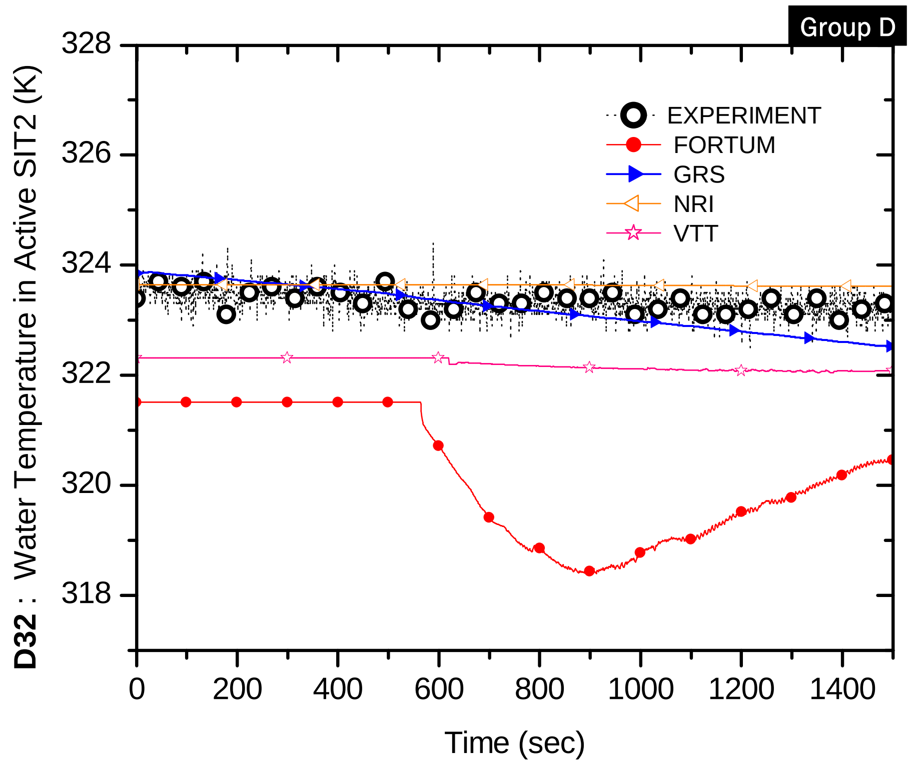

Figure B.32-DWater temperature in the SIT-2 (D32)

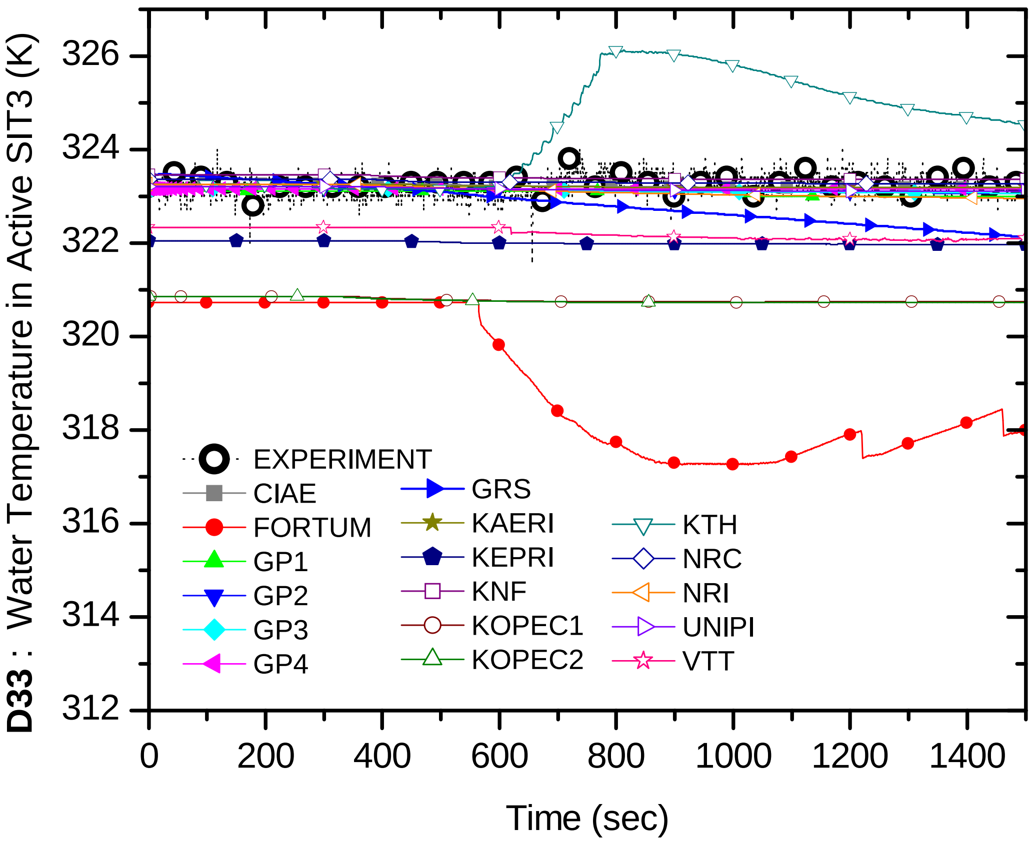

Figure B.33 Water temperature in the SIT-3 (D33)

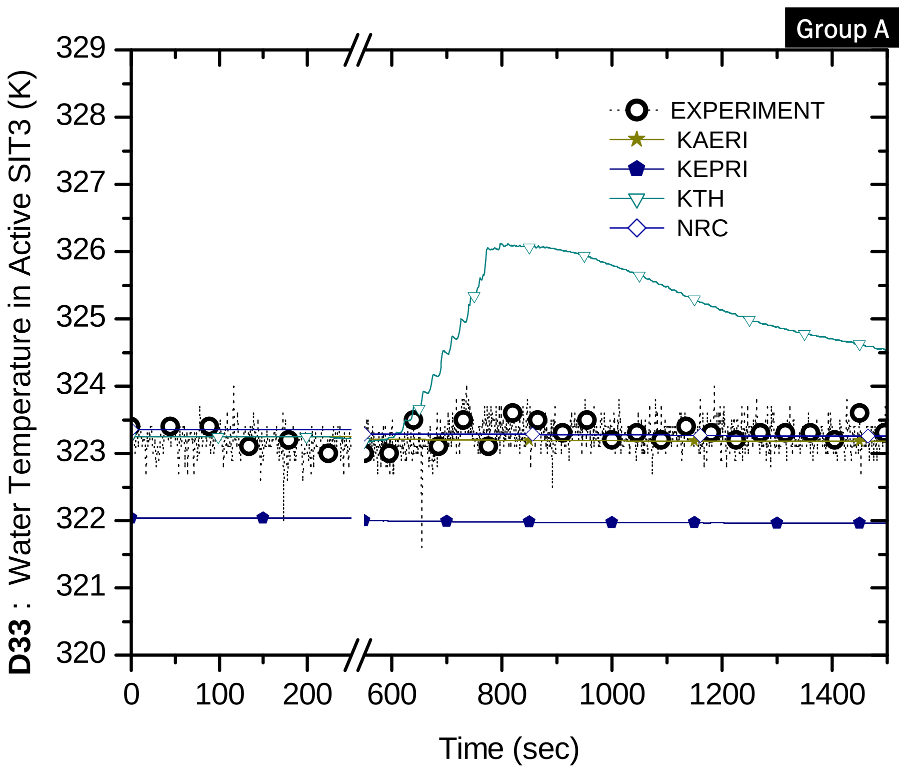

Figure B.33-A Water temperature in the SIT-3 (D33)

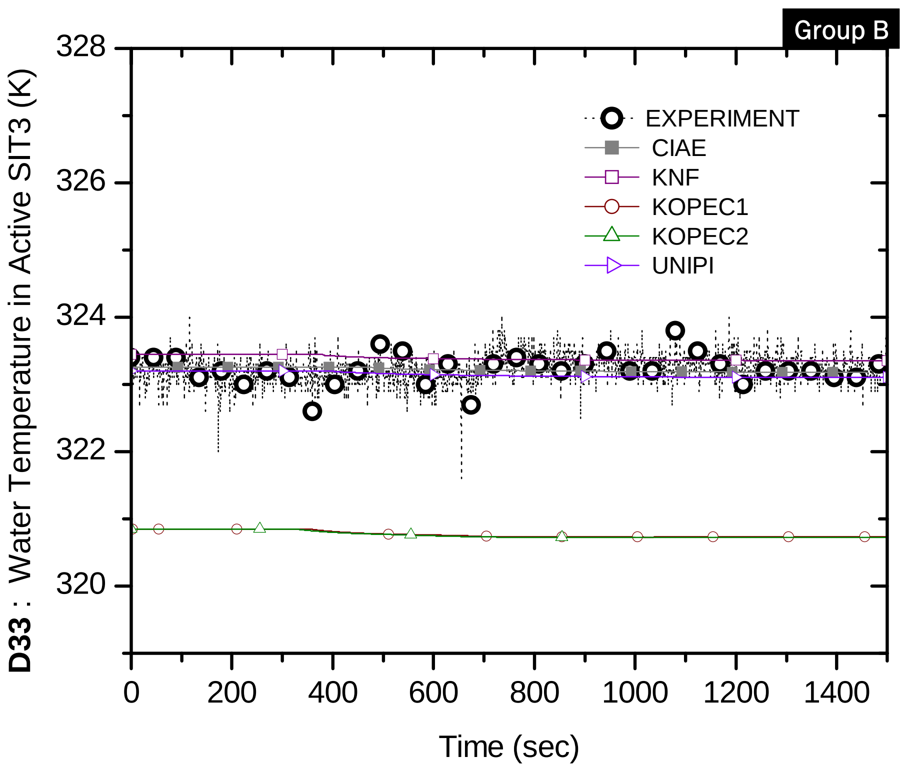

Figure B.33-B Water temperature in the SIT-3 (D33)

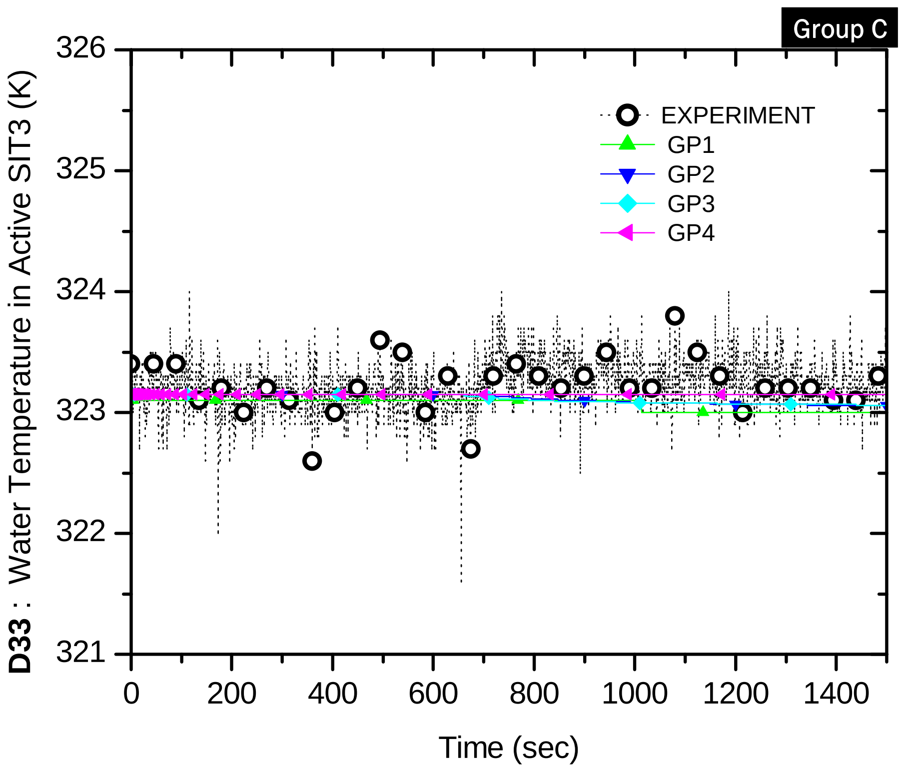

Figure B.33-C Water temperature in the SIT-3 (D33)

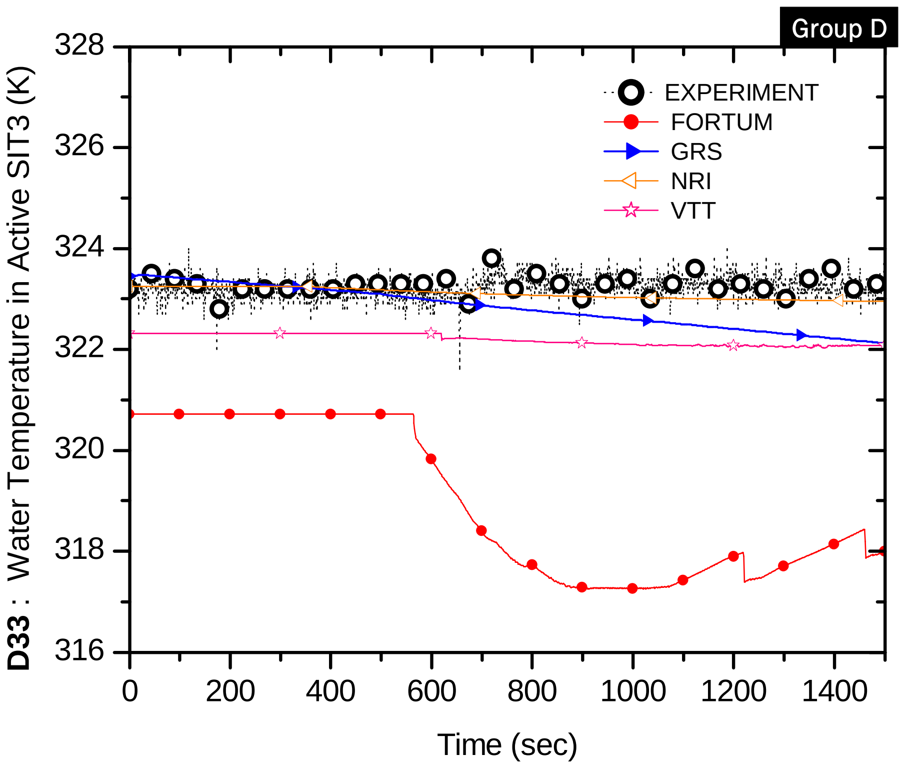

Figure B.33-D Water temperature in the SIT-3 (D33)

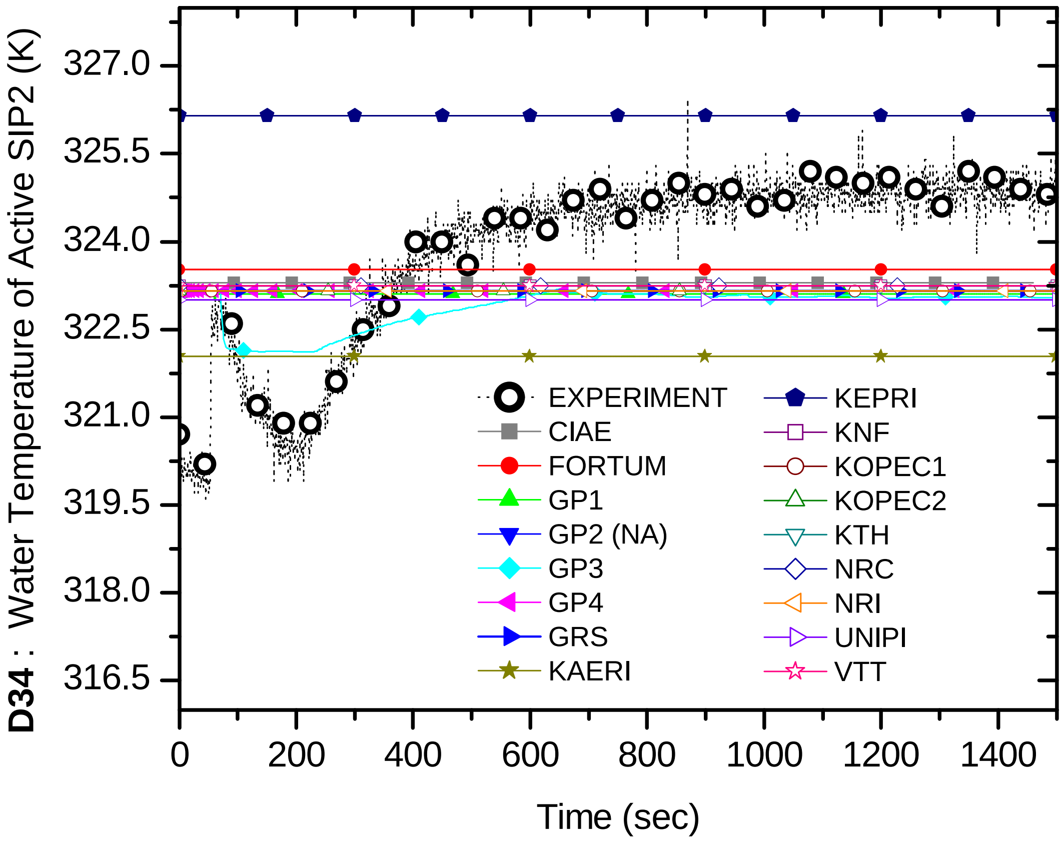

Figure B.34 Water temperature in the SIP-2 (D34)

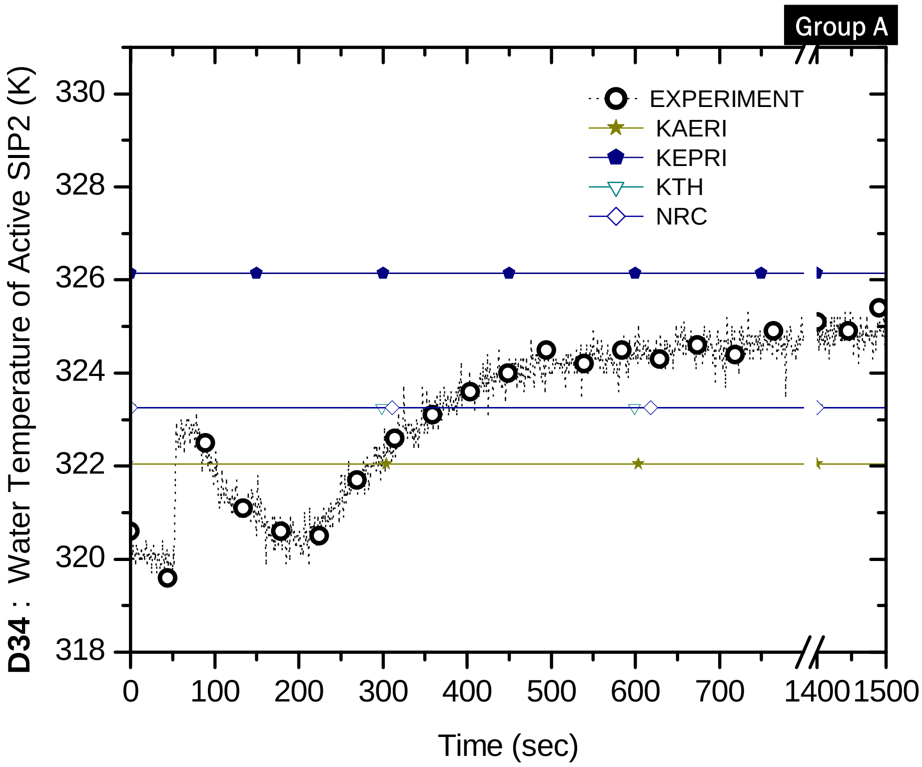

Figure B.34-A Water temperature in the SIP-2 (D34)

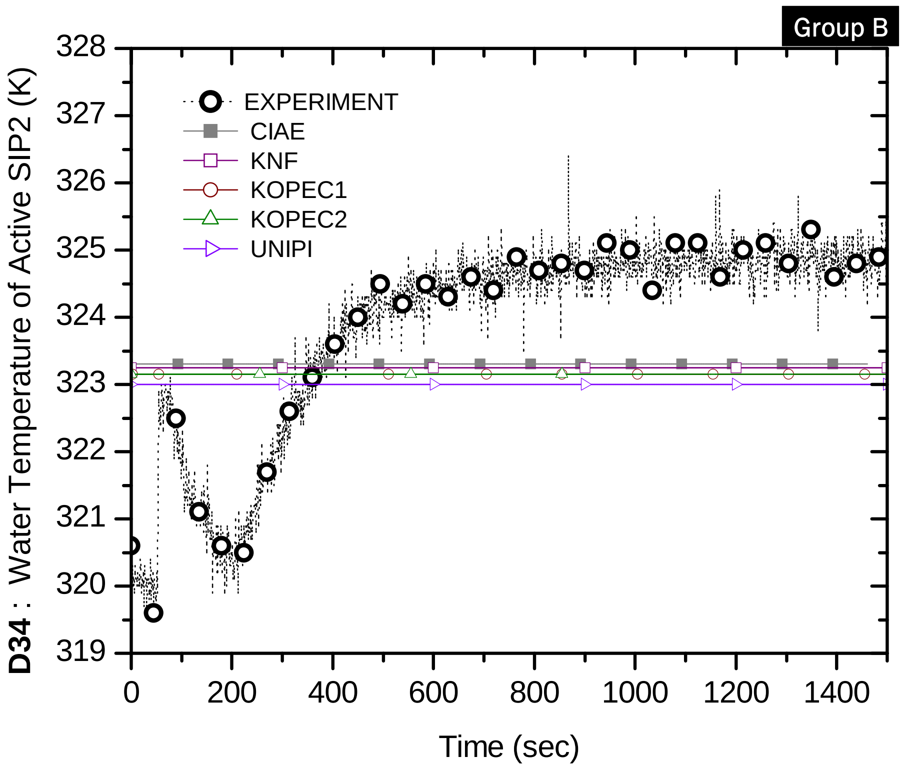

Figure B.34-B Water temperature in the SIP-2 (D34)

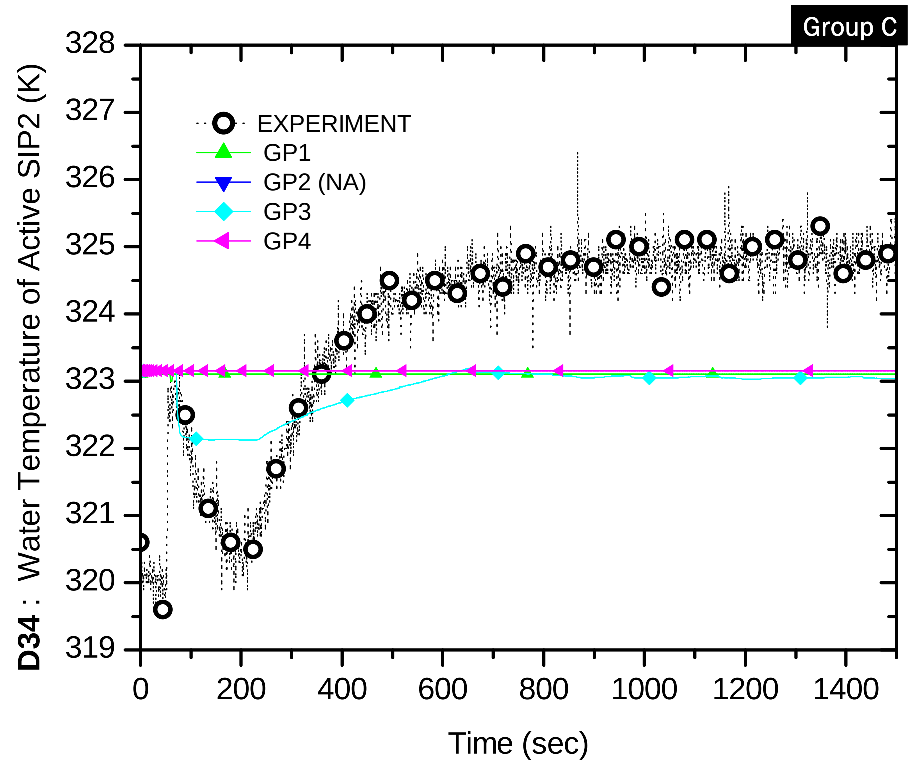

Figure B.34-C Water temperature in the SIP-2 (D34)

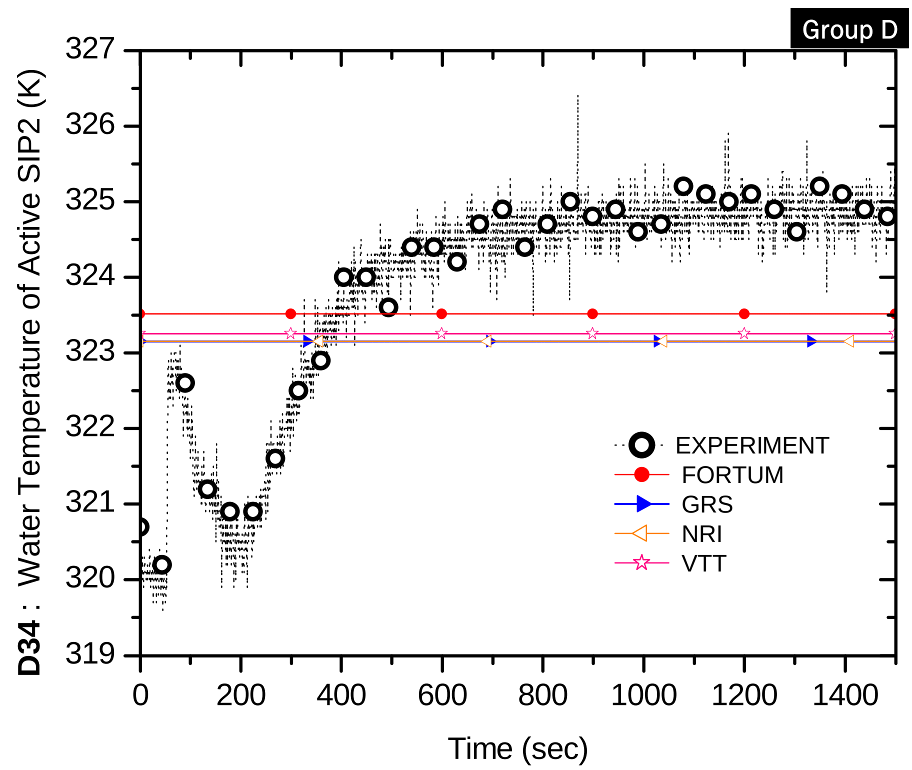

Figure B.34-D Water temperature in the SIP-2 (D34)

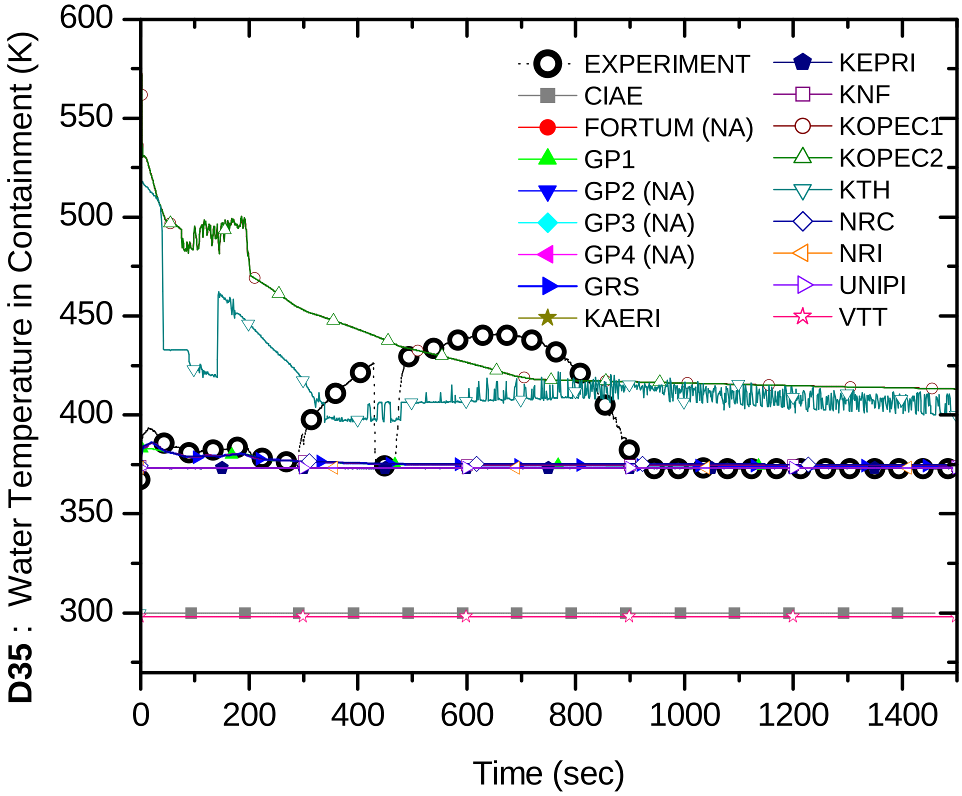

Figure B.35 Temperature in the containment (D35)

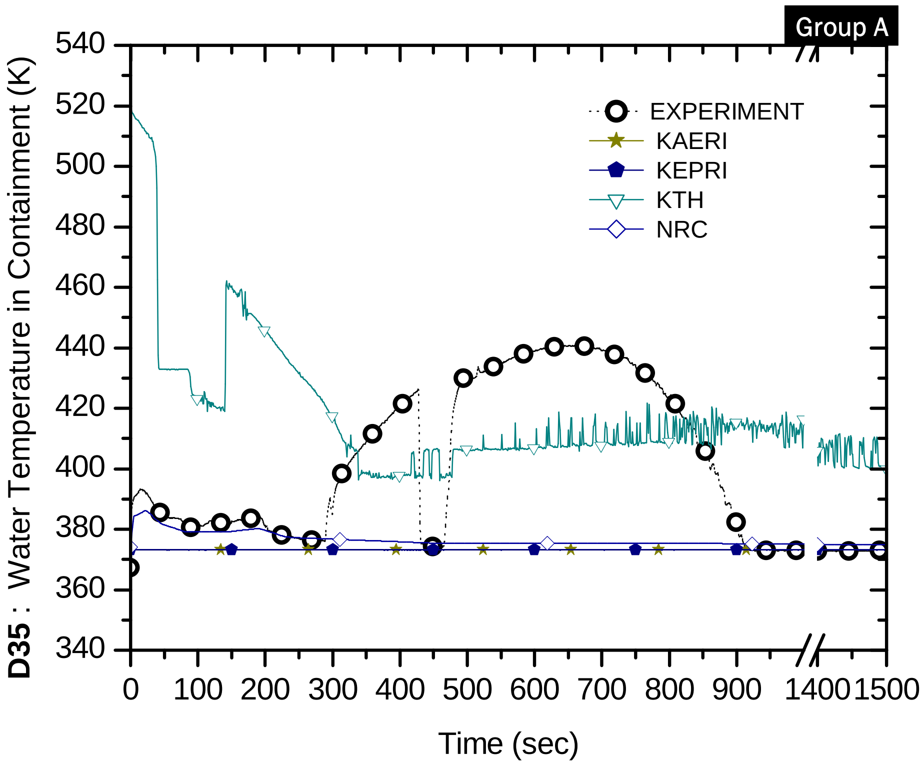

Figure B.35-A Temperature in the containment (D35)

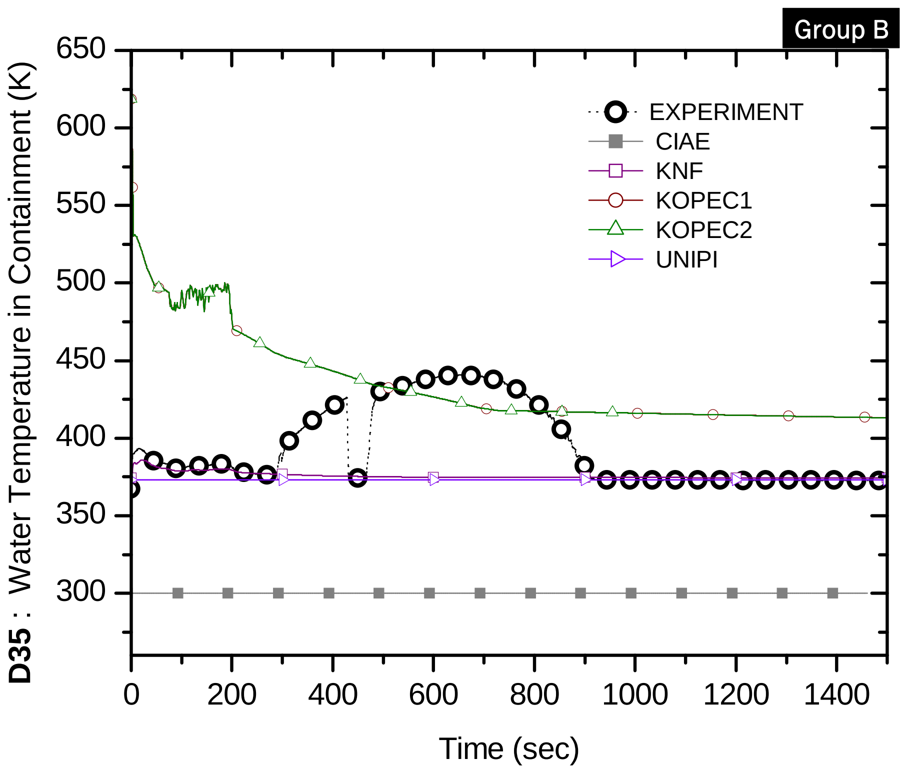

Figure B.35-B Temperature in the containment (D35)

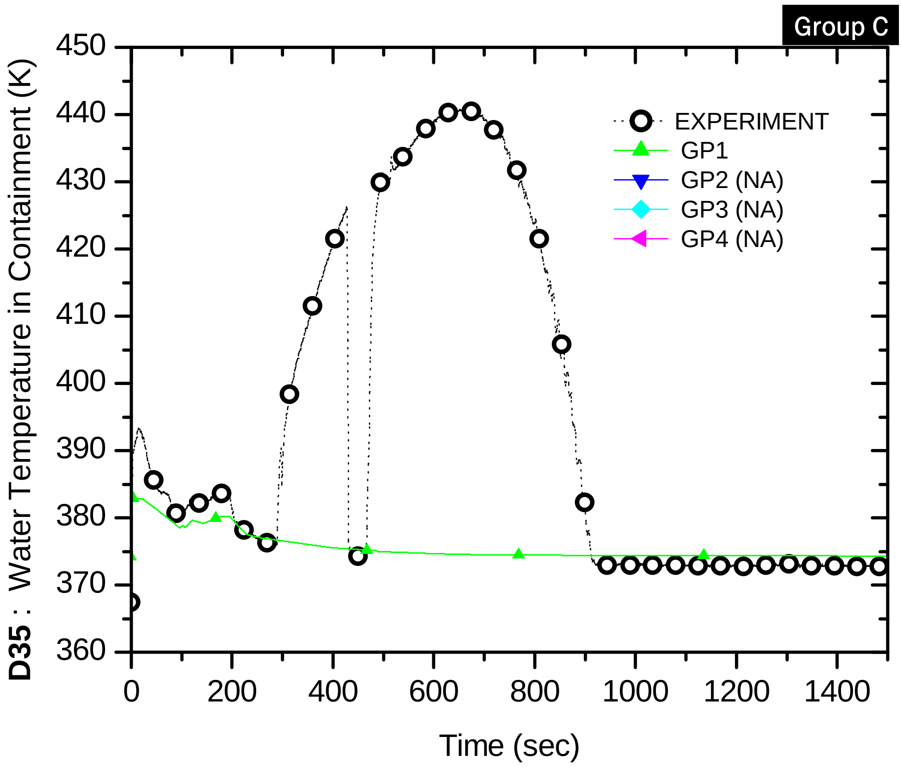

Figure B.35-C Temperature in the containment (D35)

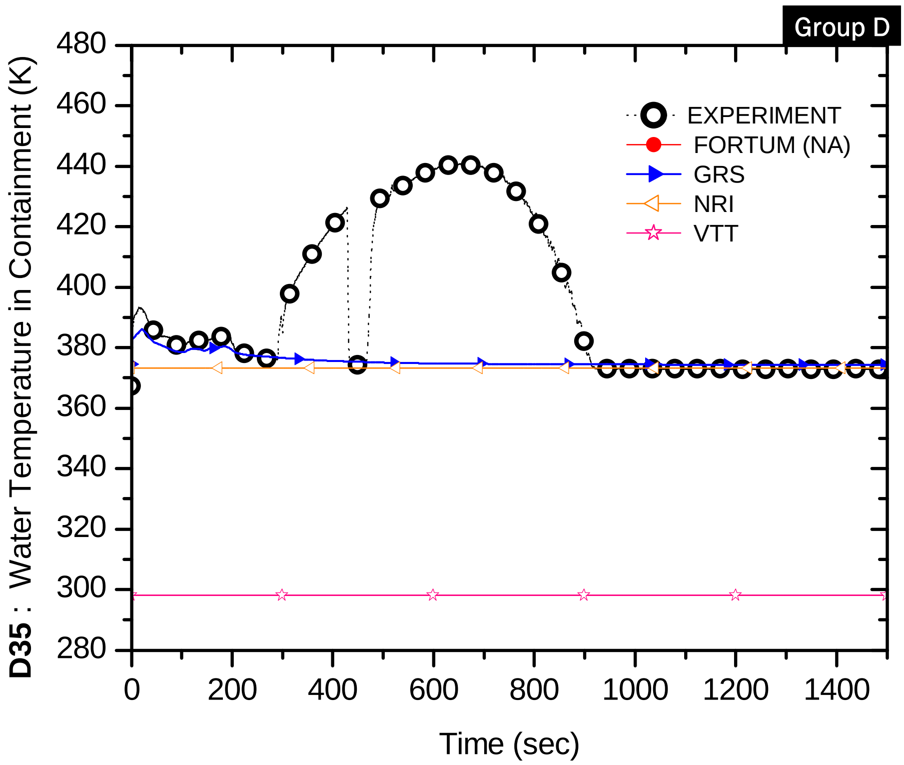

Figure B.35-D Temperature in the containment (D35)

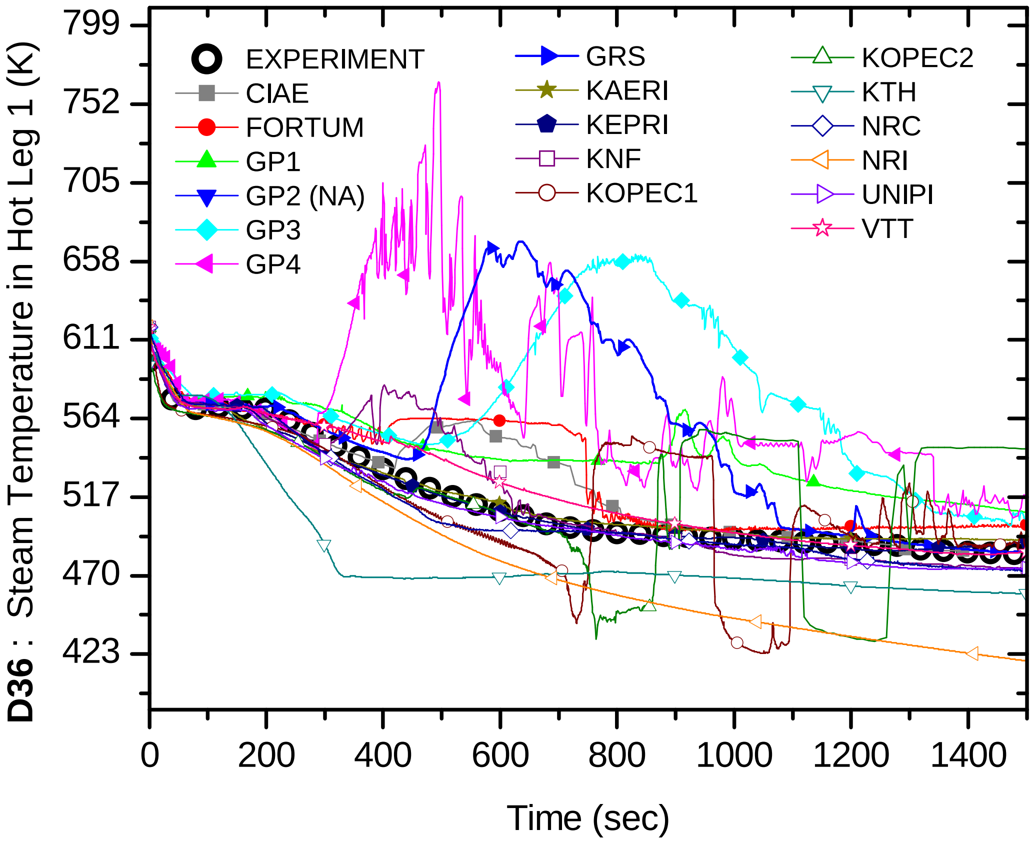

Figure B.36 Steam temperature in the hot leg 1 (D36)

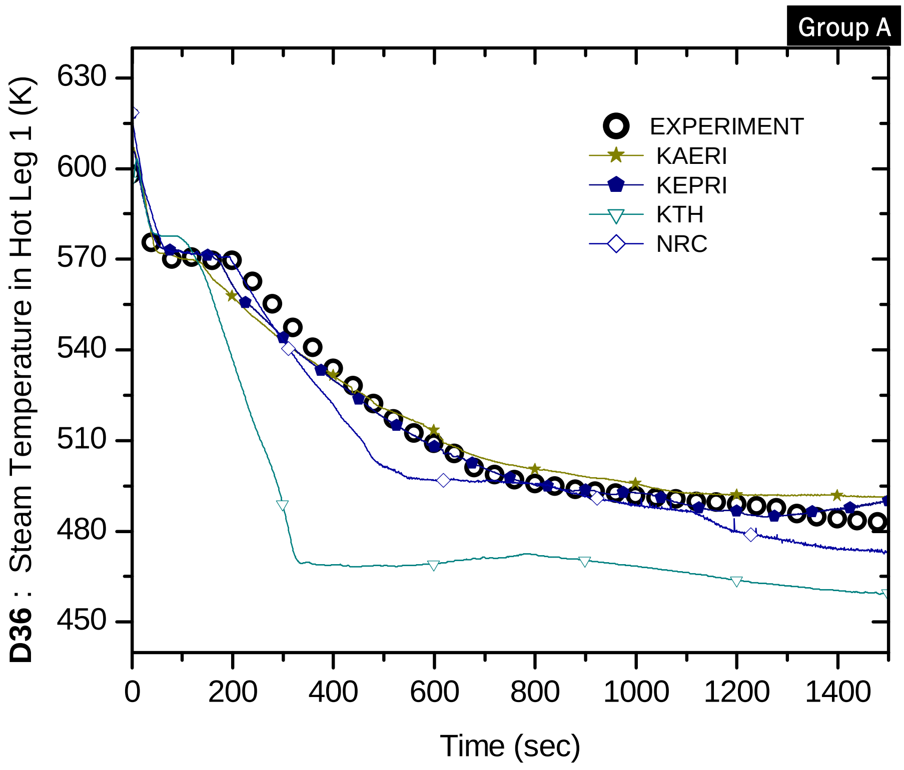

Figure B.36-A Steam temperature in the hot leg 1 (D36)

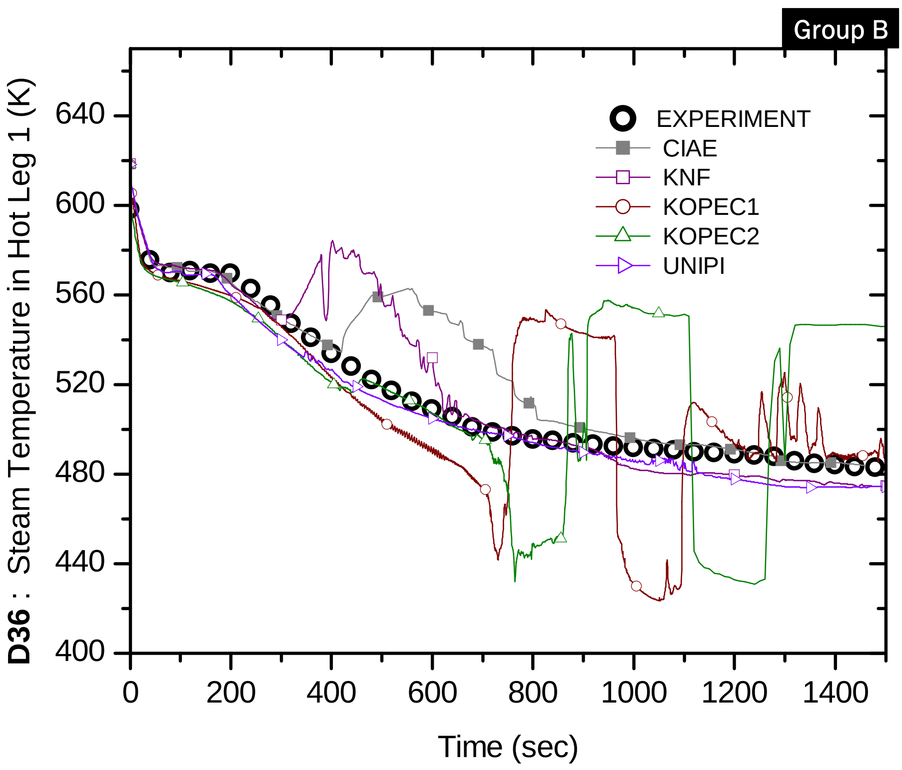

Figure B.36-B Steam temperature in the hot leg 1 (D36)

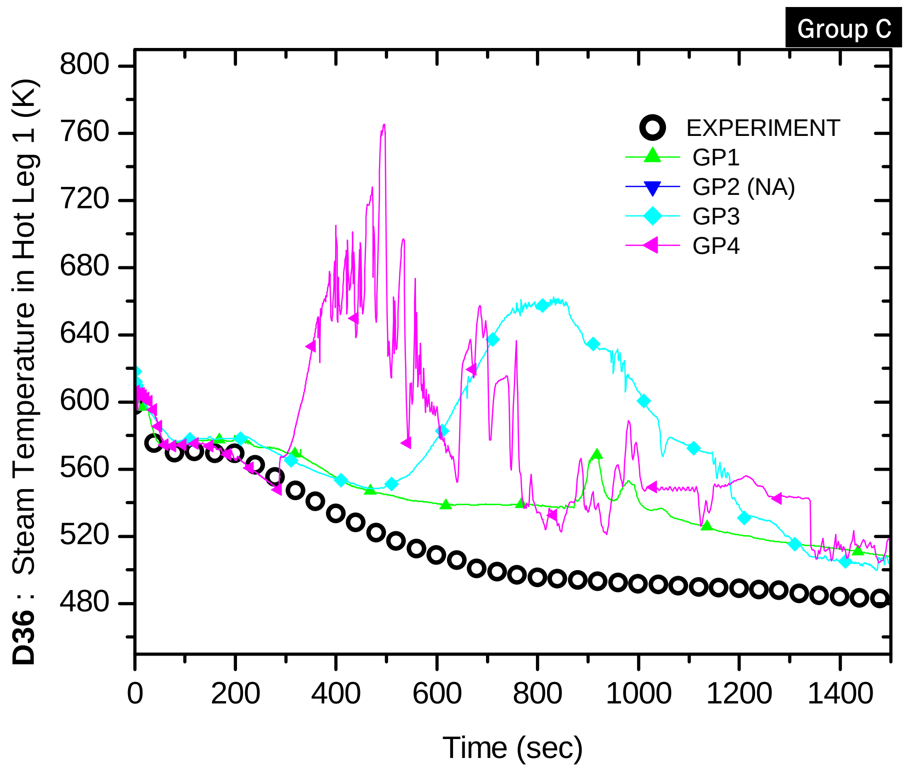

Figure B.36-C Steam temperature in the hot leg 1 (D36)

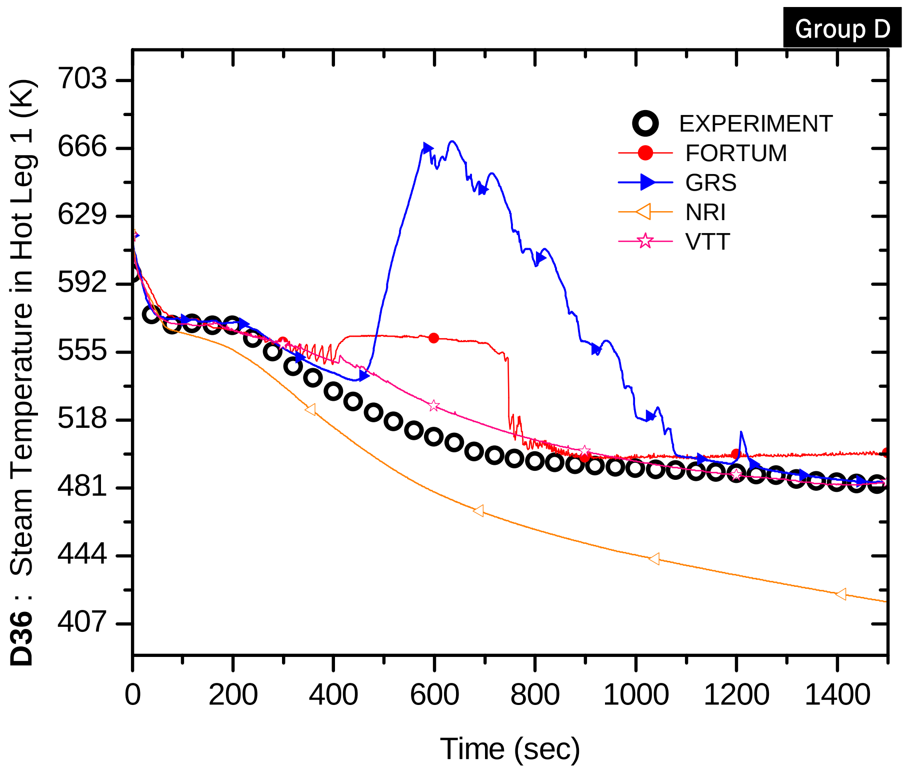

Figure B.36-D Steam temperature in the hot leg 1 (D36)

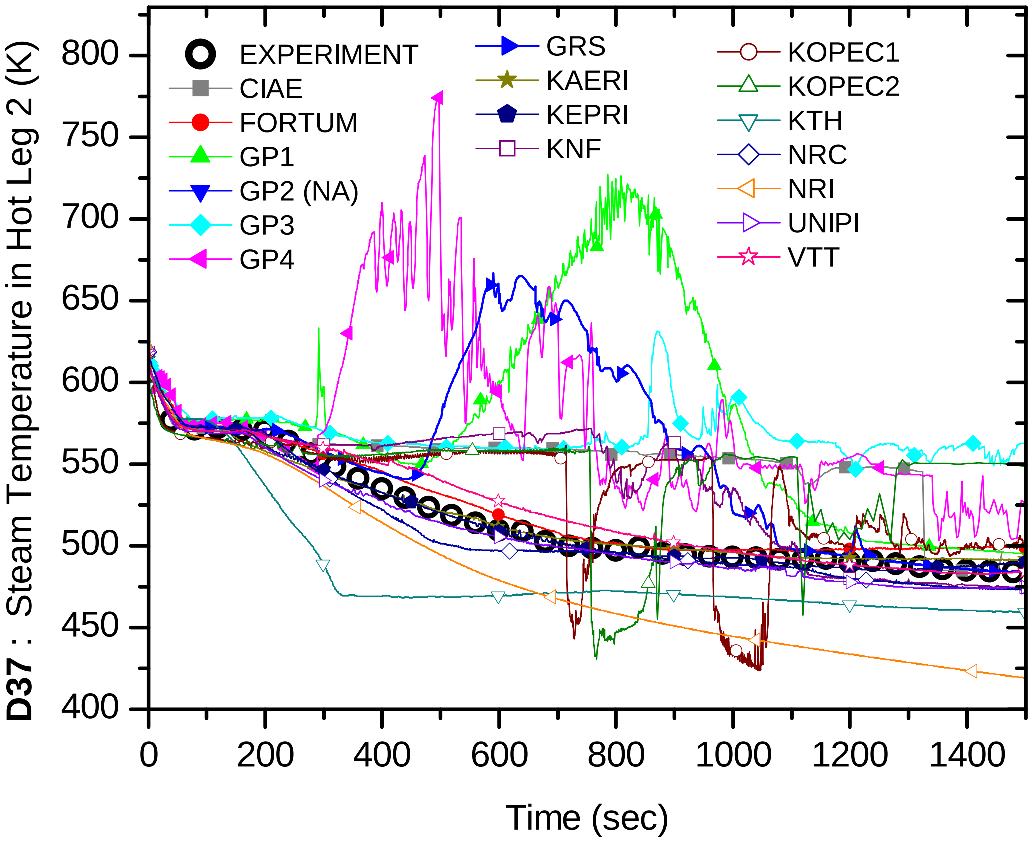

Figure B.37 Steam temperature in the hot leg 2 (D37)

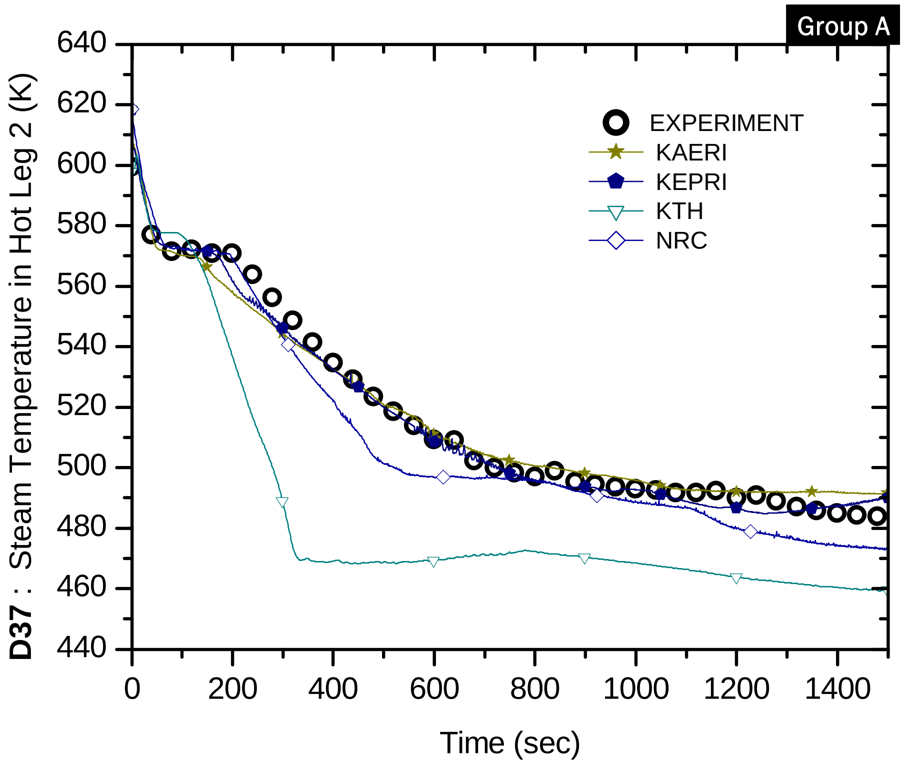

Figure B.37-A Steam temperature in the hot leg 2 (D37)

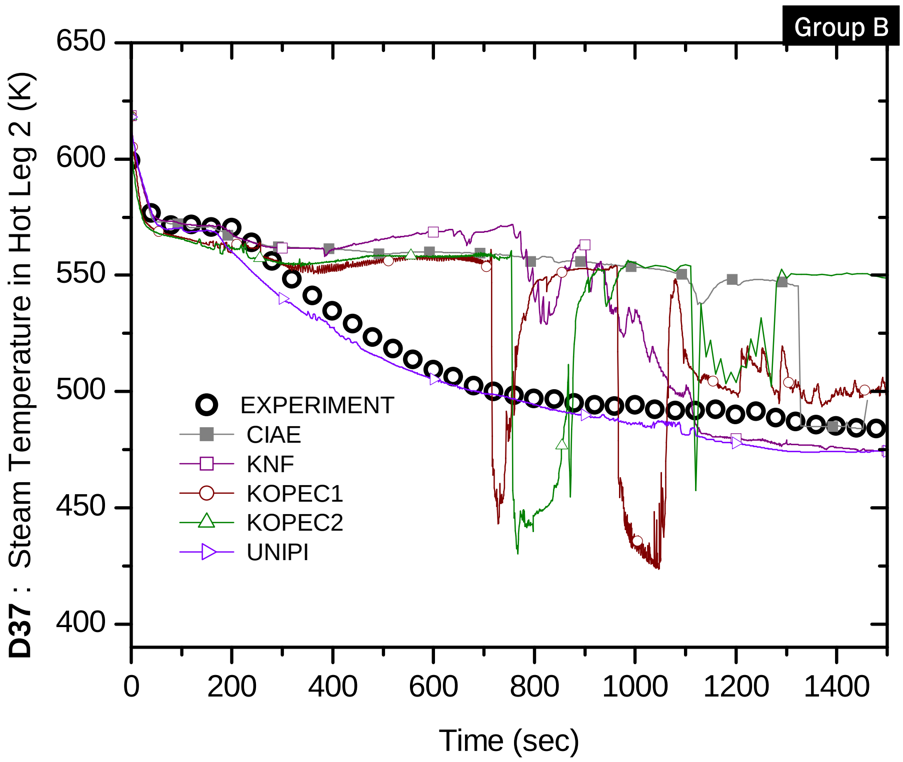

Figure B.37-B Steam temperature in the hot leg 2 (D37)

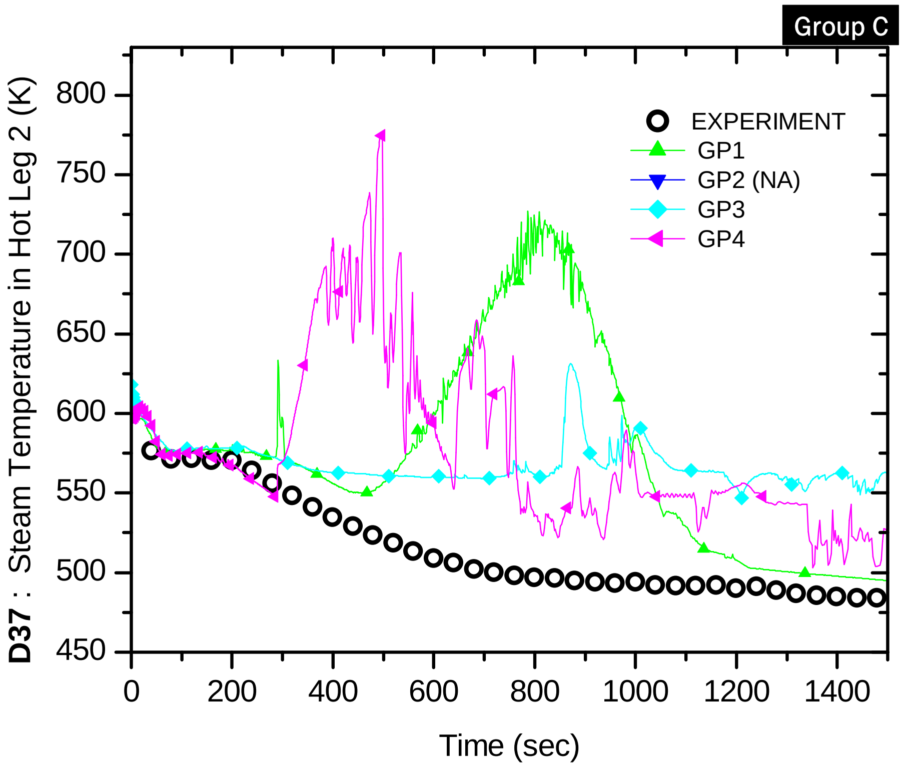

Figure B.37-C Steam temperature in the hot leg 2 (D37)

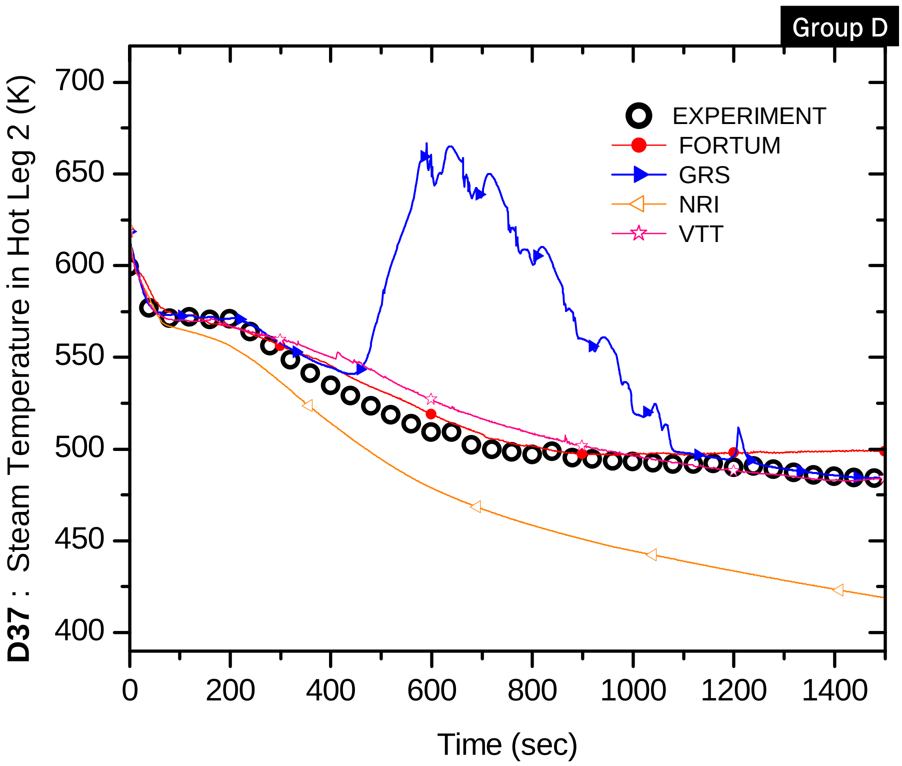

Figure B.37-D Steam temperature in the hot leg 2 (D37)

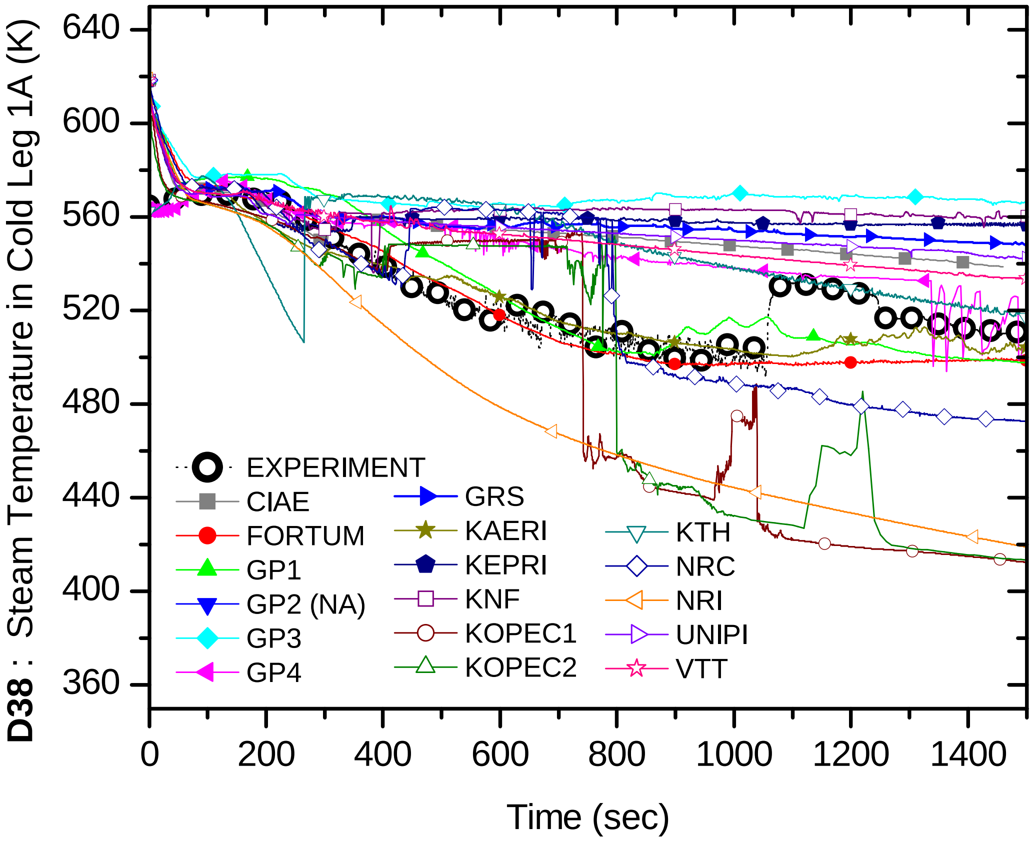

Figure B.38 Steam temperature in the cold leg 1A (D38)

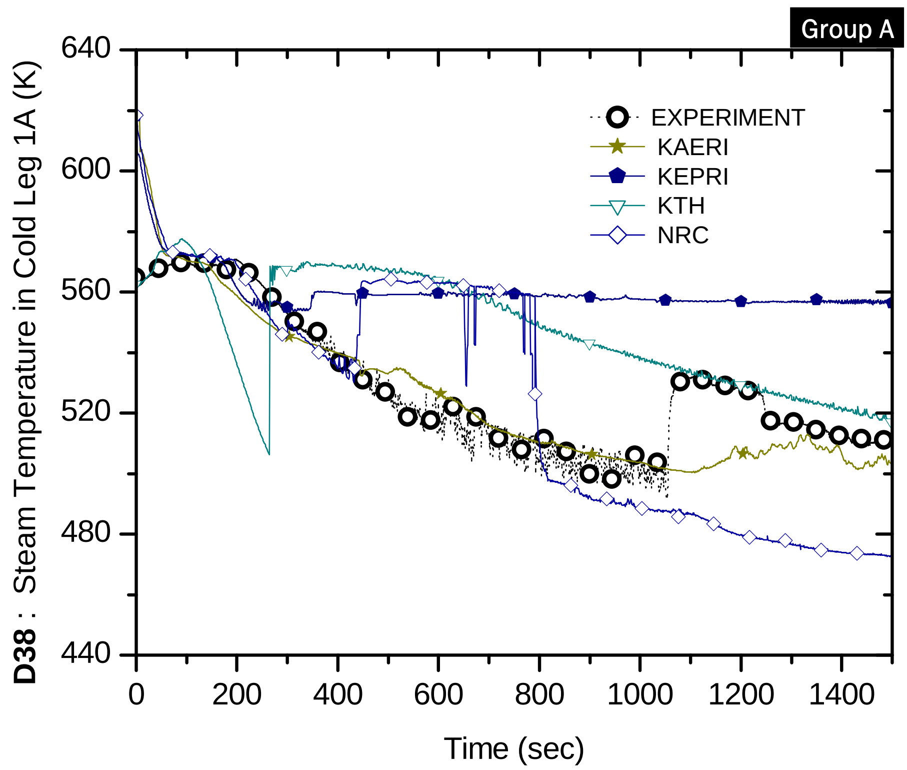

Figure B.38-A Steam temperature in the cold leg 1A (D38)

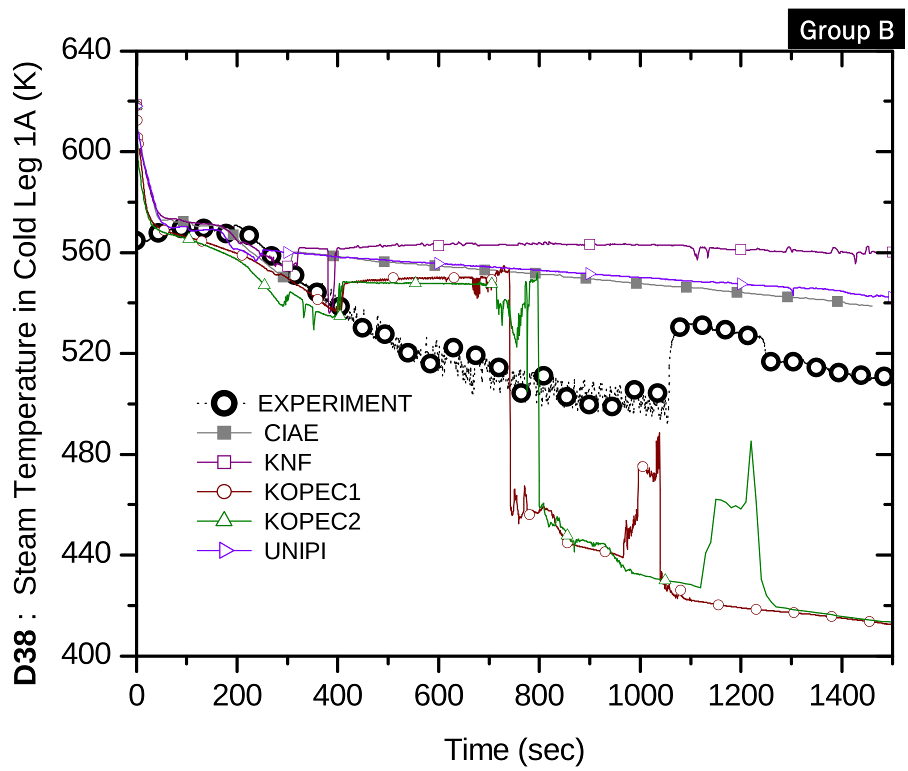

Figure B.38-B Steam temperature in the cold leg 1A (D38)

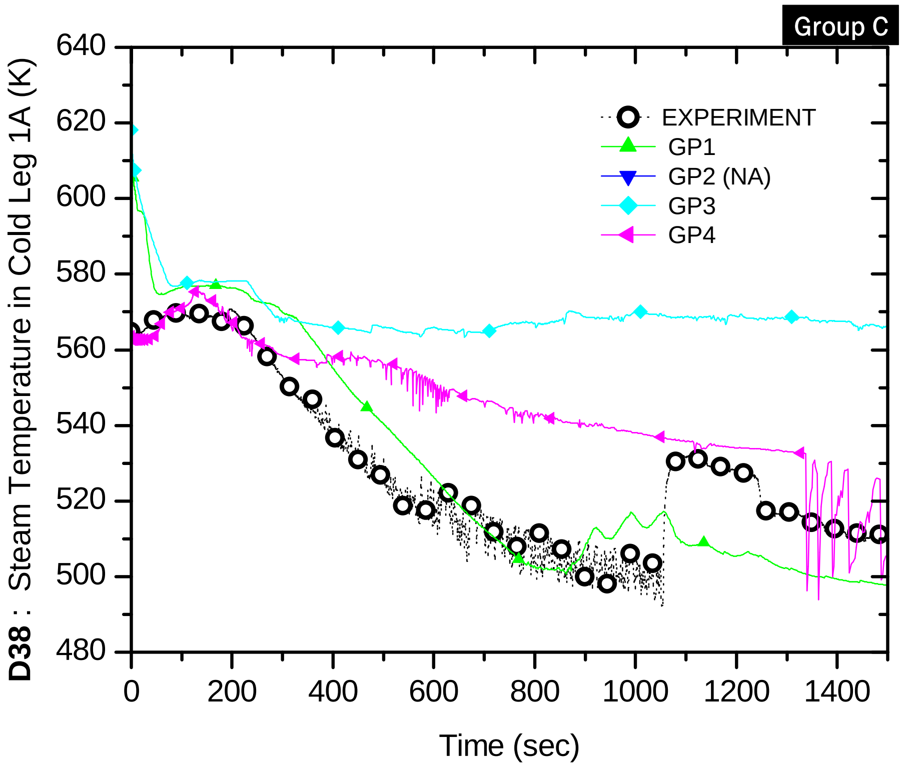

Figure B.38-C Steam temperature in the cold leg 1A (D38)

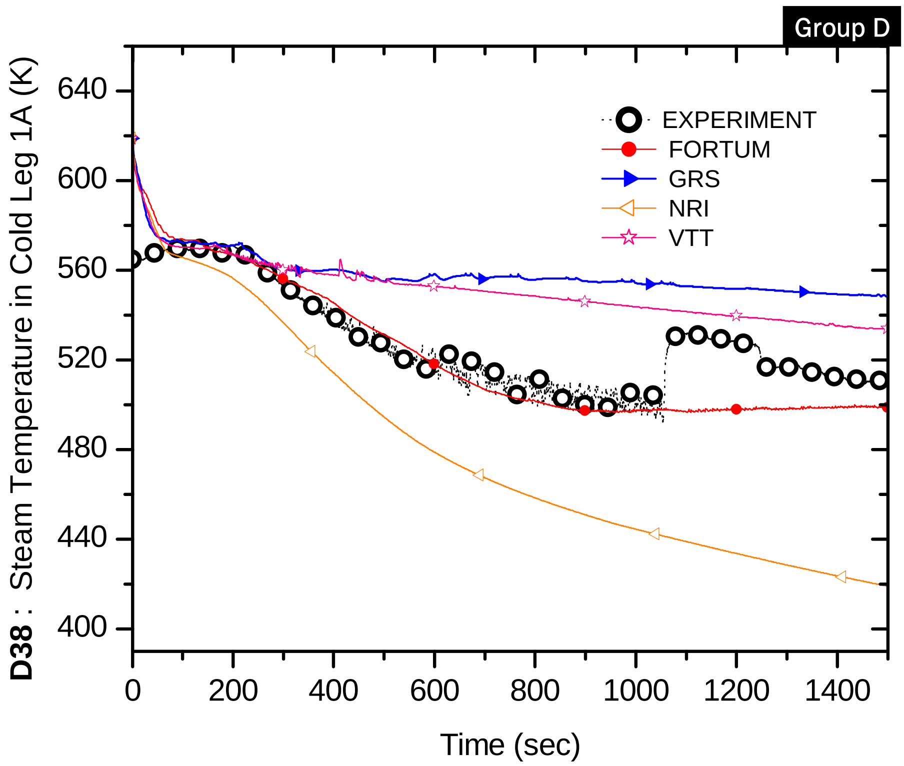

Figure B.38-D Steam temperature in the cold leg 1A (D38)

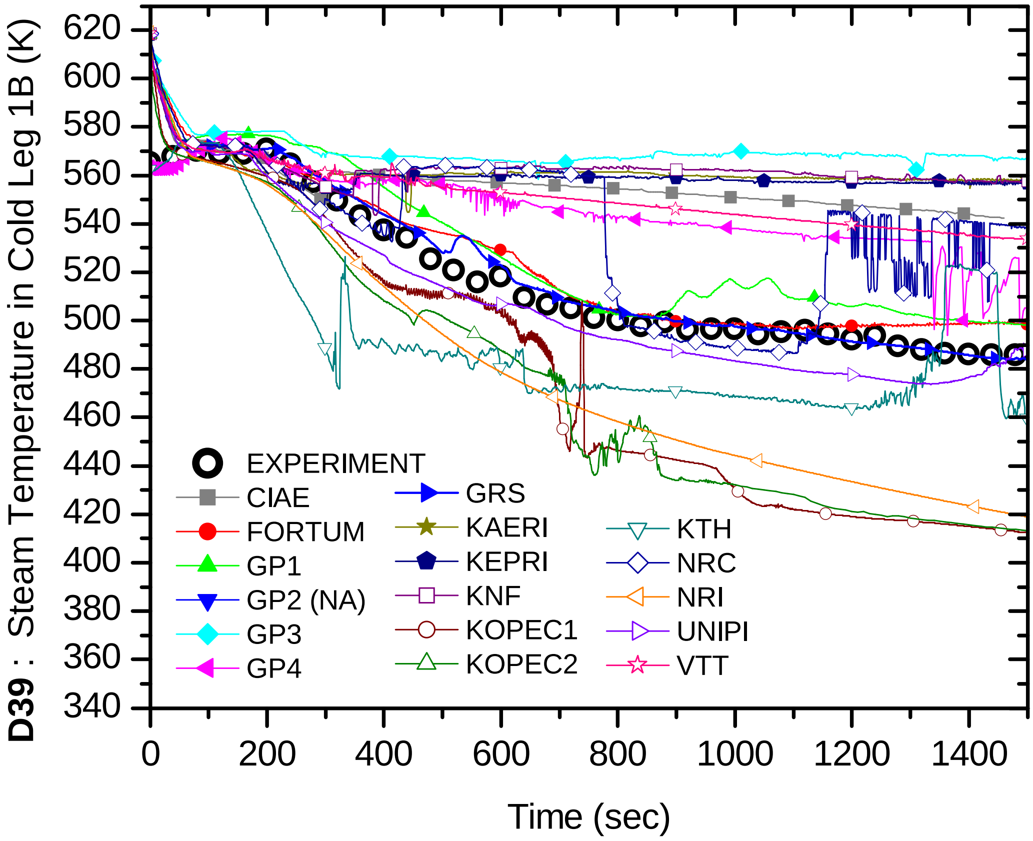

Figure B.39 Steam temperature in the cold leg 1B (D39)

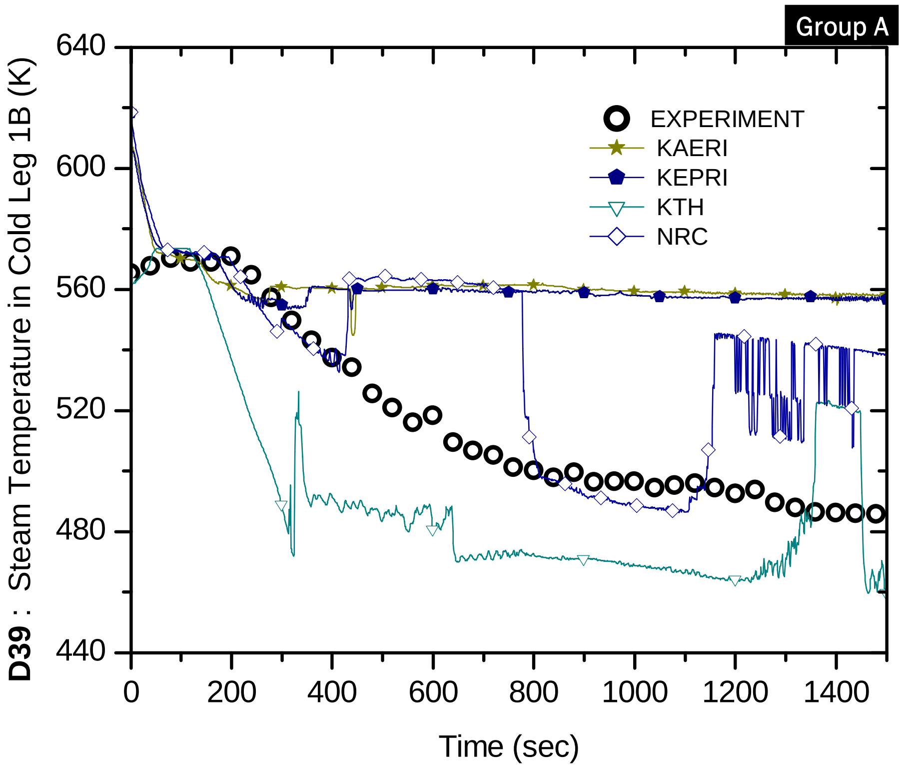

Figure B.39-A Steam temperature in the cold leg 1B (D39)

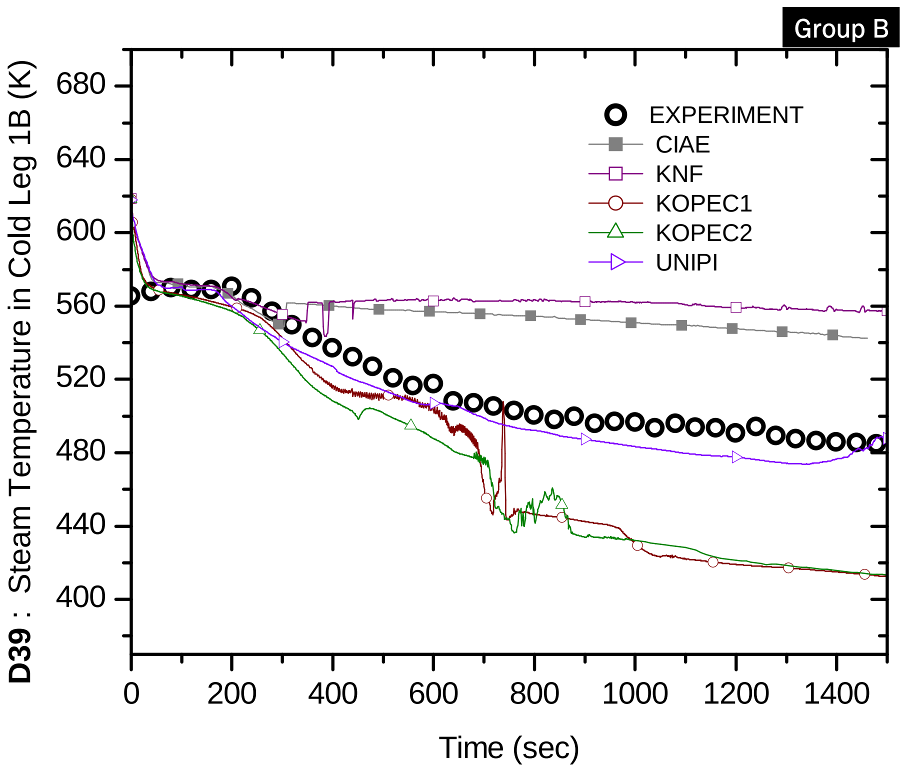

Figure B.39-B Steam temperature in the cold leg 1B (D39)

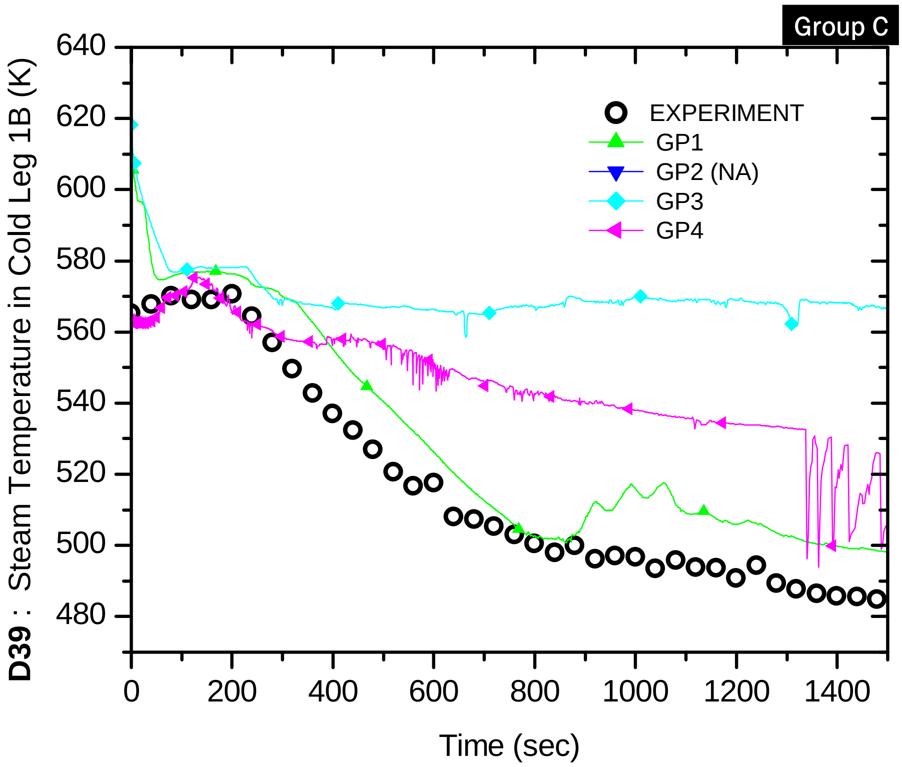

Figure B.39-C Steam temperature in the cold leg 1B (D39)

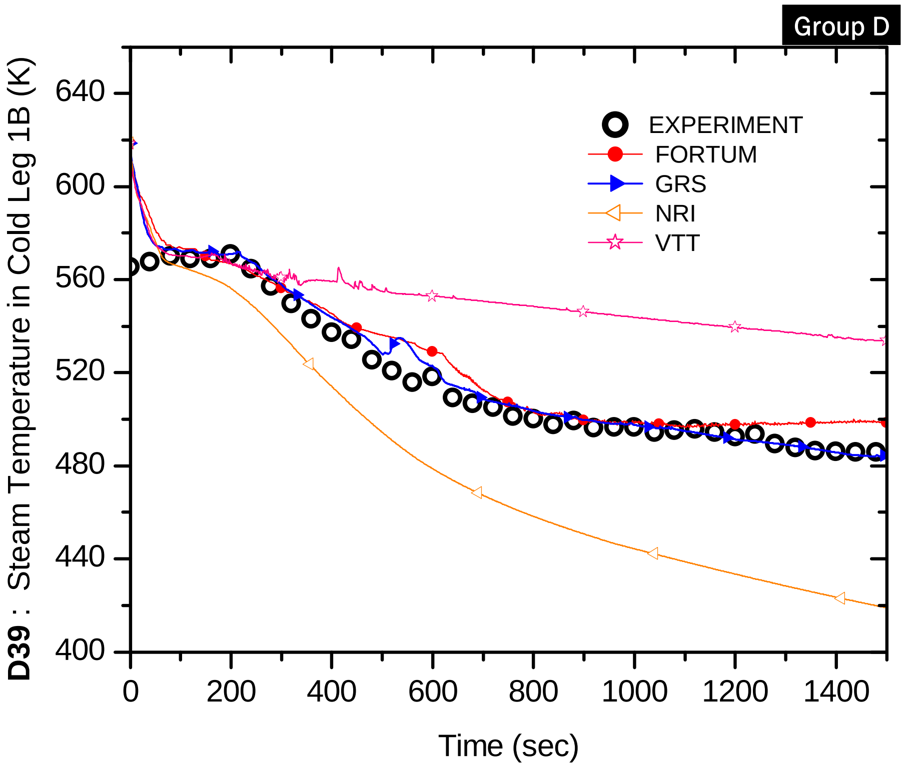

Figure B.39-D Steam temperature in the cold leg 1B (D39)

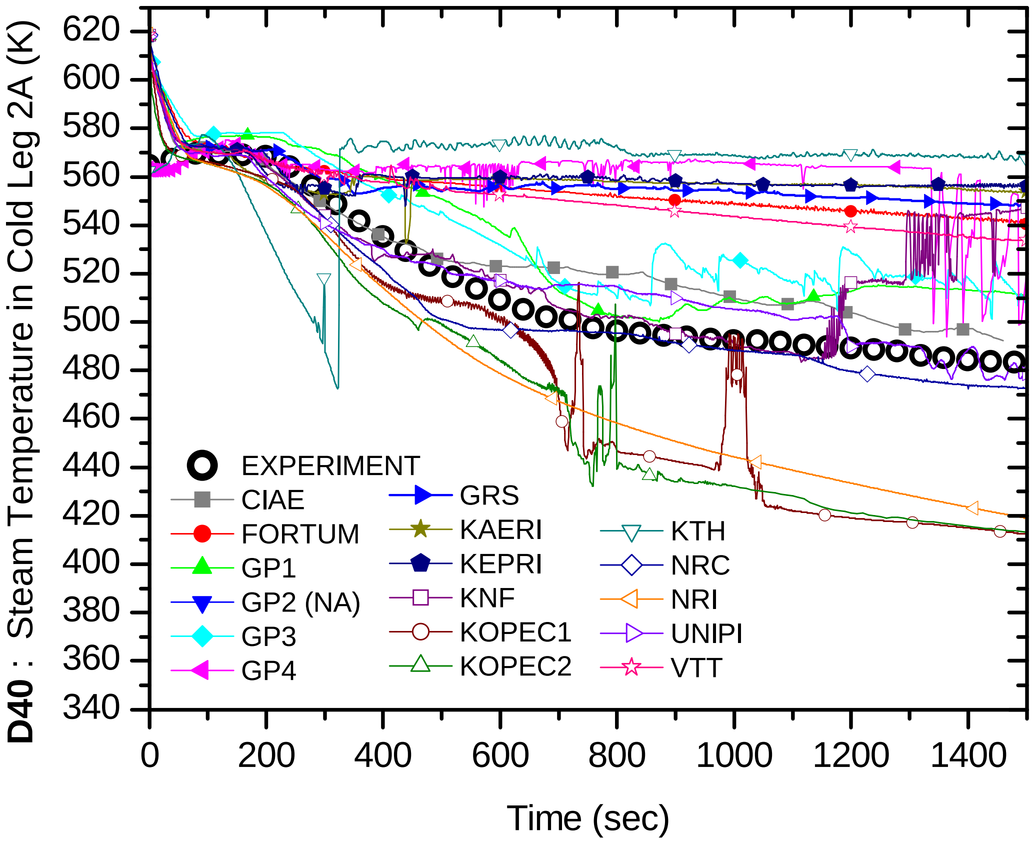

Figure B.40 Steam temperature in the cold leg 2A (D40)

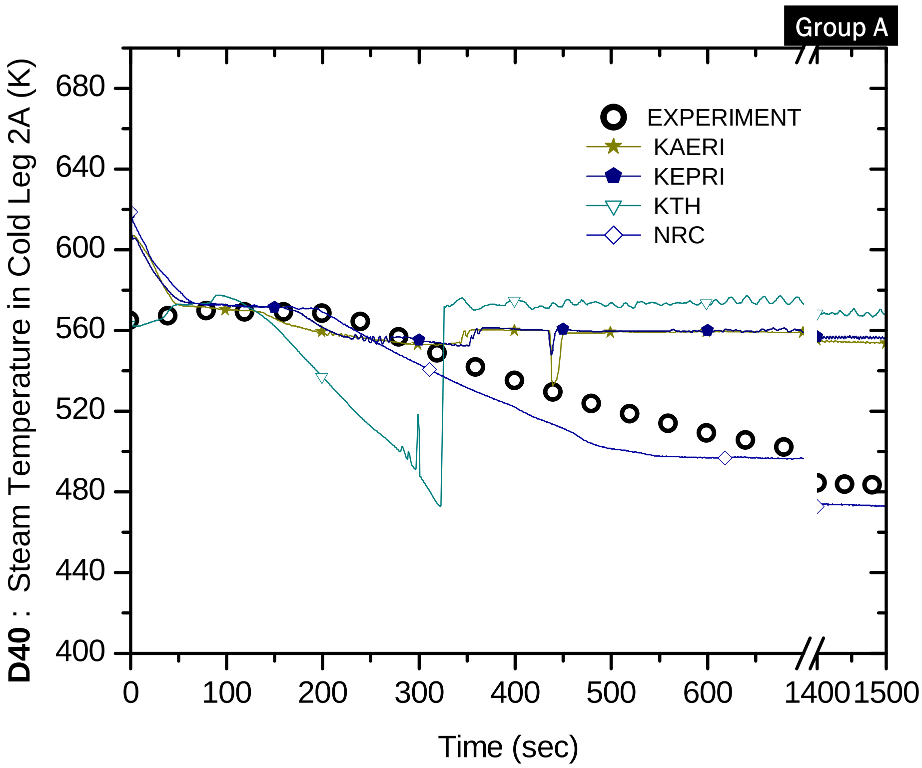

Figure B.40-A Steam temperature in the cold leg 2A (D40)

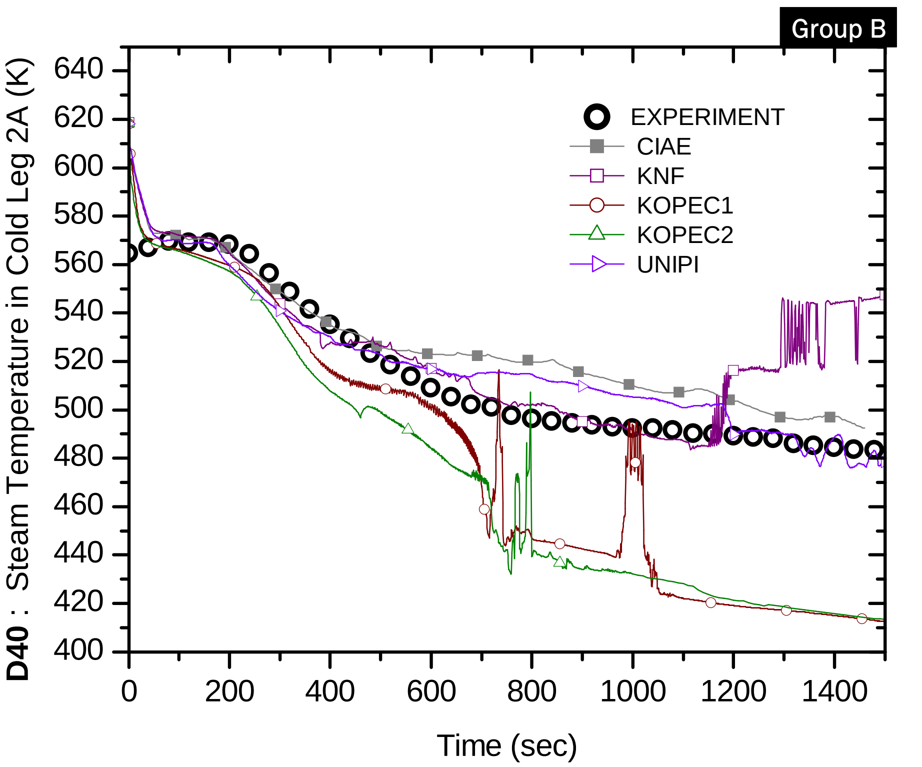

B.40-B Steam temperature in the cold leg 2A (D40)

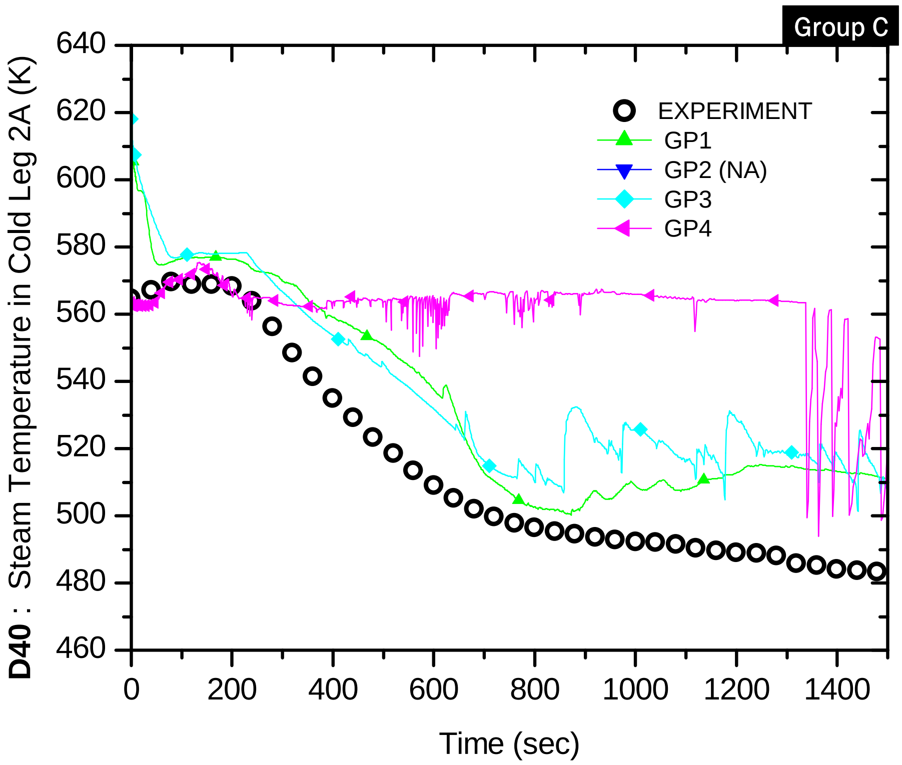

Figure B.40-C Steam temperature in the cold leg 2A (D40)

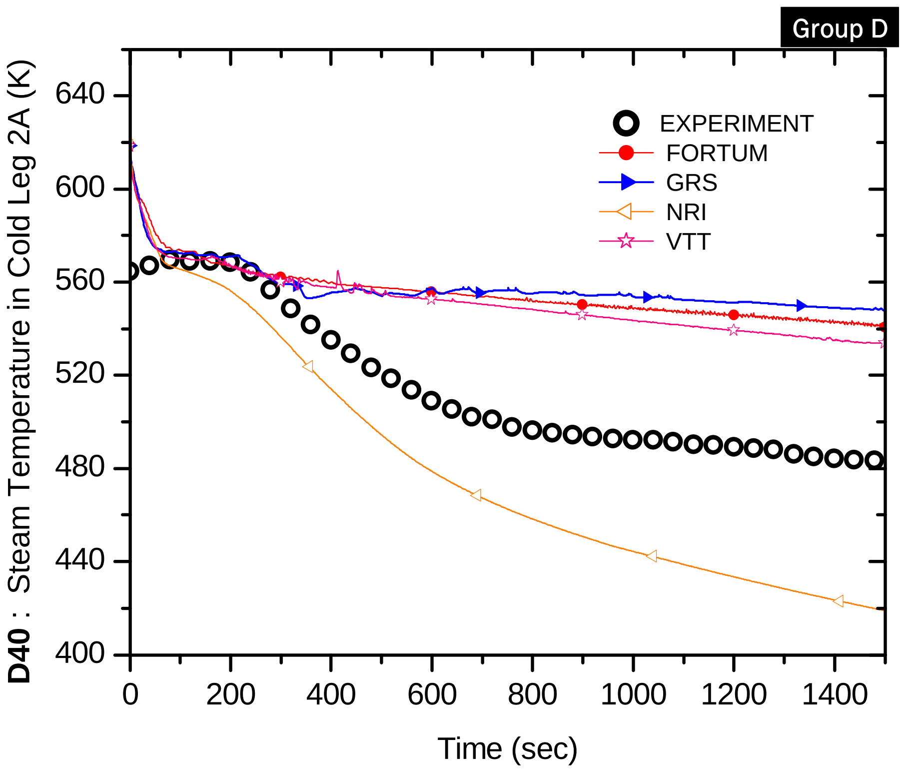

Figure B.40-D Steam temperature in the cold leg 2A (D40)

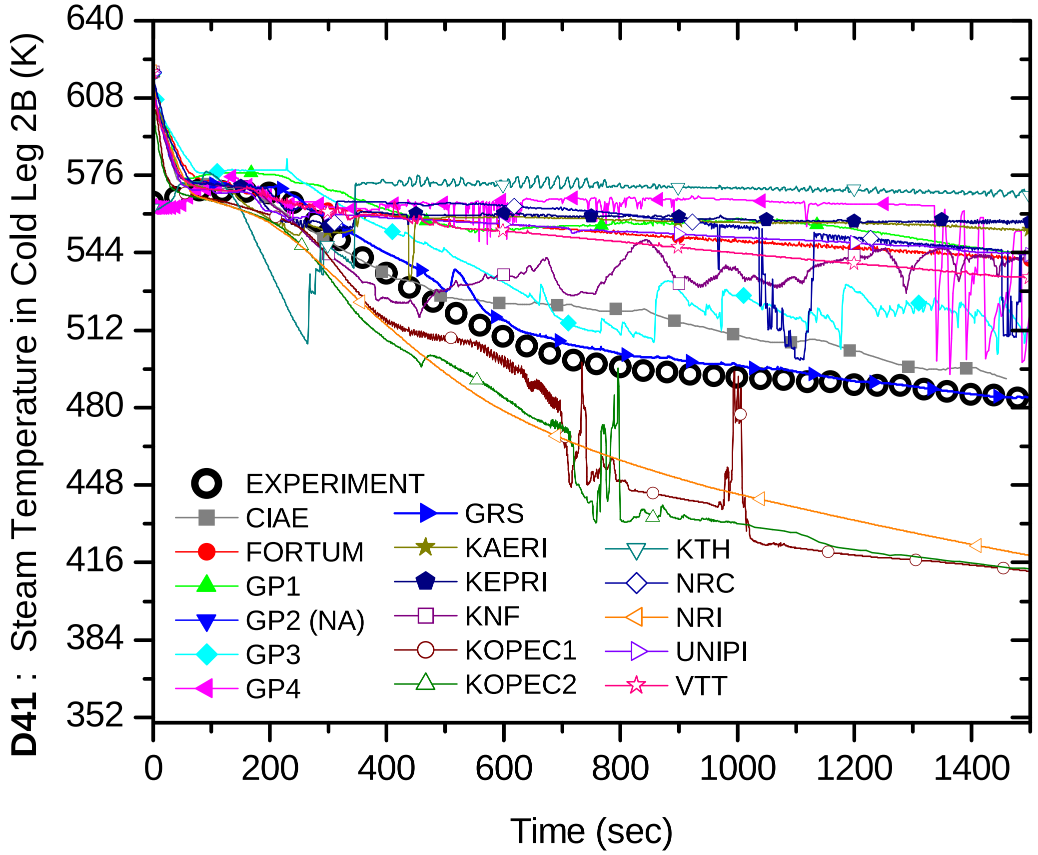

Figure B.41 Steam temperature in the cold leg 2B (D41)

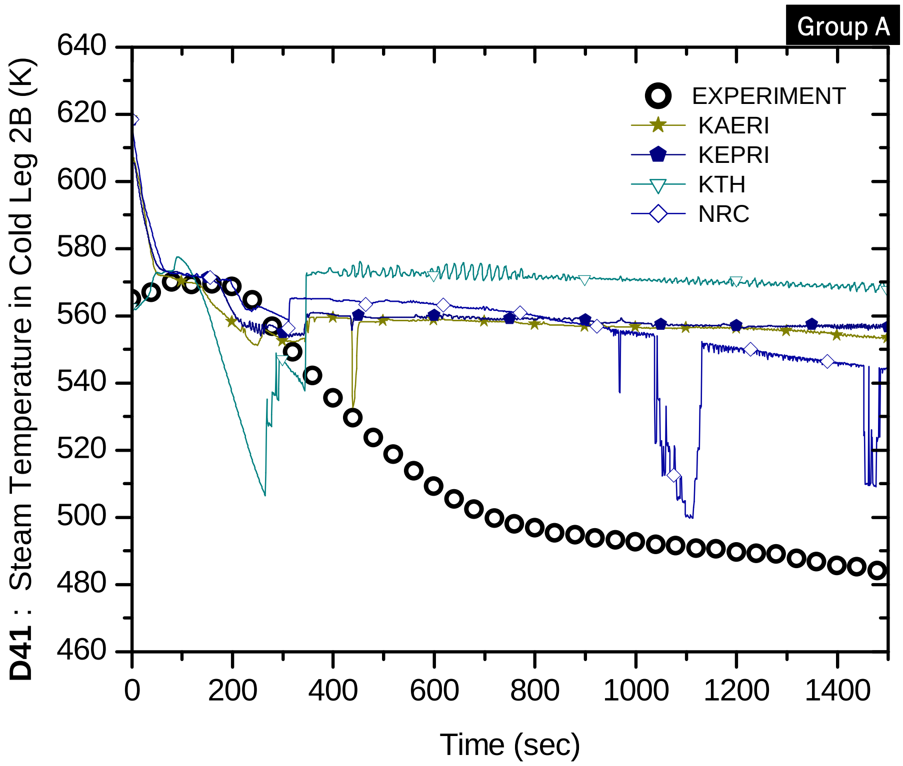

Figure B.41-A Steam temperature in the cold leg 2B (D41)

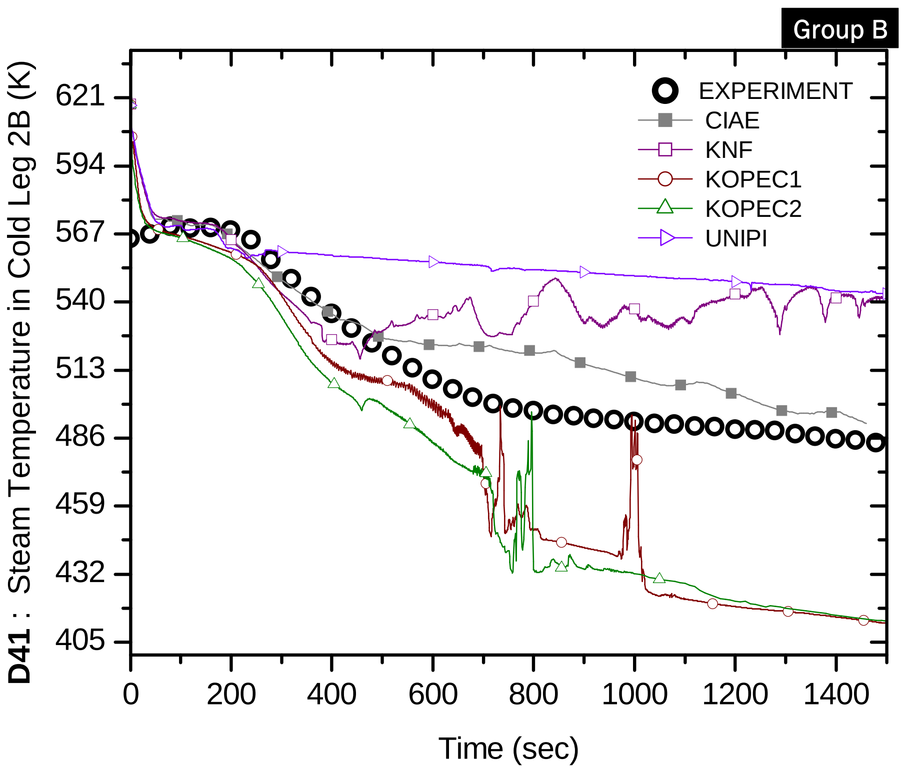

Figure B.41-B Steam temperature in the cold leg 2B (D41)

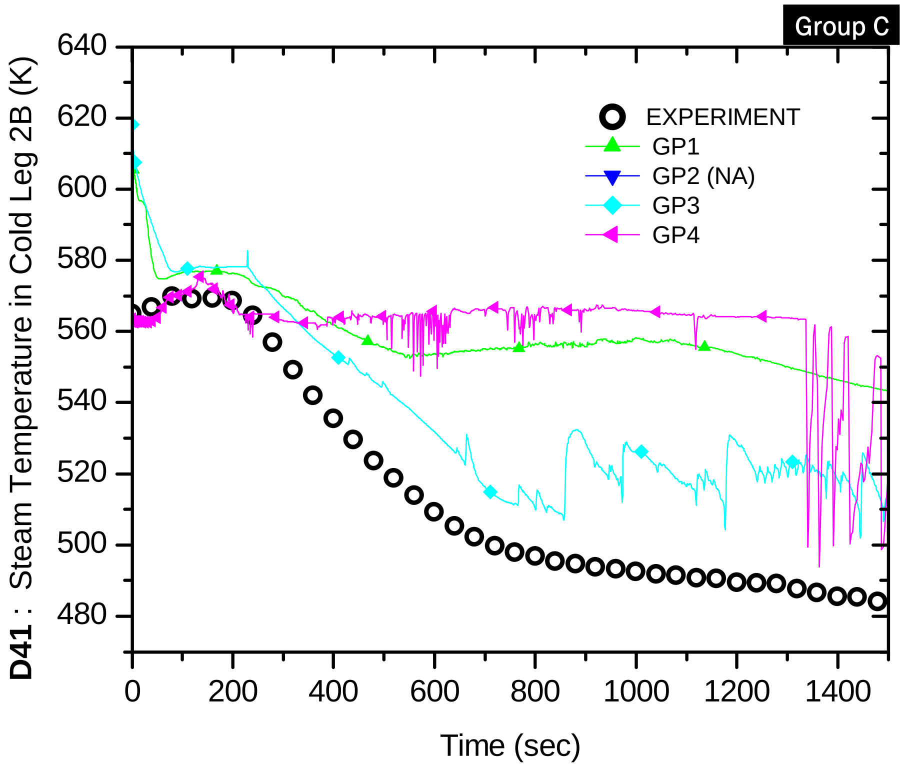

Figure B.41-C Steam temperature in the cold leg 2B (D41)

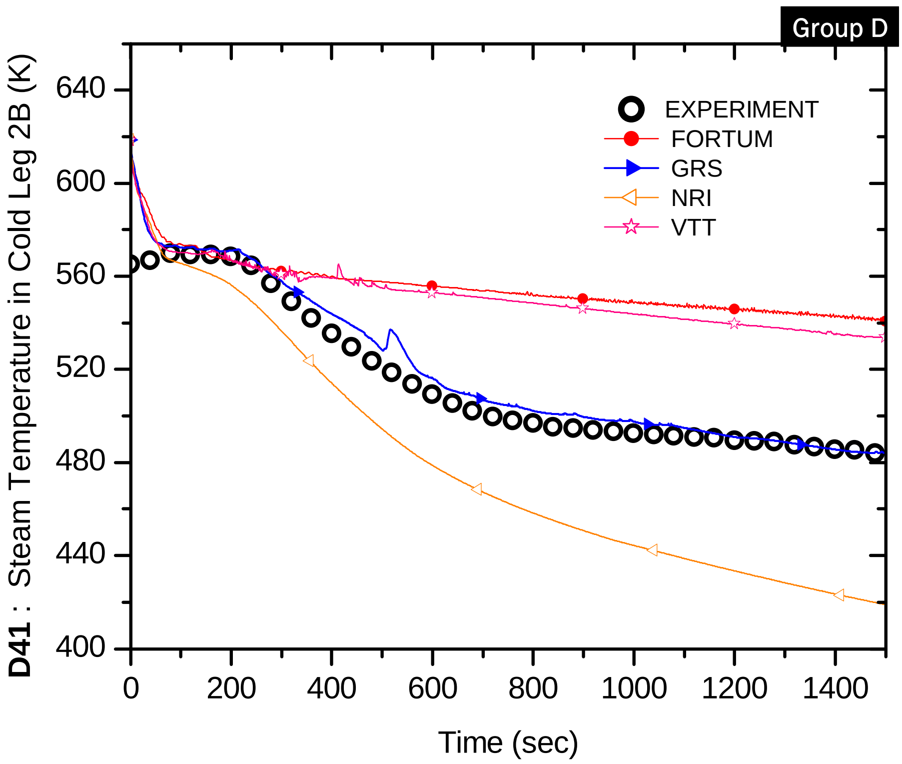

Figure B.41-D Steam temperature in the cold leg 2B (D41)

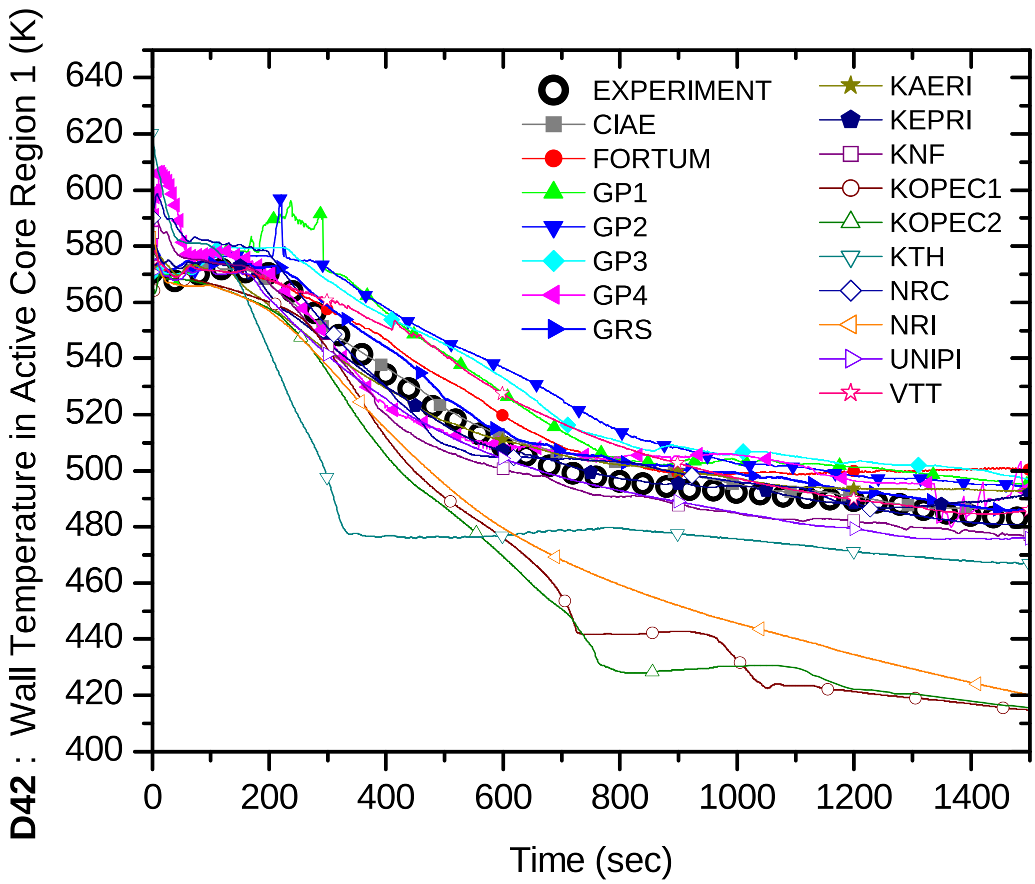

Figure B.42 Wall temperature in the active core region 1 (D42)

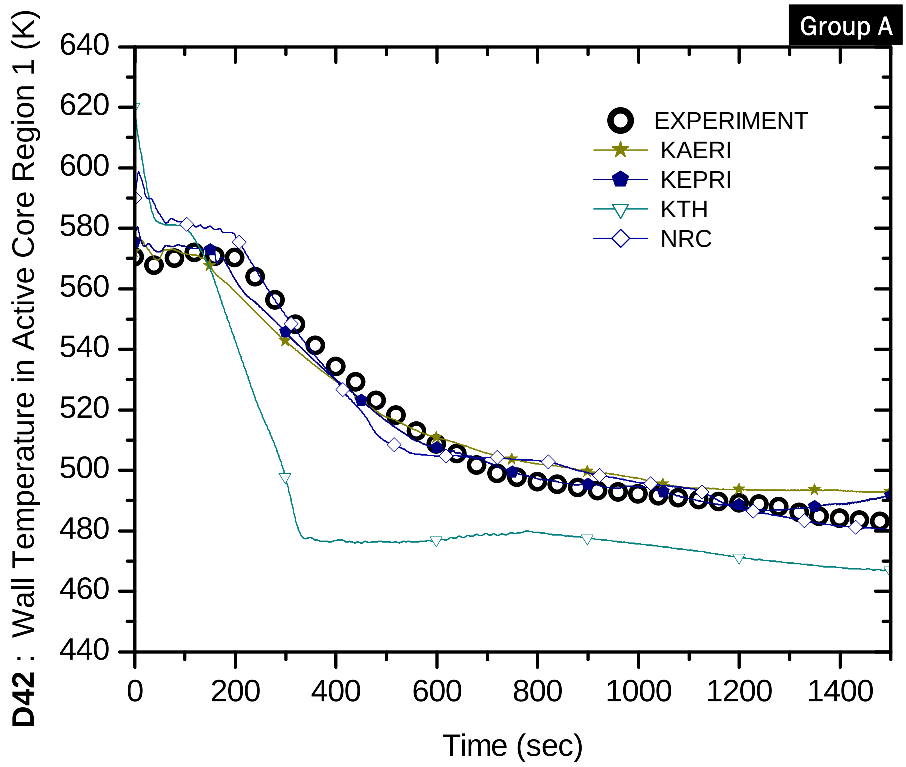

Figure B.42-A Wall temperature in the active core region 1 (D42)

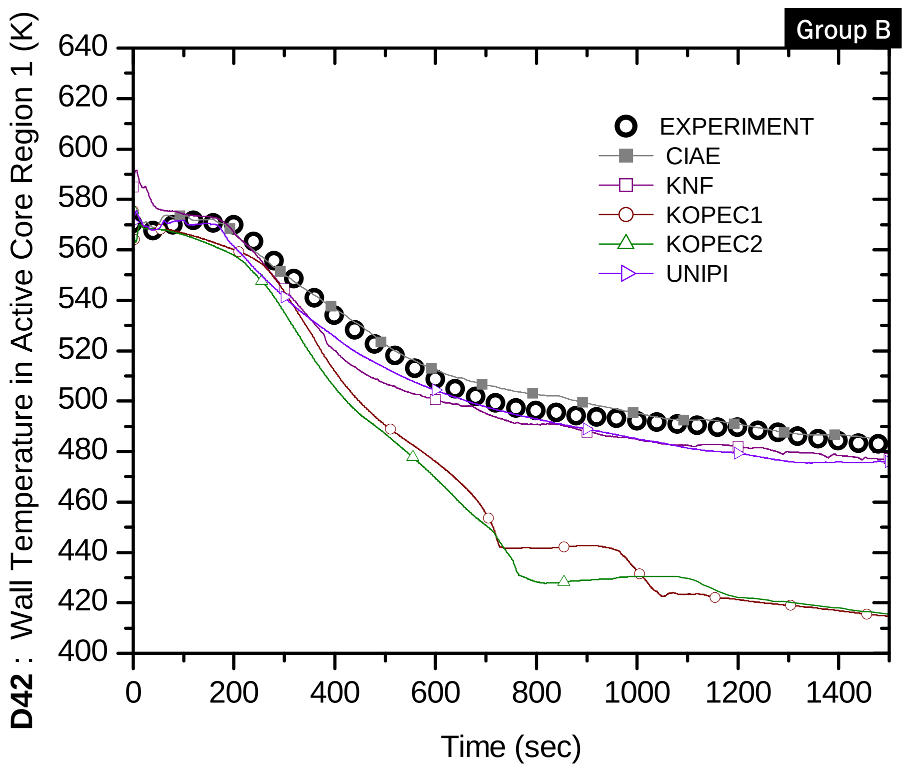

Figure B.42-B Wall temperature in the active core region 1 (D42)

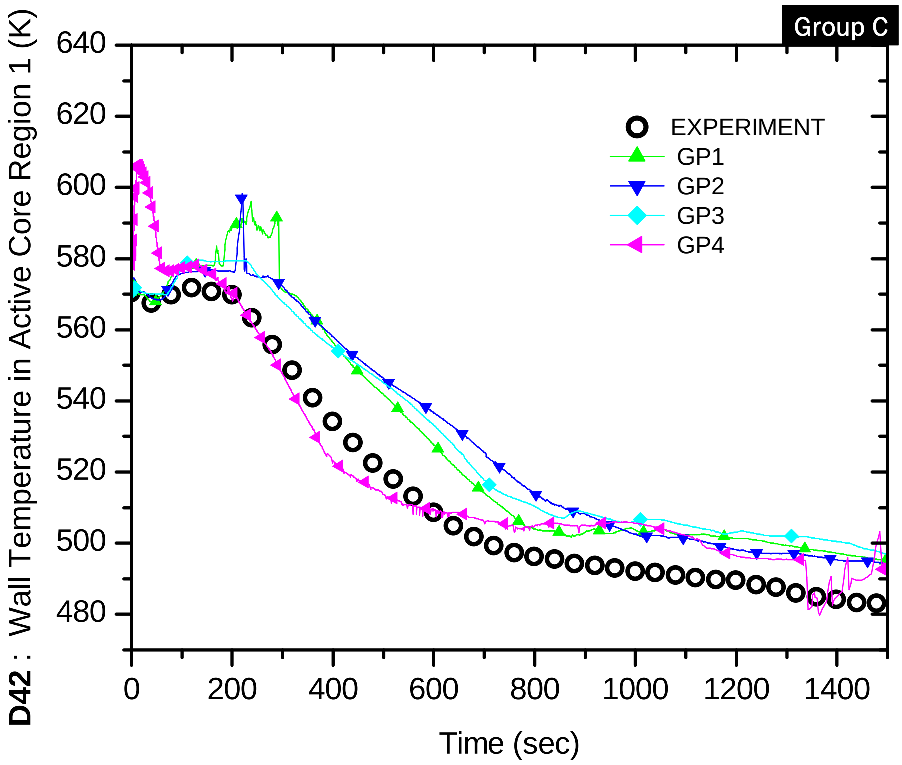

Figure B.42-C Wall temperature in the active core region 1 (D42)

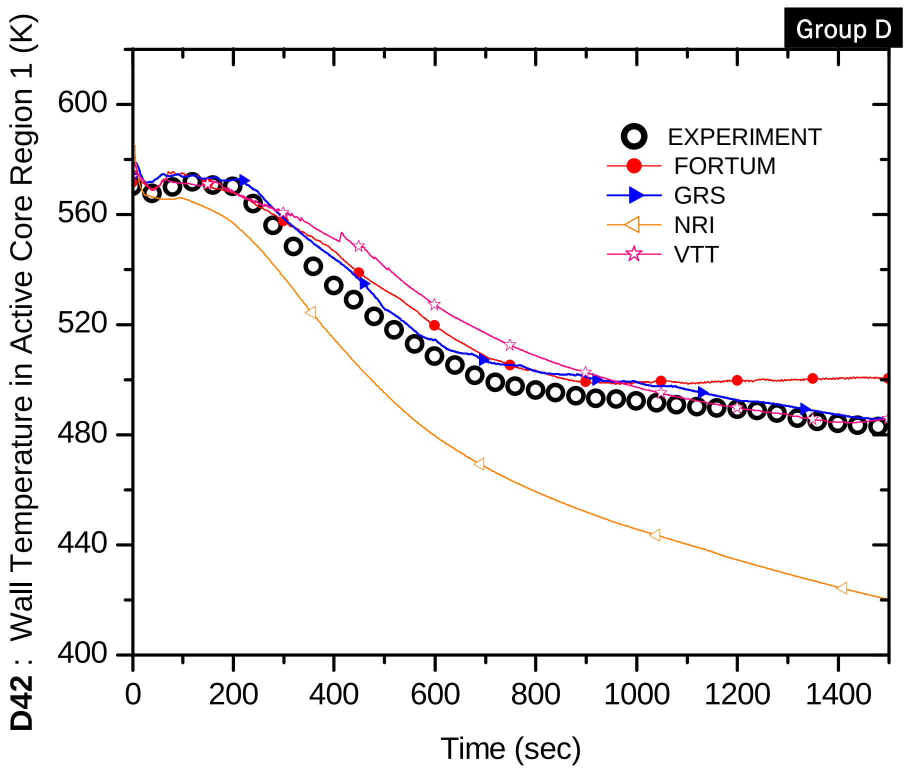

Figure B.42-D Wall temperature in the active core region 1 (D42)

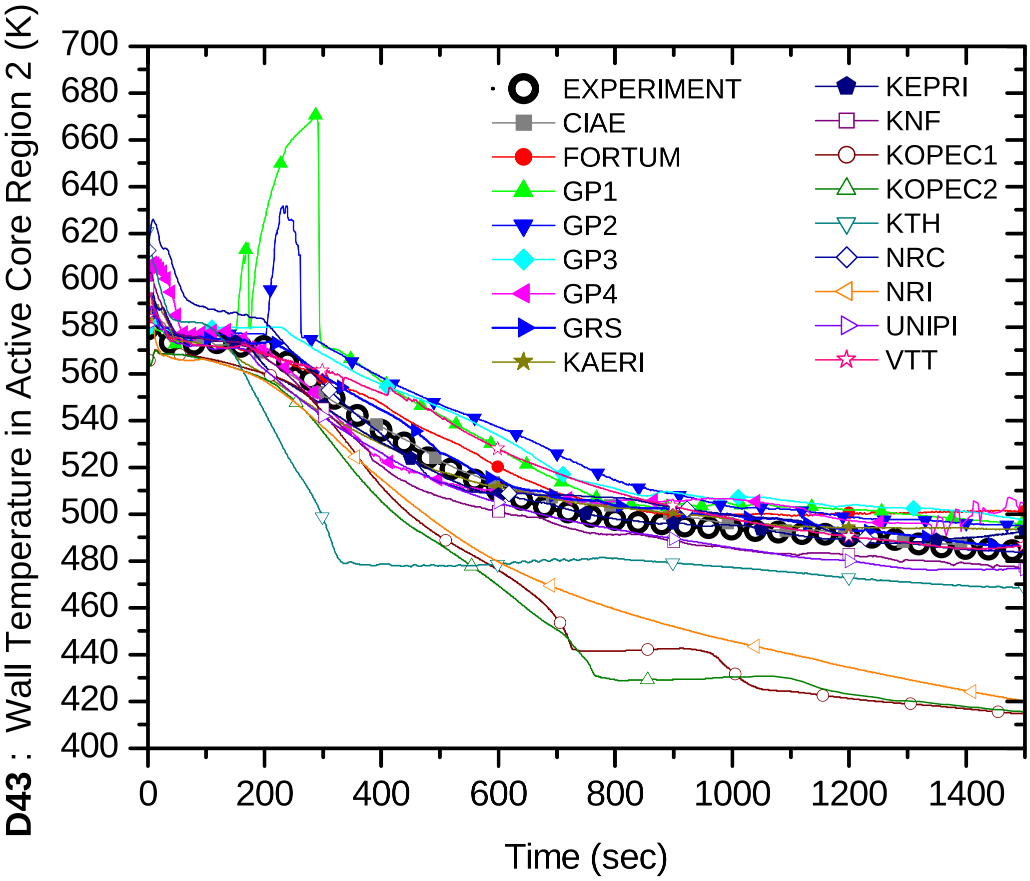

Figure B.43 Wall temperature in the active core region 2 (D43)

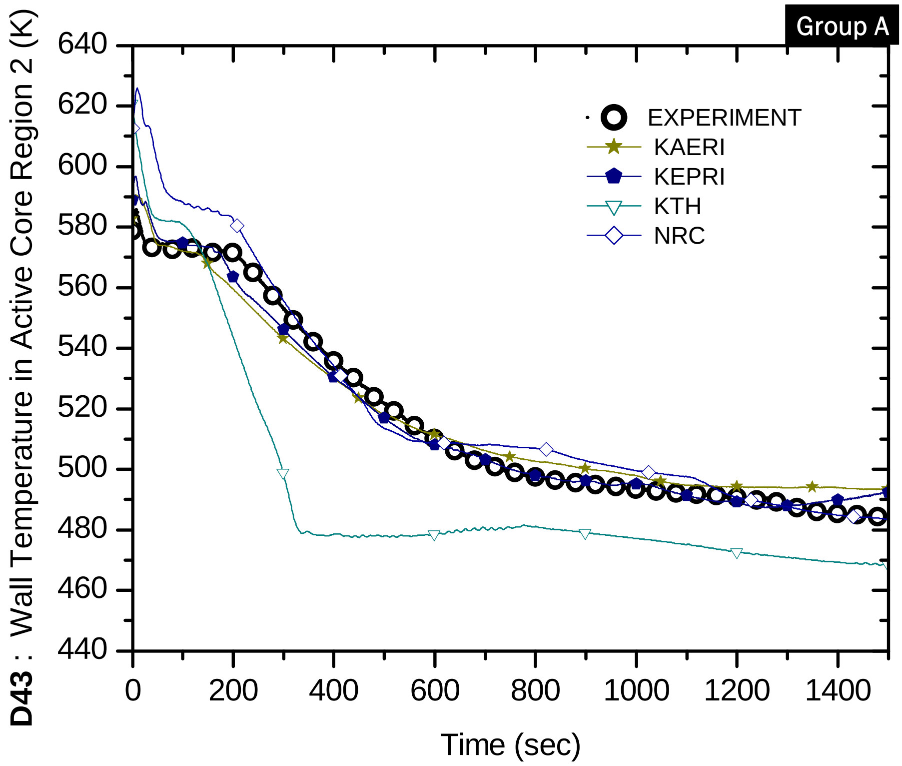

Figure B.43-A Wall temperature in the active core region 2 (D43)

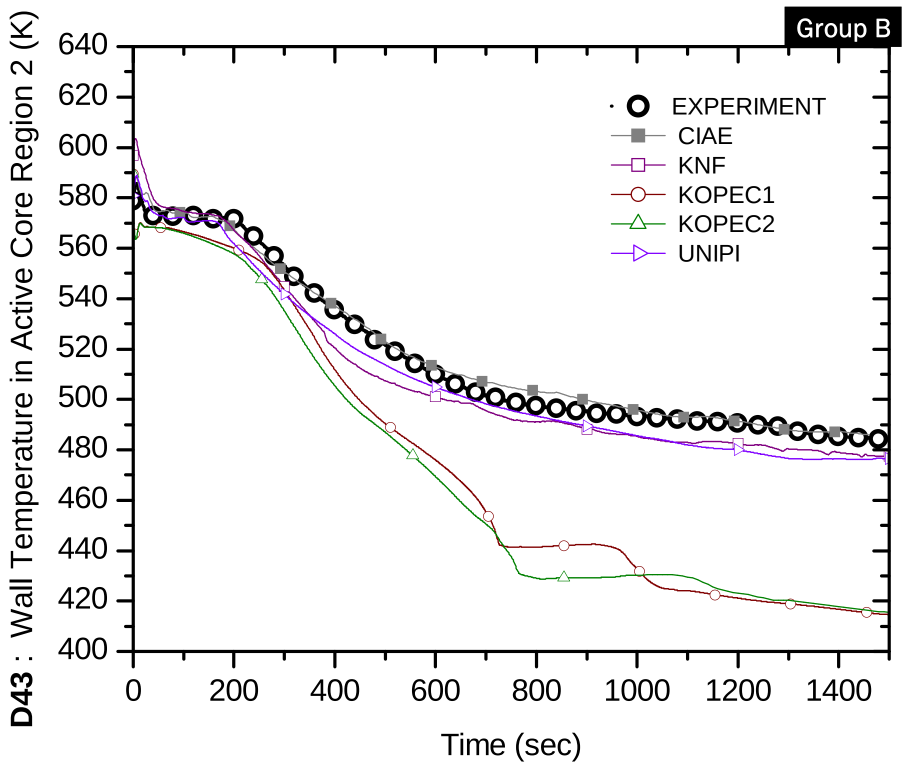

Figure B.43-B Wall temperature in the active core region 2 (D43)

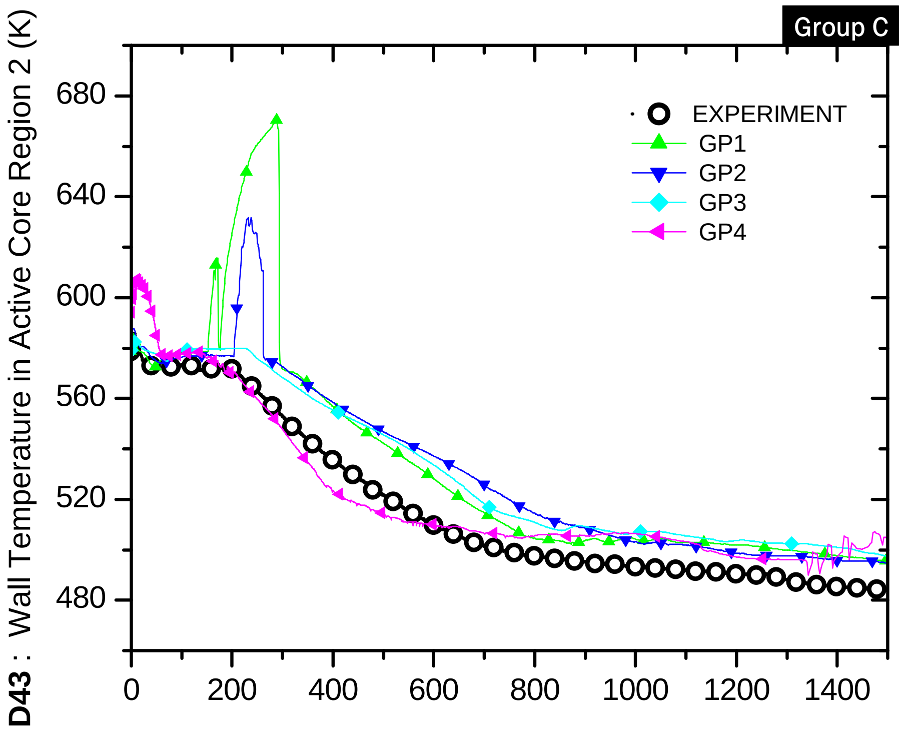

Figure B.43-C Wall temperature in the active core region 2 (D43)

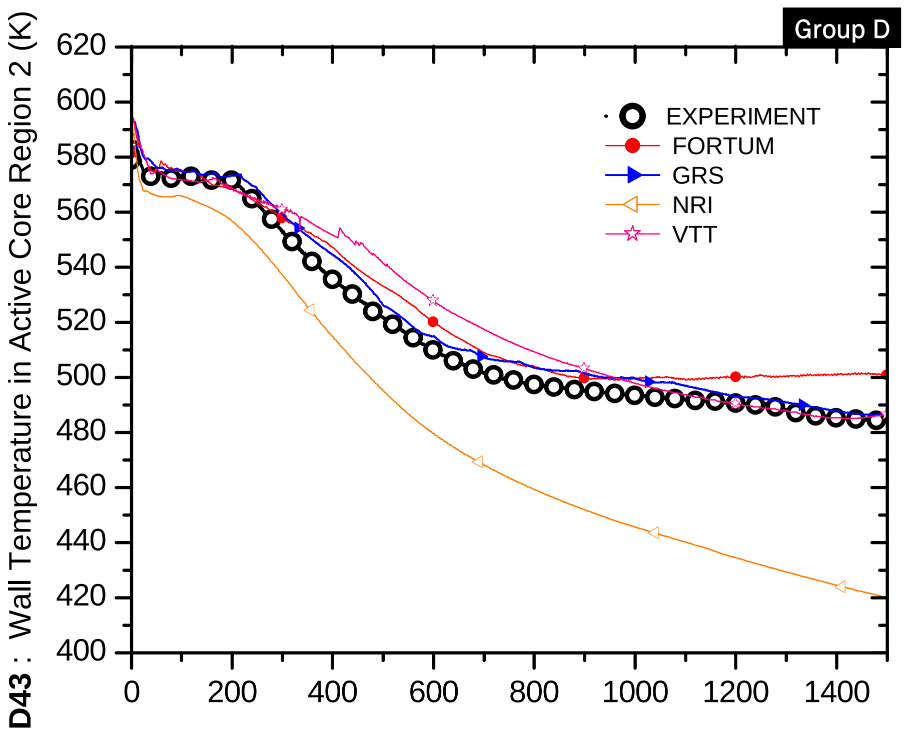

Figure B.43-D Wall temperature in the active core region 2 (D43)

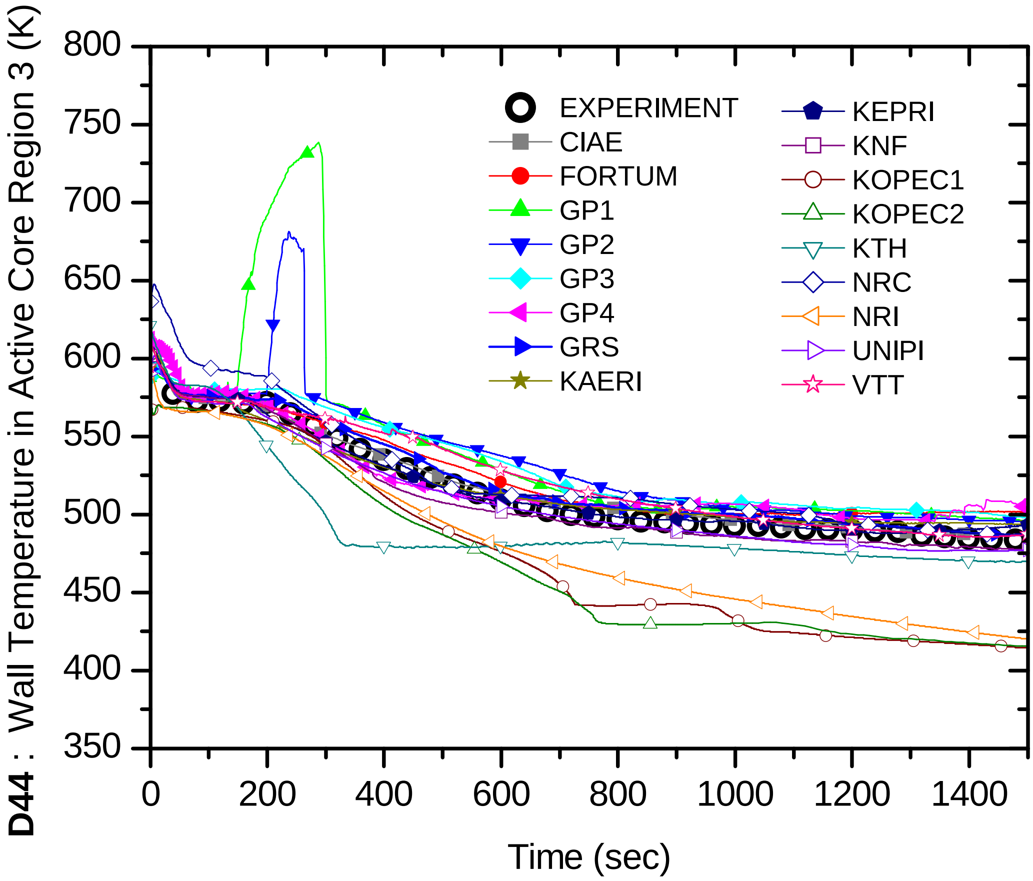

Figure B.44 Wall temperature in the active core region 3 (D44)

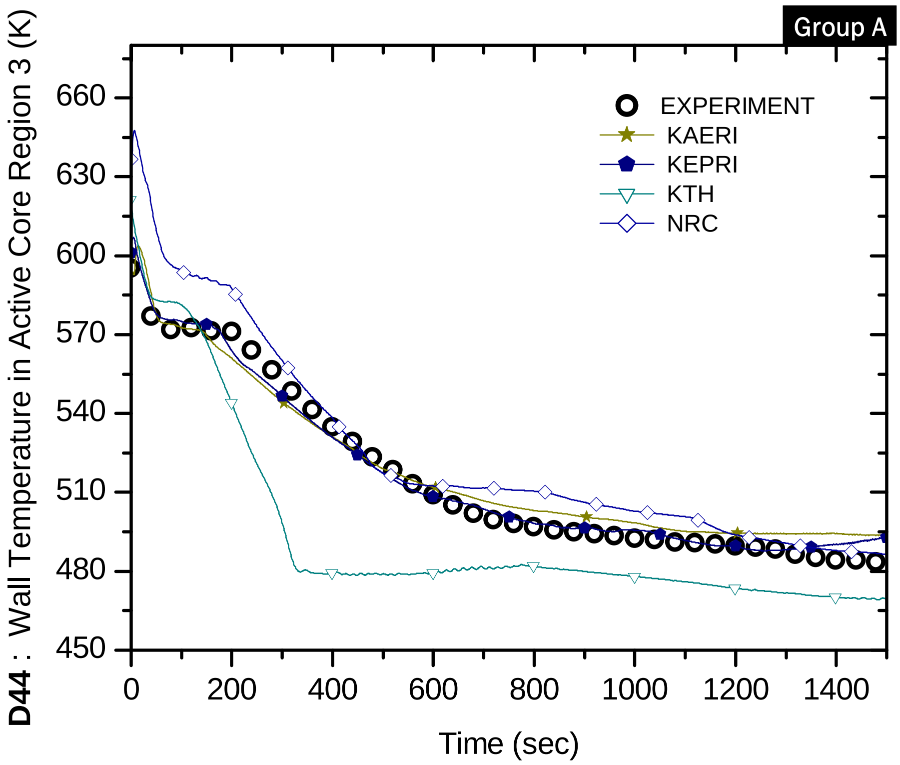

Figure B.44-A Wall temperature in the active core region 3 (D44)

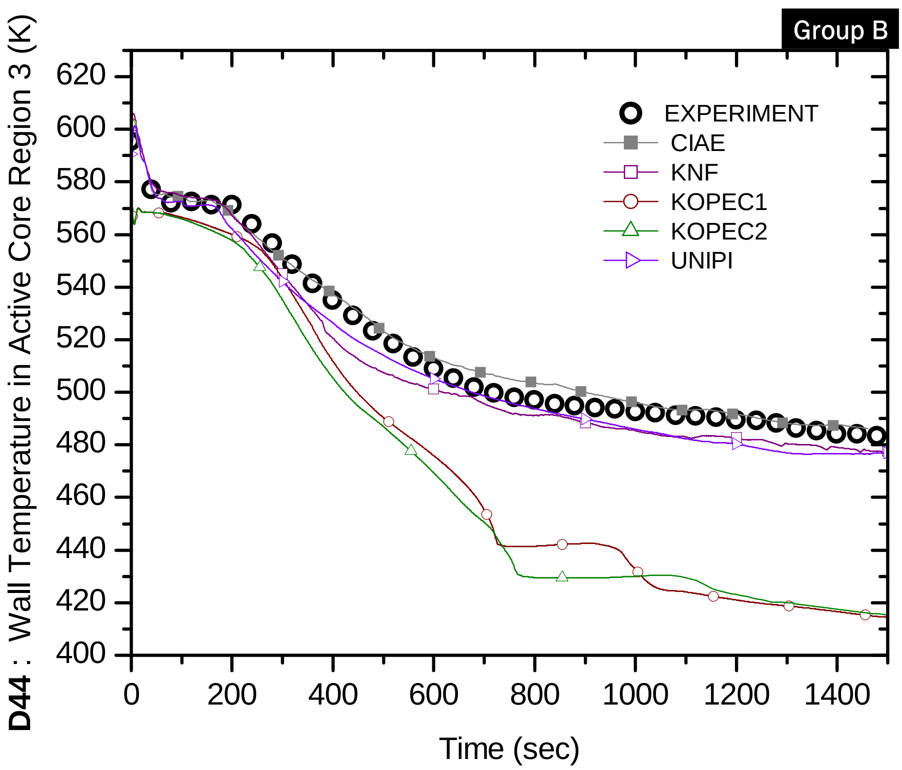

Figure B.44-B Wall temperature in the active core region 3 (D44)

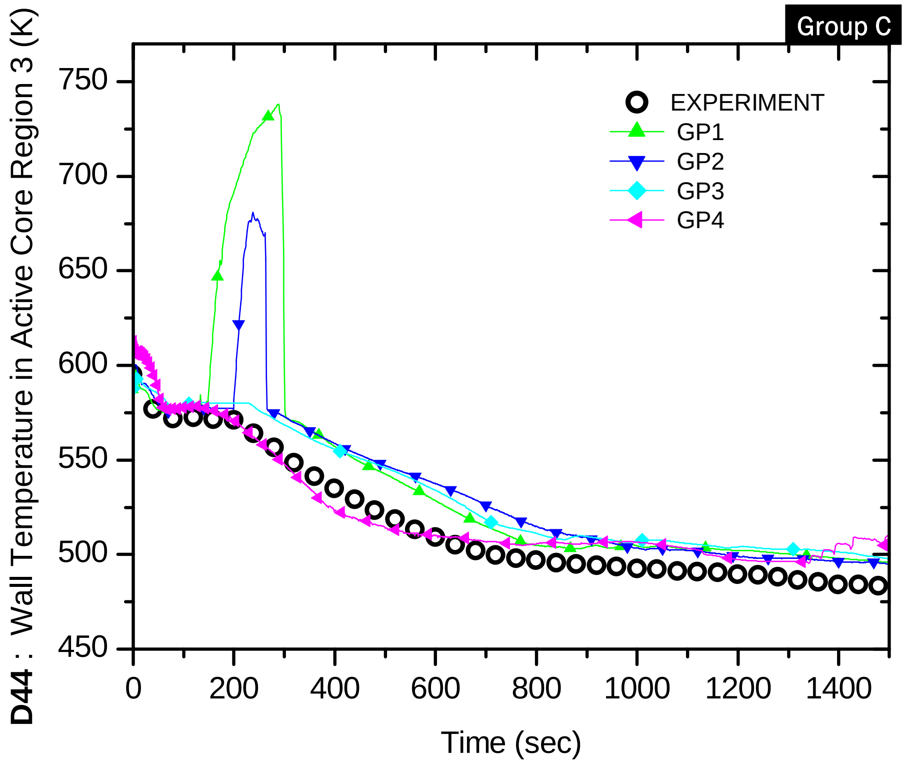

Figure B.44-C Wall temperature in the active core region 3 (D44)

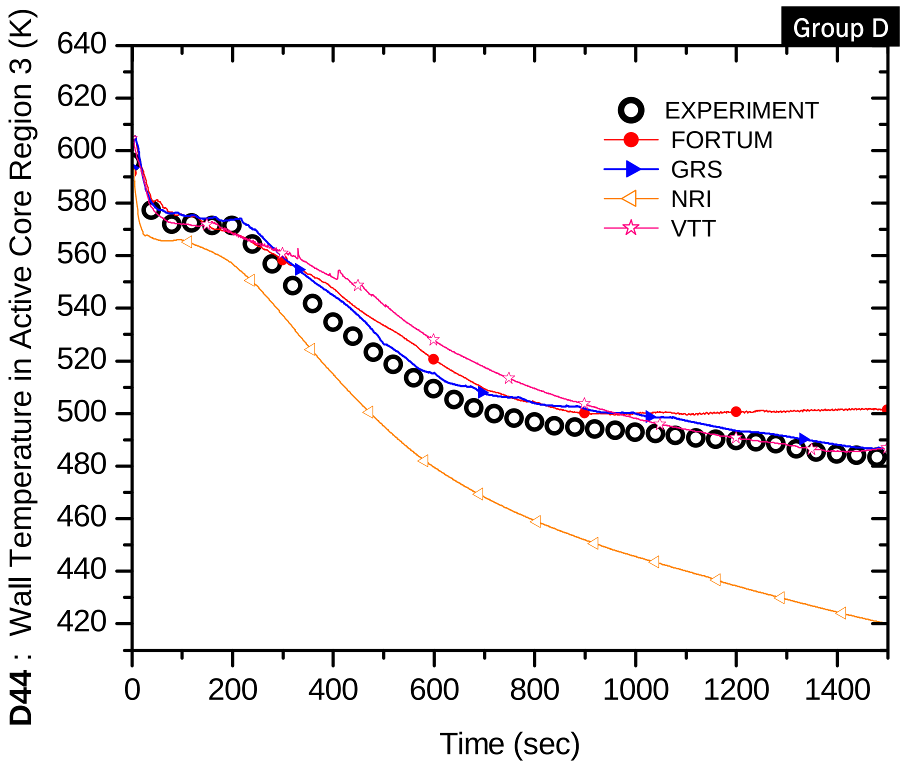

Figure B.44-D Wall temperature in the active core region 3 (D44)

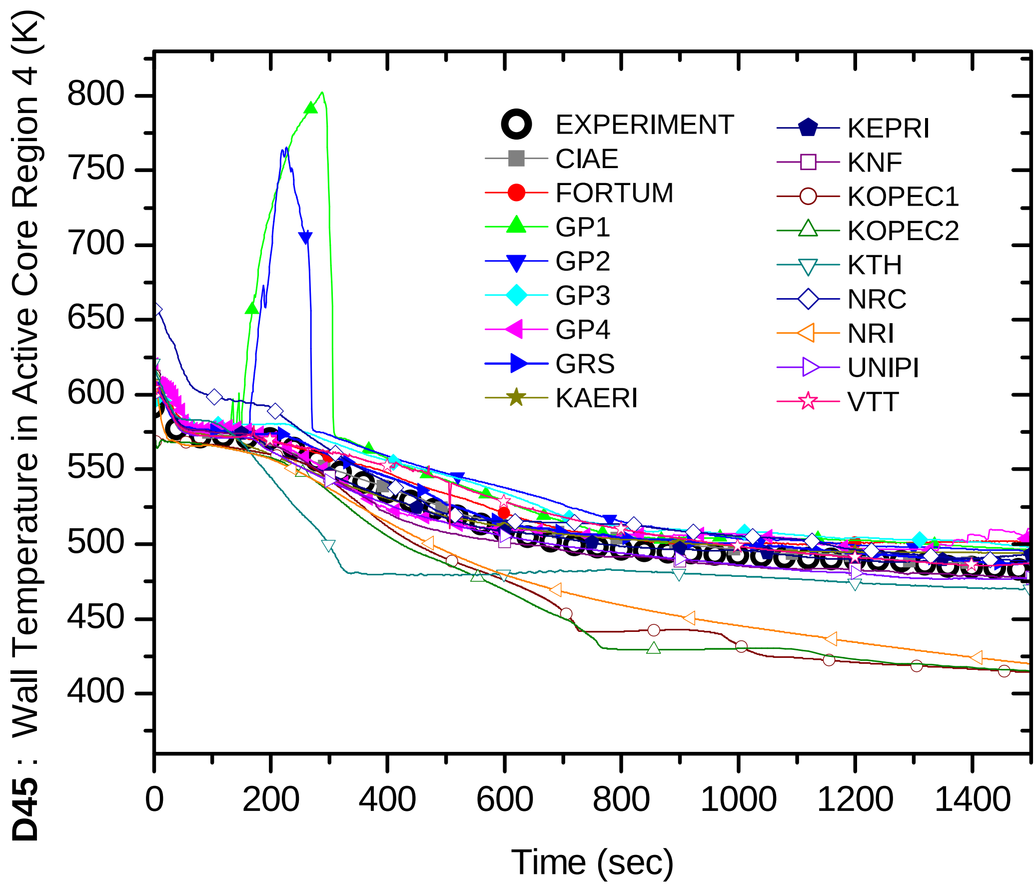

Figure B.45 Wall temperature in the active core region 4 (D45)

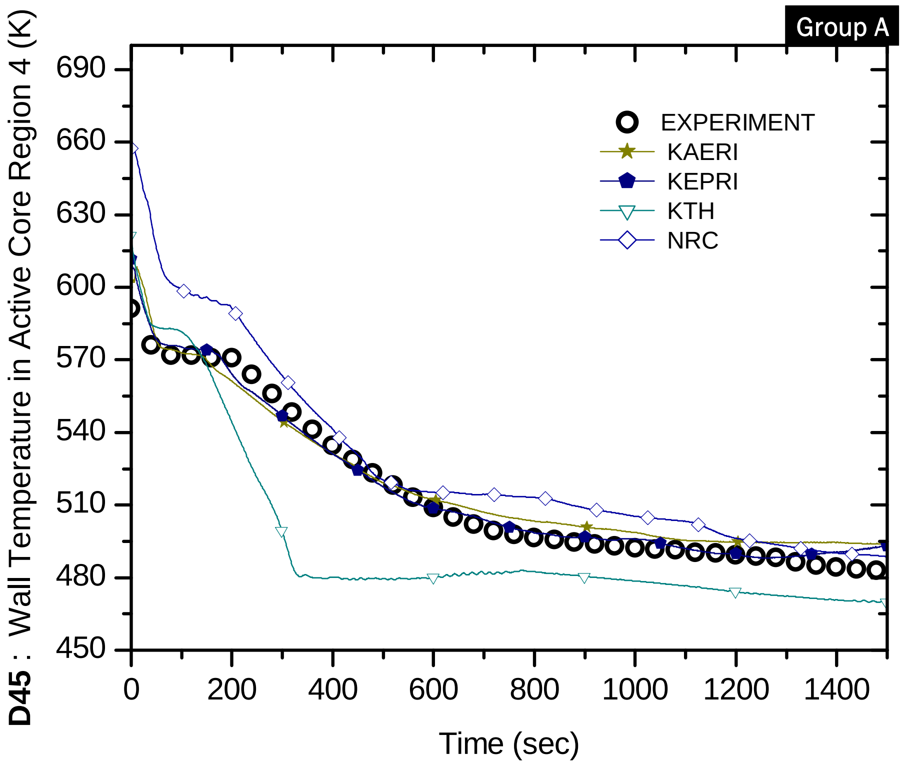

Figure B.45-A Wall temperature in the active core region 4 (D45)

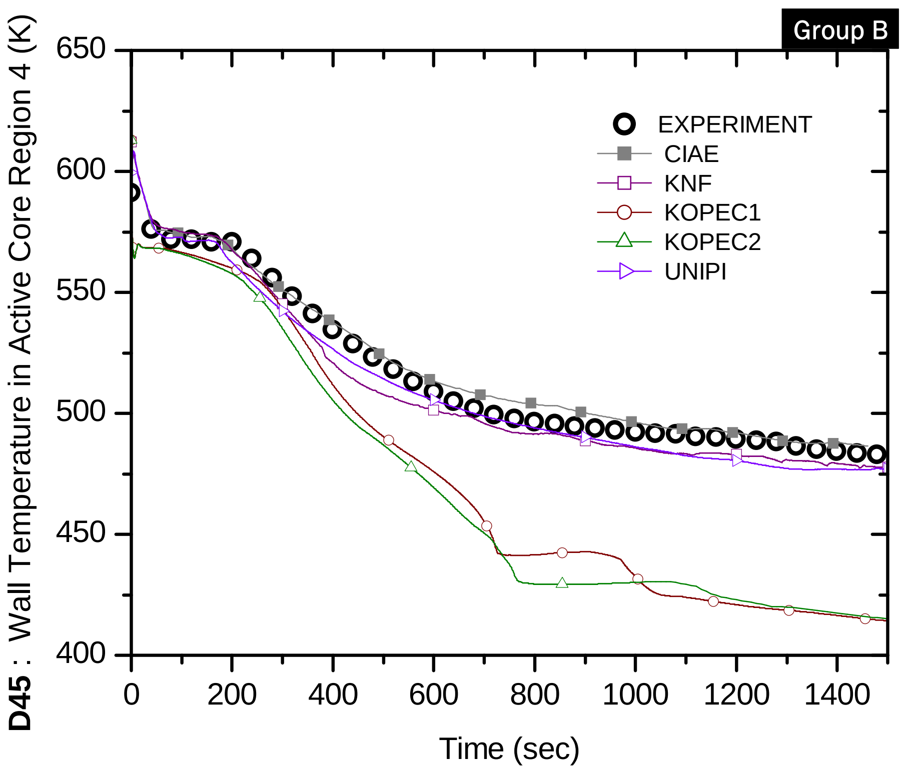

Figure B.45-B Wall temperature in the active core region 4 (D45)

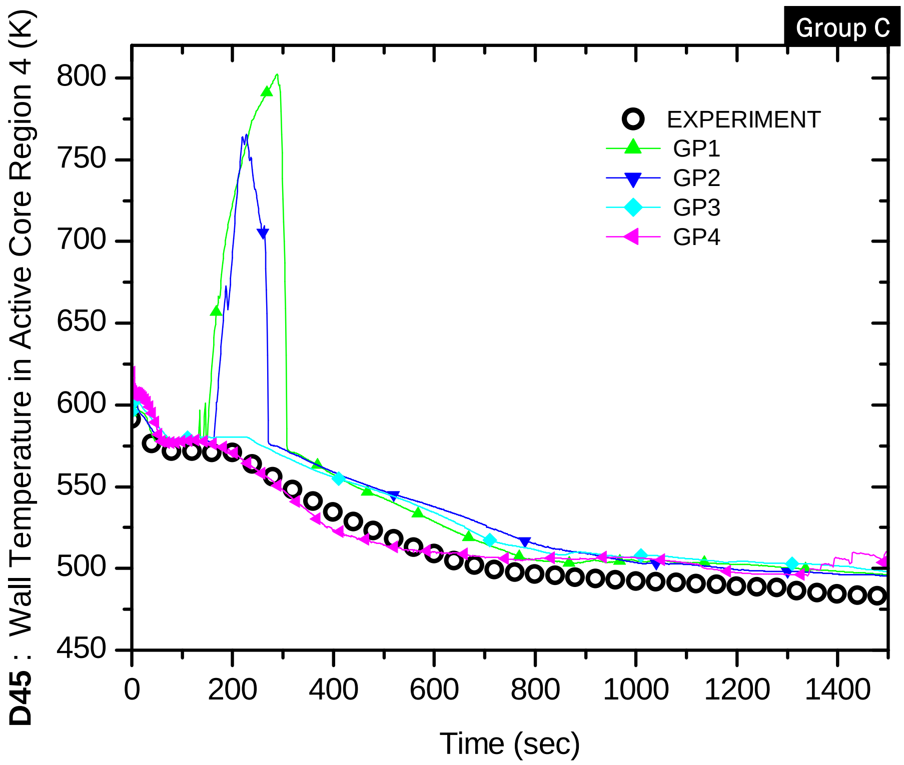

Figure B.45-C Wall temperature in the active core region 4 (D45)

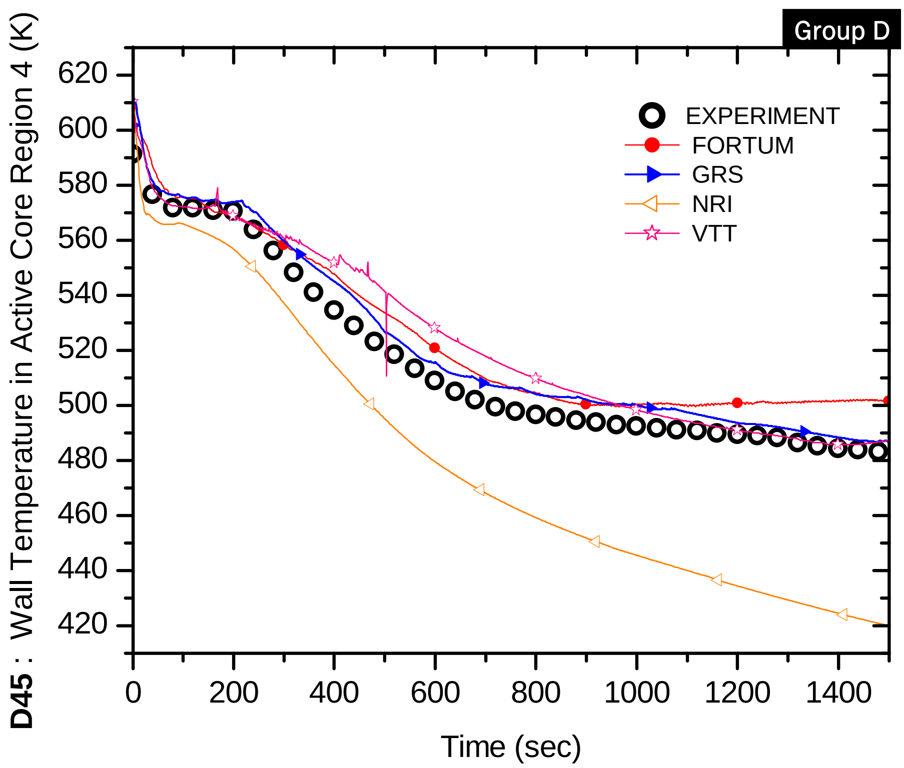

Figure B.45-D Wall temperature in the active core region 4 (D45)

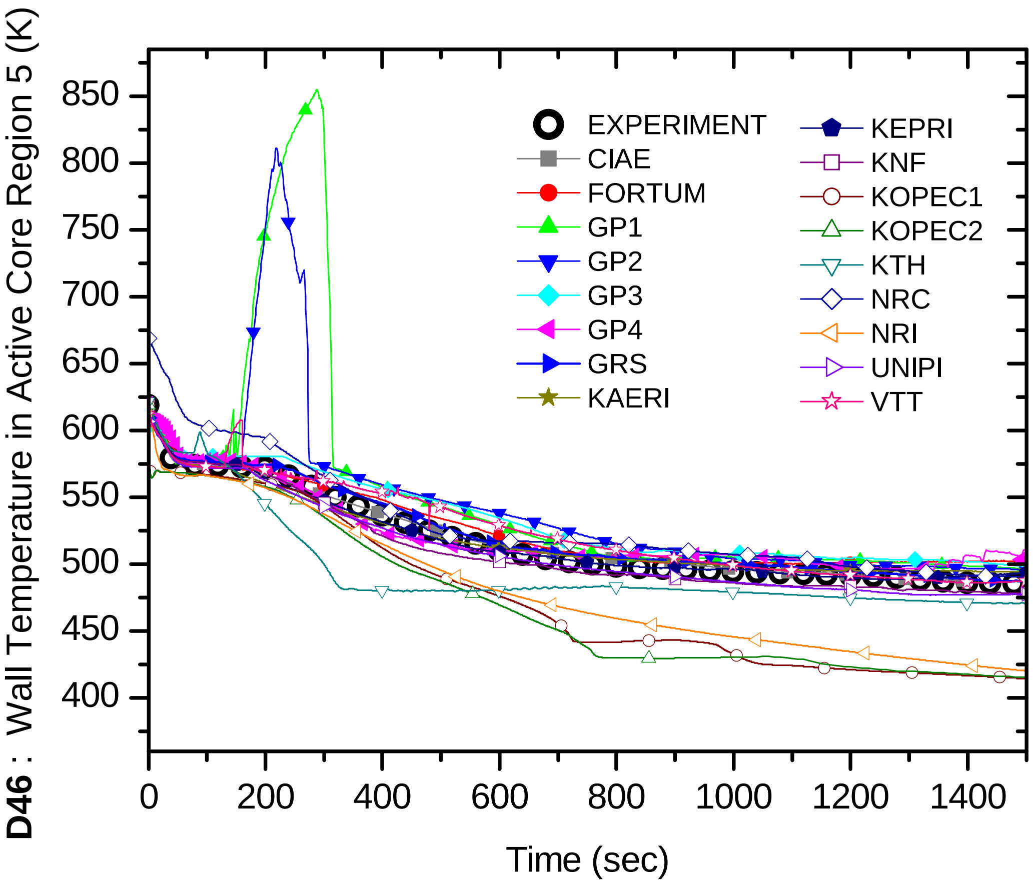

Figure B.46 Wall temperature in the active core region 5 (D46)

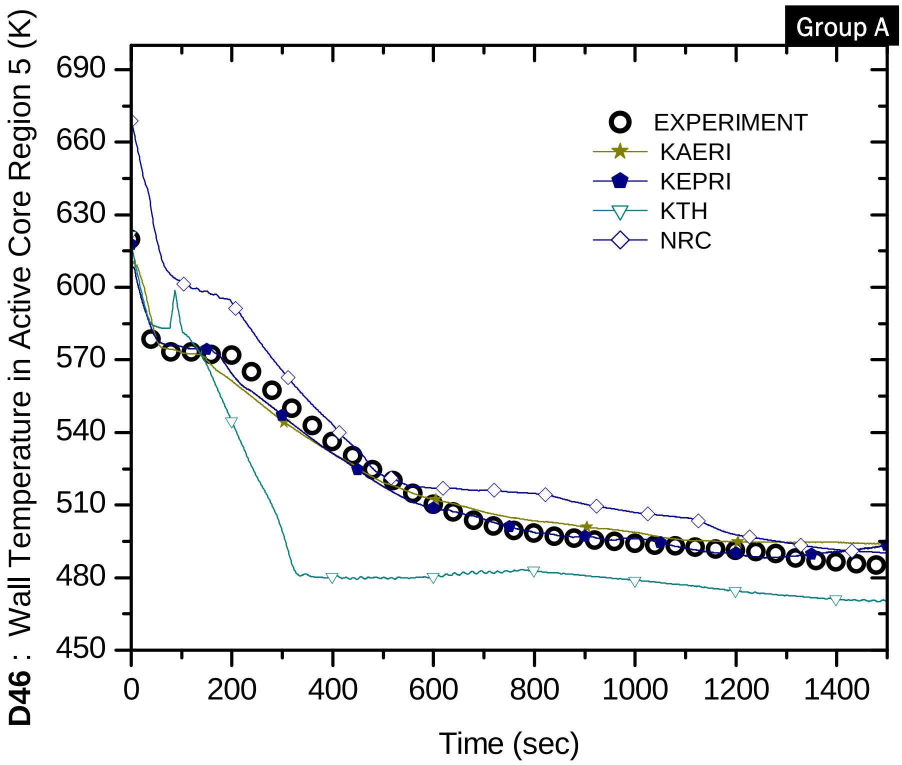

Figure B.46-A Wall temperature in the active core region 5 (D46)

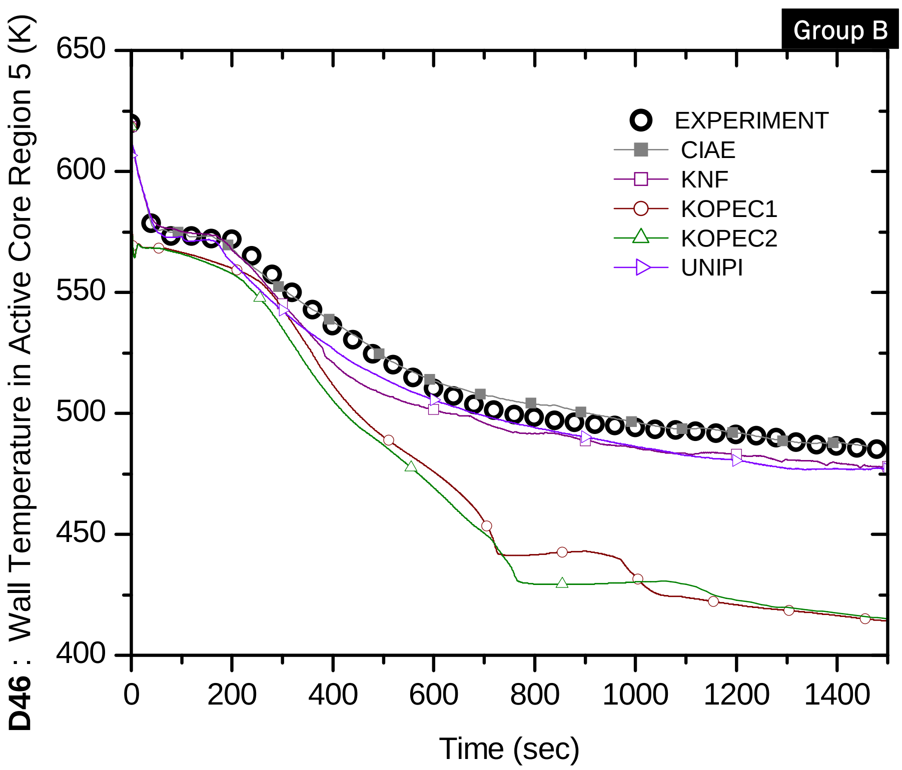

Figure B.46-B Wall temperature in the active core region 5 (D46)

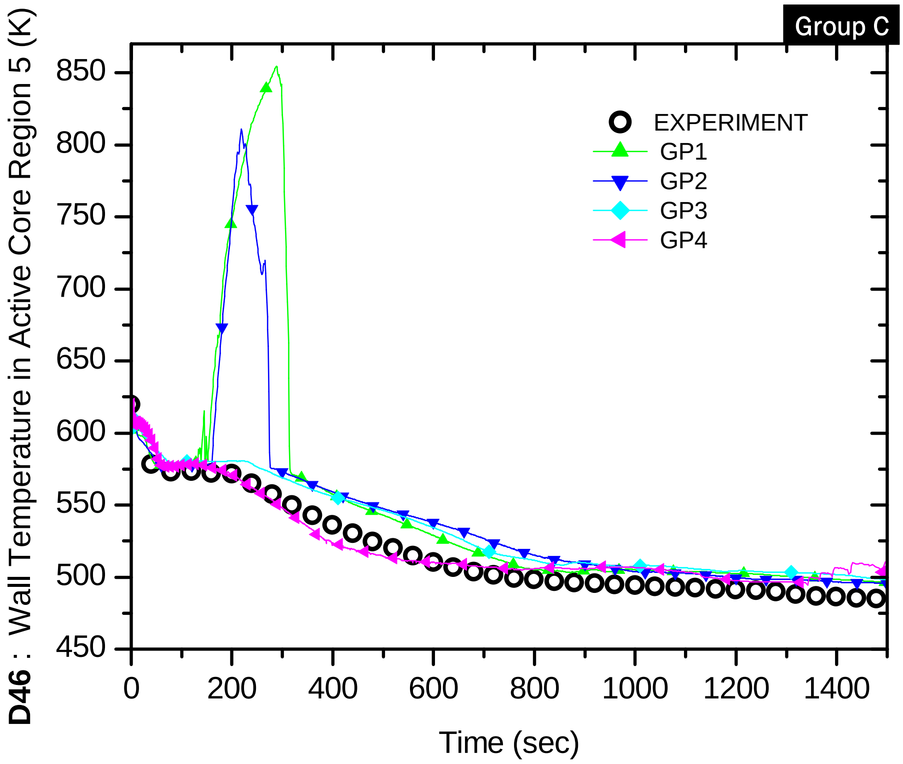

Figure B.46-C Wall temperature in the active core region 5 (D46)

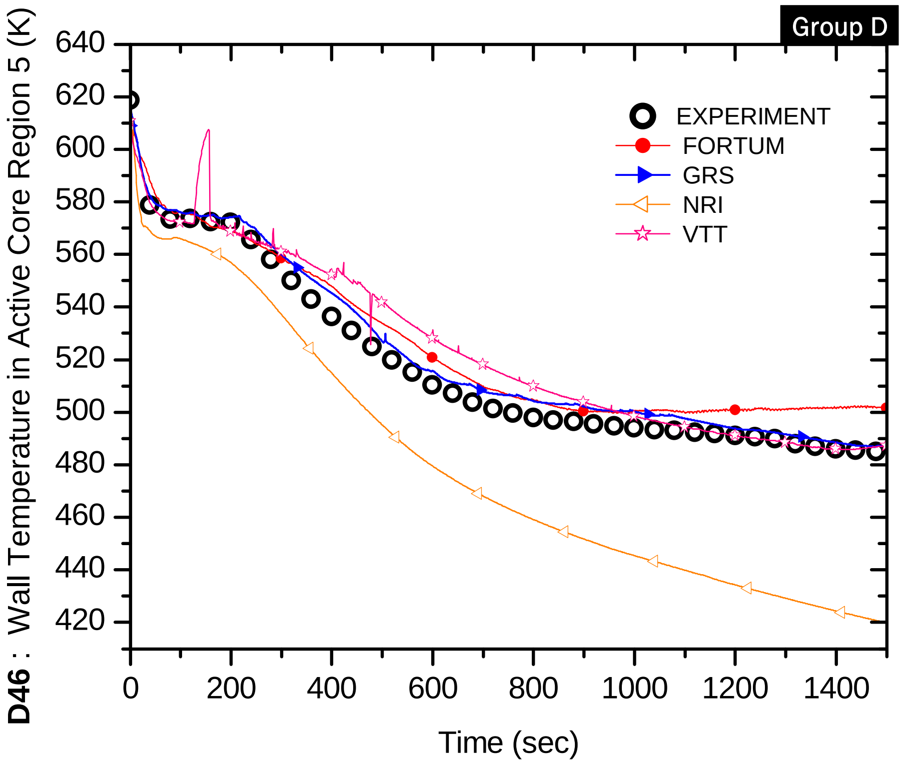

Figure B.46-D Wall temperature in the active core region 5 (D46)

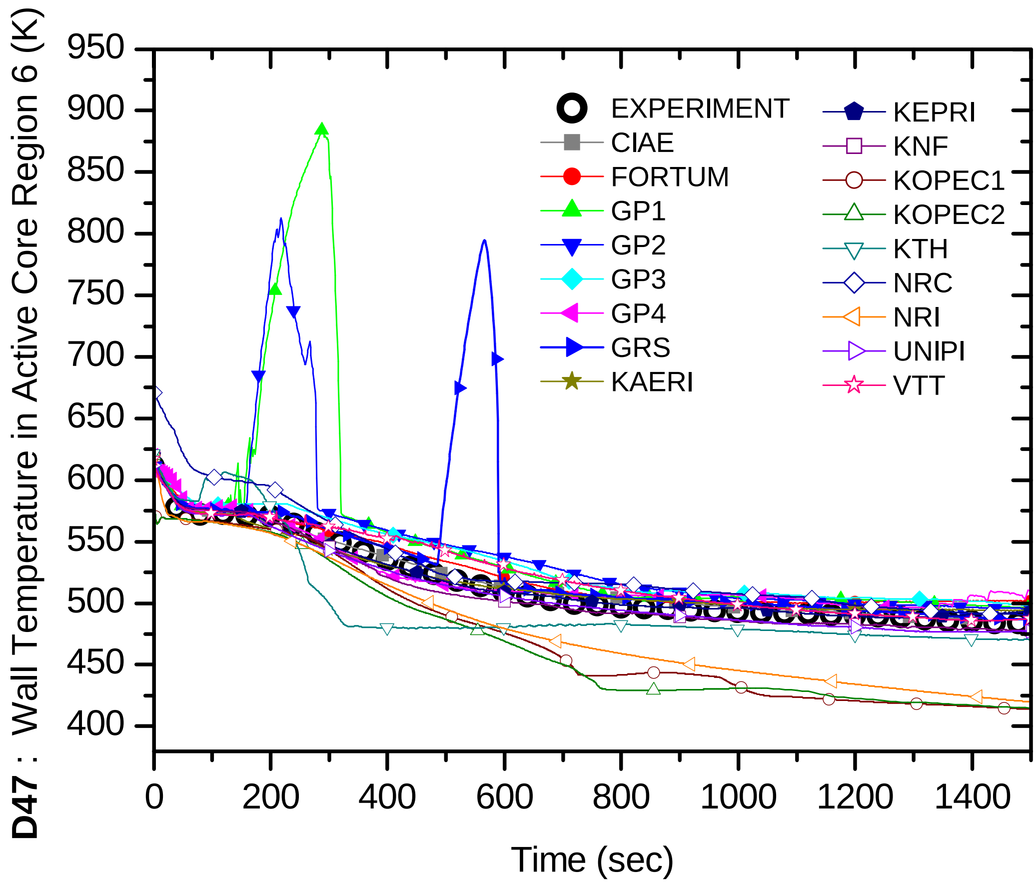

Figure B.47 Wall temperature in the active core region 6 (D47)

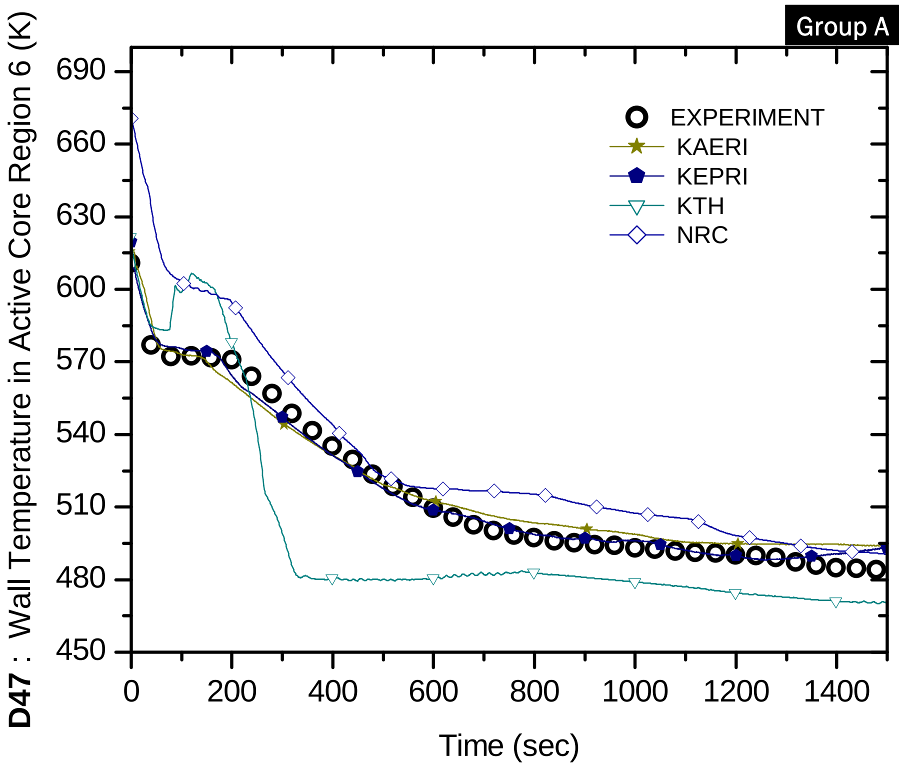

Figure B.47-A Wall temperature in the active core region 6 (D47)

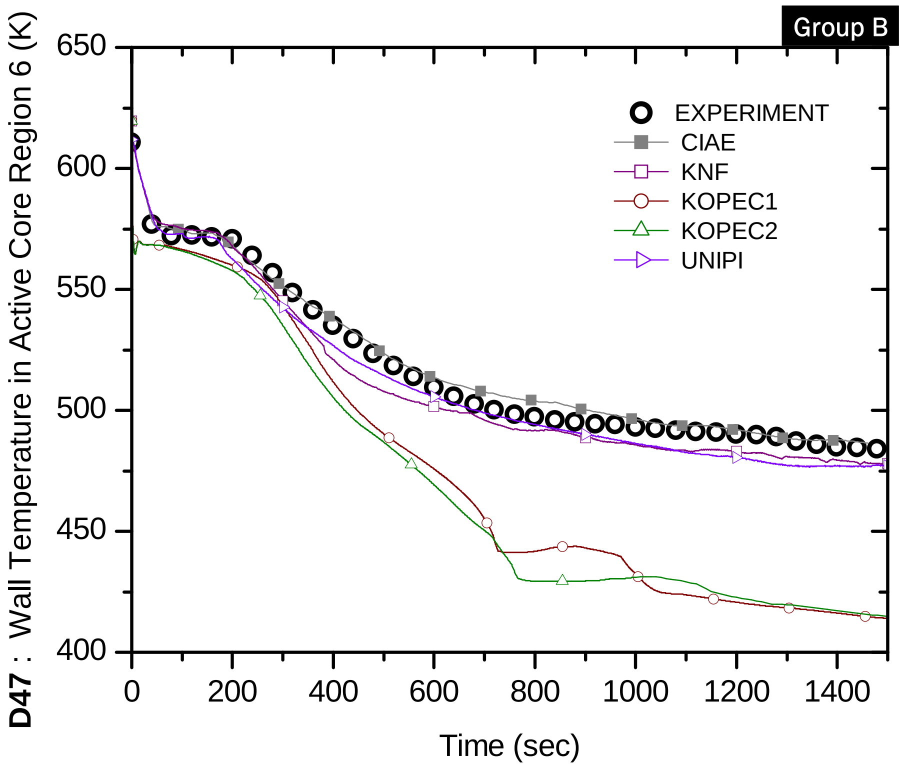

Figure B.47-B Wall temperature in the active core region 6 (D47)

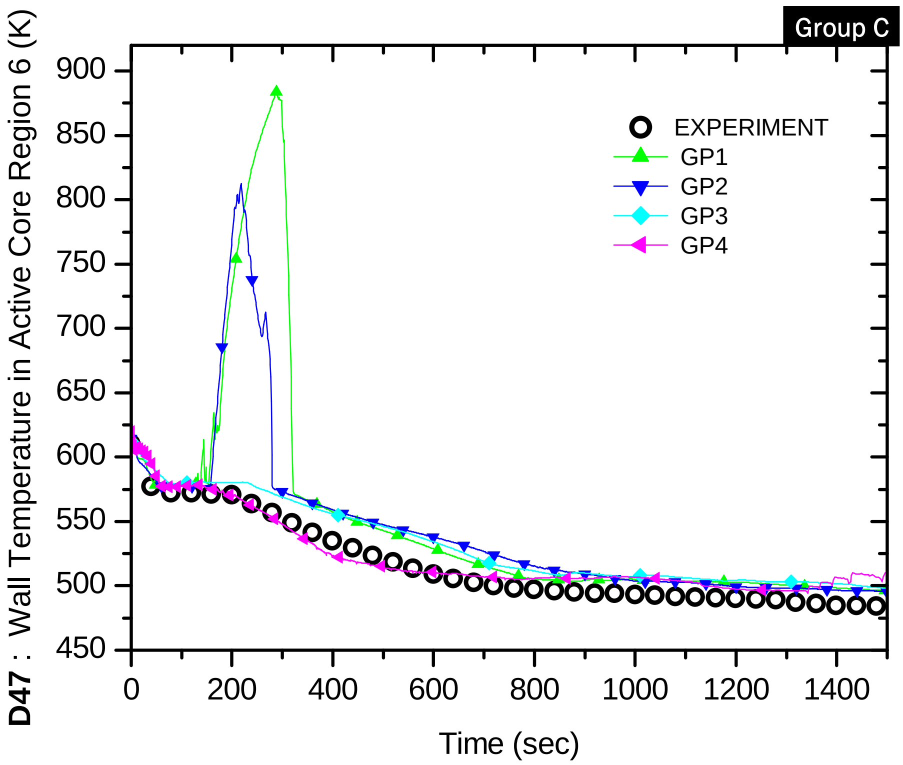

Figure B.47-C Wall temperature in the active core region 6 (D47)

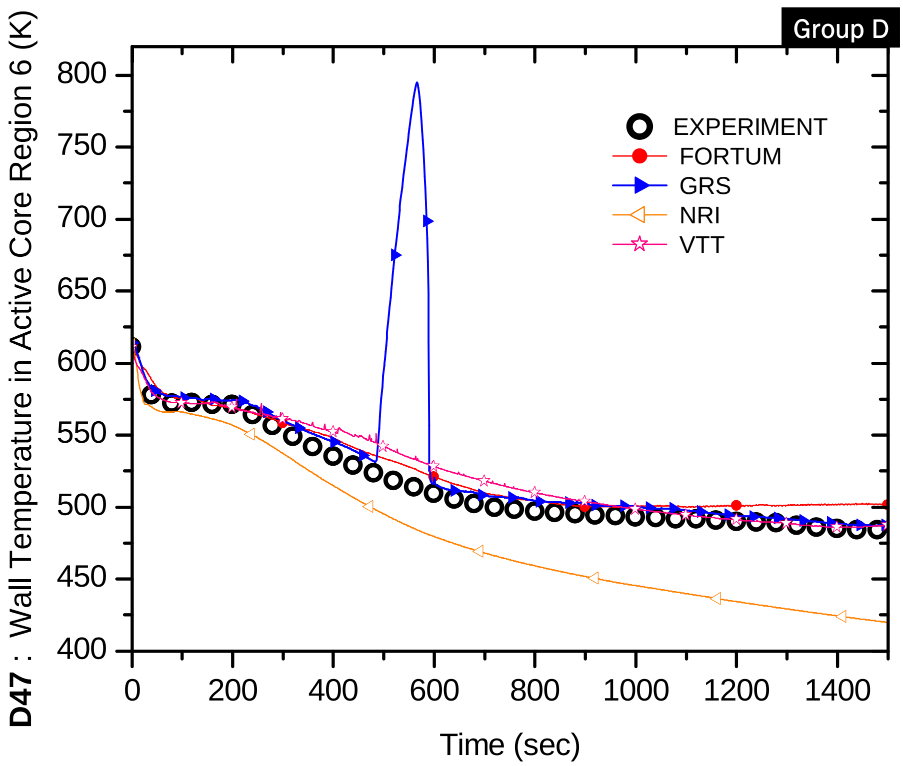

Figure B.47-D Wall temperature in the active core region 6 (D47)

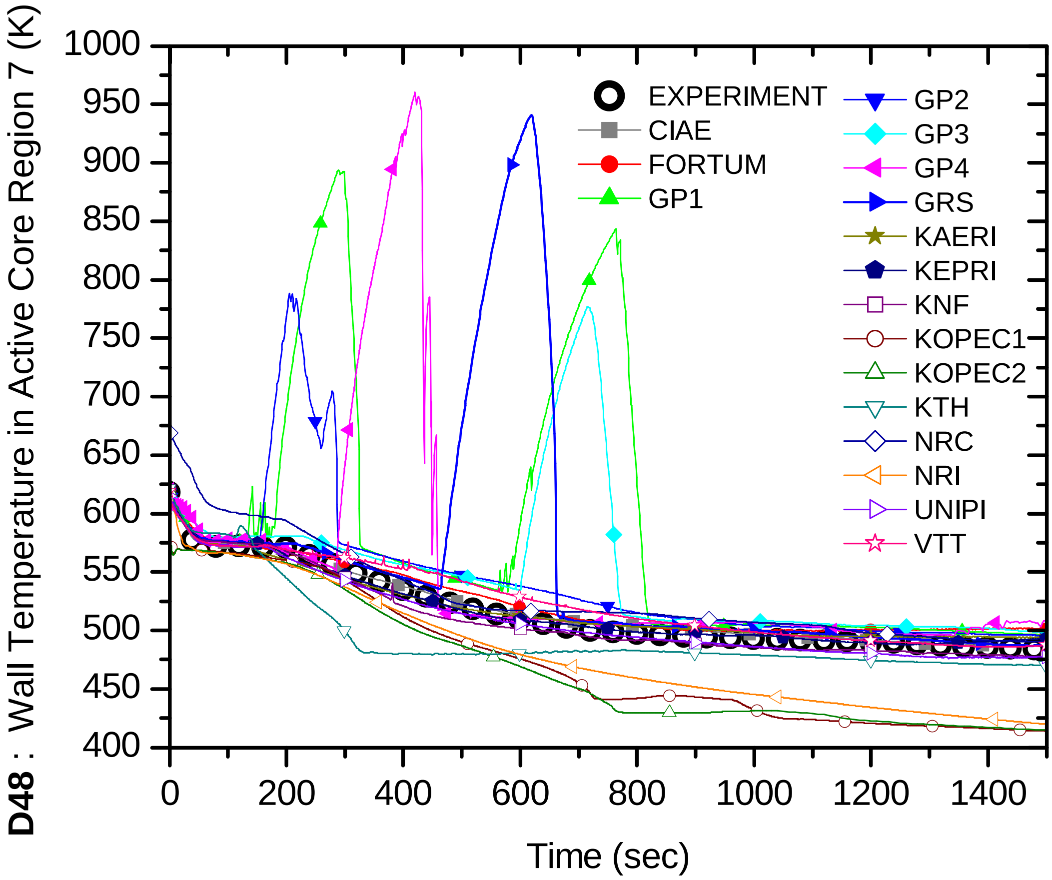

Figure B.48 Wall temperature in the active core region 7 (D48)

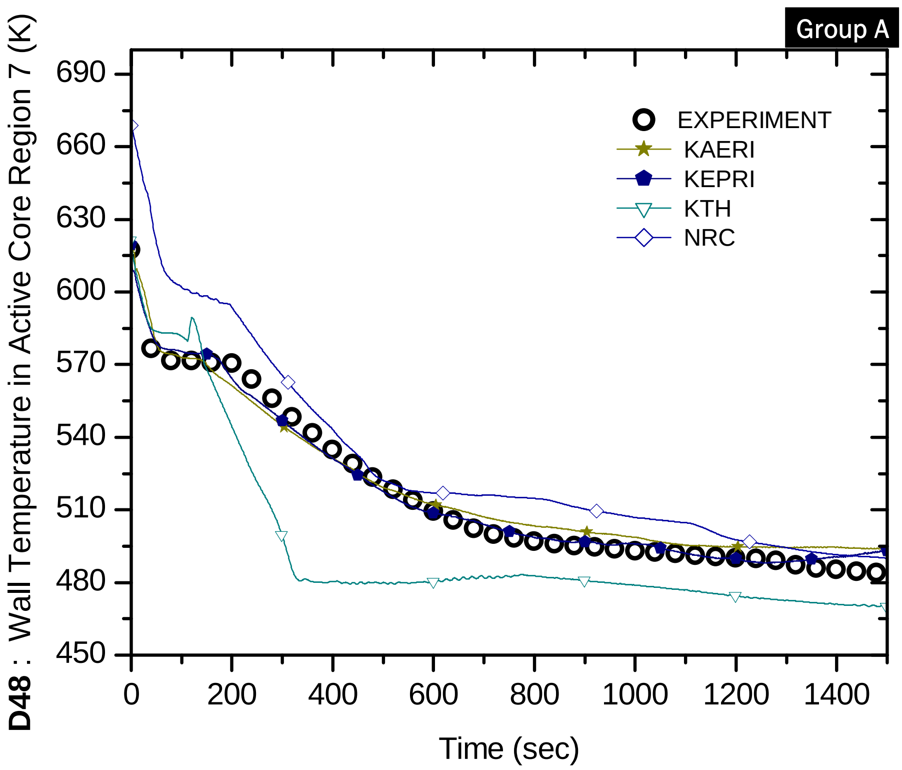

Figure B.48-A Wall temperature in the active core region 7 (D48)

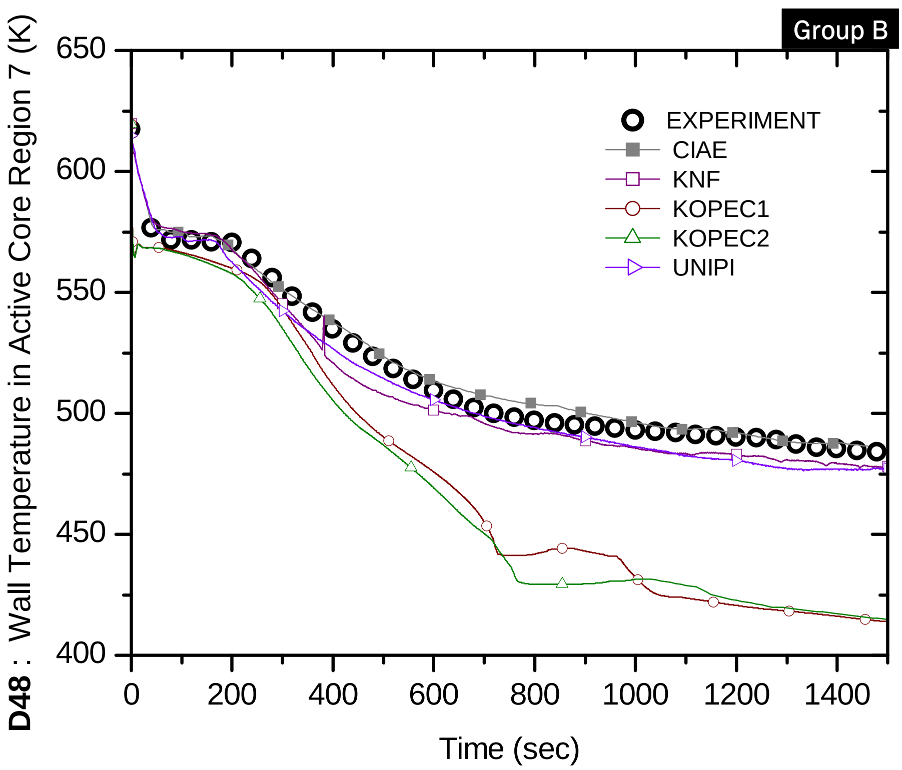

Figure B.48-B Wall temperature in the active core region 7 (D48)

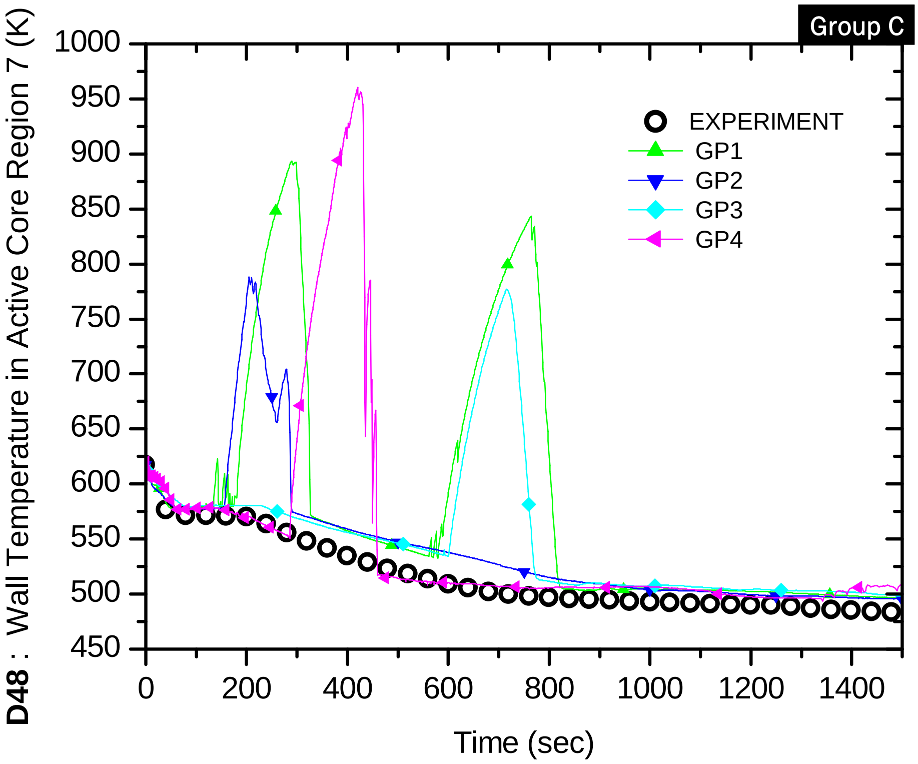

Figure B.48-C Wall temperature in the active core region 7 (D48)

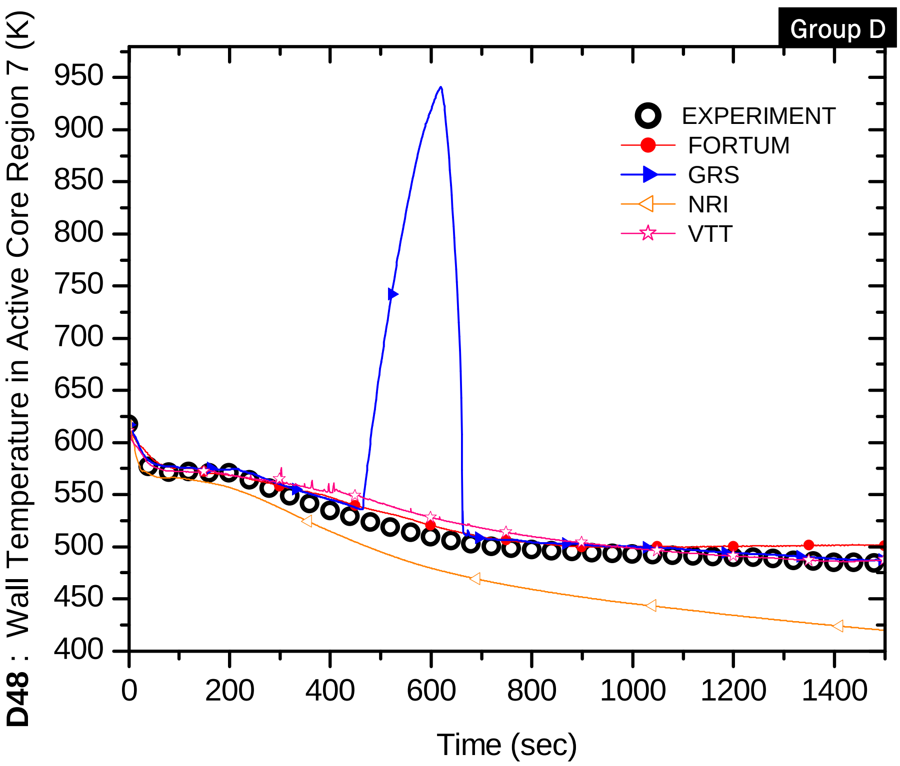

Figure B.48-D Wall temperature in the active core region 7 (D48)

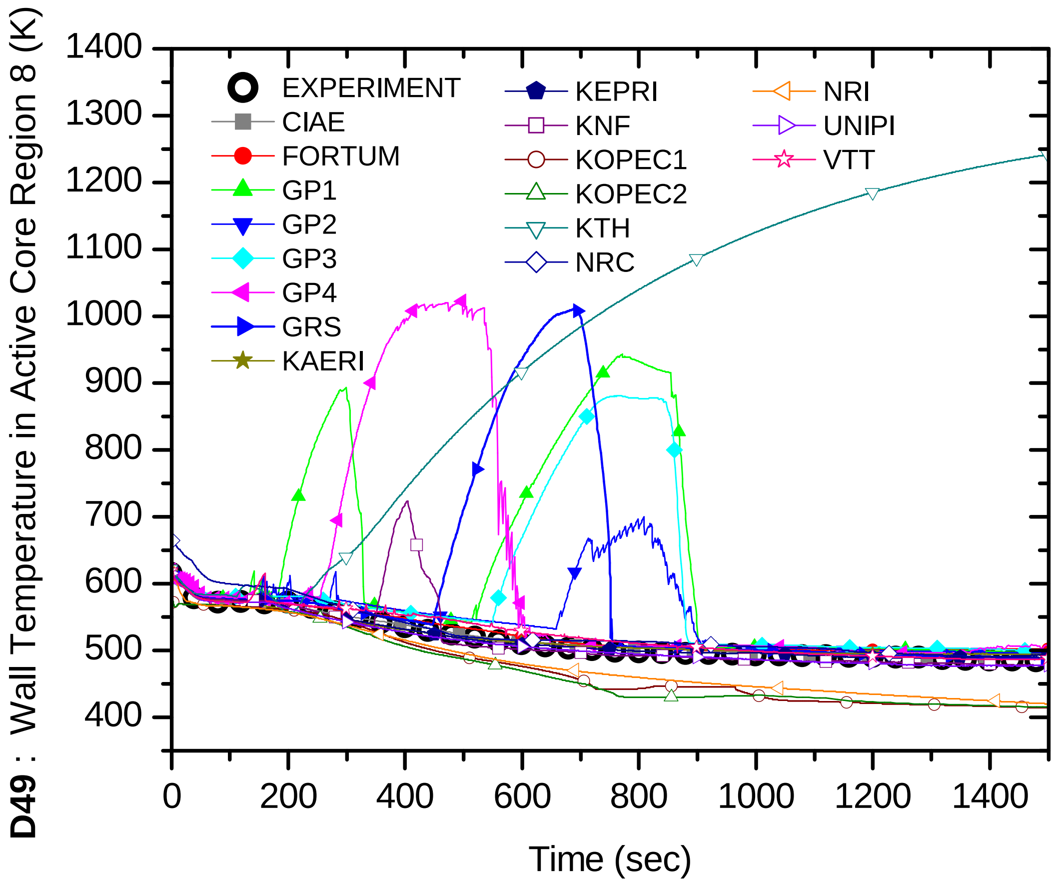

Figure B.49 Wall temperature in the active core region 8 (D49)

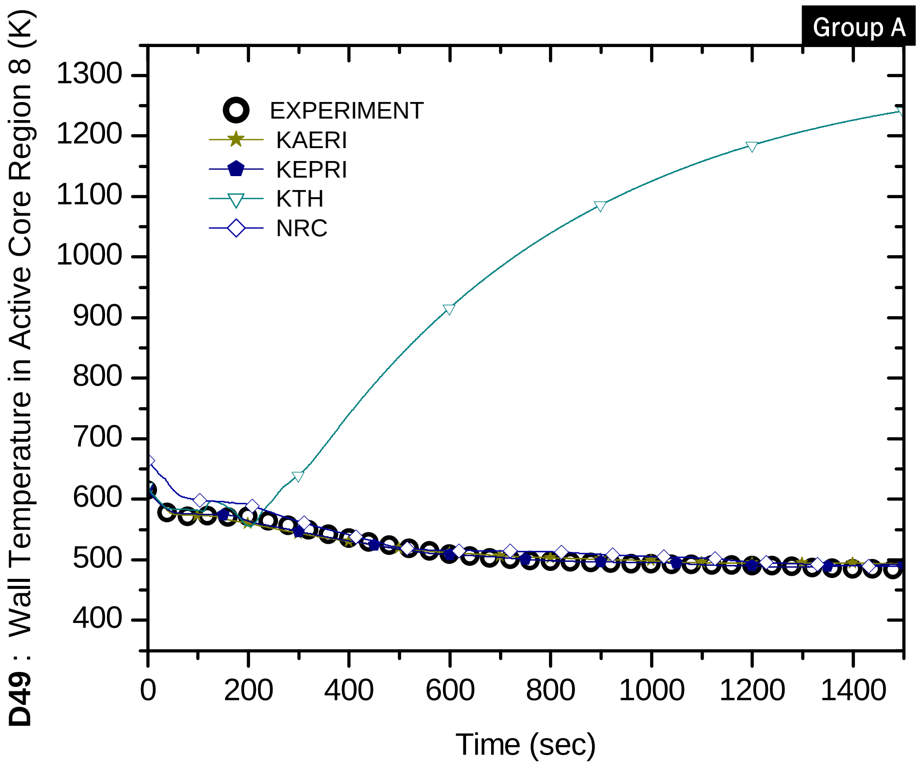

Figure B.49-A Wall temperature in the active core region 8 (D49)

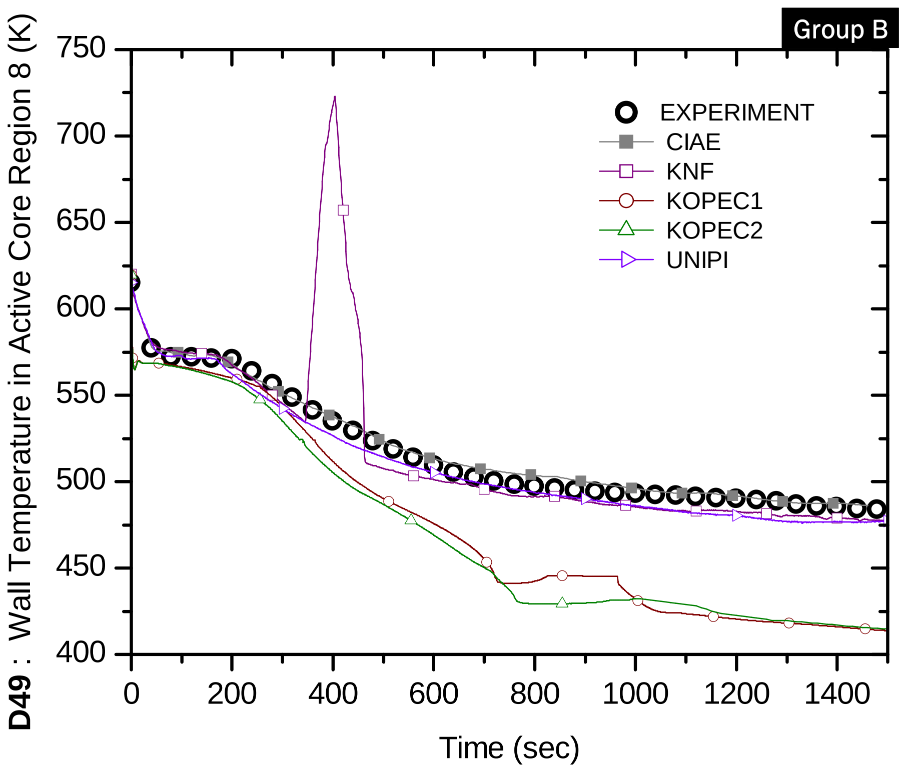

Figure B.49-B Wall temperature in the active core region 8 (D49)

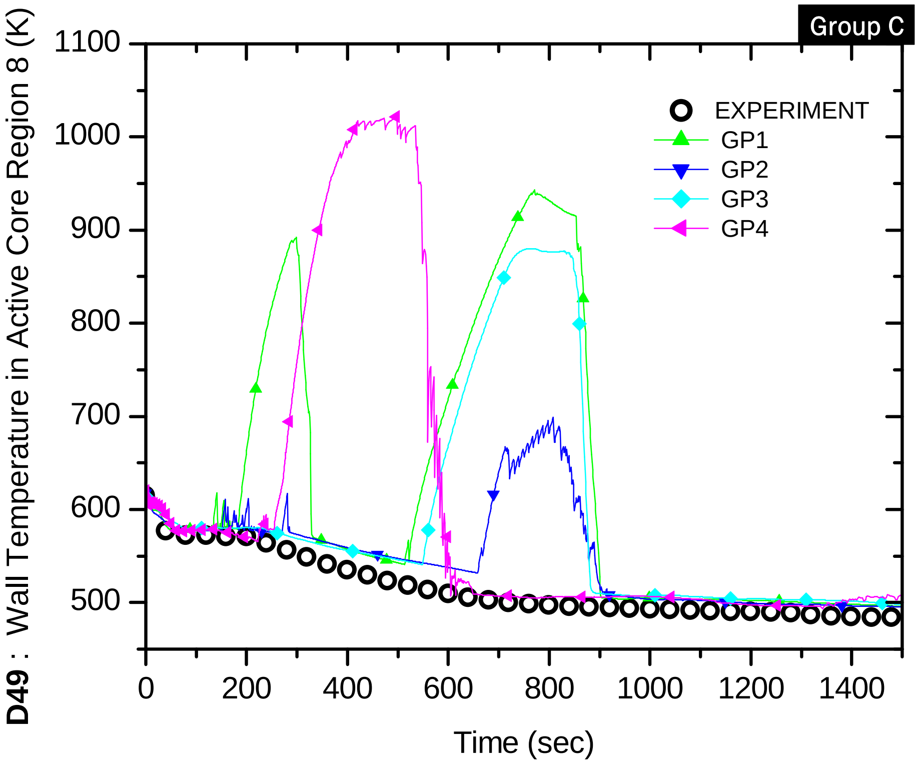

Figure B.49-C Wall temperature in the active core region 8 (D49)

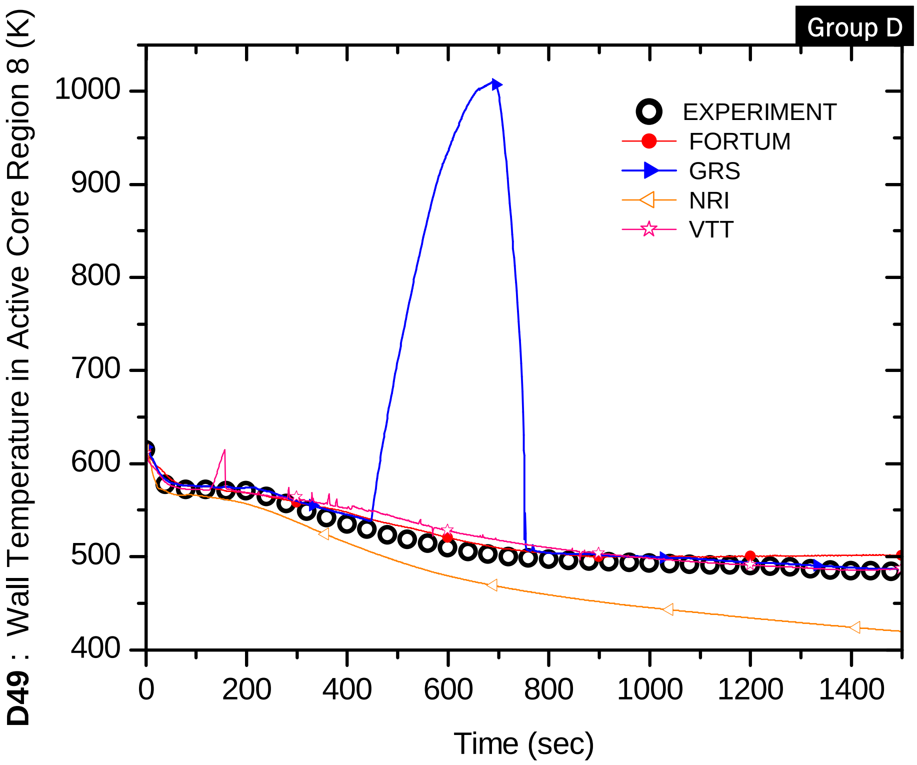

Figure B.49-D Wall temperature in the active core region 8 (D49)

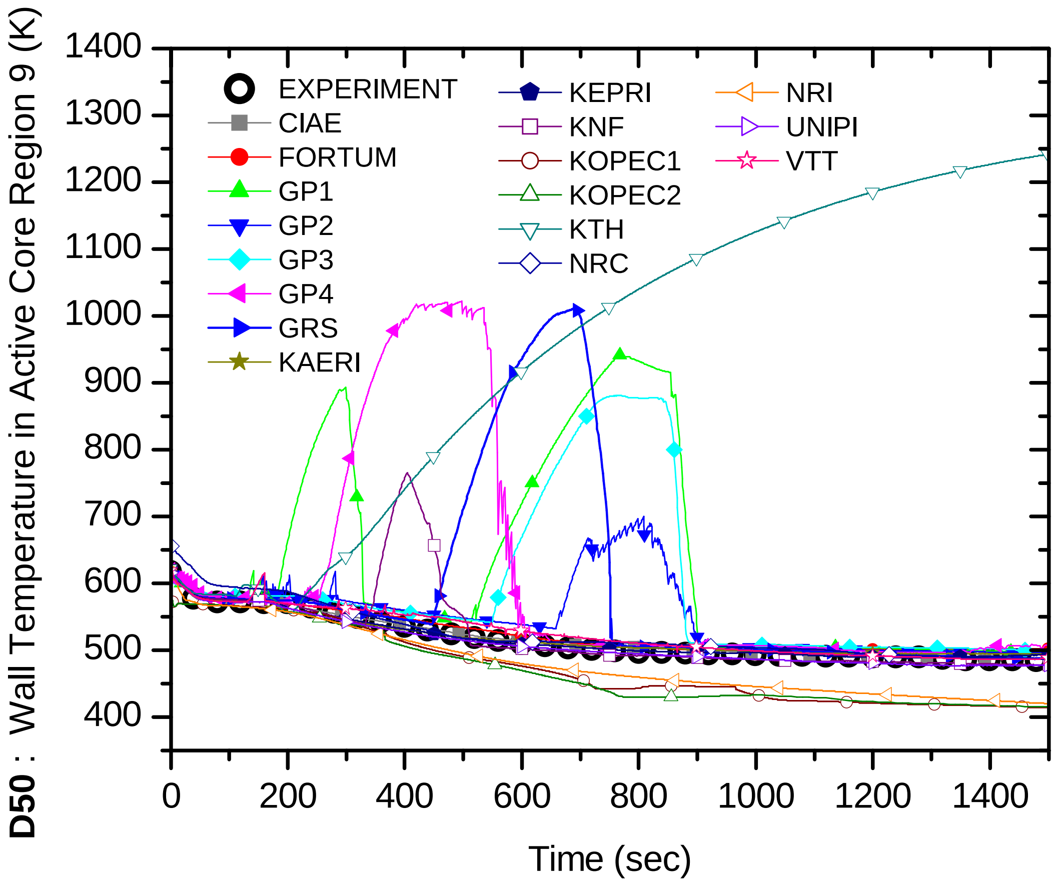

Figure B.50 Wall temperature in the active core region 9 (D50)

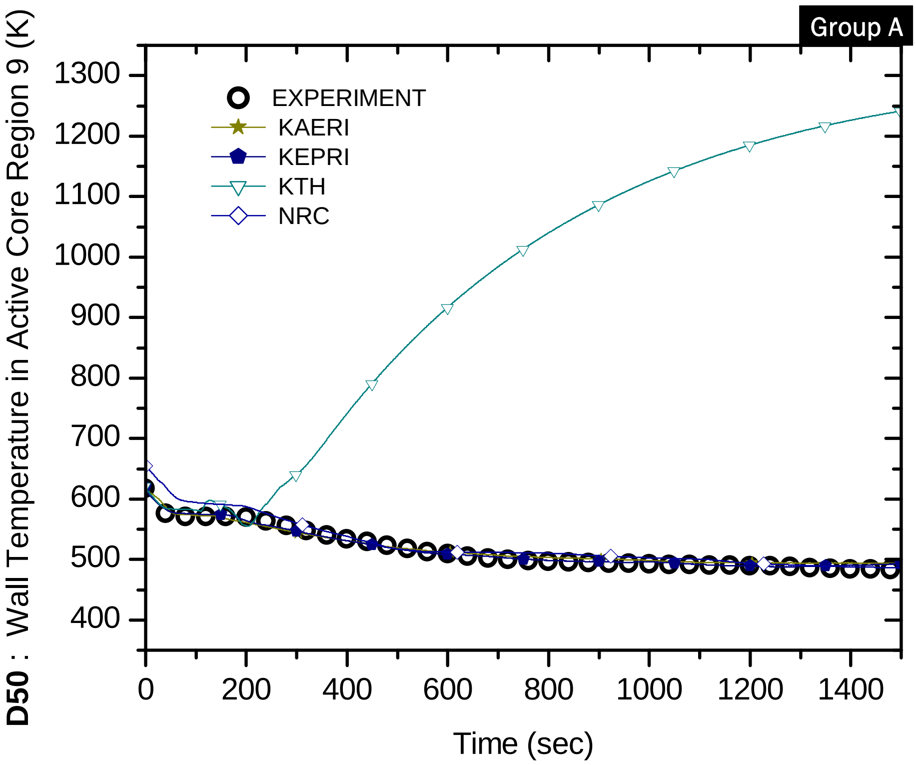

Figure B.50-A Wall temperature in the active core region 9 (D50)

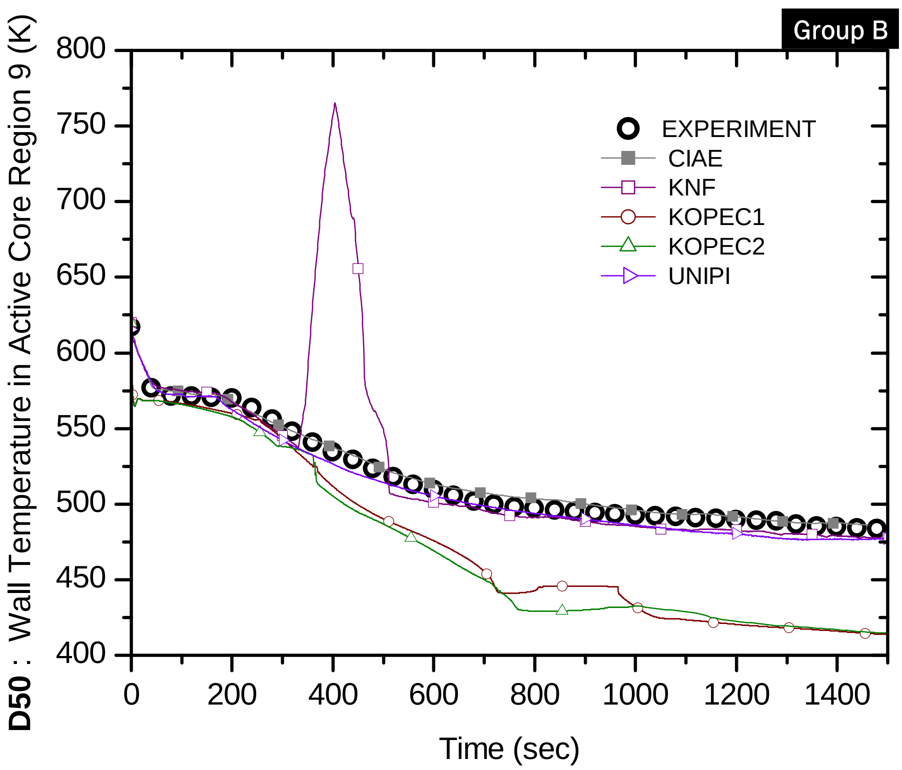

Figure B.50-B Wall temperature in the active core region 9 (D50)

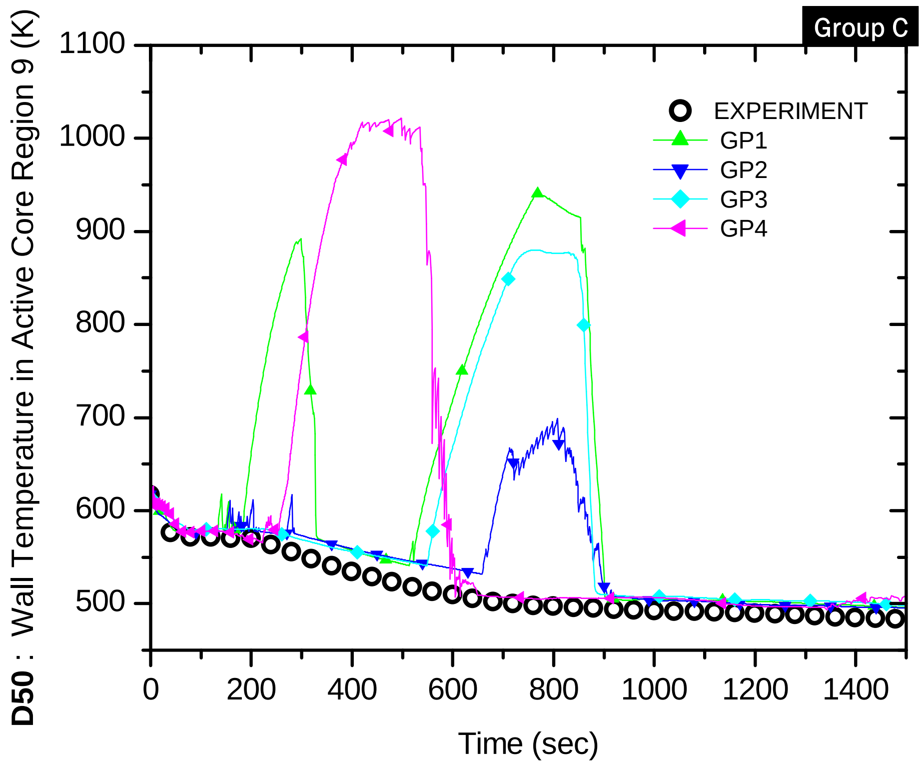

Figure B.50-C Wall temperature in the active core region 9 (D50)

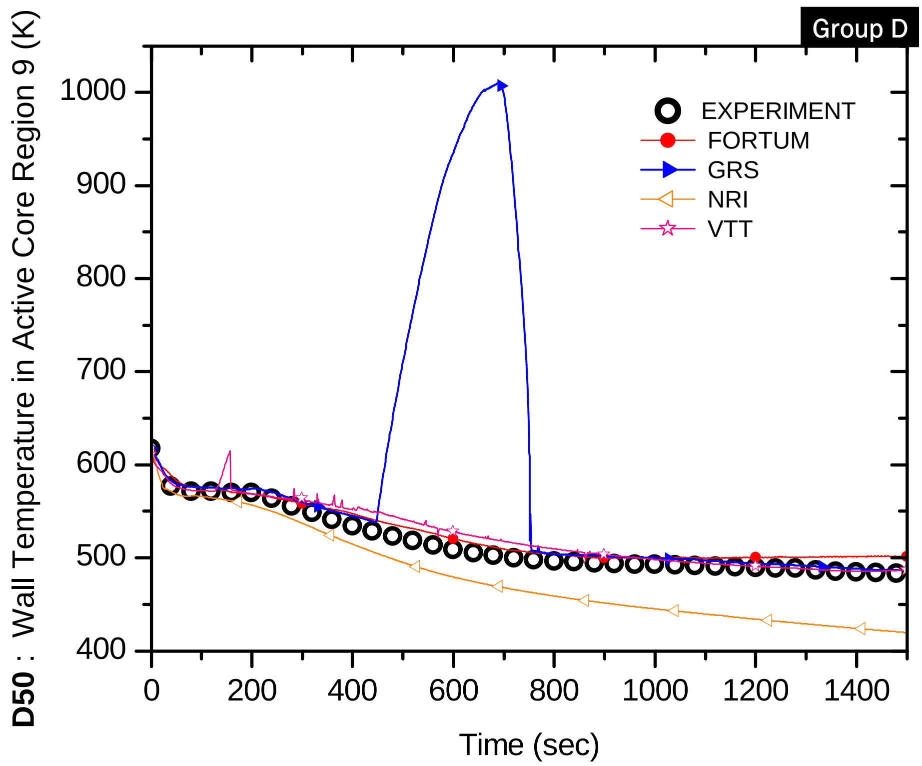

Figure B.50-D Wall temperature in the active core region 9 (D50)

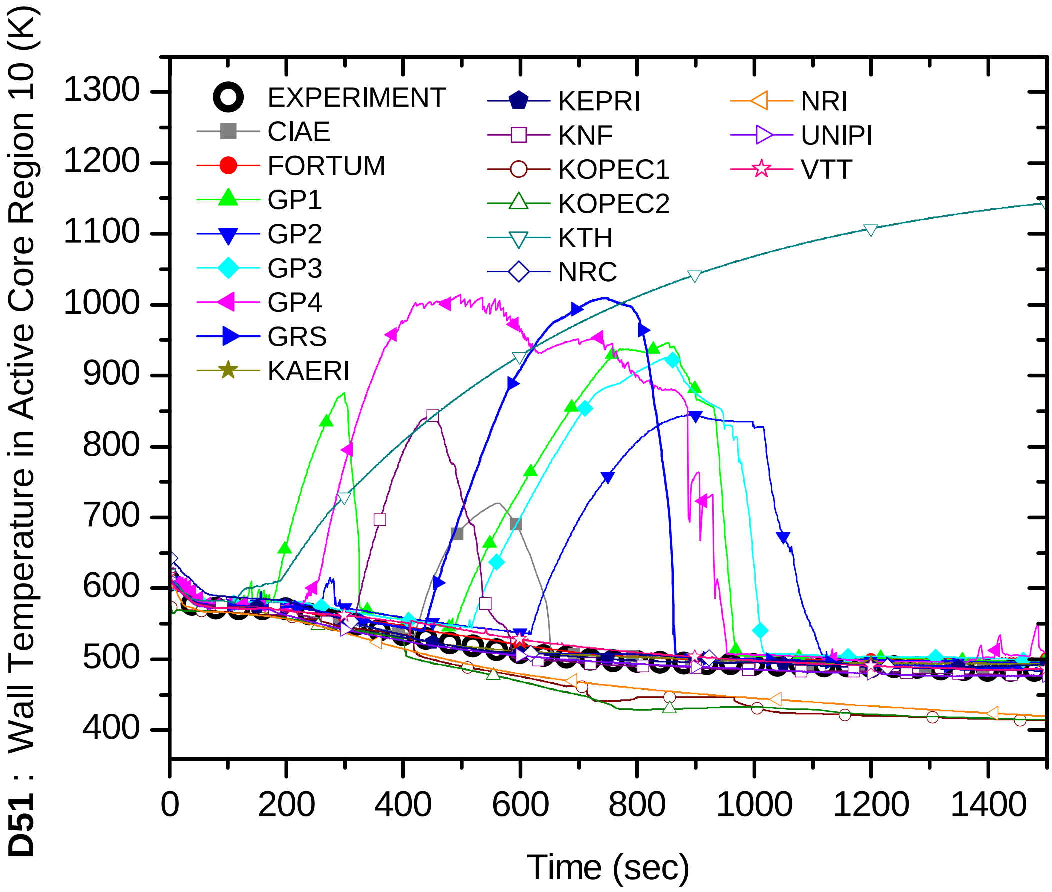

Figure B.51 Wall temperature in the active core region 10 (D51)

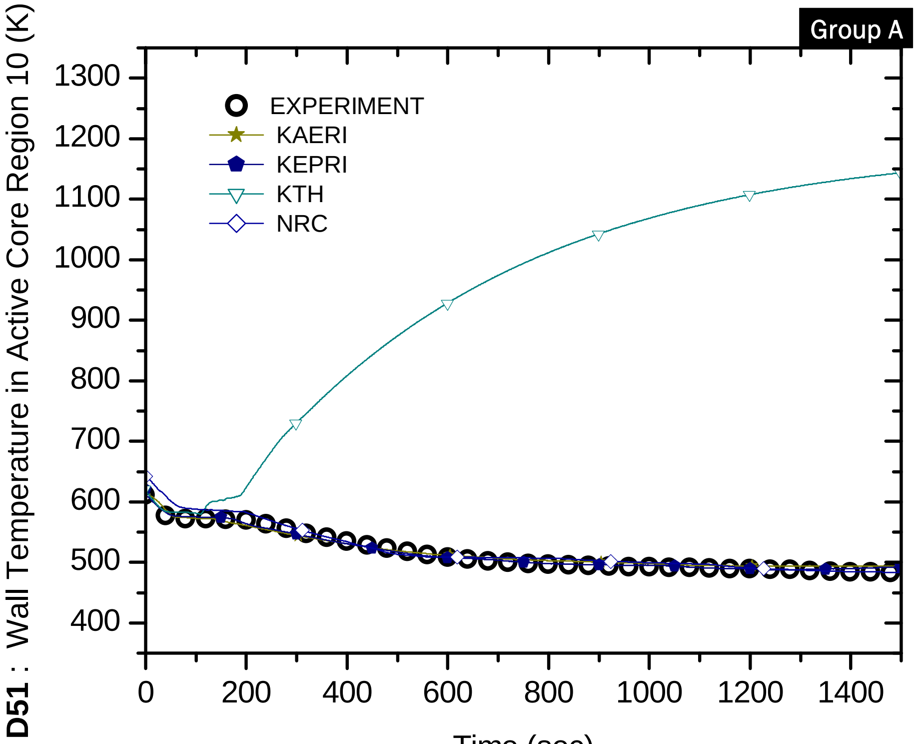

Figure B.51-A Wall temperature in the active core region 10 (D51)

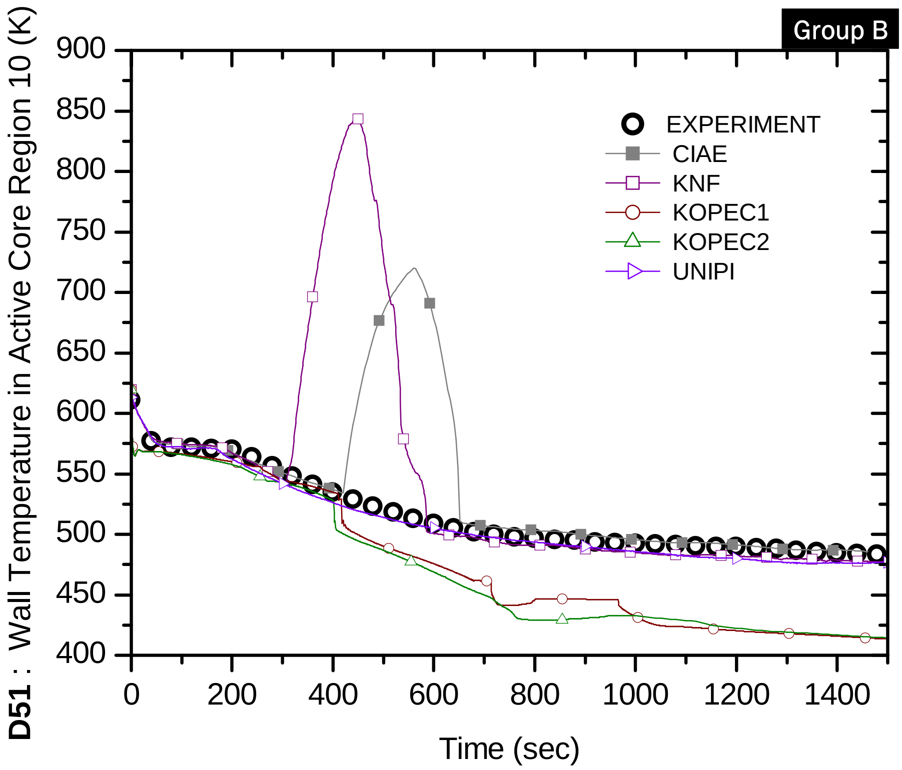

Figure B.51-B Wall temperature in the active core region 10 (D51)

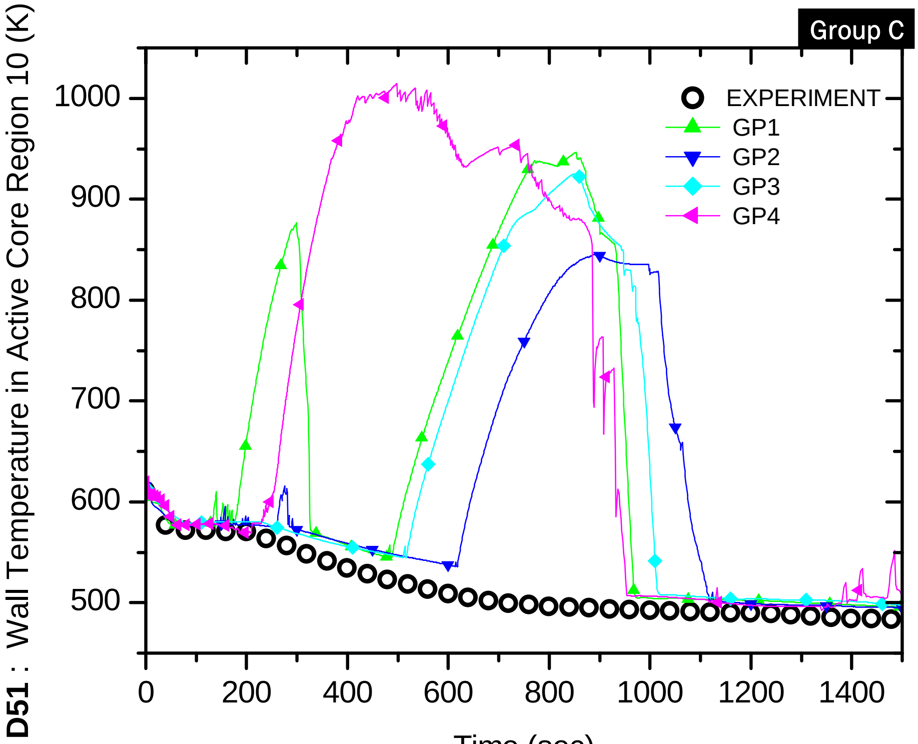

Figure B.51-C Wall temperature in the active core region 10 (D51)

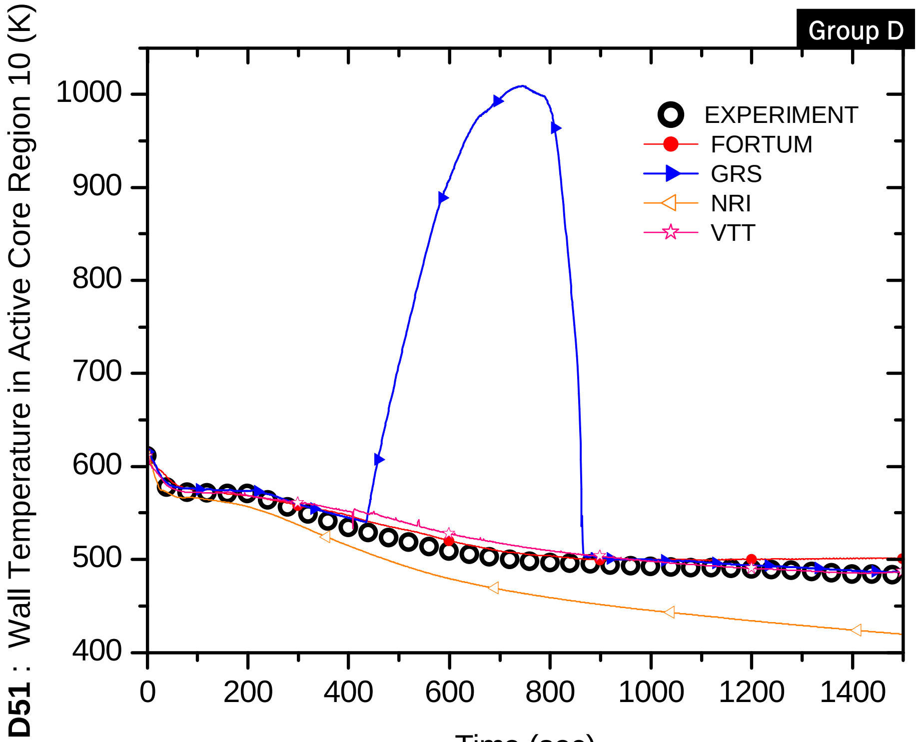

Figure B.51-D Wall temperature in the active core region 10 (D51)

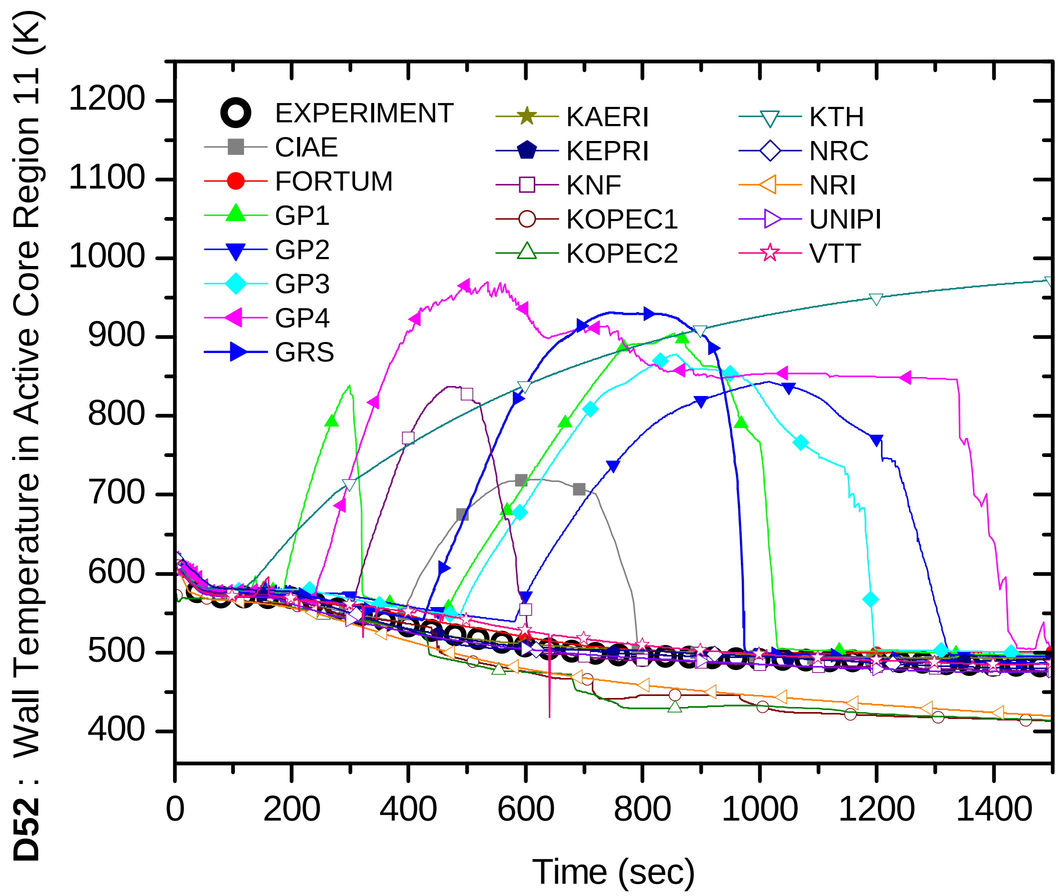

Figure B.52 Wall temperature in the active core region 11 (D52)

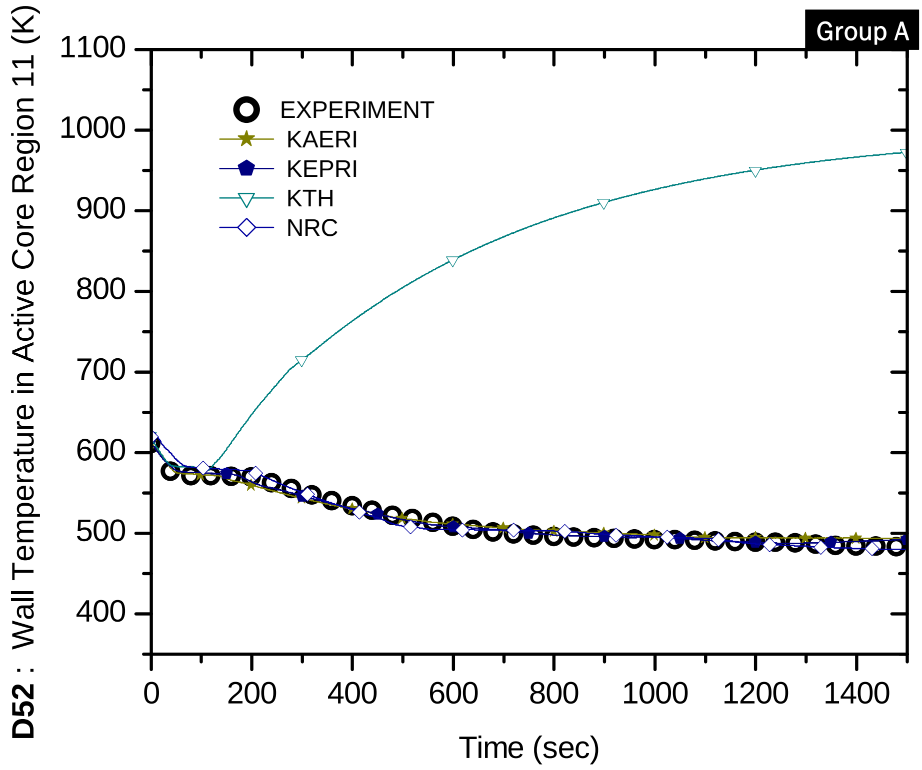

Figure B.52-A Wall temperature in the active core region 11 (D52)

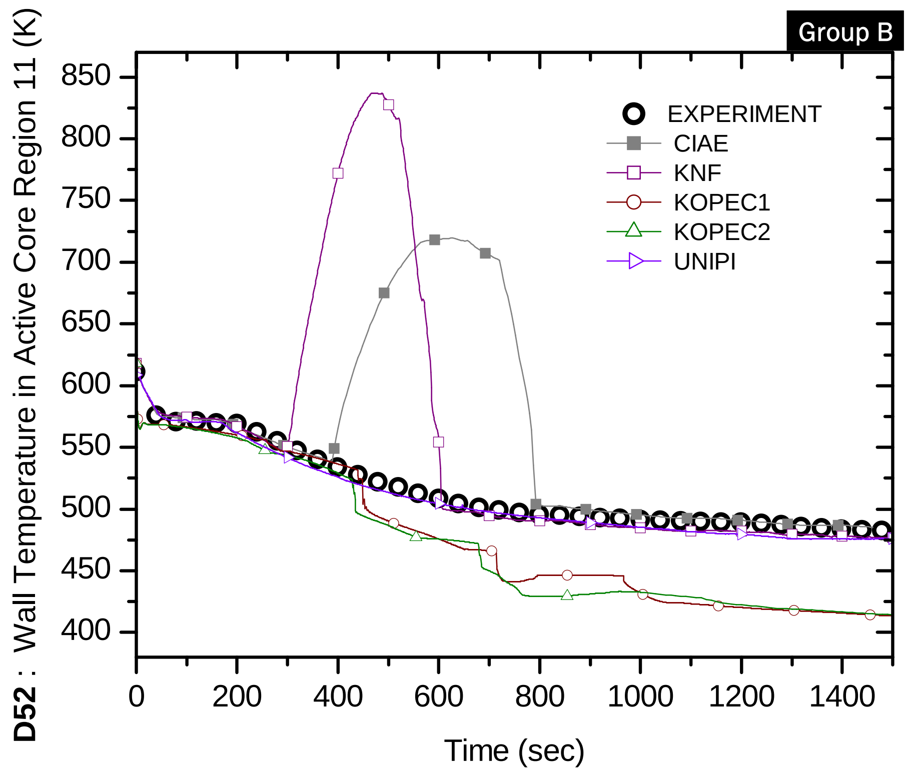

Figure B.52-B Wall temperature in the active core region 11 (D52)

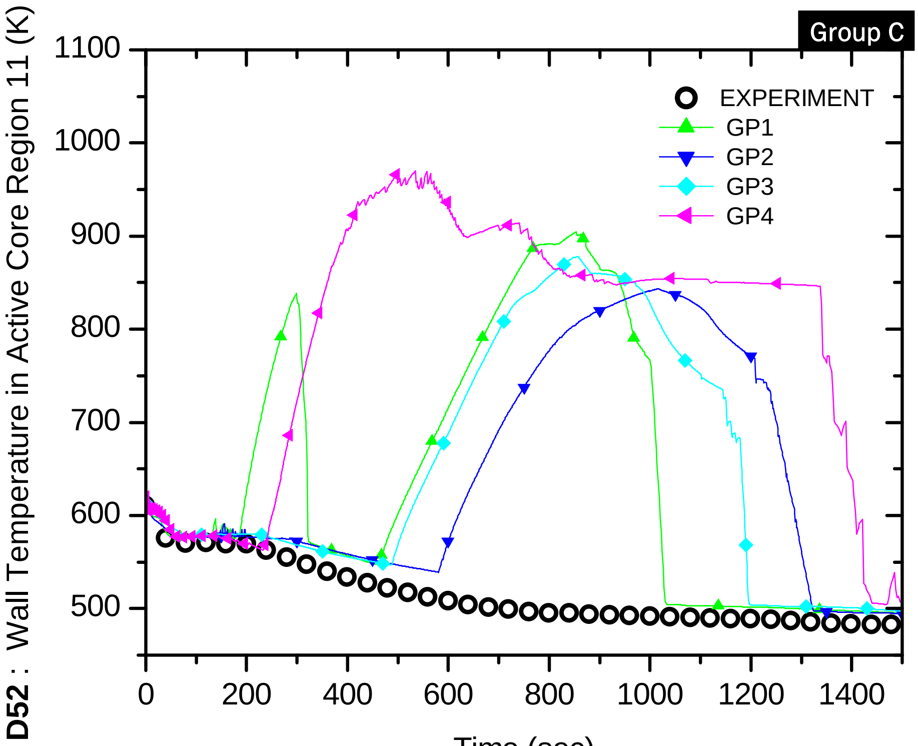

Figure B.52-C Wall temperature in the active core region 11 (D52)

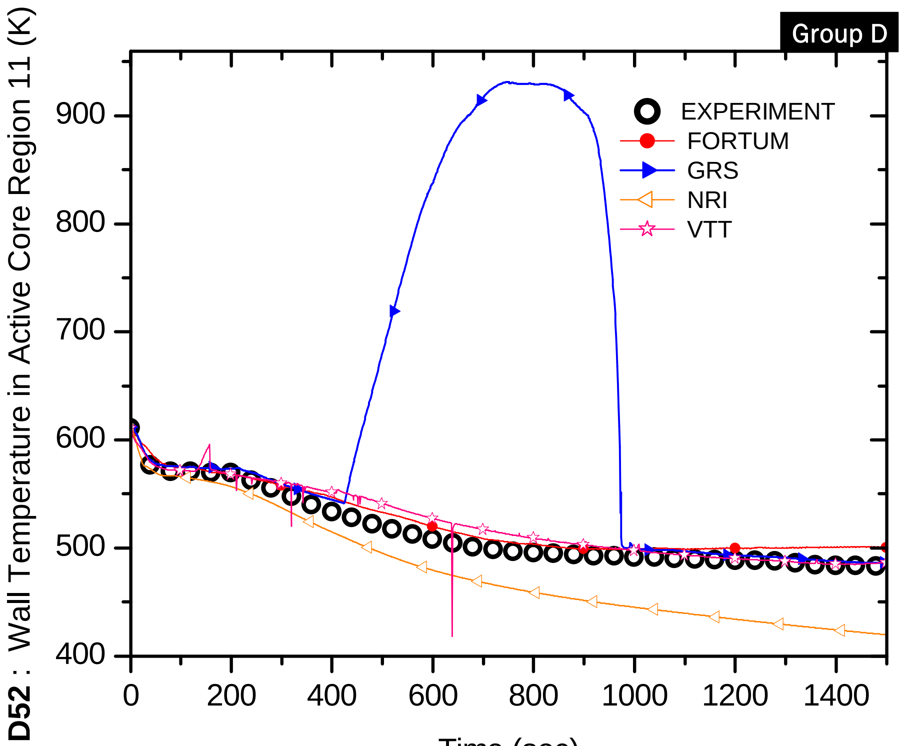

Figure B.52-D Wall temperature in the active core region 11 (D52)

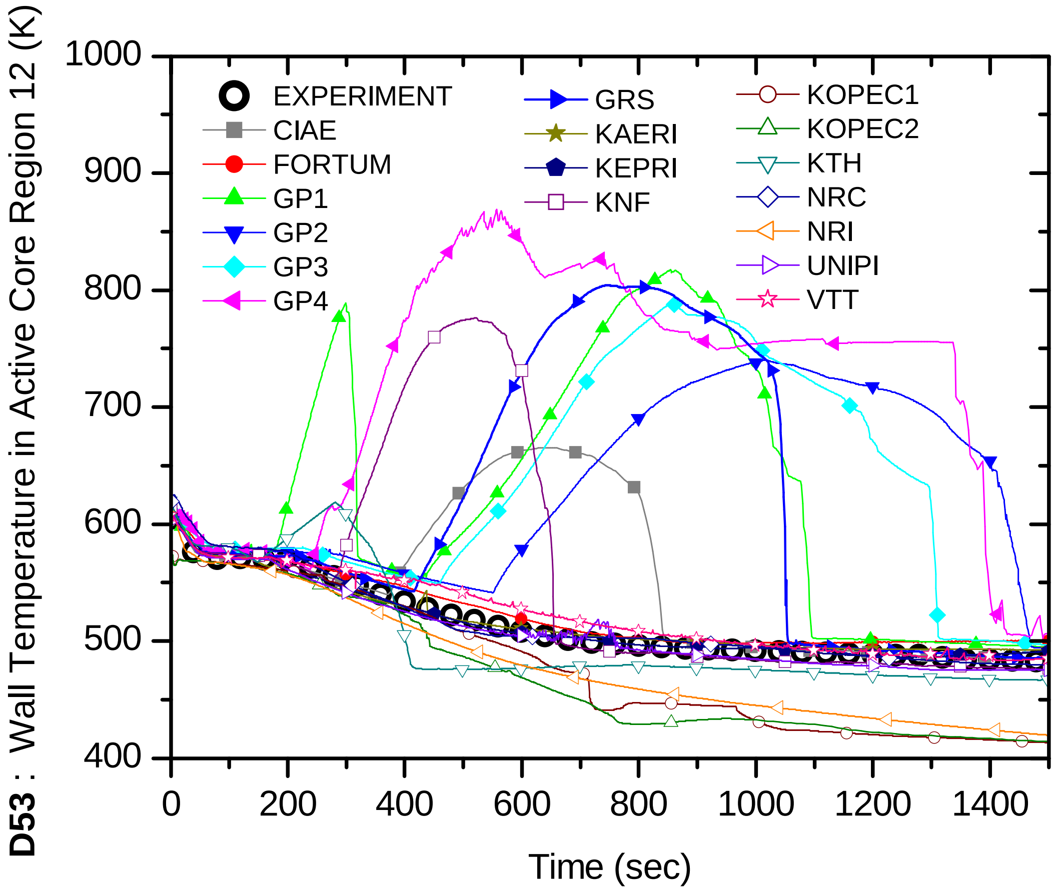

Figure B.53 Wall temperature in the active core region 12 (D53)

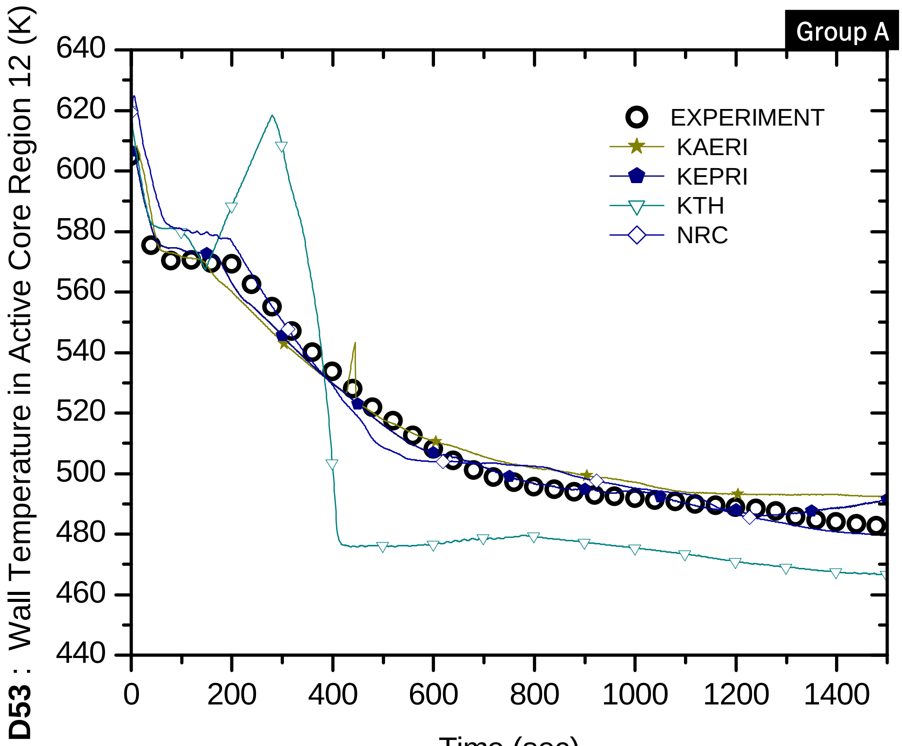

Figure B.53-A Wall temperature in the active core region 12 (D53)

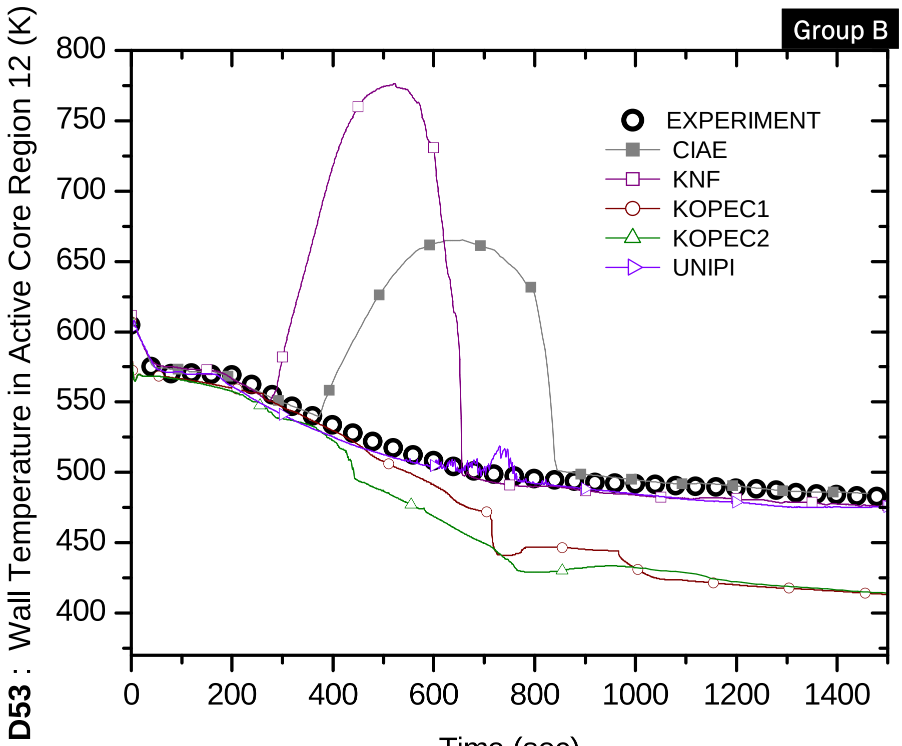

Figure B.53-B Wall temperature in the active core region 12 (D53)

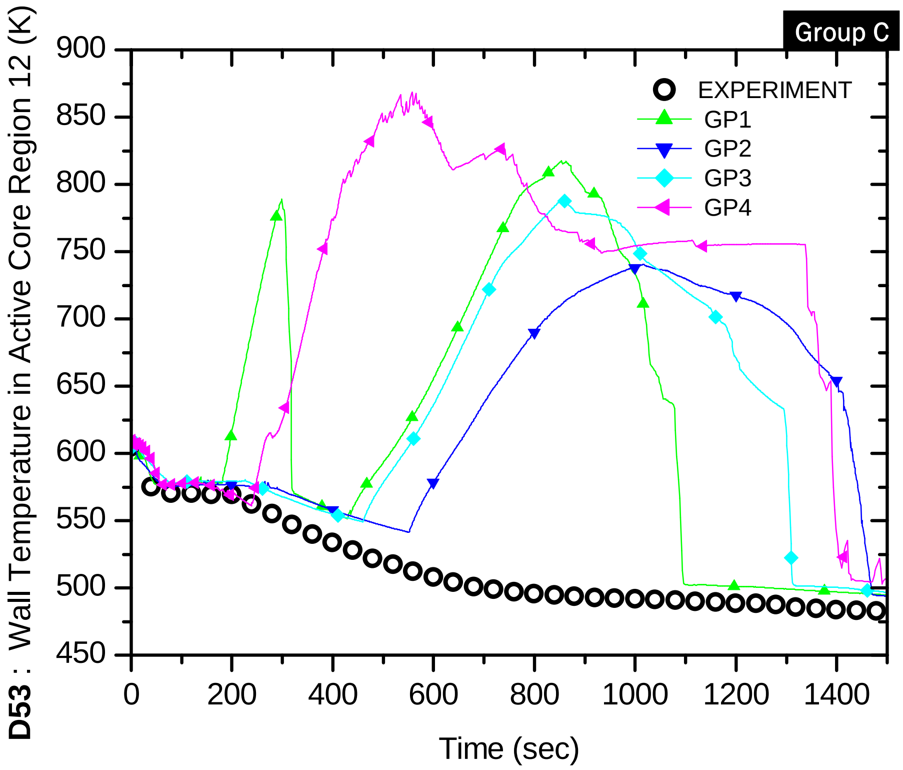

Figure B.53-C Wall temperature in the active core region 12 (D53)

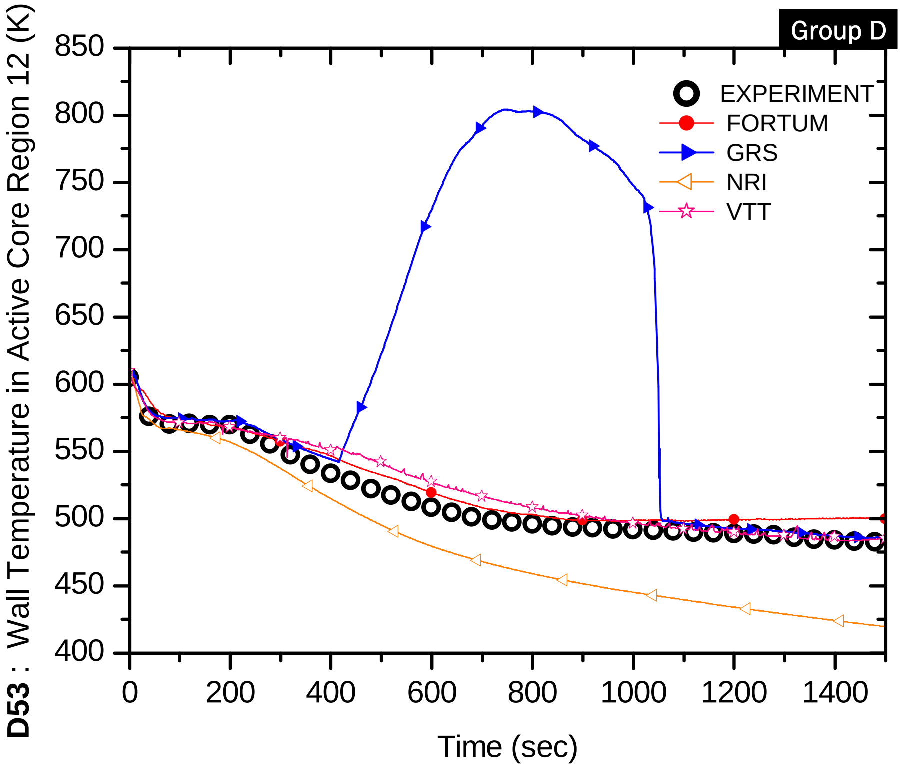

Figure B.53-D Wall temperature in the active core region 12 (D53)

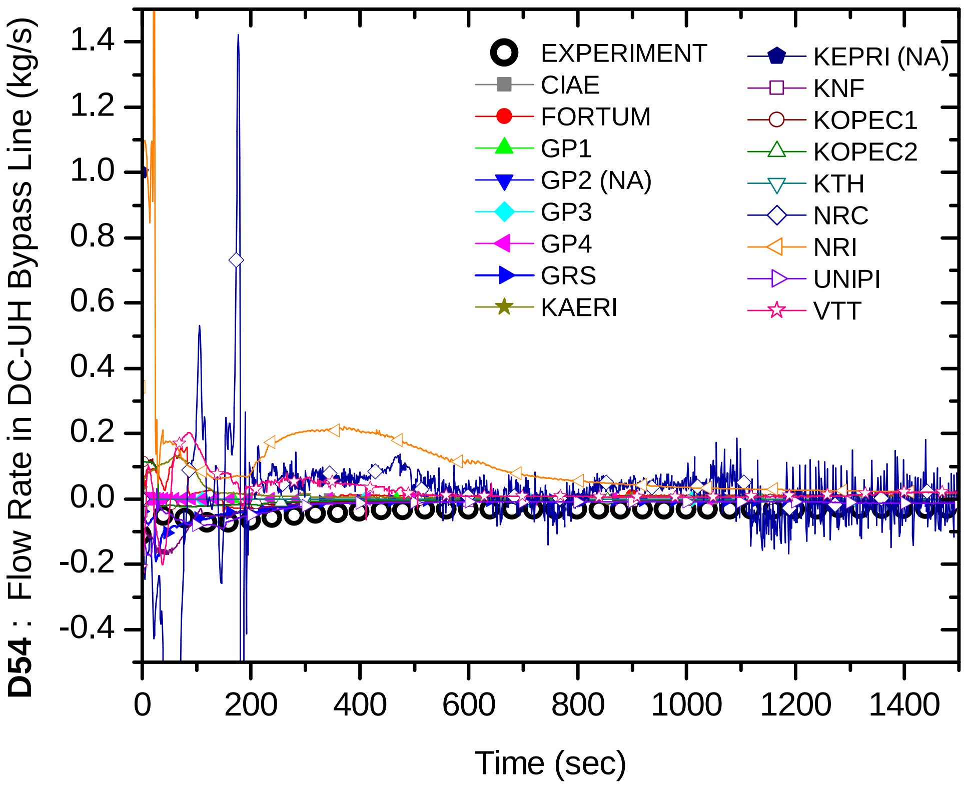

Figure B.54 Flow rate in DC-UH bypass line (D54)

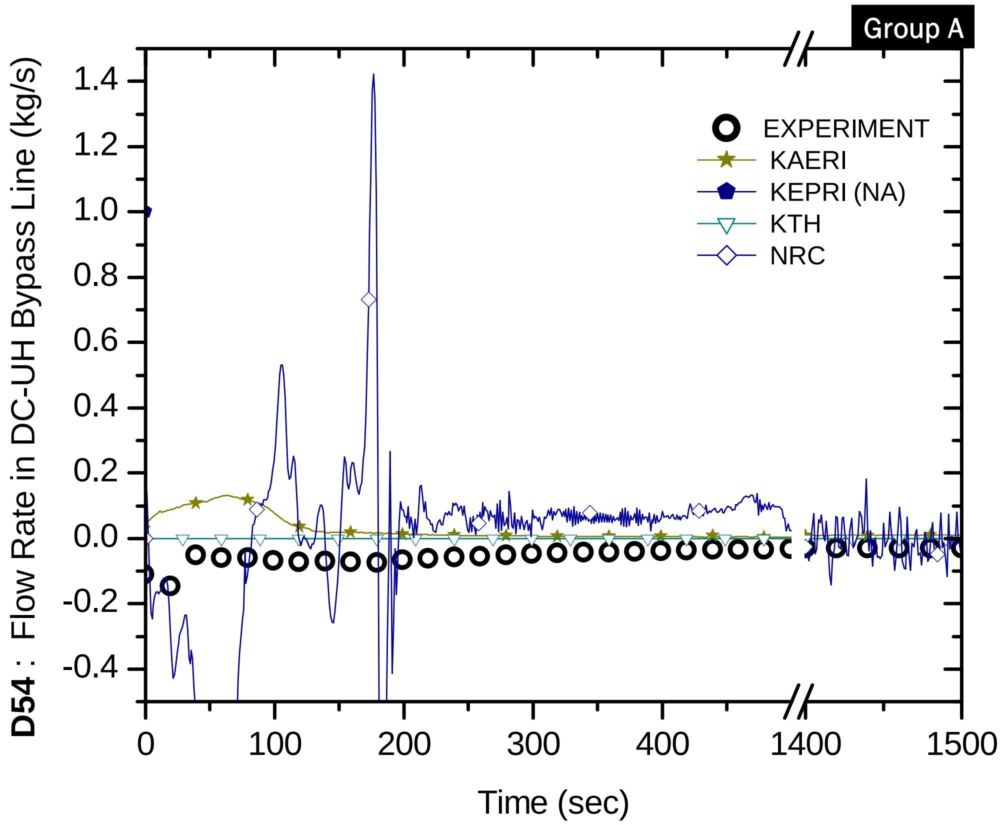

Figure B.54-A Flow rate in DC-UH bypass line (D54)

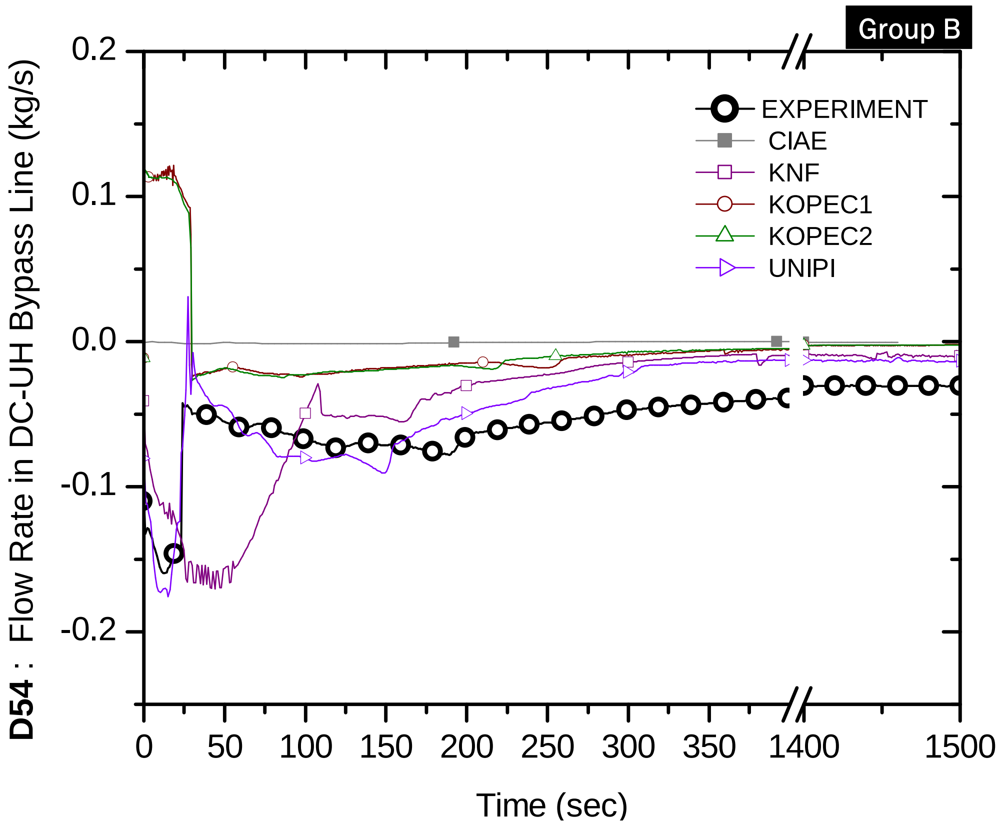

Figure B.54-B Flow rate in DC-UH bypass line (D54)

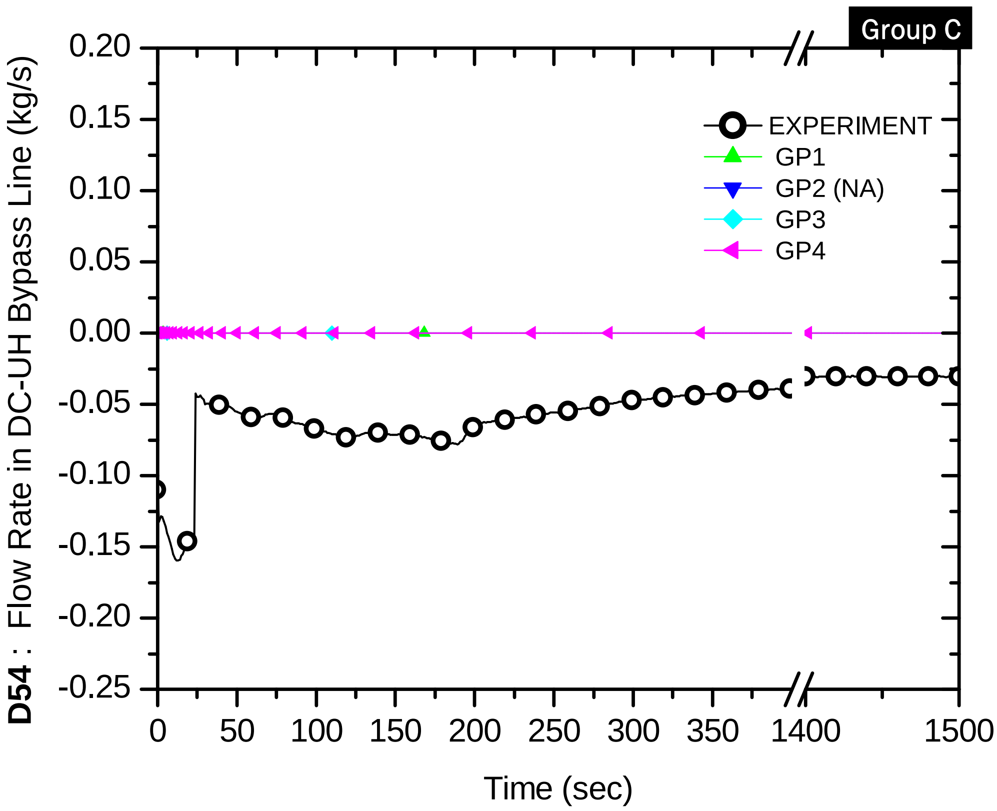

Figure B.54-C Flow rate in DC-UH bypass line (D54)

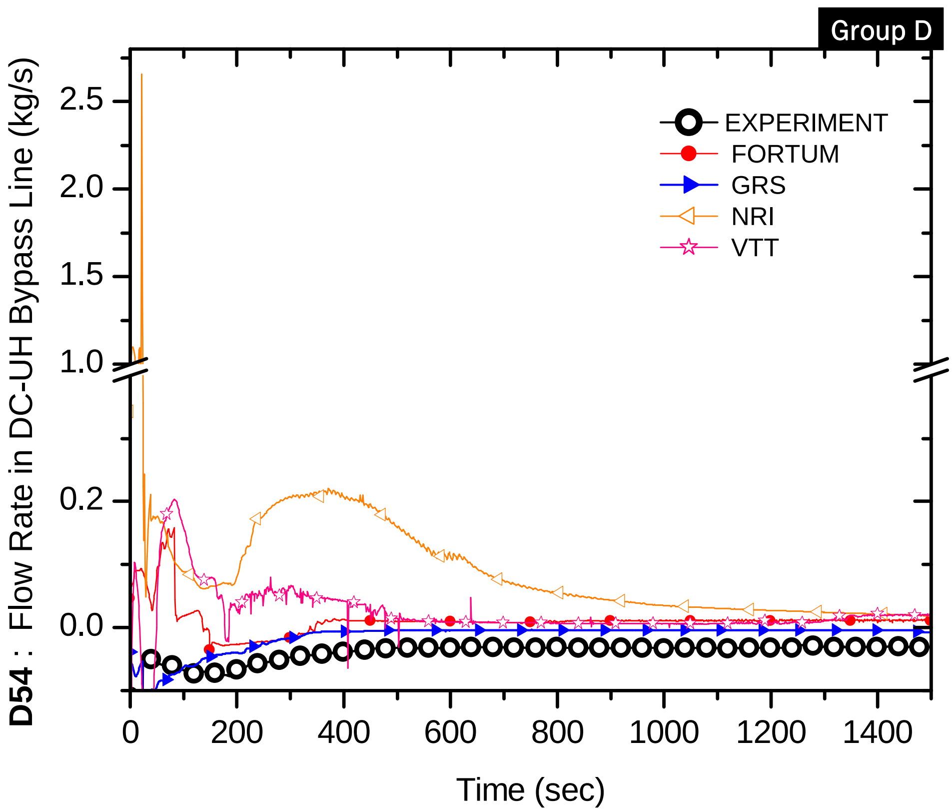

Figure B.54-D Flow rate in DC-UH bypass line (D54)

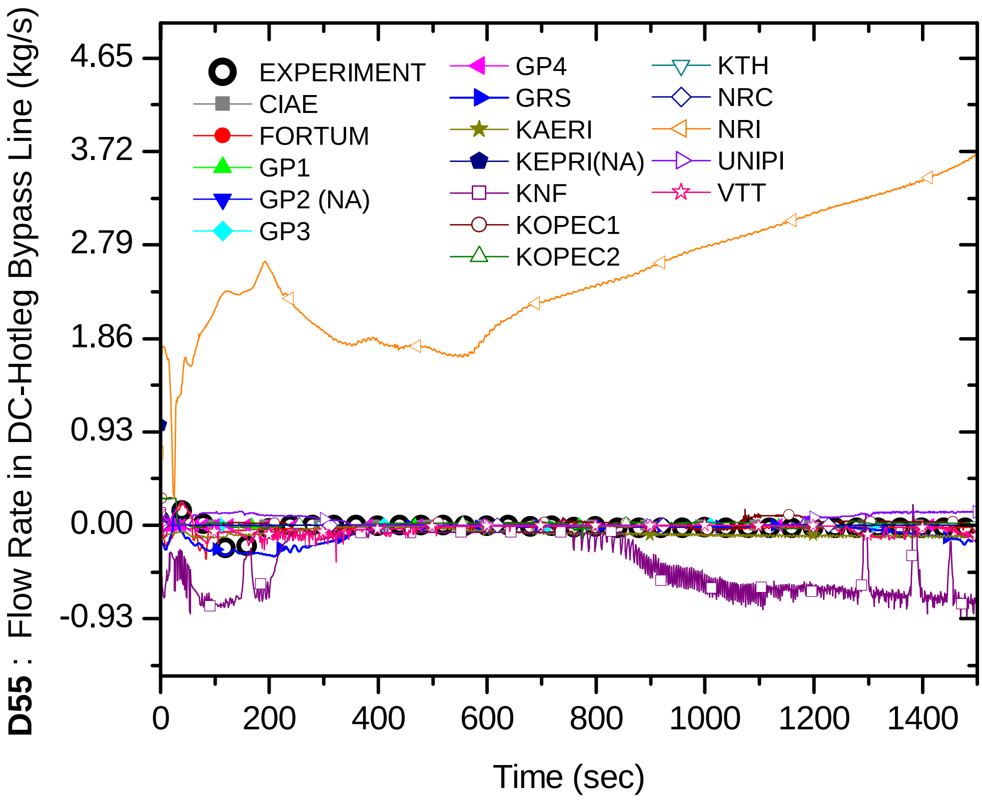

Figure B.55 Flow rate in DC-HL bypass line (D55)

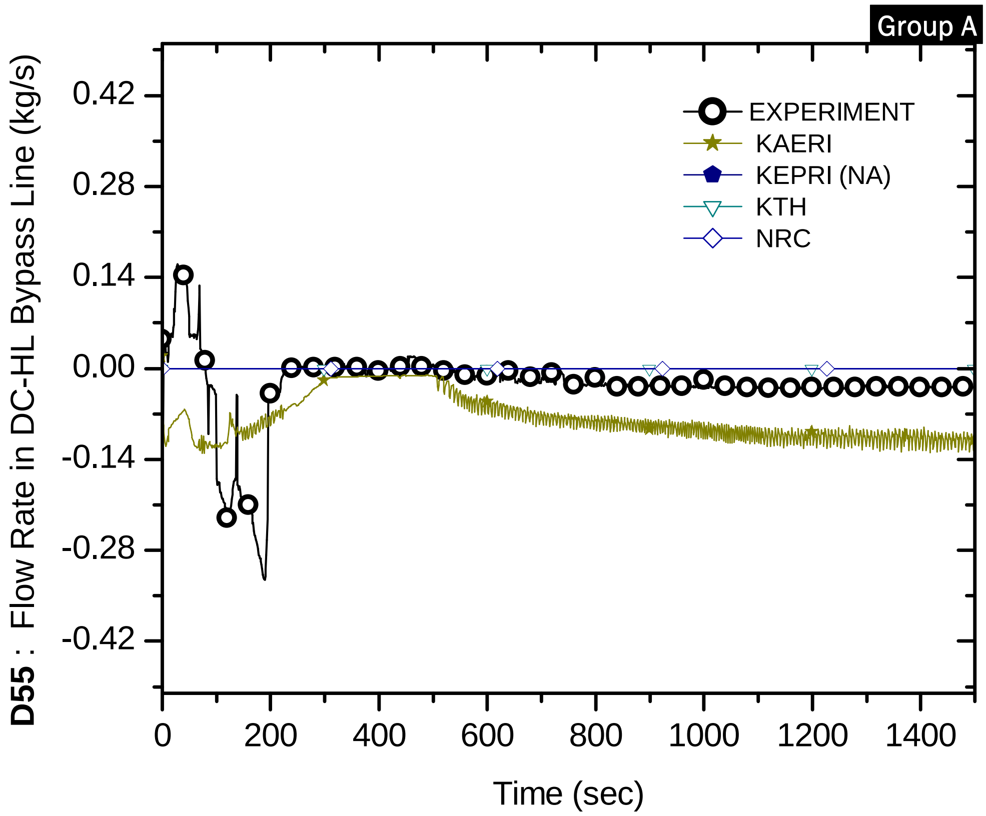

Figure B.55-A Flow rate in DC-HL bypass line (D55)

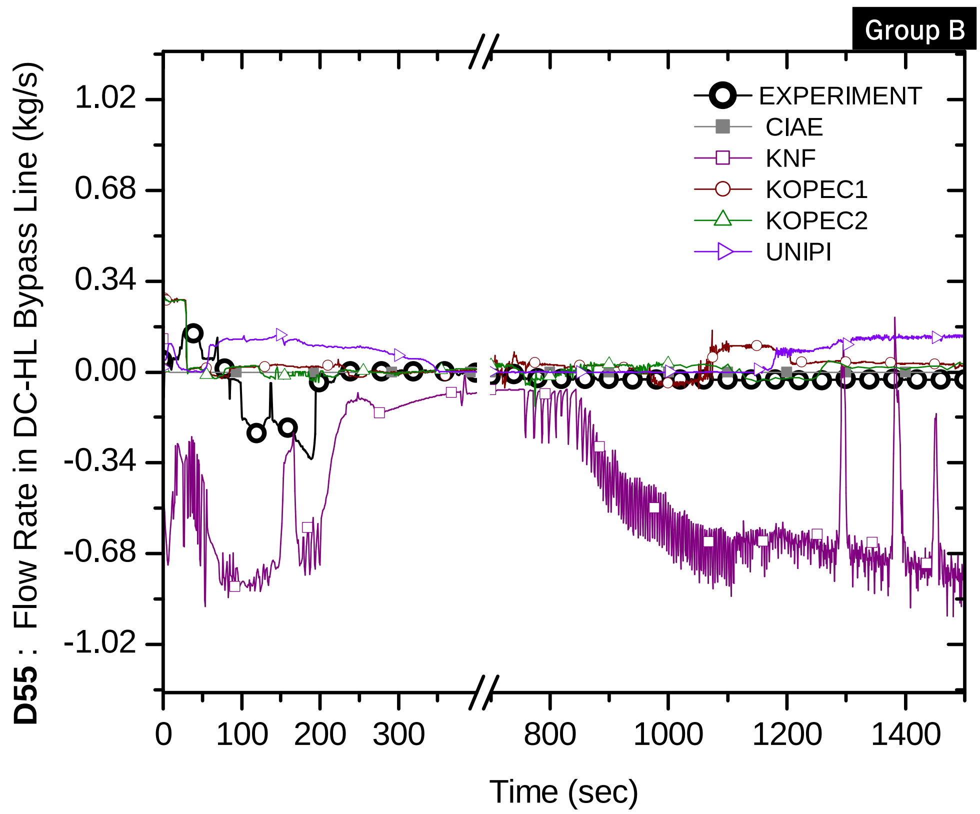

Figure B.55-B Flow rate in DC-HL bypass line (D55)

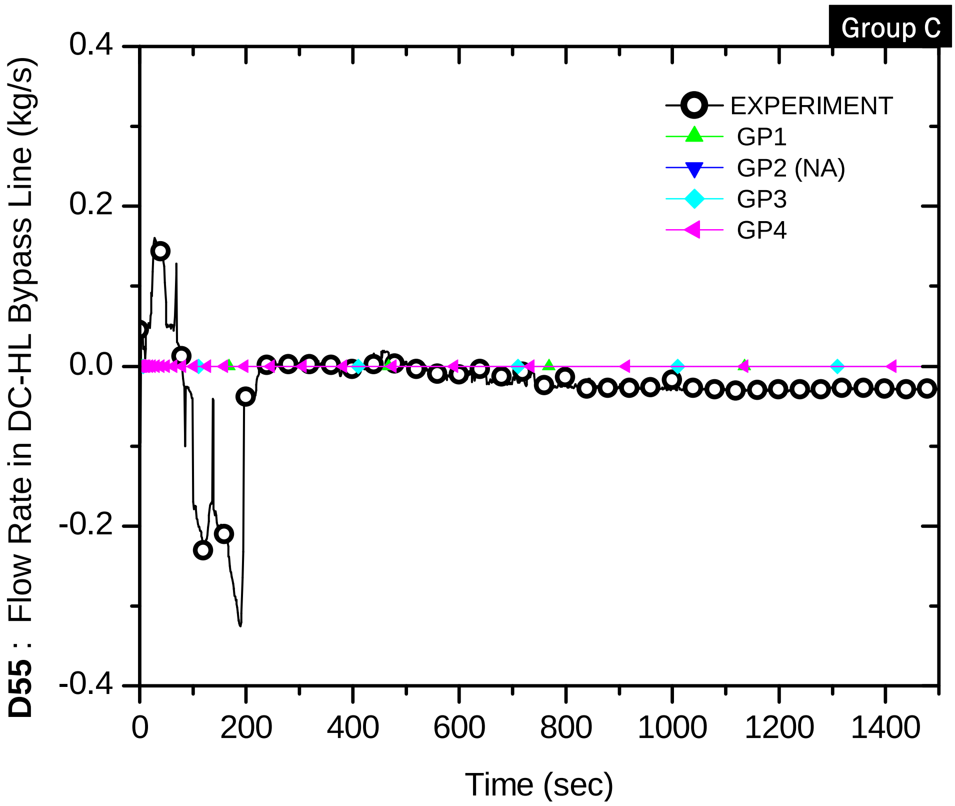

Figure B.55-C Flow rate in DC-HL bypass line (D55)

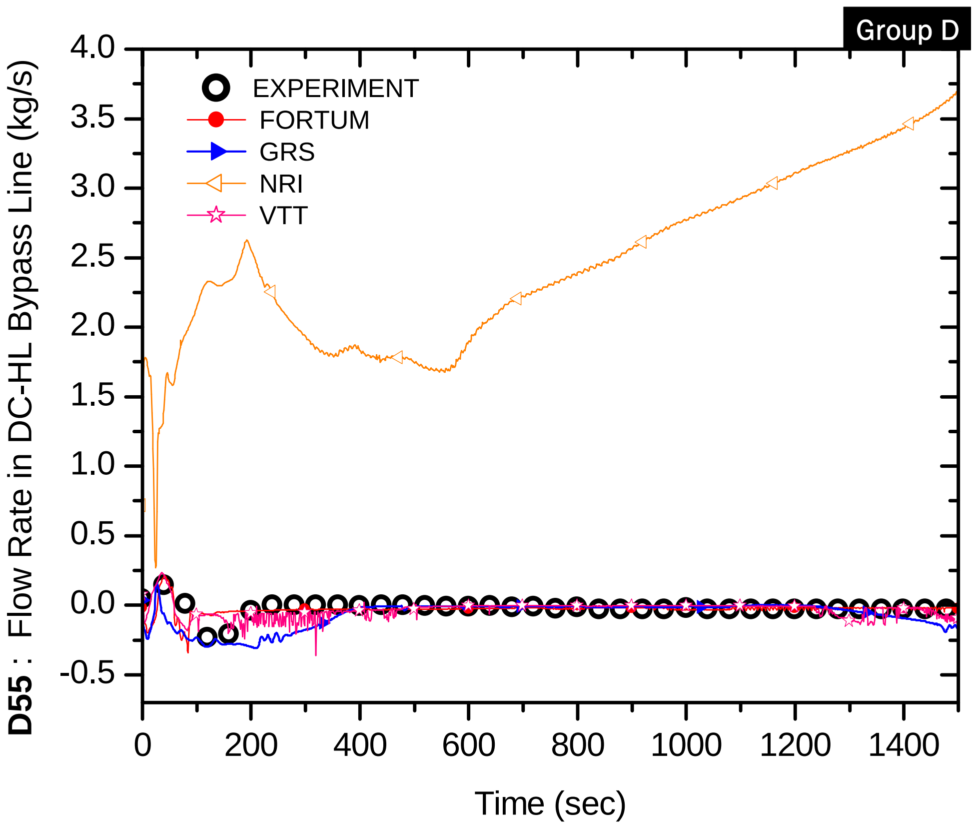

Figure B.55-D Flow rate in DC-HL bypass line (D55)

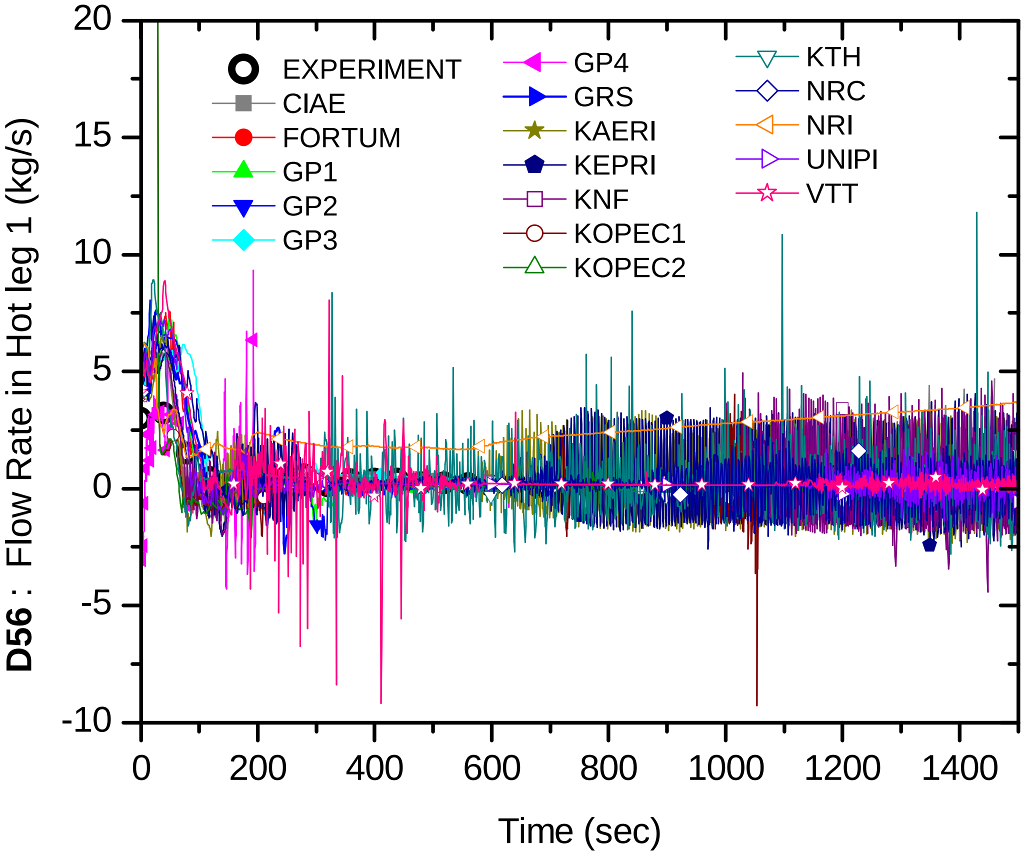

Figure B.56 Flow rate in the hot leg 1 (D56)

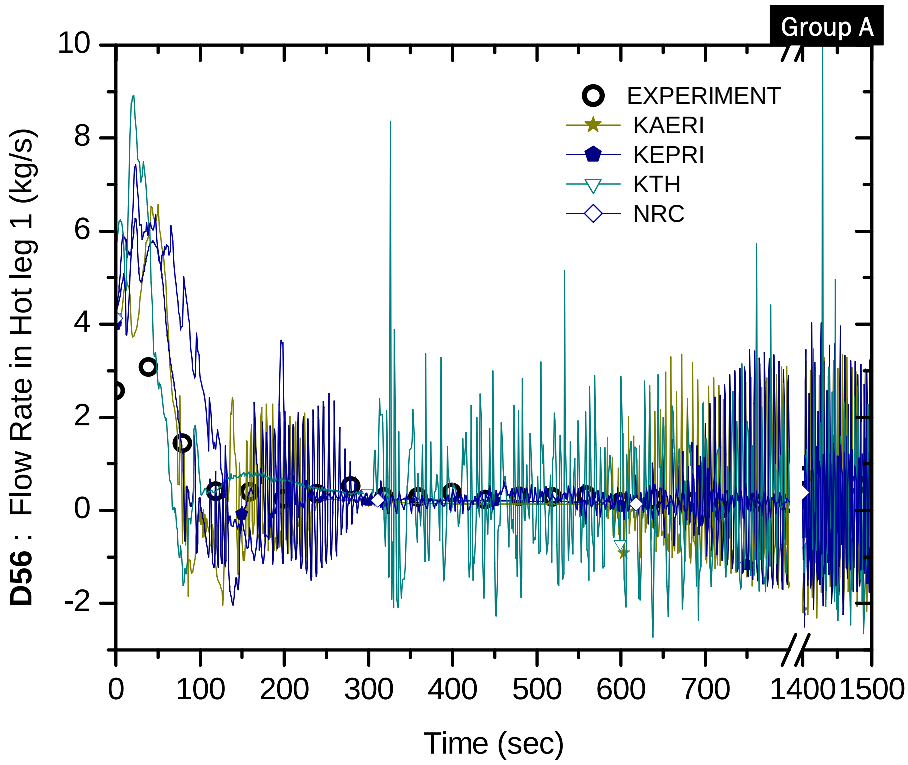

Figure B.56-A Flow rate in the hot leg 1 (D56)

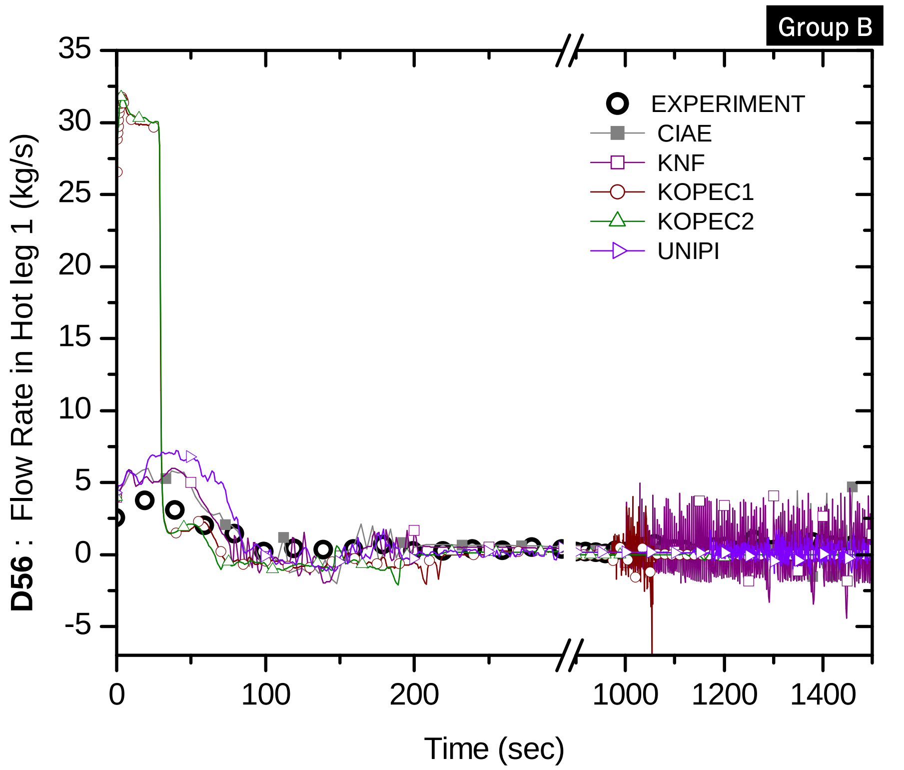

Figure B.56-B Flow rate in the hot leg 1 (D56)

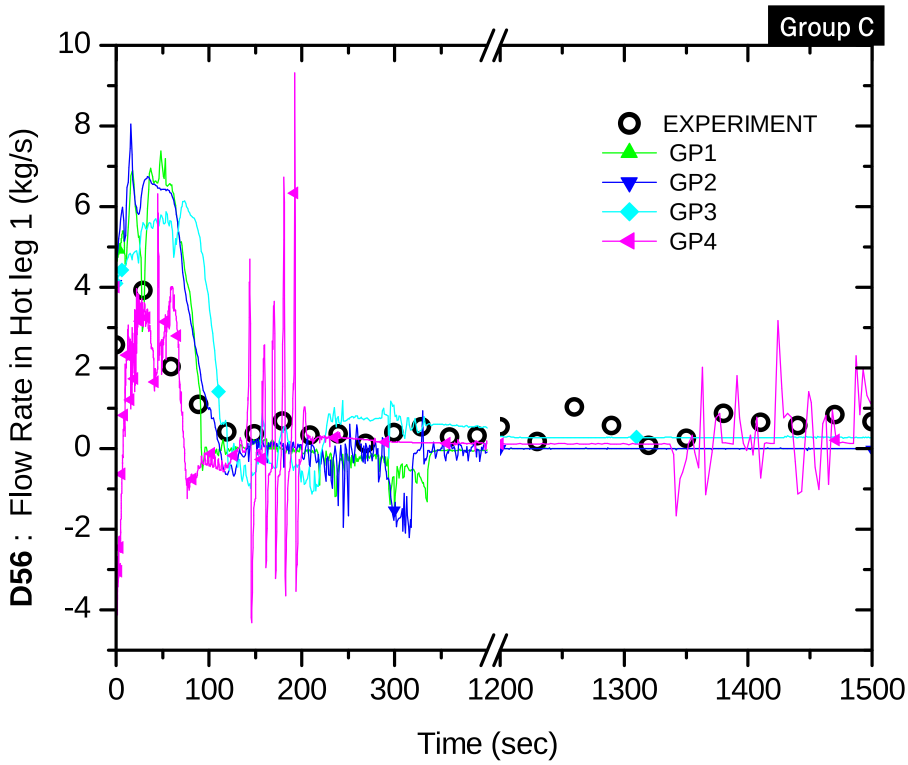

Figure B.56-C Flow rate in the hot leg 1 (D56)

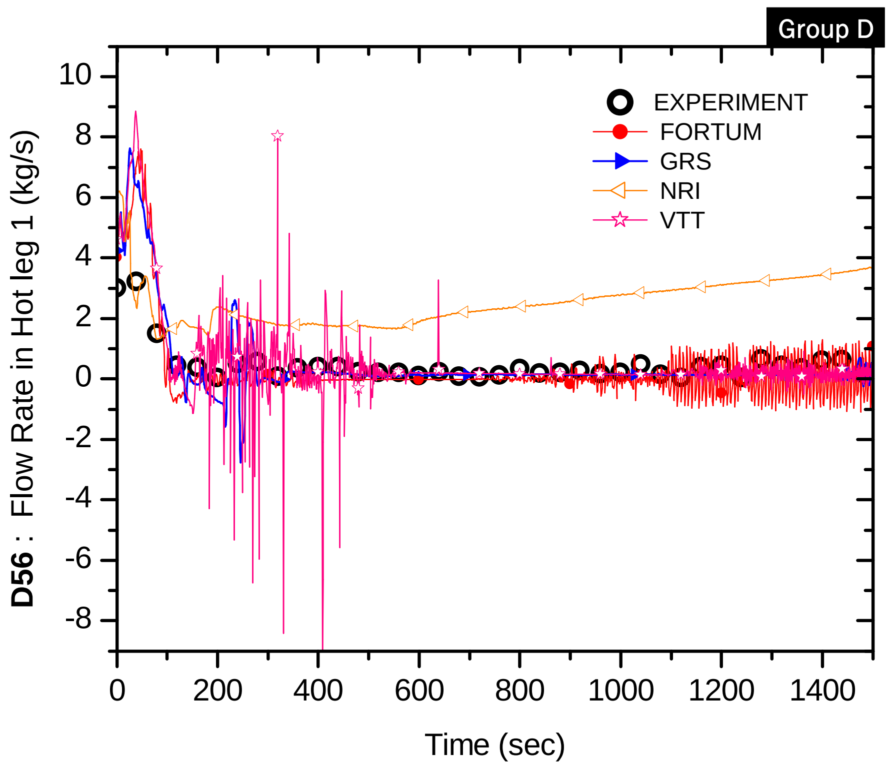

Figure B.56-D Flow rate in the hot leg 1 (D56)

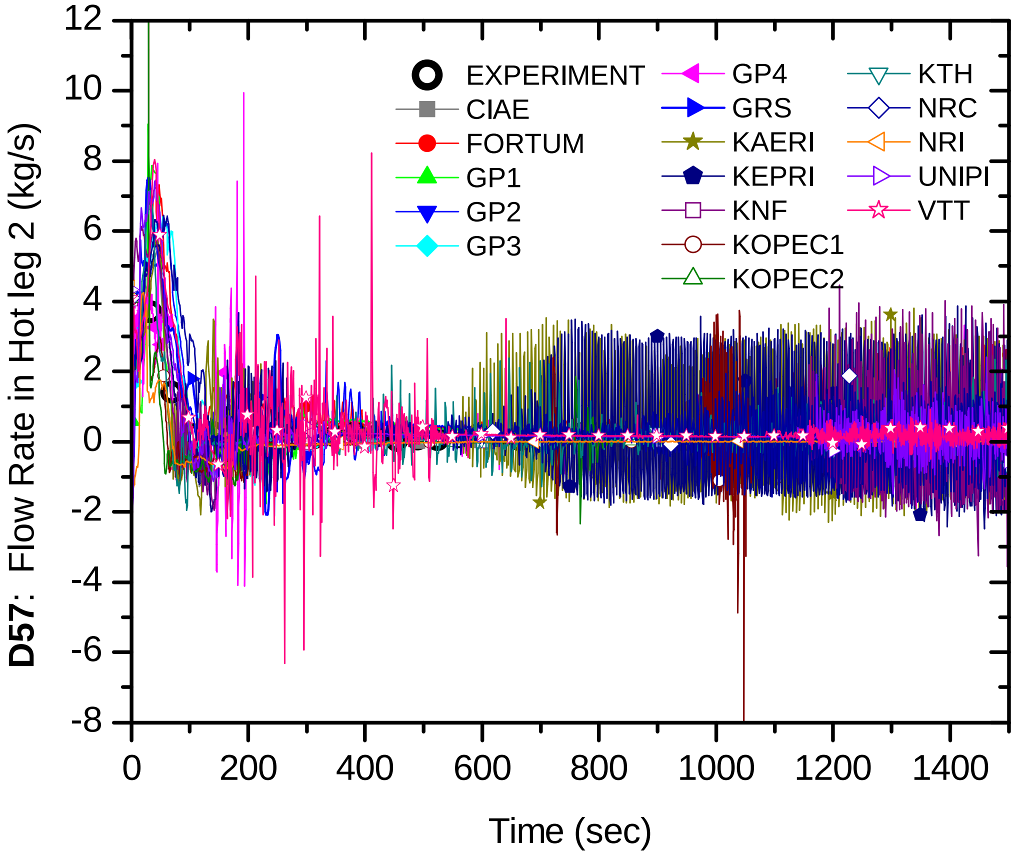

Figure B.57 Flow rate in the hot leg 2 (D57)

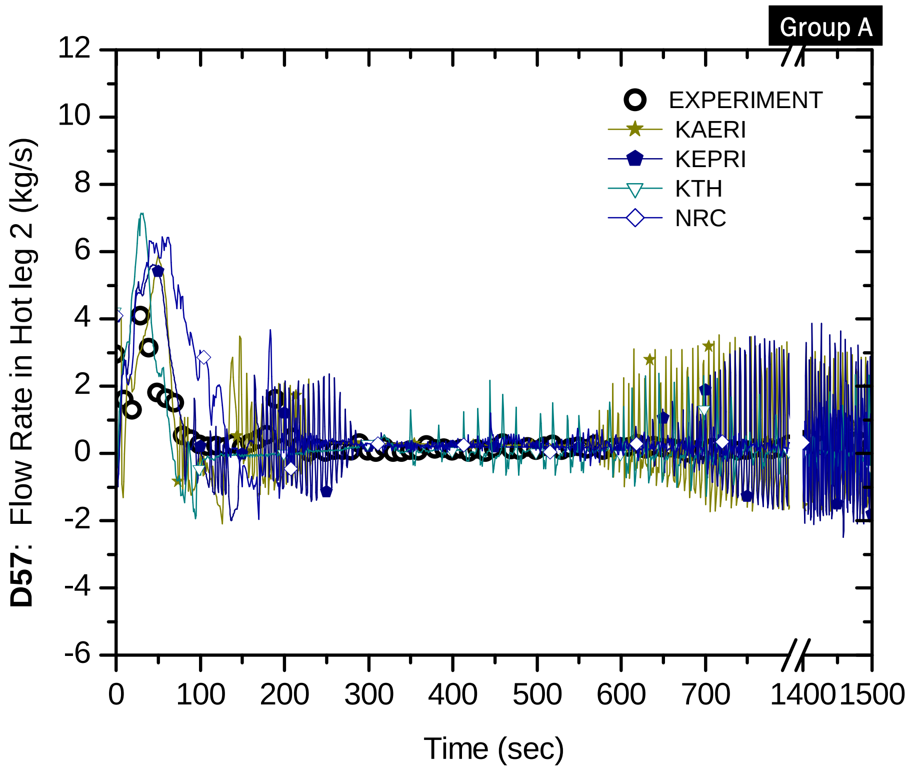

Figure B.57-A Flow rate in the hot leg 2 (D57)

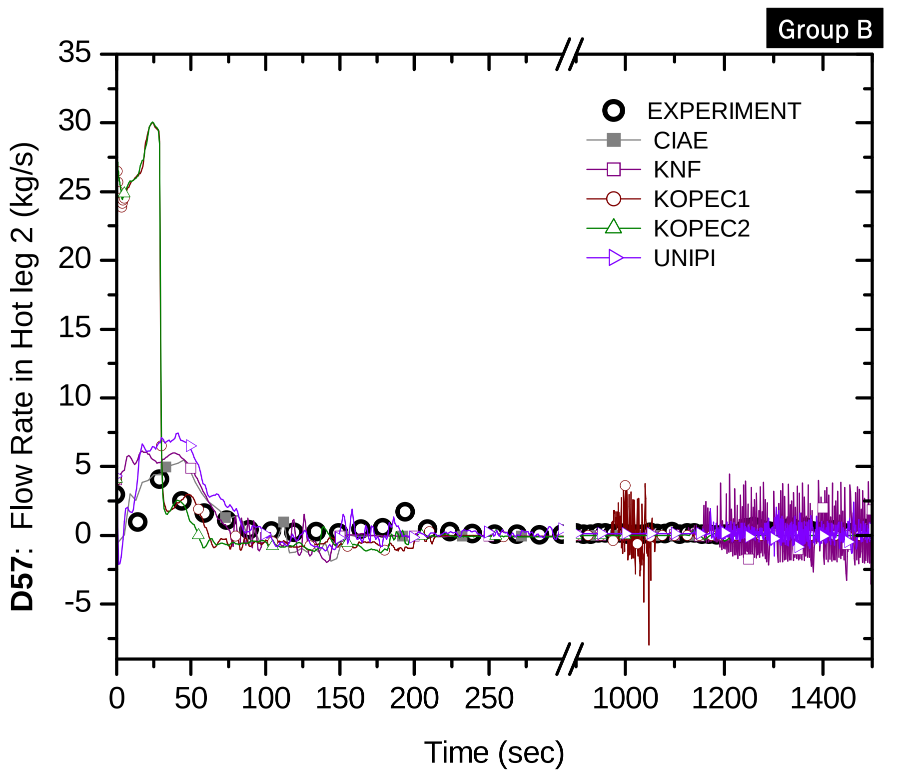

Figure B.57-B Flow rate in the hot leg 2 (D57)

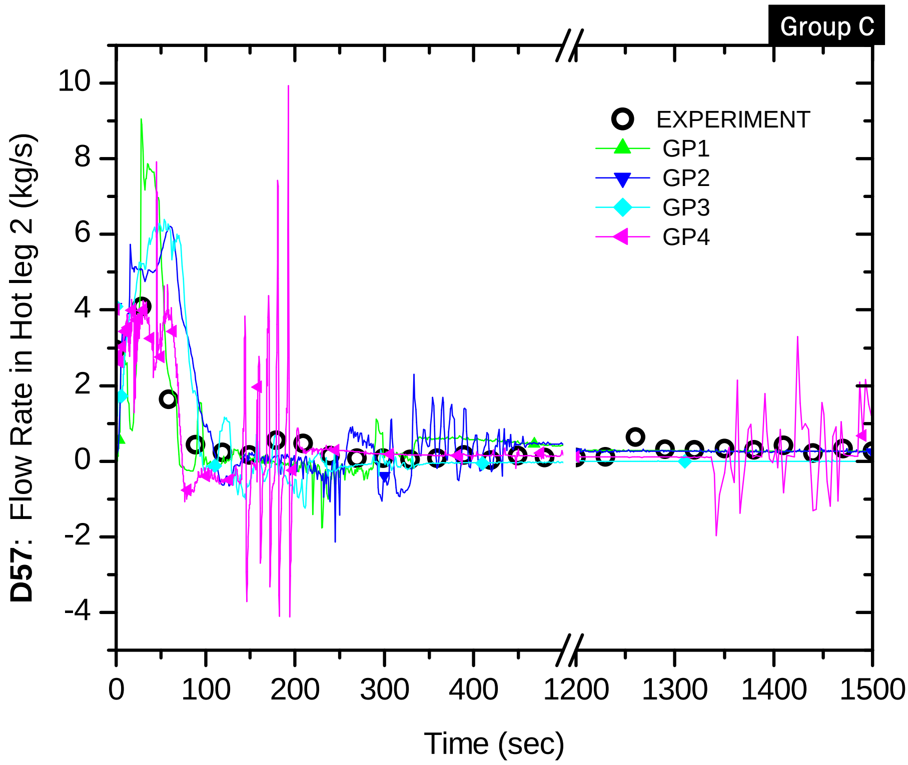

Figure B.57-C Flow rate in the hot leg 2 (D57)

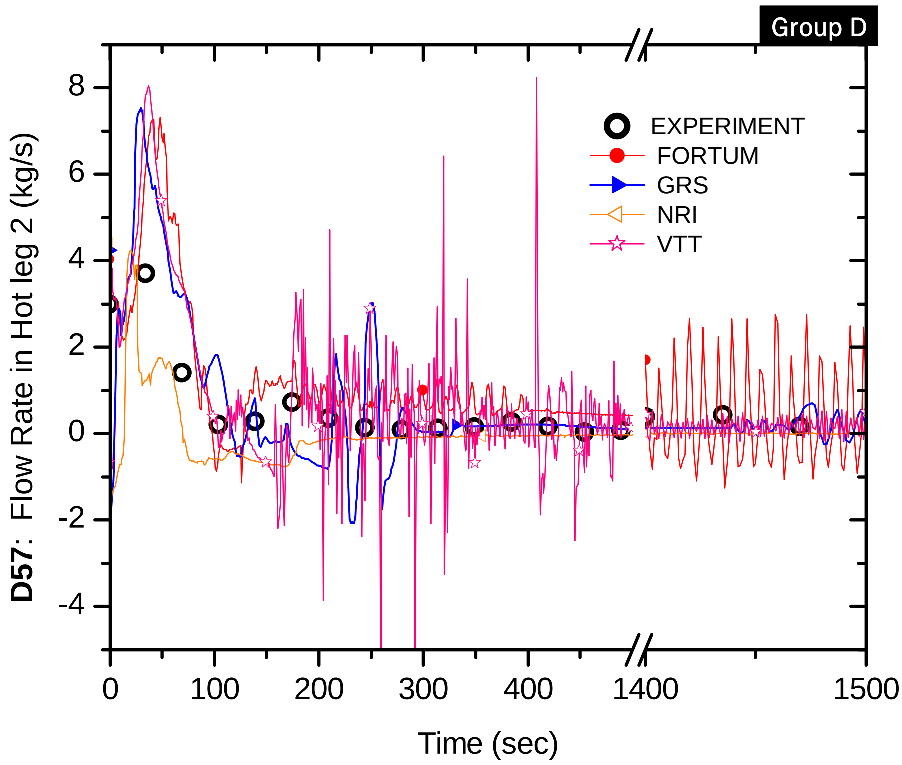

Figure B.57-D Flow rate in the hot leg 2 (D57)

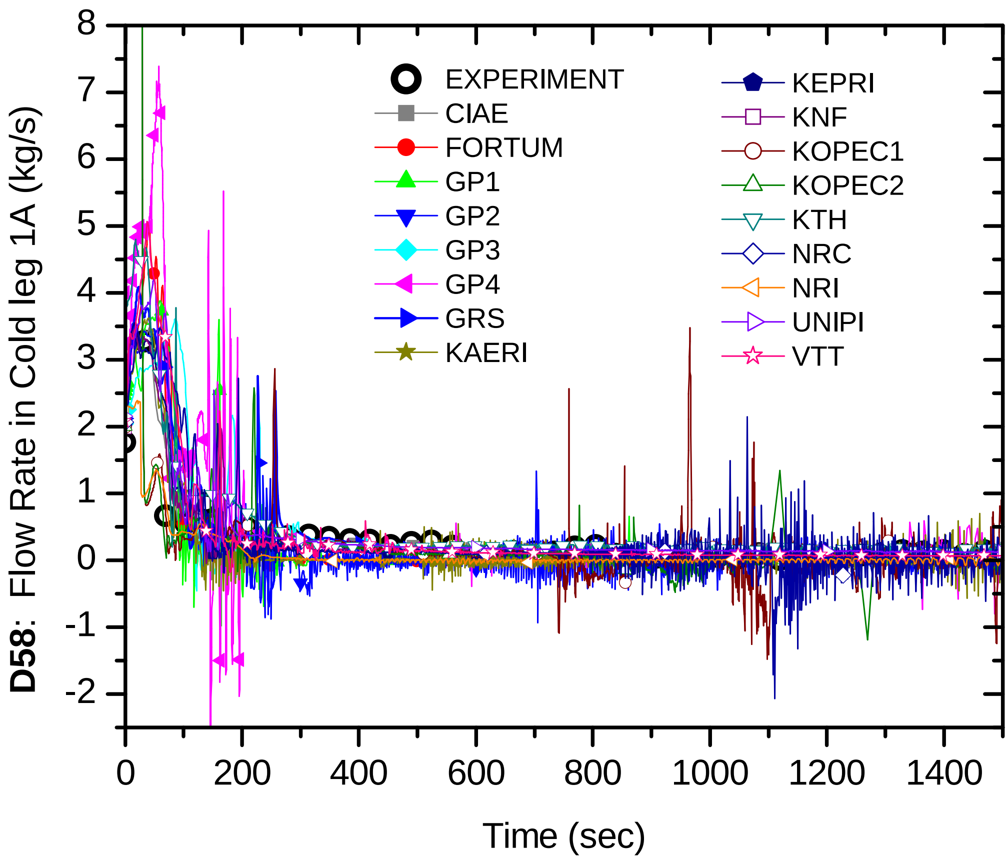

Figure B.58 Flow rate in the cold leg 1A (D58)

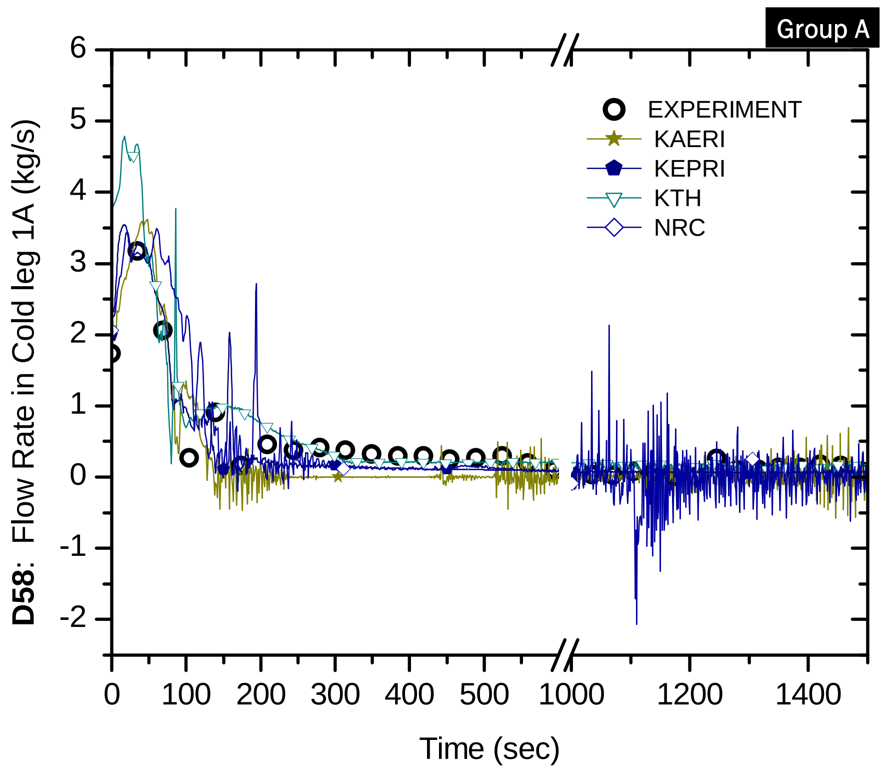

Figure B.58-A Flow rate in the cold leg 1A (D58)

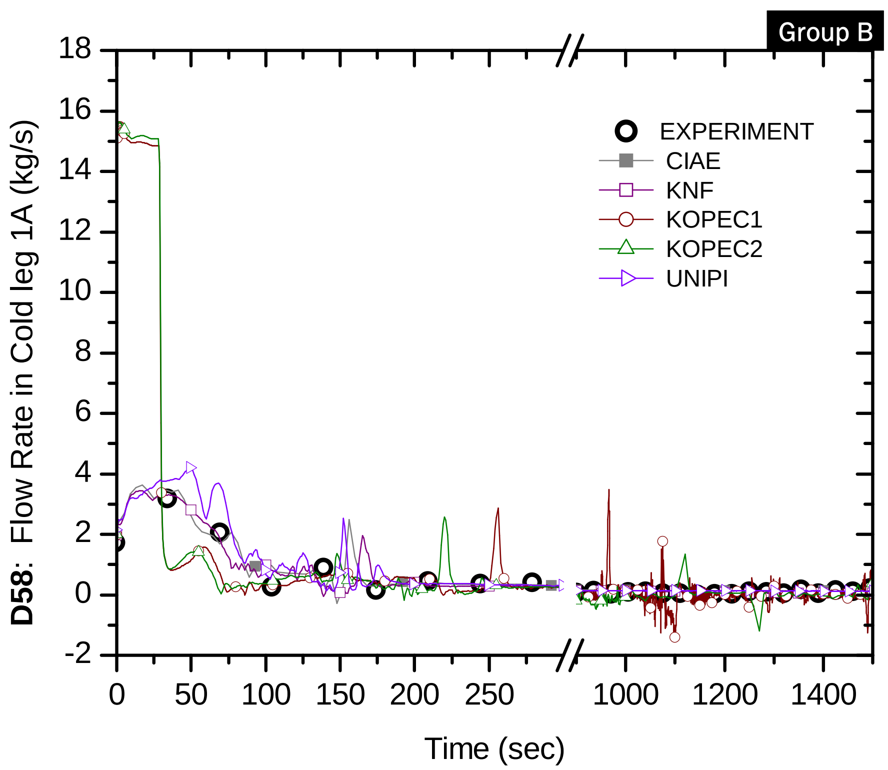

Figure B.58-B Flow rate in the cold leg 1A (D58)

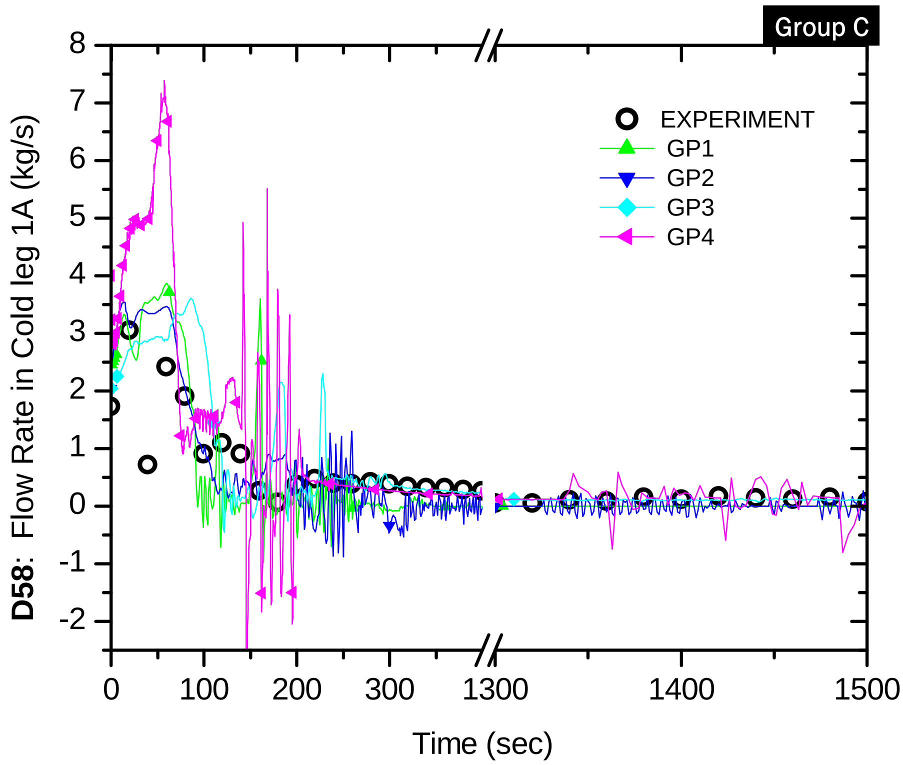

Figure B.58-C Flow rate in the cold leg 1A (D58)

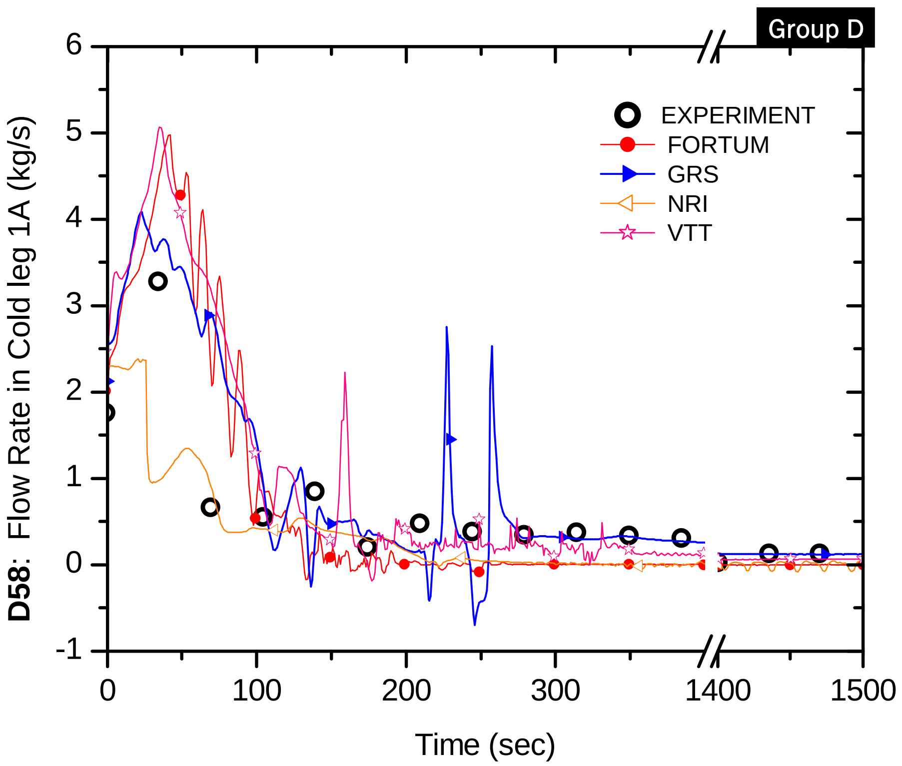

Figure B.58-D Flow rate in the cold leg 1A (D58)

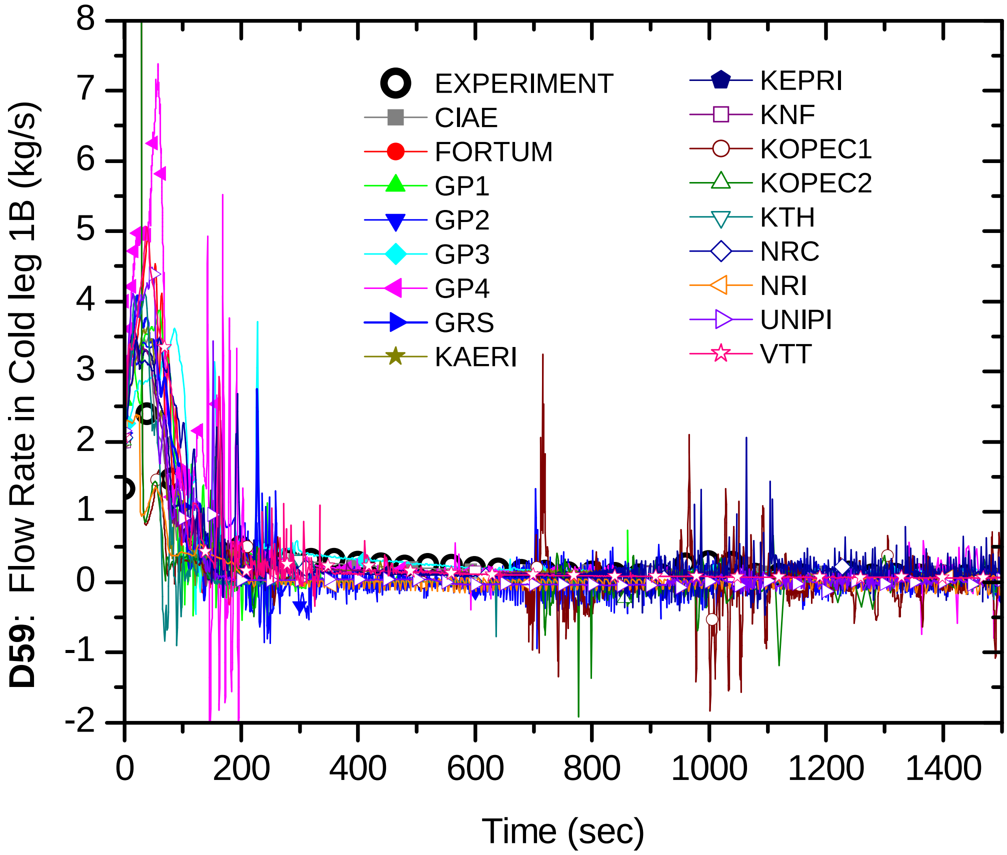

Figure B.59 Flow rate in the cold leg 1B (D59)

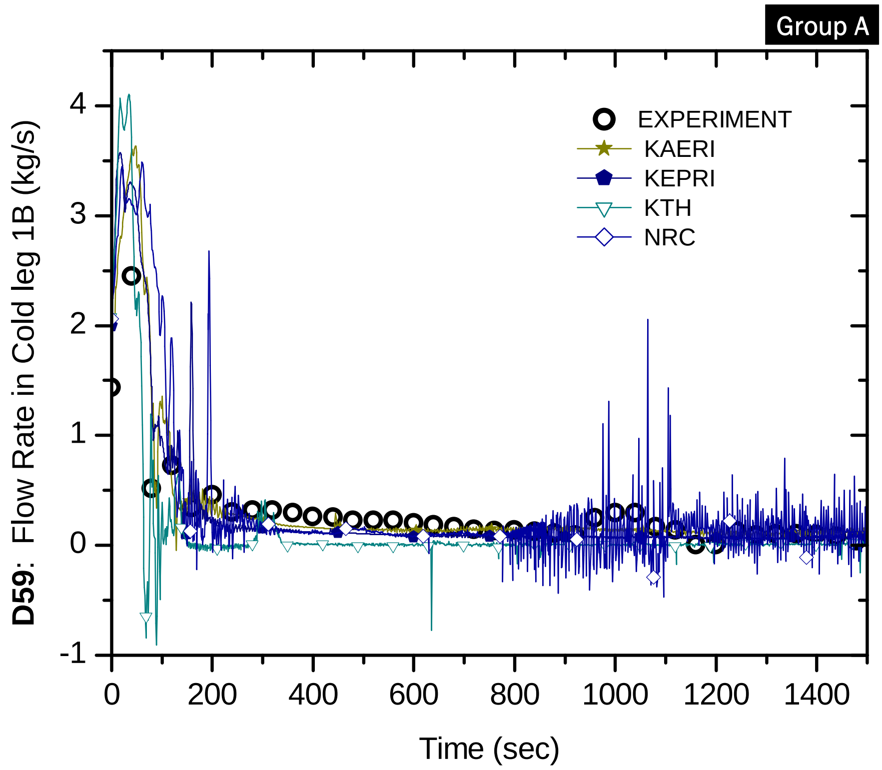

Figure B.59-A Flow rate in the cold leg 1B (D59)

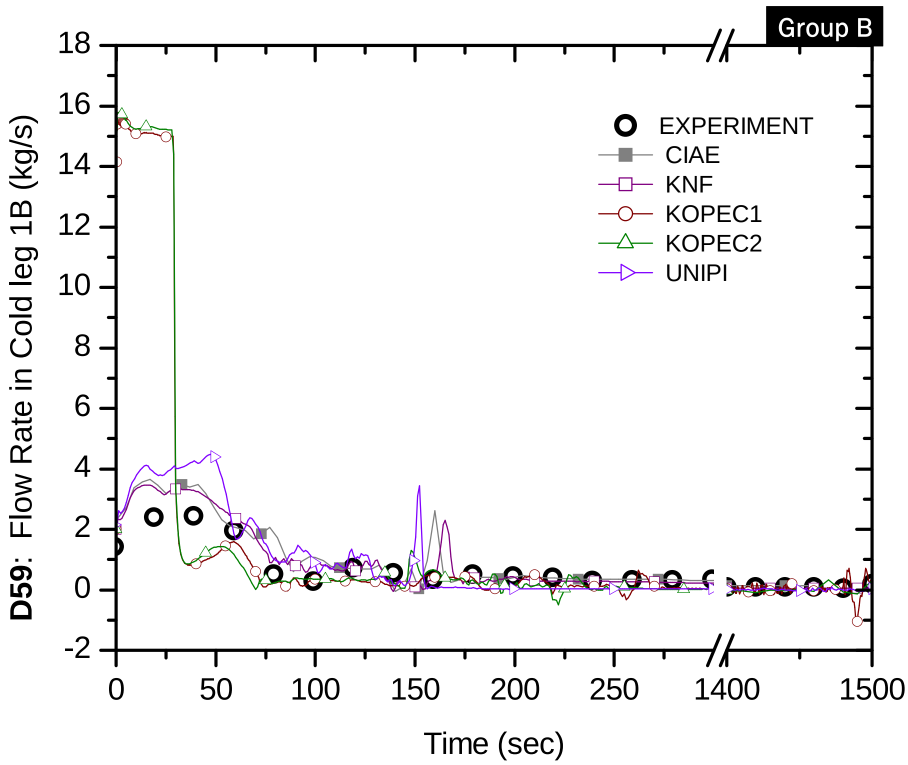

Figure B.59-B Flow rate in the cold leg 1B (D59)

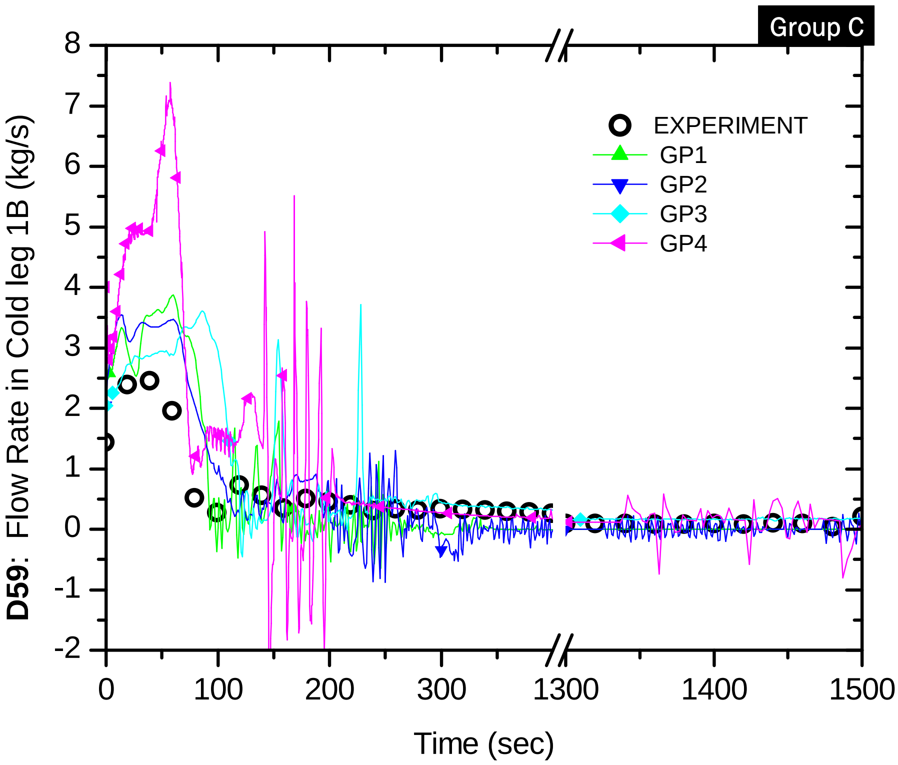

Figure B.59-C Flow rate in the cold leg 1B (D59)

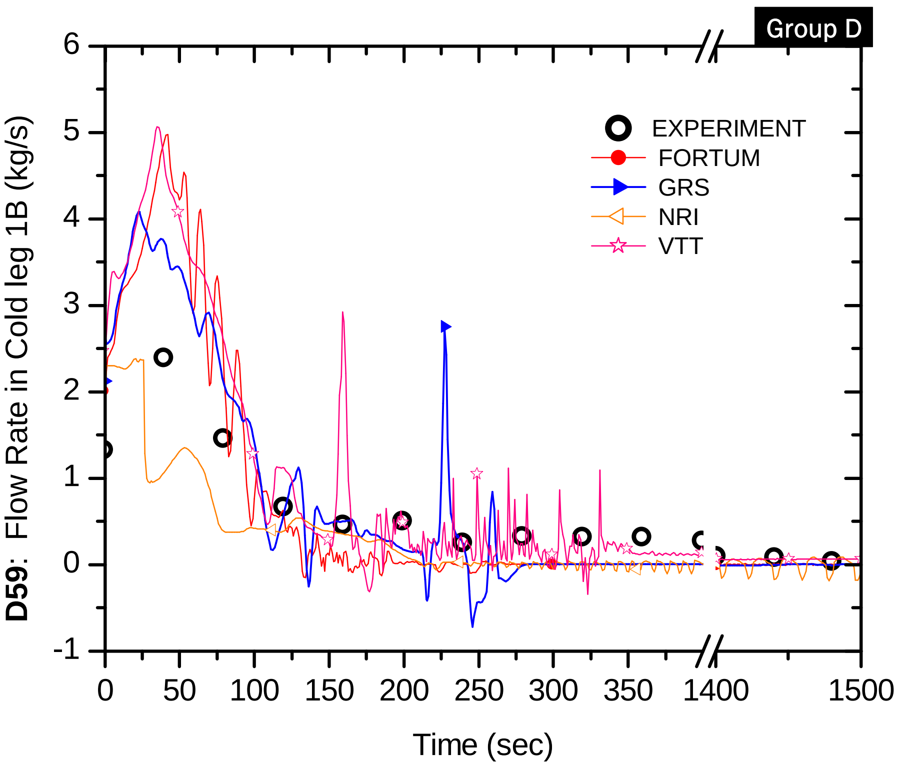

Figure B.59-D Flow rate in the cold leg 1B (D59)

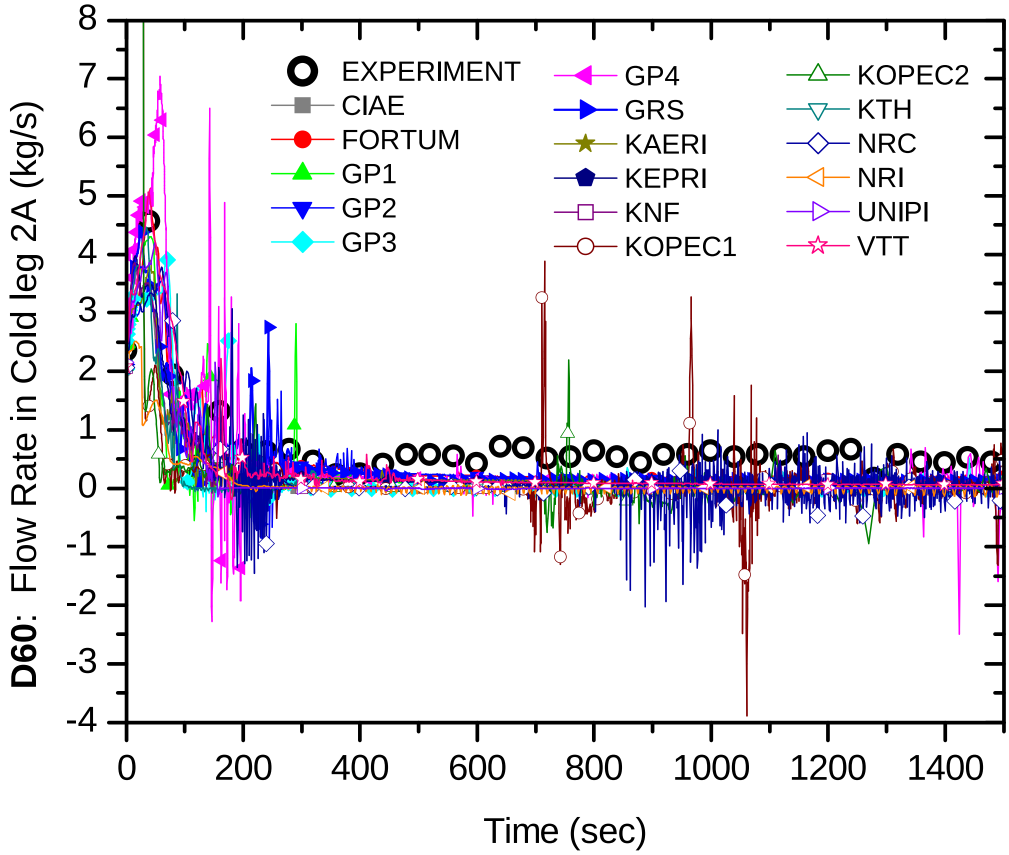

Figure B.60 Flow rate in the cold leg 2A (D60)

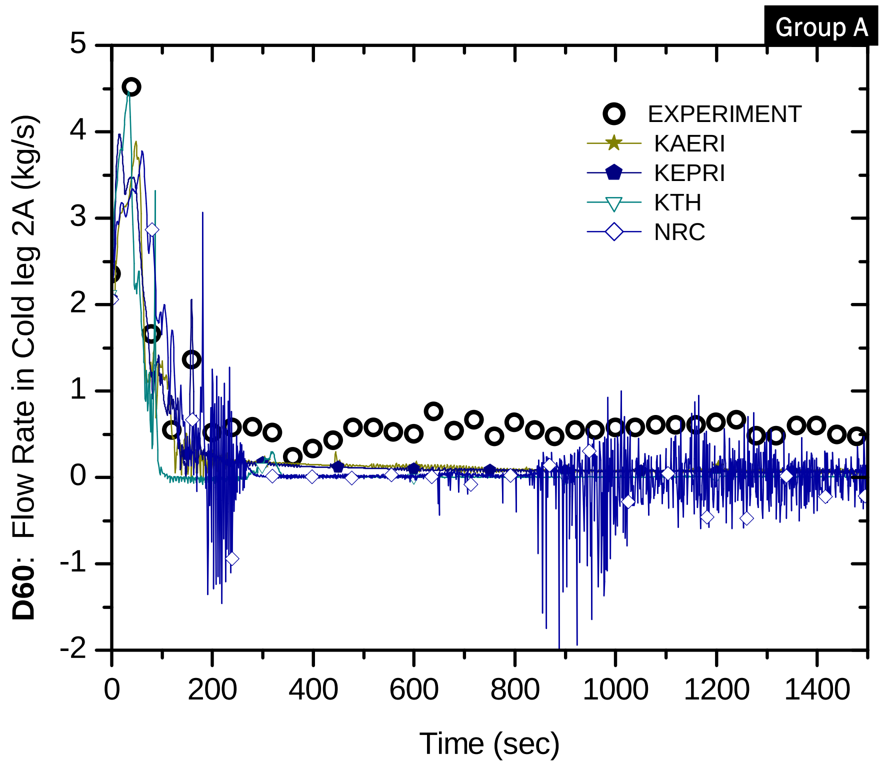

Figure B.60-A Flow rate in the cold leg 2A (D60)

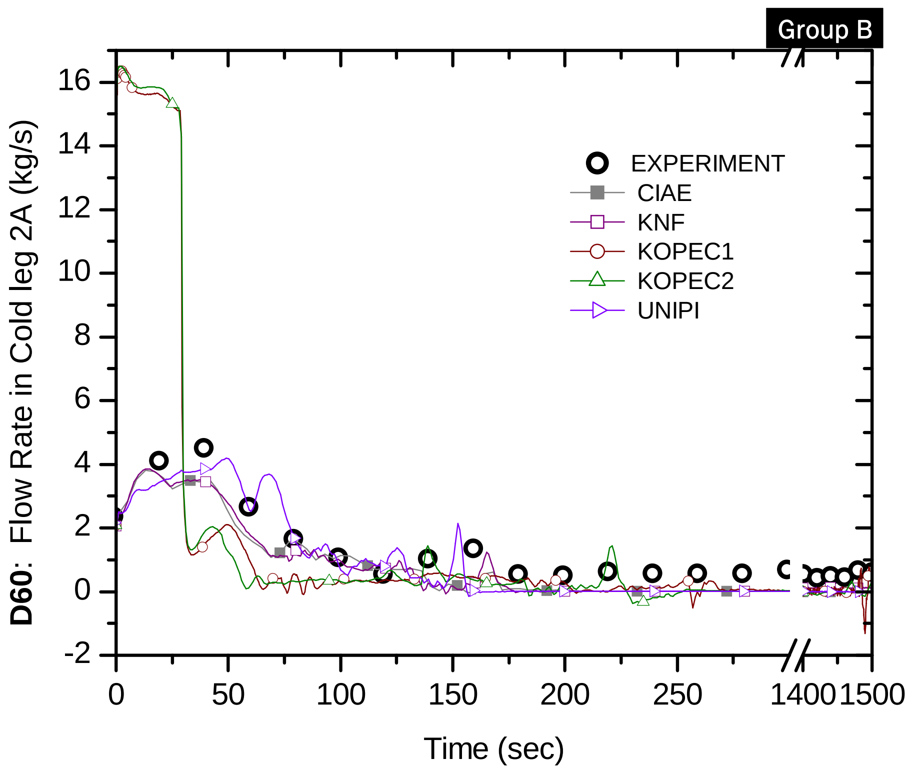

Figure B.60-B Flow rate in the cold leg 2A (D60)

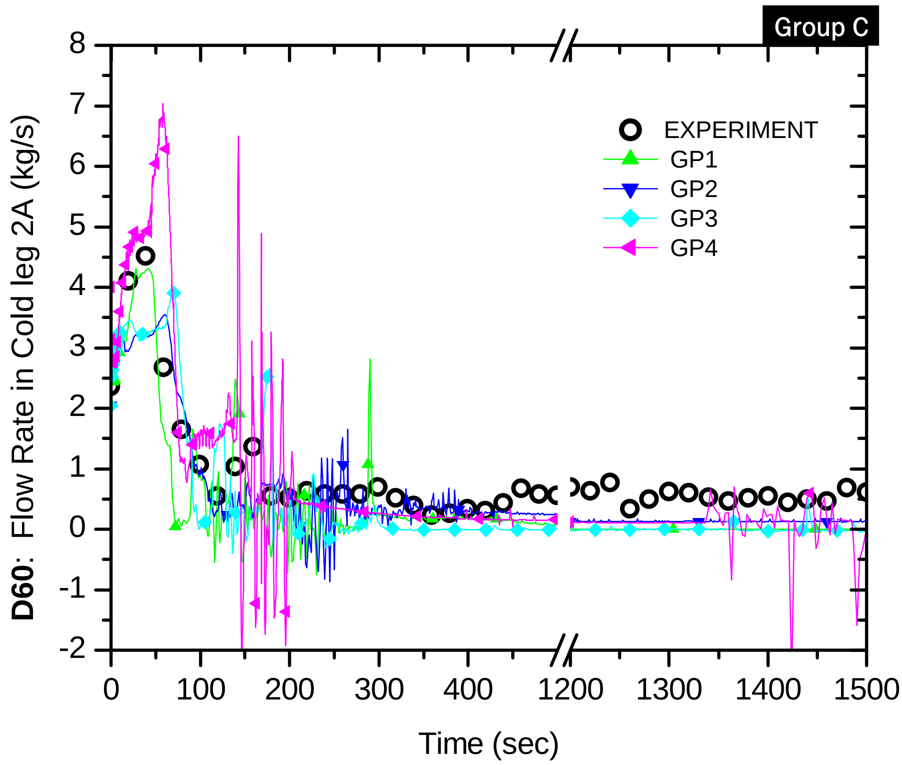

Figure B.60-C Flow rate in the cold leg 2A (D60)

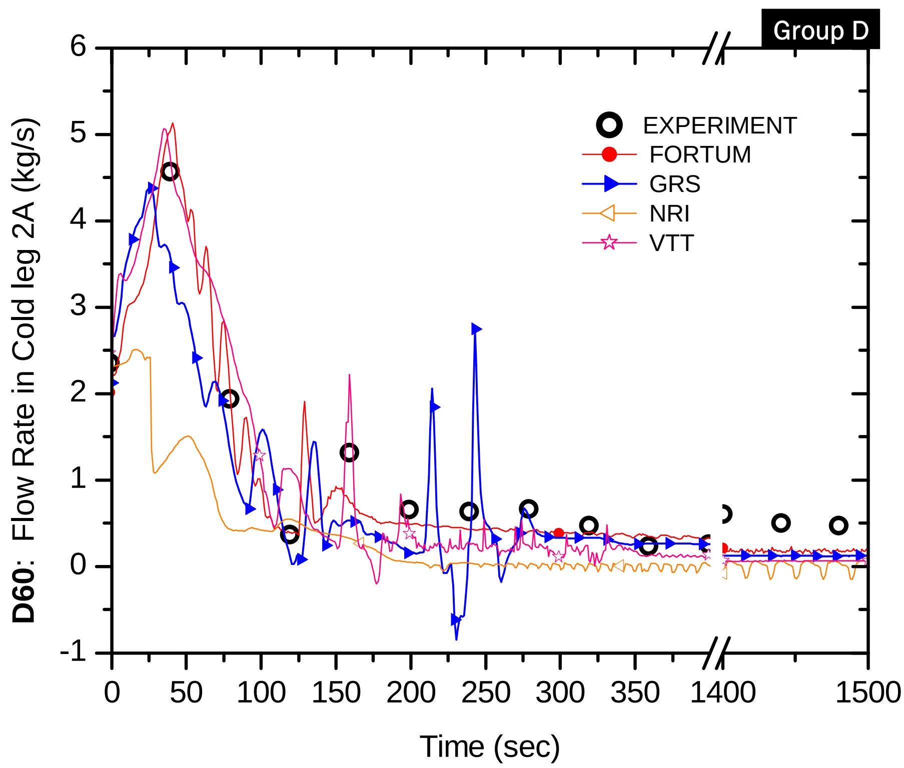

Figure B.60-D Flow rate in the cold leg 2A (D60)

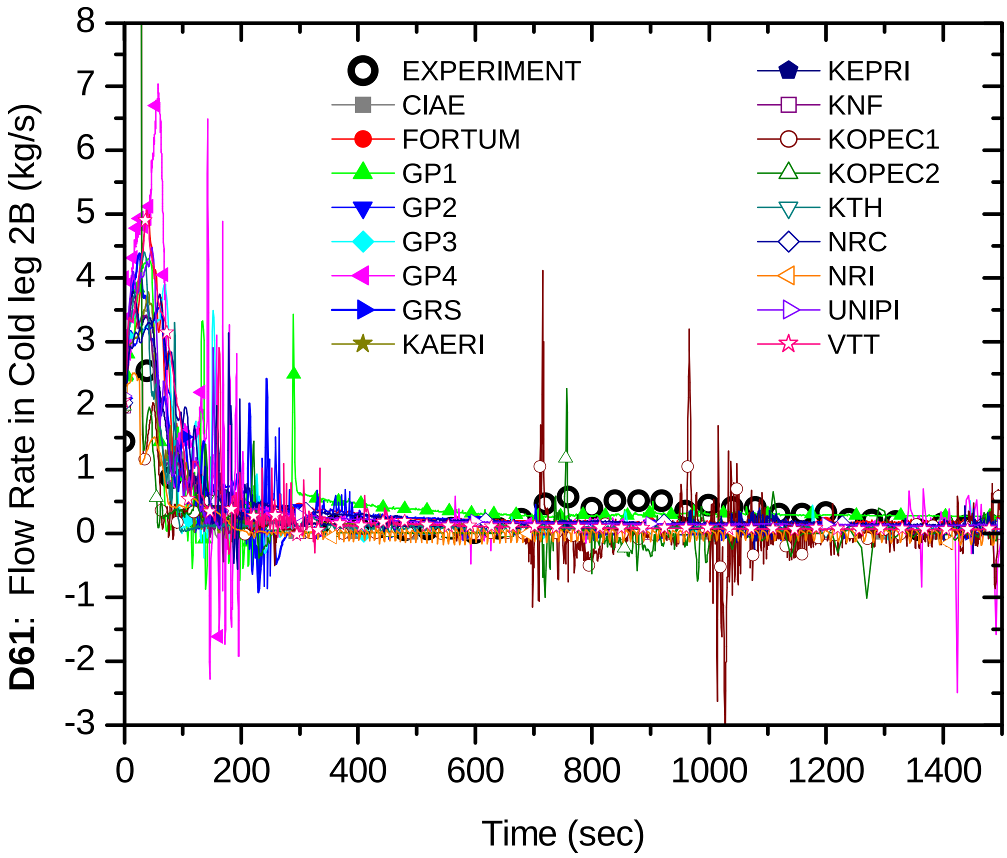

Figure B.61 Flow rate in the cold leg 2B (D61)

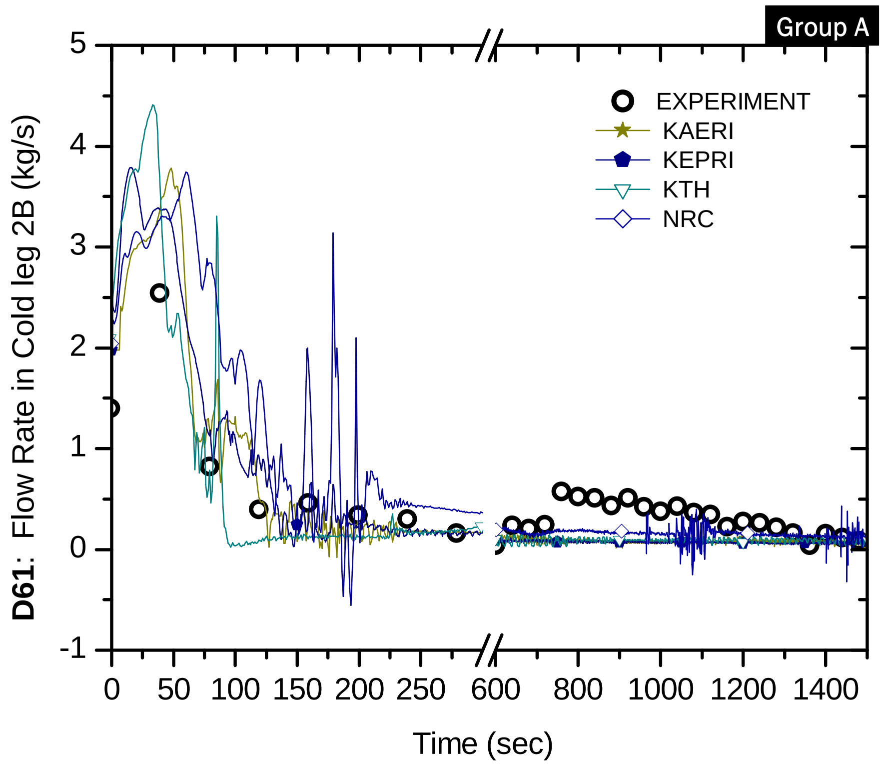

Figure B.61-A Flow rate in the cold leg 2B (D61)

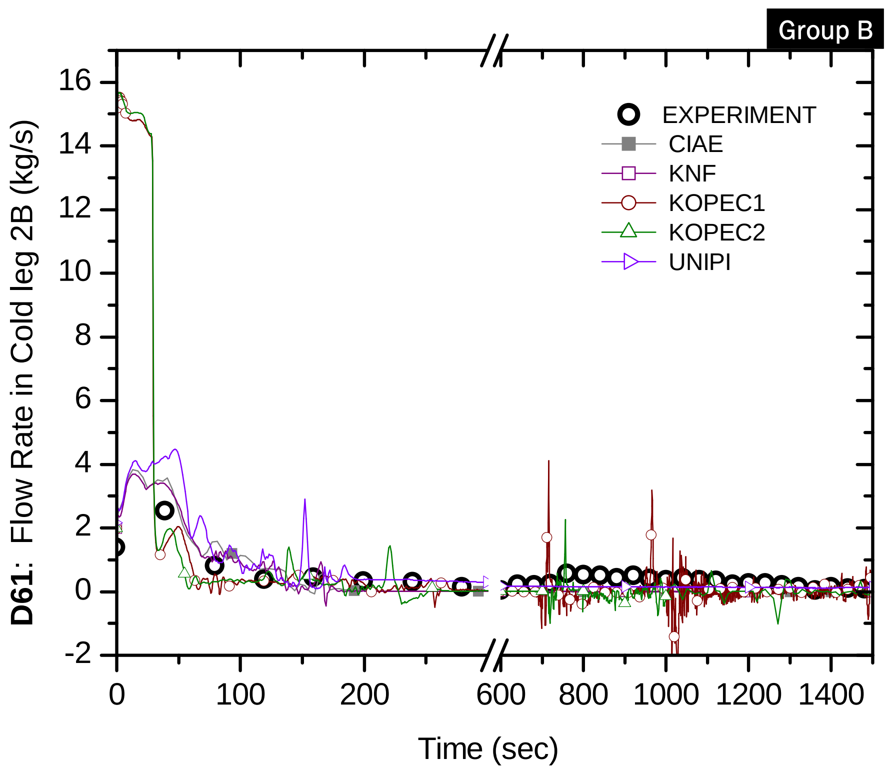

Figure B.61-B Flow rate in the cold leg 2B (D61)

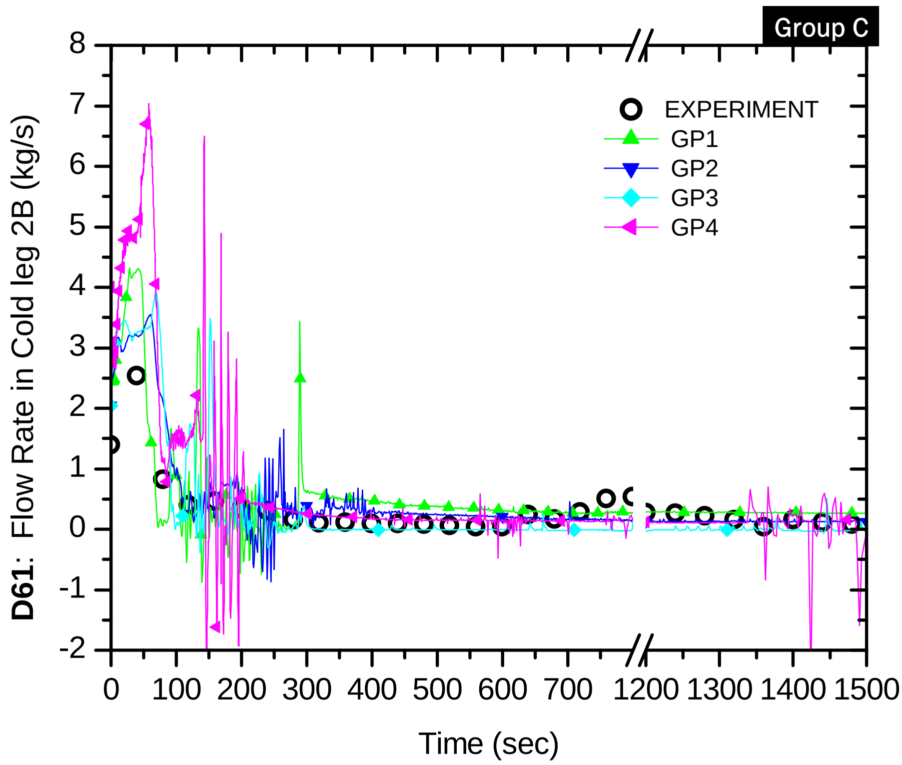

Figure B.61-C Flow rate in the cold leg 2B (D61)

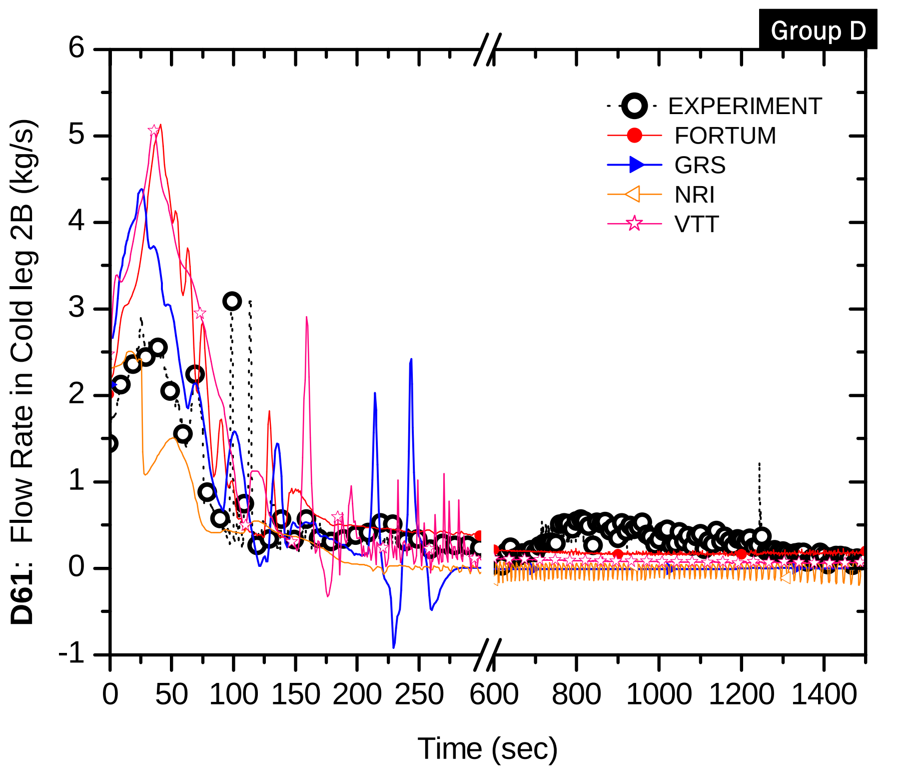

Figure B.61-D Flow rate in the cold leg 2B (D61)

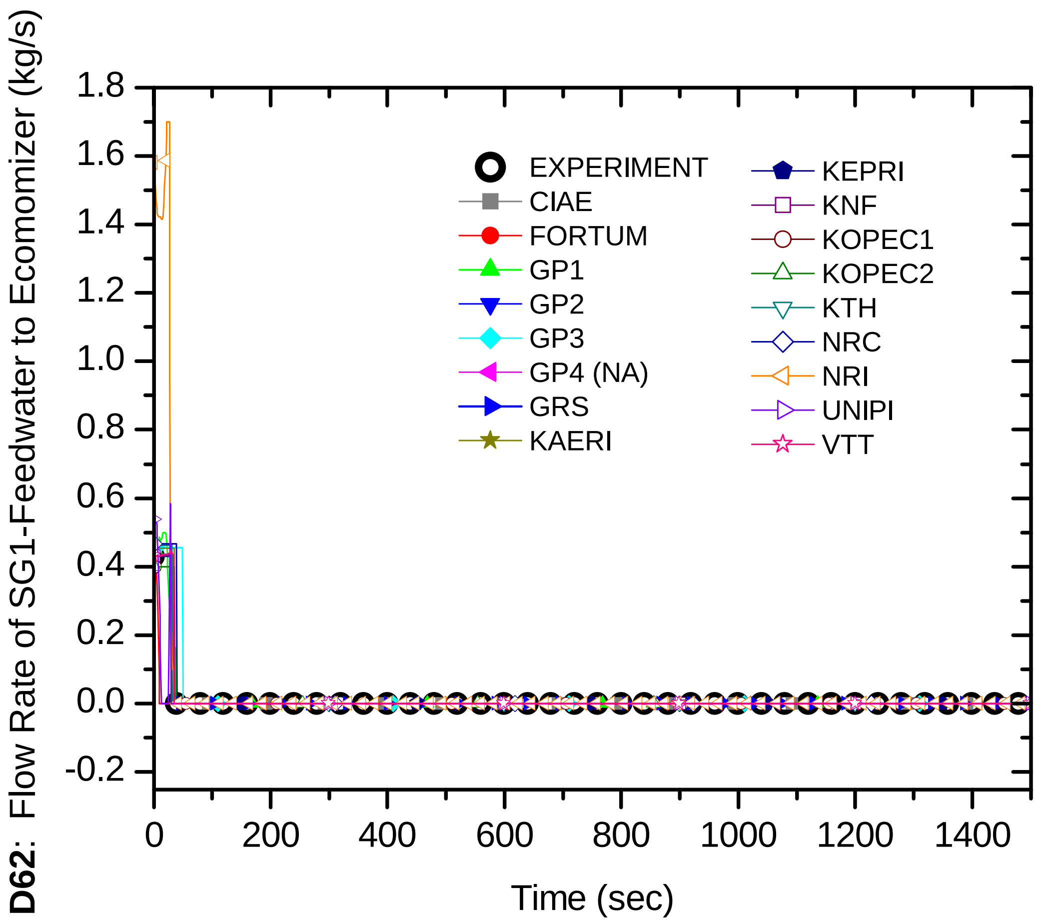

Figure B.62 Feed water flow rate to the economizer of SG-1 (D62)

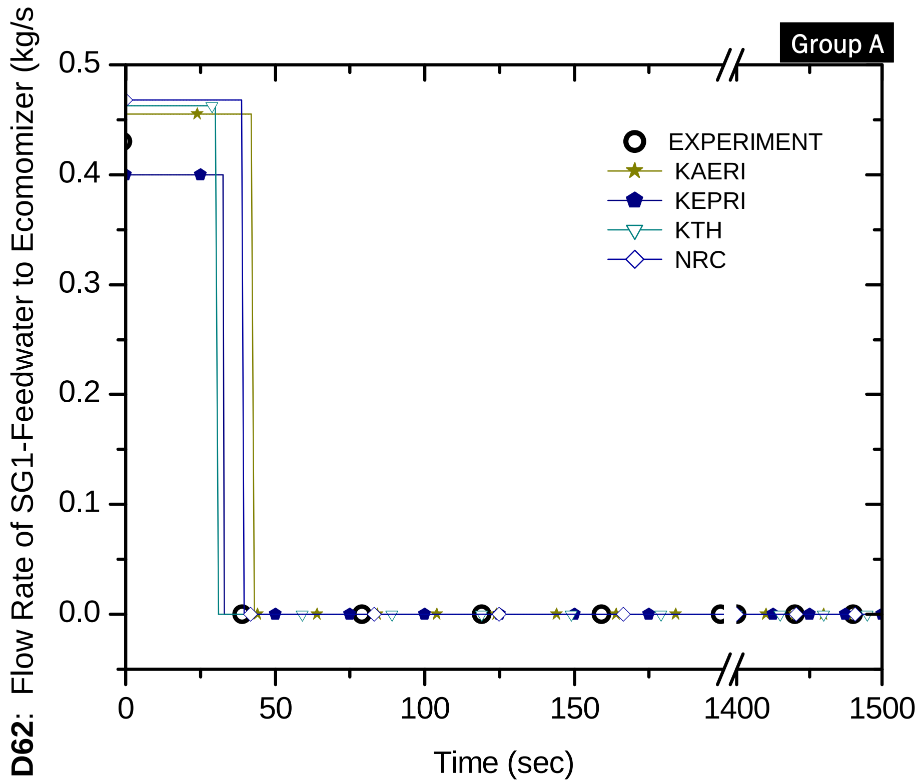

Figure B.62-A Feed water flow rate to the economizer of SG-1 (D62)

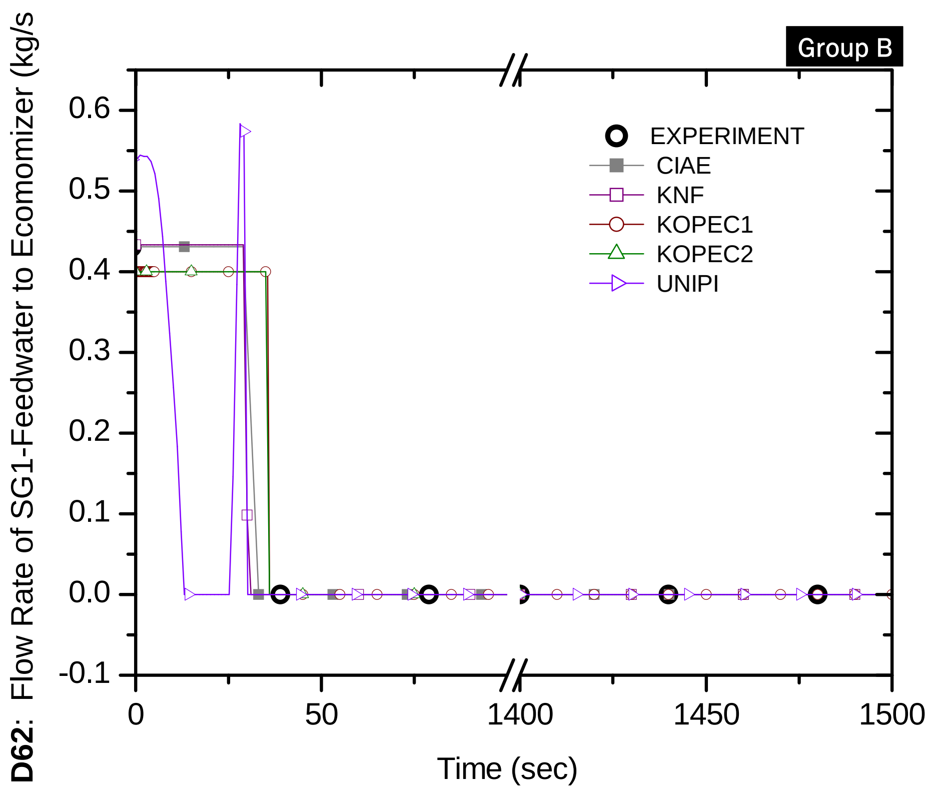

Figure B.62-B Feed water flow rate to the economizer of SG-1 (D62)

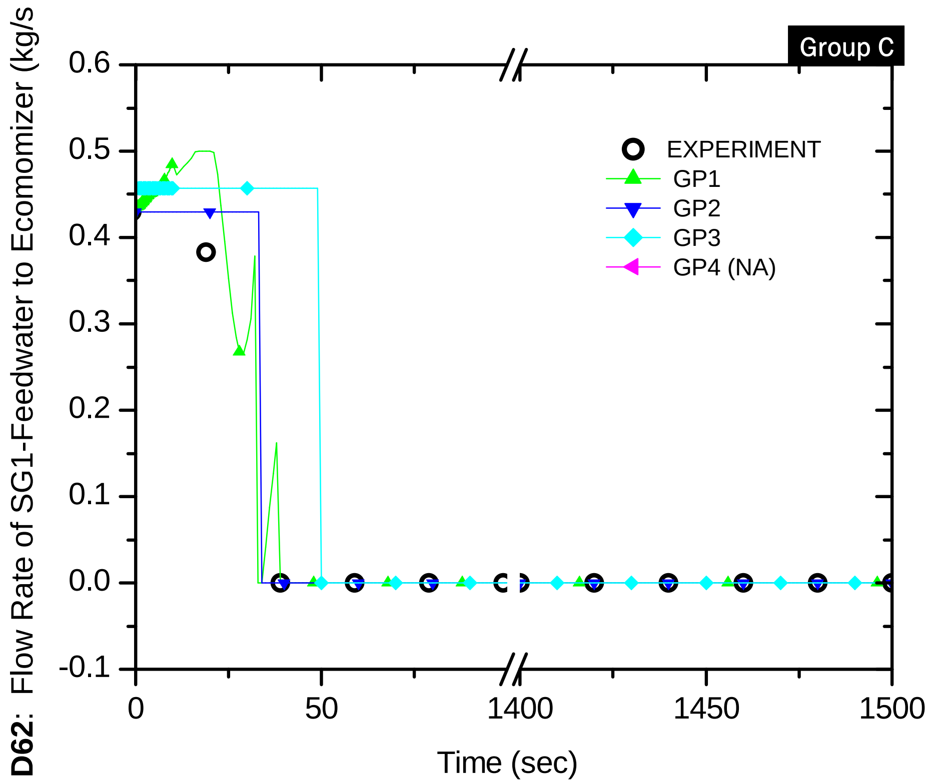

Figure B.62-C Feed water flow rate to the economizer of SG-1 (D62)

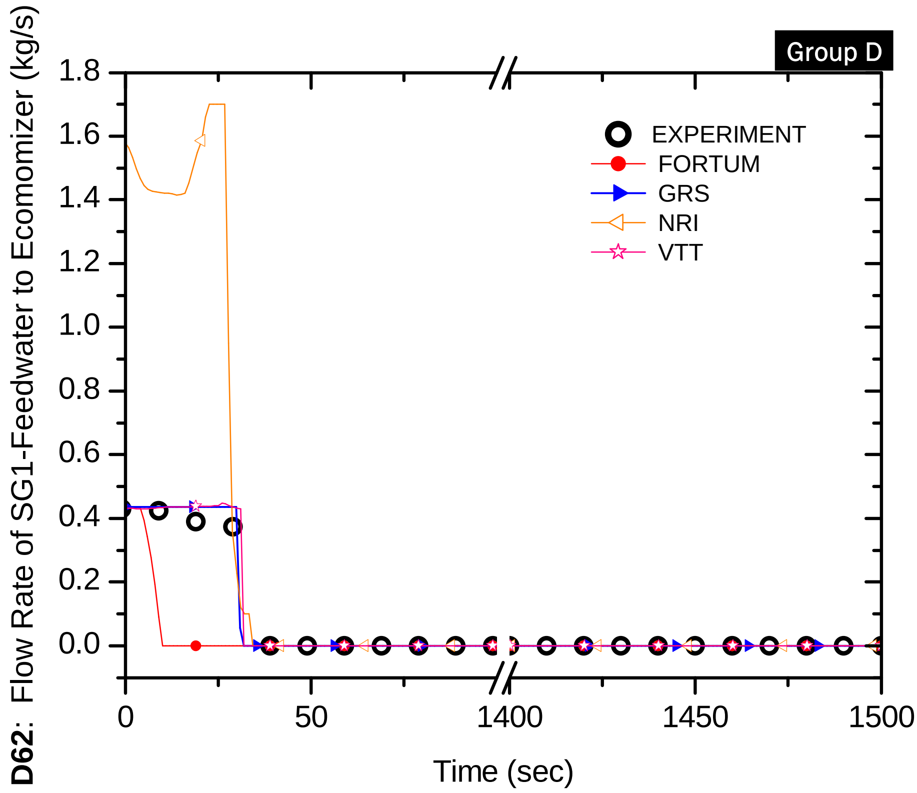

Figure B.62-D Feed water flow rate to the economizer of SG-1 (D62)

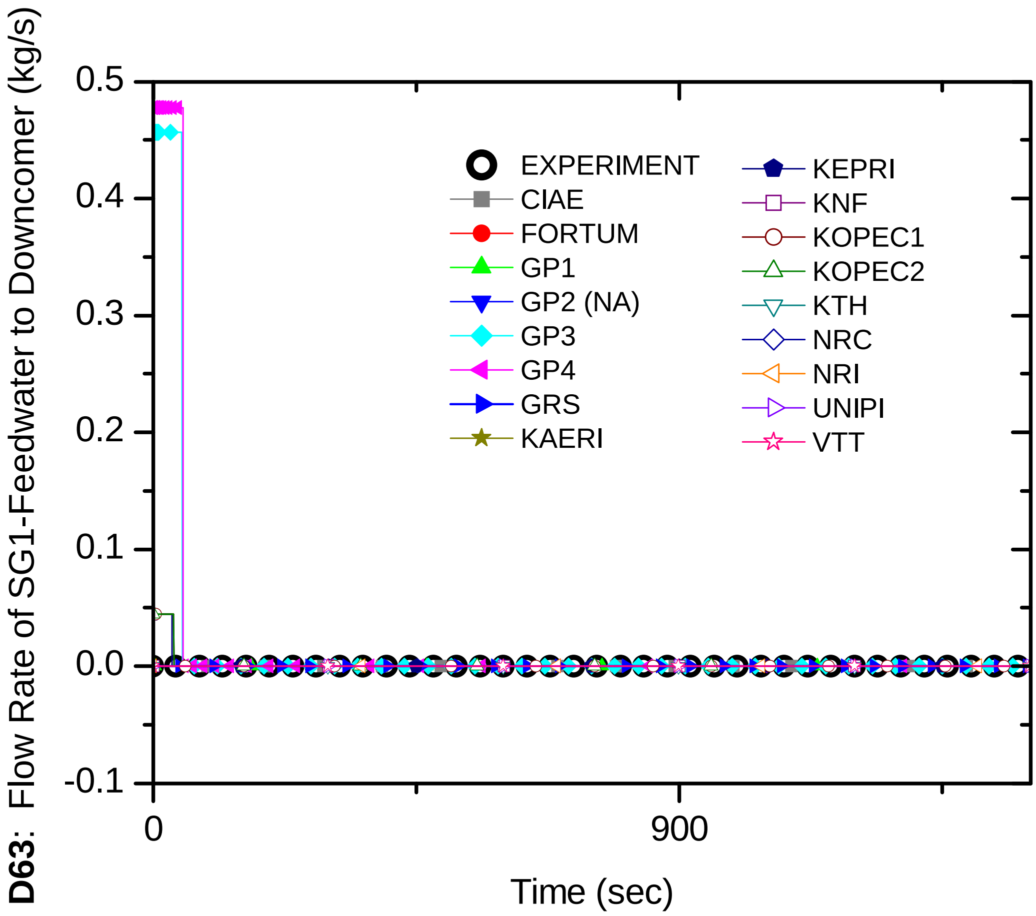

Figure B.63 Feed water flow rate to the down-comer of SG-1 (D63)

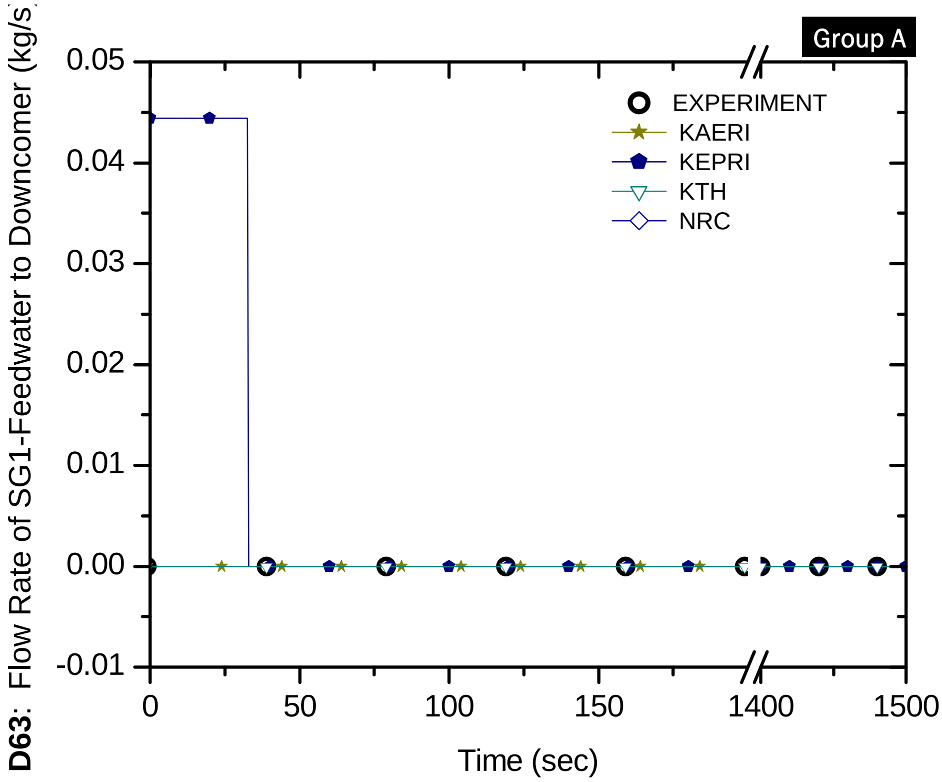

Figure B.63-A Feed water flow rate to the down-comer of SG-1 (D63)

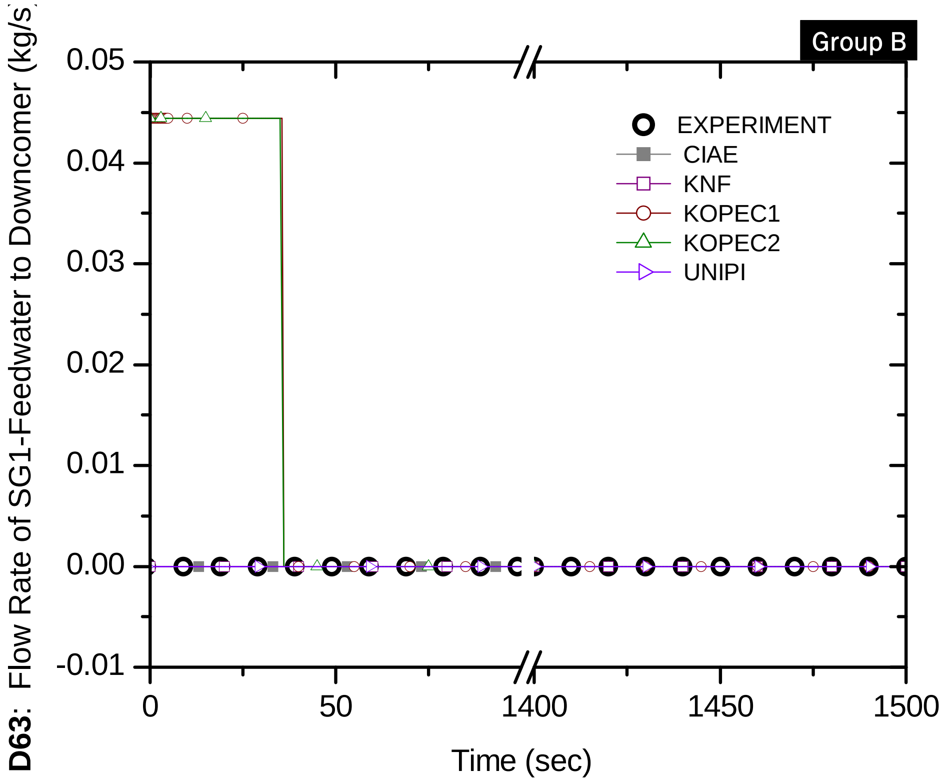

Figure B.63-B Feed water flow rate to the down-comer of SG-1 (D63)

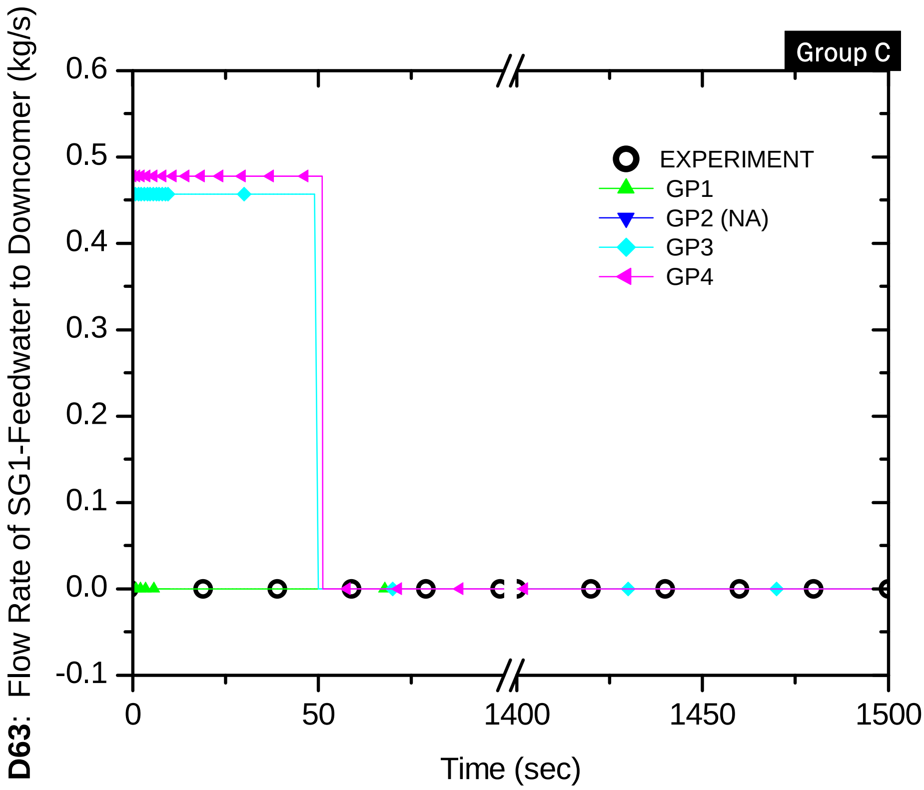

Figure B.63-C Feed water flow rate to the down-comer of SG-1 (D63)

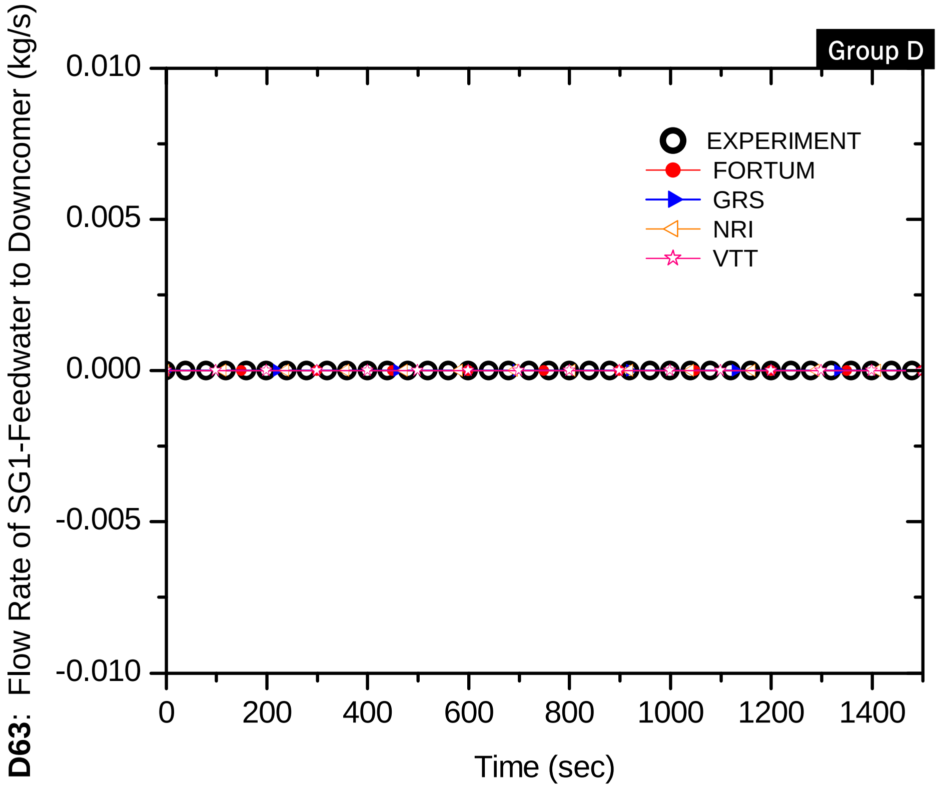

Figure B.63-D Feed water flow rate to the down-comer of SG-1 (D63)

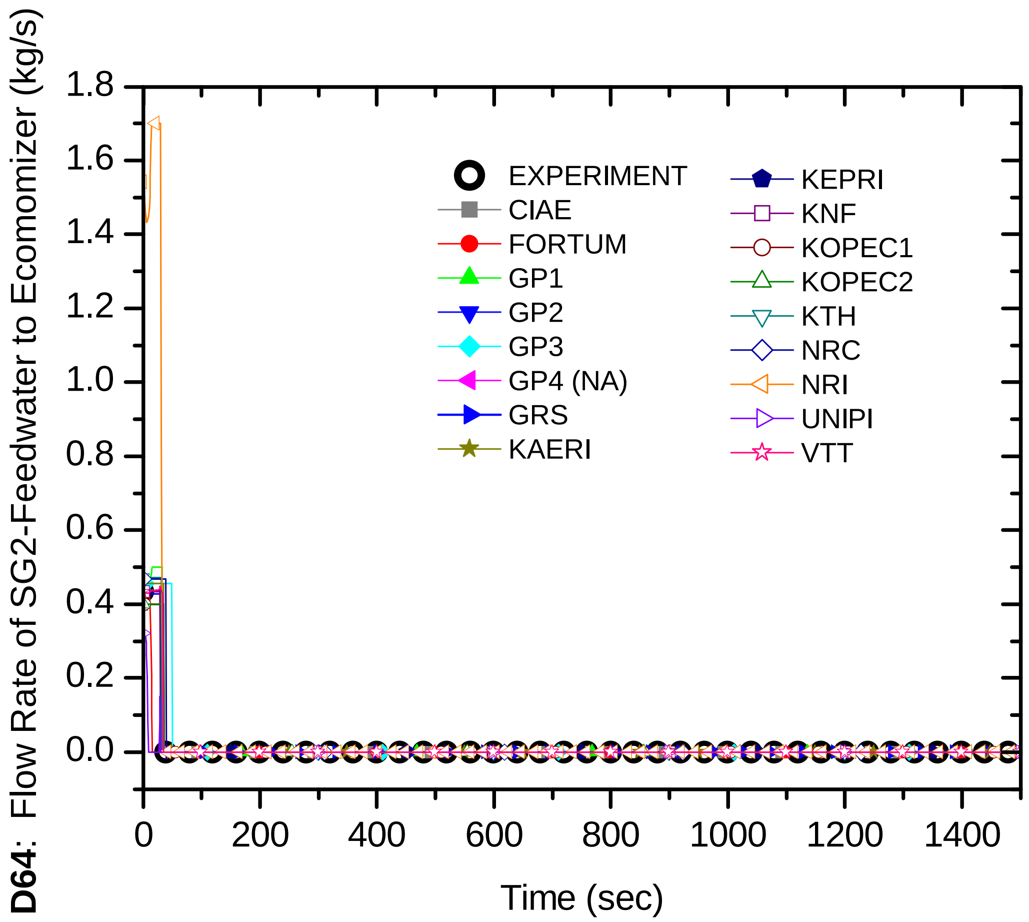

Figure B.64 Feed water flow rate to the economizer of SG-2 (D64)

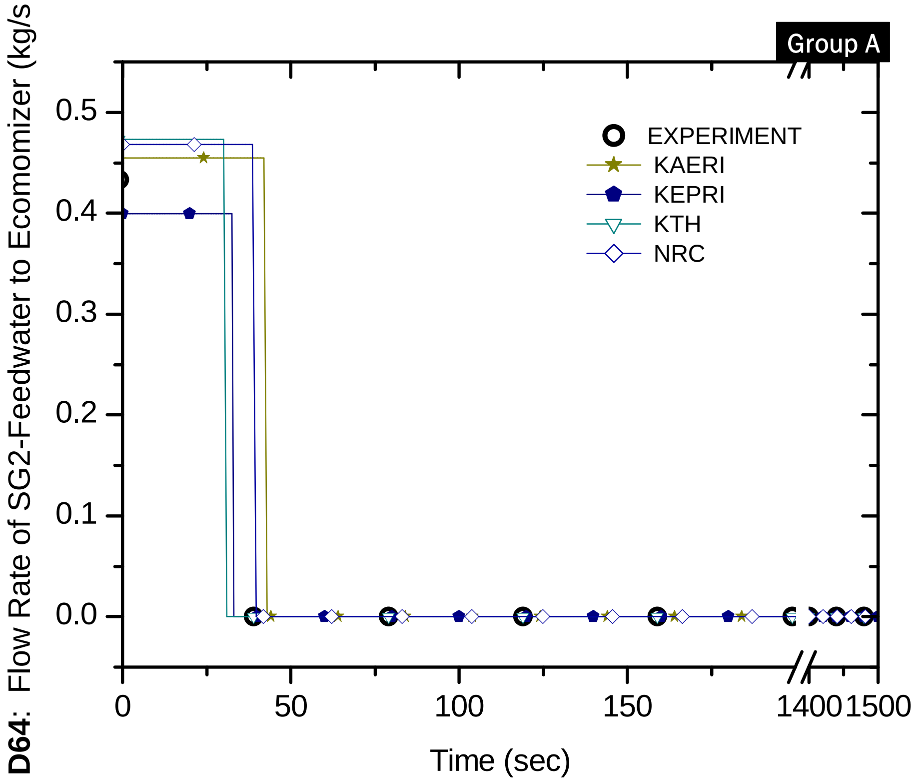

Figure B.64-A Feed water flow rate to the economizer of SG-2 (D64)

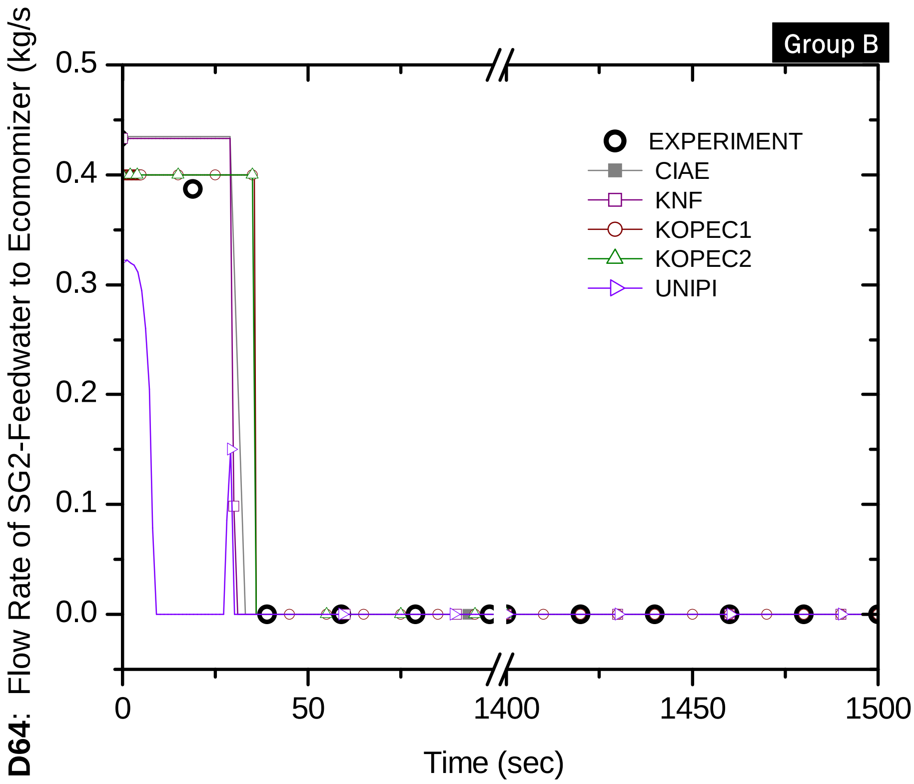

Figure B.64-B Feed water flow rate to the economizer of SG-2 (D64)

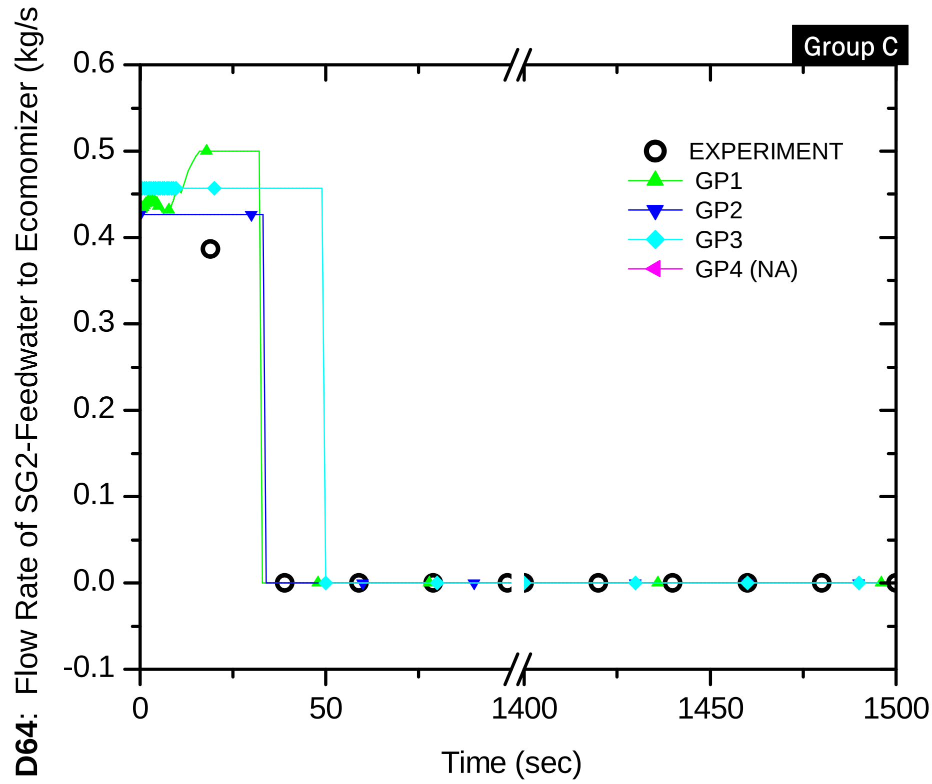

Figure B.64-C Feed water flow rate to the economizer of SG-2 (D64)

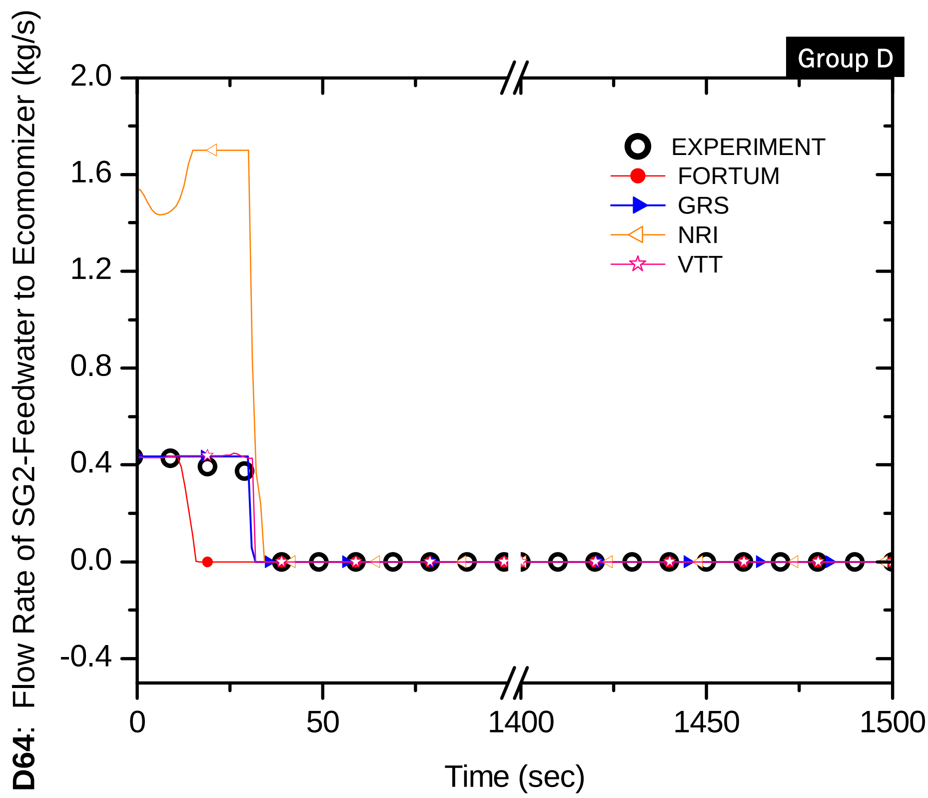

Figure B.64-D Feed water flow rate to the economizer of SG-2 (D64)

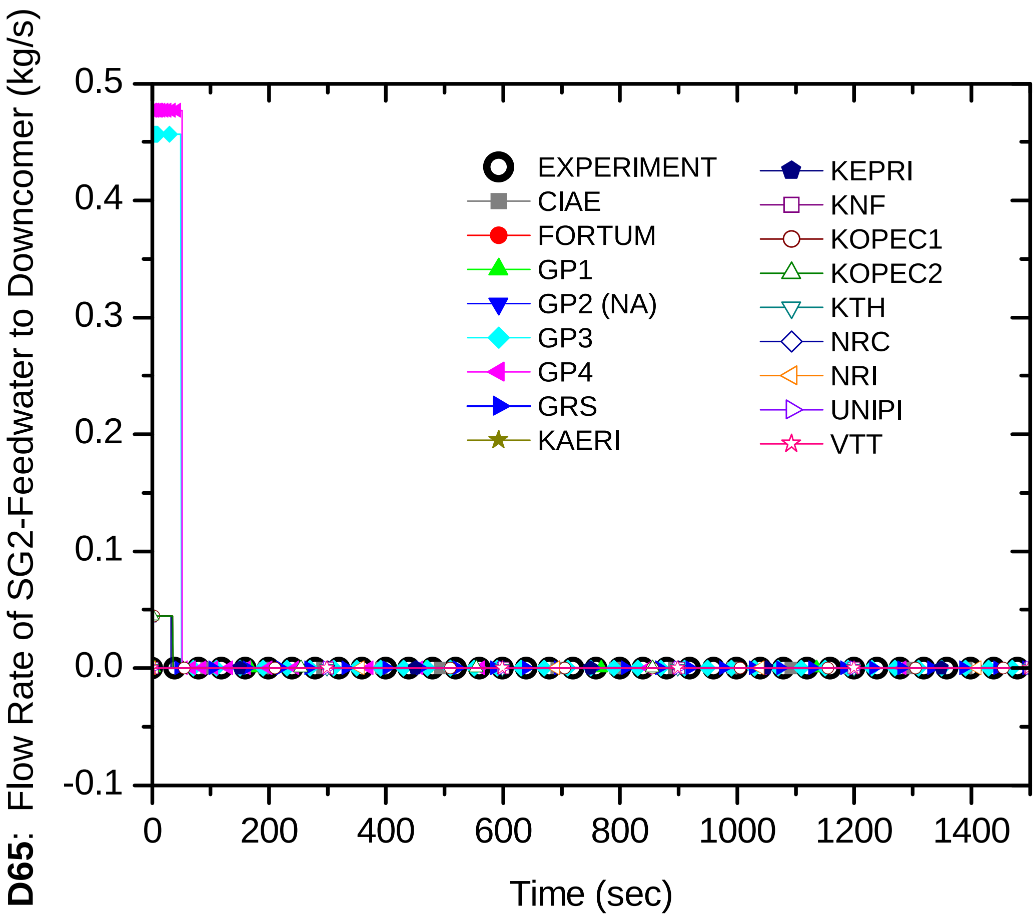

Figure B.65 Feed water flow rate to the down-comer of SG-2 (D65)

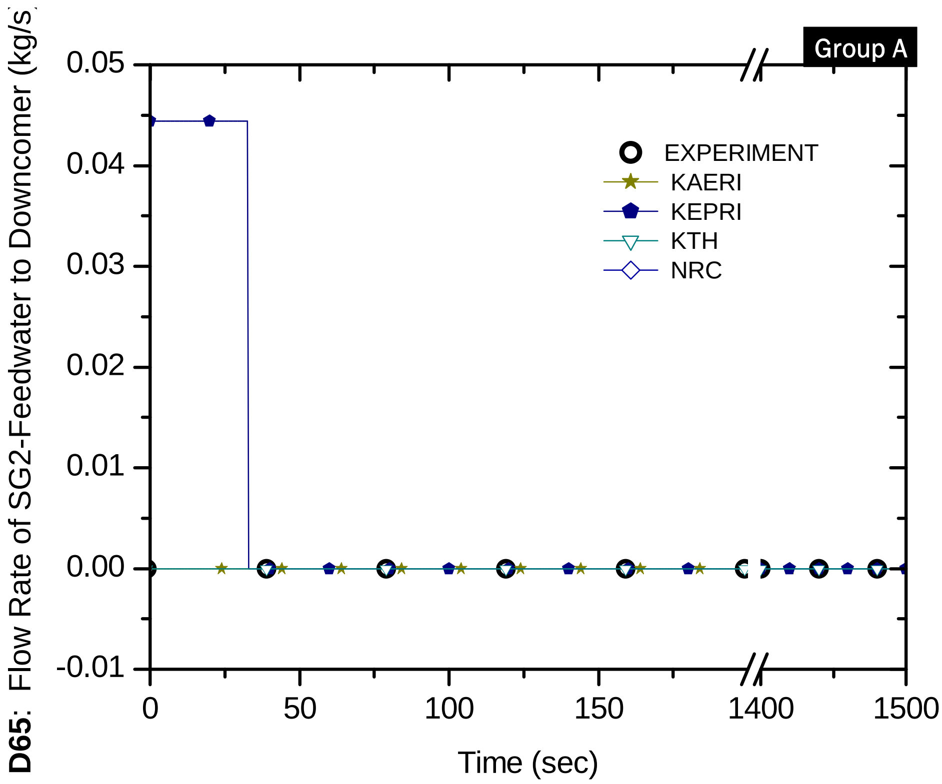

Figure B.65-A Feed water flow rate to the down-comer of SG-2 (D65)

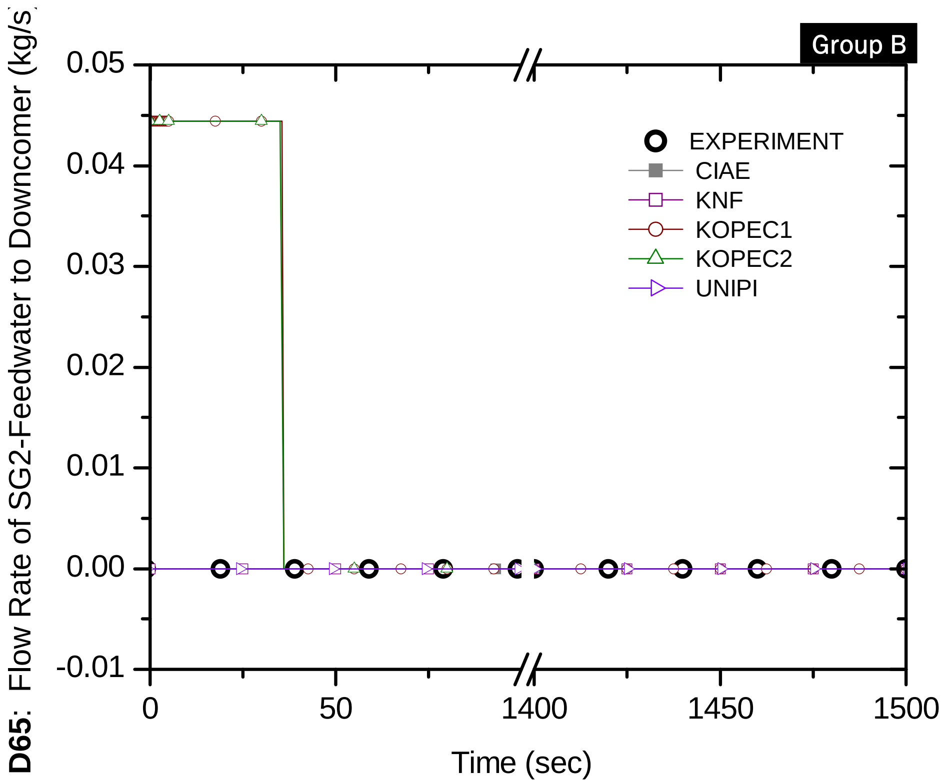

Figure B.65-B Feed water flow rate to the down-comer of SG-2 (D65)

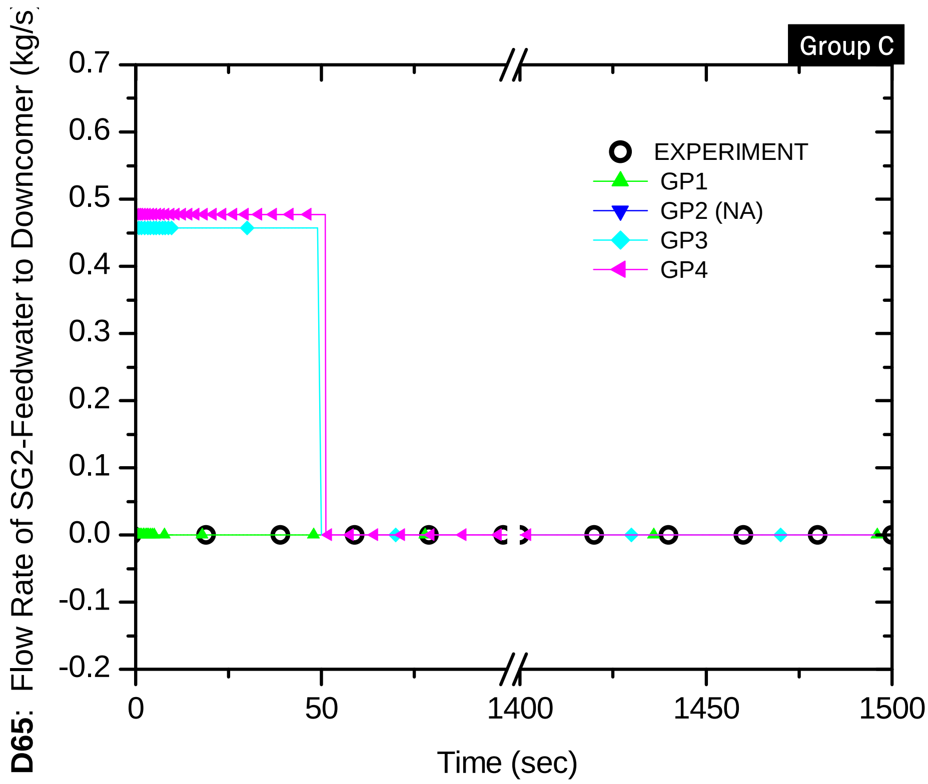

Figure B.65-C Feed water flow rate to the down-comer of SG-2 (D65)

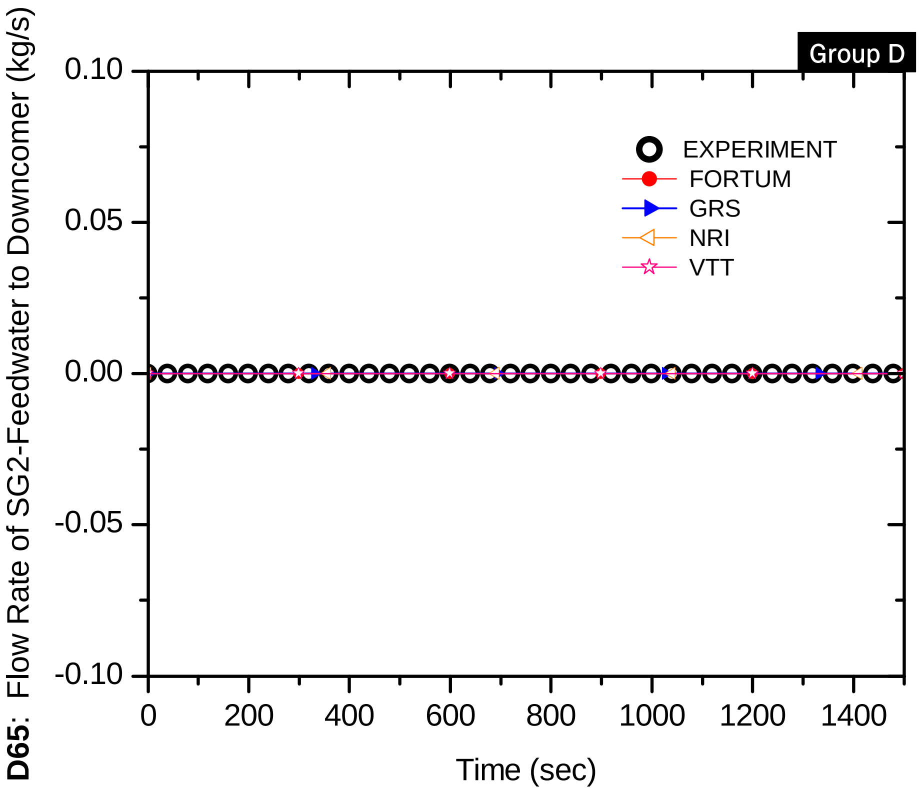

Figure B.65-D Feed water flow rate to the down-comer of SG-2 (D65)

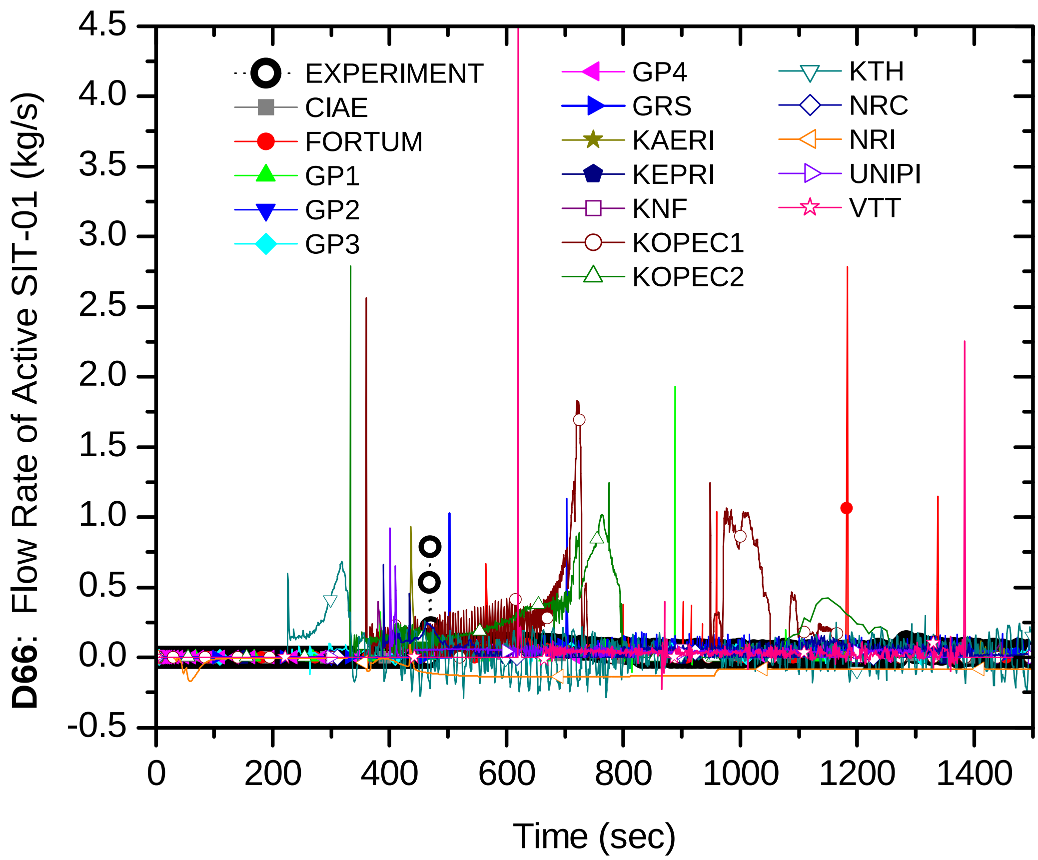

Figure B.66 Flow rate of the SIT-1 (D66)

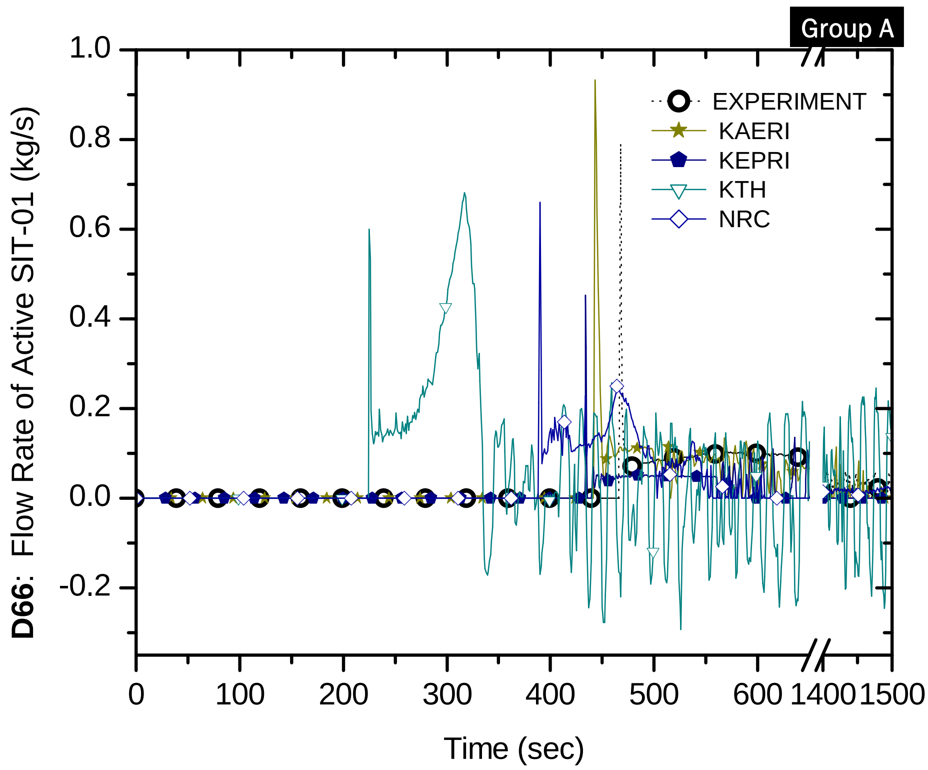

Figure B.66-A Flow rate of the SIT-1 (D66)

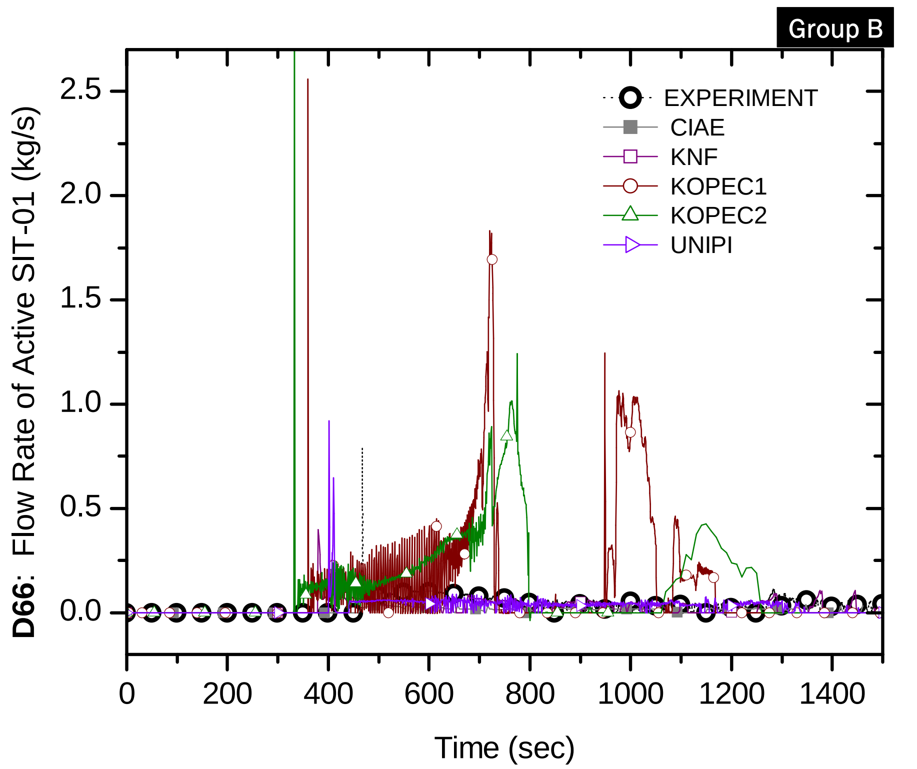

Figure B.66-B Flow rate of the SIT-1 (D66)

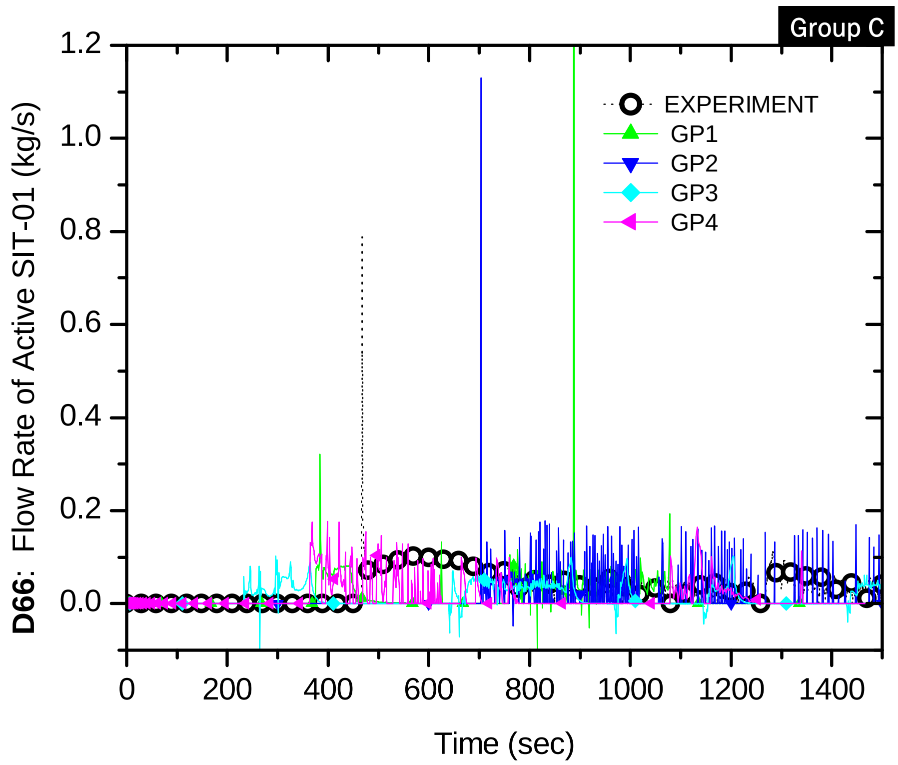

Figure B.66-C Flow rate of the SIT-1 (D66)

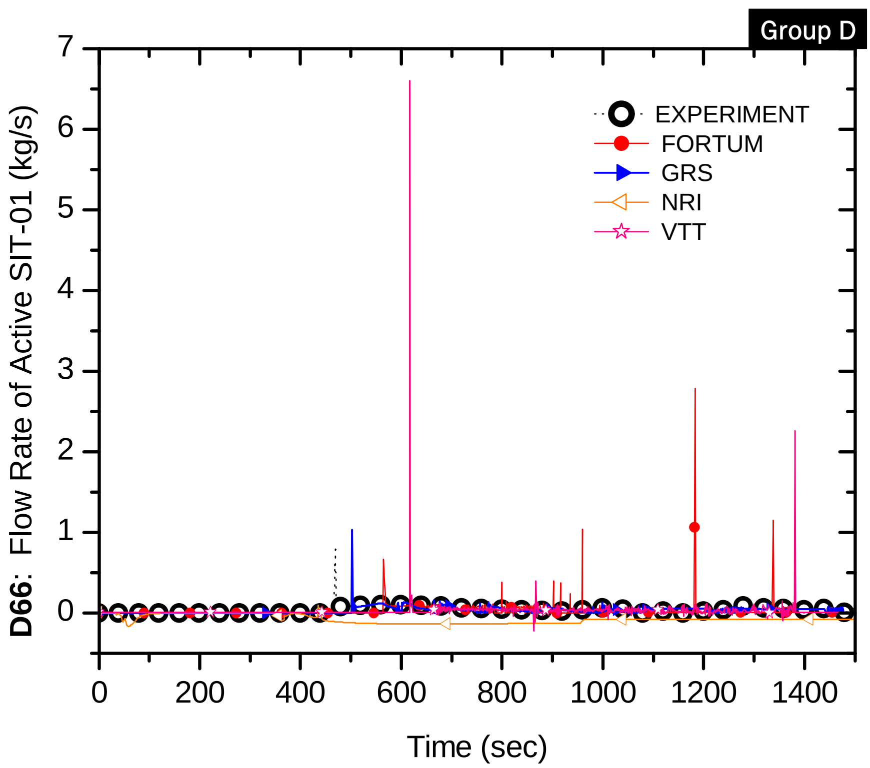

Figure B.66-D Flow rate of the SIT-1 (D66)

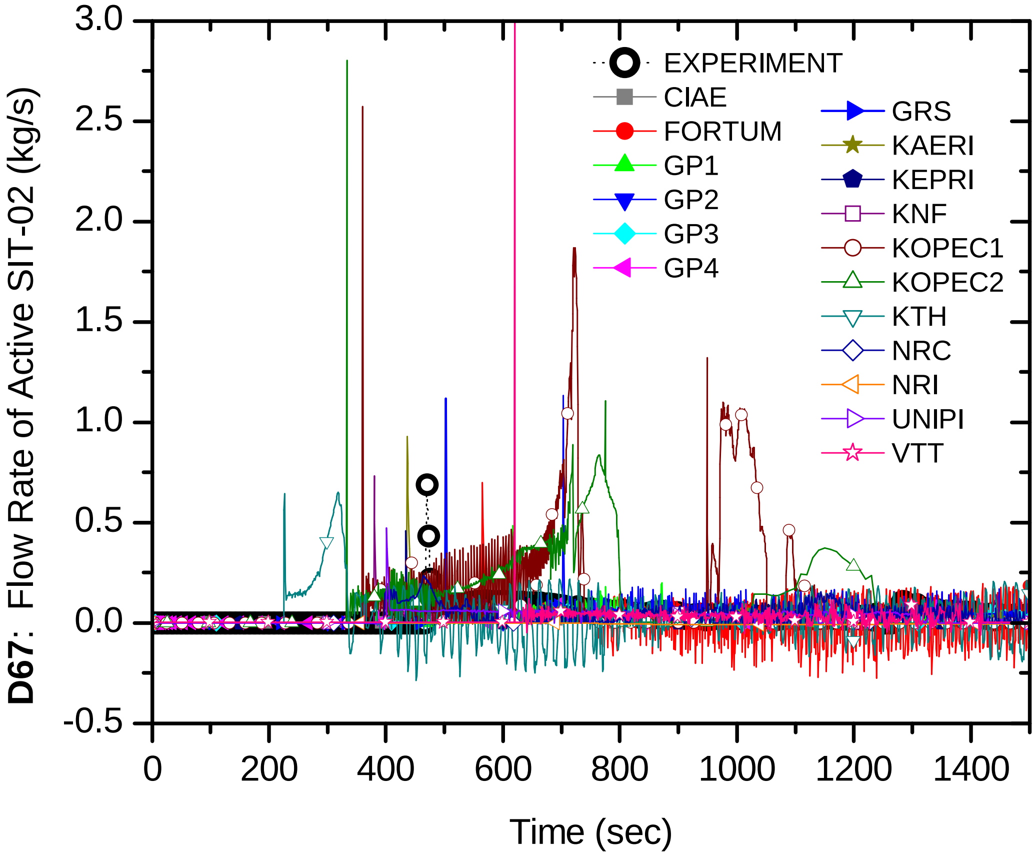

Figure B.67 Flow rate of the SIT-2 (D67)

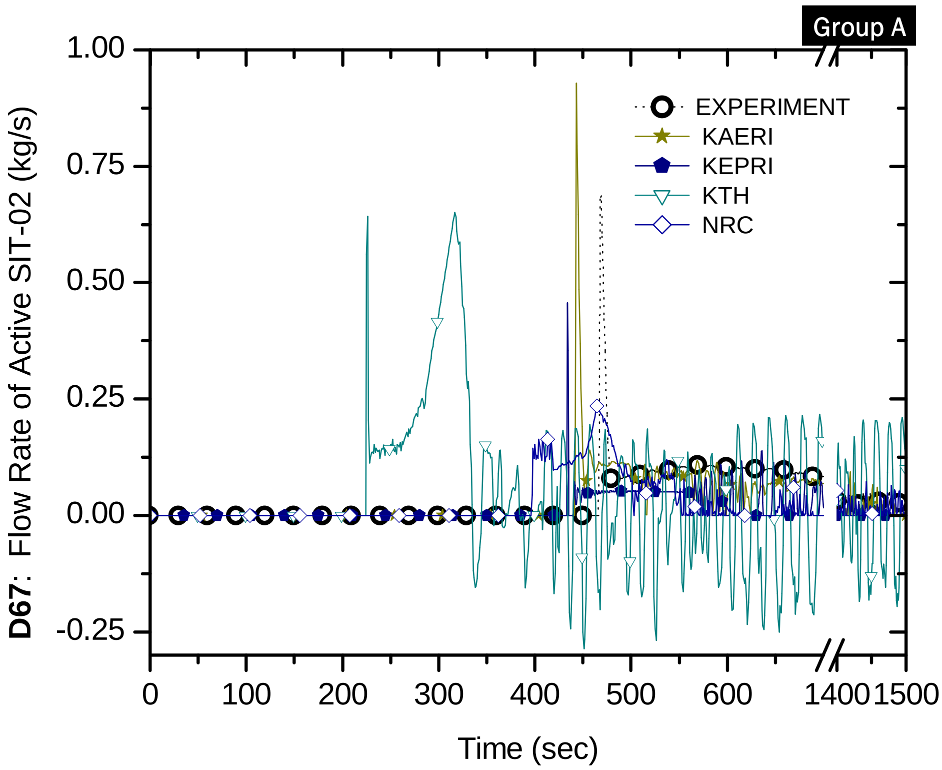

Figure B.67-A Flow rate of the SIT-2 (D67)

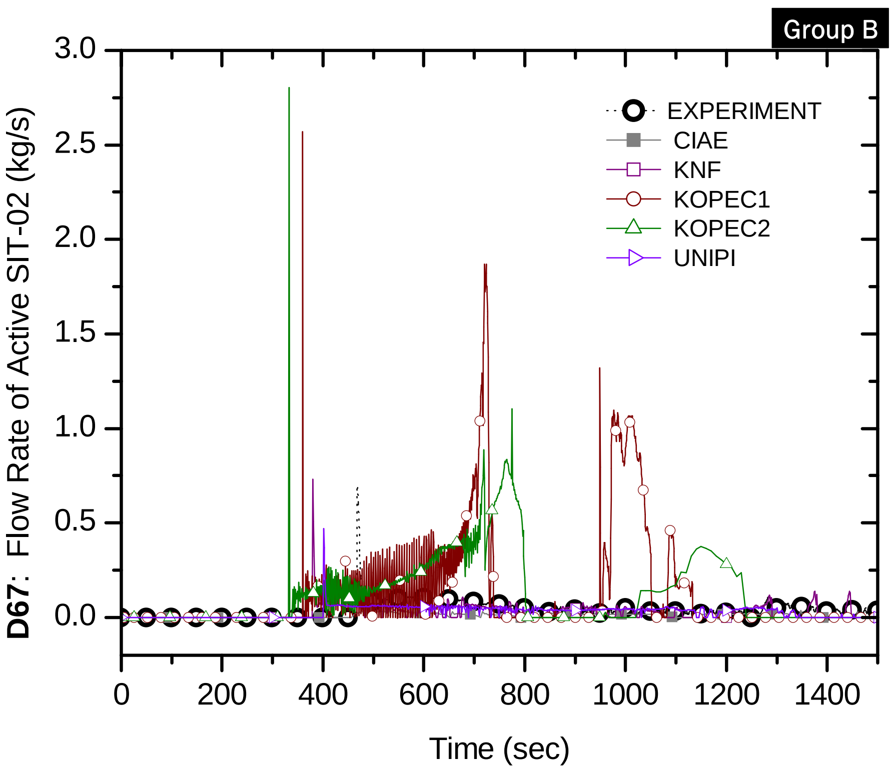

Figure B.67-B Flow rate of the SIT-2 (D67)

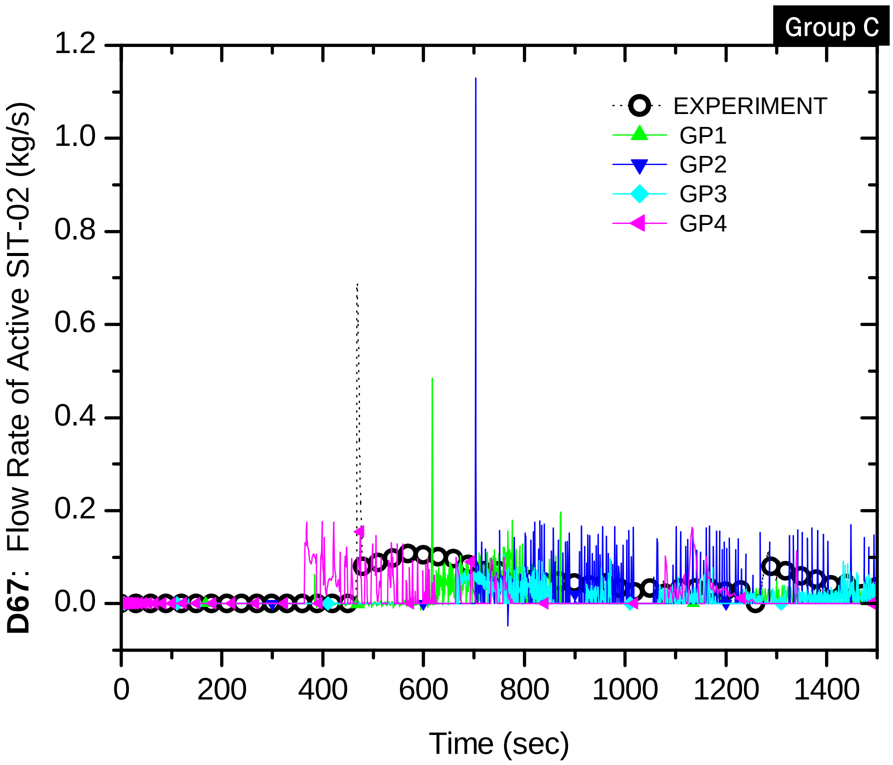

Figure B.67-C Flow rate of the SIT-2 (D67)

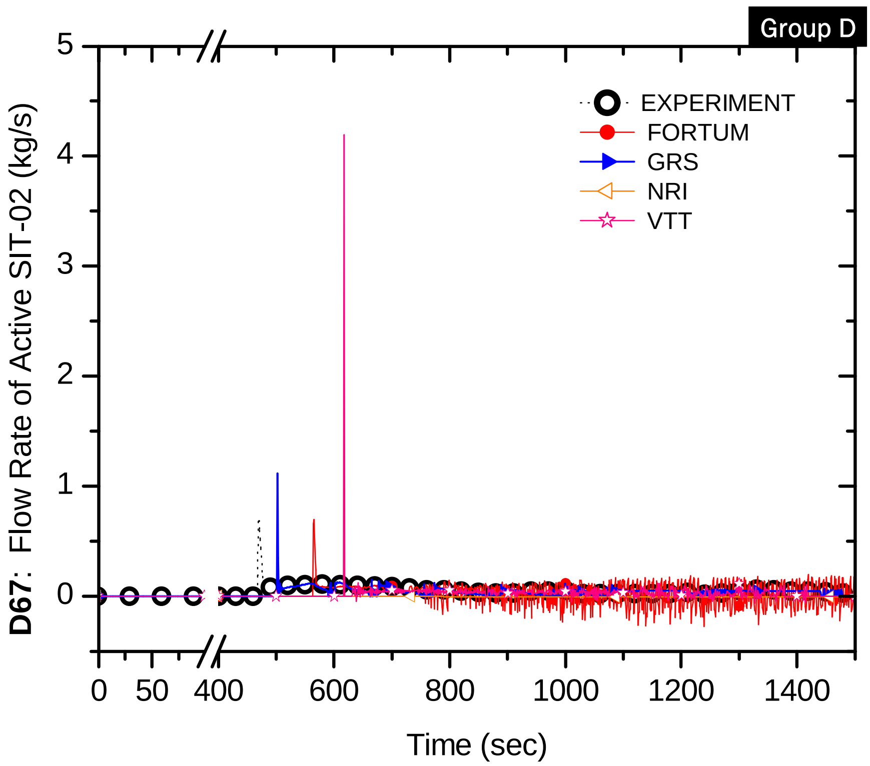

Figure B.67-D Flow rate of the SIT-2 (D67)

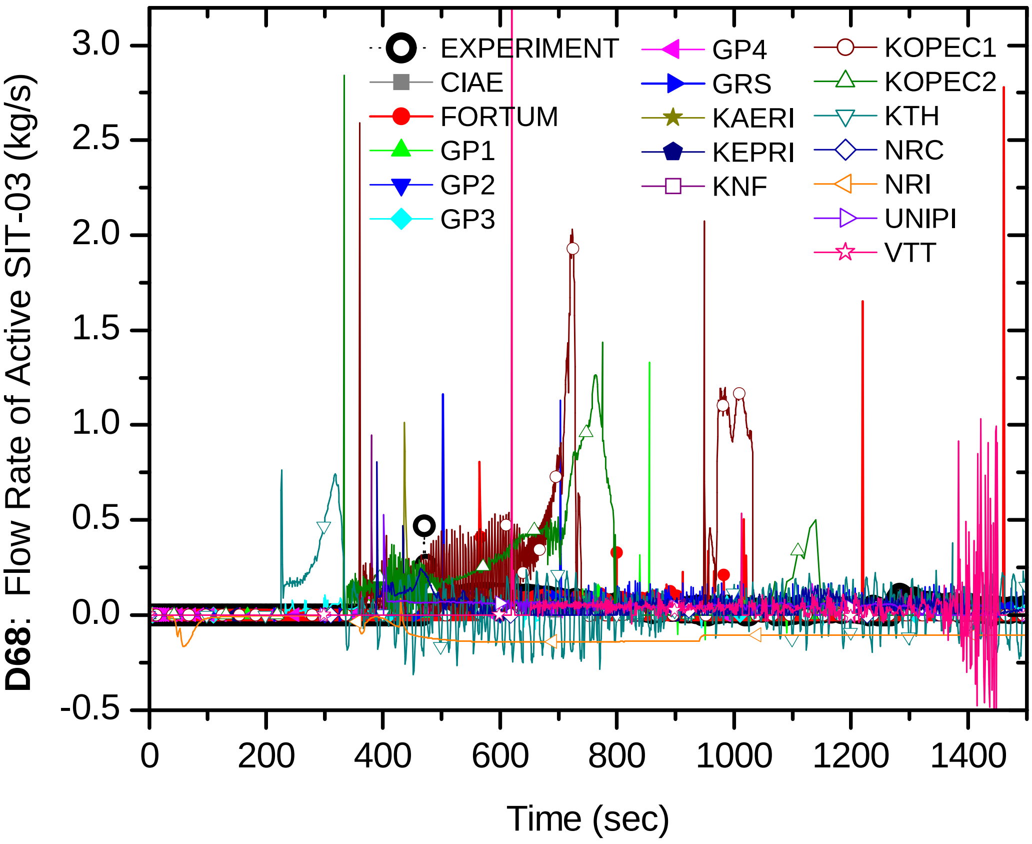

Figure B.68 Flow rate of the SIT-3 (D68)

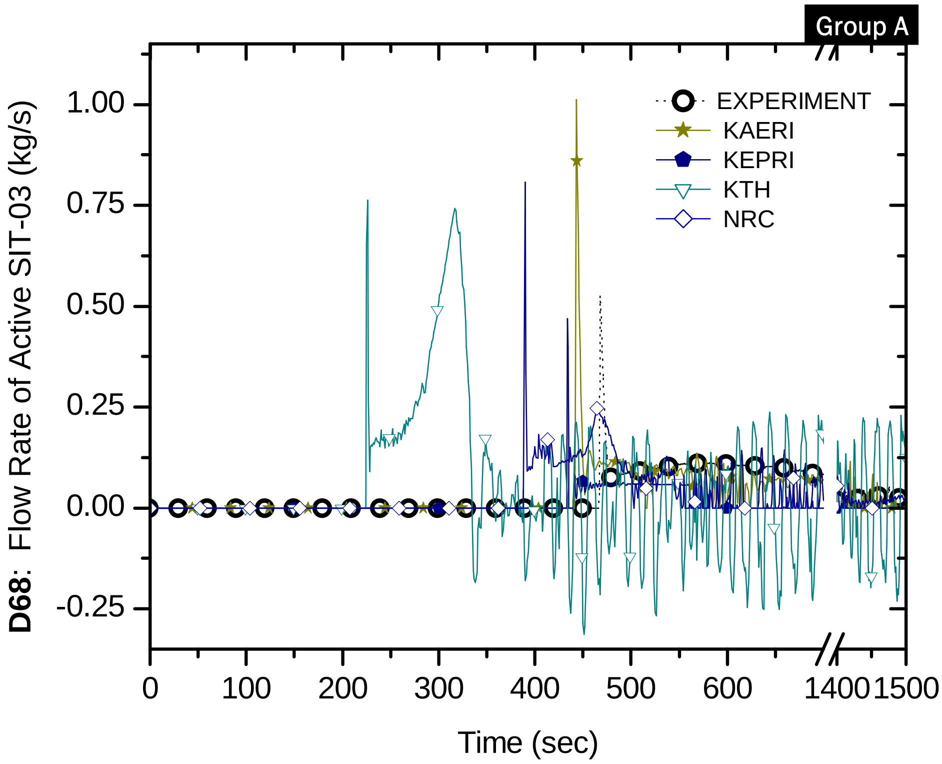

Figure B.68-A Flow rate of the SIT-3 (D68)

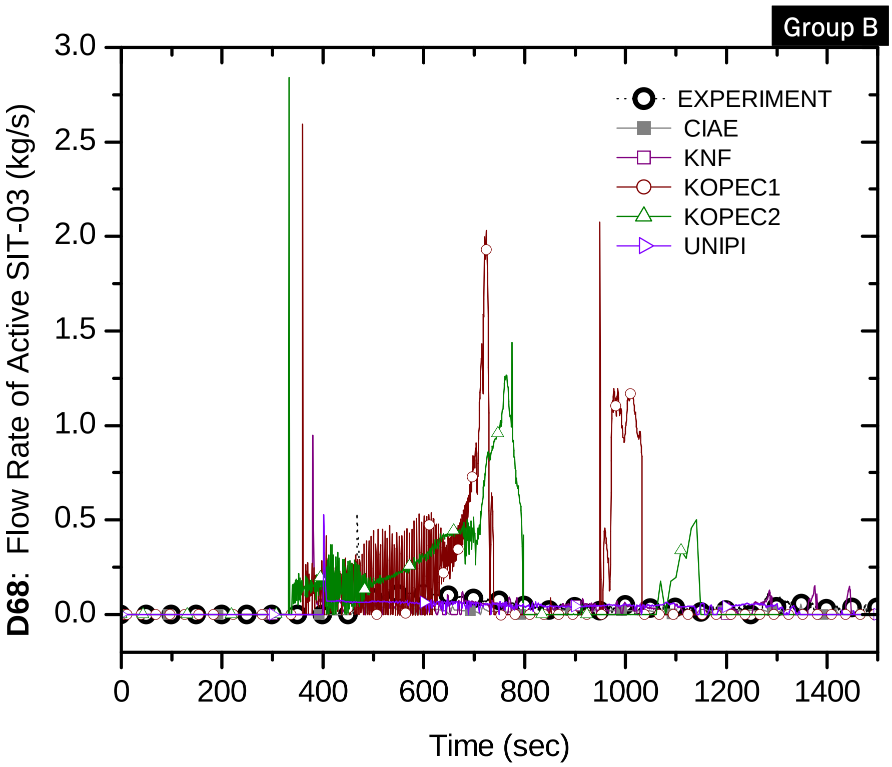

Figure B.68-B Flow rate of the SIT-3 (D68)

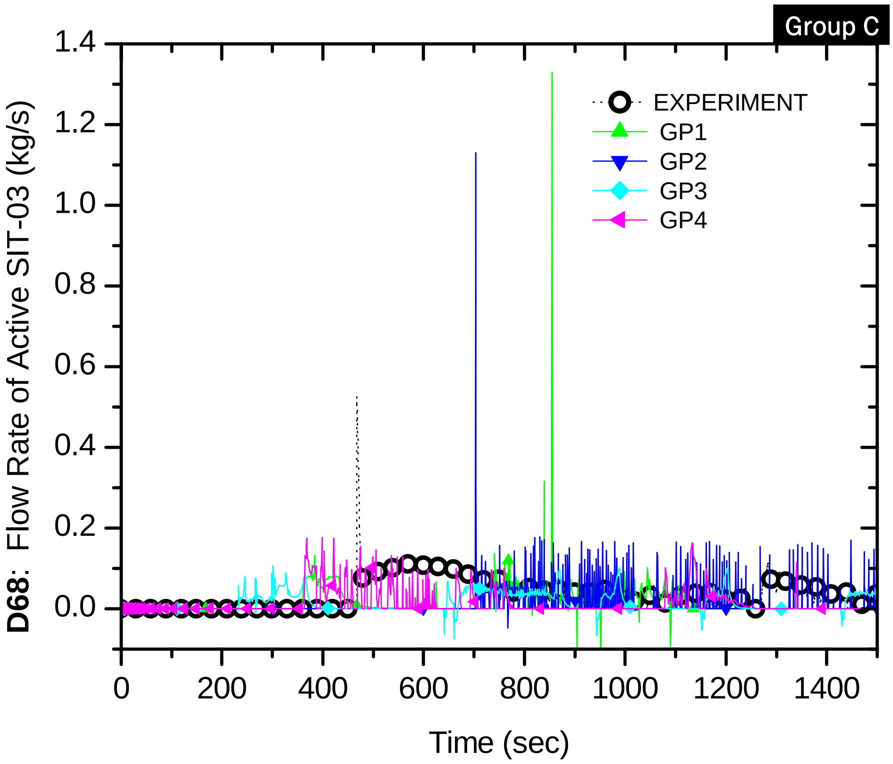

Figure B.68-C Flow rate of the SIT-3 (D68)

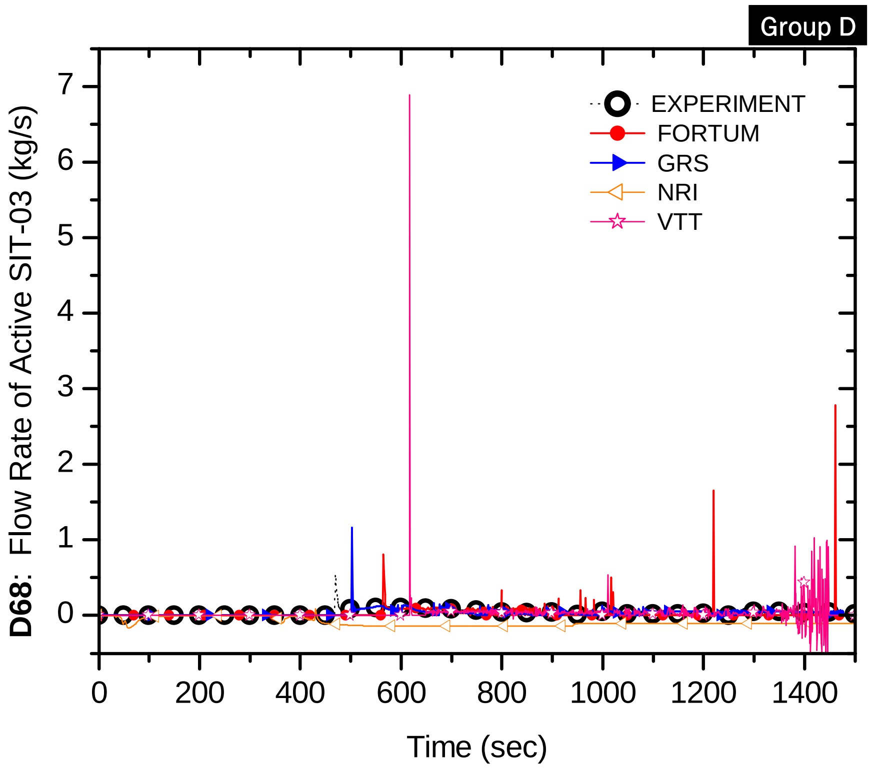

Figure B.68-D Flow rate of the SIT-3 (D68)

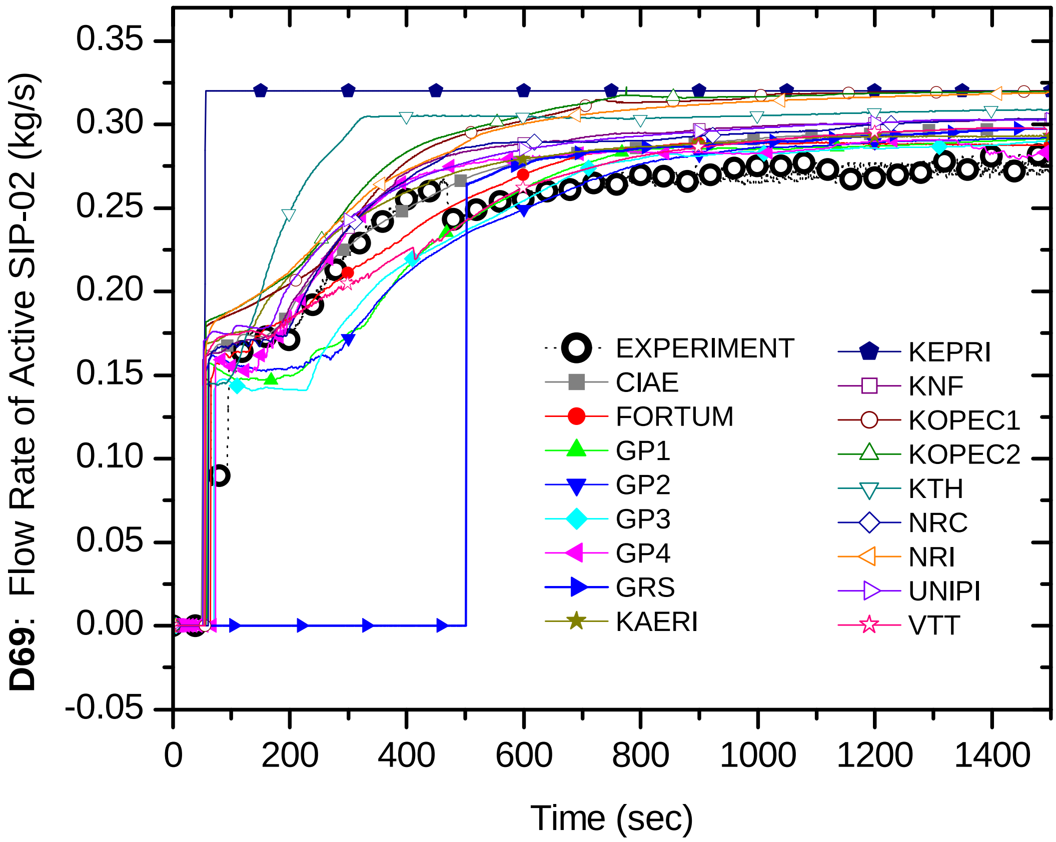

Figure B.69 Flow rate of the SIP-2 (D69)

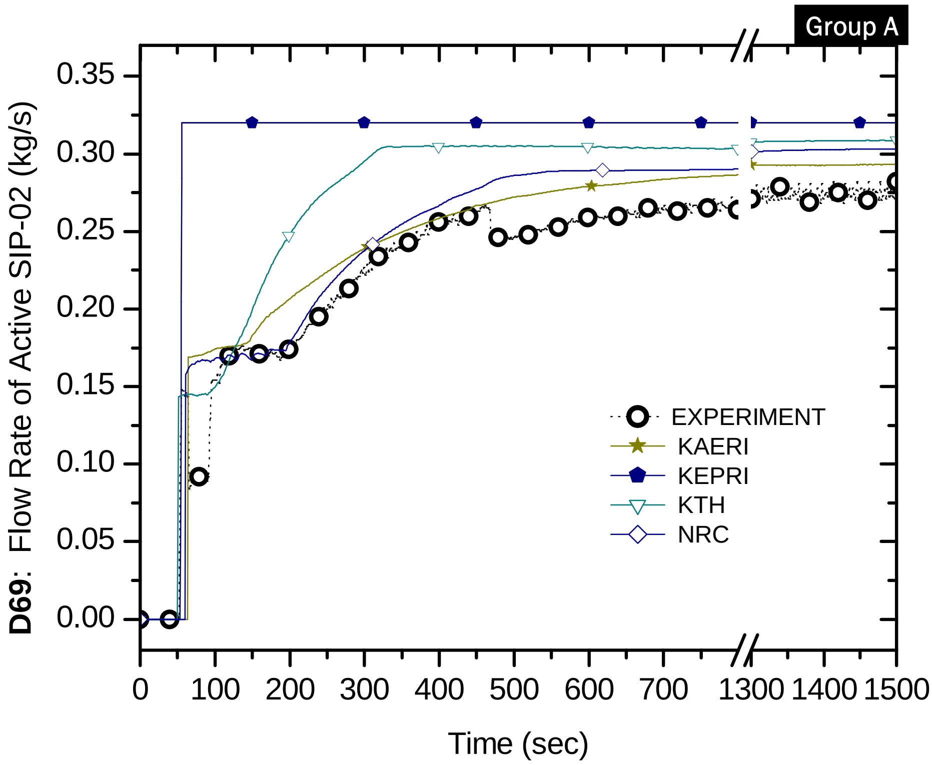

Figure B.69-A Flow rate of the SIP-2 (D69)

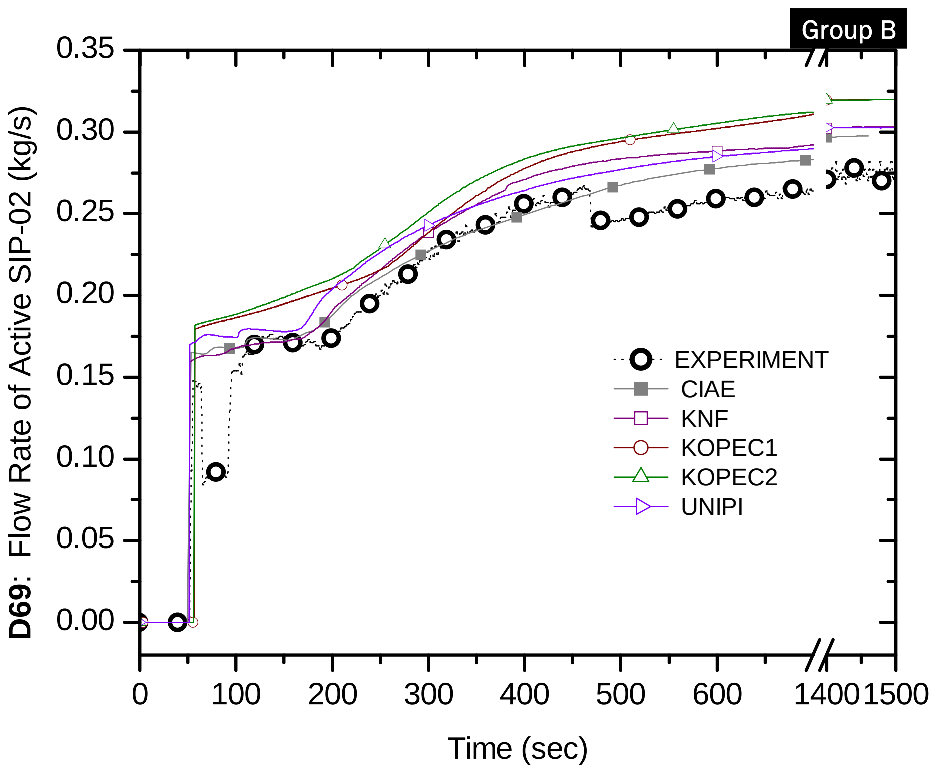

Figure B.69-B Flow rate of the SIP-2 (D69)

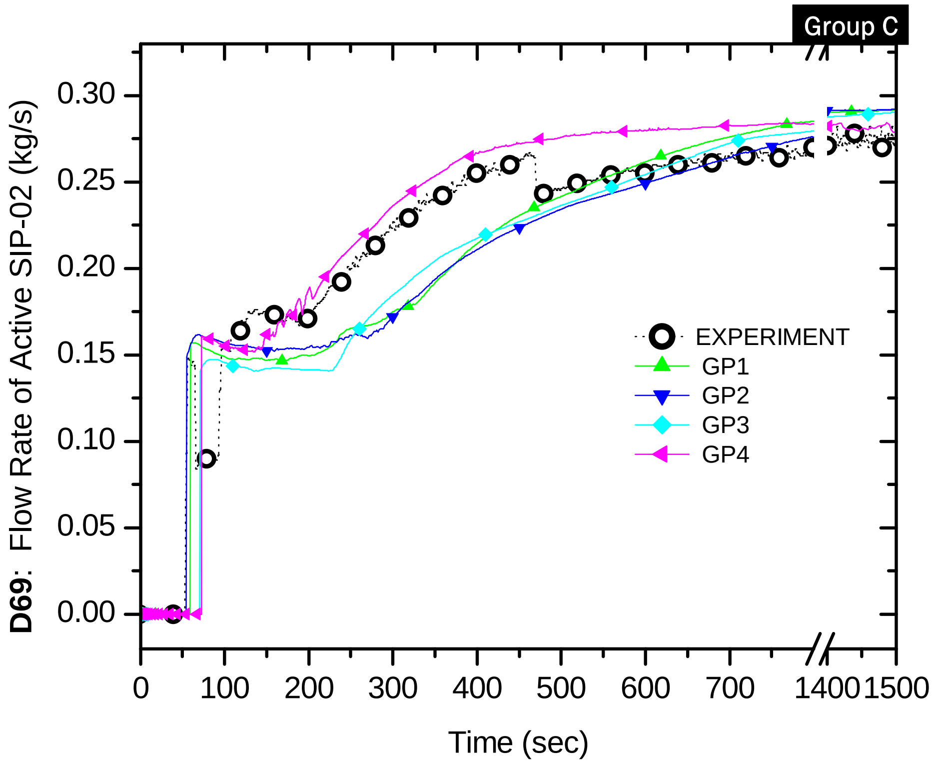

Figure B.69-C Flow rate of the SIP-2 (D69)

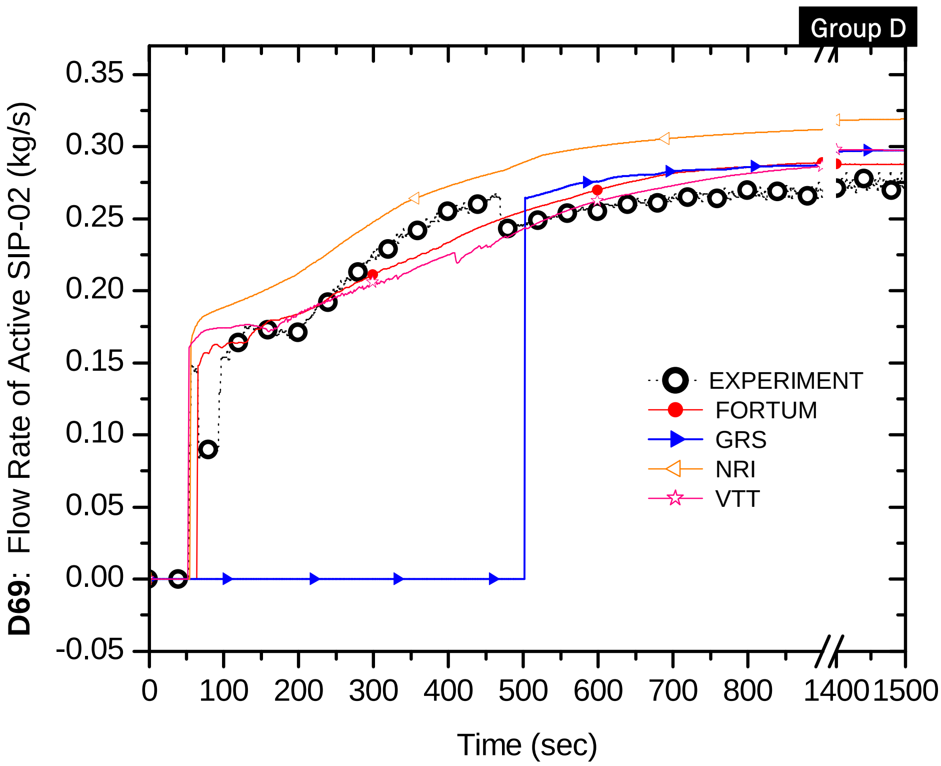

Figure B.69-D Flow rate of the SIP-2 (D69)

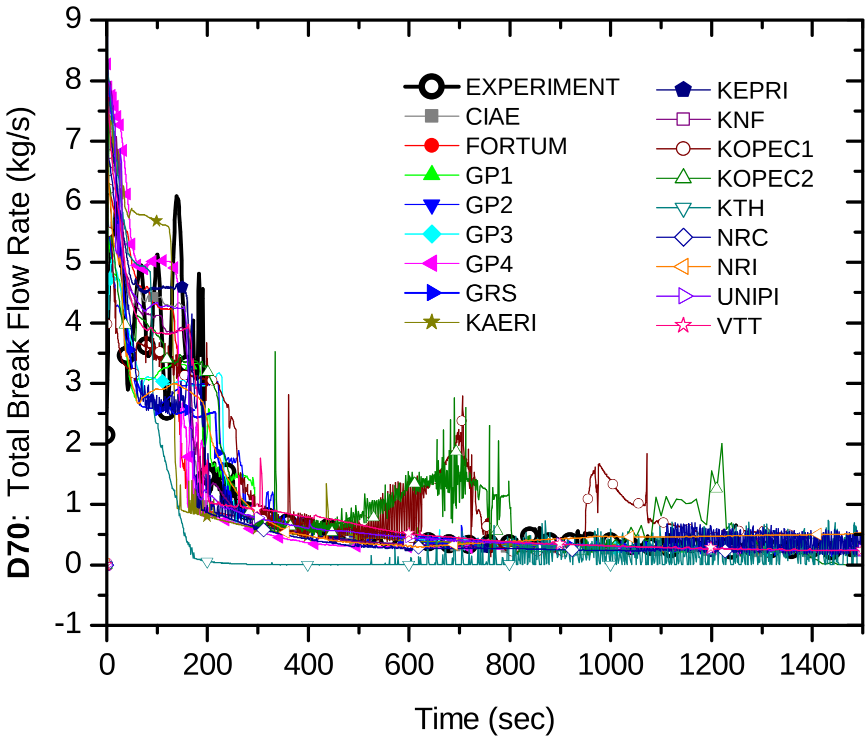

Figure B.70 Total break flow rate (D70)

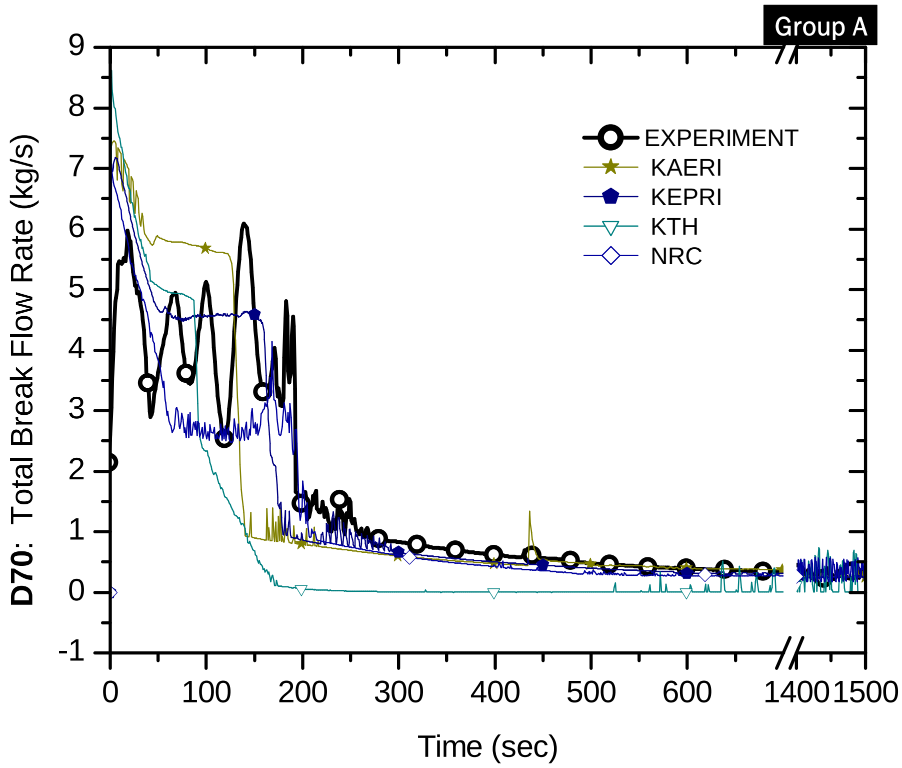

Figure B.70-A Total break flow rate (D70)

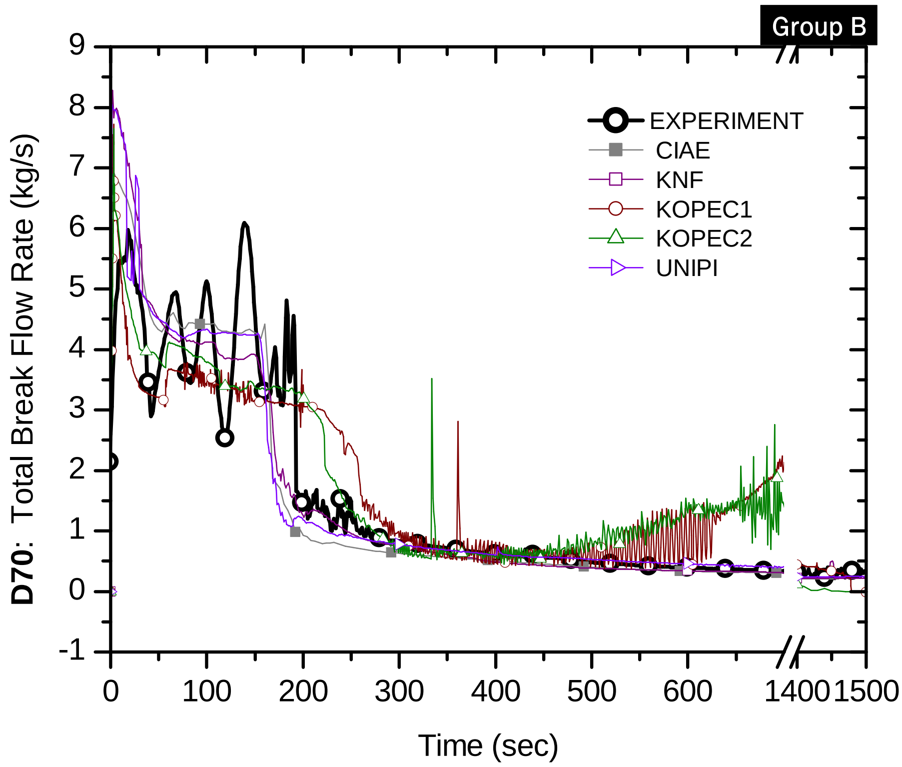

Figure B.70-B Total break flow rate (D70)

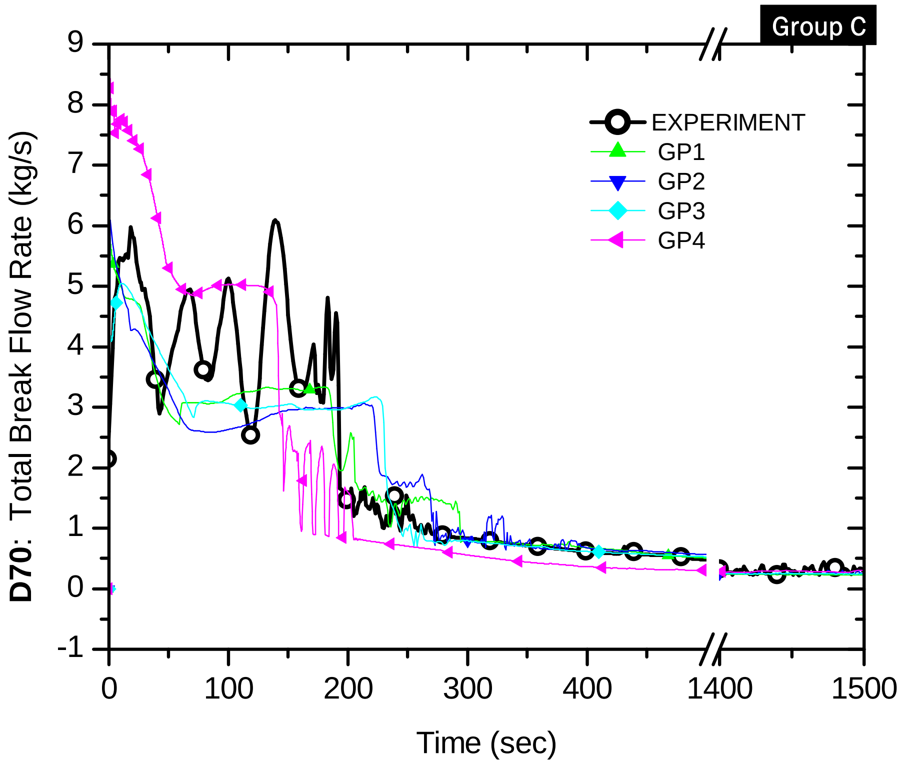

Figure B.70-C Total break flow rate (D70)

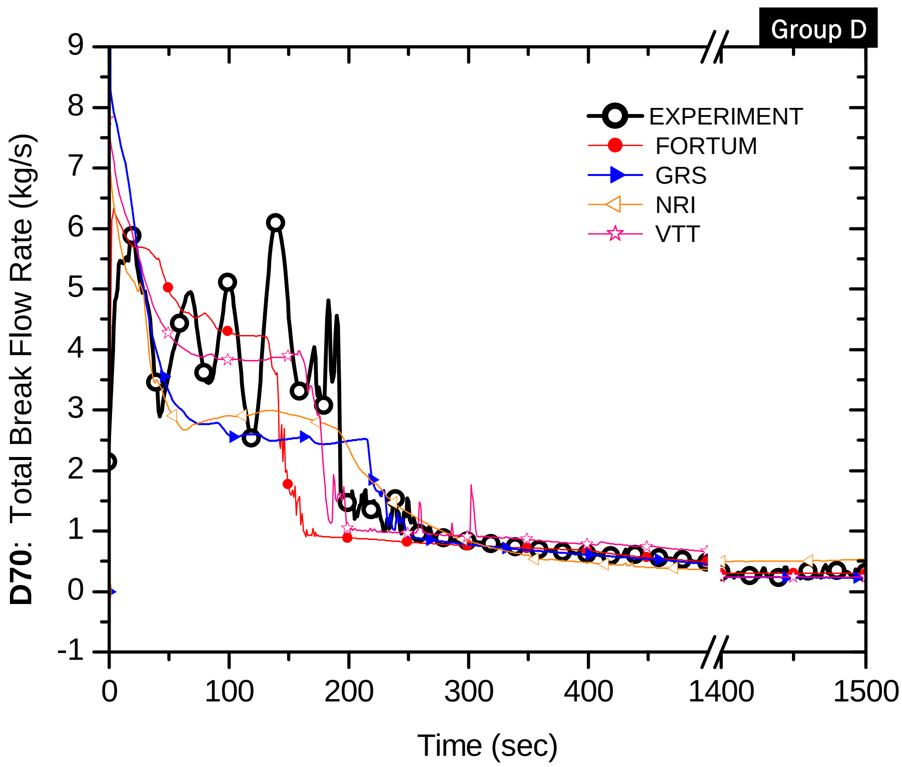

Figure B.70-D Total break flow rate (D70)

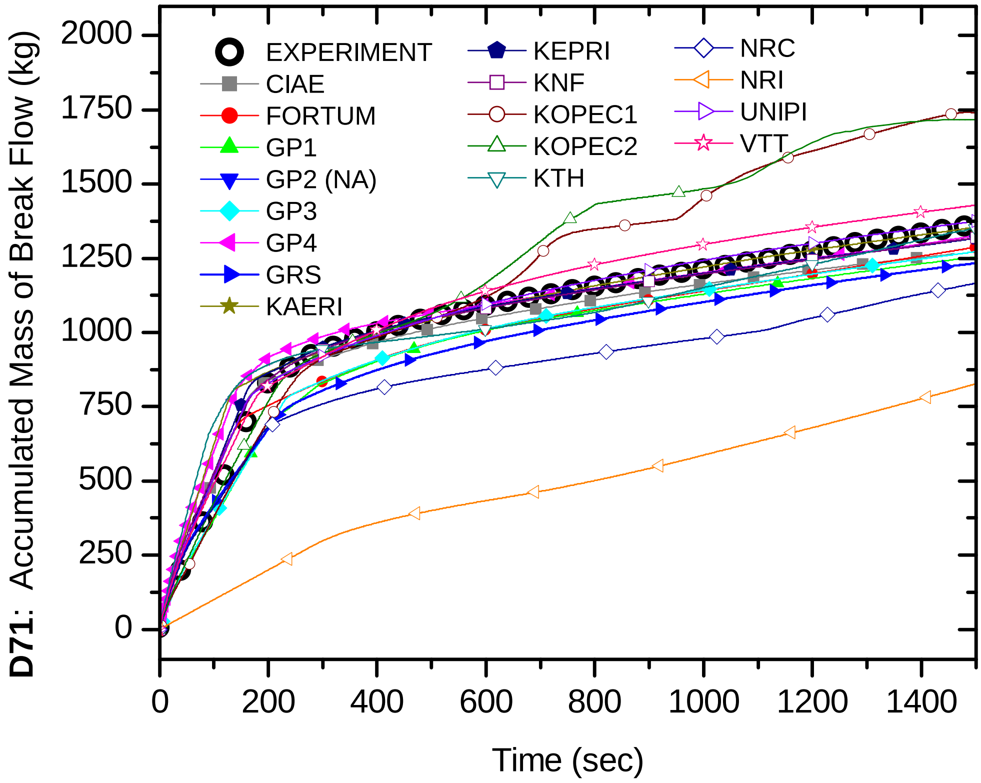

Figure B.71 Accumulated mass of the break flow (D71)

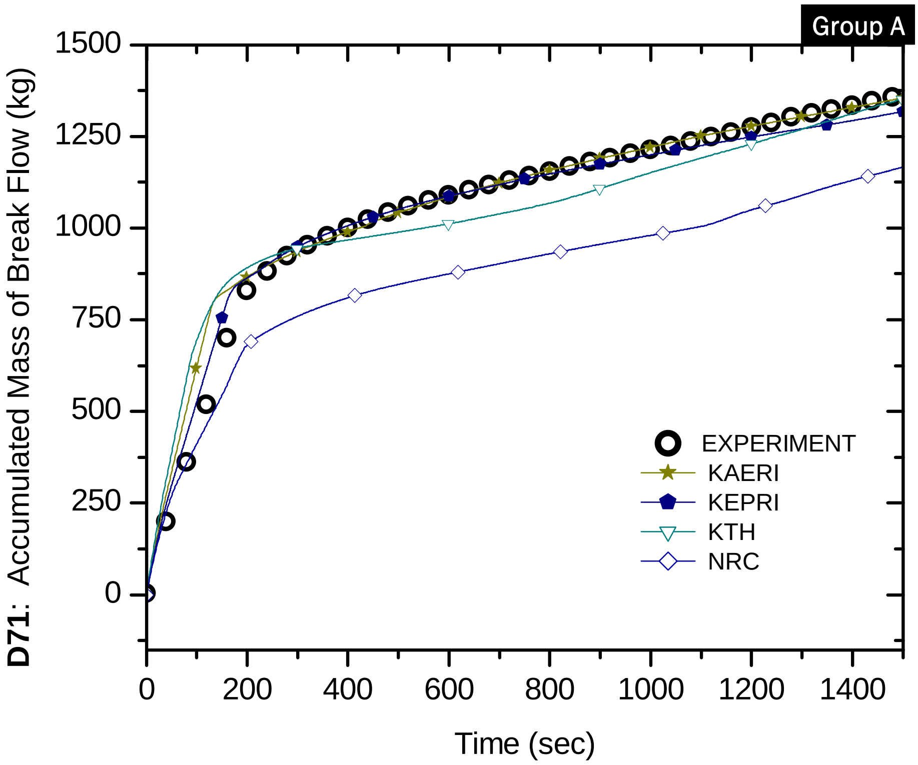

Figure B.71-A Accumulated mass of the break flow (D71)

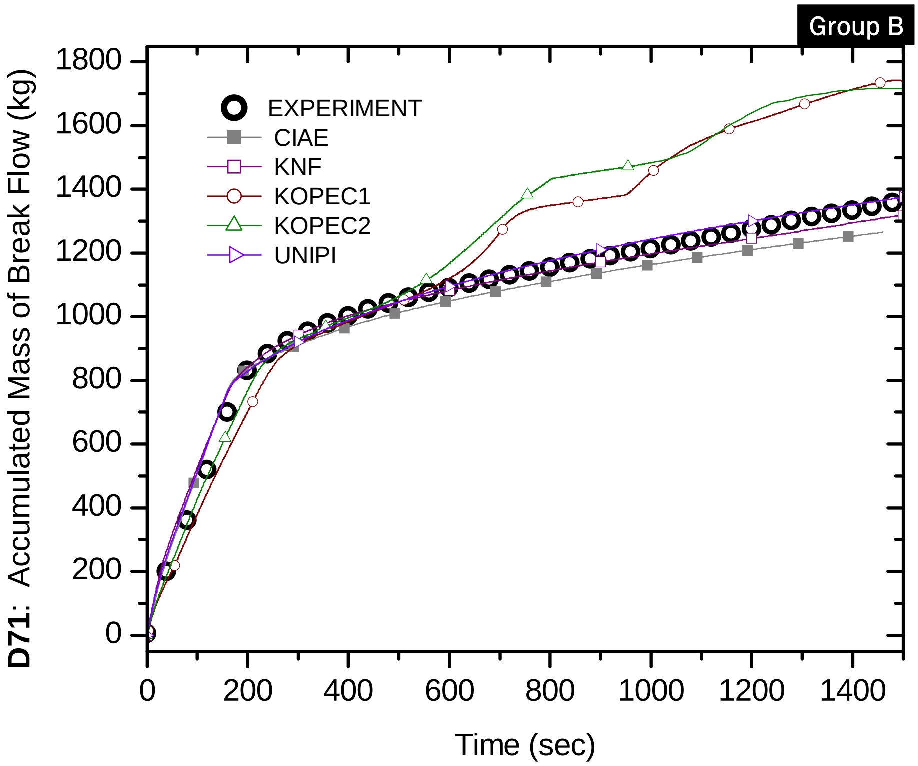

Figure B.71-B Accumulated mass of the break flow (D71)

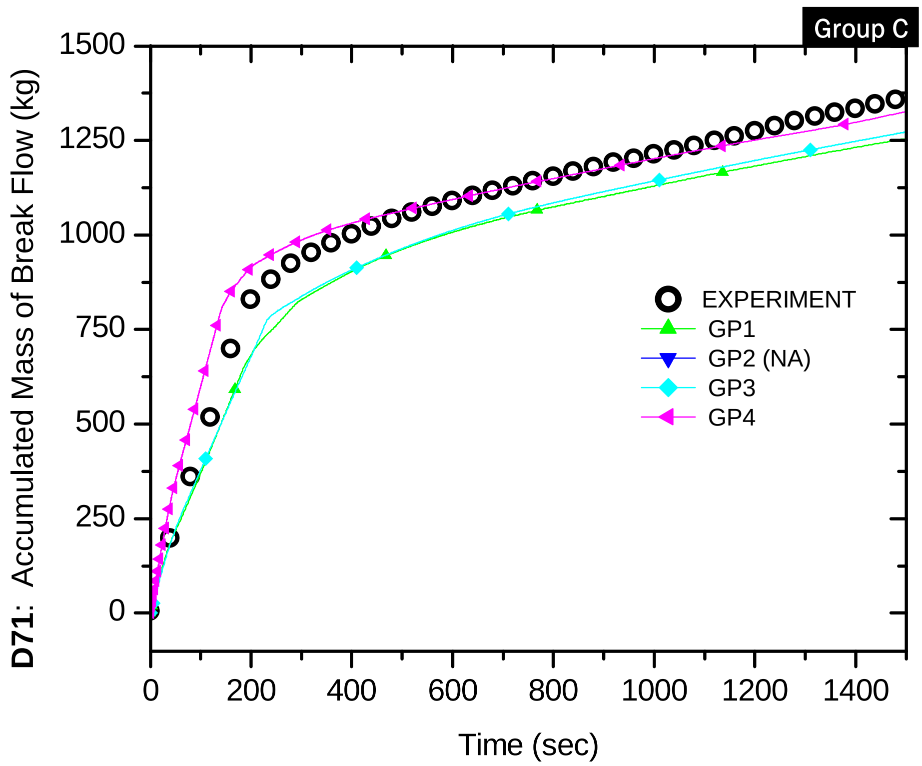

Figure B.71-C Accumulated mass of the break flow (D71)

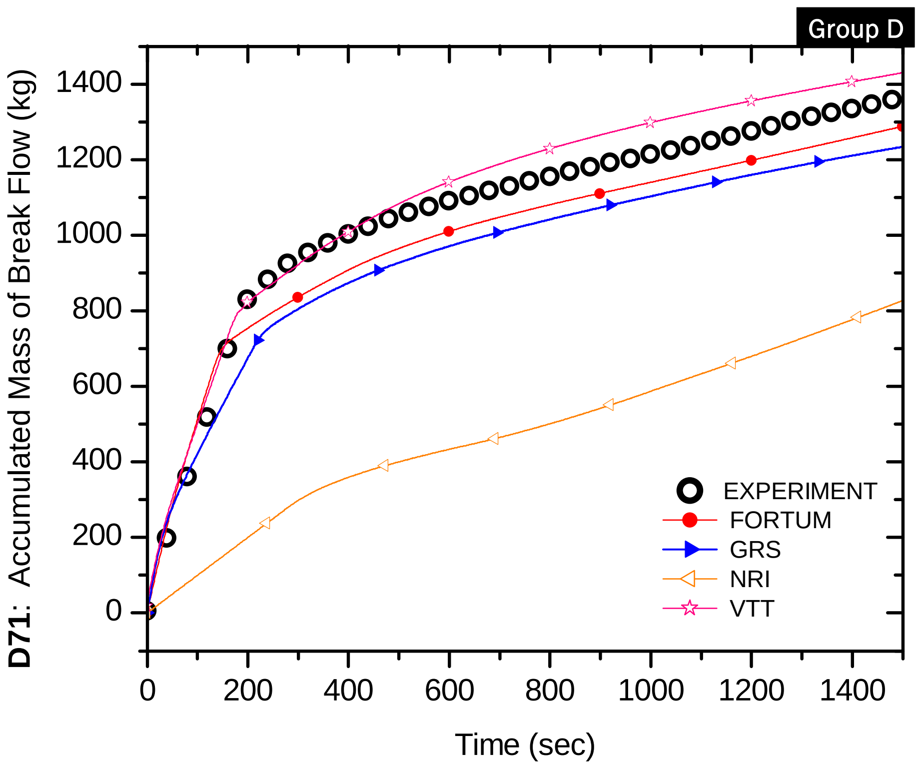

Figure B.71-D Accumulated mass of the break flow (D71)

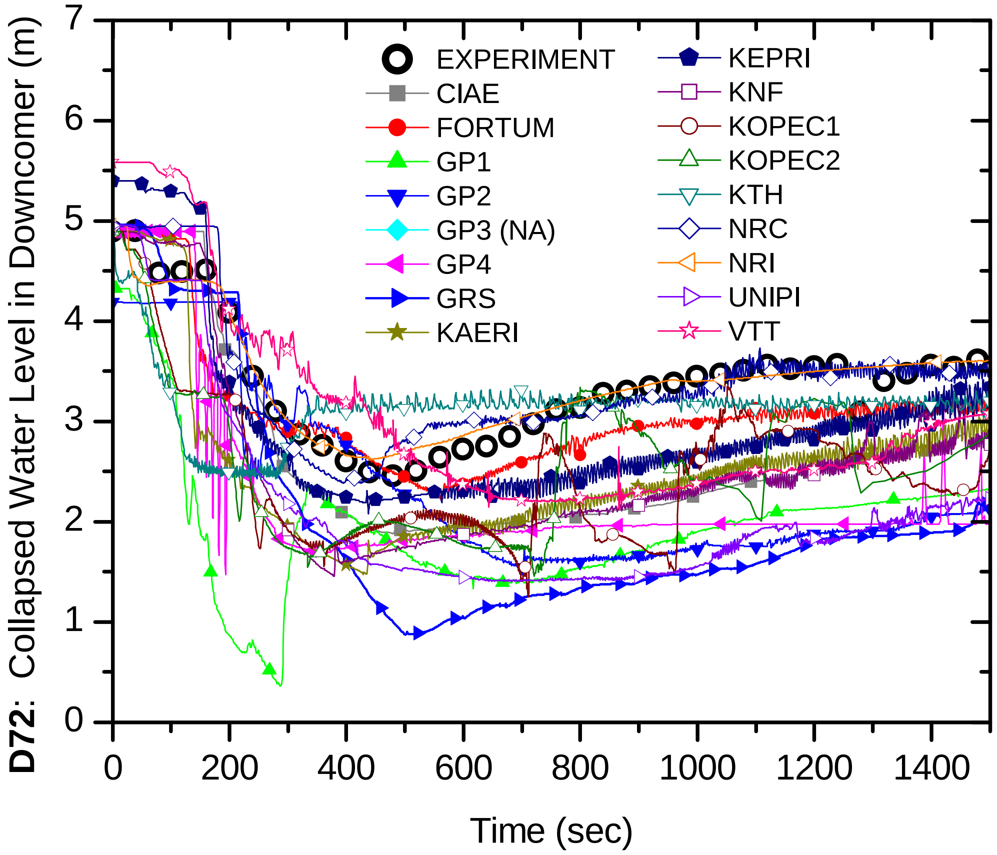

Figure B.72 Collapsed water level in the down-comer (D72)

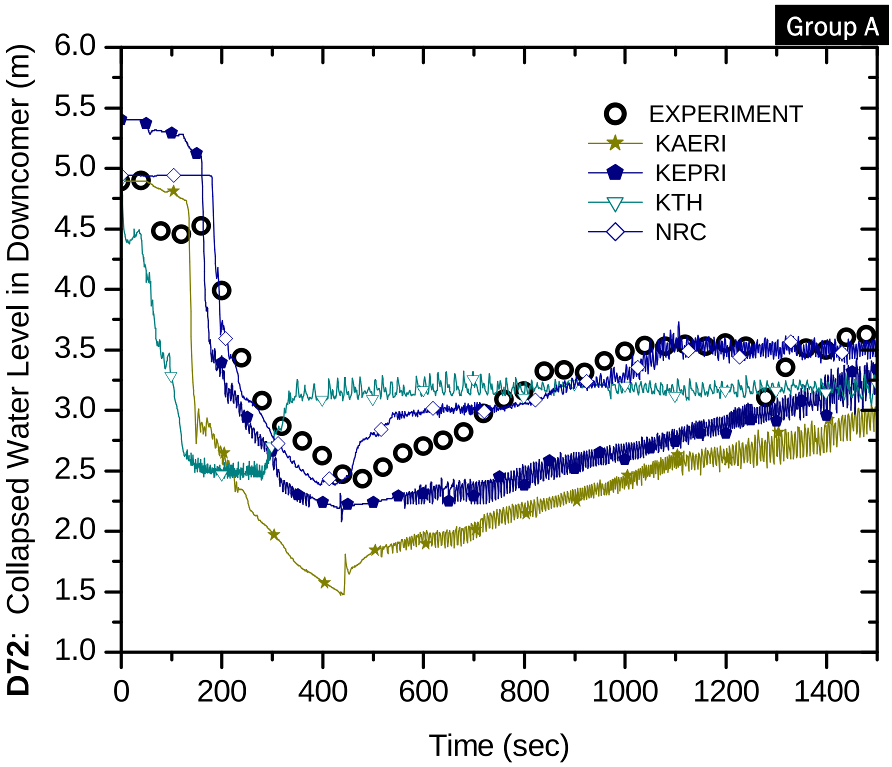

Figure B.72-A Collapsed water level in the down-comer (D72)

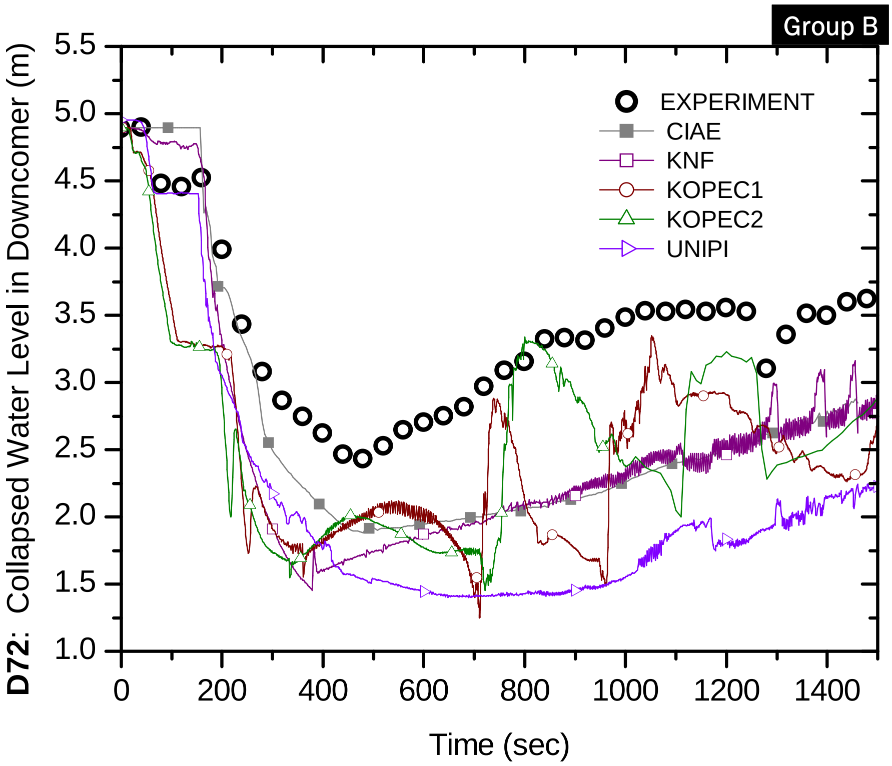

Figure B.72-B Collapsed water level in the down-comer (D72)

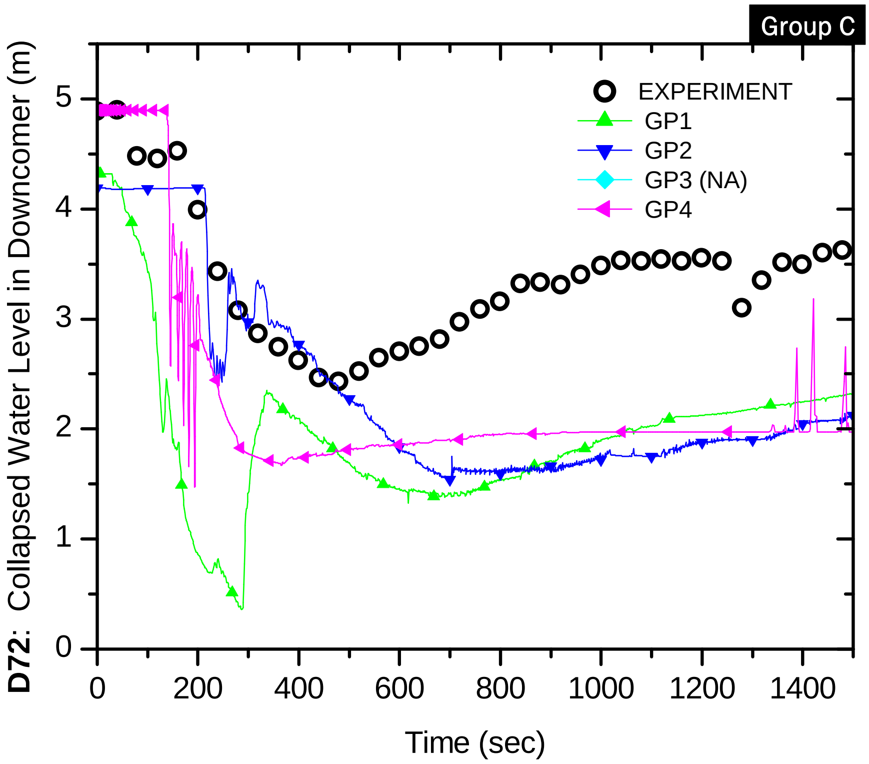

Figure B.72-C Collapsed water level in the down-comer (D72)

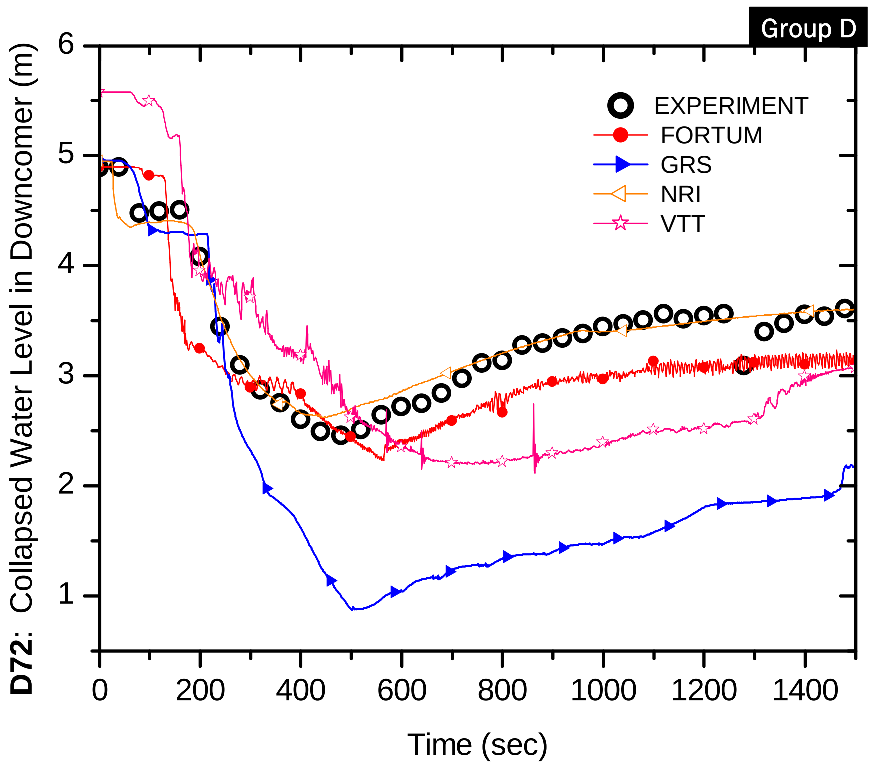

Figure B.72-D Collapsed water level in the down-comer (D72)

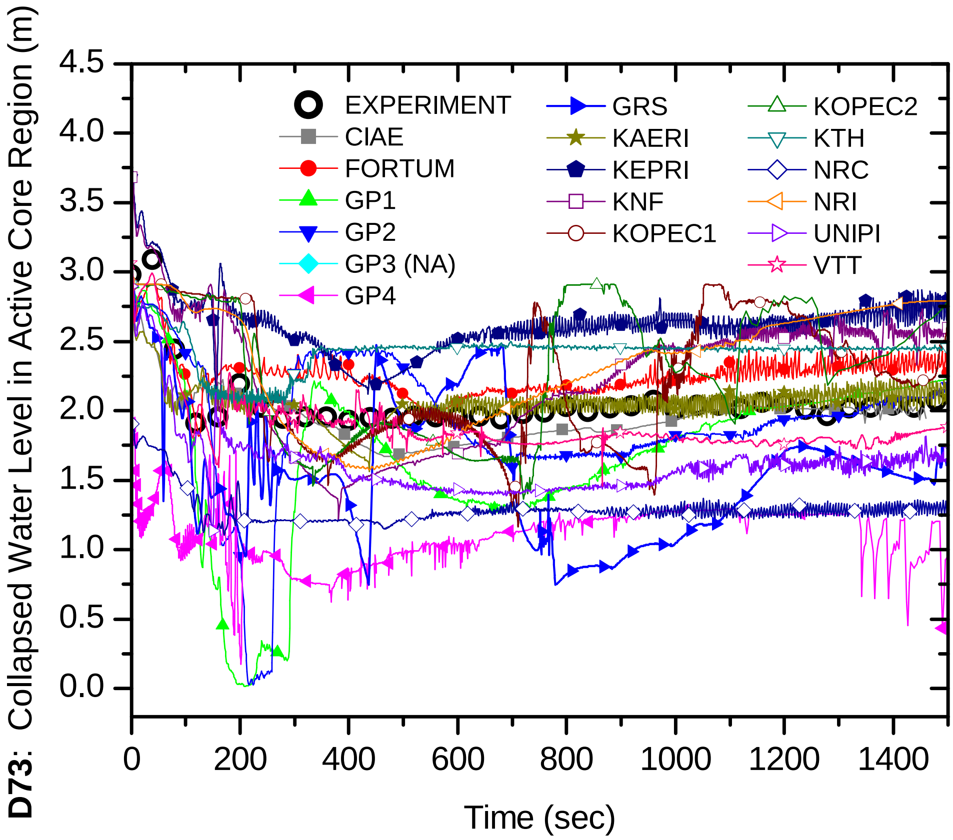

Figure B.73 Collapsed water level in the active core region (D73)

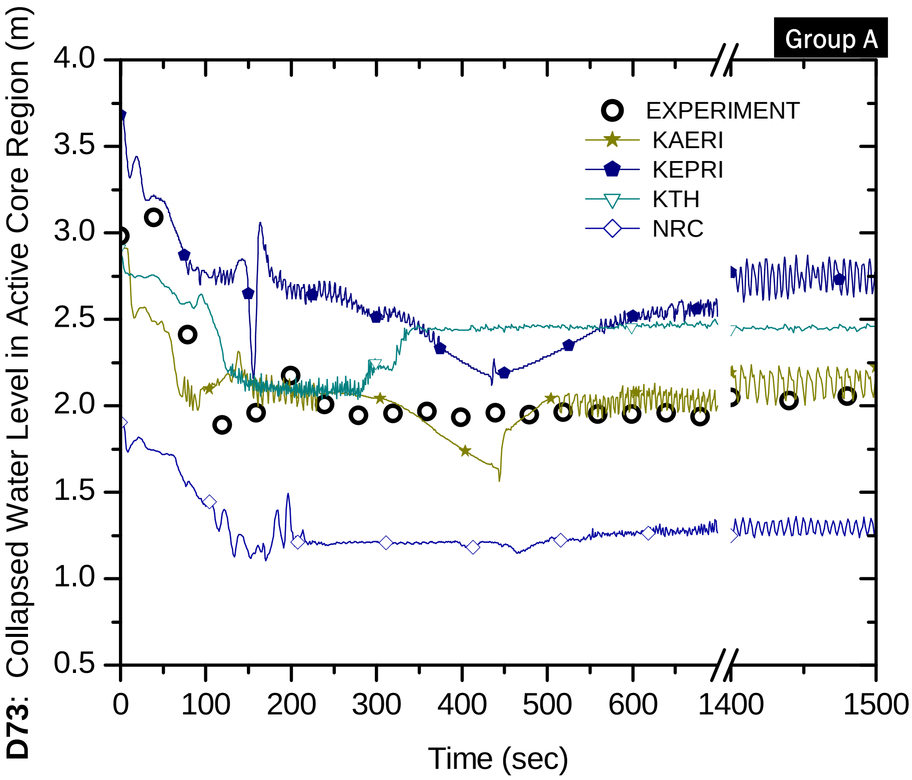

Figure B.73-A Collapsed water level in the active core region (D73)

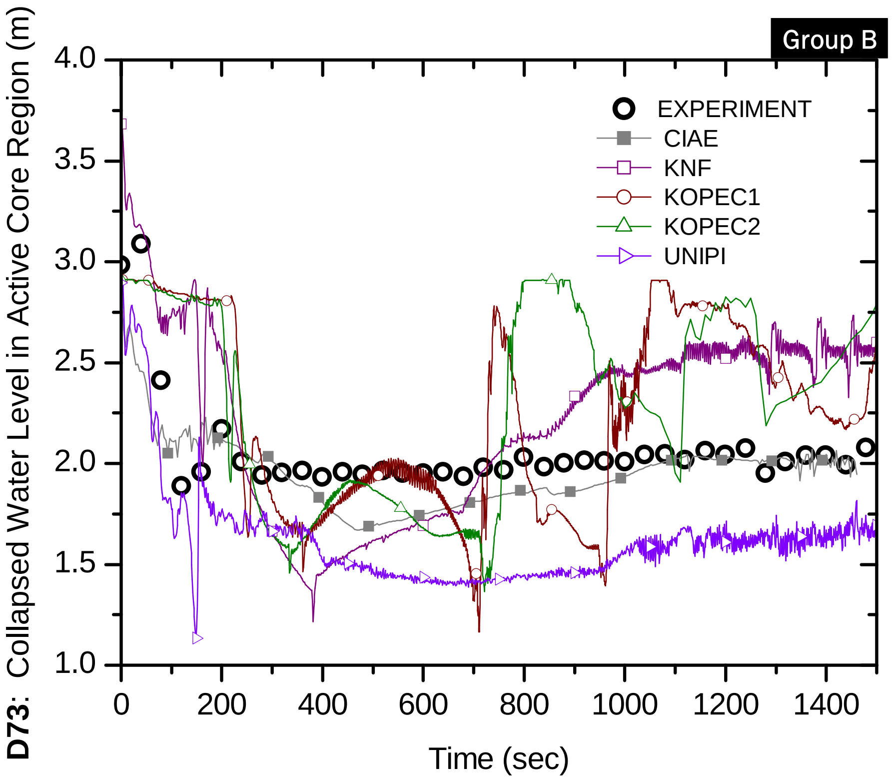

Figure B.73-B Collapsed water level in the active core region (D73)

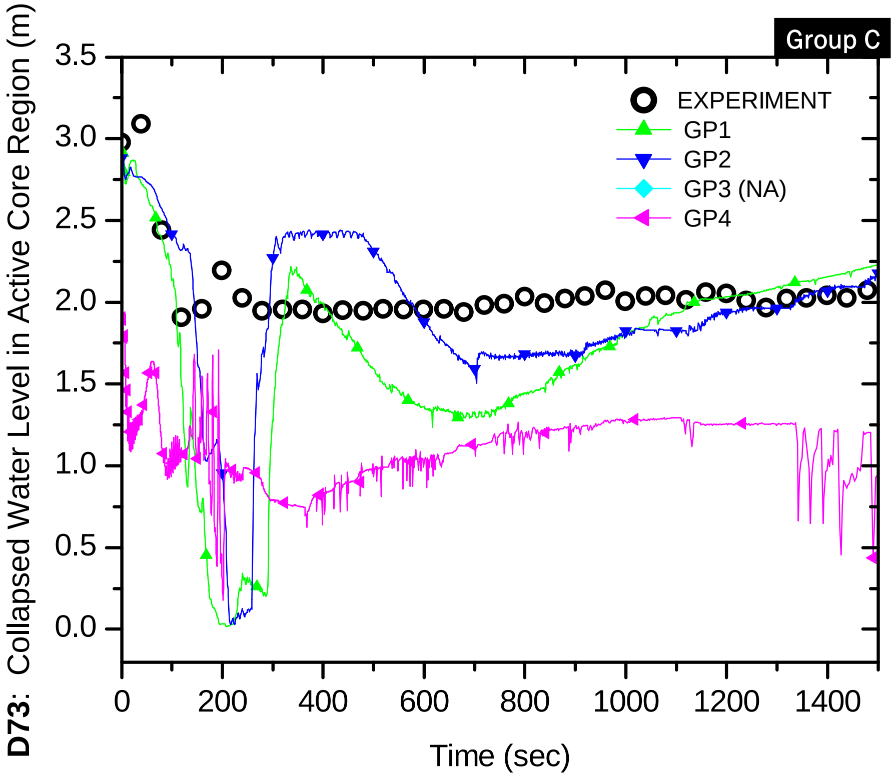

Figure B.73-C Collapsed water level in the active core region (D73)

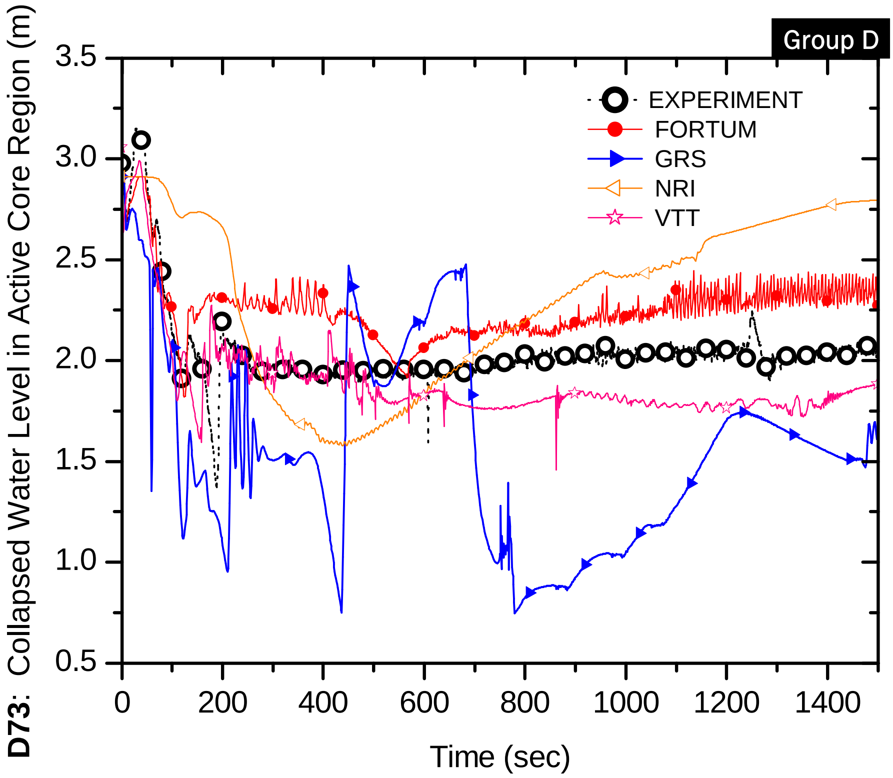

Figure B.73-D Collapsed water level in the active core region (D73)

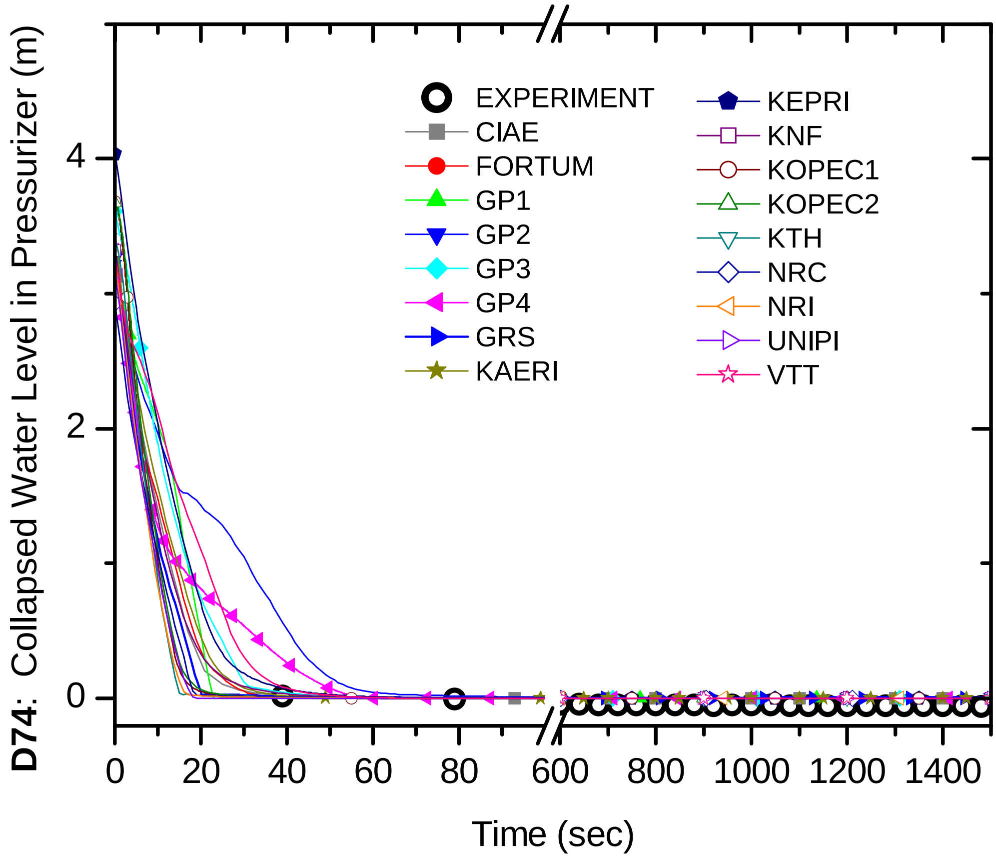

Figure B.74 Collapsed water level in the pressurizer (D74)

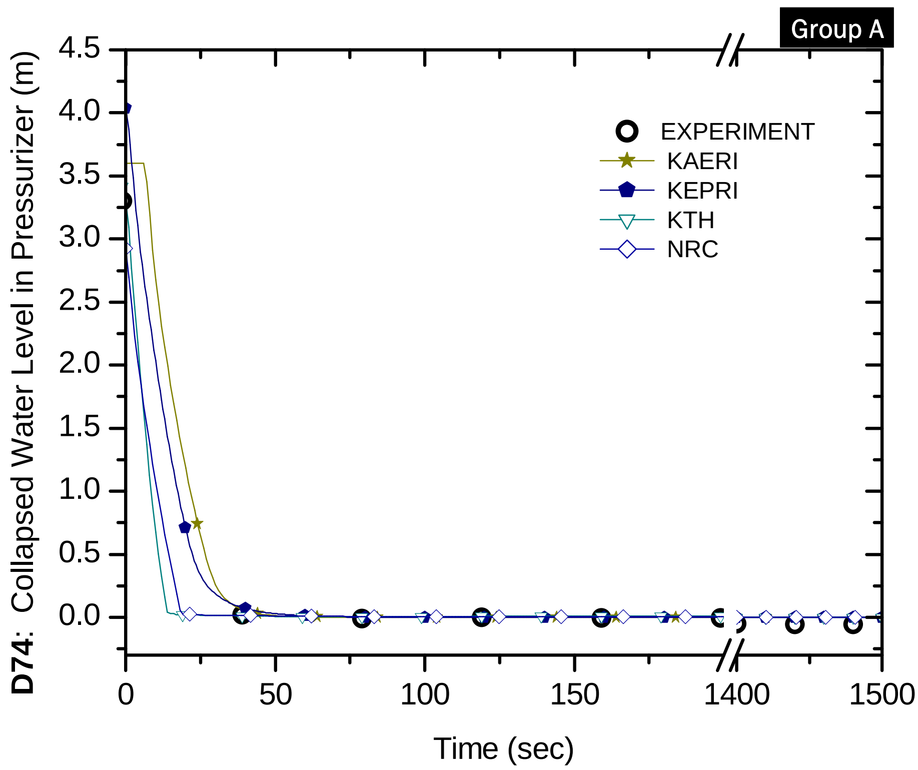

Figure B.74-A Collapsed water level in the pressurizer (D74)

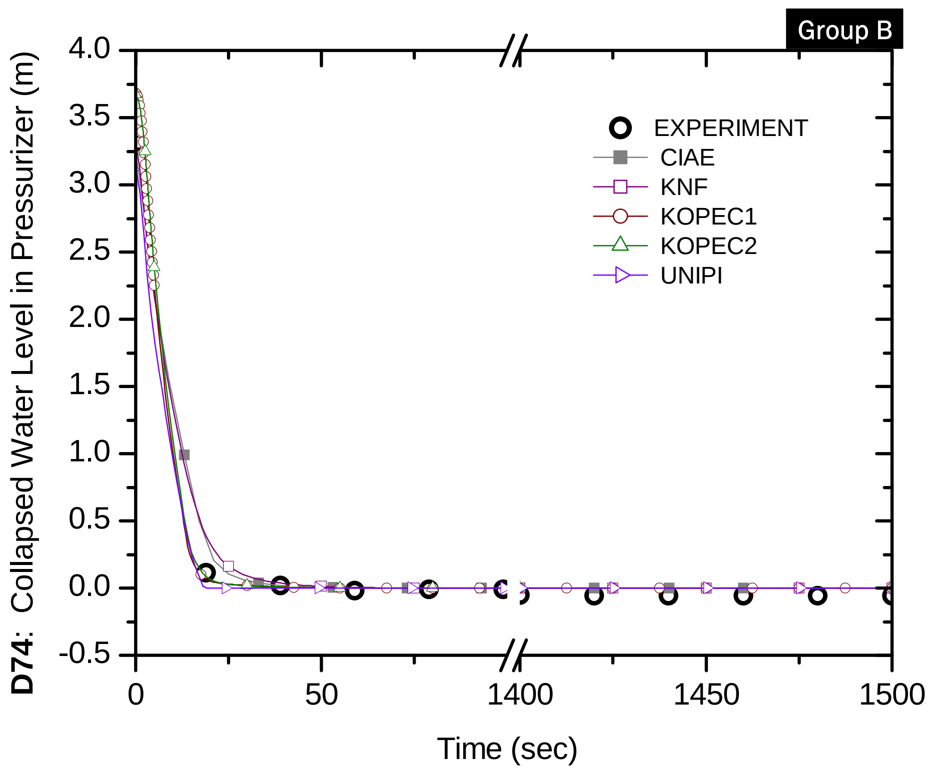

Figure B.74-B Collapsed water level in the pressurizer (D74)

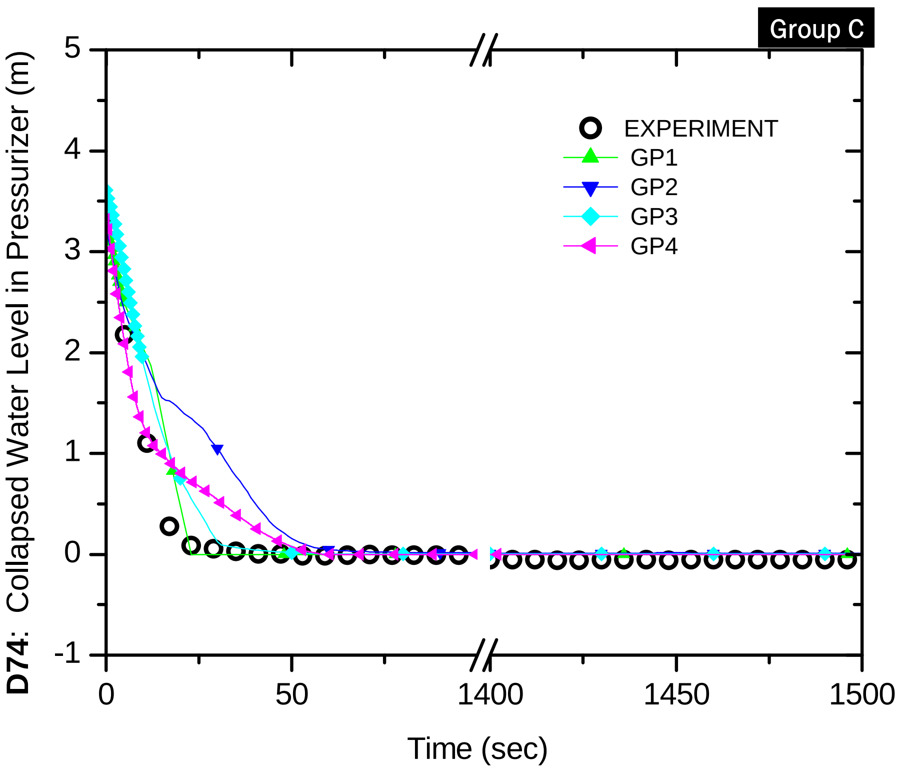

Figure B.74-C Collapsed water level in the pressurizer (D74)

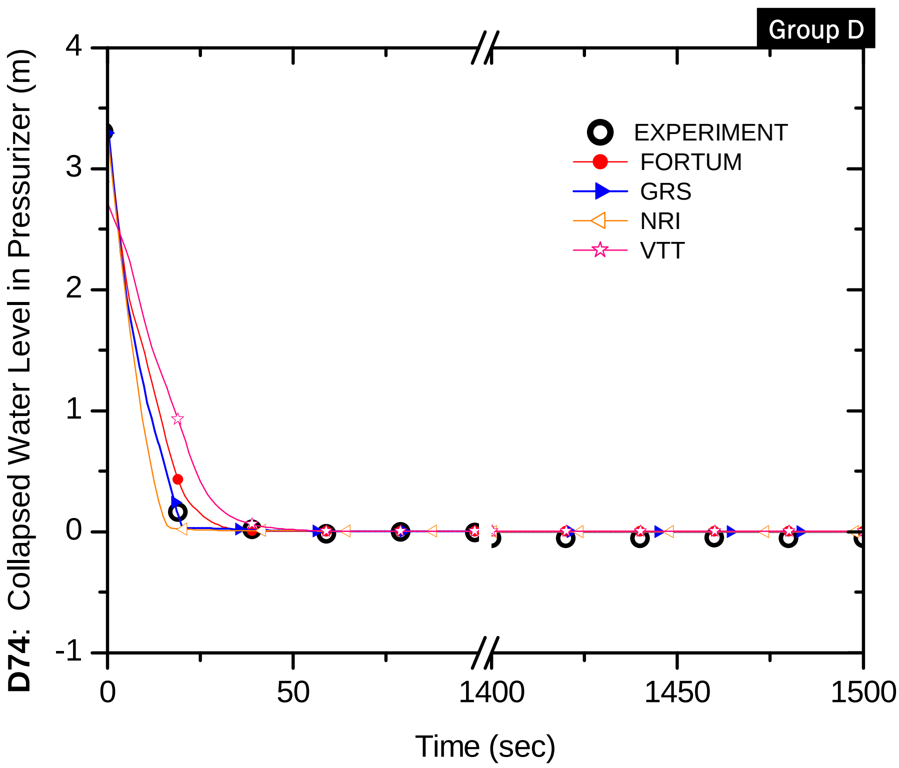

Figure B.74-D Collapsed water level in the pressurizer (D74)

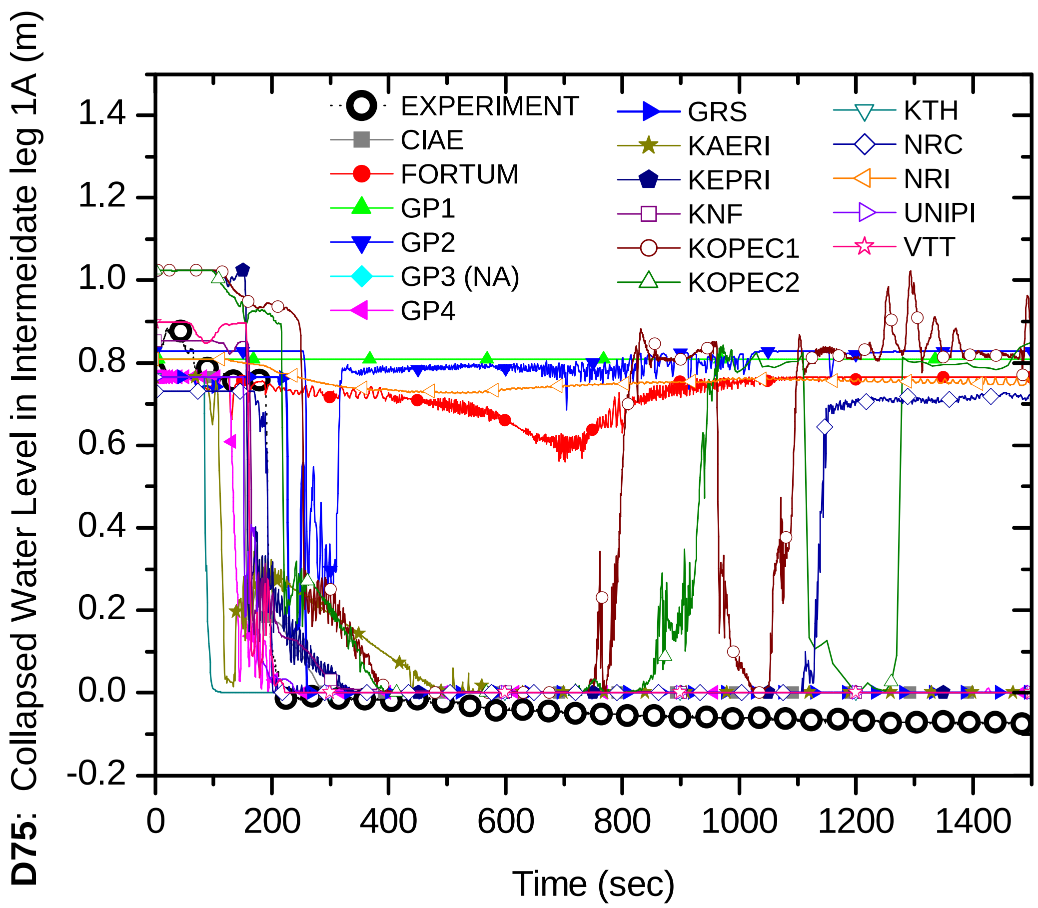

Figure B.75 Collapsed water level in the intermediate leg 1A (D75)

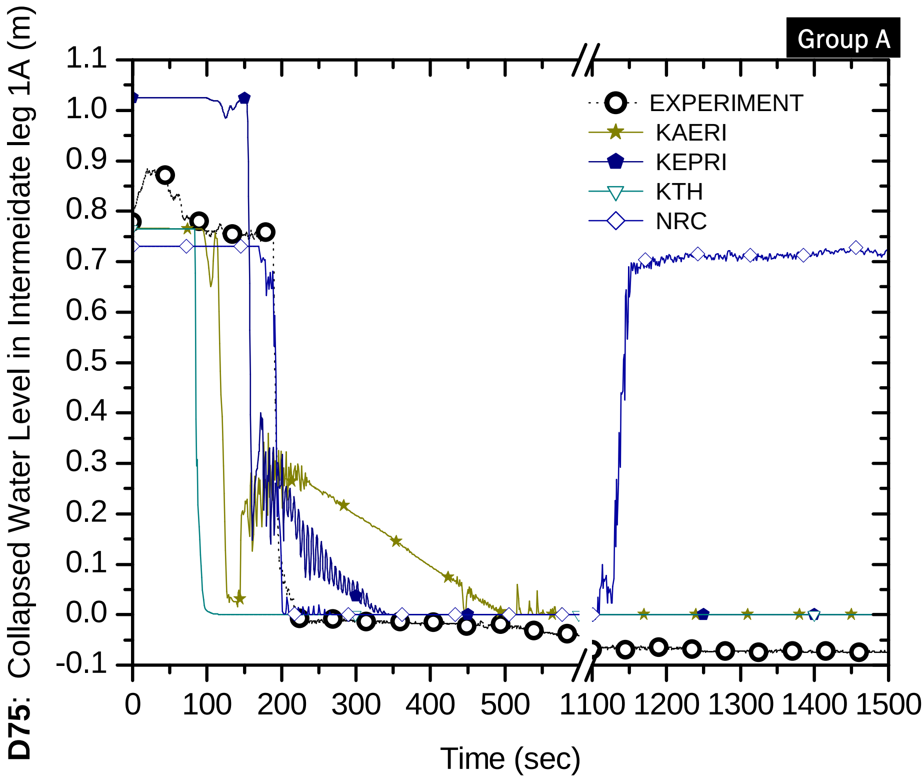

Figure B.75-A Collapsed water level in the intermediate leg 1A (D75)

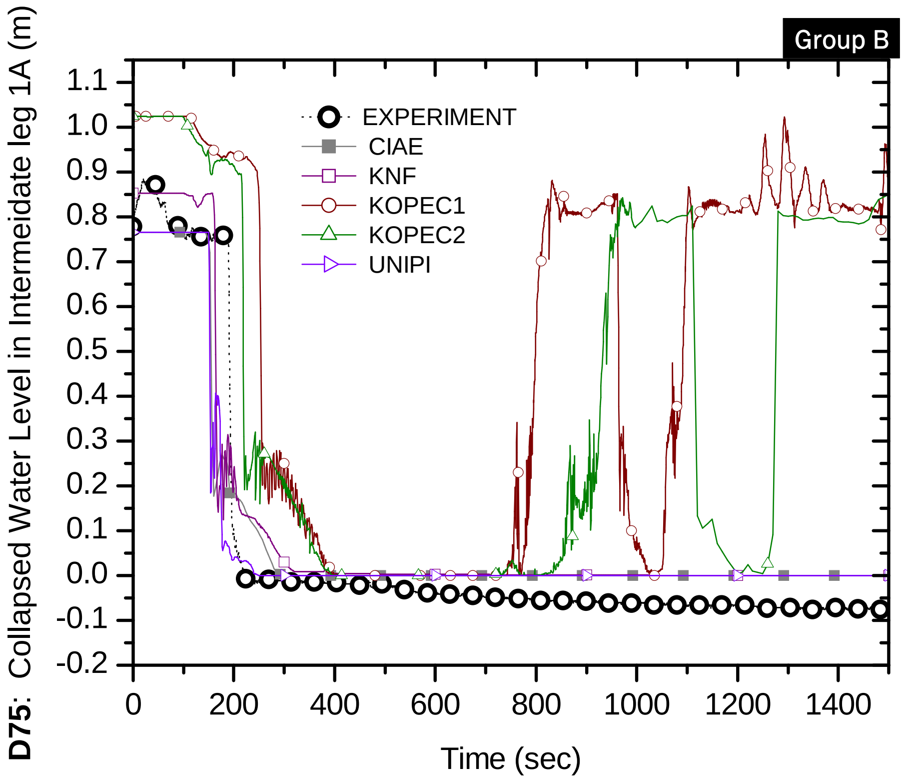

Figure B.75-B Collapsed water level in the intermediate leg 1A (D75)

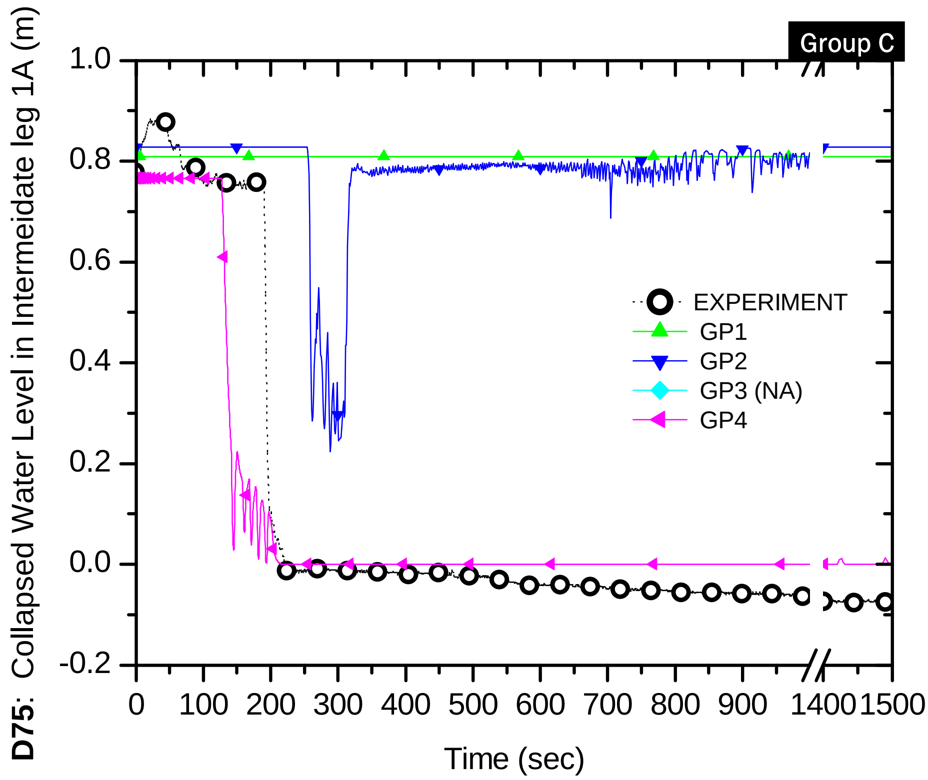

Figure B.75-C Collapsed water level in the intermediate leg 1A (D75)

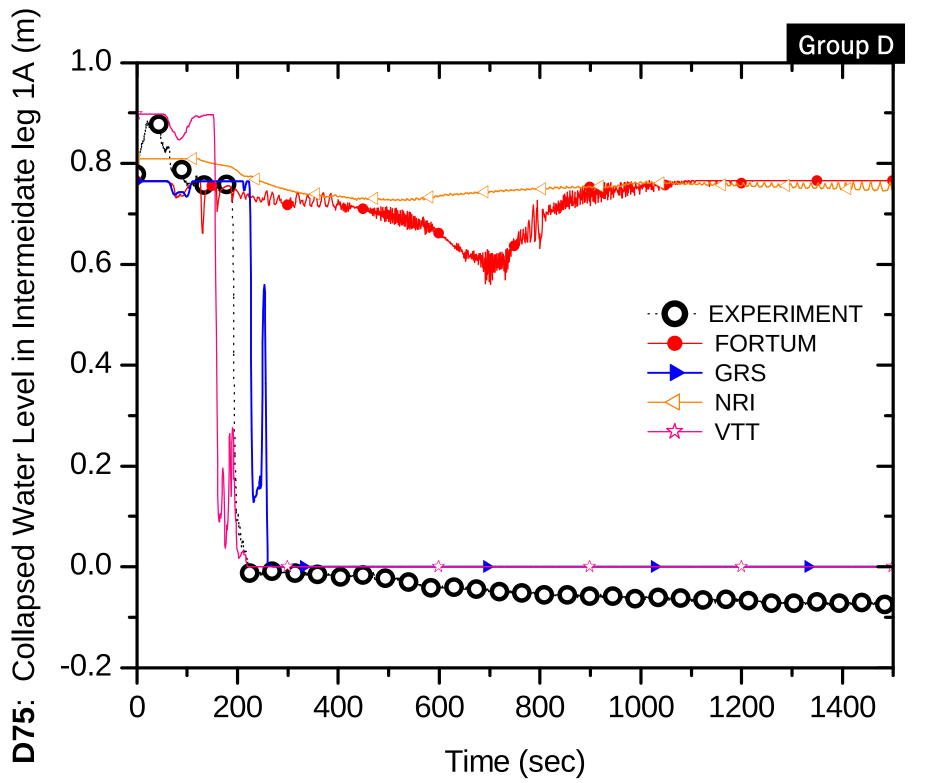

Figure B.75-D Collapsed water level in the intermediate leg 1A (D75)

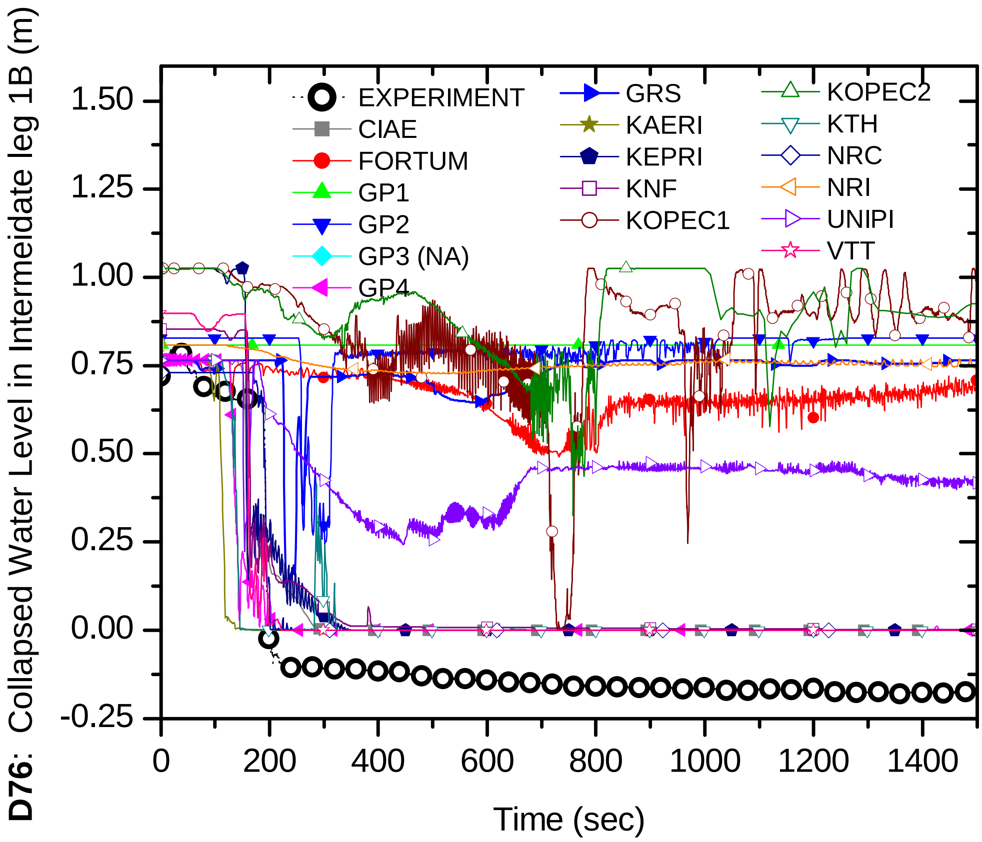

Figure B.76 Collapsed water level in the intermediate leg 1B (D76)

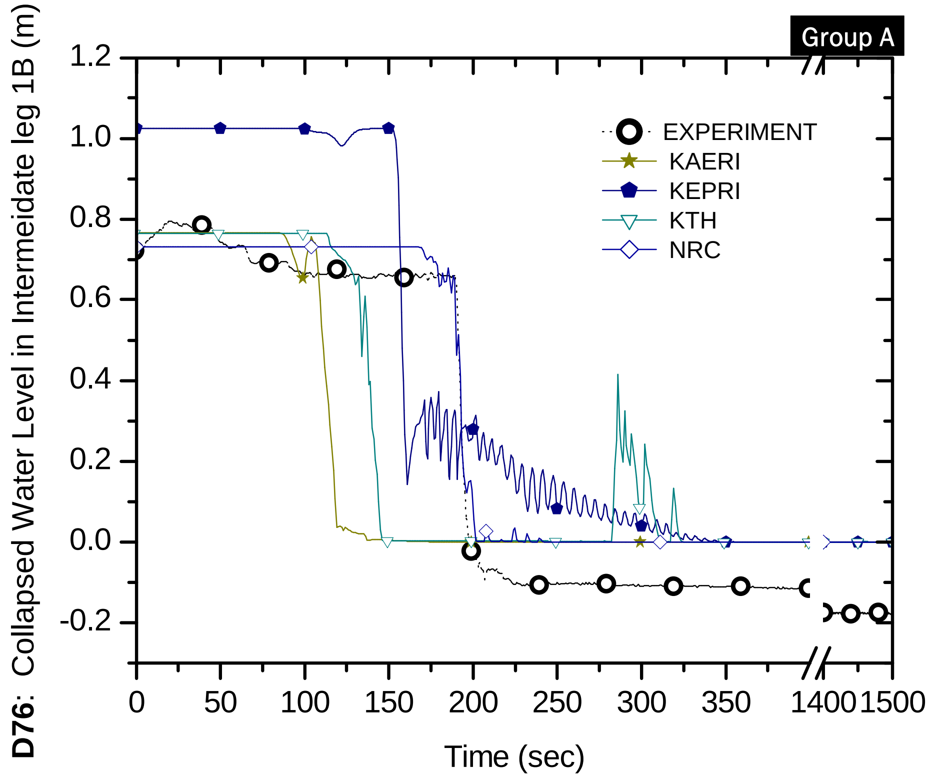

Figure B.76-A Collapsed water level in the intermediate leg 1B (D76)

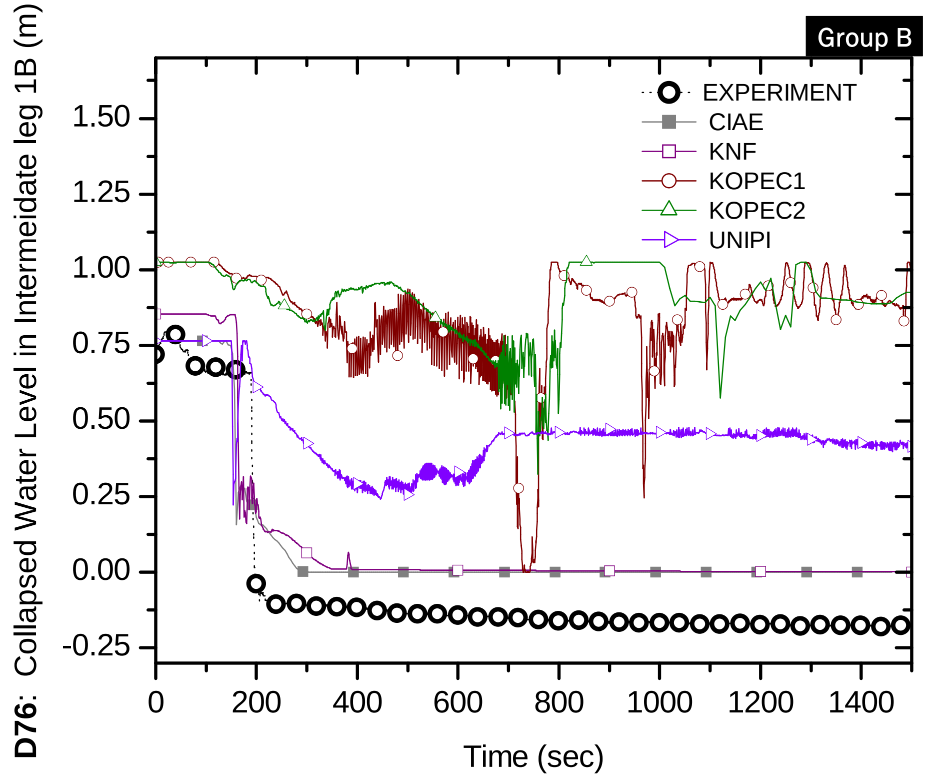

Figure B.76-B Collapsed water level in the intermediate leg 1B (D76)

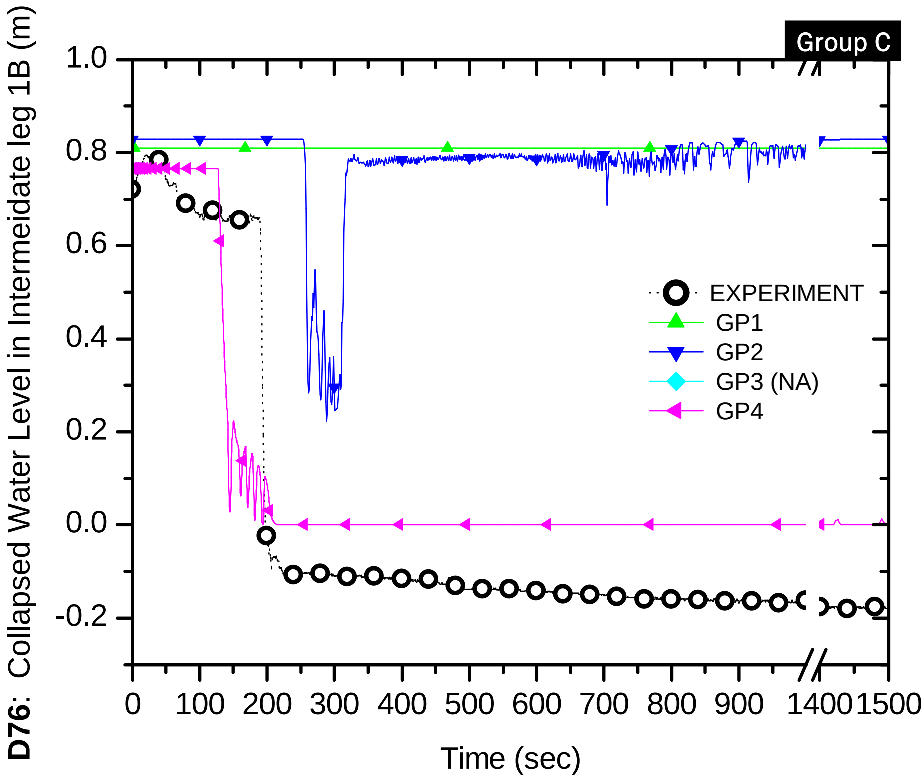

Figure B.76-C Collapsed water level in the intermediate leg 1B (D76)

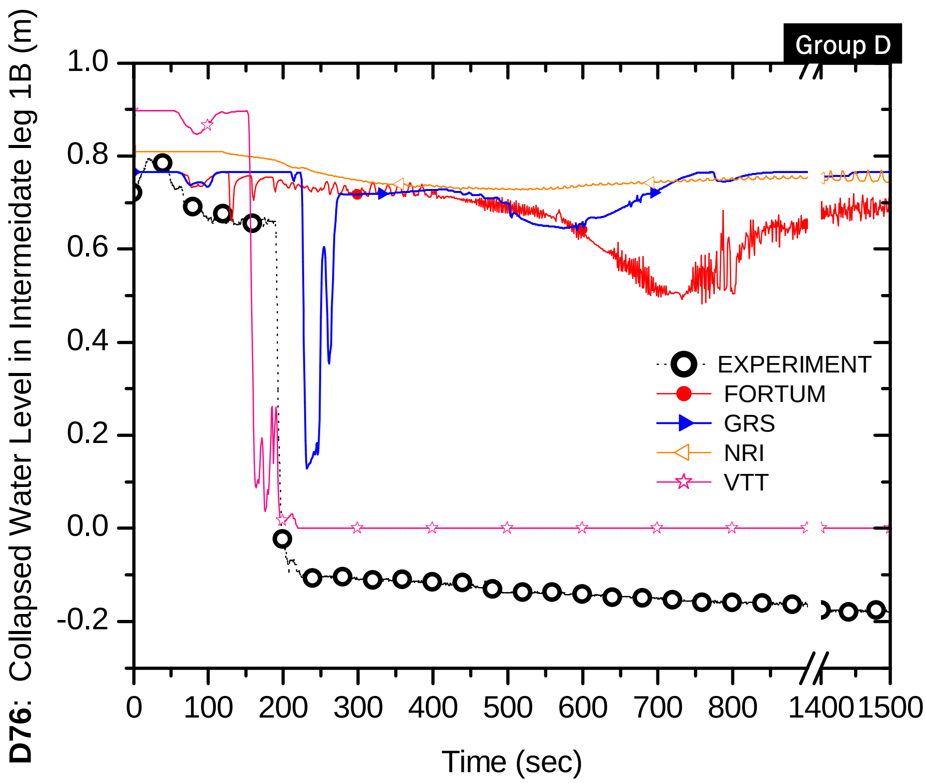

Figure B.76-D Collapsed water level in the intermediate leg 1B (D76)

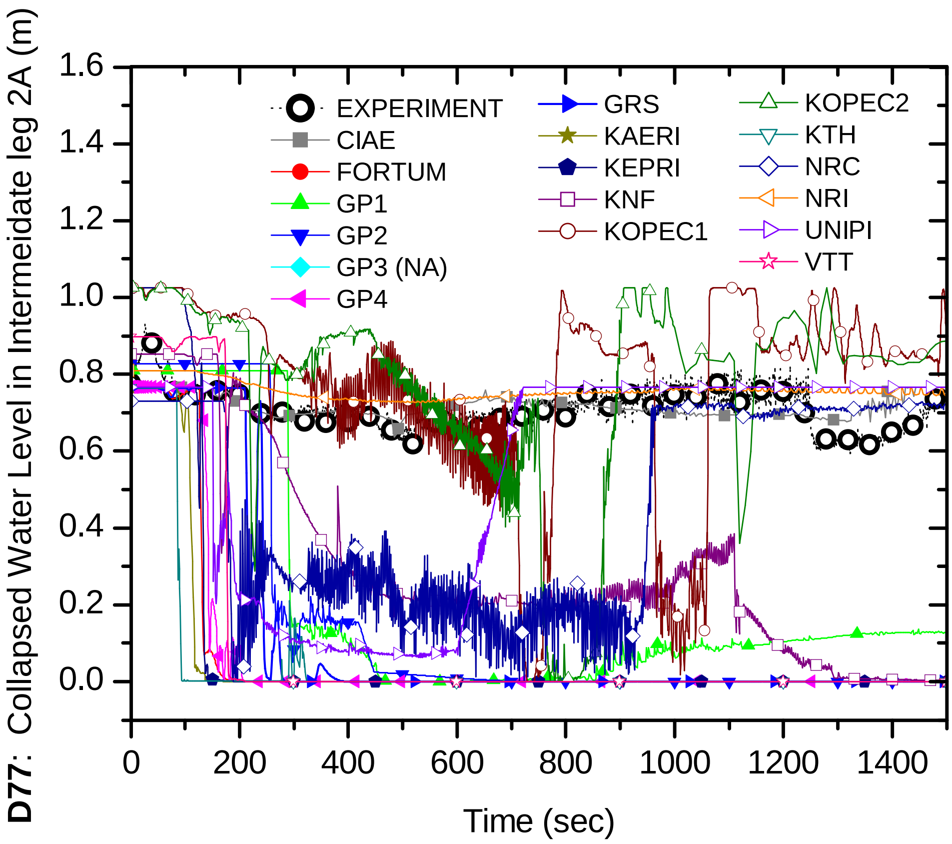

Figure B.77 Collapsed water level in the intermediate leg 2A (D77)

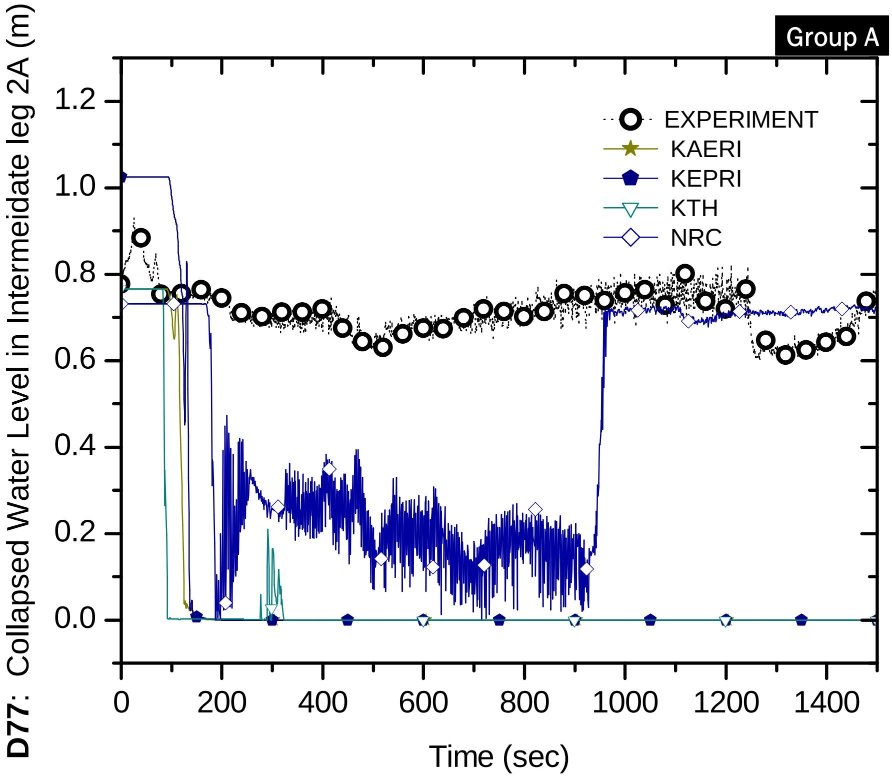

Figure B.77-A Collapsed water level in the intermediate leg 2A (D77)

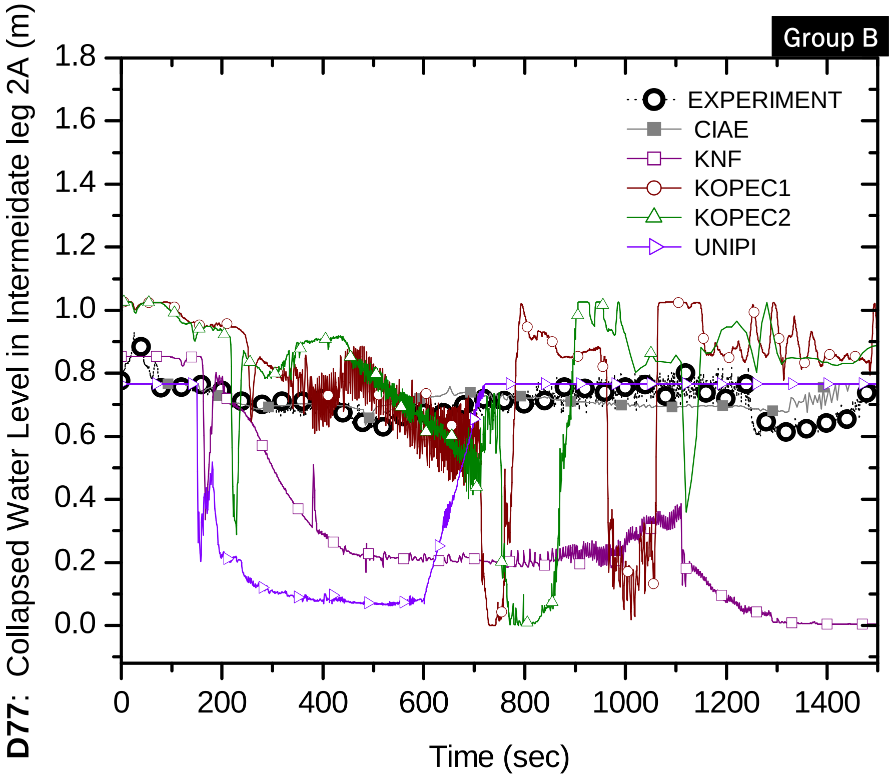

Figure B.77-B Collapsed water level in the intermediate leg 2A (D77)

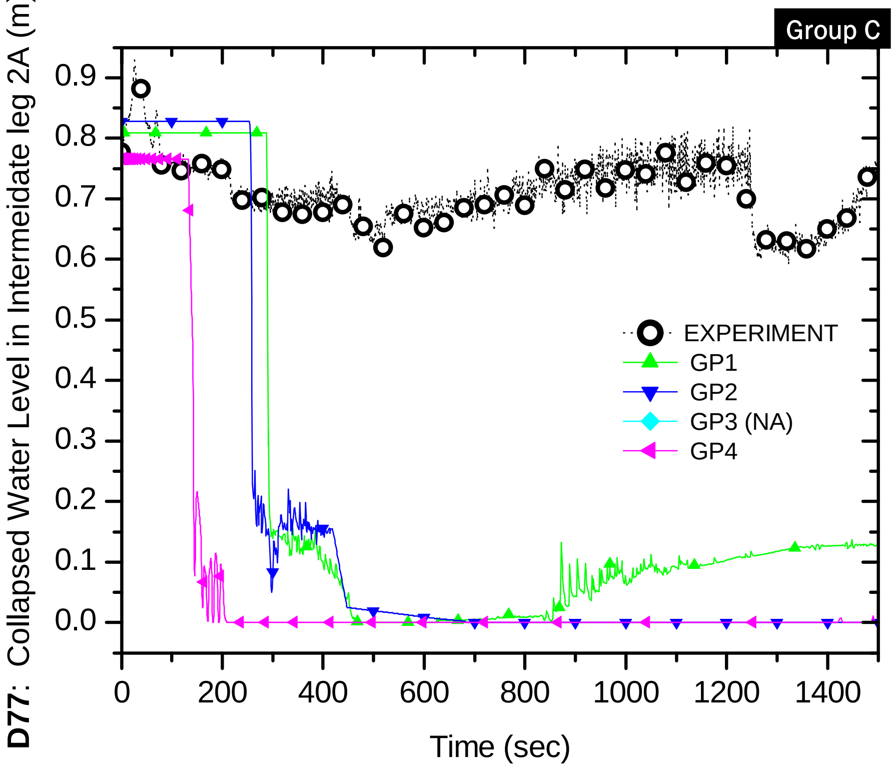

Figure B.77-C Collapsed water level in the intermediate leg 2A (D77)

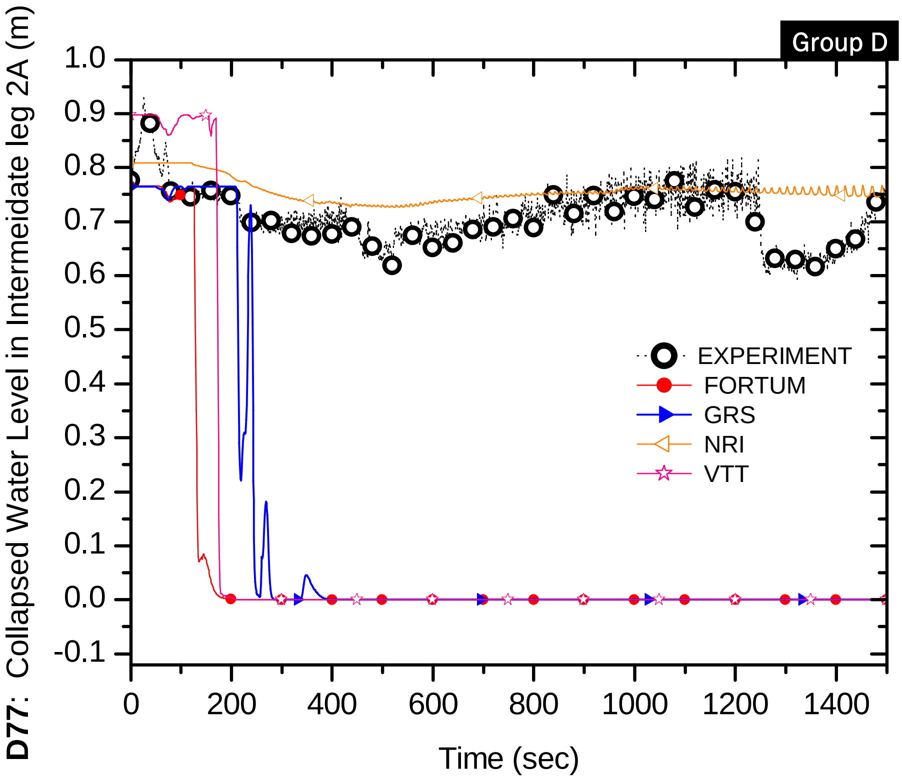

Figure B.77-D Collapsed water level in the intermediate leg 2A (D77)

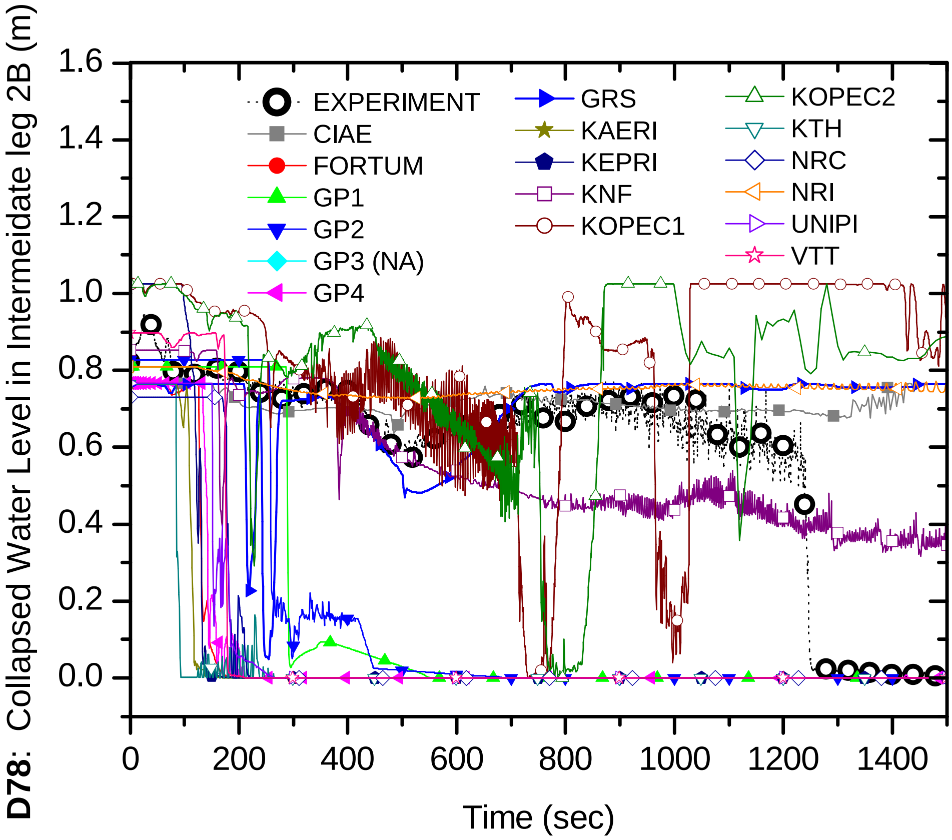

Figure B.78 Collapsed water level in the intermediate leg 2B (D78)

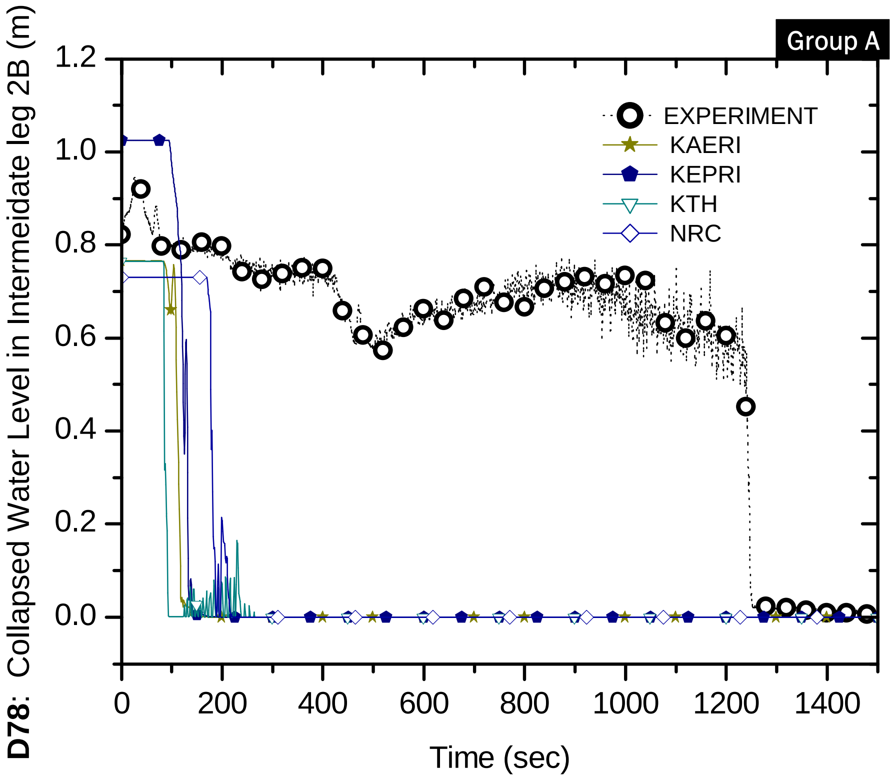

Figure B.78-A Collapsed water level in the intermediate leg 2B (D78)

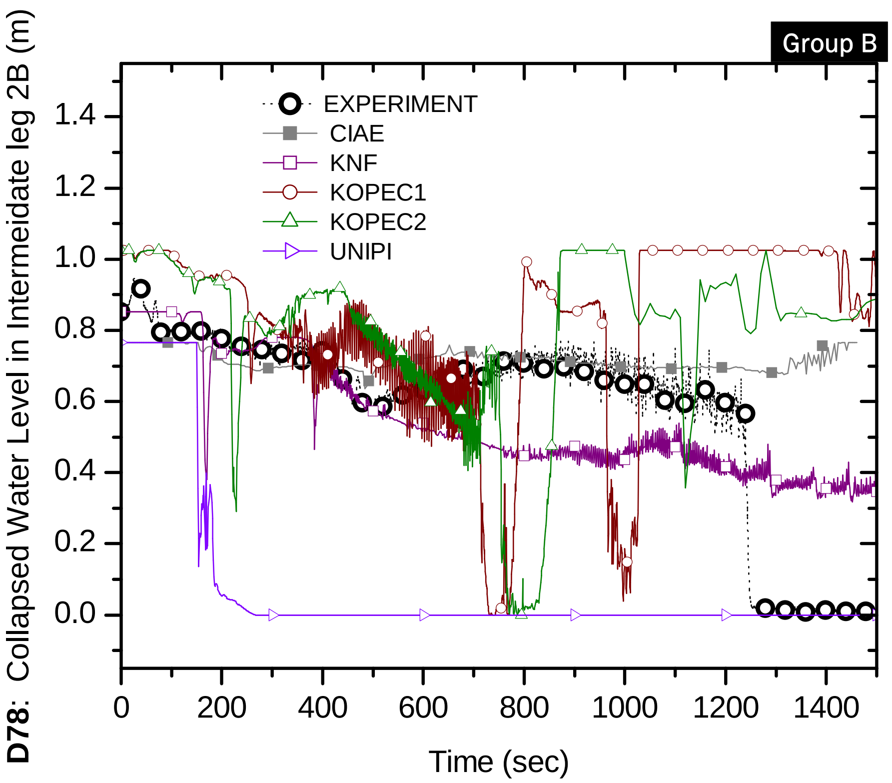

Figure B.78-B Collapsed water level in the intermediate leg 2B (D78)

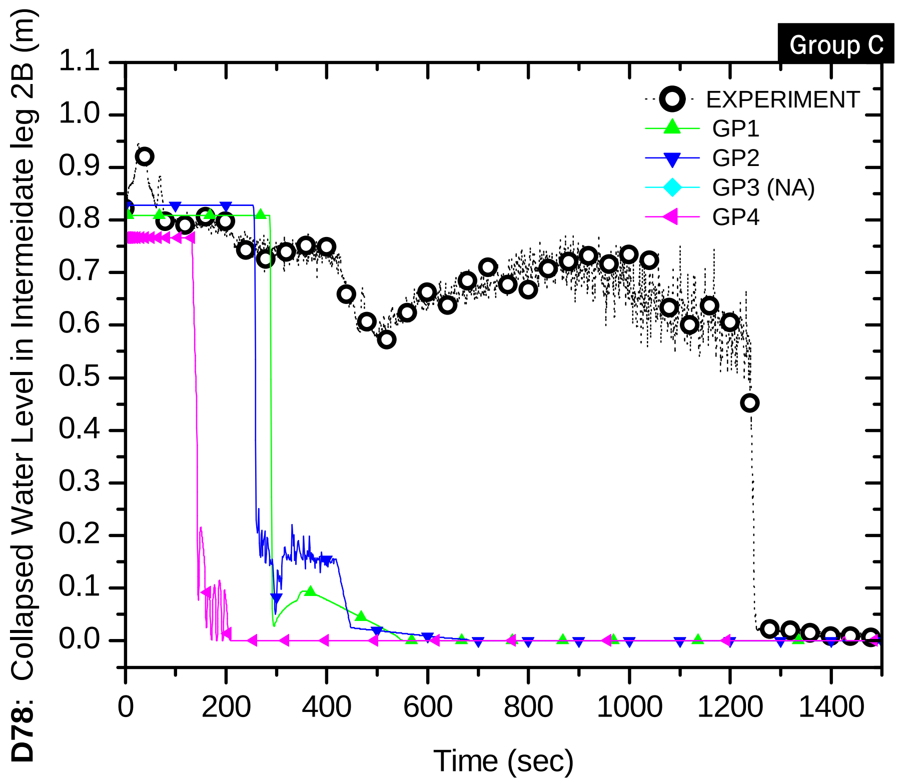

Figure B.78-C Collapsed water level in the intermediate leg 2B (D78)

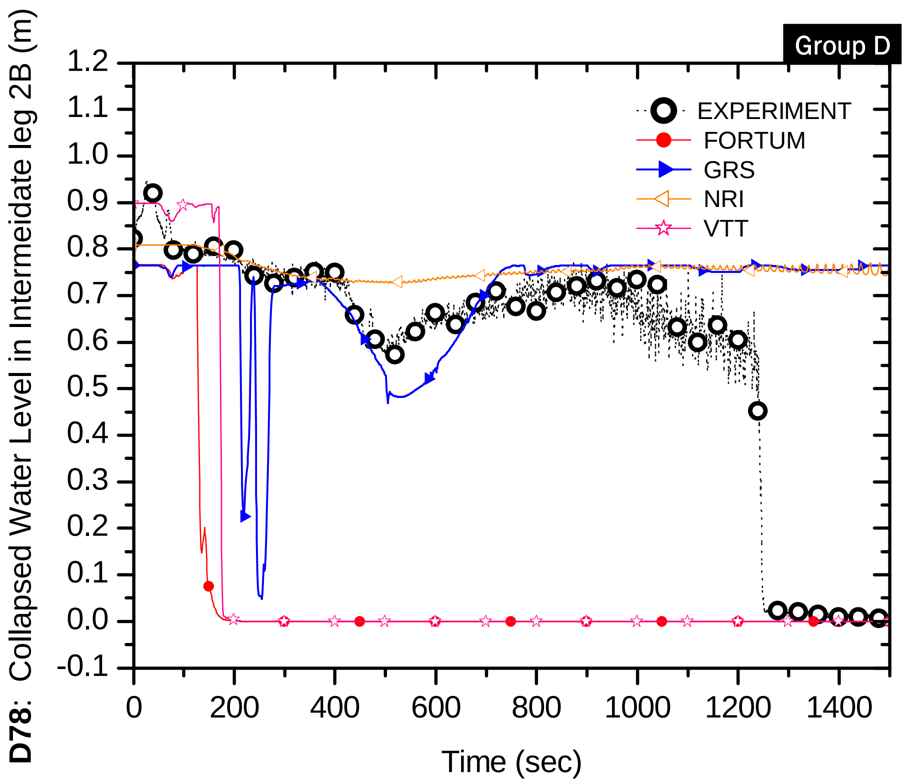

Figure B.78-D Collapsed water level in the intermediate leg 2B (D78)

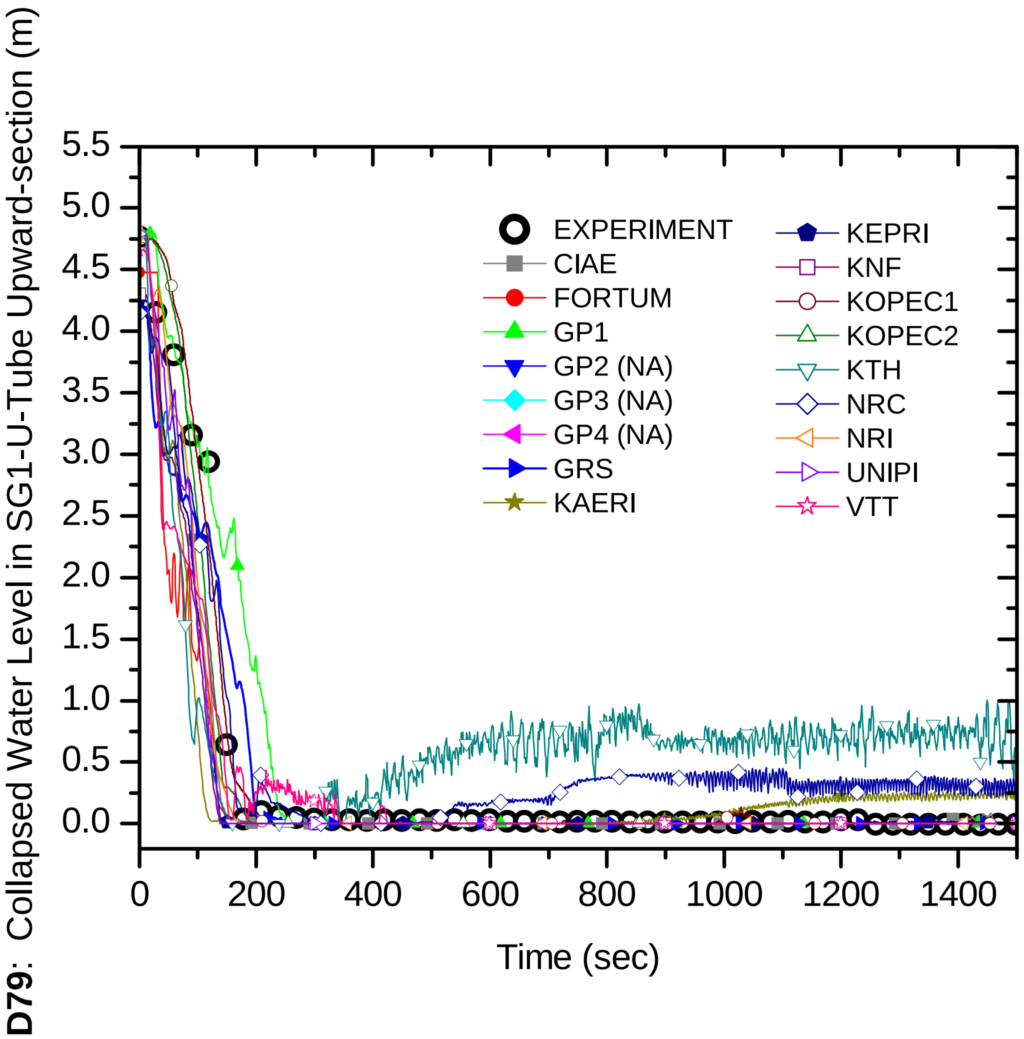

Figure B.79 Collapsed water level in SG-1 U-tube upward section (D79)

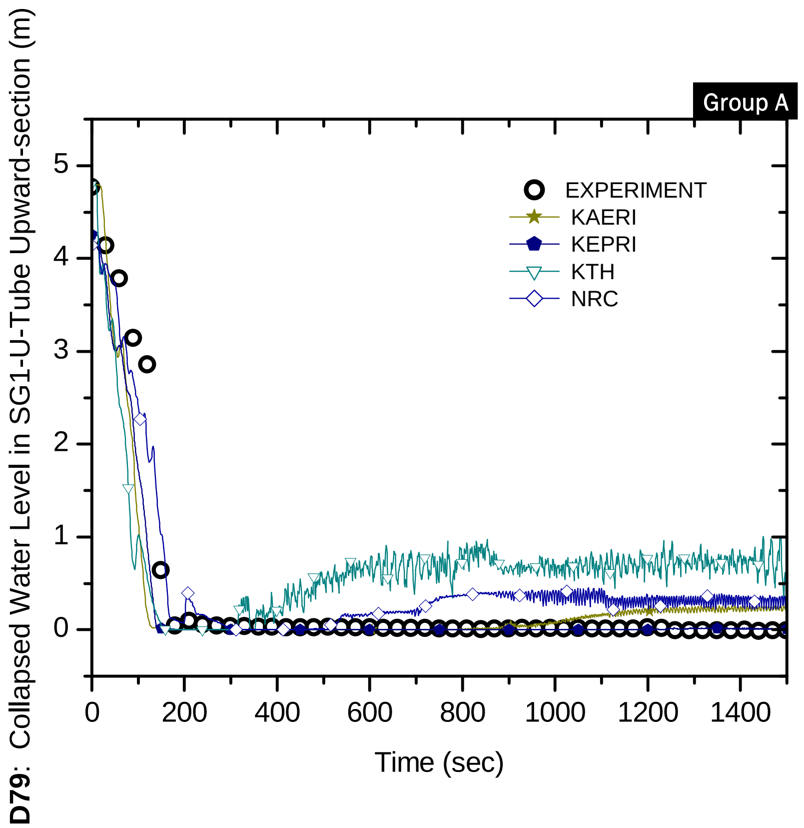

Figure B.79-A Collapsed water level in SG-1 U-tube upward section (D79)

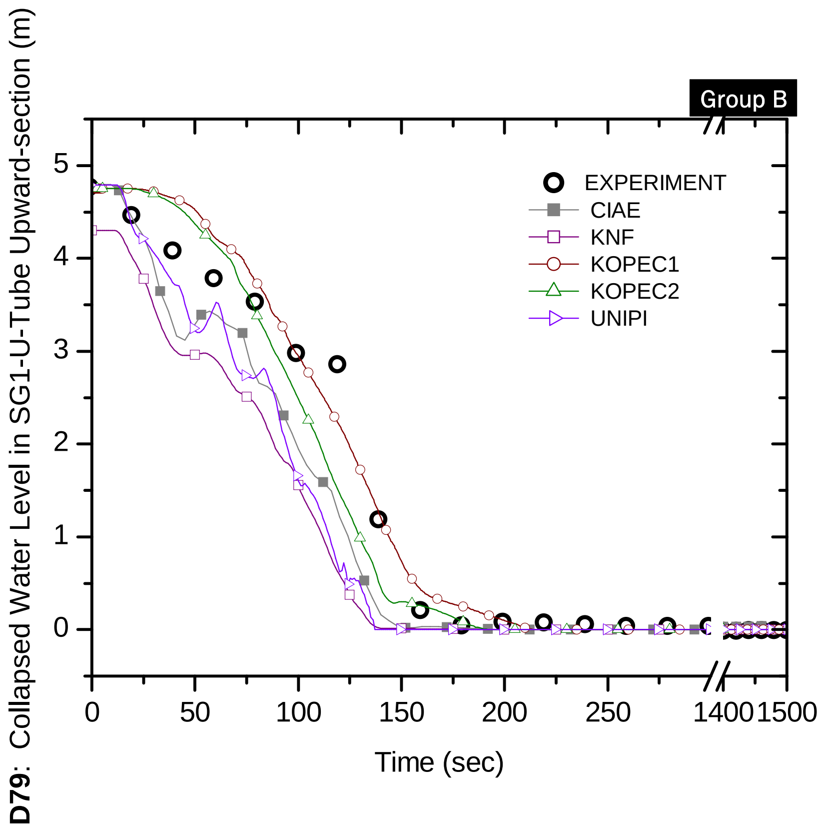

Figure B.79-B Collapsed water level in SG-1 U-tube upward section (D79)

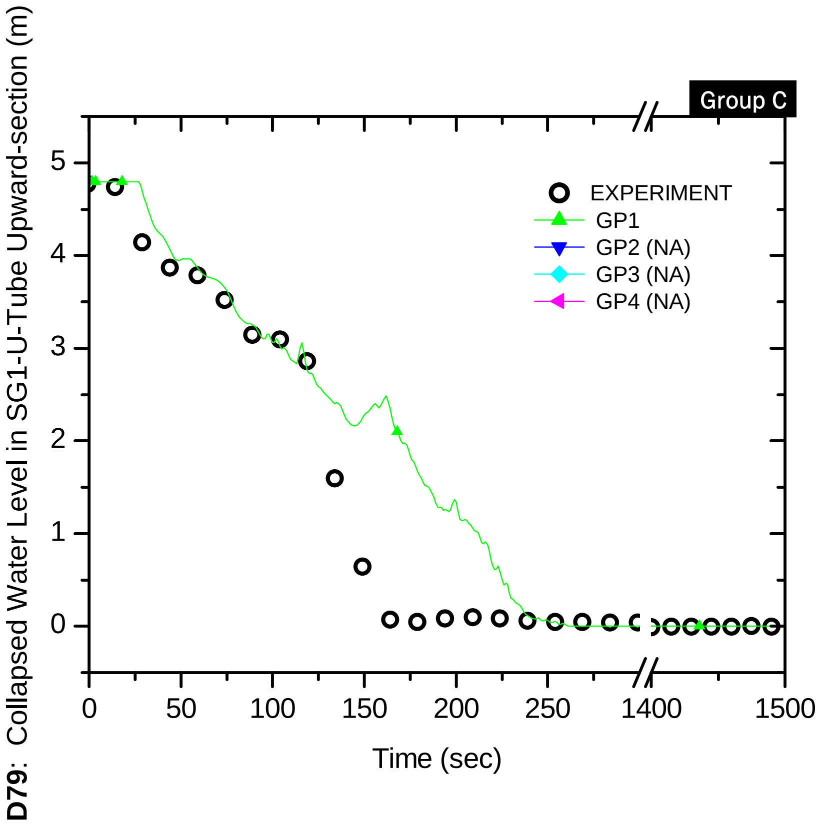

Figure B.79-C Collapsed water level in SG-1 U-tube upward section (D79)

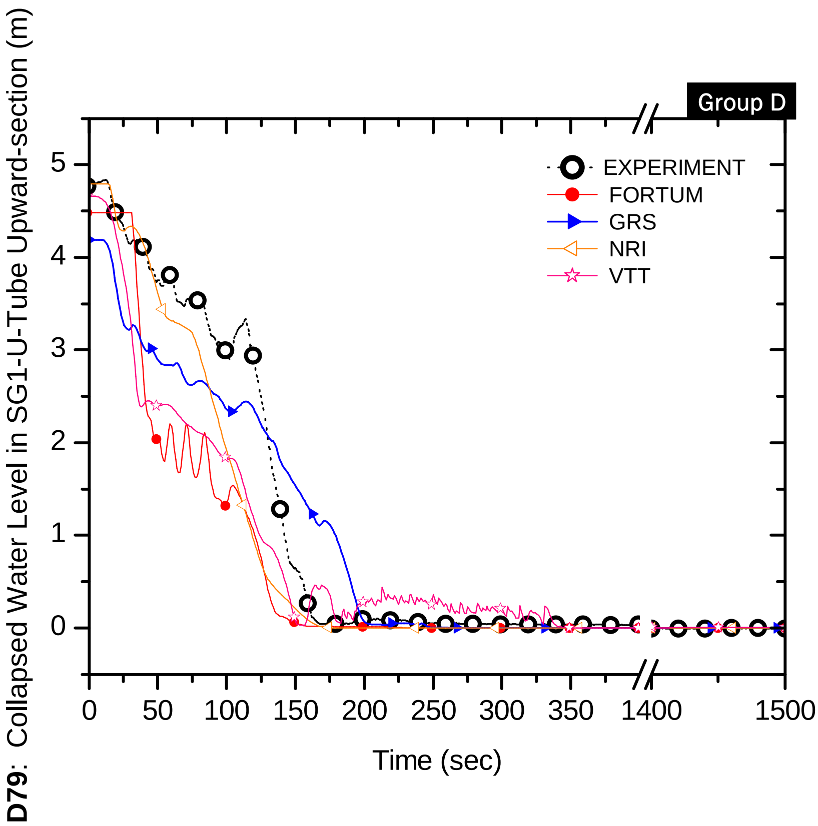

Figure B.79-D Collapsed water level in SG-1 U-tube upward section (D79)

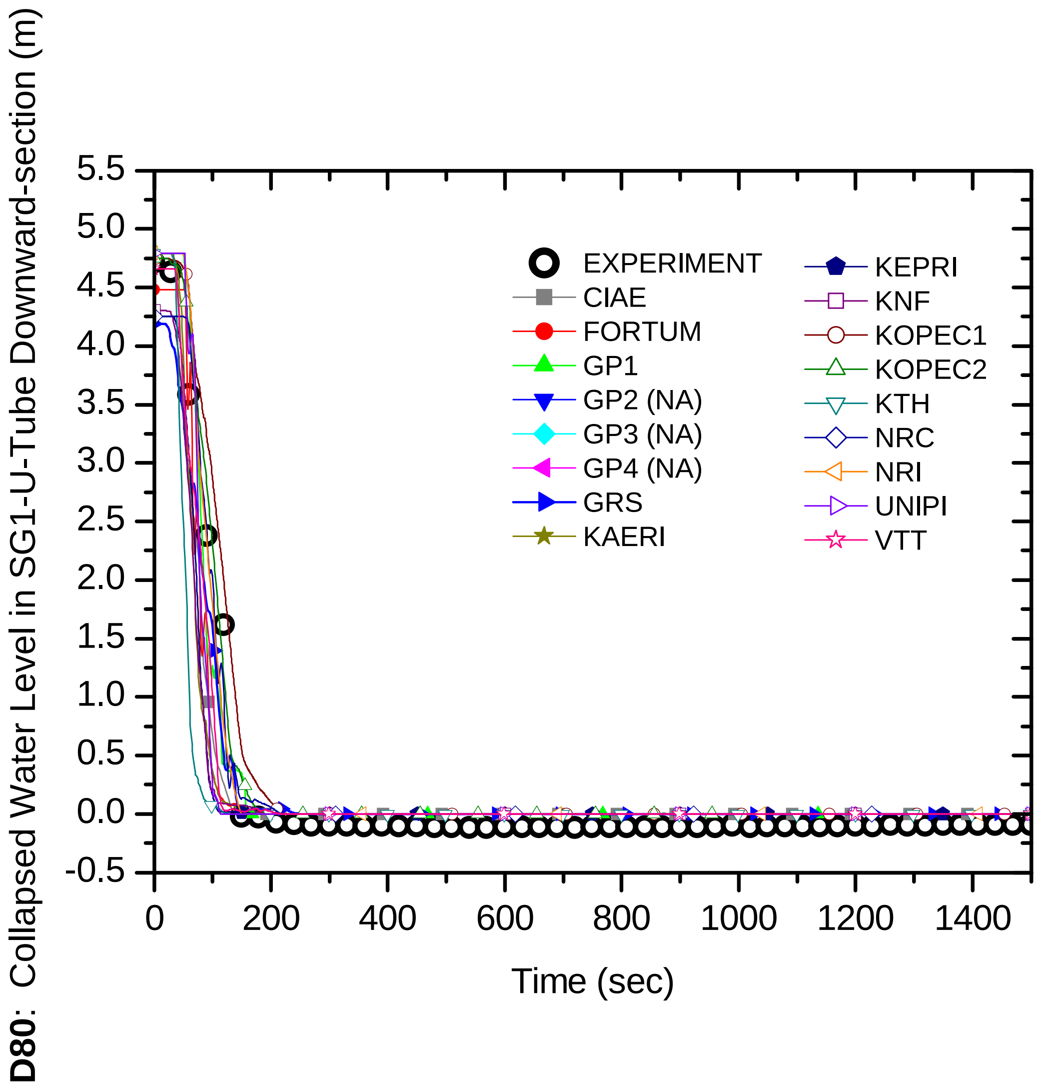

Figure B.80 Collapsed water level in SG-1 U-tube downward section (D80)

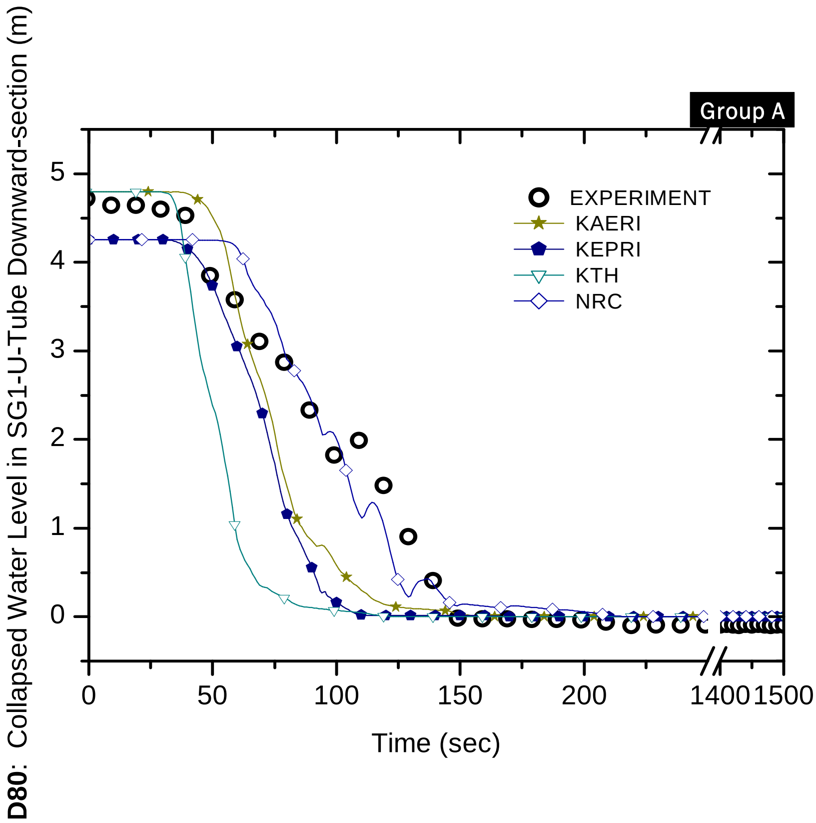

Figure B.80-A Collapsed water level in SG-1 U-tube downward section (D80)

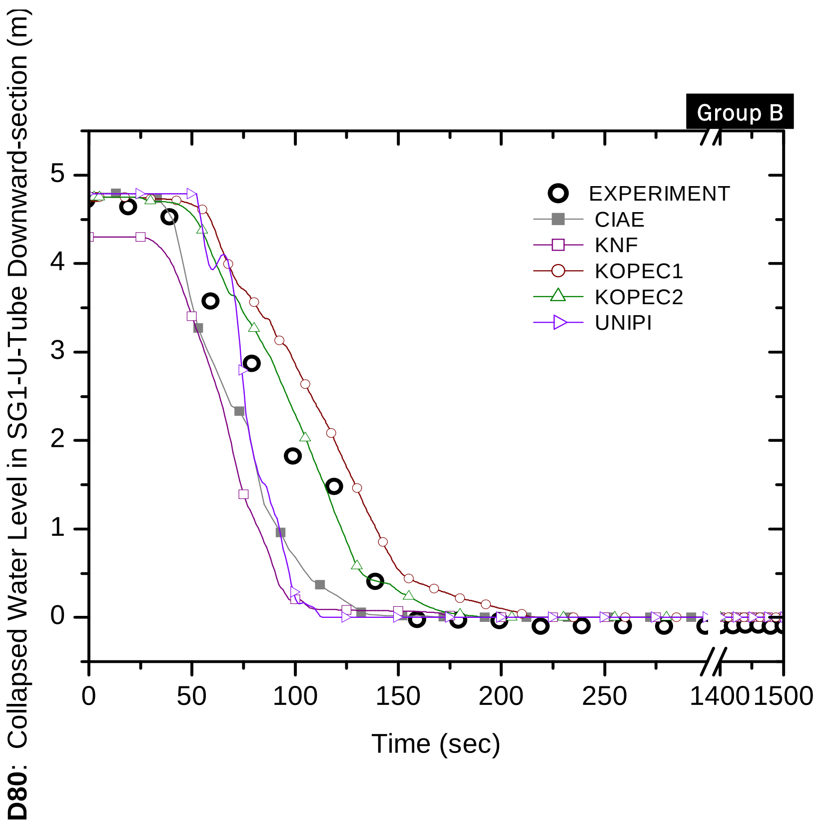

Figure B.80-B Collapsed water level in SG-1 U-tube downward section (D80)

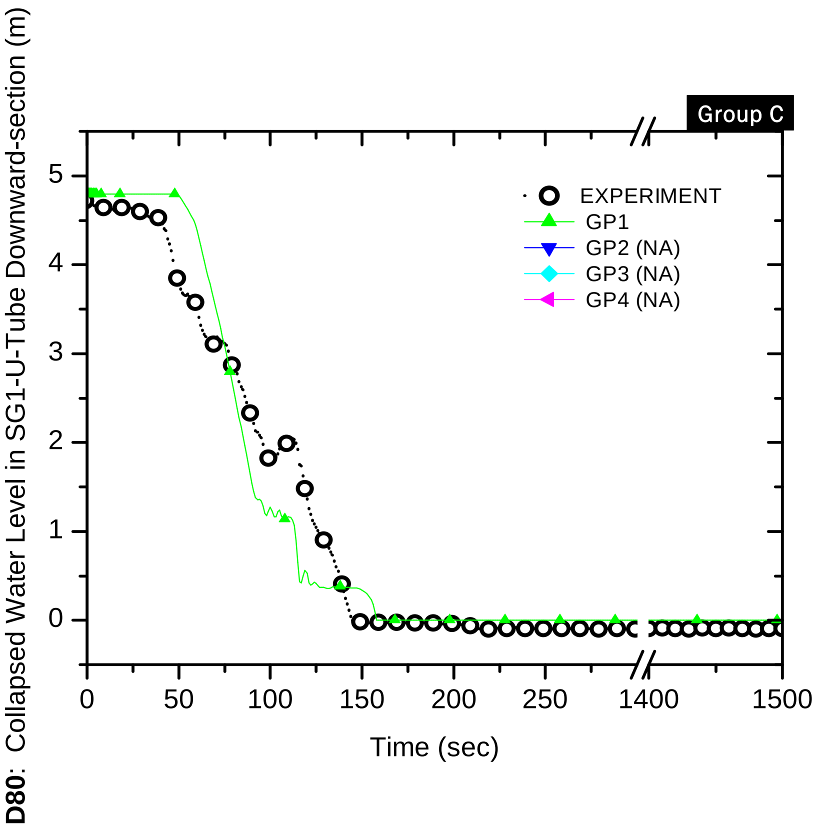

Figure B.80-C Collapsed water level in SG-1 U-tube downward section (D80)

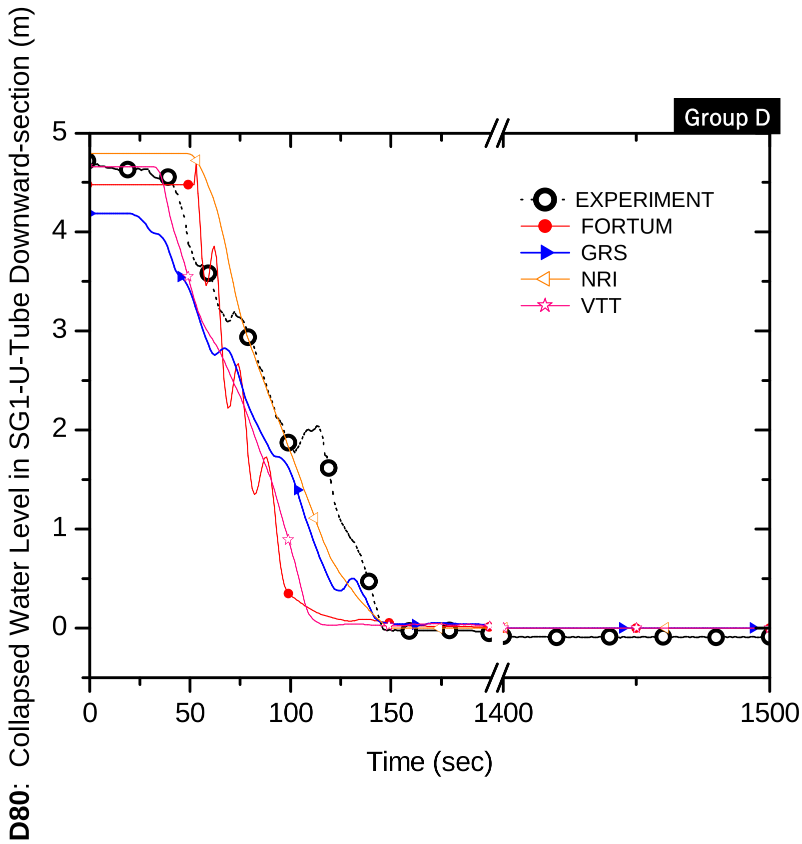

Figure B.80-D Collapsed water level in SG-1 U-tube downward section (D80)

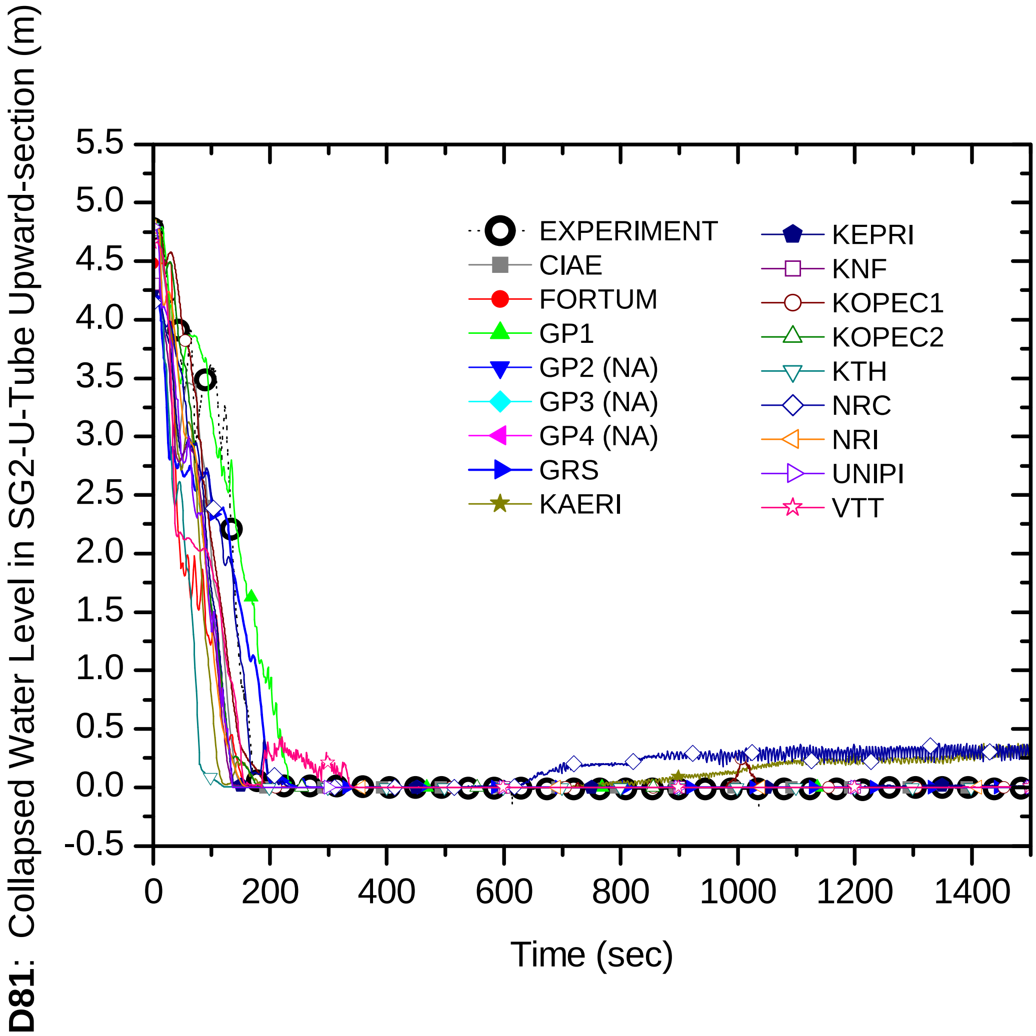

Figure B.81 Collapsed water level in SG-2 U-tube upward section (D81)

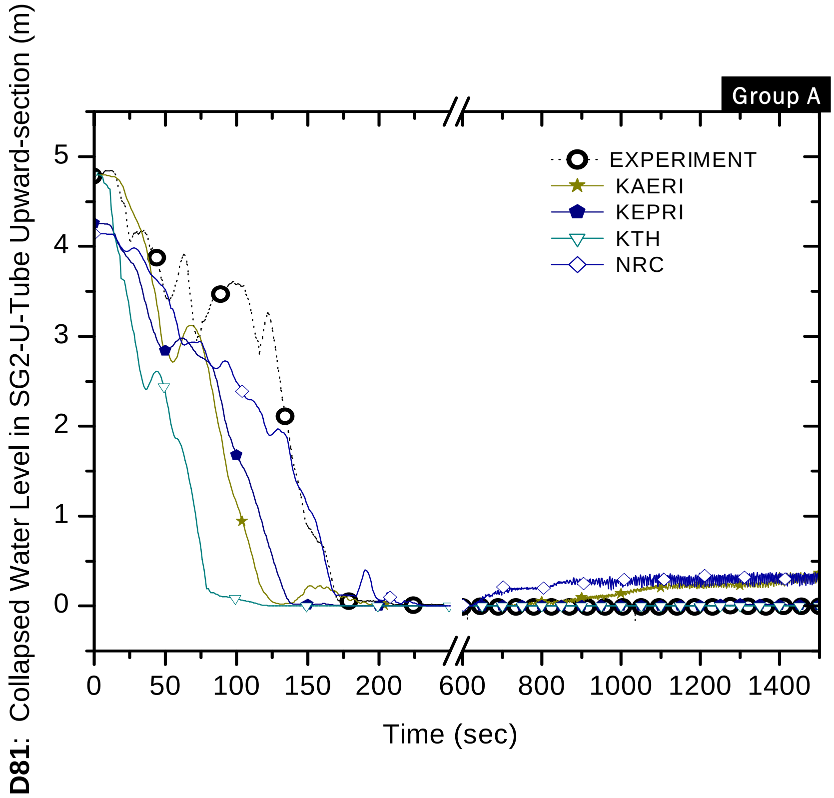

Figure B.81-A Collapsed water level in SG-2 U-tube upward section (D81)

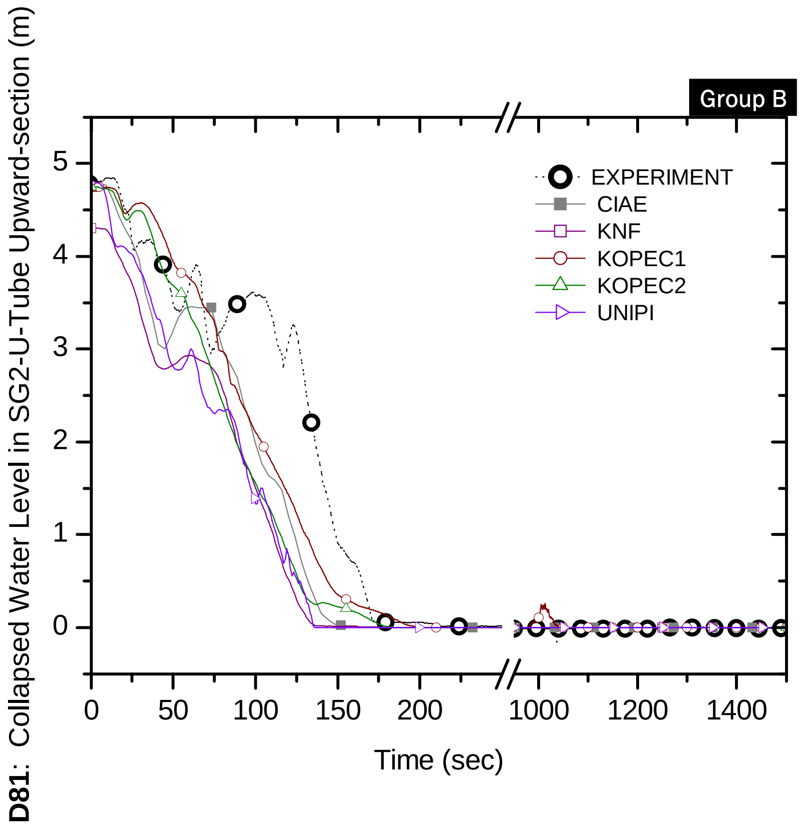

Figure B.81-B Collapsed water level in SG-2 U-tube upward section (D81)

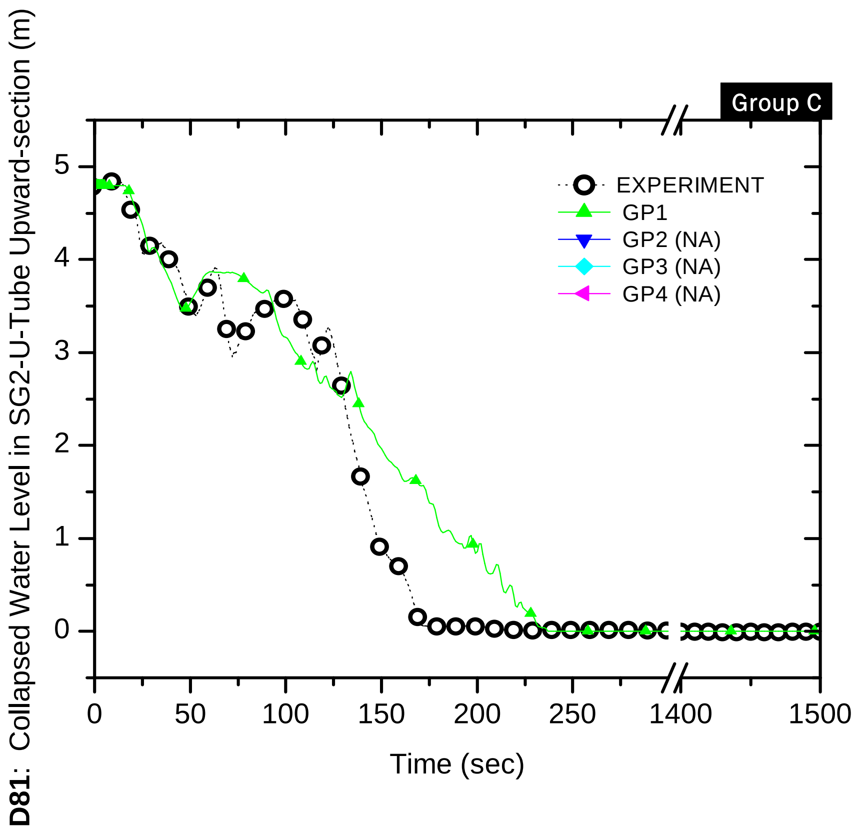

Figure B.81-C Collapsed water level in SG-2 U-tube upward section (D81)

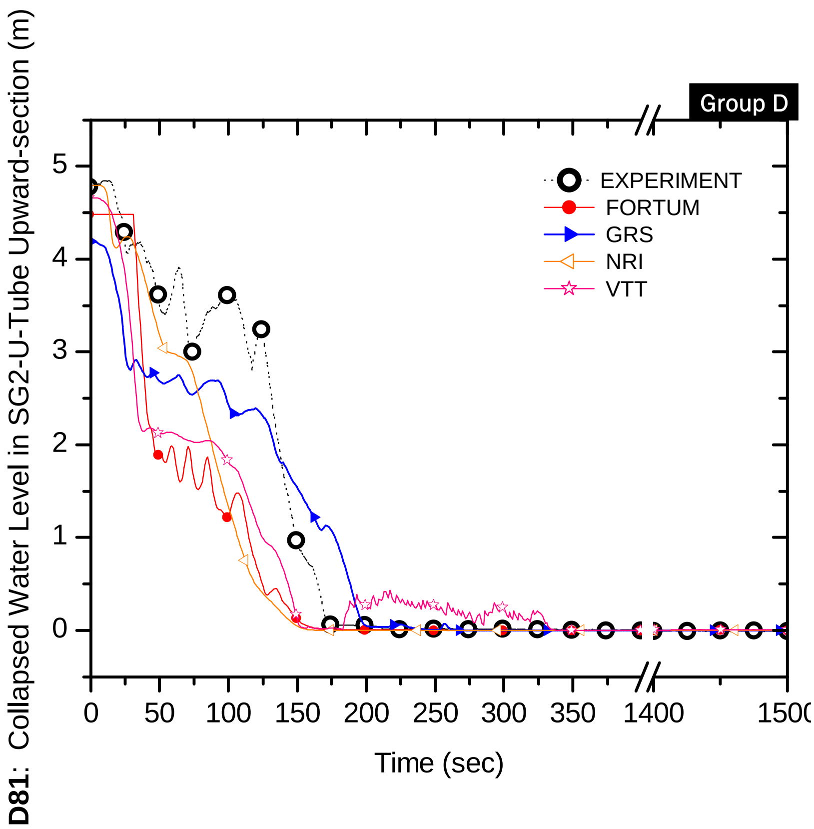

Figure B.81-D Collapsed water level in SG-2 U-tube upward section (D81)

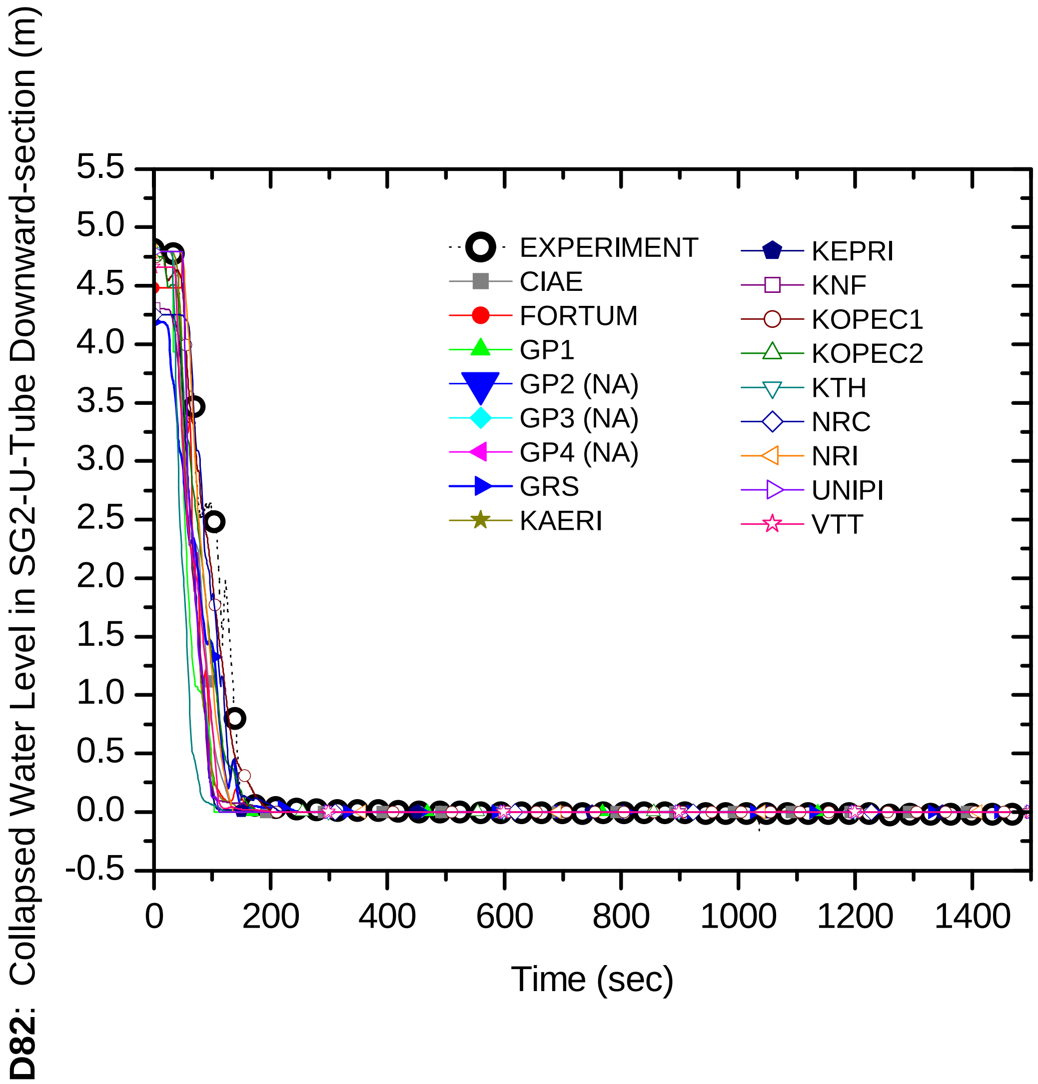

Figure B.82 Collapsed water level in SG-2 U-tube downward section (D82)

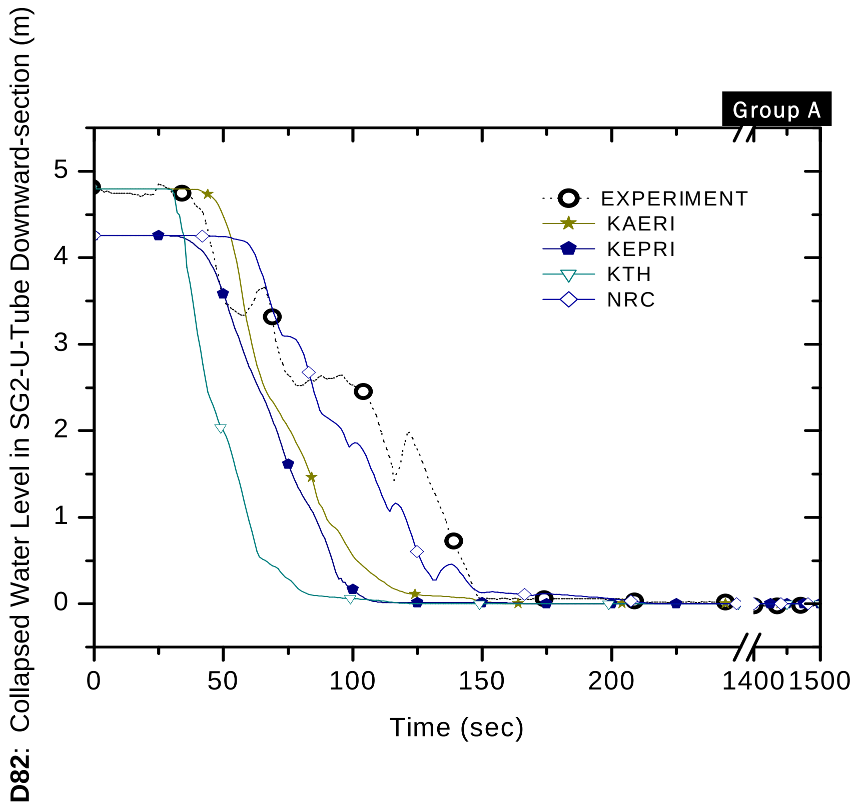

Figure B.82-A Collapsed water level in SG-2 U-tube downward section (D82)

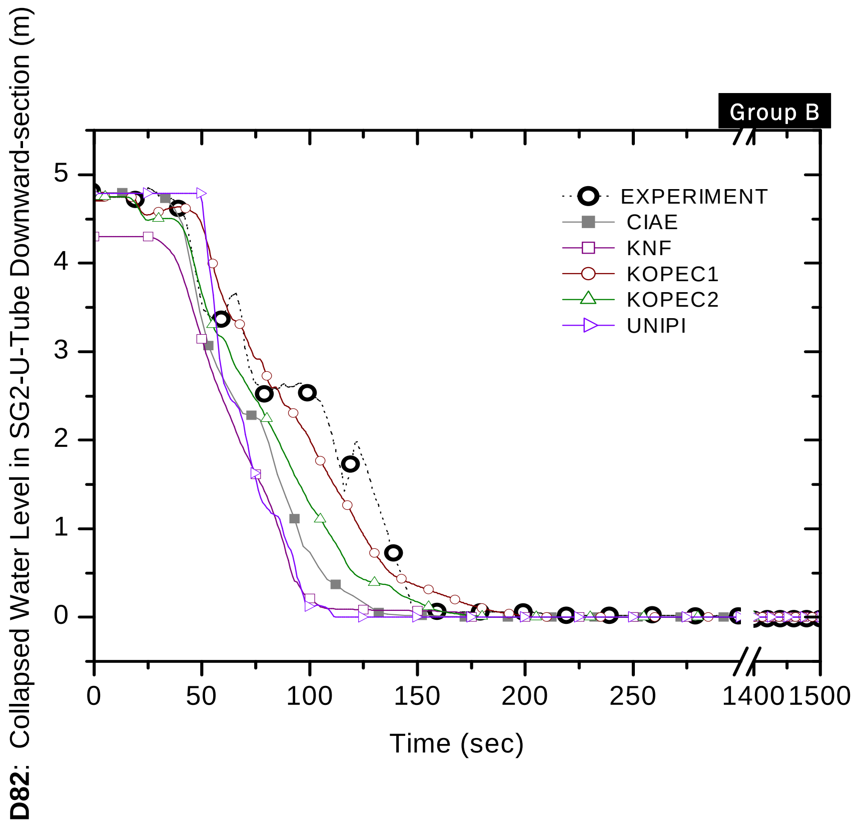

Figure B.82-B Collapsed water level in SG-2 U-tube downward section (D82)

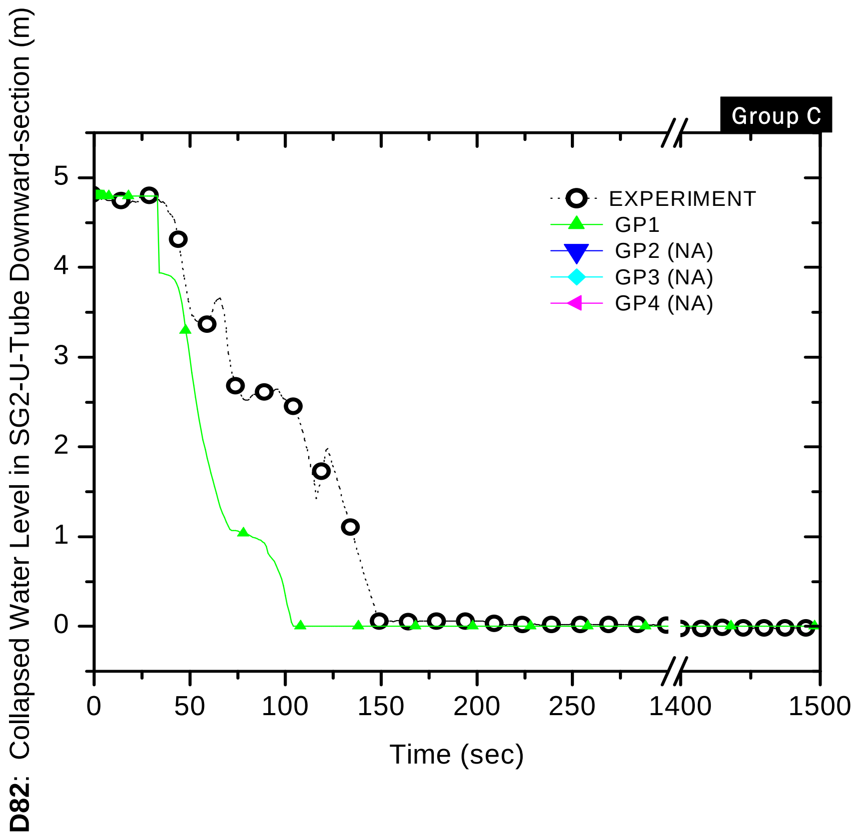

Figure B.82-C Collapsed water level in SG-2 U-tube downward section (D82)

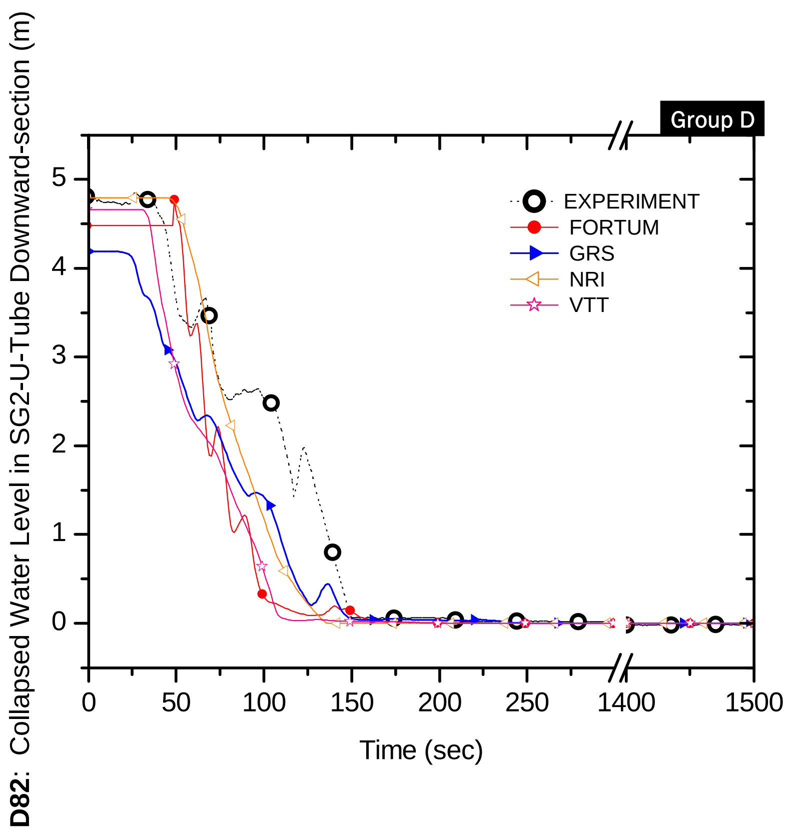

Figure B.82-D Collapsed water level in SG-2 U-tube downward section (D82)

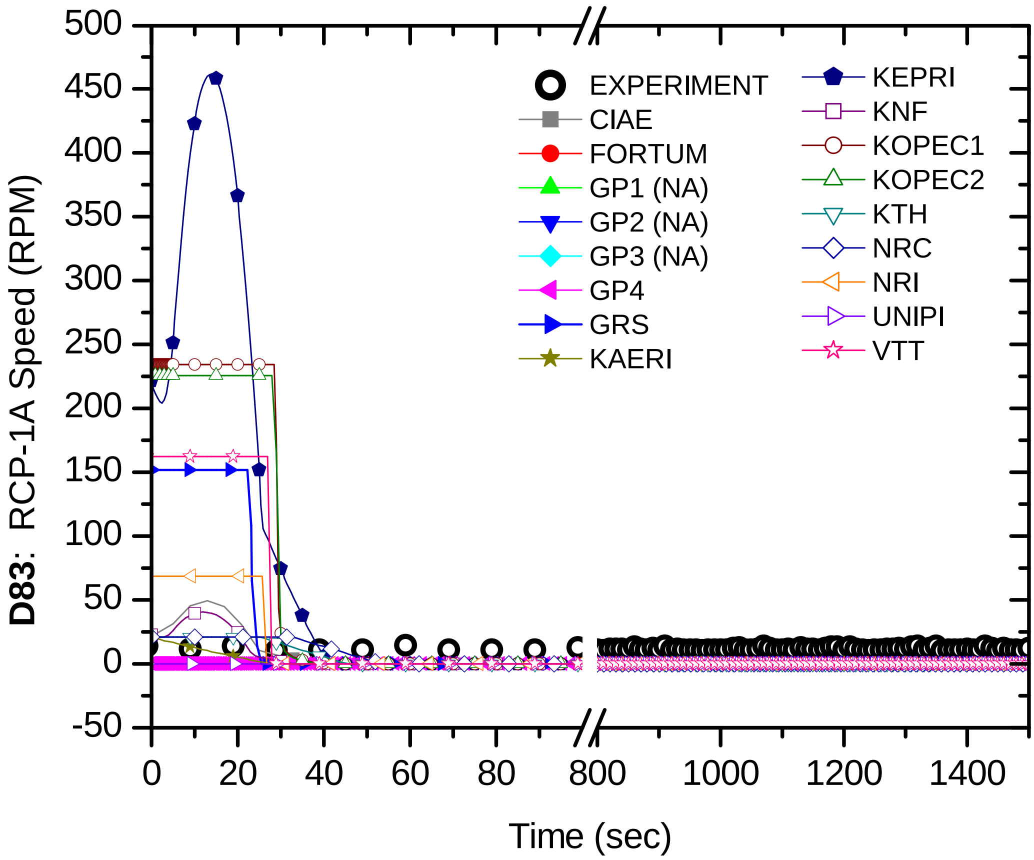

Figure B.83 RCP 1A speed (D83)

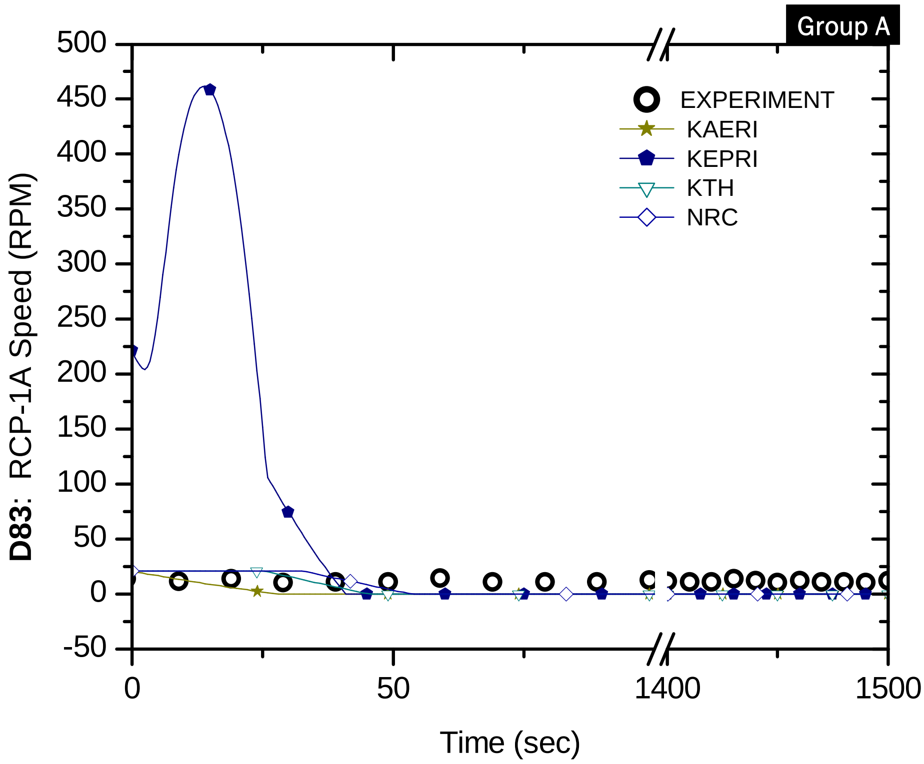

Figure B.83-A RCP 1A speed (D83)

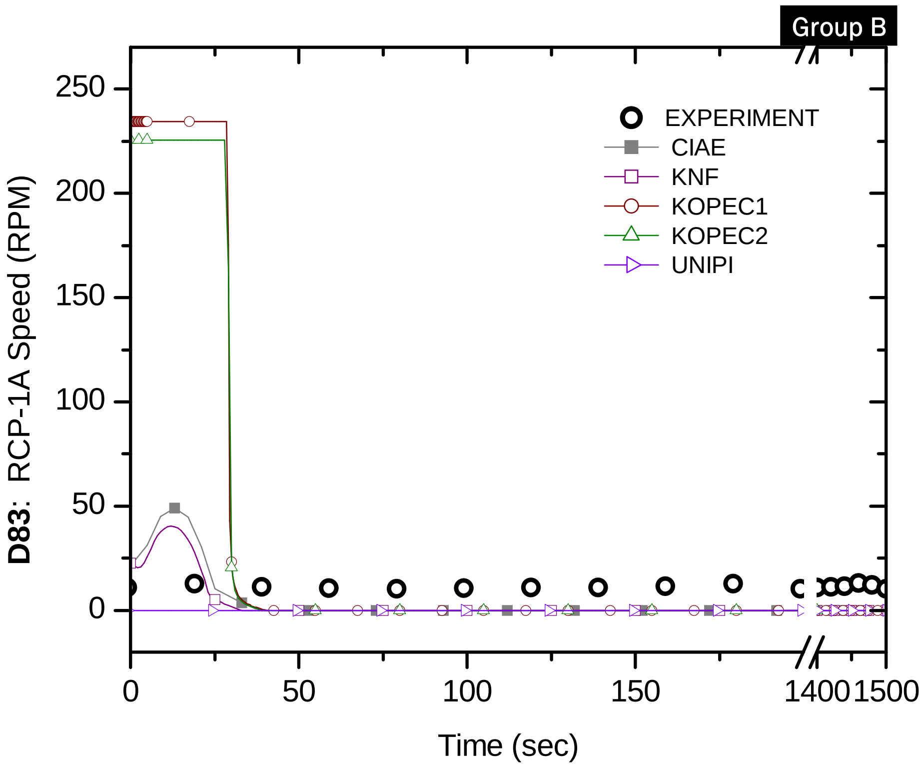

Figure B.83-B RCP 1A speed (D83)

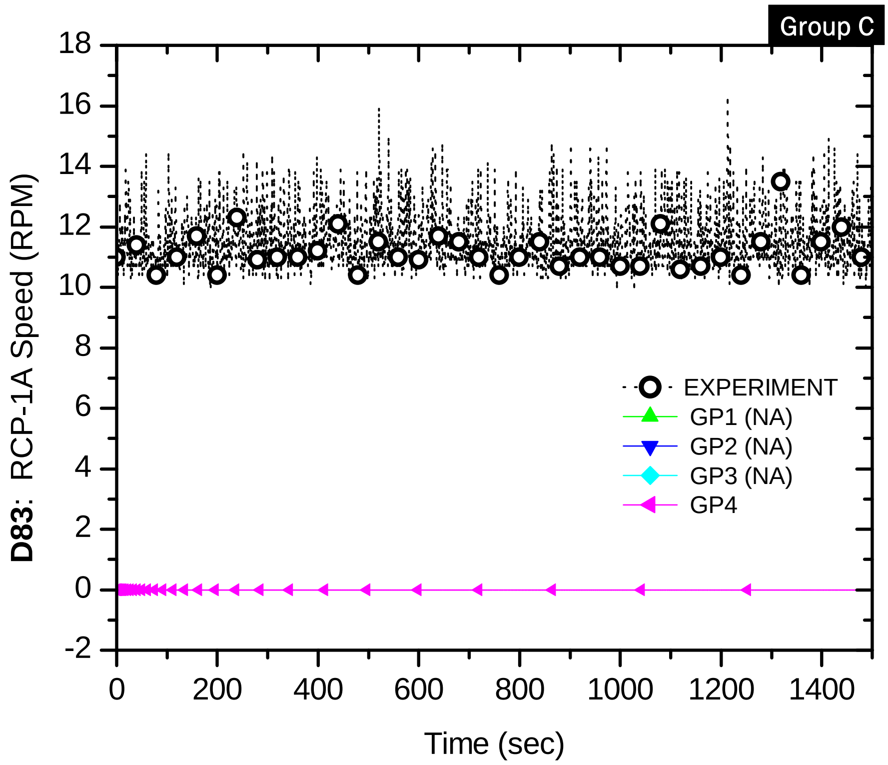

Figure B.83-C RCP 1A speed (D83)

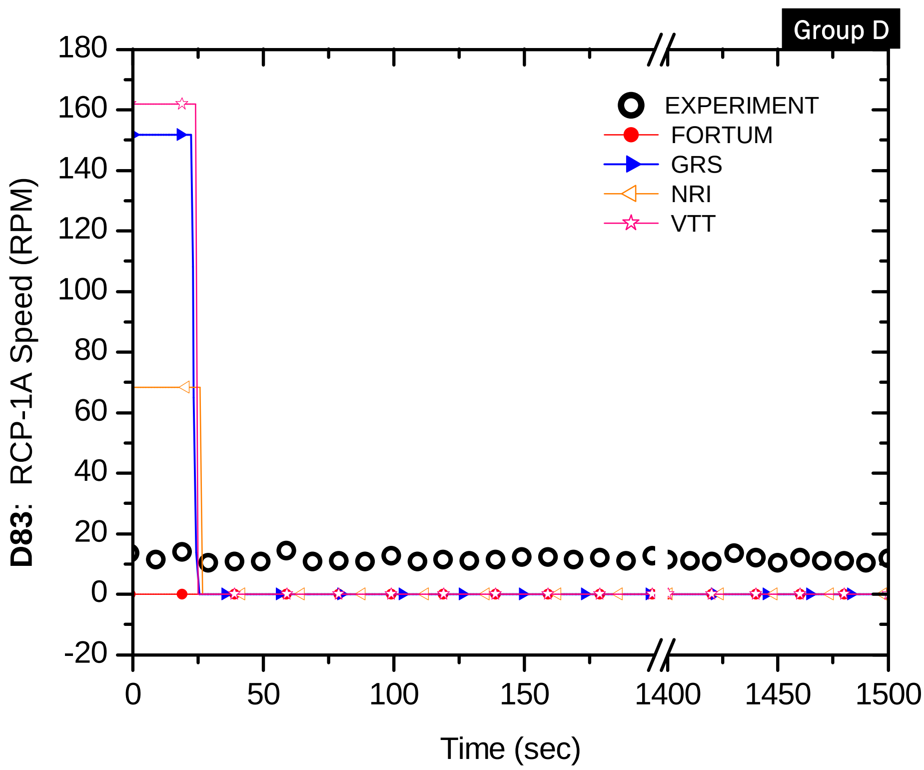

Figure B.83-D RCP 1A speed (D83)

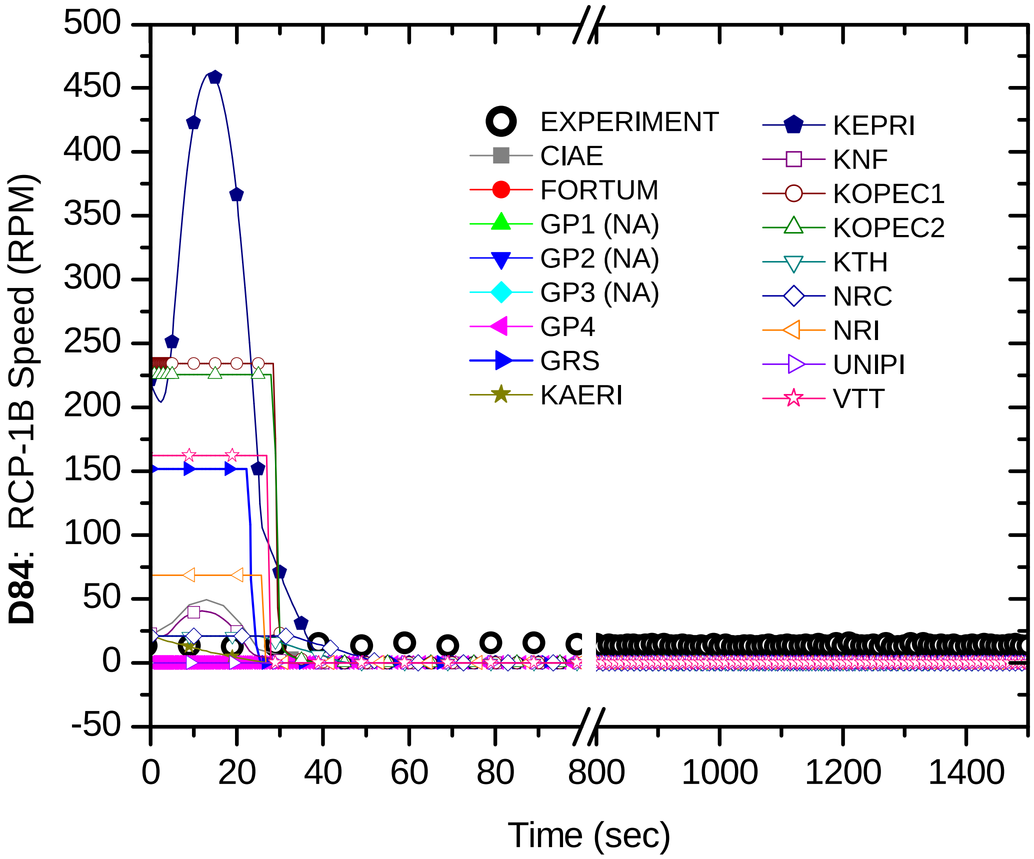

Figure B.84 RCP 1B speed (D84)

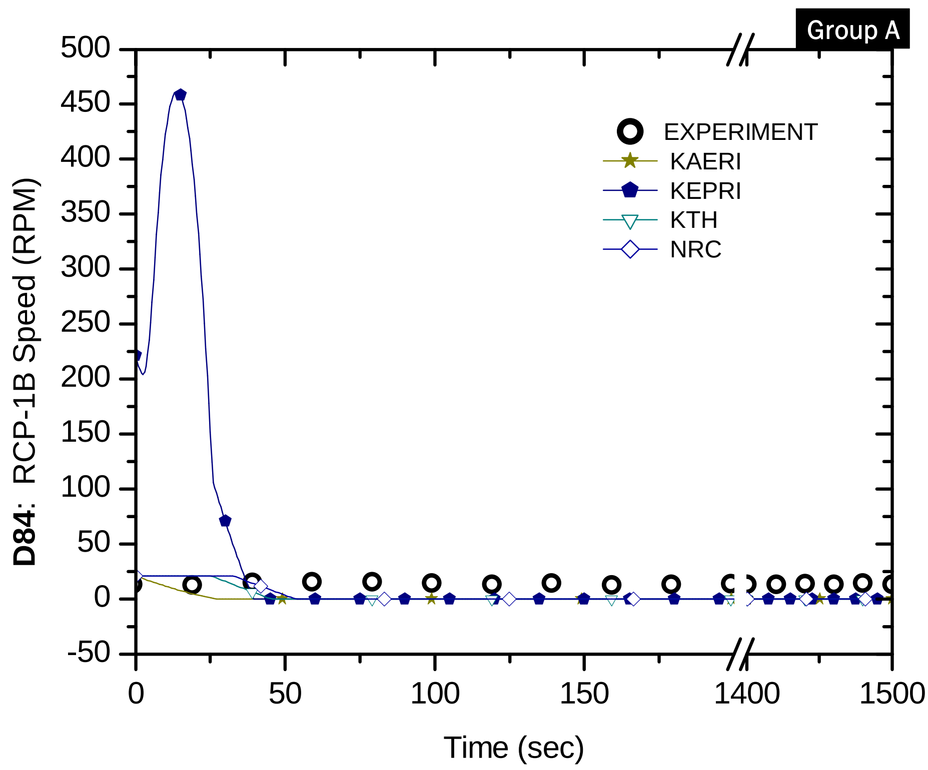

Figure B.84-A RCP 1B speed (D84)

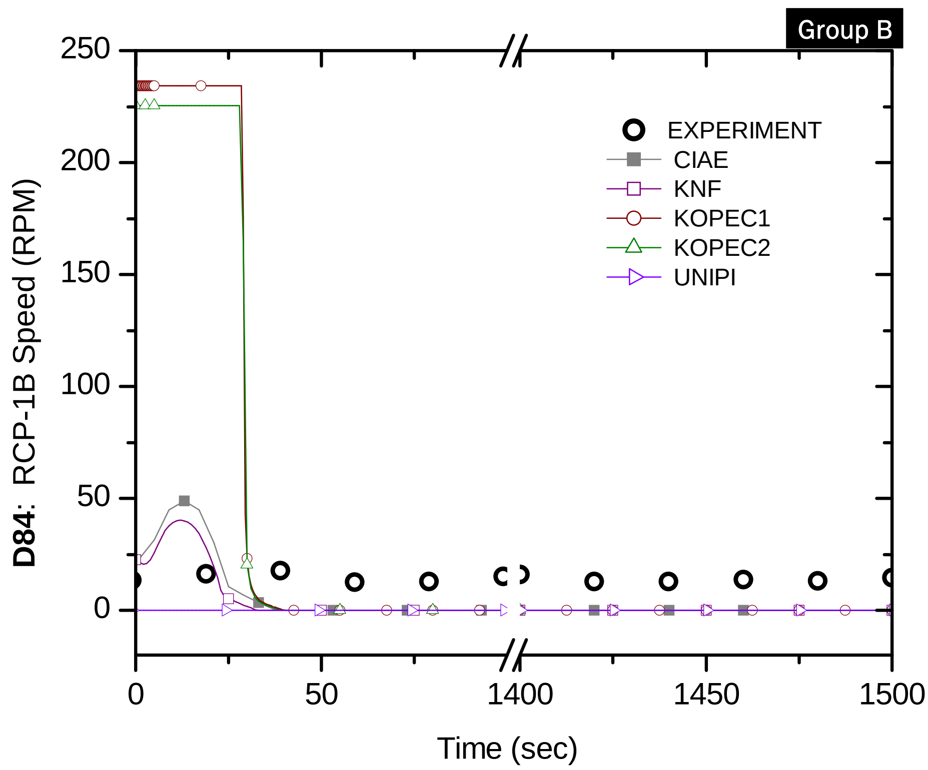

Figure B.84-B RCP 1B speed (D84)

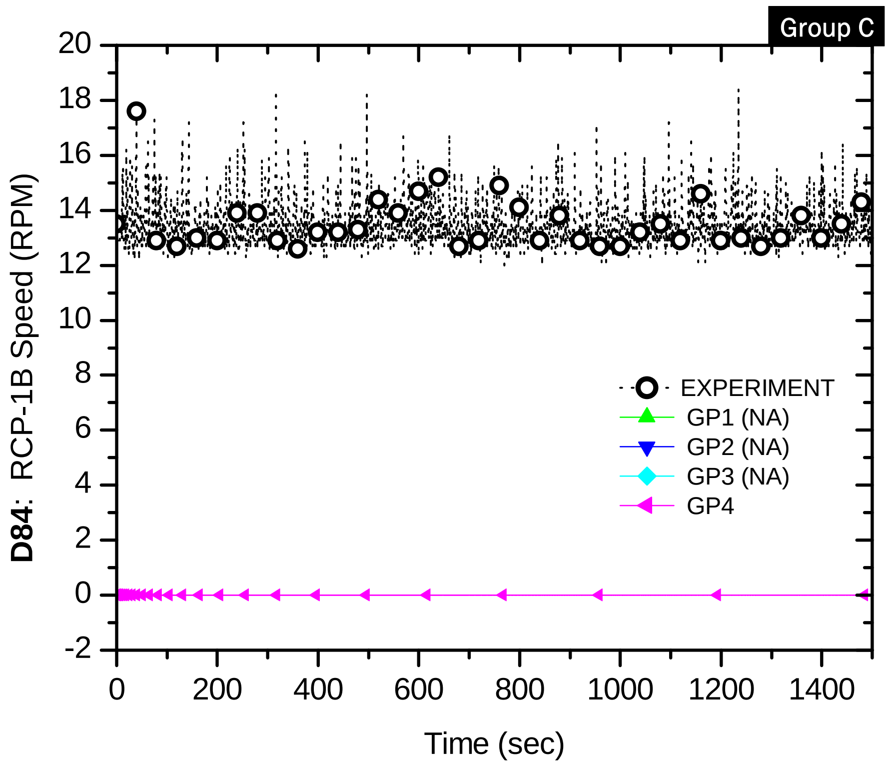

Figure B.84-C RCP 1B speed (D84)

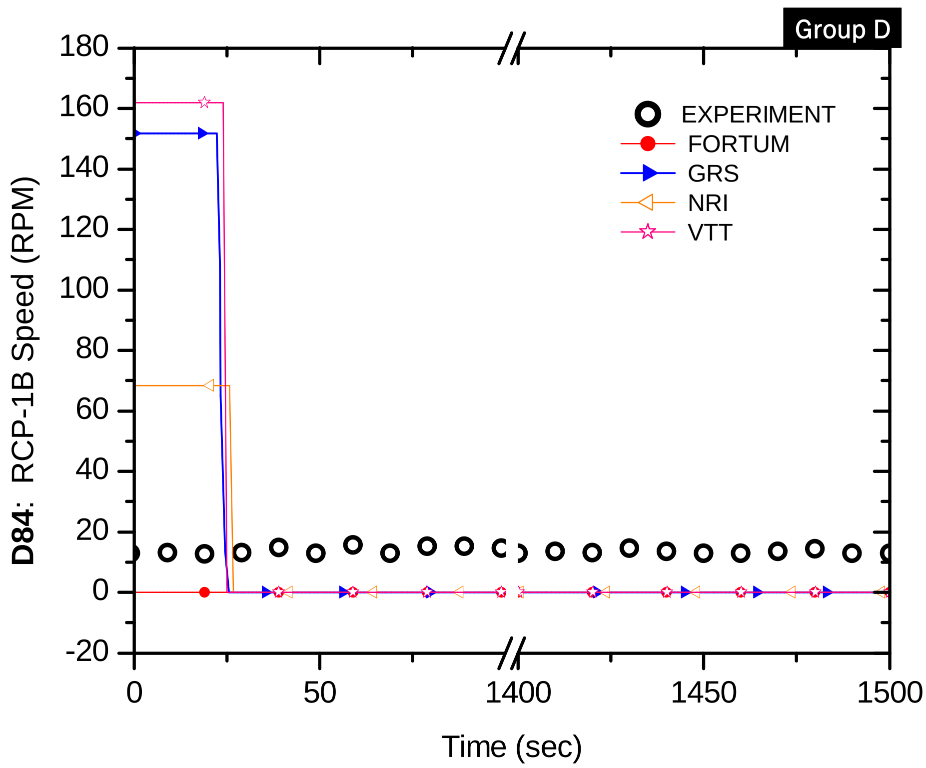

Figure B.84-D RCP 1B speed (D84)

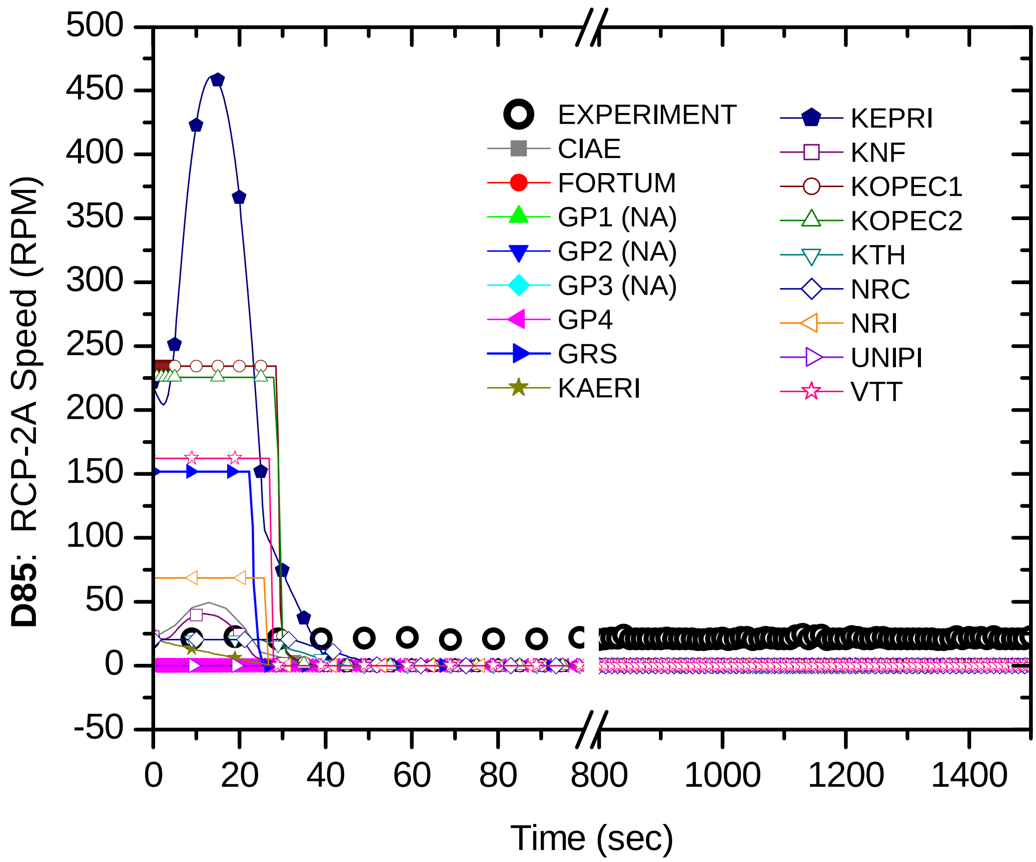

Figure B.85 RCP 2A speed (D85)

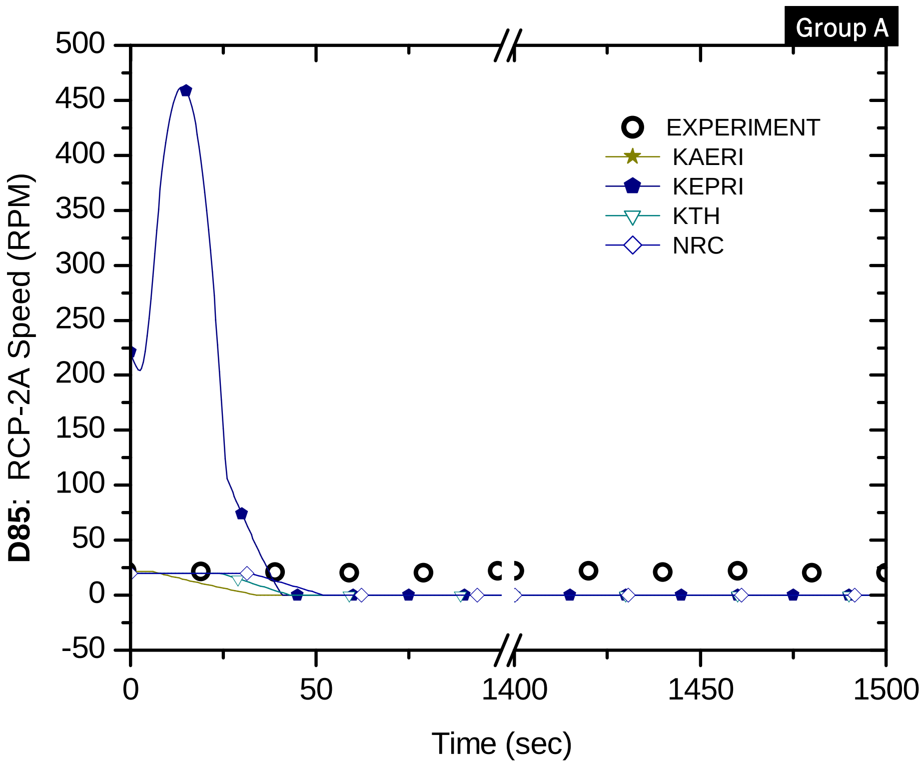

Figure B.85-A RCP 2A speed (D85)

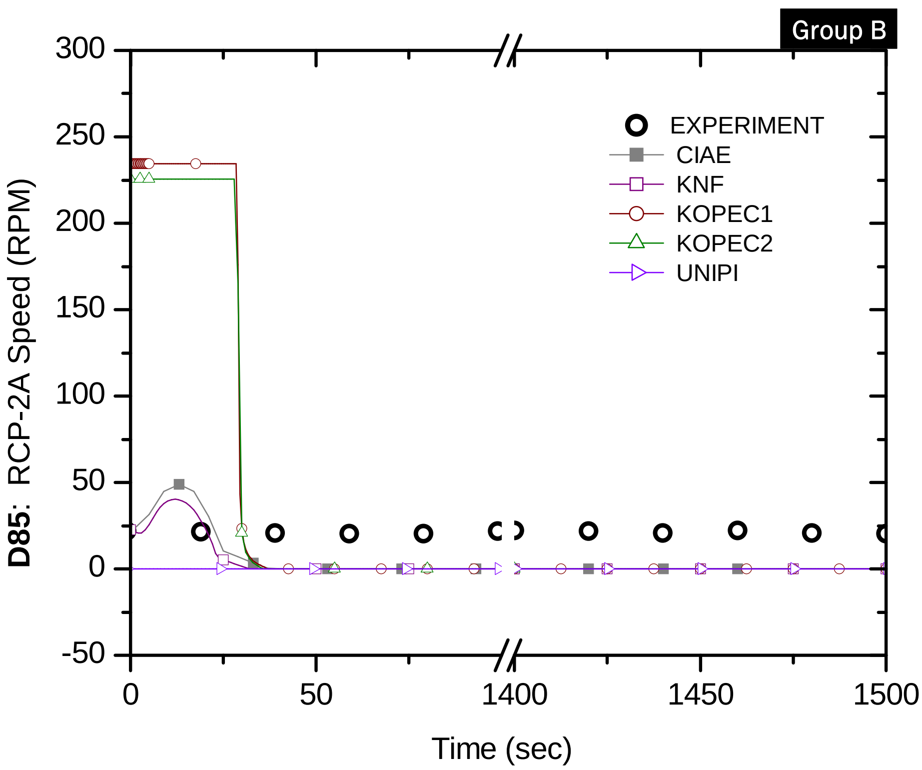

Figure B.85-B RCP 2A speed (D85)

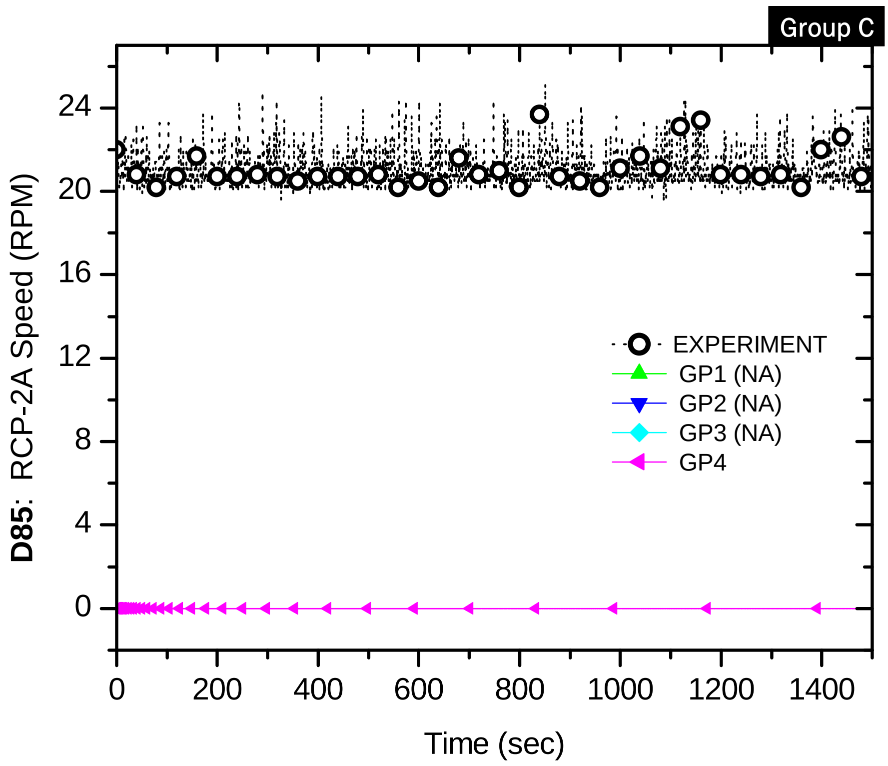

Figure B.85-C RCP 2A speed (D85)

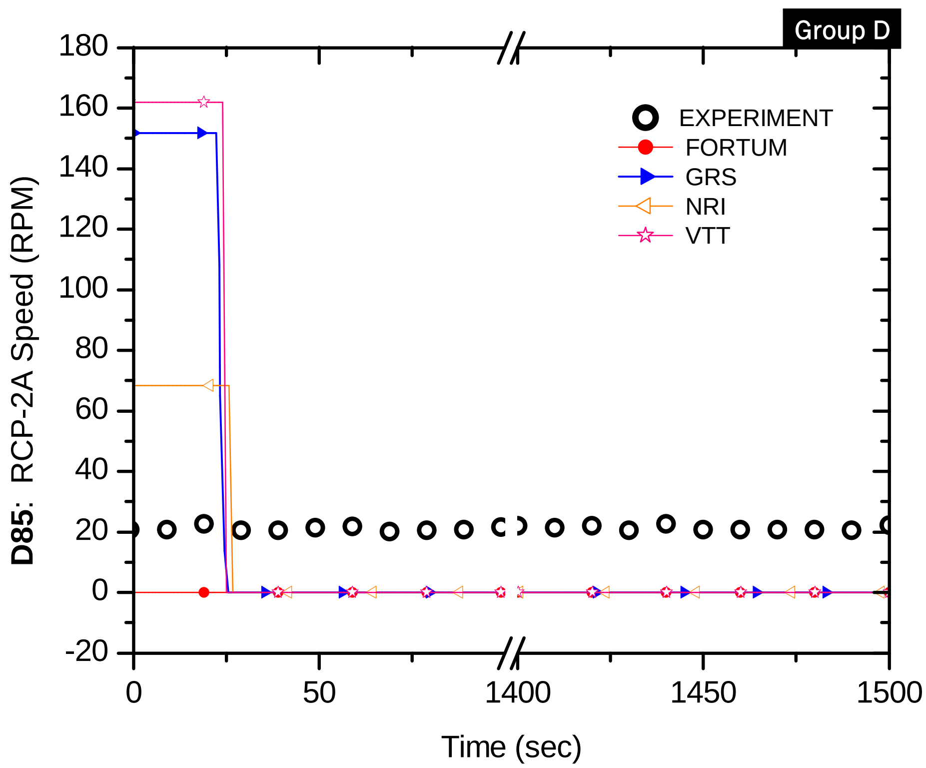

Figure B.85-D RCP 2A speed (D85)

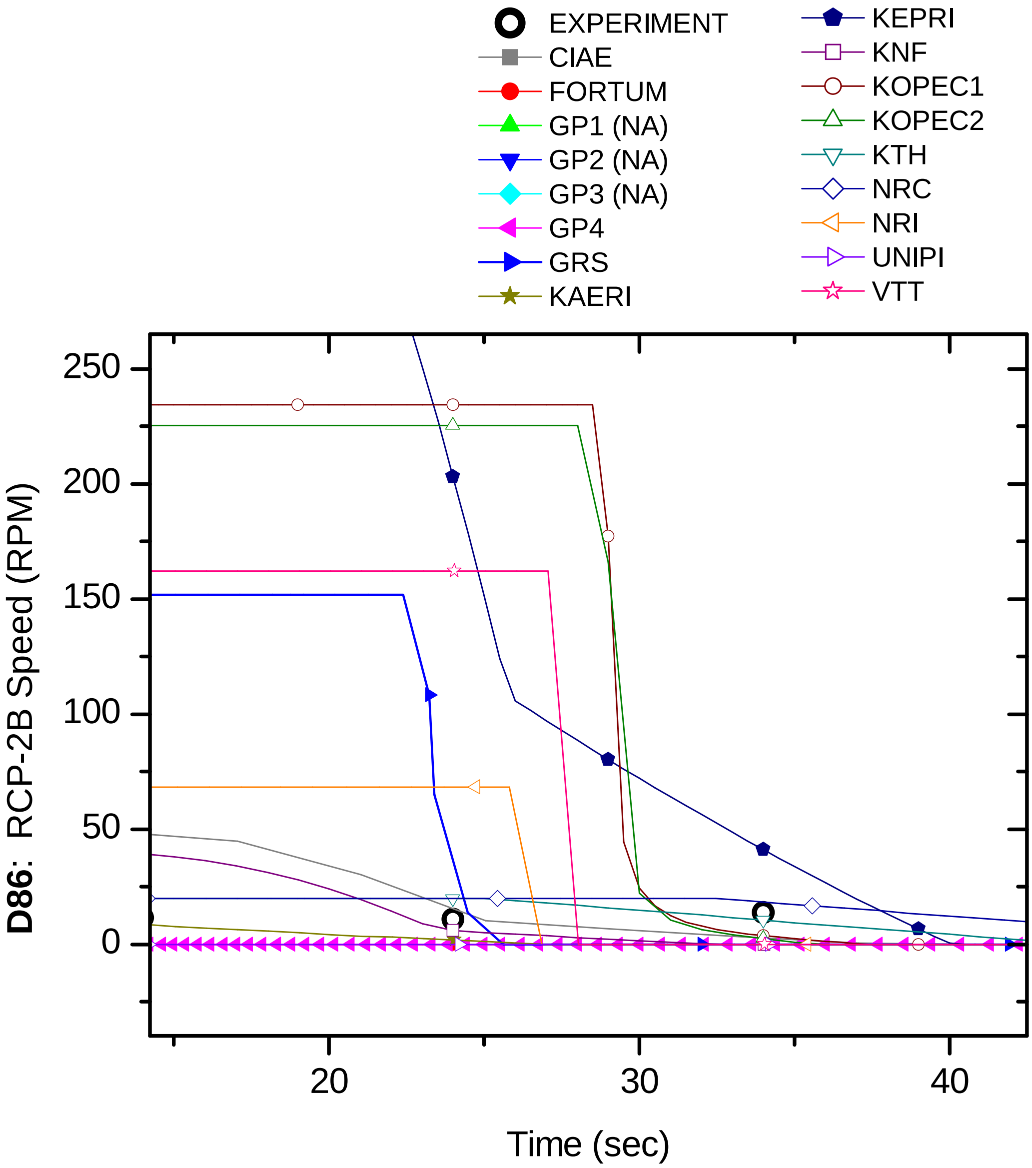

Figure B.86 RCP 2B speed (D86)

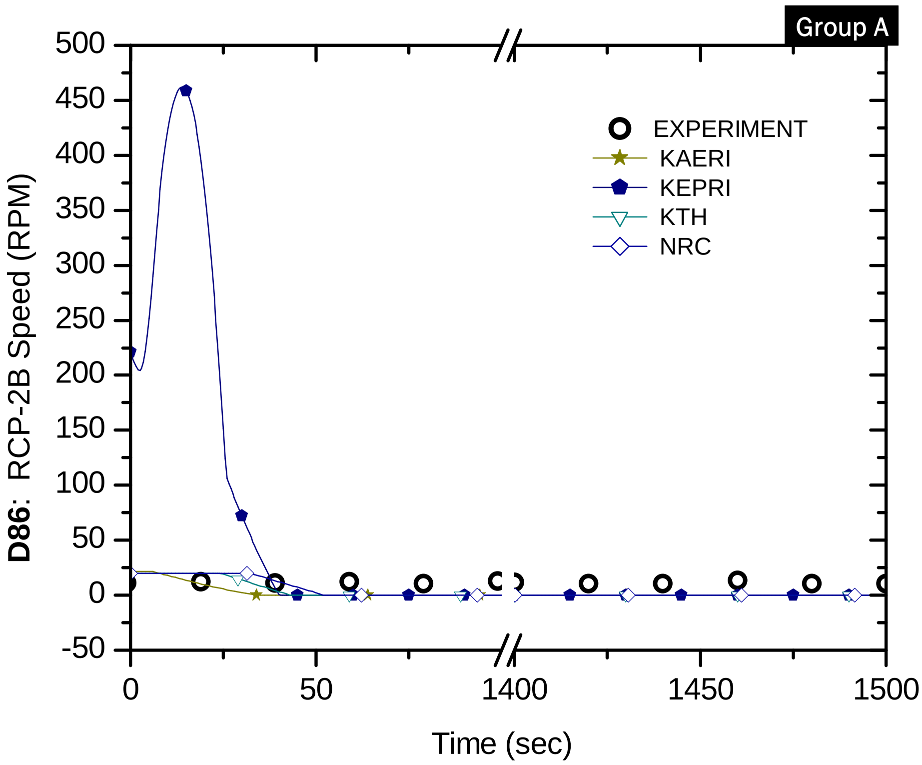

Figure B.86-A RCP 2B speed (D86)

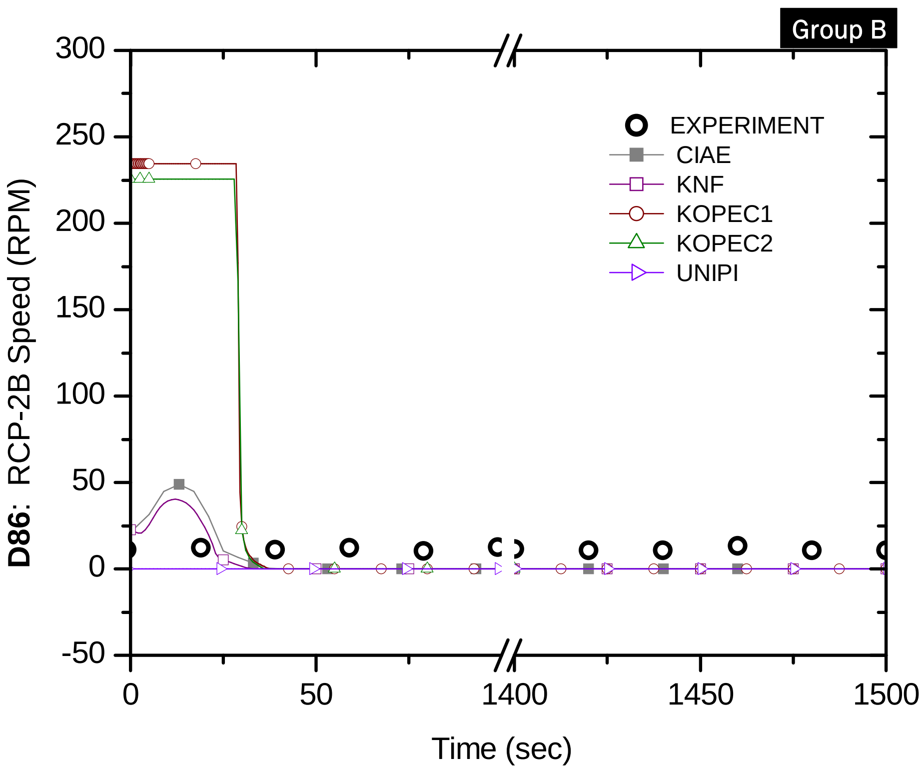

Figure B.86-B RCP 2B speed (D86)

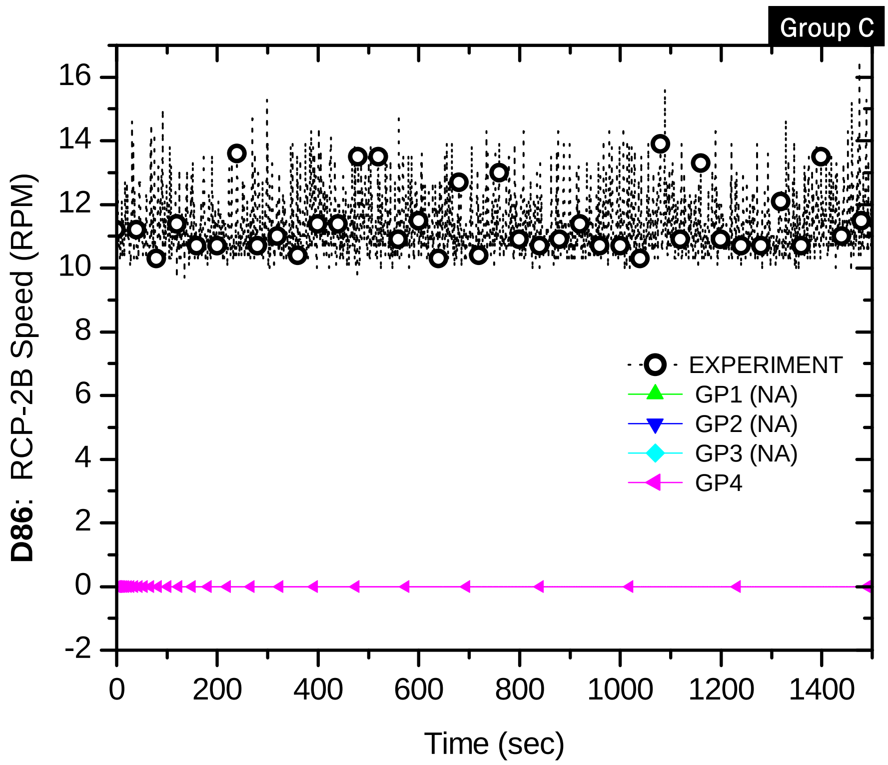

Figure B.86-C RCP 2B speed (D86)

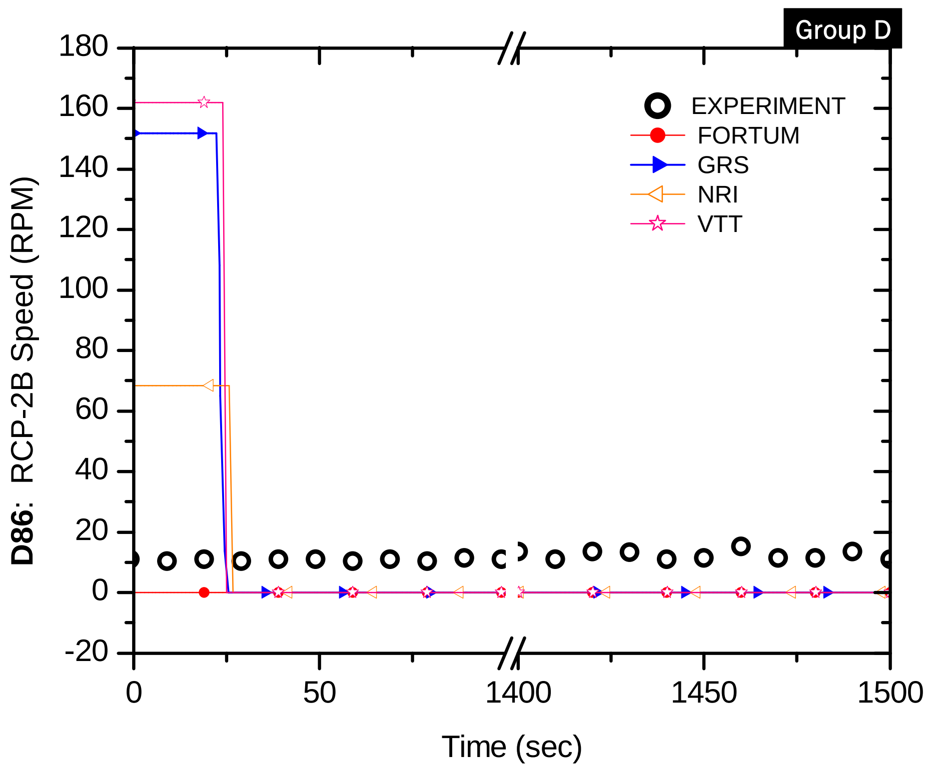

Figure B.86-D RCP 2B speed (D86)

Appendix-C:
Blind Reports Provided by Participants

1. FORTUM (prepared by Aino Ahonen)

1.1 Introduction

This report includes code and model description and discussion of the major events during the blind calculation. The ISP-50 exercise was conducted in Finland by Fortum Nuclear Services. Fortum Nuclear Services provides consultant and engineering services and system supplies for the nuclear power industry. The modelling and calculation was conducted by Aino Ahonen M.Sc. (Tech.).

1.2 APROS simulation software

The tool used for the ISP-50 blind calculation was advanced process simulation software APROS version 5.08. The development of APROS was initiated 1986 in co-operation by Fortum Nuclear Services Ltd and VTT Technical Research Centre of Finland. APROS is a multifunctional simulation tool, which is suitable for various tasks during a complete project cycle of a nuclear and thermal power plant from the plant design to operator training. It can be used e.g. in conceptual design, detailed process and automation design, testing, engineering and safety analysis as well as training simulator applications. APROS is used in 25 countries and the users are e.g. nuclear and combustion power plants, automation suppliers, paper mills and solid oxide fuel cell system developers. In the nuclear field, APROS has been used to simulate many different plant concepts, including both boiling and pressurised water reactors. References are available in APROS web page Ref. 1.

APROS power plant library consists of comprehensive simulation models. The component library includes an extensive set of ready-made unit operation or process component models for the simulation of different kind of processes, such as nuclear reactor and boiler plants, including automation and electrical systems.

The thermal hydraulic library contains 3- , 5- and 6-equation models for the calculation of one-dimensional two-phase flow. Fast access material property tables are used for the computation of the water and steam material properties.

The six equation model is based on the conservation equations of mass, momentum and energy for the two phases. The equations are coupled with empirical correlations describing various two-phase phenomena, like friction and heat transfer for wall and interface. The pressures and velocities, volume fractions and enthalpies of each phase are solved from the discretized equations using an iterative procedure.

The performance of the APROS code has been validated extensively in more than 70 cases by modelling different test facilities and comparing calculations to a large set of selected transients, detailed information in Ref. 1. The validity of the APROS power plant applications ranges from cold start-up to normal operation modes, normal and emergency shutdown, load rejections and other disturbances as well as to failures of any combination of process, automation or electrical components.

For Loviisa Nuclear Power Plant, owned by Fortum, APROS is the main analyses tool for thermohydraulic transients. For example APROS is the main tool for the analyses calculated for the Final Safety Analysis Report (FSAR) of the Loviisa Nuclear Power Plant. During the Loviisa automation renewal project (2008-2014) also the full scale operator training simulator of Loviisa will be replaced by a new APROS based simulator.

1.3 APROS model of ATLAS facility

The data of the input model is based on Ref. 2, Ref. 3, Ref. 4, Ref. 5 and Ref. 6. The available input deck for RELAP5 was not requested in order to make an independent model preparation and calculation.

Nodalization of the reactor pressure vessel is shown in Figure 1. The downcomer has been divided horizontally into 6 symmetrical sectors connected with cross flow branches. Only exception is the cold leg inlet elevation where there are only four horizontal nodes because the hot legs partly fill the downcomer volume. Vertically the downcomer has been divided into 34 nodes.

Lower plenum, core and upper plenum have only one flow channel which is divided vertically following mostly the division of the downcomer. Below and above the fuel alignment plate the outlet plenum is divided into two flow channels, one in the center of the outlet plenum and the other surrounding it. Vertically the outlet plenum from the core outlet to the upper guide structure support plate is divided into 8 nodes. Lower plenum consists of five vertical nodes and the active core area from 22 even nodes. Upper plenum is divided into 15 vertical nodes. Four bypasses of the core have been modelled according to the given data, two from the downcomer to the hot leg and two from the downcomer to the upper head.

Reactor core has been modelled with ready made component to which heat structures of heat rods are connected to. The axial power profile of the core is entered into the heat structure nodes with boundary conditions.

Heat structures of the pressure vessel include pressure vessel wall, core shroud, flow baffle, guide tubes, dummy rods, fuel alignment plate, upper guide structure support plate and UGS barrel. The outer surface of the heat structures of the pressure vessel wall have been connected to a containment node with boundary condition of temperature 30 °C and pressure 0,1 MPa.

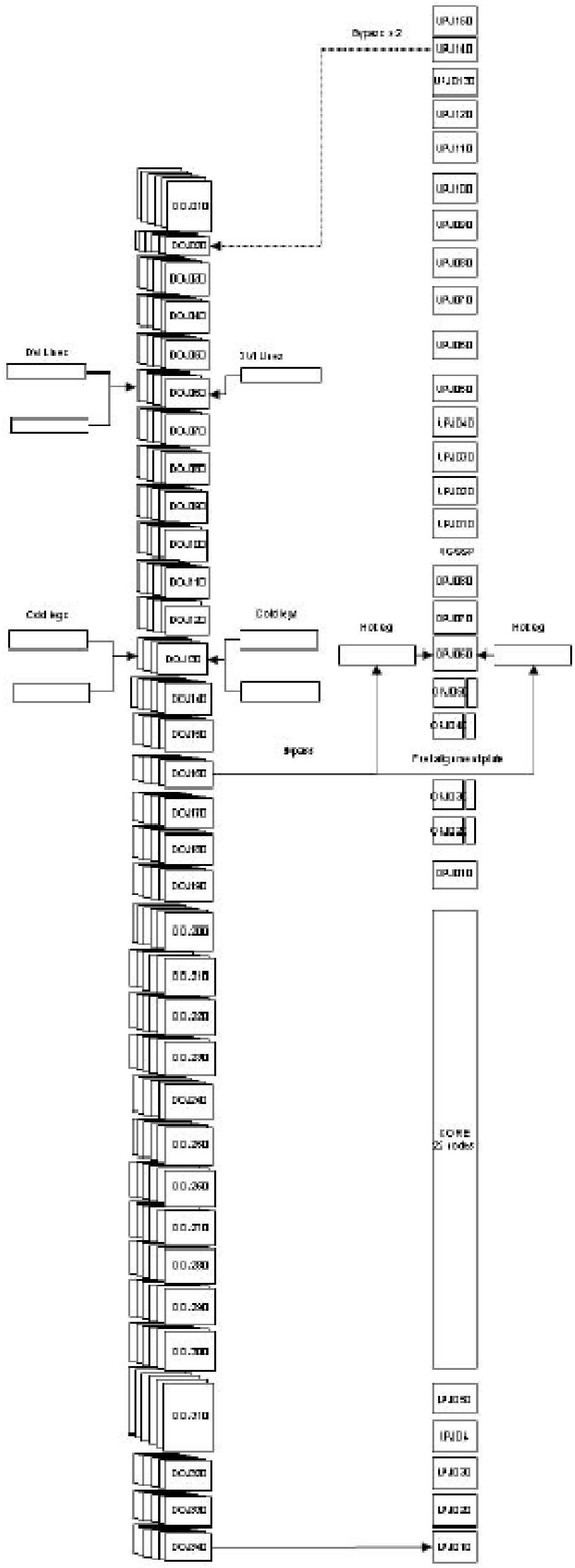

Figure 1 Nodalization of the reactor vessel

The pressurizer component is divided into 20 vertical nodes and the heat structures representing the walls are connected to the containment node. The pressure of the pressurizer is controlled with a PI-controller attached to the pressurizer heaters.

Primary loops, pressurizer surge line and emergency core cooling safety injection lines have been modelled with heat pipe modules including the heat structure for pipe walls. The pipe lines include nodes according to the Table 1. A view of the primary circuit in shown in Figure 2 and view of one safety injection line in Figure 3. Safety injection pump was modelled with pipe component with mass flow boundary condition with respect to primary pressure according to the given data.

Table 1. Nodalization of the pipe lines

	Nodes per line	Total nodes
Hot legs	11	22
Intermediate legs	19	76
Cold legs	13	52
Surge line	13	13
DVI lines	34	102

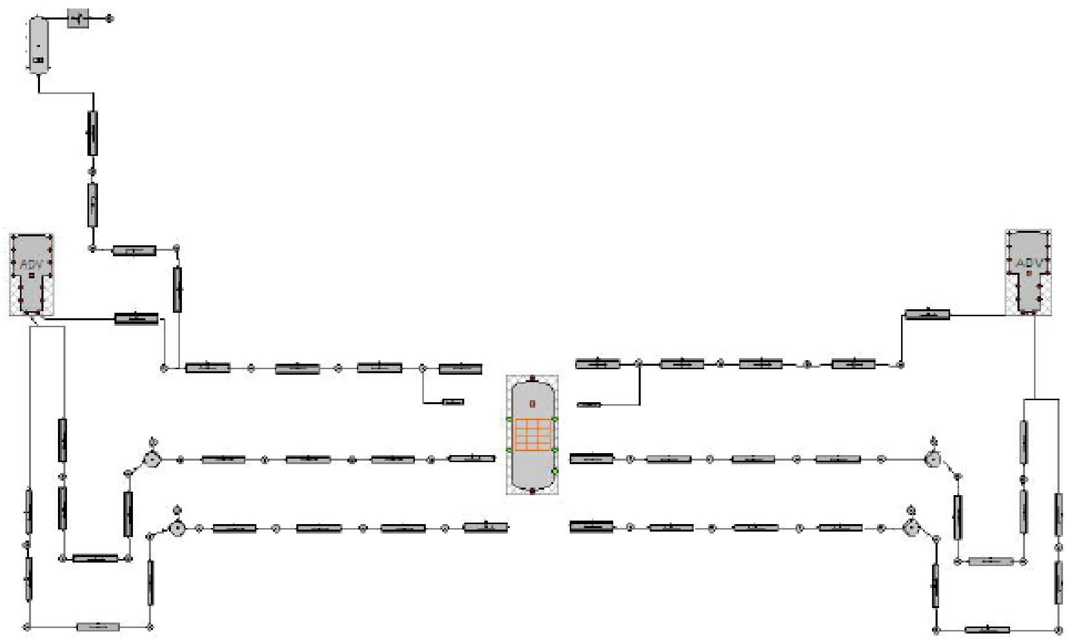

Figure 2. Primary system of ATLAS

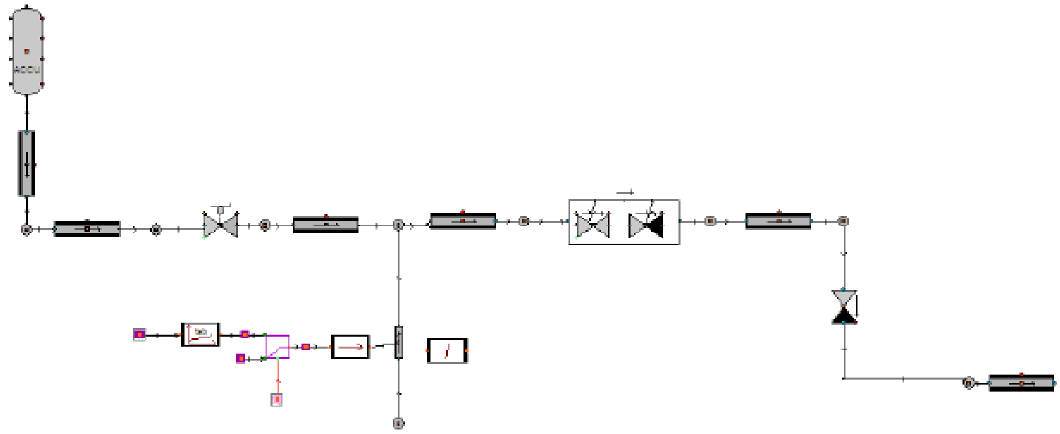

Figure 3. Safety Injection line 2

The form loss coefficients of the primary circuit were adjusted according to the given pressure drop characteristics with the mass flow rate of 100 % pump capacity in non-heated condition.

The form loss coefficients in the safety injection line were taken from the given data, expect for the flow orifice, for which no form loss coefficient was available. Therefore the form loss coefficient of the orifice was tuned with respect to the discharge test data of the ATLAS safety injection tanks.

Ready made component of APROS for advanced vertical steam generator was used to model the steam generators. Nodalization of the steam generators is shown in Figure 4. The feedwater is fed to the economizer of the steam generator. The downcomer inlet of steam generator feed water was not modelled because it was not used in the test case. Liquid level of the steam generator is kept in its set point with control valve steered by PI-controller. Steam lines include three safety valves which are modelled according to the given data.

In steady state the core is operating at constant power and the loops are in natural circulation. In order to achieve the given initial conditions in flow rates and temperature distribution, the loss coefficient of stopped reactor coolant pumps was modified. The given heat losses at steady state were achieved by modifying the heat transfer coefficient from pipe, pressure vessel and steam generator outer walls to the containment.

The break line flow nozzle was modelled with a pipe component having the given dimensions. Critical flow limitation was used for the break branch and the upwind density of the branch was used in calculation of break flow. Value 1 was used for discharge coefficient of the critical flow.

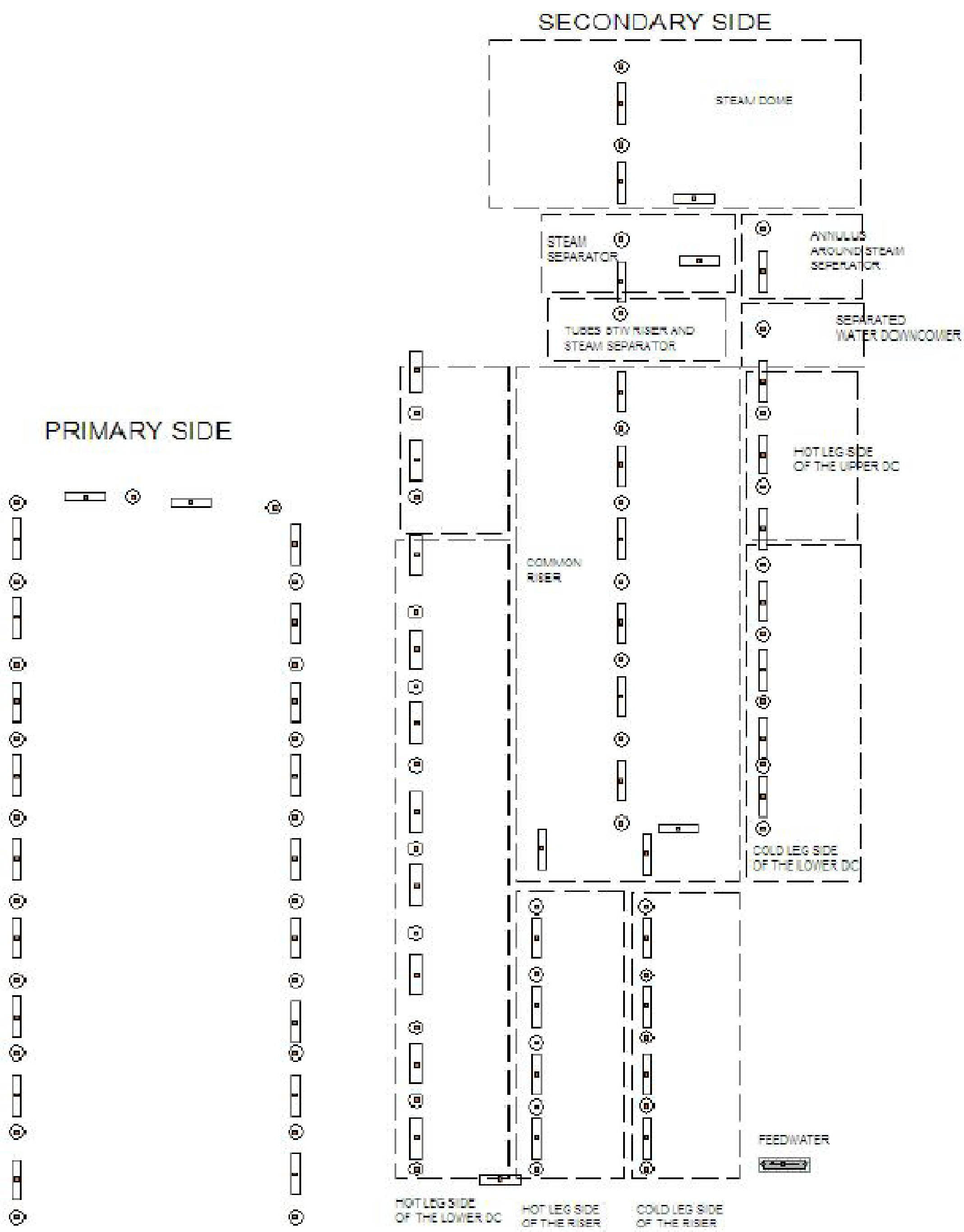

Figure 4. Nodalization of the Steam Generator

1.4 Calculation of DVI line break

The calculated transient was a 50 % break in direct vessel injection line. Steady state was first calculated for 193 seconds, after this the break was initiated by taking the given boundary condition of the downstream pressure of the break nozzle in use. The maximum time step during the transient was in the very beginning of the break 0,001s and then it was increased to 0,01 s . The minimum number of iterations during one time step was 9. Major events of the transient are show in Table 2.

Table 2. Major events during the transient

Time (s)	
193	Break initiated
229	Pressurizer pressure < 10,72 MPa Reactor Scram, Turbine isolation
234	SG safety valves open for the first time
235	Feedwater isolation
258	SIP start
756	SIT start, downcomer pressure < 4,03 MPa
2200	Calculation stopped

In the beginning of the accident leak mass flow rate reaches 6,2 kg/s. Mass flow rates in loops increase momentarily as the water is discharged through the leak. The pressurizer drains and primary pressure starts to decrease and reaches 10,72 MPa at 228 seconds. Followed by Low Pressurizer Pressure (LPP) signal the reactor is tripped and steam lines and feedwater lines isolated and one safety injection pump started with given the delays. The reactor trip is executed by taking the given boundary condition for core power in use. Following the steam line isolation, pressure in steam generators rises to safety valve opening set point in a few seconds. Void formation in upper head and reactor core occurs already before the reactor trip but after the core power drops the bubbles in core area collapse.

Pressure drop in primary circuit calms down for minute (around 280 s…320 s) as the water in reactor starts to boil again. At this point primary pressure is around 8,8 MPa. Also in upper plenum vaporization begins. Mass inventory continues decreasing as the break mass flow rate is about 4.2 kg/s. As the boiling in reactor core increases the pressure the water is pushed to the downcomer side, which together with the boiling effect causes a rapid drop of liquid level in core region. The collapsed water level in the core region (LT-RPV-01) reaches its lowest value 1,82 m at around 320 seconds, but the core is not overheated. At around 320 seconds the downcomer reaches its saturation point and void formation slows down pressure degradation and pushes the water from the downcomer to the core and core liquid level rises. The leak mass flow turns into steam and primary pressure degradation increases again.

This is followed by stable phase. Primary pressure and temperature decrease as the core boils the water with the diminishing decay heat power. The steam generated in the core is carried trough one hot leg to the cold legs and then through the downcomer into the leak. In the cold legs 1A and 1B loop seals are blocking the steam flow.

The water inventory is still decreasing slowly because the flow rate from one safety injection pump is not enough to compensate the water loss out of the leak. During this phase also the water from the upper plenum is drained to the outlet plenum, from where it is partly carried to hot legs and partly flowing down to the reactor core. The water drops carried with the steam flow to the steam generators are vaporized and the steam superheated, which consequently cools down the steam generator.

The oscillation shown in mass flow rates of hot legs results from mass flow oscillation in reactor core. The core is modelled with only one flow channel which means that during one time step water can flow to one direction only. So in order obtain back flow of water in reactor core the mass flow has to oscillate. The code calculates liquid penetration from outlet plenum to the core using CCFL correlation.

At 756 seconds downcomer pressure decreases below the discharge limit of the safety injection tanks pressure and the discharge from three safety injection tanks begins. Liquid levels in reactor pressure vessel begin to rise and shortly after this also the primary mass inventory starts to rise again. Primary pressure and temperature continue to decrease.

At about 1100 seconds a steady state in calculation is reached. The primary pressure settles down to about 2,5 MPa. The continuous flow from the safety injection tanks ends and the operating safety injection pump is enough to compensate the leak.

1.5 Conclusion

This report presents the ISP-50 analysis results calculated with APROS 5.08 simulation software. The analysis was carried out as a blind calculation. The available RELAP5 input deck of the ATLAS test facility was not utilized. During the APROS input deck preparation some shortcomings concerning needed input data was discovered and discussed with the organizer.

The model preparation and performing of the calculations on the blind ISP-50 has been extremely educational task. It will be very interesting to compare the results with the measured data and thereafter carry out the post test analysis.

1.6 References

1. Homepage of APROS simulation software http://www.apros.fi/
2. ISP-50 specifications for a Direct Vessel Injection Line Break Test with the ATLAS, Korea Atomic Energy Research Institute, June 2009.
3. ATLAS Facility and Instrumentation description Report,

4. Detailed Information on Actual Test Conditions and Procedures for ISP-50, Korea Atomic Energy Research Institute, August 2009.
5. ATLAS Facility and Instrumentation description Report (Addendum 4), Korea Atomic Energy Research Institute, December 2009.
6. Summary of ISP-50 Q&As, Korea Atomic Energy Research Institute, December 2009.

2. GRS (prepared by Henrique Austregesilo)

2.1 General information

1	Name of participants	Henrique Austregesilo
2	Organization's name	Gesellschaft für Anlagen- und Reaktorsicherheit (GRS)mbH
3	Country	Germany
4	Code version	ATHLET Mod 2.2 Cycle A
5	PC/operating system/compiler	CRAY LINUX Server under SLES 9.2 (64 bit/Opteron) INTEL FORTRAN Compiler Version 9.1 and Windows PC with INTEL Core 2, 2.4 GHz INTEL FORTRAN Compiler Version 10.0
6	Number of files submitted	2: GRS-ISP-50.pdf (this document) GRS-ISP-50.xls

2.2 Description of the computer code

The thermal-hydraulic system code ATHLET (Analysis of THermal-hydraulics of Leaks and Transients) is being developed by GRS for the analysis of the whole spectrum of leaks and transients in light water reactors. The code is applicable for western reactor designs as well as for Russian VVER and RBMK reactors. The main code features are:

- advanced thermal-hydraulics,
- modular code architecture,
- separation between physical models and numerical methods
- pre- and post-processing tools,
- portability to the prevalent computer platforms.
-

ATHLET is composed of several basic modules for the simulation of the different phenomena involved in the operation of a light water reactor:

- thermo-fluiddynamics (TFD)
- heat transfer and heat conduction (HECU)
- neutron kinetics (NEUKIN)
- and control and balance-of-plant (GCSM)

together with the fully implicit numerical time integration method FEBE. Other independent modules (e.g. 3-D neutron kinetics or containment modules) can be coupled by means of a general interface.

The thermo-fluid-dynamic module is based on a six-equation model, with fully separated balance equations for liquid and vapour, complemented by mass conservation equations for up to 5 different non-condensable gases and by a boron tracking model. Alternatively, a five-equation model, with a mixture momentum equation and a fullrange drift-flux formulation for the calculation of the relative velocity between phases is also available. Specific models for pumps, valves, separators, mixture level tracking, critical flow etc. are also included in ATHLET. The system configuration to be simulated is modeled just by connecting basic thermo-fluid dynamic elements, called thermo-fluid (TF) and heat conduction (HC) objects. Multi-dimensional processes are simulated by parallel channels with cross flows. The systematic validation of ATHLET is based on a well balanced set of integral and separate effects tests derived from the CSNI code validation matrices.

Reference:

G. Lerchl, H. Austregesilo, ATHLET Mod 2.2 Cycle A – User's Manual, GRS-P-1/Vol. 1, July 2009.

2.3 Nodalization of the ATLAS facility

Main features:

- detailed 2-loop dataset
- downcomer region represented by 4 parallel channels with cross-connection junctions (90° symmetry)
- core region represented by three parallel channels: two concentric rings (one inner core ring with 174 heated and 2 unheated rods, and one outer core ring with 216 heated and 4 unheated rods, connected by cross-connection junctions) and one channel representing the 5 guide tubes. The active core region was modeled with 11 axial nodes. Sensitivity studies with 20 axial nodes did not show any significant changes with respect to the peak cladding temperatures.
- the six-equation, two-fluid model was used in the primary system; the five-equation model together with mixture level calculation was applied in the pressurizer and in the secondary sides of the steam generators
- critical discharge flow rates calculated with the ATHLET finite-difference model CDR1D
- altogether 130 TF-Objects (101 pipes and 29 branches) and 129 HC-Objects,

corresponding to 247 control volumes, 327 junctions and 331 heat slabs.

Fig. 1 depicts the used nodalization for the primary system (pressure vessel, loops 1 and loop 2 with the pressurizer). A more detailed description of the pressure vessel is given in Fig. 2, with the downcomer split in four parallel channels (PV-DC-XX1A, -XX1B, XX2A, XX2B), the inner core ring (PV-CORE1), the outer core ring (PVCORE2), the guide tubes (PV-GUIDE) and the CEA tie tubes (PV-UP-GT). The bypasses between the downcomer and the hot legs, respectively the upper plenum, have been simulated as pipe components. Fig. 3 shows the nodalization of the SIT tanks and the corresponding injection lines, as well as the break line connected to the containment tank, which was simulated as a time-dependent volume with the given measured pressure (PT-CS-03). The SIP injection was modeled by a fill junction connected to the injection line PV-SIL-2. Finally fig. 4 depicts the nodalization used for the secondary side of the steam generators. The downcomer pipe S1-DC-B1 is connected to S1-LP, whereas the pipe S1-DC-B2 is connected to S1-RISIN. The economizer feedwater flow is injected into S1-ECO. The downcomer feedwater (S1-FW) was not used in the experiment. The SG relief valves, modeled as a fill junction connected to the main steam line (S1-MSL) were simulated within the control simulation module GCSM.

All four pictures have been generated from the input data set using the pre-processing tool AIG (ATHLET Input Graphics). In these pictures the elevation 0 m corresponds to the centerline of the hot legs. Tab. 1 presents the volume distribution of the ATLAS facility as applied in the ATHLET calculation. Since the pump model in ATHLET is a junction-related model, the actual pump volumes have been split between the intermediate and the cold legs. The volumes of the hot leg nozzles inside the pressure vessel have been assigned to the components P1-HL and P2-HL.

Table 1: Volume distribution in the ATLAS facility

Component	KAERI-TR-3779 (m^3)	ATHELET (m^3)
Primary system		
RPV – core, lower and upper plenum	0.3860	0.3765
RPV - downcomer	0.1670	0.1670
Hot leg (2x)	0.0190	0.0253
SG inlet plenum (2x)	0.0709	0.0709
SG U-tubes (2x) – active region	0.1633	0.1637
SG outlet plenum (2x)	0.0709	0.0709
Intermediate leg (4x)	0.0161	0.0179
Pumps (4x)	0.0068	
Cold leg (4x)	0.0100	0.0148
Pressurizer	0.2726	0.2735

Surge line	0.0047	0.0041
Total RCS	1.6101	1.6135
Secondary system (2x)		
SG downcomer	0.2471	0.2457
Riser	0.6739	0.6739
Separator	0.0628	0.0628
Steam dome	0.1868	0.1868
Total	1.1706	1.1692

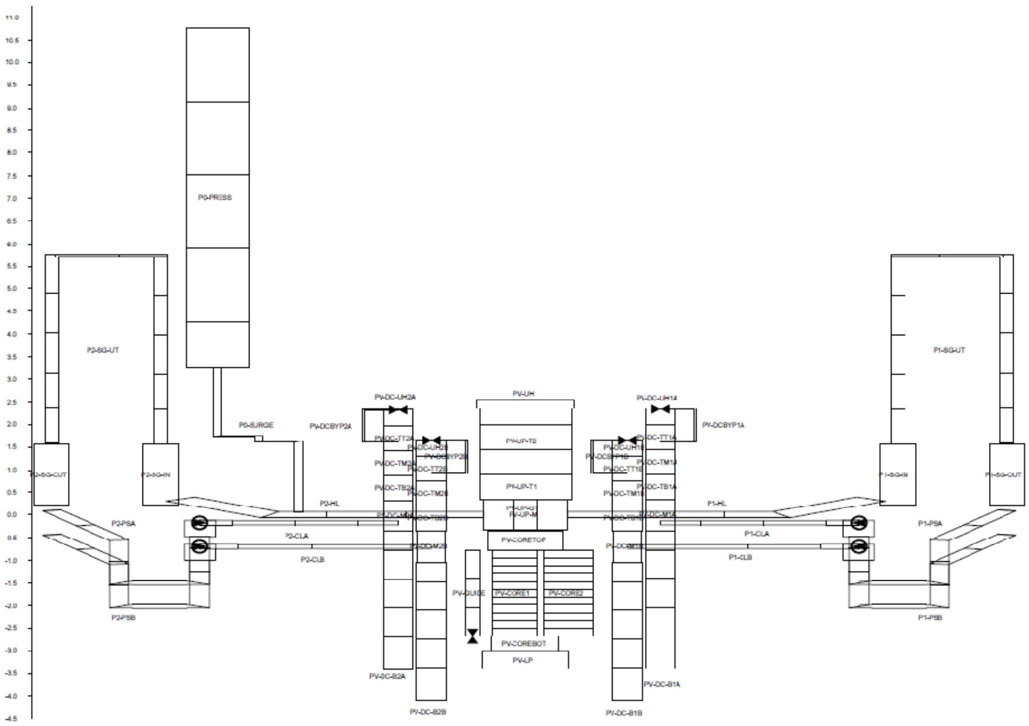

ATHLET Nodalization for the ATLAS Facility (primary circuit)

Fig. 1: ATHLET Nodalization for the ATLAS Facility (primary circuit)

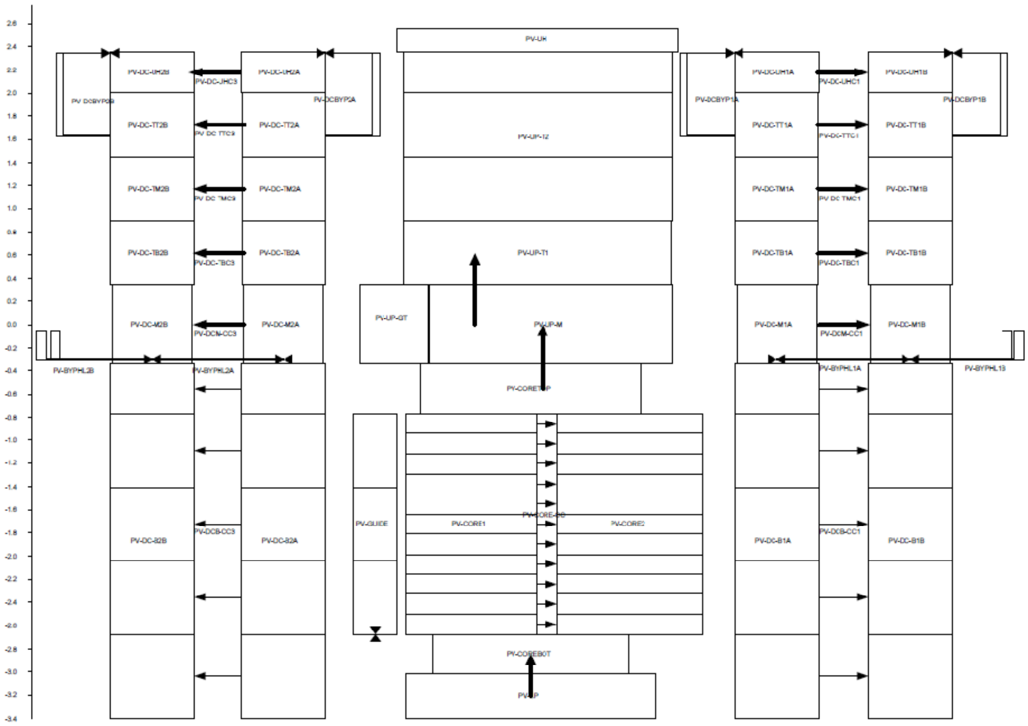

ATHLET Nodalization for the ATLAS Test Facility (Reactor Vessel)

Fig. 2: ATHLET Nodalization for the ATLAS Facility (pressure vessel)

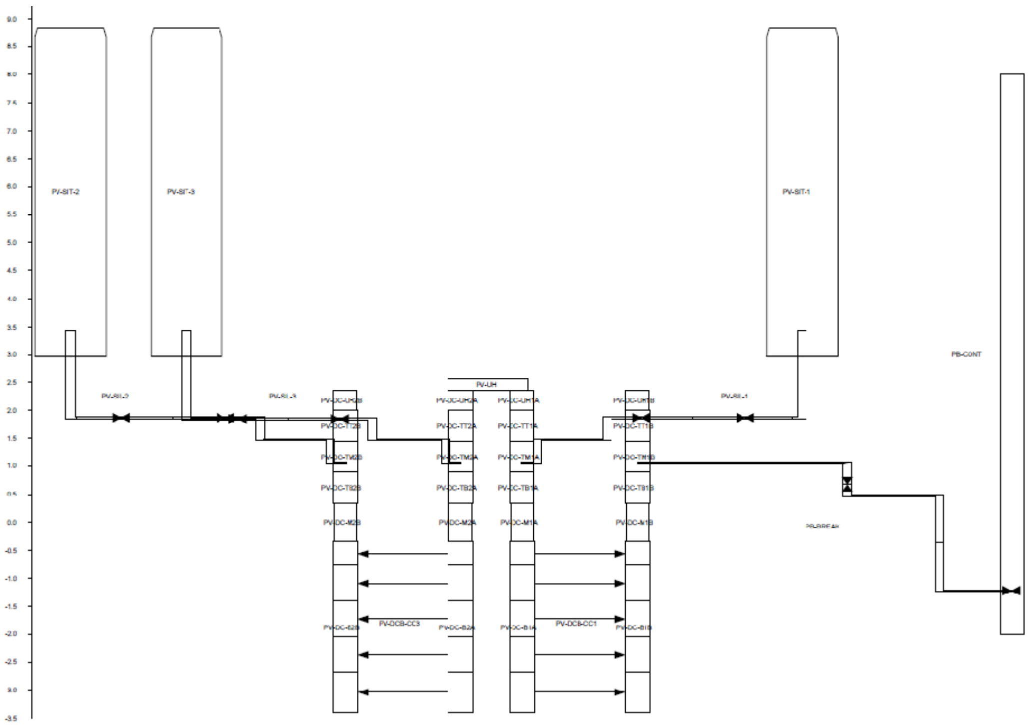

ATHLET Nodalization for the ATLAS Test Facility (SIS)

Fig. 3: ATHLET Nodalization for the ATLAS Facility (SIT tanks, injection lines and break line)

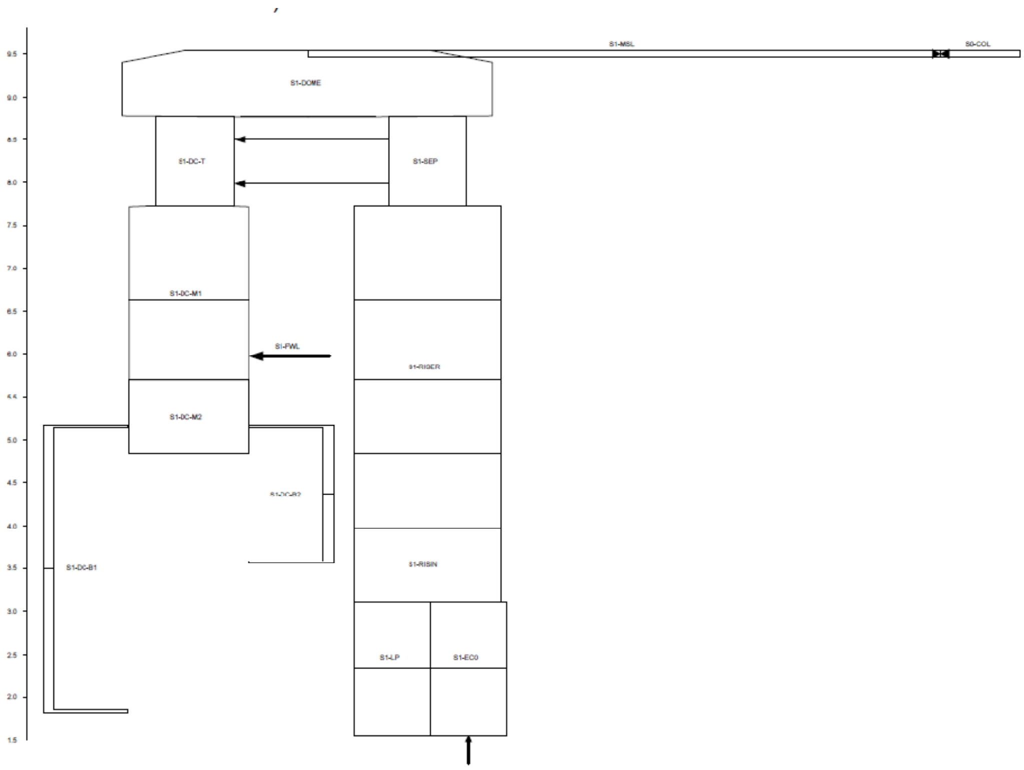

Fig. 4: ATHLET Nodalization for the ATLAS Facility (SG secondary side – loop 1)

2.4 Initial conditions

ATHLET provides a steady state calculation which initializes the complete system starting from a limited number of user-supplied initial and boundary conditions, performing mass, energy and momentum balances for the whole system. In order to check the adequacy of the calculated initial conditions, a zero-transient of about 200 s has been performed before break opening. Table 2 presents the calculated initial conditions shortly before break opening, in comparison with the measured values in the facility.

Parameter	Experiment	ATHLET
Primary system		
Core power (MW)	1.636	1.636
Heat losses (kW) - estimation	83.5	83.59
Pressurizer pressure (MPa)	15.596	15.60
Core inlet temperature (°C)	290.0	292.5
Core exit temperature (°C)	325.0	325.7
Hot leg temperatures (°C) – Loops 1 / 2	324.4 / 325.3	325.3 / 325.3
Cold leg temperatures (°C) – 1A/1B/2A/2B	292.2 / 292.1 291.8 / 292.0	292.0 / 292.0 292.0 / 292.0
RCS flow rates (kg/s) – 1A/1B/2A/2B	2.2 / 2.2 2.3 / 2.2	2.12 / 2.12 2.12 / 2.12
Bypass – downcomer to upper head (kg/s)	~ 0.0	-0.038
Bypass – downcomer to hot legs (kg/s)	~ 0.0	0.034
Pressurizer level (m)	3.32	3.29
Pump speed (RPM)	-	152
Secondary system	**SG1 / SG2**	**SG1 / SG2**
Pressure (MPa)	7.83 / 7.83	7.833 / 7.833
Steam dome temperature (°C)	295.4 / 295.6	293.6 / 293.6
FW temperature – economizer (°C)	234.4 / 235.2	235.0 / 235.0
FW flow rate (kg/s)	0.431 / 0.435	0.435 / 0.435
Water level (m)	2.03 / 1.97	2.054 / 2.053
Heat removal (MW)	0.693 / 0.774	0.790 / 0.790
Heat losses (kW) - estimation	28.5 / 28.5	28.26 / 28.26

Table 2: Comparison between measured and calculated initial test conditions

3. KEPRI (prepared by S. W. Kim)

3.1 Code environment

ISP-50 analyses were carried out with the MARS-KS safety analysis code [Ref.1]. The one-dimensional model of MARS 3.0a version was used in the analyses. The MARS-KS code is a best estimate code developed by KAERI through unifying and restructuring the RELAP/MOD 3.2.1 and COBRA-TF. The analyses were performed on the operating system of Microsoft Windows XP (32bit) and a transient calculation took about 20 hours with Intel CPU of Core i5 2.67GHz.

3.2 Modeling information

Based on the provided steady state input file of MARS code, transient input for 50% break of DVI line was prepared. To analyze DVI line break accident, a break pipe line, SITs, SIP and IRWST should be modeled. The provided steady-state model for the 8% power condition of ATLAS facility was adopted and additional safety-related components are modeled according to the given description of test facility tabulated in Table X-1. The nodalization diagram for the DVI-04 pipe line and the break simulation system is presented in Figure X-1.

Table X-1 Major parameters of the break simulation system

No.	Type	Area	Length	Hydraulic diameter	Inclined angle	Elevation change	K_f	K_r	Inner diameter
575	Sngljun	0.0	-	3.81E-02	-	-	0.5	1.0	3.81E-02
576	pipe	1.14009E-03	0.47	3.81E-02	0.0	0.0			3.81E-02
		1.14009E-03	0.4	3.81E-02	0.0	0.0	0.63	0.63	3.81E-02
		1.14009E-03	0.29	3.81E-02	-90.0	-0.29			3.81E-02
577	Sngljun	0.0	-	1.08E-02	-	-			
578	pipe	9.16088E-05	0.07	1.08E-02	-90.0	-0.07			1.08E-02
		9.16088E-05	0.07	1.08E-02	-90.0	-0.07			1.08E-02
579	Sngljun	0.0	-	1.08E-02	-	-			
580	pipe	1.14009E-03	0.15	3.81E-02	-90.0	-0.15	0.63	0.63	3.81E-02
		1.14009E-03	0.37995	3.81E-02	0.0	0.0	0.63	0.63	3.81E-02
		1.14009E-03	1.69	3.81E-02	-90.0	-1.69	0.63	0.63	3.81E-02
		1.14009E-03	0.4965	3.81E-02	0.0	0.0			3.81E-02

Three available safety injection tanks and the passive control of discharge flow with the fluidic devices (FD) were modeled with the "accumulator" component in MARS according to the descriptions as tabulated in Table X-2. A safety injection pump was simulated with boundary condition of "time-dependent junction" of MARS code and an IRWST connected to

SIP was modeled with "time-dependent volume" of MARS code. The provided conservative 1973 ANS decay heat curve with a 1.2 multiplication factor was considered with the tables for power vs. time to simulate the decay heat in transient calculation. The sequence of major events, include LPP trip, and the delay time of component activation were modeled with trip according to the specifications. The feedwater junctions were replaced for the simulation of the feedwater isolation activated by the trip signal. The main steam isolation valve was modeled with a "trip valve" activated by turbine isolation signal.

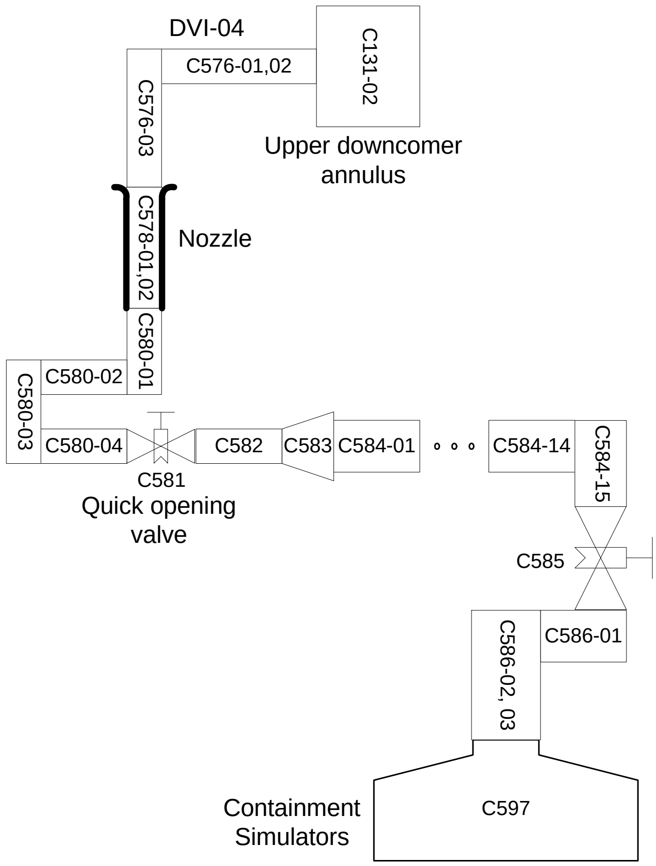

Figure X-1 Nodalization diagram for the DVI pipe line and the break simulation system

Table X-2 Major parameters of the safety injection tanks

	SIT1	SIT2	SIT3
Length of stand pipe	1.45288	1.45288	1.45288
Level of liquid	3.00872	3.02016	3.05448
Effective liquid volume	0.186740	0.186740	0.186348
Liquid volume	0.205923	0.206706	0.209055
Surgeline length	12.8920	13.0020	12.8750
Elevation	4.25128	4.24984	4.18552

3.3 Steady state analysis results

The steady state condition was calculated with the provided steady state input file of MARS code. For a sensitivity study on the critical flow models, several steady state conditions were calculated with the options for Henry-Fauske model, Ransom-Trapp model and Moody model. Despite the critical flow model has no effect on steady state condition, the MARS code does not allow a user to switch between the two critical flow models in the middle of a problem. The plotted analysis result on MARS user interface screen of user-selected variables in the steady state analysis 8% power condition of ATLAS facility is depicted in Figure X-2.

Figure X-2 Steady state analysis result on MARS user interface

3.4 Transient analysis results

The transient calculations were carried out for 2000 seconds. The break occurs at 0.0 second. For the reference case which adopts Henry-Fauske critical flow model, calculated major sequence of events are summarized in Table X-3. The pressure of primary system reached a set point of low pressurizer pressure (LPP) trip at 25 seconds. The high pressure safety injection (HPSI) started to inject ECC water through the intact DVI nozzle after LPP trip signal with a delay of 28.28 seconds.

Table X-3 Calculated major sequence of events

Event	Time[s]	Remarks
Initiation of break	0.0	
LPP trip	25.44	
MSIV closure	25.54	
Reactor scram	25.79	
RCP trip	25.79	
Turbine trip	25.89	
Main feedwater isolation	32.51	
SIP activation	53.72	HPSI-2
SIT valve open	422.58	SIT-1,2,3

And three safety injection tanks were activated at 422.58 seconds when the pressure of upper annular plenum decreased to 4.04MPa.

The generated power in core and the power removed by primary coolant and steam generators are depicted in Figure X-3. In the steady-state condition, the decay heat and the removed heat by primary coolant in core subchannels were balanced, however the removed heat abruptly increases mainly due to increase of mass flowrate of suchannels. The removed heat in the steam generators becomes zero in 200 seconds.

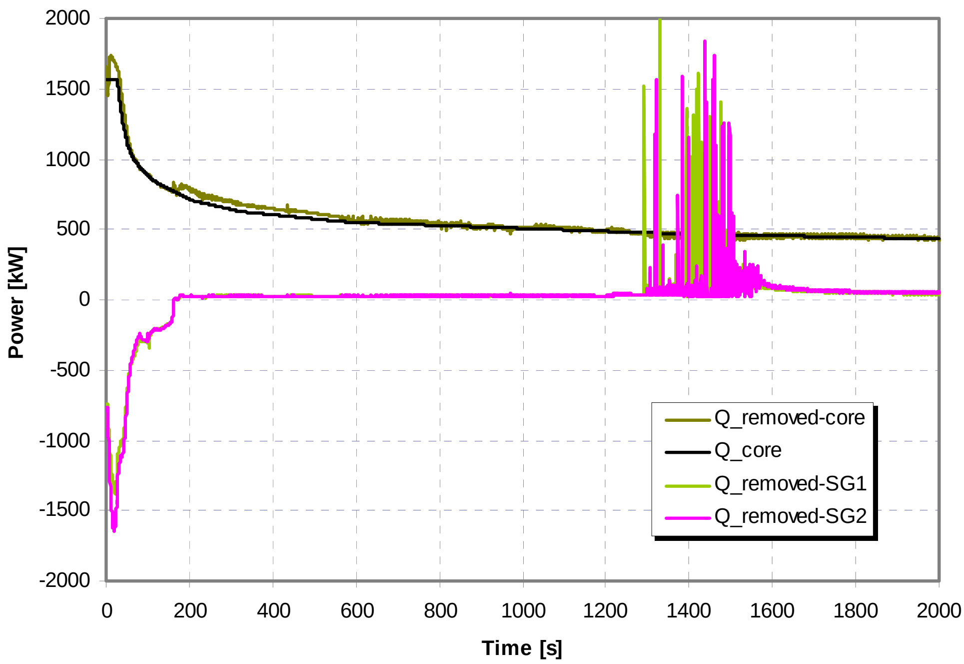

Figure X-3 Transient power behavior in reference case

The transient behaviors of pressure are presented in Figure X-4. The primary coolant pressure shows rapid decrease in 50 seconds before the activation of safety injection. After the activation of the safety injection pump at 54 seconds and the opening of safety valves at 423 seconds, the pressure decrease asymptotically.

The pressure of steam generator steamdome increases at 26 seconds due to MSIV closure and decreases gradually due to cooling of secondary system as shown in Figure X-5. The pressure of the SIT shows exponential decrease after 423 seconds and the pressure of the downstream of the break nozzle decreases caused by break and choking phenomena.

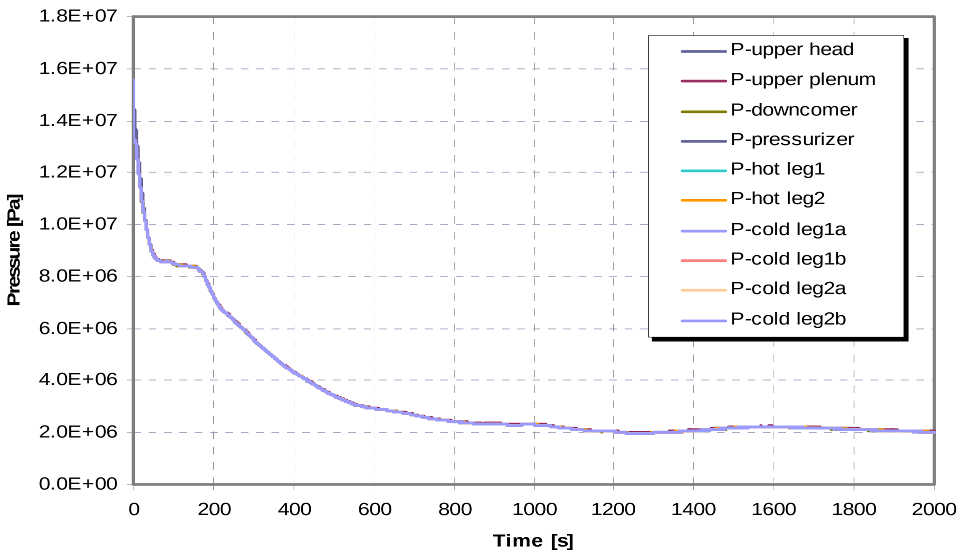

Figure X-4 Transient pressure of primary system

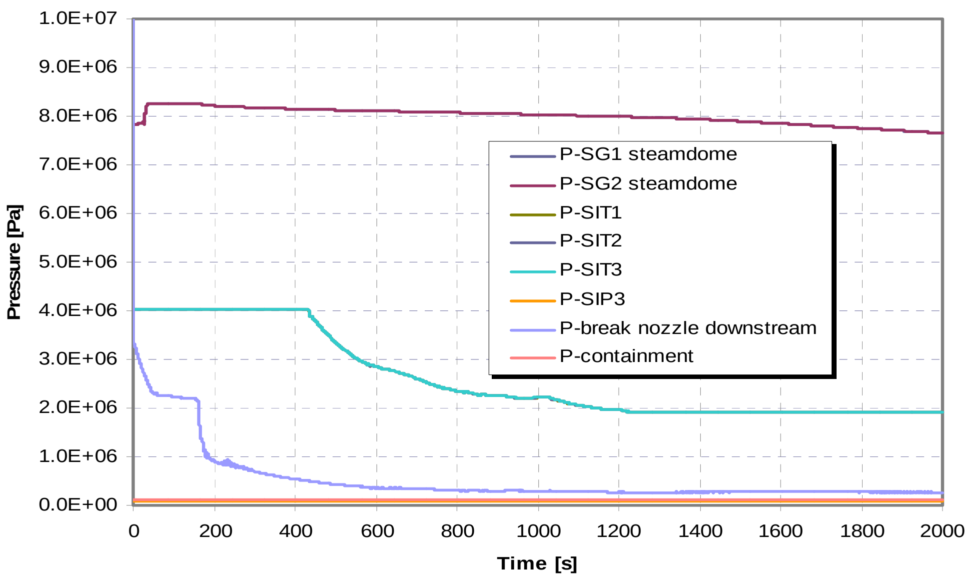

Figure X-5 Transient pressure of SG, SIT, break and containment

The liquid temperatures of primary and secondary coolant are presented in Figure X-6 and X-7. Due to the depressurization of systems and power decay, the temperature of system decreases rapidly before 70 seconds and slowly in later phase of the transient. In the steam generators, the temperature gradually decreases except the primary-secondary interfaces for the absence of heat sink.

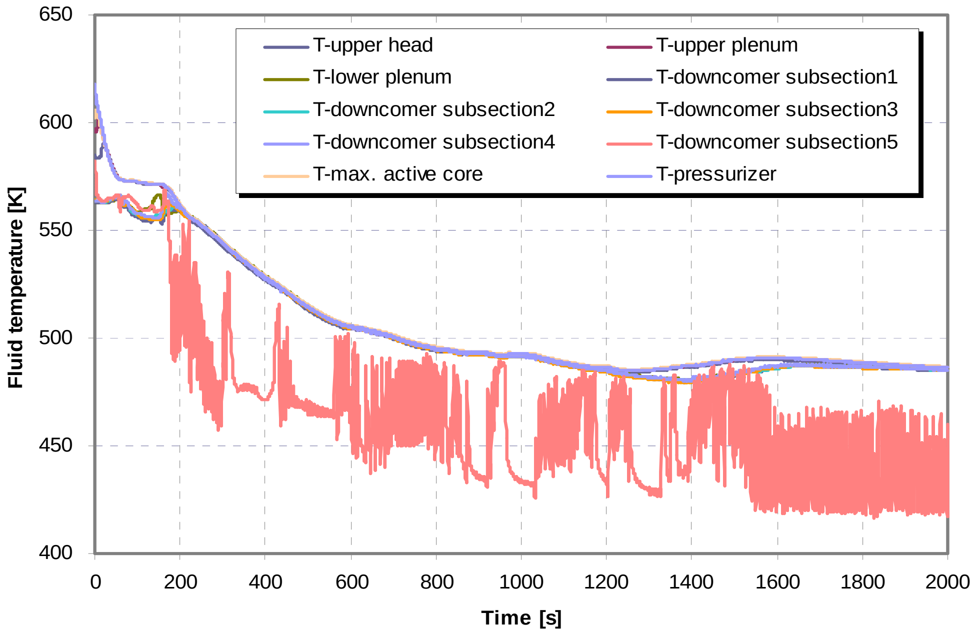

Figure X-6 Transient temperature of primary system

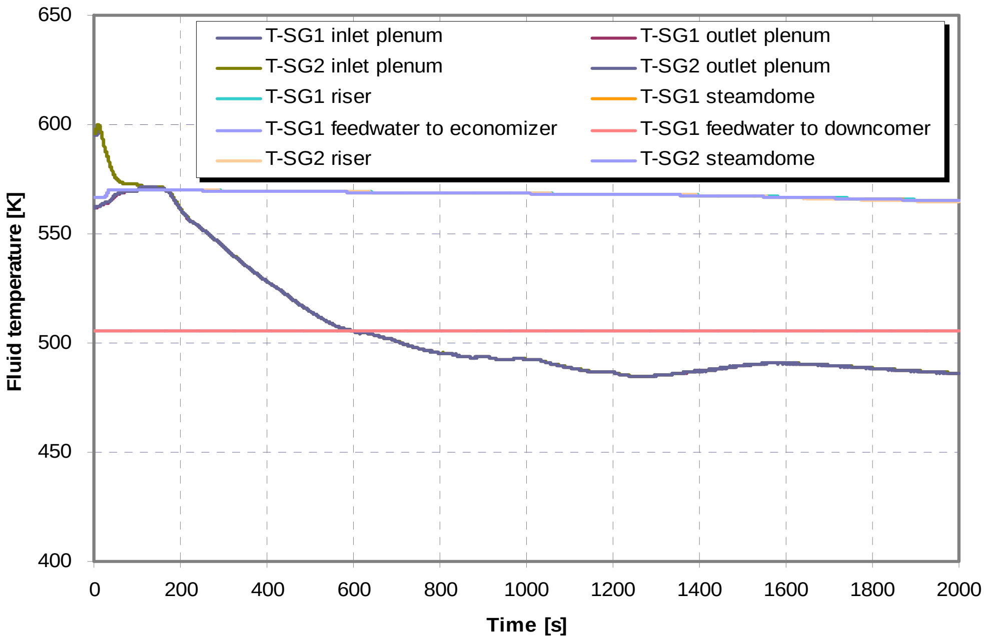

Figure X-7 Transient temperature of secondary system

The wall temperatures of downcomer and the maximum temperatures of heat structure in core are depicted in Figure X-8. Because the peak cladding temperature (PCT) dosen't appear in the calculation, the general trend of wall temperature decrease is similar with the transient behavior of the fluid temperature. Therefore, no meaningful phenomena of level change in downcomer and core region are observed.

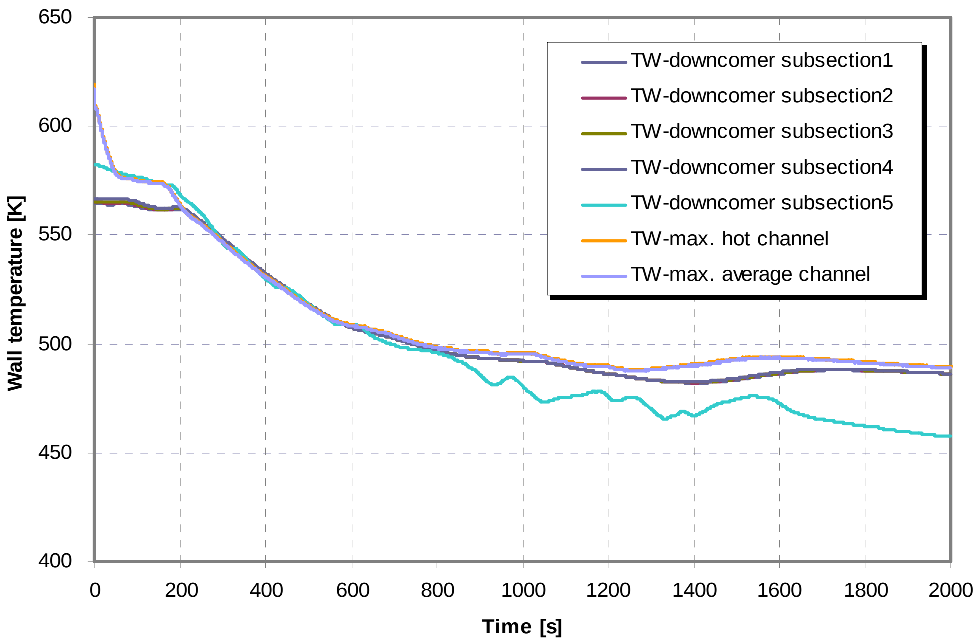

Figure X-8 Transient temperature of cladding and downcomer wall

The transient behaviors of mass flowrates of coolant are shown in Figure X-9 and X-10. Due to the DVI line break, the mass flowrates of primary system show peak and fluctuation caused by abrupt pressure transient. The main reason of frequent fluctuation of mass flowrate of hot leg after 600 seconds is the abrupt phase change in the control volumes.

At the view point of the mass balance at the upper downcomer which the broken DVI line is connected, the major inflow sources of the break flow are the crossflows from horizontally connected neighbor volumes as depicted in Figure X-10. The pressure difference between the upper downcomer and the DVI line is the most dominant force when compared to the gravity. About 160 seconds, the water level cross the upper downcomer volume and the volume is filled with vapor as presented in Figure X-11. At the downstream of the break nozzle, the void fraction is nearly 1.0 in the early phase of the transient due to the evaporation in the volume because of the depressurization. The vaporization in the nozzle downstream is mainly caused by the expansion process in flow direction.

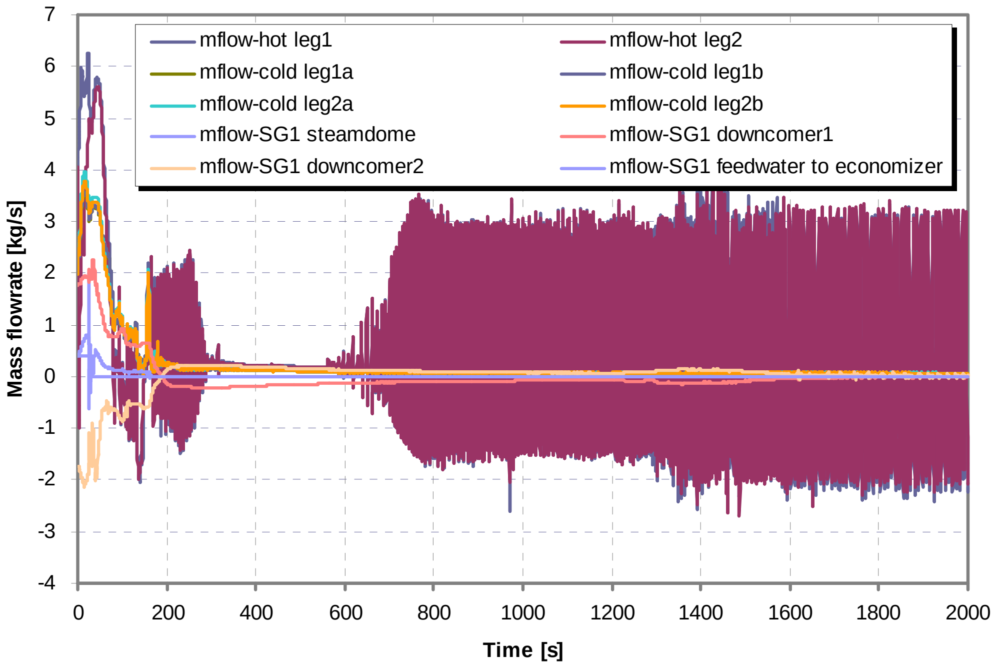

Figure X-9 Transient mass flowrate in system

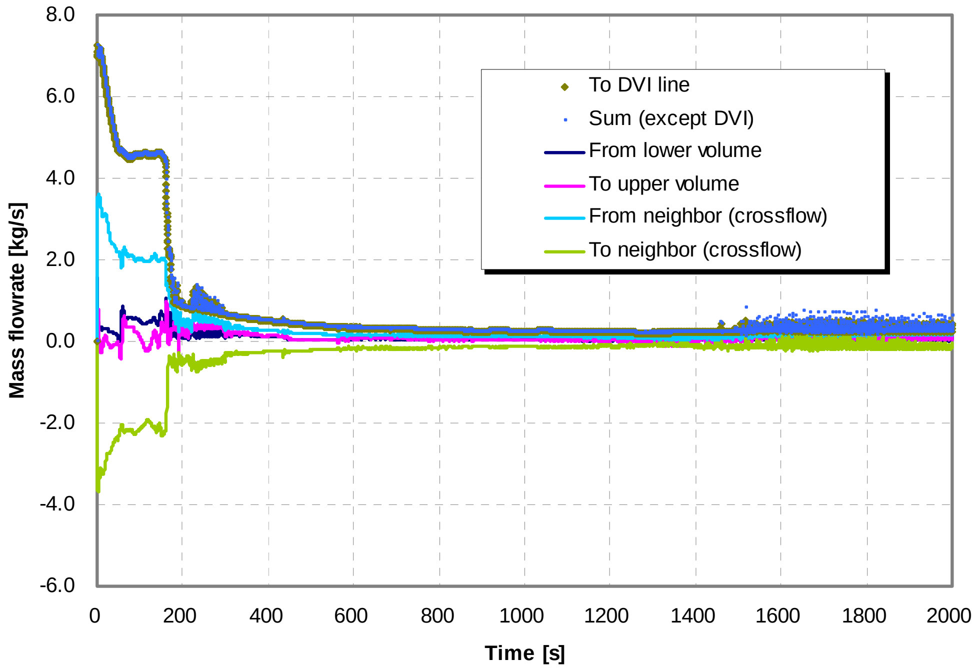

Figure X-10 Transient mass flowrate at upper downcomer volume

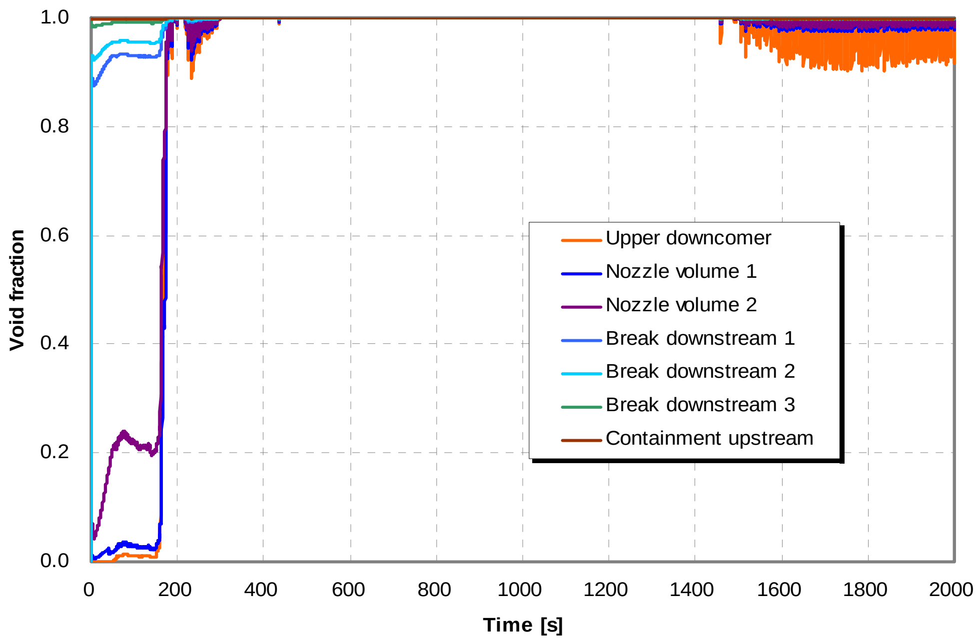

Figure X-11 Transient behavior of void fraction in broken pipe

The transient behavior of the accumulated mass budget of primary system is calculated with the inflow mass which includes the transient SIT and SIP massflow and the outflow mass through break nozzle. For 160 seconds, the mass of primary system rapidly decreases as shown in Figure X-12. After the SIP activation at 54 seconds and SIT valve open at 423 seconds, the water inventory balances on -790 [kg], that is 1590 [kg] in total mass.

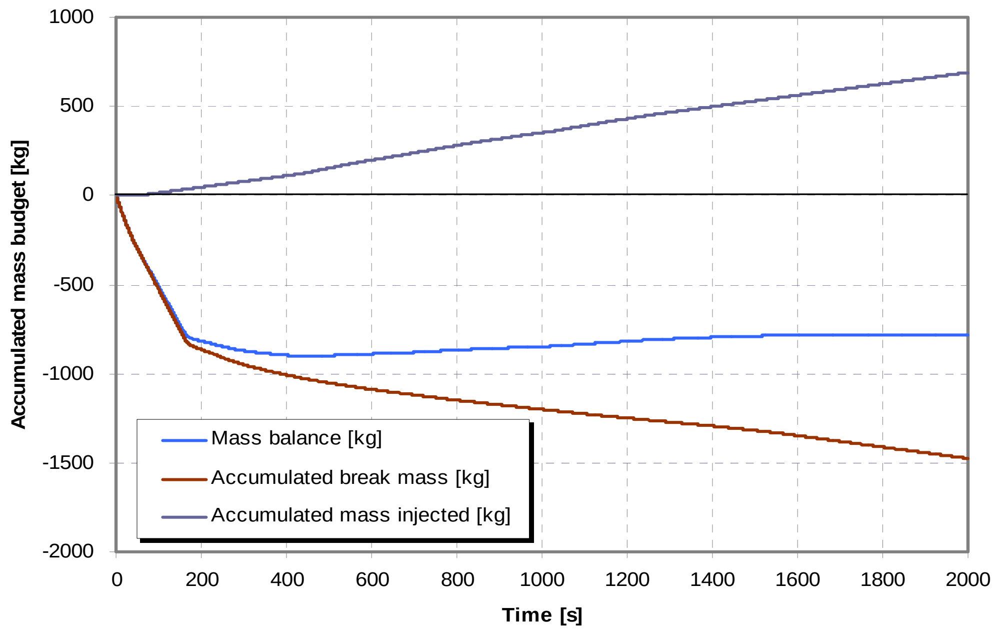

Figure X-12 Transient behavior of accumulated mass budget of primary system

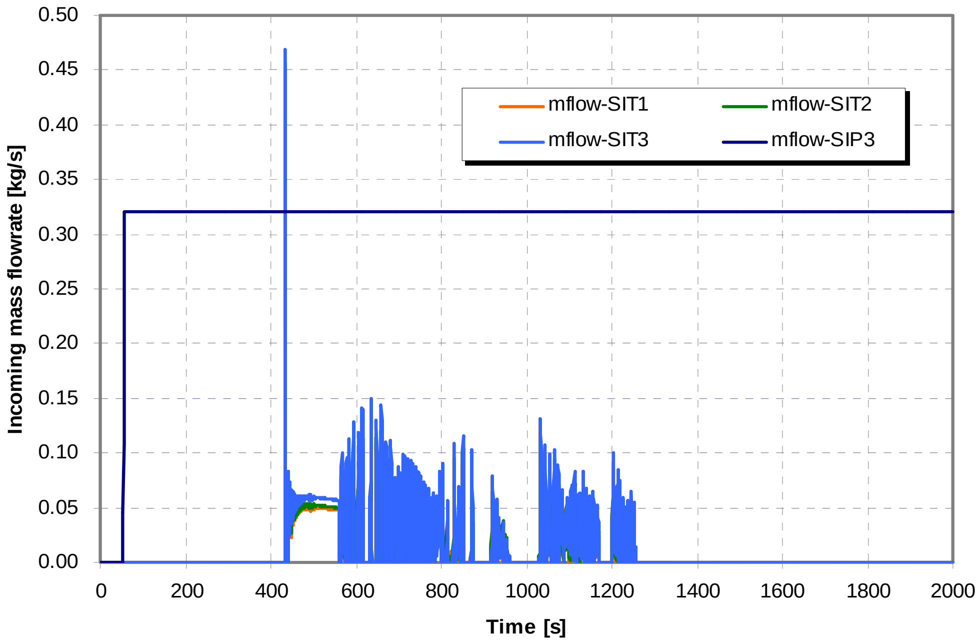

Figure X-13 Transient behavior of incoming mass flowrate

When compared to the SIP mass flowrate, the SIT mass flowrate is intermittent and the magnitude is relatively small as shown in Figure X-13. Therefore, role of SIP in the transient is dominant.

3.5 Sensitivity studies

Table X-4 Comparison of major sequence of events

Event	Ransom-Trapp	Moody	Modified Cd(Case1)	Modified Cd(Case2)	No break downstream
LPP trip	51.13	24.68	25.40	37.37	25.44
MSIV closure	51.24	24.78	25.50	37.47	25.54
Reactor scram	51.48	25.03	25.75	37.72	25.79
RCP trip	51.48	25.03	25.75	37.72	25.79
Turbine trip	51.59	25.13	25.85	37.82	25.89
Main feedwater isolation	58.20	31.75	32.47	44.44	32.51
SIP activation	79.42	52.96	53.68	65.65	53.72
SIT valve open	464.03	494.74	456.07	942.77	423.72

For a sensitivity study of the break flow and the transient behavior on critical flow conditions, several calculations were carried out. For the critical flow model, the options for Ransom-Trapp model and Moody model were used. And for the Henry-Fauske model, that is reference case, the discharge coefficient for liquid and vapor were varied as 0.9 and 7.6 times respectively (case1) and as 0.5 and 2.0 times respectively (case2).

To investigate the effect of pipe model of the break downstream, a calculation in which the break nozzle was directly connected to the containment was carried out also. The calculated major sequences of events in five cases are summarized in Table X-4.

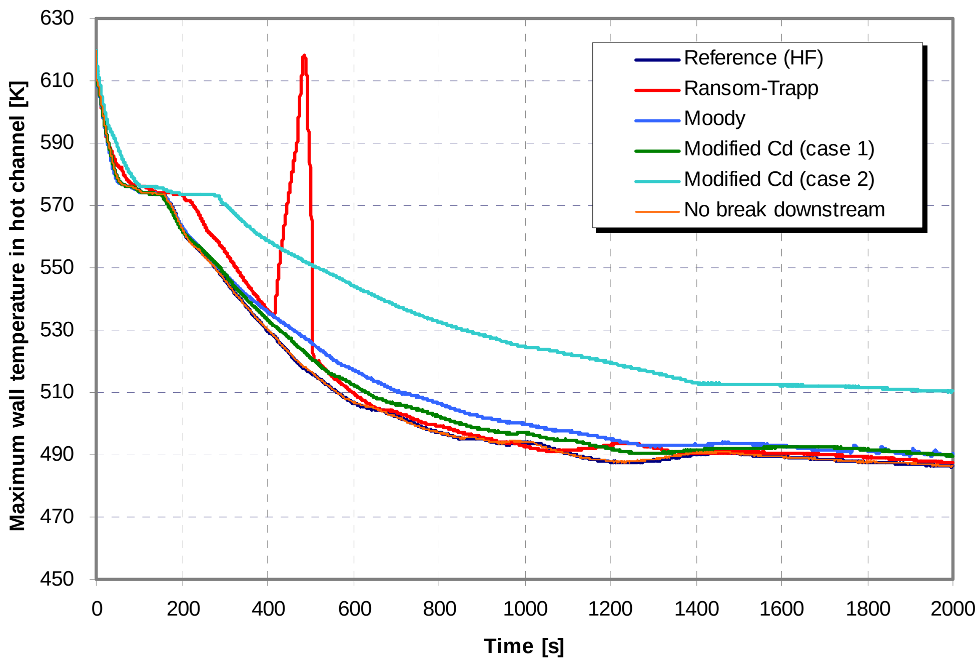

Figure X-14 Comparison of maximum cladding temperature

In Figure X-14, the calculation results for the maximum cladding temperature are presented. The peak cladding temperature is observed only in the case using Ransom-Trapp critical flow model. At 400 seconds, the collapsed water level in active core become lower than 1.9 [m] and the core uncovery occurs. When compared to the reference case, the water inventory in case using Ransom-Trapp critical flow model is slightly smaller (about 0.4%) than that of the reference case. The mass flowrates at break nozzles are in similar range for the cases of the reference, Henry-Fauske model with modified discharge coefficient (case 1), no break downstream and Moody model as presented in Figure X-15. However, for the case of Henry-Fauske model with half liquid discharge coefficient (case 2) the mass flowrate is almost half but sustains twice period. As a result, the accumulated break mass of the case 2 differs from that of the reference case about 40% at early phase and 6% at later phase. However, the significant characteristics of transient break flow are observed also in the simulation of case 2. The accumulated break mass of the case using Ransom-Trapp critical flow model become similar to that of the reference case, the difference is about 1% at 500 seconds. Without break downstream model, the pressure of the break downstream is lower than that of reference case about 12% for 150 seconds of the early phase of the accident. However, the difference of the mass flowrate through the break nozzle is about 2% in average value compared to the reference case due to the choking phenomenon. The pipe model of the break downstream has effect on the pressure of the near downstream of the break nozzle but on the general transient behavior of the systems.

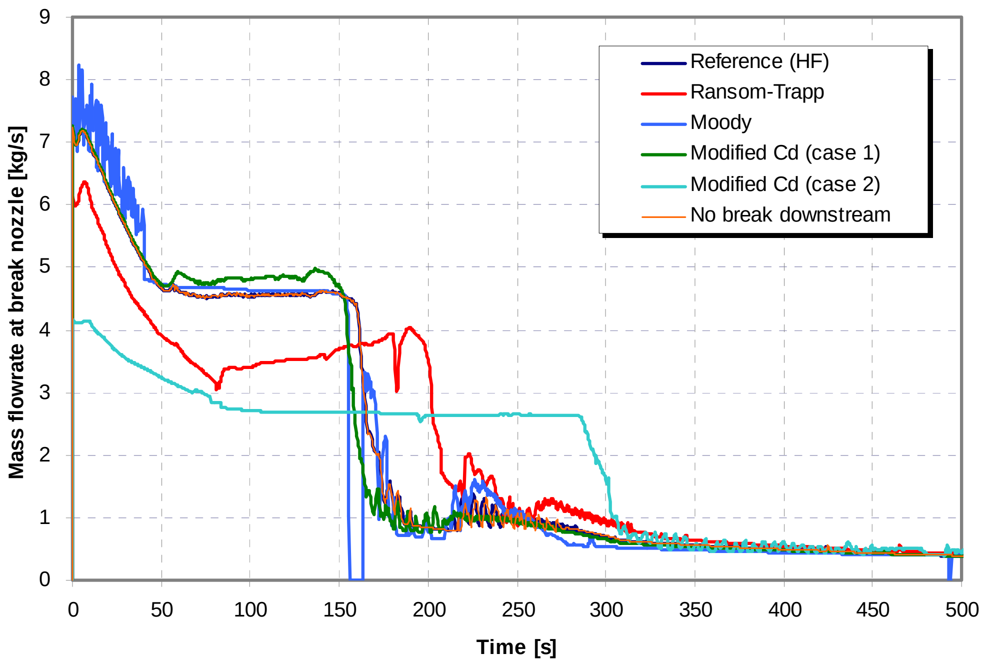

Figure X-15 Comparison of break mass flowrate

3.6 Summary and comments

With the MARS-KS safety analysis code, transient analysis for 50% break of DVI line was carried out. The provided steady-state model for the 8% power condition of ATLAS facility was adopted and additional safety-related components are modeled according to the given description of test facility. The transient calculations were carried out for 2000 seconds. The low pressurizer pressure trip signal generated at 25 seconds.

The transient behavior of primary coolant pressure shows rapid decrease in 50 seconds before the activation of safety injection. After the activation of the safety injection pump at 54 seconds and the opening of safety valves at 423 seconds, the pressure decrease asymptotically.

The pressure of steam generator steam dome increases at 26 seconds due to MSIV closure and decreases gradually due to cooling of secondary system. The pressure of the SIT shows exponential decrease after 423 seconds and the pressure of the downstream of the break nozzle decreases caused by break and choking phenomena. In the steam generators, the temperature gradually decreases except the primary-secondary interfaces for the absence of heat sink. Because the peak cladding temperature (PCT) doesn't appear in the calculation, the general trend of wall temperature decrease is similar with the transient behavior of the fluid temperature. At the upper downcomer to which the broken DVI line is connected, the major inflow sources of the break flow are the cross flows from horizontally connected neighbor volumes. At the downstream of the break nozzle, the evaporation occurs due to the expansion process. In early phase of transient the mass of primary system rapidly decreases, and the water inventory balances after the SIP and the SIT activation. In the mass budget of system, role of SIP in the transient is dominant when compared with the contribution of the SIT. In the sensitivity analyses, the effect of the critical flow model on the transient behavior was studied. Six case of the break flow model were investigated. For the case using Ransom-Trapp critical flow model, the peak cladding temperature is observed. The pipe model of the break downstream has effect on the pressure of near downstream of the break nozzle but on the general transient behavior of the systems. The other case of sensitivity studies, no significant effect of variation of critical flow was observed.

3.7 Reference

[Ref.1] Korea Institute of Nuclear Safety, Expert training course for the regulatory auditing safety analysis, KINS/TR-143, 2007

4. Gidropress (GP1 and GP2)

GP1: prepared by Igor Cheremisov

GP2: prepared by Vladimir Shchekoldin

4.1 Brief KORSAR/GP features description

KORSAR/GP is a best-estimate code and intended for calculation analysis during stationary, transient and accident conditions for nuclear facilities. KORSAR/GP is approved by Russian authorities and widely used in VVER design practice. KORSAR/GP thermohydraulic processes bases on absolutely non-equilibrium two-fluid model (three conservation equation for each phase: steam and water) in 1-D approach. Calculation of neutron physics processes is provided using of point or 3D neutron kinetics model. Problem formation in KORSAR/GP is realized in the ideology of flexible topology scheme, i.e. various problem solving does not require recompiling of code executable file. Coding of initial data is made by means of special DLC language (Data Language for Codes) designed for KORSAR/GP. KORSAR/GP code consists of a set of specialized program modules. Behaviour of each equipment component is calculated by means of these modules.

Input data file is a text file written as a DLC language program according to user developed nodalization scheme. The file consists of a set of procedures that allow to describe links between elements and unique conditions for each element of a nodalization scheme. Special features are provided to program control system operation, movements of elements of thermohydraulic systems (e.g. executive mechanisms of flaps, valves and so on). Real physical systems are simulated in KORSAR/GP code by means of hydrodynamic and thermodynamic models. Main of them are given in Table 1.

Table 1. Main KORSAR/GP models

Name	Application domain	Program name
Channel	Pipelines, tanks, pressuriser	CH
Simplified channel	Breaks, relief devices	SCH
Collector	Several channel junctions, link between channel and simplified channels	COL
User defined boundary volume	Boundary condition definition, huge tanks	BVOL_T
Hydro accumulator	Closed tanks with gas partially filled with water	ACCUM
Steam water vessel	Steam generator, separator, pressurizer	SLVES
Blind junction	Dead end conditions	BLJUN
Connection-branch	Critical flow, throttling orifices	JUNB

Name	Application domain	Program name
Local resistance	Local resistance	LR
Slide-valve	Valve	VAL
User defined mass source	Source, bleed of medium	SMASS_T
Heat conducting structure	Metal walls, power sources, fuel rods	HCS
User defined heat generation	Specified power in heat conducting structure	QHCS_T
User defined boundary condition on heat exchange	Thermal boundary conditions set up	BHEAT

4.2 KORSAR/GP input file description

Input data files for ATLAS facility were developed according to [1]. Each of three input files has specific features, but in the whole ATLAS models was made in similar way. Brief description of version schemes is given below.

Nodalization schemes of variant GP1 are given in Figures 1-4. Reactor nodalization scheme is given in figure 1. The core consists of three independent thermohydraulic channels with different power according to power group given in specification (3.2.1.2). Loop with pressurizer nodalization scheme is given in Figure 2. Both cold legs are identical, so only one is presented. Loop without pressurizer is similar. Figure 3 shows DVI-2 scheme. DVI-1, DVI-3 are identical except of SIP. Secondary side scheme is given in Figure 4. Steam generator consists of two economizer parts (ch6130, ch6131, ch6110, ch6111), main heat exchange part (ch6120) and separator (slves6140). Tubes of steam generator are simulated by one U-tube. Safety system elements are given in table 2. SIP is simulated by boundary condition – specified flow rate depending on pressure in connection point.

Table 2 Safety system elements (GP1)

Name	Designation		
Channel number	1	2	3
Tank	accum4110	accum4210	accum4310
Tank pipelines	ch4110	ch4210	ch4310
Pump		smass_t4010	

ATLAS nodalization scheme of variant GP2 is given in Figure 5. Hydraulic reactor model consists of several ch elements simulating different reactor components: downcomer, core, upper plenum. The core is simulated by one channel (ch3) comprising all fuel rod groups. HCS element simulates the rods axially divided into 11 levels and corresponding to power profile.

Cold legs are identical and set by ch elements (ch15001-ch15004). Pressurizer (ch140) is connected to the hot leg of loop 2 (ch12902). The loop without pressurizer is modeled by one element ch12901. There are 3 SIT and 1 SIP channels that are connected to reactor downcomer. SIP is simulated by boundary condition – specified flow rate depending on pressure in connection point.

Steam generators are simulated by slves elements (slves1, slves2). Primary to secondary side heat exchange is modeled by a set of ch and hcs elements (176 U-tubes). Feed water is supplied only to economizer. Break is simulated by sch500. Containment is modeled as a boundary volume with constant pressure.

The key points of nodalization differences are summarized below. There are no collectors in GP1 scheme all channels are connected directly. It results in different ways of numerical solution inside the code. Figures 4, 5, 10 show that there are some difference in SG modeling. GP2 has more detailed SG primary side model and simple secondary side. Slves is a point element, so water inside this element has a single temperature. Water temperature is close to SG saturation temperature in this case. Roughly, core inlet temperature cannot be lower than SG water temperature. That is why in GP2 secondary side pressure was reduced in order to obtain required core inlet temperature. GP1 SG models consist of spatially distributed elements (ch) so in these cases there is spatial distribution of water temperature inside SGs. Hence core inlet temperature depends not only on SG pressure but feed water temperature and flow rate.

Initial steady state conditions for variants and the experiment are given in table 4 in comparative way. RCS flow rate is based on energy balance according to Korean side answer (Summary Q&A, p.22), that is why it was reduced in comparison to measured experimental value.

Table 4. Initial steady state conditions.

Parameter	Experimental value*)	Calculated values	
		GP1	GP2
Core power, MW	1,636	1,636	1,636
PRZ Pressure , MPa	15,596	15,61	15,55
Core inlet temperature, °C	290	290,5	290
Core outlet temperature, °C	325	324,8	325.1
Hot leg temperature, loop 1, °C	324,4	324,6	325
Hot leg temperature, loop 2, °C	325,3	324,6	325
Cold leg temperature, loop 1A, °C	292,2	290,3	290,2
Cold leg temperature, loop 1B, °C	292,1	290,3	290,2
Cold leg temperature, loop 2A, °C	291,8	290,3	290,2
Cold leg temperature, loop 2B, °C	292,0	290,3	290,2

RCS flow rate, kg/s	2,2	2,0	2,0
Pressurizer level, m	3,32	3,32	3,22
Steam generator pressure, MPa	7,83	7,86	7,44
Feed water temperature, °C	234,4/235,2	232,2	-
Economizer feed water temperature, °C		235,0	225
Feed water flow rate, kg/s	0,0	0,0	0,0
Feed water flow rate to economizer, kg/s	0,431/0,435	0,434	0,425
Steam generator water level, m	2,03/1,97	2,0	2,0
SIT pressure, MPa	4,19/4,21/4,23	4,2	4,2
SIT temperature, °C	50,2/50,5/50,1	50	50
SIT Levels, %	95,0/95,2/94,3	95,0/95,2/94,3	95,0/95,2/94,3

*) according to [2] (table 2 page 5).

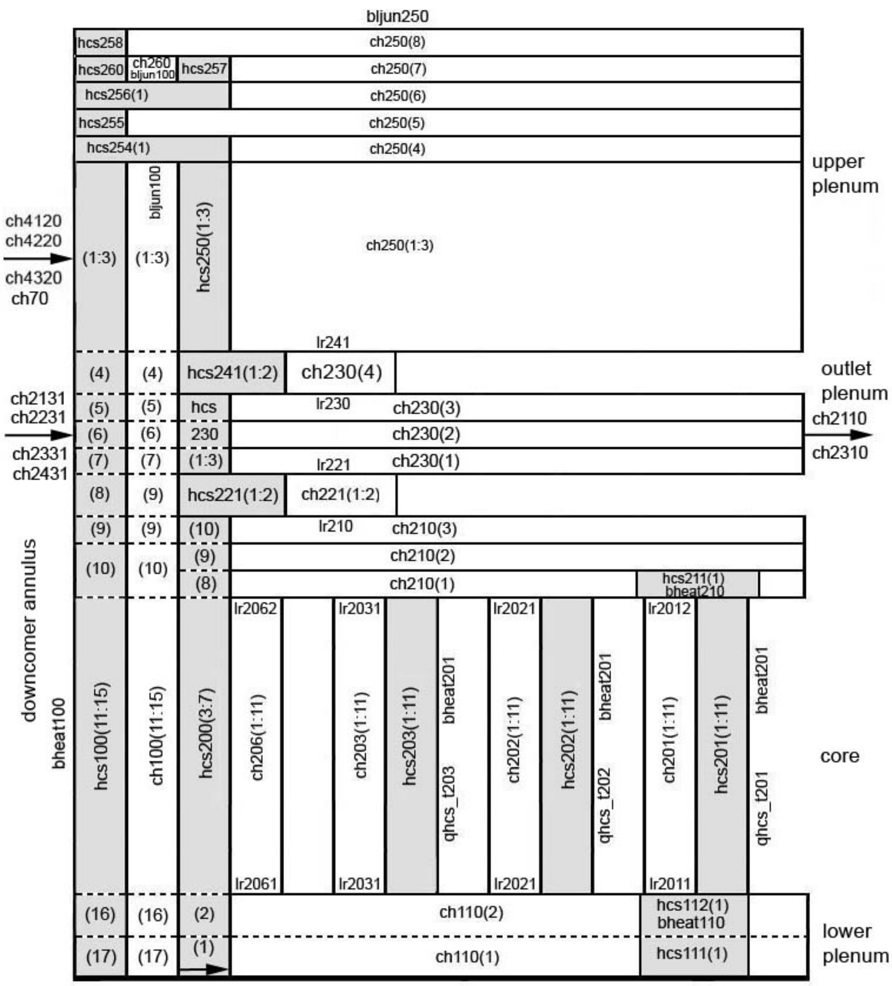

Figure 1 – Reactor nodalization scheme

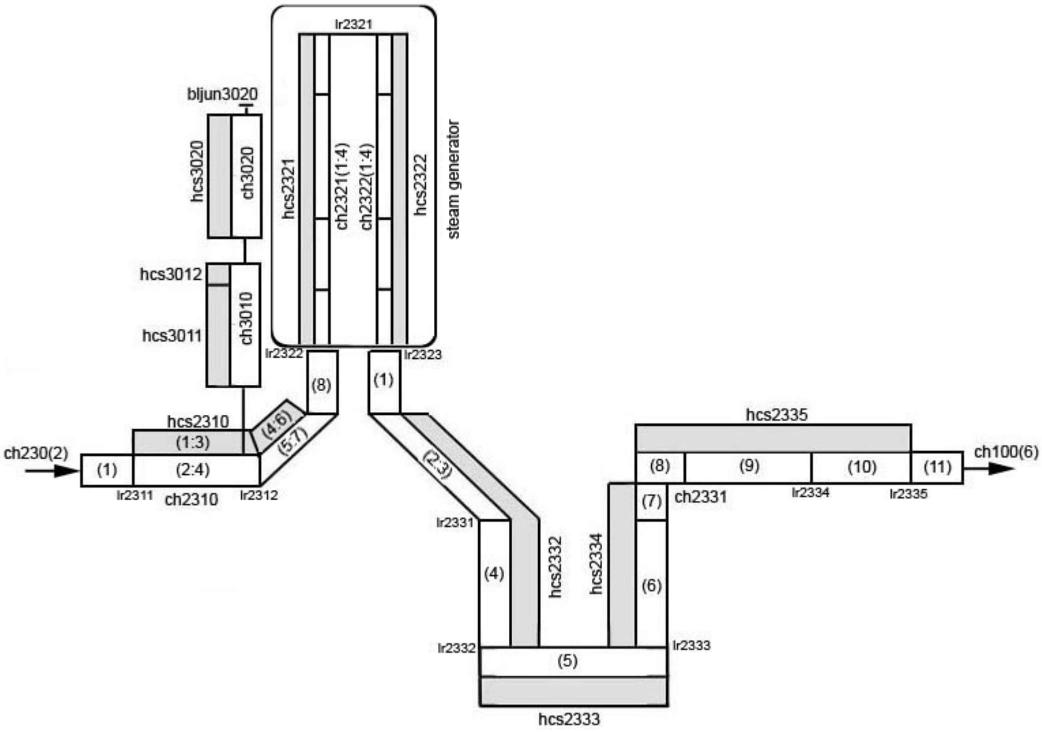

Figure 2 – Primary circuit nodalization scheme

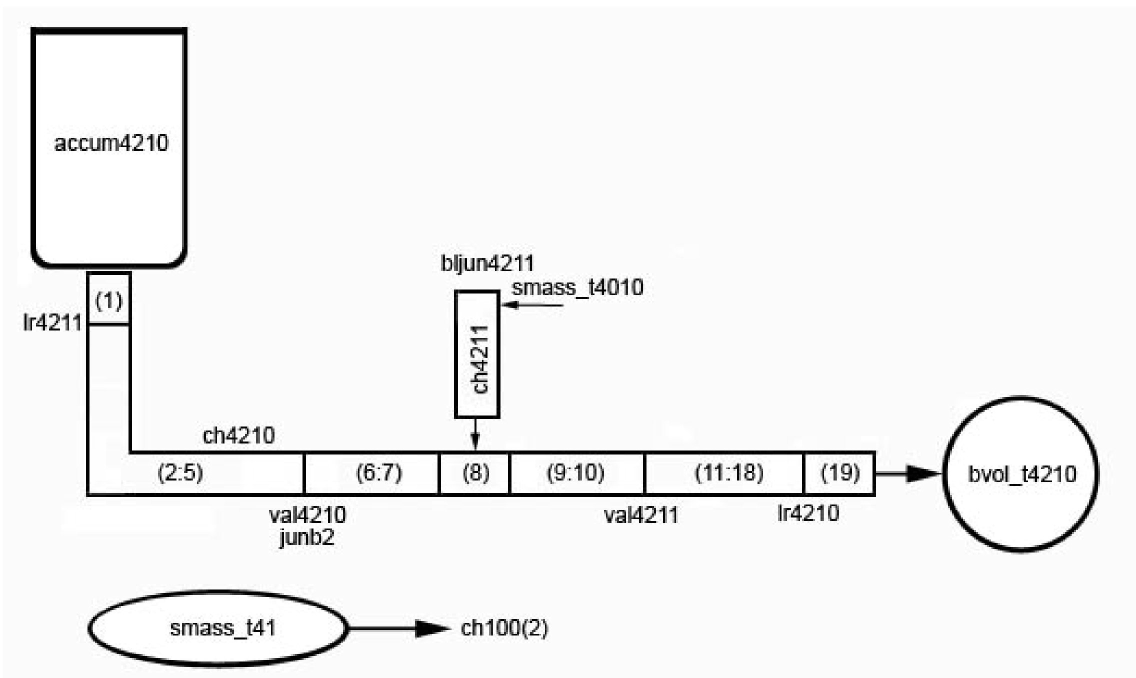

Figure 3 – DVI-2 nodalization scheme

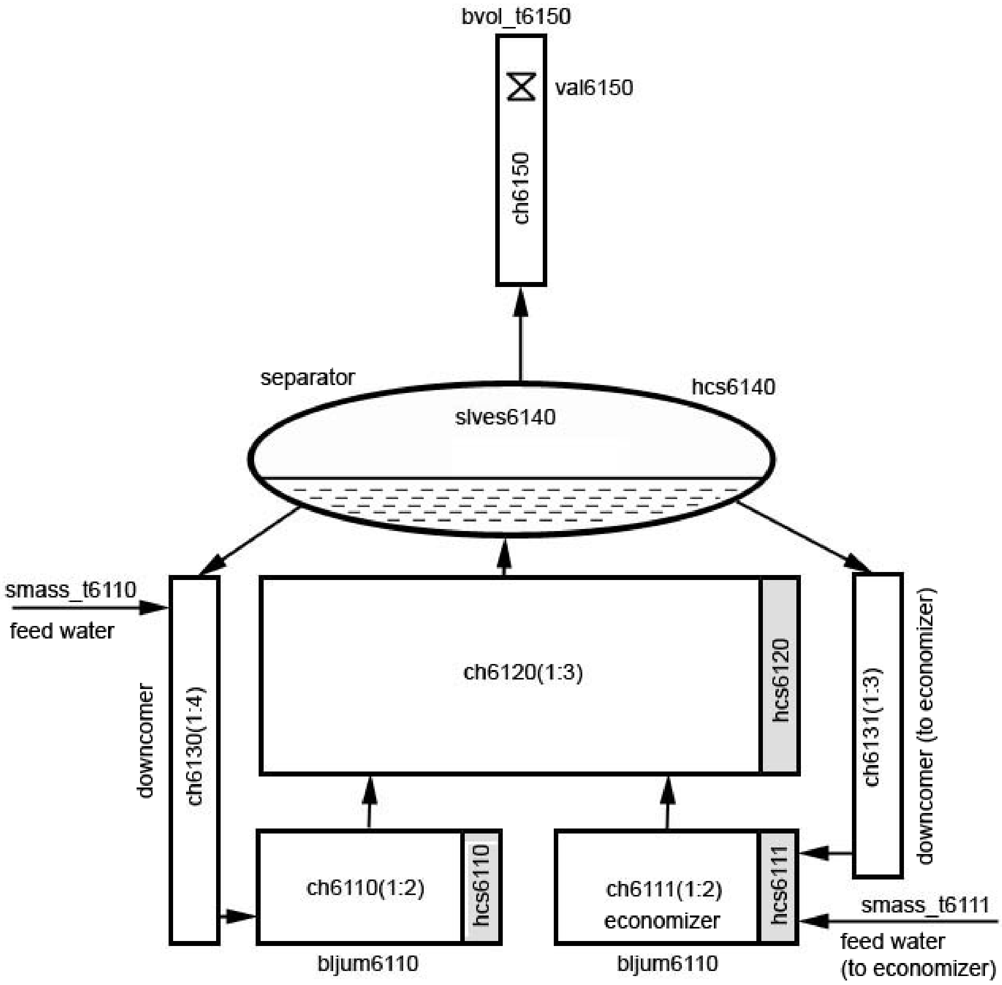

Figure 4 – Steam generator nodalization scheme

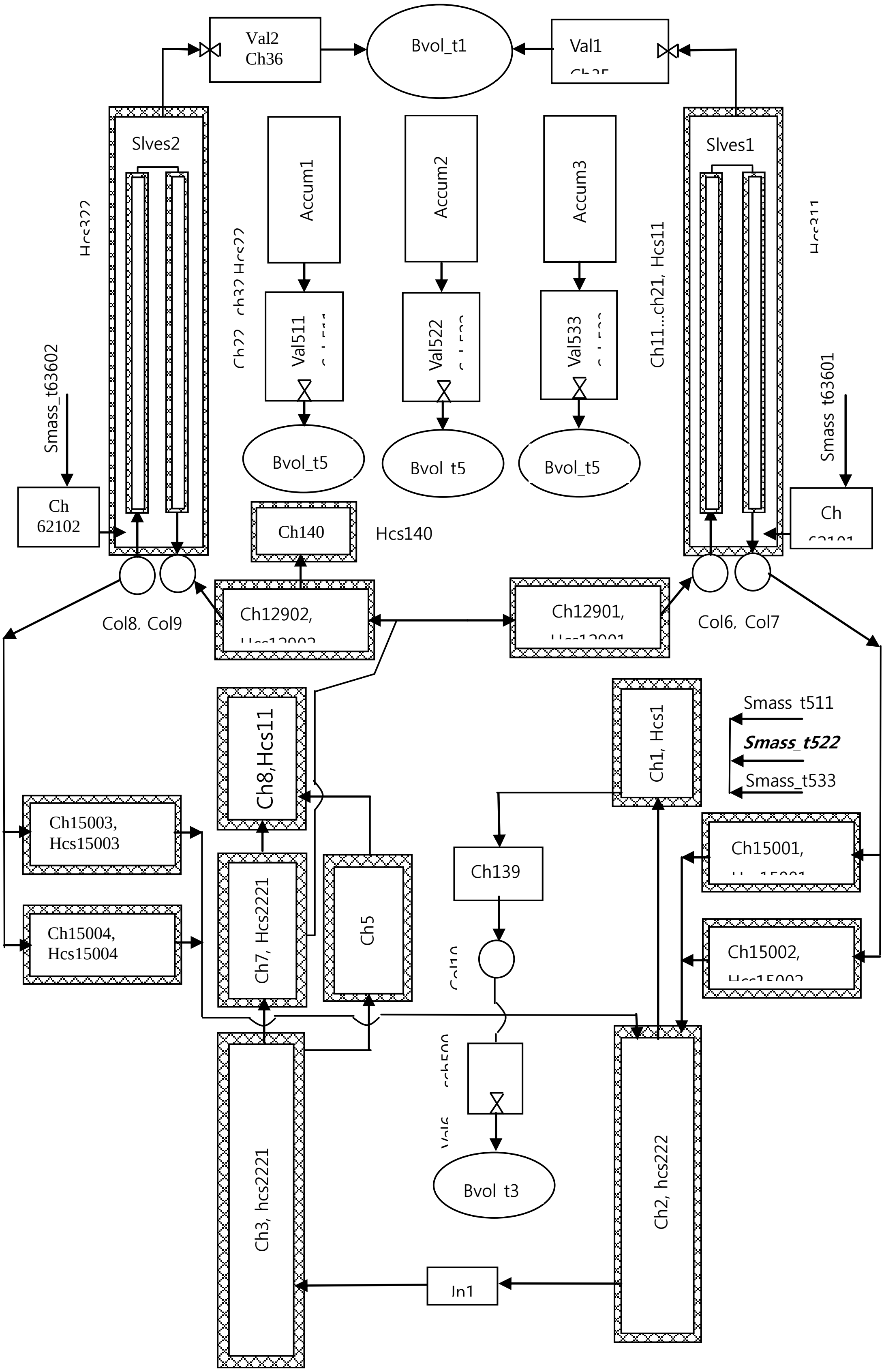

Figure 5 – ATLAS nodalization scheme

4.3 Calculation results

Transient based on [2]. Safety systems model description was taken from [3].

Time sequence of events is given in Table 5.

Table 5 – Time sequence of events

Time, s			Event
GP1	GP2	exp *	
0,0	0,0	0,0	Break open
31,39	26,9	LLP	Pressurizer pressure below 10,72 MPa
31,39	26,9	LLP+0,0	Pressurizer heater trip
31,46	27,0	LLP+0,07	Turbine isolation
31,74	27,4	LLP+0,35	Reactor scram
38,46	34,0	LLP+7,07	Main feedwater isolation
59,67	55	LLP+28,28	Safety injection pump start
615,99	684	LUDP	Reactor downcomer pressure below 4.03MPa
615,99	684	LUDP+0,0	Safety injection tank (SIT) start
3000,0	3000		End of calculation

*) according to [2] data (page 3).

REFERENCES

1. ATLAS Facility and Instrumentation Description Report, KAERI, 2009
2. Detailed Information on Actual Test Conditions and Procedures for ISP-50, KAERI, 2009
3. ISP-50 Specifications for a Direct Vessel Injection Line Break Test with the ATLAS, KAERI, 2009

5. Gidropress (GP3, V. Yudakhin)

5.1 Input file description

Nodalization schemes of variant GP3 are given in Figures 1-5. Reactor nodalization scheme is given in figure 1. The core consists of three independent thermohydraulic channels with different power according to power group given in specification (3.2.1.2). Loop with pressurizer nodalization scheme is given in Figure 2. Both cold legs are identical, so only one is presented. Loop without pressurizer is identical. Figures 3,4 show DVI-1, DVI-2 scheme. DVI-3, DVI-4 are identical to DVI-1 except of SIP. Secondary side scheme is given in Figure 5. Steam generator consists of economizer (ch6120), main heat exchange part (slves6110). Tubes of steam generator are modeled by one U-tube. Safety system elements are given in table 1. SIP is simulated by boundary condition – specified flow rate depending on pressure in connection point.

Table 1. Safety system elements (GP3)

Name	Designation		
Channel number	1	2	3
Tank	accum1	accum2	accum3
Tank pipelines	ch4110	ch4210	ch4310
Pump		smass_t4010	

The key points of nodalization differences are summarized below. There are no collectors in GP1 scheme all channels are connected directly. It results in different ways of numerical solution inside the code. Figures show that there are some difference in SG modeling. Primary to secondary side heat exchange models in GP1 and GP3 are similar. GP2 has more detailed SG primary side model and simple secondary side. Slves is a point element, so water inside this element has a single temperature. Water temperature is close to SG saturation temperature in this case. Roughly, core inlet temperature cannot be lower than SG water temperature. That is why in GP2 secondary side pressure was reduced in order to obtain required core inlet temperature. GP1 and GP3 SG models consist of spatially distributed elements (ch) so in these cases there is spatial distribution of water temperature inside SGs. Hence core inlet temperature depends not only on SG pressure but feed water temperature and flow rate.

Initial steady state conditions for variants GP1-3 and the experiment are given in table 2 in comparative way. RCS flow rate is based on energy balance according to Korean side answer (Summary Q&A, p.22), that is why it was reduced in comparison to measured experimental value.

Table 2. Initial steady state conditions.

Parameter	Experimental value*)	Calculated values		
		GP1	GP2	GP3
Core power, MW	1,636	1,636	1,636	1,636
PRZ Pressure , MPa	15,596	15,61	15,55	15,53
Core inlet temperature, °C	290	290,5	290	290,15
Core outlet temperature, °C	325	324,8	325.1	324,87
Hot leg temperature, loop 1, °C	324,4	324,6	325	324,49
Hot leg temperature, loop 2, °C	325,3	324,6	325	324,49
Cold leg temperature, loop 1A, °C	292,2	290,3	290,2	289,58
Cold leg temperature, loop 1B, °C	292,1	290,3	290,2	289,58
Cold leg temperature, loop 2A, °C	291,8	290,3	290,2	289,58
Cold leg temperature, loop 2B, °C	292,0	290,3	290,2	289,58
RCS flow rate, kg/s	2,2	2,0	2,0	2,044
Pressurizer level, m	3,32	3,32	3,22	3,32
Steam generator pressure, MPa	7,83	7,86	7,44	7,86
Feed water temperature, °C	234,4/235,2	232,2	-	225,5
Economizer feed water temperature, °C	225,5/256,3	235,0	225	225,5
Feed water flow rate, kg/s	0,0	0,0	0,0	0,0
Feed water flow rate to economizer, kg/s	0,431/0,435	0,434	0,425	0,457
Steam generator water level, m	2,03/1,97	2,0	2,0	1,98
SIT pressure, MPa	4,19/4,21/4,23	4,2	4,2	4,2
SIT temperature, °C	50,2/50,5/50,1	50	50	50
SIT Levels, %	95,0/95,2/94,3	95,0/95,2/94,3	95,0/95,2/94,3	95,0/95,2/94,3

*) according to [2] (table 2 page 5).

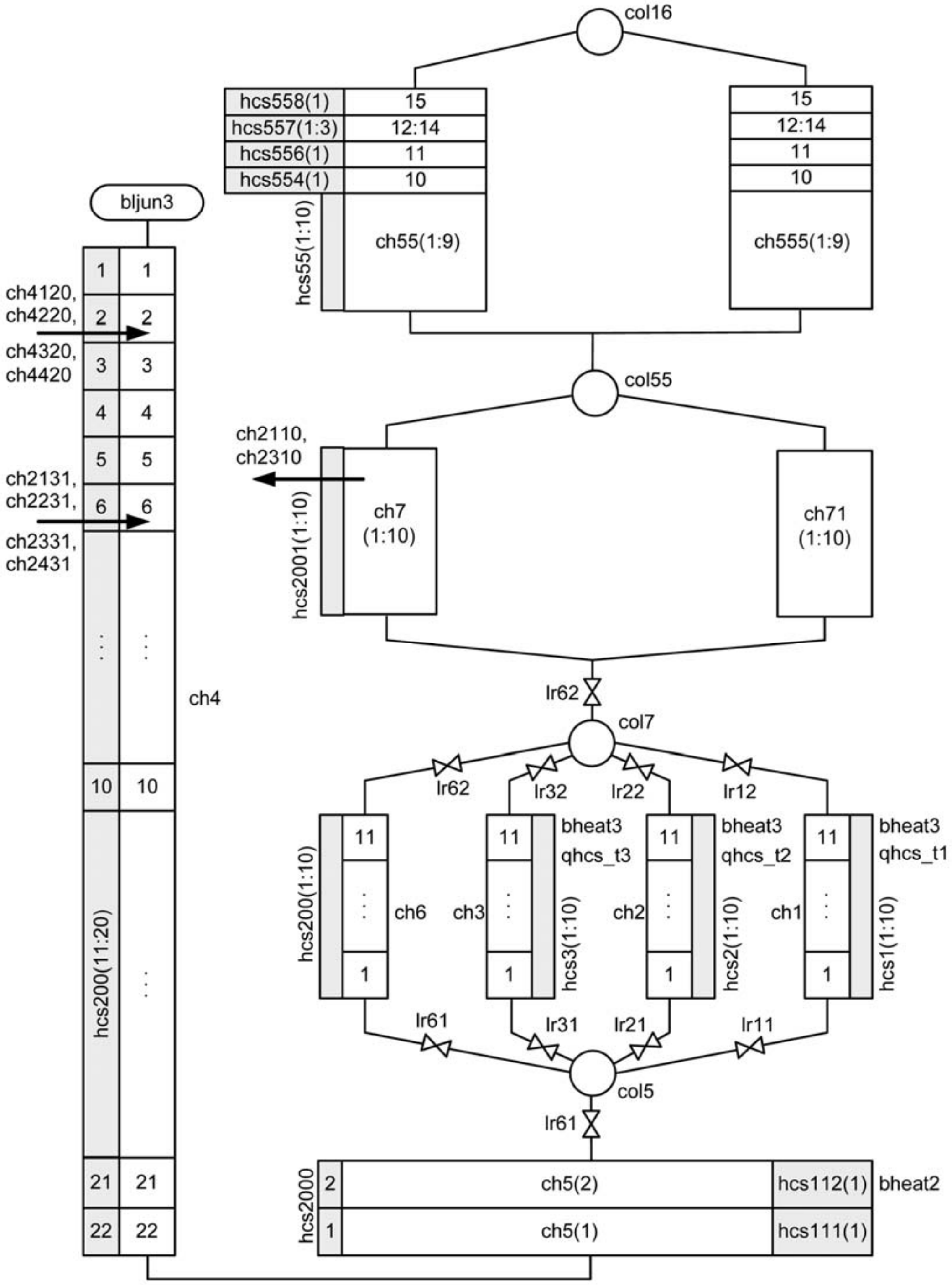

Figure 1 - Reactor nodalization scheme

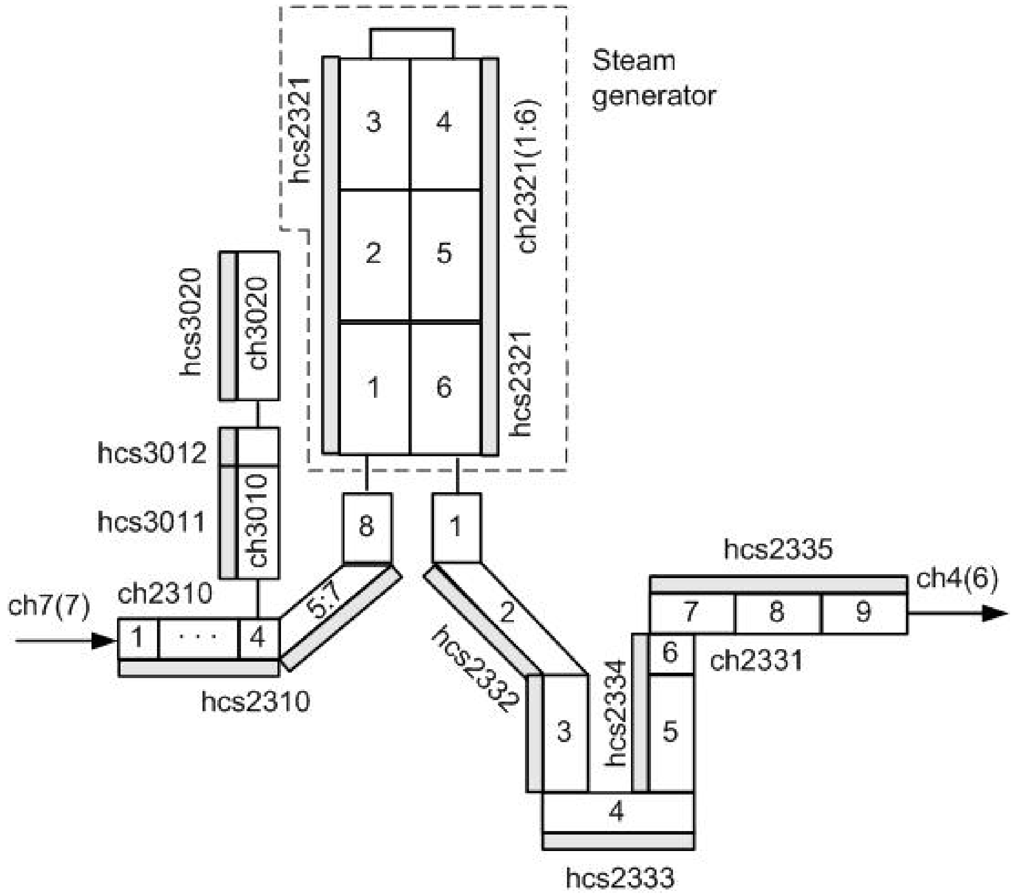

Figure 2 - Primary circuit nodalization scheme

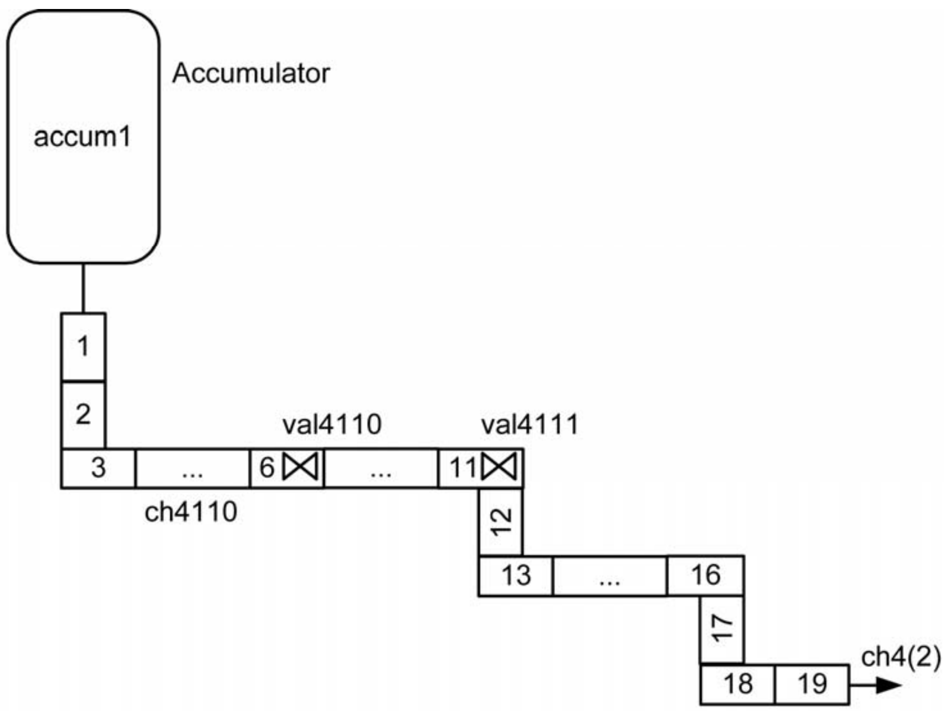

Figure 3 – DVI-1 nodalization scheme

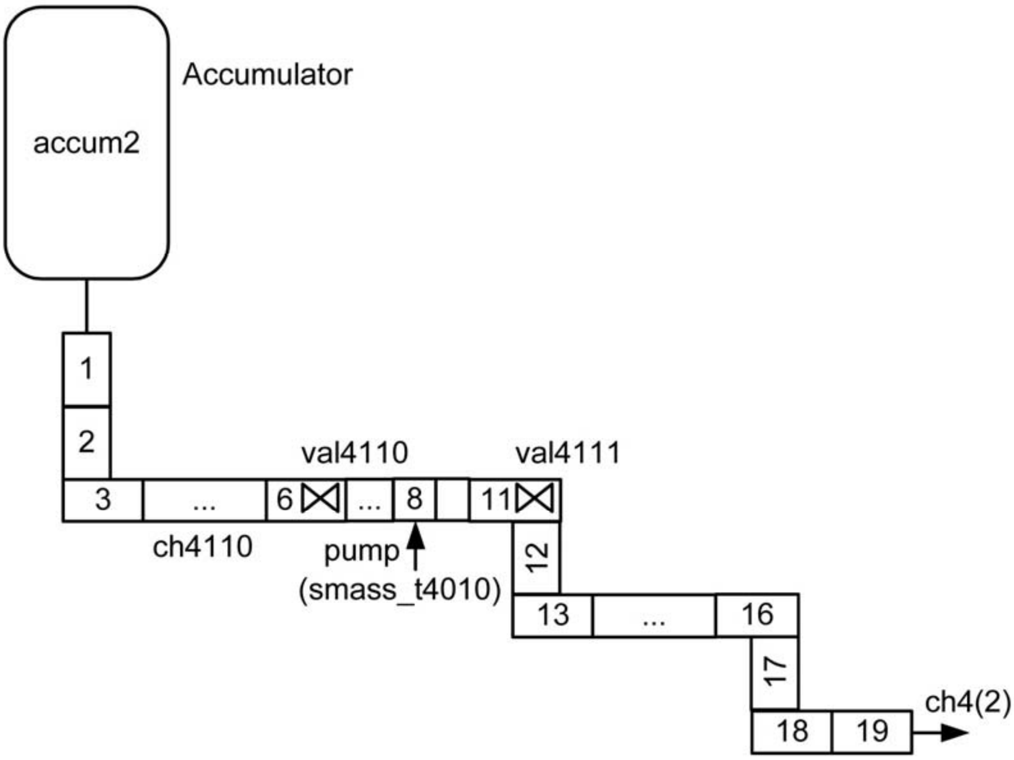

Figure 4 – DVI-2 nodalization scheme

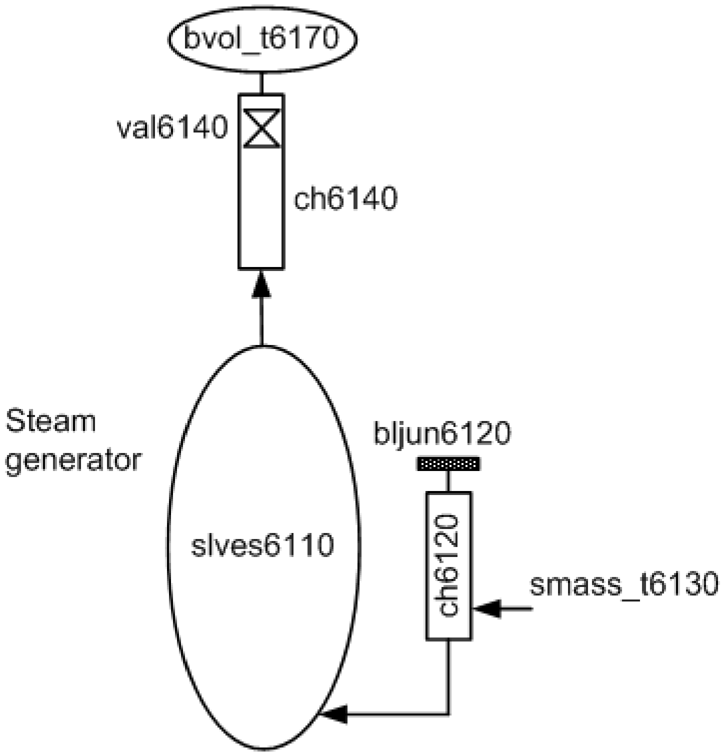

Figure 5 – Steam generator nodalization scheme

5.2 Calculation results

Transient based on [2]. Safety systems model description was taken from [3].

Time sequence of events is given in Table 3.

Table 3 – Time sequence of events

Time, s				Event
GP1	GP2	GP3	exp *	
0,0	0,0	0,0	0,0	Break open
31,39	26,9	42,1	LLP	Pressurizer pressure below 10,72 MPa
31,39	26,9	42,1	LLP+0,0	Pressurizer heater trip
31,46	27,0	42,17	LLP+0,07	Turbine isolation
31,74	27,4	42,45	LLP+0,35	Reactor scram
38,46	34,0	49,17	LLP+7,07	Main feedwater isolation
59,67	55	70,38	LLP+28,28	Safety injection pump start
615,99	684	658,6	LUDP	Reactor downcomer pressure below 4.03MPa
615,99	684	658,6	LUDP+0,0	Safety injection tank (SIT) start
3000,0	3000	2905,0		End of calculation

*) according to [2] data (page 3).

REFERENCES

1. ATLAS Facility and Instrumentation Description Report, KAERI, 2009
2. Detailed Information on Actual Test Conditions and Procedures for ISP-50, KAERI, 2009
3. ISP-50 Specifications for a Direct Vessel Injection Line Break Test with the ATLAS, KAERI, 2009